

**Ultimate and Proximate Causes behind Evolutionary Plastic
Response in the Nematode Genus *Pristionchus*
(A Natural Isolates' Perspective)**

Dissertation

der Mathematisch-Naturwissenschaftlichen Fakultät
der Eberhard Karls Universität Tübingen
zur Erlangung des Grades eines
Doktors der Naturwissenschaften
(Dr. rer. nat.)

vorgelegt von
Mohannad Dardiry
aus Giza, Ägypten

Tübingen
2022

Ultimate and Proximate Causes behind Evolutionary Plastic Response in the
Nematode Genus *Pristionchus* (A Natural Isolates' Perspective)

Dissertation

der Mathematisch-Naturwissenschaftlichen Fakultät
der Eberhard Karls Universität Tübingen
zur Erlangung des Grades eines
Doktors der Naturwissenschaften
(Dr. rer. nat.)

vorgelegt von
Mohannad Dardiry
aus Giza, Ägypten

Tübingen
2022

Gedruckt mit Genehmigung der Mathematisch-Naturwissenschaftlichen Fakultät der Eberhard Karls Universität Tübingen.

Tag der mündlichen Qualifikation:	28.11.2022
Dekan:	Prof. Dr. Thilo Stehle
1. Berichterstatter:	Prof. Dr. Ralf J. Sommer
2. Berichterstatter:	Prof. Dr. Oliver Bossdorf
3. Berichterstatter:	Prof. Dr. Ehab Abouheif

Table of contents

Table of contents	3
I. Acknowledgments	6
II. Summary	7
III. Deutsche Zusammenfassung	8
IV. List of publications	10
1. General introduction	11
1.1. On the meaning of causation	11
1.1.1. The driving question and its dimensions	11
1.1.2. The first pillar (On the nature and properties of the cause)	12
1.1.3. The second pillar (The logical link between the cause and the effect)	15
1.1.4. The third pillar (The epistemological approach)	17
1.2. On the nature of biological causation	19
1.2.1. Platonic causation	19
1.2.2. Aristotelian four causes	21
1.2.3. Ernst Mayr and the concept of proximate and ultimate causes	24
1.2.4. Nicolaas Tinbergen and his four questions	26
1.3. A very short leap on the history of causation behind biological diversity	28
1.3.1. Pre-Darwinian thoughts	28
1.3.2. Post-Darwinian evolutionary theories	32
1.4. On the meaning of phenotypic plasticity	36
1.4.1. Universality of phenotypic plasticity	36
1.4.2. Genetic basis of plasticity	39
1.4.3. Phenotypic plasticity as a driver for evolutionary novelties	41
1.5. <i>Prisitonchus pacificus</i> : a model for phenotypic plasticity	44
1.5.1. <i>Prisitonchus pacificus</i> as a model organism for studying plasticity	44
1.5.2. Natural variants approach to understand the evolutionary “why” and the mechanistic “how” of mouth-form phenotypic plasticity	46
2. Thesis aims	48
3. Results	49
3.1. The genetics of phenotypic plasticity in nematode feeding structures	49

3.1.1. Synopsis	49
3.2.1. Own contribution	49
3.2. Environmental influence on <i>Pristionchus pacificus</i> mouth-form through different culture methods	50
3.2.1. Synopsis	50
3.2.2. Own contribution	50
3.3. A developmental switch generating phenotypic plasticity is part of a conserved multi-gene locus	51
3.3.1. Synopsis	51
3.3.2. Own contribution	52
3.4. Adult influence on juvenile phenotypes by stage-specific pheromone Production	53
3.4.1. Synopsis	53
3.4.2. Own contribution	53
3.5. Crowdsourcing and the feasibility of manual gene annotation: a pilot study in the nematode <i>Pristionchus pacificus</i>	54
3.5.1. Synopsis	54
3.5.2. Own contribution	54
3.6. Sex or cannibalism: Polyphenism and kin recognition control social action strategies in nematodes	55
3.6.1. Synopsis	55
3.6.2. Own contribution	56
3.7. Experimental and theoretical support for costs of plasticity and phenotype in a nematode cannibalistic trait.	57
3.7.1. Synopsis	57
3.7.2. Own contribution	58
3.8. Cost of adaptive plasticity and spatial heterogeneity in <i>Pristionchus pacificus</i> : a computational perspective	59
3.8.1. Synopsis	59
3.8.2. Own contribution	59
3.9. Dissecting the genetic architecture underlying mouth dimorphism in <i>P. pacificus</i>	

identifies cis-regulatory variations in a multi-gene locus	60
3.9.1. Synopsis	60
3.9.2. Own contribution	61
4. Discussion	62
5. References	68
6. Appendix	85

I. Acknowledgments

I would like to thank all the Sommer lab members for all the support through the years. I would like to thank all collaborators I have worked with; it would be impossible to learn and produce knowledge without any of them. A special thanks to Dr. Bogdan Sieriebriennikov; not only that he introduced me to the lab and guided me in my early times, but he was as well a good friend. Another special thanks to Dr. James Lightfoot for sharing a significant part of my Ph.D. journey as a colleague and supportive friend. I also would like to thank Dr. Ata Kalirad for his vital contribution to my Ph.D. journey through collaboration, discussions, philosophical talks, and friendship. I am also very thankful to Dr. Christian Rödelsperger for his bioinformatics support and insightful conversations. The same applies to Dr. Neel Prabh and Dr. Kohta Yoshida for helpful discussions and friendship. Much gratitude and respect to Dr. Michael S. Werner for being an honest and fair scientist. I am also thankful to my colleague Tobias Theska for helping in writing the German summary of the thesis. Much appreciation for the technical staff for their continuous support, especially Hanh Witte, Gabi Eberhardt, and Heike Haussmann. They were instrumental in keeping the workflow in the best shape.

I am genuinely grateful and thankful to my supervisor Prof. Dr. Ralf J. Sommer, for guidance and support through my Ph.D. time. He gave me the space to grow intellectually and practically. I indeed appreciate and respect his management and efforts. The time I spent in the Sommer lab has made me a more mature scientist and person. My one-to-one talks with Ralf and our daily regular kitchen talks were more than learning how to do science; I have acquired wisdom and vision from these times.

Finally, I would like to warmly thank my family: my parents, my brother, my two lovely boys (Nour and Seraj); with their smiles, I appreciated every moment I have. But above all, I am genuinely grateful and thankful to my beautiful wife, Lamia Abdraboh. She tolerated my long absence and endless hours of working and reading. Indeed, this journey would not be possible without her strength and support. She is a gorgeous representation of partnership and generosity.

II. Summary

Phenotypic plasticity is the ability of a single genotype to produce several phenotypes responding to environmental stimuli. Phenotypic plasticity is widely spread, with its evolutionary consequences being under investigation in several taxa. However, a clear insight into the evolutionary significance of plasticity requires an integrative understanding of this phenomenon. A cornerstone for such insight is the molecular machinery underlying plastic responses. The nematode genus *Pristionchus* provides an opportunity for exploring such evolutionary significance in an integrative framework. The feeding structures in *Pristionchus* display a dimorphic switch response to environmental conditions. Furthermore, the affordability of genetic manipulations, the accessibility to a vast collection of isolates, and the ecological significance of the dimorphism, makes *Pristionchus* a promising system for investigating the significance of genetic switches in evolution. *Pristionchus* worms can develop either a wide mouth-form with two teeth, (Eurystomatous), or a narrow mouth-form with a single tooth, (Stenostomatous). This morphological plasticity is associated with behavioral plasticity. The Eu form enables predation on other nematodes, while St worms are strictly microbivorous. Among more than 40 species, the hermaphrodite *P. pacificus* and its 'wild type' strain PS312 have served as a reference, and genetic investigations have identified many components in the network underlying the morphological switch. This genetic network revealed the involvement of the *eud-1*/sulfatase as the master regulator of switch control. In my thesis, I aimed to follow a natural isolates' perspective to understand the evolutionary significance of mouth-form plasticity, morphologically and behaviorally. On the mechanistic side, I revealed the involvement of *eud-1* cis-regulation in controlling mouth-form responses in natural isolates. I was also involved in identifying that *eud-1* is part of a multi-gene locus, with several of these genes being involved in the regulation of mouth-form. On the adaptive value side, I investigated the role of the costs of plasticity and costs of phenotype in shaping the population dynamics in *P. pacificus* natural isolates. I also majorly contributed to revealing the social action strategies in the genus *Pristionchus*, demonstrating that mouth-form dimorphism, kin-recognition, and relatedness shape competitive or cooperative strategies in this genus.

III. Deutsche Zusammenfassung

Phänotypische Plastizität beschreibt die Fähigkeit eines einzelnen Genotyps, als Reaktion auf Stimuli der Umwelt, mehrere Phänotypen zu produzieren. Phänotypische Plastizität ist weitverbreitet und ihre evolutionären Konsequenzen werden derzeit in mehreren Taxa untersucht. Allerdings bedarf ein klarer Einblick in die evolutionäre Signifikanz dieser Plastizität eines integrativen Verständnisses dieses Phänomens. Ein Grundstein für ein solches Verständnis ist die molekulare Maschinerie, die der plastischen Reaktion zugrunde liegt. Die Nematodengattung *Pristionchus* bietet die Gelegenheit, eine solche evolutionäre Signifikanz in einem integrativen Rahmen zu studieren. Die Mundstrukturen von *Pristionchus* weisen eine dimorphe Schaltantwort auf verschiedene Umweltkonditionen auf. Die Erschwinglichkeit von genetischen Manipulationen, die Zugänglichkeit zu Sammlungen zahlreicher Wildnis-Isolate und die ökologische Signifikanz des zuvor genannten Dimorphismus', machen *Pristionchus* zu einem vielversprechenden System für Studien zur Signifikanz von genetischen Schaltern in der Evolution. *Pristionchus*-Würmer können entweder eine breite Mundform („eurystomat“) mit zwei Zähnen, oder eine schmale Mundform („stenostomat“) mit einem einzelnen Zahn ausbilden. Diese morphologische Plastizität geht mit einer verhaltensbezogenen Plastizität einher. Die eurystomate Form ermöglicht die Prädation anderer Nematoden, wohingegen die stenostomaten Würmer ausschließlich mikrobivor leben. Unter den mehr als 40 beschriebenen Arten diente die hermaphroditische *P. pacificus*, speziell der Wildtypstamm PS312, als Referenz in genetischen Untersuchungen welche eine Vielzahl von Komponenten des Netzwerkes enthüllten, das dem morphologischen Schalter zugrunde liegt. Dieses genetische Netzwerk offenbarte die Beteiligung der Sulfatase *eud-1* als Hauptregulator des Schaltnetzwerkes. Ziel meiner Arbeit war, die evolutionäre Signifikanz der Mundformplastizität, speziell in Würmern die aus der Wildnis isoliert wurden, auf morphologischer und verhaltensbiologischer Ebene zu verstehen. Auf der mechanistischen Seite konnte ich aufzeigen, dass die *cis*-Regulation von *eud-1* eine wichtige Rolle in der Kontrolle der Mundformplastizität wild-isolierter Würmer spielt. Ich war außerdem an der Identifikation des Multi-Gen-Locus' involviert, der *eud-1* und weitere Gene beinhaltet die an der Regulation der Mundformen

beteiligt sind. Auf der Seite des adaptiven Wertes untersuchte ich die biologischen Kosten der Plastizität und des Phänotyps, und wie diese Faktoren die Populationsdynamik wild-isolierter *P. pacificus* beeinflussen. Weiterhin war ich maßgeblich an der Entschlüsselung sozialer Strategien von *Pristionchus* Nematoden beteiligt, die demonstrieren, dass der Mundformdimorphismus, die Fähigkeit Verwandte zu erkennen und der Verwandtschaftsgrad die kompetitiven oder kooperativen Strategien dieser Nematoden formen und beeinflussen.

IV. List of publications

1. Sommer RJ, **Dardiry M**, Lenuzzi M, Namdeo S, Renahan T, Sieriebriennikov B, Werner MS. The genetics of phenotypic plasticity in nematode feeding structures. *Open Biol.* 2017;7. doi:10.1098/rsob.160332
2. Werner MS, Sieriebriennikov B, Loschko T, Namdeo S, Lenuzzi M, **Dardiry M**, Renahan T, Sharma DR, Sommer RJ. Environmental influence on *Pristionchus pacificus* mouth form through different culture methods. *Sci Rep.* 2017;7: 7207.
3. Sieriebriennikov B, **Dardiry M***, Prabh N*, Witte H, Röseler W, Kieninger MR, Rödelsperger C, Sommer RJ. A Developmental Switch Generating Phenotypic Plasticity Is Part of a Conserved Multi-gene Locus. *Cell Rep.* 2018;23: 2835–2843.e4.
4. Werner MS*, Claaßen MH*, Renahan T*, **Dardiry M**, Sommer RJ. Adult Influence on Juvenile Phenotypes by Stage-Specific Pheromone Production. *iScience.* 2018;10: 123–134.
5. Rödelsperger C, Athanasouli M, Lenuzzi M, Theska T, Sun S, **Dardiry M**, Wighard S, Hu W, Sharma DR, Han Z. Crowdsourcing and the feasibility of manual gene annotation: A pilot study in the nematode *Pristionchus pacificus*. *Sci Rep.* 2019;9: 18789.
6. **Dardiry M***, Lightfoot JW*, Kalirad A, Giaimo S, Eberhardt G, Witte H, Wilecki M, Rödelsperger C, Traulsen A, Sommer RJ. Sex or cannibalism: Polyphenism and kin recognition control social action strategies in nematodes. *Sci Adv.* 2021;7. doi:10.1126/sciadv.abg8042
7. **Dardiry M**, Piskobulu V*, Kalirad A*, Sommer RJ. Experimental and theoretical support for costs of plasticity and phenotype in a nematode cannibalistic trait. Submitted.
8. Kalirad A, **Dardiry M**, Sommer RJ. Cost of adaptive plasticity and spatial heterogeneity in *Pristionchus pacificus*: a computational perspective. Ready for submission.
9. **Dardiry M**, Lightfoot JW, Rödelsperger C, Witte H, Eberhardt G, Sommer RJ. Dissecting the genetic architecture underlying mouth dimorphism in *P. pacificus* identifies cis-regulatory variations in a multi-gene locus. In preparation.

1. General introduction

1.1. On the meaning of causation

'I think; therefore, I am'¹

–Rene Descartes, *Discourse on the Method*

1.1.1 The driving question and its dimensions

What are the causes behind biological diversity? This question has been a significant driving force for a contemporary comprehension of knowledge in recent decades, although it resembles an unadorned inquiry^{2,3}. Moreover, it profoundly influenced social, cultural, economic, and political thinking⁴⁻⁷. For instance, the idea of improving the human “stock” by promoting the reproduction of individuals with favorable survival abilities while eliminating ones with unfavorable disabilities, *i.e.*, eugenics⁸, is considered by numerous historians to be a dreadful reflection of solving social and political issues by employing biological knowledge⁹⁻¹¹. Exquisitely, it is not a unidirectional process rather a bidirectional one. For instance, the evolutionary geneticist Eva Jablonka suggested that postmodernism, an intellectual skeptic movement established in the 20th century¹², has affected the narrative of genetic determinism and its implications¹³. Thus, despite questioning the source of biological variation appears as a curious intention for understanding life, the inferences created out of it had real ramifications on the structure of the modern world.

A comprehensive insight for answering this question requires a deep understanding of three main pillars: i) The nature of the causal link between the source of variation and the displayed effect. ii) The logical framework inferring results from premises to reach justifiable conclusions. iii) The epistemological approach of which the method for obtaining knowledge is determined and evaluated¹⁴. While these three aspects are seemingly distinct, they have evolved simultaneously and are undoubtedly linked.

Causality is a prodigious concept; however, many historians and philosophers refer to Ancient Greek philosophy as the first systematic attempt to understand causation¹⁵⁻¹⁷. Nevertheless, if we restrict the notion of causality solely on defining the

causal link without considering the nature of the cause, prehistoric hunting paintings might be one of the earliest attempts to record the human plumb for causation. In this case, causal cognition is suggested to drive technical reasoning¹⁸⁻²¹. Chronologically, many historians credit the first formal and systematic theory of causality to the great Greek philosopher Aristotle in his treatise *Physics* and *Metaphysics*^{15,16}. However, causation has been conceptually inspected pre-Aristotle, mainly by Aristotle's predecessors Socrates and Plato^{17,22,23}. Subsequently, the Ancient Greek philosophy immensely affected the Arabic and Islamic golden age causal philosophy (e.g., Ibn Sina "Avicenna", Ibn Rushd "Averroes")²⁴, as well as the philosophy of the Middle ages (e.g., Thomas Aquinas, William of Ockham)²⁵, to finally reach modern history thoughts (e.g., Descartes, Hume, Bacon, Mill)^{14,17,26}.

Therefore, in this introductory essay, I will first shed light on the three previously mentioned pillars: the nature of the cause, the logical reasoning framework, and the epistemological approach¹⁴. Afterwards, I will briefly highlight the significant contribution of four major leading characters regarding biological causality: Plato, Aristotle, Ernst Mayr, and Nikolaas Tinbergen. Subsequently, I will discuss the development of thoughts explaining biological diversity pre-Darwinian, and post-Darwinian. I will then focus on the main topic of the thesis, phenotypic plasticity, as a potential cause of phenotypic diversity and a driver of evolutionary novelty^{27,28}. Finally, I will explain the advantages of using the model organism *Pristionchus pacificus* to dissect both ultimate and proximate causes behind the evolution and the maintenance of the plastically dimorphic mouth-form. But note that for an empirically driven thesis like mine, this philosophical and historical introduction is solely scratching the tip of the iceberg.

1.1.2 The first pillar (On the nature and properties of the cause)

What is the nature of the cause? In principle, this question represents an ontological query. It attempts to define causal entities' *essence* and *properties*, besides identifying their *relation* to the proceeding effect^{14,29,30}. *Ontology* could be defined as the branch of philosophy concerned with studying what entities exist and the features of these entities³⁰. Assuming each *event* Y has a temporal predecessor X and a temporal

successor Z, such a proposal would indicate two assumptions: i) There are three *events*. ii) There is a temporal order of these *events* regarding one another³¹⁻³³. These assumptions require clarification of what an *event* is first and then asking if the cause-effect observation between the three *events* is repetitive or, in other words, if these *events* enjoy some *properties* and *relations*.

First, *events* are subject to significant ontological disagreement as to their nature³⁴. The criteria implemented to distinguish between different entities and rank them have evolved from Aristotle to the modern era generating different conceptual paradigms³⁵. For instance, there is an ontological disagreement if *events* would possess *properties* and how *events* are different from another entity named *objects*³⁴⁻³⁷. Thus, the nature of an *event* is seemingly paradigm-dependent.

Secondly, the *relation* between the cause and the effect was also under a vast body of inspection. However, one of the most influential philosophers who scrupulously dissected this *relation*, is David Hume (1711-1776)³⁸. Hume identified three cause-effect *relation* conditions: i) First, temporal priority, where the cause would precede its effect. ii) Second, contiguity; that is, a cause should be in a spatiotemporal vicinity to its effect. iii) Third, the cause and the effect should represent a regularity; thus, if a cause (c) is followed by an effect (e), all similar (c) causes would be in a similar *relation* to alike (e) effects; in what is known as a regularity theory of causality^{14,26,31,38-40}.

Before explaining these conditions in detail, it is important to note that a conceptual key in the Humean theory is the realization of the causal link as solely experience-dependent, mainly as repeated experience³⁹. Indeed, for Hume, causal links are inferred from observations, and thus, they are subjected to change according to perceptions and beliefs^{39,40}. Therefore, he argued against necessity in the actual world. Nevertheless, this regular association is indeed in the minds³⁹.

This theory of regularity invoked few objections to its explanatory power. First, the temporal priority of the cause to the effect would suggest causal asymmetry, where the cause would always be *a priori* to its effect. However, this assumption does not consider simultaneous causation and retro-causality theories, where mathematical propositions stand against sequential causation and directionality⁴¹⁻⁴². Moreover, the second

assumption, contiguity, was questioned as it disbars distal causation³⁹. Nevertheless, Hume addressed this issue in his book “*A treatise of human nature*” by arguing for a chain of contiguous causal links between the first cause and the final effect⁴³. More importantly, it has been a matter of debate between Hume’s scholars on connecting causation in the minds to causation in the actual world^{39,44}.

Hume’s regularity theory has been a subject for several enhancements reaching modern times. For instance, John Stuart Mill (1806-1873), an English philosopher, refined Hume’s theory by defining a set of positive and negative factors representing causes, *i.e.*, he defined *tokens* that represent particular *instances*. He argued that the totality of these factors would be sufficient to produce the effect^{39,40,45}. Moreover, these *tokens* might be grouped in classes of *types*, of which similar *tokens* from the same *type* would produce similar effects³⁹. Afterward, the Australian philosopher John Leslie Mackie (1917-1981) updated Hume’s and Mill’s theory proposing INUS condition, *i.e.*, an insufficient but non-redundant part of an unnecessary but sufficient condition^{39,40}. Mackie principally accounted for the clusters of causes that together lead to an effect. Each cluster of these causes is sufficient to produce the effect; however, each is unnecessary if another cluster of causes is actual. To explain this, let us suppose different causes of a burning house. The first cluster of causes might be represented by a spark of fire, oxygen in the air, and the absence of water sprinklers. A second cluster would be a fire-raiser and the use of gas. A third cluster would be a burning tree falling and flammable material in the house. Each part of each cluster is non-redundant and insufficient to initiate the burning of the house, but each cluster is sufficient by itself to initiate the effect; however, it is unnecessary if the other cluster does happen^{39,40}. All of this would occur under natural laws³⁹. Nevertheless, it remains firm that conditional causality theories, such as Mackie’s theory, rely on a deterministic explanation of causality, while another school for envisioning causal links is the probabilistic school⁴⁰.

In the actual world, an essential distinction between the two schools is that in the deterministic perception of causality, the cause will always be followed by its effect when it occurs. Under this assumption, probabilities are represented as a lack of knowledge about the causal link. On the other hand, proponents of probabilistic causation argue that the cause would only increase the chance of the effect to follow. However, it is not

imperative⁴⁰. Probabilistic causation has been the leading theory of causation in the second half of the 20th century and is still applied during the current time through probabilistic models⁴⁶.

In conclusion, defining the nature of the cause and its relation to the effect has been under extensive investigation by numerous scholars. Moreover, two primary schools in comprehending causality are interpreting causation either as a deterministic relation or a probabilistic one. Supposedly the cause was identified, what would be the logical reasoning framework at which this cause could be inferred? This inquiry would represent the second pillar.

1.1.3 The second pillar (The logical link between the cause and effect)

Logical reasoning aims at reaching a coherent argument and justifiable claims^{47,48}. In turn, this argument is used for inferences about the issue under investigation^{47,48}. In principle, arguments can take three forms; deductive, inductive, and abductive. However, some authors would append argumentation via analogy^{47,48}. An argument can be defined as a statement of two structures, premises and conclusions. Simply put, premises might either guarantee the truthfulness of the conclusion or make the conclusion more acceptable or more probable^{47,48}.

A critical distinction between deductive reasoning on one side and inductive, besides abductive reasoning, is that conclusions in the latter two types go beyond the premises. In deductive reasoning, valid and sound arguments are the arguments where the truth of premises necessitates the truth of the conclusions; *e.g.*, premise 1: All animals are living organisms, premise 2: all living organisms are mortal; thus, the conclusion: all animals are mortal. A crucial feature of deductive reasoning is monotonicity^{49,50}. Monotonicity implies the inability to invalidate a previously valid conclusion via adding opposite premises⁴⁸⁻⁵⁰. Deductive reasoning has faced several philosophical issues. In principle, to be described as not ampliative, not flexible to new information, which puts the usefulness of this approach in question⁴⁸. In addition, many scholars question the nature of the necessity involved in the deduction; for instance, can it be metaphysical⁴⁸?

On the other hand, inductive reasoning uses past instances of observation to conclude about future instances and produce general principles⁴⁸. For example, past observations of the sun rising from the east predict that the sun will rise from the east the next day, which will generalize that the sun always rises from the east⁴⁸. In contrast to deductive reasoning, in induction, the truth of the premises does not necessarily imply the truth of the conclusion. Rather it provides a degree of support for the truth of the conclusion⁴⁸. In addition, one commonly known type of inductive reasoning is induction by enumeration⁵¹. It is simply a statistical estimation, such as when a random sample of 200 squirrels are shown to be brownish, inductively, this strongly supports a conclusion that all squirrels are brownish⁵¹. Moreover, unlike deductive reasoning, accumulating new information might change the degree of support to the final conclusion⁴⁸. Therefore, several scholars argue that inductive reasoning is mostly used in modern scientific methodology⁴⁸. However, such an approach has its own back draws as well. For instance, David Hume wondered what defines the correctness of inductive inference and what justifies the generality “Uniformity Principle” of the conclusion⁵². As a result, Hume concluded inductive arguments could not be justified in what is known as the problem of induction⁵². A third, however, a latecomer in the inferential framework, is abduction. Abduction is usually referred to as “inference of the best explanation”⁵³. Like induction, but unlike a deduction, abductive inferences are non-monotonic, meaning that it does not necessarily preserve the truth. Nevertheless, unlike induction, abduction does not generalize *a priori* observation, but rather it seeks to explain something that already happened^{48,53}. The last type of argument is arguing through Analogy. In this case, when A and B are similar, what is true regarding A; is most likely true regarding B. However, this reasoning methodology does not supply how much similarity between A and B would be sufficient to agree if what is true to A is similarly true to B⁴⁸.

Together, these four major directions would represent reasoning frameworks in which a causal argument would fall. Therefore, after discussing the nature of the cause, its properties, and in which framework it would constitute a reasonable argument, comes the question of how the cause would be methodologically identified; and this is the third pillar.

1.1.4 The third pillar (The epistemological approach)

The third pillar answers the question: how to obtain justifiable knowledge? Furthermore, a branch of philosophy considered with knowledge, its limits, its sources, and its comprehension is epistemology^{54,55}. In the highly cited paper, 'Epistemology', the authors argue that epistemology, by one way or the other, seeks to identify cognitive success⁵⁴. The definition of cognitive success and which entities (agents) can achieve such success is a matter of debate⁵⁴. However, here I restrict these entities to theories, where success might be evaluated by being established on all available kinds of evidence, and how conclusive it might be to acquire this evidence⁵⁴. Most scholars argue that knowledge of something requires the justification of the truthfulness of the proposition to this knowledge; it requires a belief⁵⁶. But what justifies a proposition to be true? Note that here, I do not discuss theories of justification such as internalism vs. externalism or foundationalism vs. coherentism⁵⁴. Instead, I will discuss two knowledge paradigms, rationalism, and empiricism⁵⁵, focusing on the evolution of the scientific methodology as a justification tool for knowledge truthfulness, considering that all of these theories are connected.

Arguably, one significant distinction between rationalism and empiricism is the source of knowledge⁵⁴. Scholars suggest five sources of reliable knowledge, not including emotional needs or desires; namely, perception, memory, reason, testimony, and introspection⁵⁴. In the rationalistic approach, the source of knowledge is reason, while in the empirical approach, perception, memory, and introspection are the sources of knowledge. The disagreement between the two approaches is mainly about how we can gain justifiable knowledge^{54,55}. In principle, empiricism relies on experience, either sensible or not, where this justification procedure is called "*a posteriori*"; *i.e.*, the justification of a belief comes after the experience⁵⁴. On the other hand, when the justification is independent of experience, it is called "*a priori*"⁵⁴. Nonetheless, a strict vision of experience would solely restrict the "*a posteriori*" definition to perceptual experience. However, how would knowledge be justified without experience?

Rationalists suggest three main arguments on how to obtain knowledge without experience. First, the intuition/deduction argument, where we understand a proposition

just when seeing it as true, then deduce our belief from these premises to conclusions. For instance, mathematics is considered to be known by intuition and deduction.

The second and the third arguments are the innate knowledge and the innate concept arguments. These assertions suggest that we are born with some knowledge, without the need for experience to grasp this knowledge; however, experiences might bring this knowledge to consciousness⁵⁴. In conclusion, several rationalists rely on the assertion of reason superiority or the indispensability of reason explaining knowledge without the need to experience⁵⁴.

Another school of thought is the empirical school. I will focus more on knowledge obtained through perceptual experience and the methodology of acquiring such knowledge in this school, *i.e.*, scientific knowledge and scientific methodology.

In the highly influential book '*What is this thing called science*⁵⁷', the author states that defining scientific knowledge would not be an easy task giving how this term evolved historically. However, scientific knowledge could be defined as knowledge representing facts based on unbiased observations and experiments perceived by our senses⁵⁷. When these facts are structured systematically and justified reasonably, they constitute laws and theories⁵⁷. This definition is adequate with how scientific knowledge was perceived after the 17th century⁵⁷. After acquiring facts through observations and experiments, inductive reasoning sets theories and laws. Afterwards, deduction is used to draw explanations and prediction⁵⁷. Nevertheless, since the relationship between experiments and theories is circular and evidently subjected to updating and refining, observations need skillful training agents to be performed⁵⁷. Furthermore, two features of science were the subject of discussion through various entailments of history and philosophy of science. Specifically, pluralism of the scientific knowledge and falsification of the scientific methodology⁵⁷.

First scientific pluralism. In brief, despite the seemingly robust and universal approach of scientific methodology, many scholars argue for scientific pluralism⁵⁷. In simple epistemic terms, scientific pluralism refers to the heterogeneity of explanations, the variety of the models, theories, and approaches that can explain a natural phenomenon^{58,59}. For instance, a biological phenomenon might have a historical

evolutionary explanation and a functional molecular explanation⁶⁰. Secondly, in the book ‘*The logic for scientific discovery*’ (1959), Karl Popper discussed the nature of scientific knowledge in detail. He argued for the falsifiability of scientific knowledge to be demarcated from non-scientific one^{61,62}. Under this perspective, a piece of knowledge needs to disprove theories rather than support hypotheses inductively; therefore, it qualifies to be scientific^{59,61}. Furthermore, he argues that observations are selective and never pure⁵⁹. In his opinion, it is impossible to use experience to verify a universal proposition; however, with a single authentic opposite instance, one could refute a theory; thus, scientific knowledge progresses by improving existing theories through falsifying them⁵⁹. Indeed, both features have their proponents and opponents along with the historical development of scientific knowledge.

To conclude, it is apparent from the previous analysis that evaluating a source of knowledge and the methodological approach taken to define causal links, genuinely depends on the epistemological paradigm. Hence, after briefly discussing the three pillars by which causality could be understood, I move into highlighting four figures that influenced the current comprehension of biological causation. Each might have defined the nature of the cause and its properties in their perspective. Some have generated (Plato, Aristotle) a logical reasoning framework and an epistemological approach to support their propositions, while others have followed (Mayr, Tinbergen) pre-existing once. In the end, their enterprise has been immensely influential in understanding the causes behind biological diversity.

1.2. On the nature of biological causation

‘We think we do not have knowledge of a thing until we have grasped its why,
that is to say, its cause’¹⁶

–Aristotle, *Physics*

1.2.1 Platonic causation

Plato (429? –347 B.C.E.) is one of the most influential figures in the history of philosophy⁶³. For many historians, he is regarded as the first person who structured philosophy systematically in Ancient Greek time⁶³. In *Phaedo*, on the soul, Plato argues

for "*the thing responsible*," keeping the essence of the "*thing*" ambiguous²³. However, Phillip Delacy's paper "The problem of causation in Plato's philosophy" asserts that Platonic causation was utterly transcendent, *i.e.*, metaphysical⁶⁴. Moreover, in his paper Platonic cause, David Sedley argues that Plato defines a successful candidate for causation as the "*thing*" for which a logical connection to the effect could be established²³. However, this might appear straightforward; it is anything but plain. For Plato, the sensible physical effect reflects the metaphysical Form or Idea; an *essence*, *e.g.*, "It is because of the [causal dative] beautiful that all beautiful things are beautiful"²³. Thus, the nature of the cause is not the imperfect material rather the intelligible Form⁵⁹. Moreover, for Platonic causation, "*how*" this cause will lead to its effect is secondary²³. To illustrate the "*how*" issue, Sedley gave an example with a jury judging a murder, therefore first they need to judge if a person is "*responsible for*" the murder, but then "*how*" the murder was executed, *e.g.*, poisoning, starvation is secondary²³. This separation elucidates a genuine distinction between science and philosophy. Regarding causal relationships, philosophical studies attempt to define the nature of the cause and its essence, while scientific methodology examines empirical practices to provide evidence for the connection between the cause and its effect⁴⁰. Moreover, Plato argued for the causative incongruity of the "*thing responsible*." For instance, when *y* is causing anything to be *G* (whose opposition is *un-G*), first, *y* must not be *un-G*. Second, *y*'s opposite must not cause anything to be *G*. Finally, *y* must not cause anything to be *un-G*²³. Therefore, the platonic causation identified the nature and properties of the cause. Epistemologically, Plato argues that Forms are the only objects of knowledge, and this knowledge could be reached by deductive reasoning while minimizing the role of observation⁵⁹. Ernst Mayr (1904-2005), an influential German-raised evolutionary biologist, had strongly argued that the current understanding of evolutionary biology had been historically undermined by the essentialist view of Platonic causation. Moreover, he described Plato as "the great anti-hero of evolutionism"^{65,66}. However, this accusation is a matter of debate⁶⁶.

Plato's one brilliant student who challenged his teacher's thoughts, agreed with some and developed others, and was one of the most influential thinkers who shaped many philosophical arguments throughout history is Aristotle; who was named by the Arabic and Islamic philosophers as "The first teacher".⁶⁷

1.2.2 Aristotelian four causes

The term scientist with its empirical meaning is a relatively young term. It was coined in the 19th century by the English polymath William Whewell⁶⁸. However, long before this time, the dichotomy in the methodological aspects between empirical sciences and philosophical reasoning was not strict; namely, natural scientists were referred to as natural philosophers^{69,70}. Additionally, empiricism as an epistemological direction was formulated, by its modern state, in the 17th century by the British philosopher Francis Bacon⁷¹; therefore, no wonder Aristotle writings about causality is not scientific in the modern sense. However, it constructed a framework that was majorly shaping numerous current biological causal explanations; including Ernst Mayr's enterprise^{65,72,73}.

In short, Aristotle defined four leading causes (*aitia*) in his theory of causality, noting that those were not restricted to biology¹⁶. Aristotle's four causes can be depicted in the metaphor of the bronze statue. Following Aristotle's argument, a bronze statue requires four causes; therefore, it materializes. First is the *material cause*; the bronze from which the statue is made. Second, *the formal cause*; the shape and the pattern that the statue would posit. Third, *the efficient cause*; describing the art of making the statue; *i.e.*, casting principles. However, it is debatable whether the efficient cause signifies the art itself, or rather the artist. Fourth, *the final cause*; quoting Aristotle's phrase defining the final cause 'as for the sake of which a thing is done; the end aim of a procedure (*telos*)'^{16,73}.

In *Physics*, Aristotle explains his vision for understanding nature by stating that the purpose of every student of nature is to bring back natural phenomena to their four causal explanations; however, referring to all types of causes for every phenomenon is not pivotal^{16,73}. Aristotle's vital contributions to the conceptualization of causality are myriad. In biology, specifically, the study of animals was of great importance to him⁷⁴. He indeed implanted the first seed for the scientific methodology⁵⁹. Nevertheless, diving into Aristotelian heritage would foster enormous conceptual and methodological aspects; here, I explicitly and shortly highlight a few of his logical, methodological legacies for causality.

Starting with logic, in basic terms, logic is the study of inferences and their relationships⁷⁵. Thus, logical reasoning and the search for causality are indispensable. Splendidly, Aristotle set the earliest systematic, rational frameworks recorded⁷⁶. Aristotle's logical treatise was put together by his followers, *peripatetic*, in one collection; named the *Organon*, "the instrument." Remarkably, the given name to the collection of these writings displays the precise and insightful comprehension of the role of logic in constructing human intellectuality. The collection comprises six of Aristotle's writings about logical reasoning; *Categories*, *On Interpretation*, *Prior Analytics*, *Posterior Analytics*, *Topics*, and *On Sophistical Refutations*⁷⁷. Aristotle's logical arguments were based on deductive reasoning, *Syllogisms*. Such logical arguments are composed of a premise (*protasis*) besides the conclusion (*sumperasma*). Hence, reaching a conclusion out of the premise is a necessity.

Moreover, the premise might be composed of a minor and a major premise^{59,77}. Aristotle's other logical reasoning school was inductive reasoning, which generalized a particular finding to a universal truth. However, Aristotle did not touch upon such a school of reason as he thoroughly contemplated *Syllogisms*⁷⁷. In conclusion, Aristotle established one of the earliest reasoning arguments to explore causality.

Epistemologically, one of the relevant arguments about how Aristotle considered knowledge and the methodology to acquire it, is Aristotle's theory of demonstration^{77,78}. In *Posterior Analytics*, the main subject is (*epistêmê*), which can be translated to knowledge. However, many authors refer to it as science, as the definition of knowledge by demonstration, is more relevant to what is currently known as scientific knowledge⁷⁷. Unlike his predecessor, Plato, Aristotle gives more significance to observing physical entities⁶⁴. In brief, the demonstration theory starts with an observation that needs to reach a conclusion through deductive movement between premises. It starts with a primary premise that is already known to be true "to us" to reach in the end a conclusion that was already "better known to itself." With this methodology, we transfer "better known to itself" to "better known to us"⁷⁷. This first premise comes from imprecise knowledge, non-scientific, due to a different cognitive state (*nous*), meaning an insight, intelligence, or intuition⁷⁷. In his argument, these primary premises are potentialities in the mind that become actualized by sensible experiences⁷⁷. The actualization starts with perceiving

what is present, then memorizing it. Afterwards, repetition of the same memory becomes an experience (*empeiria*), and finally, repetition of the same experience becomes knowledge⁷⁷.

Indeed, these logical arguments were massively influential and later evolved thoroughly to reach what is known now as the scientific method. First, going through Francis Bacon (1561–1626) *Novum Organum* and his solid arguments for inductive reasoning to be leading scientific methodology. Then, consequently, moving to William Wheel (1794–1866) *Novum Organon Restorum*, and John Stuart Mill (1806–1873) *A system of logic*, with the discourse on the nature of inductivism to reach scientific theories and laws. Finally, reaching the 20th century and using modern statistics and probability theory for hypothesis testing and justification⁵⁹. However, Thomas Kuhn, in his book *the structure of scientific revolution* (1962), does argue against the Whig interpretation of the scientific methodology, as the evolution of the scientific methodology was not a chronologically structured movement; instead, it had a pattern of alternating phases. Kuhn argues that science starts with a normal science phase, where scientists are busy solving different puzzles of a current paradigm, *i.e.*, theories, concepts, methods, and problems. When these puzzles accumulate and are incapable of being solved, this initiates a shift to a new paradigm and, consequently, back again to a normal science phase⁷⁹.

Aristotle's contribution to the current understanding of biological causality was not restricted to setting first stones for the empirical framework and scientific knowledge. More importantly, he signified the role of the material cause dissimilar to Plato intelligible causality. In addition, three of his works about biology have reached us: *History of Animals*, *Parts of Animals*, and *Generation of Animals*, besides shorter essays describing different aspects of animals like motion and life and death⁷⁴. Shortly, he argued that we need to start with an inquiry about the differences between all animals and then try to find the causes behind these distinctions, systematically relying on observation⁷⁴; thus, he was exploring biological diversity.

After introducing two prominent, influential figures that shaped the current understanding of causation and the current understanding of causes behind biological diversity. I will next discuss the contribution of two recent scientists, who suggested an

inquiry-driven framework to understand causes behind biological diversity, the American evolutionary biologist Ernst Mayr, and in fewer details, the Dutch Nobel laureate ornithologist Nicolaas Tinbergen (1907-1988).

1.2.3 Ernst Mayr and the concept of proximate and ultimate causes

In 1961, Ernst Mayr published the substantially influential paper "*Cause and Effect in Biology*"^{80,81}. It is believed that Mayr was mainly motivated to publish his thoughts for two reasons: first, to counteract the upcoming molecular biology wave in the face of systematics and evolutionary biology, and second, to cast off the link between vitalism and evolutionary biology⁸². Mayr did not explicitly define biological causation but instead set remarks for its properties. He assigned three logical properties to causal meanings: explanation of past events, prediction of future events, and teleological inferences⁸³.

Firstly, Mayr disengaged teleological reasoning from biological causality^{82,83}. While teleological inferences in biology are considered with purposiveness of form and behavior in biological systems⁸²⁻⁸⁴, natural selection in a Darwinian sense is a non-purposive process. Mayr argues for a teleonomic rather than a teleological feature driving biological evolution^{82,83}. The word teleonomy was coined by the British biologist Colin Pittendrigh in 1958⁸⁵. It simply dismisses the apparent goal-directed ends of biological evolution; it is not the rejection of ends in nature; ends always exist; it is the rejection of purposiveness of these ends, the rejection of a pre-planned process by a controlling entity⁸⁵. It suggests natural selection upon the variation in populations as a driving force for self-replication of biological entities⁸⁵. Mayr and Pittendrigh were not the only opponents of teleological reasoning in biology; other scientific and philosophical figures, including George Gaylord Simpsons, Ernst Neagl, and Anne Roe, strongly advocated for teleonomic reason in biological causality⁸⁵. Considering that this teleological explanation of causation was argued by several authors to be supported by Aristotelian formal and final causes^{86,87}.

After arguing against the role of end-directedness of a final cause in biology, Mayr discussed the second property of causality from a biological point of view, predictability. Mayr argued for the prevalence of unpredictability in the behavior of biological systems⁸³. He defined four reasons for indeterminacy in biology: First, the randomness of events,

like spontaneous DNA mutations and chromosomal segregation, concerning their biological significance. Second, high complexity of biological systems, including feedback loops and developmental homeostasis at the molecular level. Third and fourth, higher levels of organization that seem to be primarily systems unique, and the emergence of new properties of the system that were lacking in lower levels of organization⁸³. Although Mayr correctly stated that prediction, and therefore causality, in biology stand a long distance from the predictive power of causes in classical mechanics, he argues that the precision of predictability is not uniform along with different biological fields⁸³. Furthermore, he elaborated that predictive power at the molecular and taxonomic level is much higher than at the ecological and evolutionary level⁸³. Finally, he argued for the independence of explanation and predictability in evolutionary theory^{83,88}.

Nevertheless, his most significant and debatable contribution was related to the third aspect of causality; explanation, what kind of questions does causality as a concept attempt to explain in a biological sense. To achieve this, Mayr suggested a branching of biology into two conceptually and methodologically separate fields beyond the descriptive measure of structural biology. These fields are functional biology and evolutionary biology⁸³. In his view, functional biology takes a simplified, however, justifiable approach to investigate cause and effect on a biochemical and biophysical level. It tries to answer the question “*how*”. On the other hand, evolutionary biology tries to answer “*why*”. Thus, it is concerned with the history of an organism⁸³. However, Mayr referred to the ambiguity of the question “*why*”, which created waves of debates later^{80–82}. This “*why*” might mean either the finalist “*what for*” or the historical “*how come*”; Mayr himself favored the historical “*how come*”^{82,83}. He exquisitely illustrated the difference in the meaning of causality between functional and evolutionary biology in the four reasons of Warbler bird migration. The Warbler needs to migrate from New Hampshire towards the south by the end of August as, ecologically, if it stays north, it will not find insects to consume. In contrast, when a Warbler migrates, the Screech owl that nests just beside the Warbler will not migrate, presumably, because of the genetic constitutes of these birds. This genetic element makes the two birds differentially respond to the same stimuli. A third reason is the intrinsic physiological cause, where a photoperiodicity response controls the migration behavior. Furthermore, the migration behavior might be attributed to an extrinsic

cause. The cold northern wind will initiate a sudden drop in temperature in late August when the birds will migrate⁸³.

Mayr designated both intrinsic and extrinsic physiological responses of the birds as immediate reasons for migration and called them 'proximate' causes. He considered both ecological and genetic bases for migration as historical causes implemented in the biological system through hundreds of years of natural selection. Moreover, he called these reasons the 'ultimate' causes. Mayr argued that functional biology is concerned with understanding and explaining proximate causes, while evolutionary biology is concerned with the ultimate explanation of biological causality⁸³.

In the end, it was clear that Mayr argued against biological causality through teleological reasoning, argued for indeterminacy in biology, and finally saw a dichotomy between evolutionary biology and functional biology on the questions that they can explain for biological causality, the "why" and the "how" respectively. Although, Mayr's arguments have been heavily debated, the terms 'proximal' and 'ultimate' causation are still in use in contemporary biology.

1.2.4 Nicolaas Tinbergen and his four questions.

Two years after Mayr's paper was published, in 1963, the Dutch Nobel laureate Nicolaas Tinbergen published his paper "*On the aims and methods of Ethology*"⁸⁹. Although Tinbergen was mainly concerned with explaining behaviors, his questions apply to different biological fields⁹⁰.

Tinbergen's questions are named the four whys; they attain features of similarities to Ernst Mayr's proximate/ultimate causation. Moreover, they also display similarities to other biological causal inquiries proposed before Tinbergen, namely by Julian Huxley (1887-1975) and Konrad Lorenz (1903-1989)⁹¹. Huxley was one of the 20th century leading figures in evolutionary biology. He coined the term "Evolutionary Modern Synthesis" by advocating for one paradigm that combines Darwinian evolution and Mendelian inheritance⁹²⁻⁹⁴. In his book "*Evolution: the modern synthesis*" (1942), he argued for understanding three different biological aspects to grasp biological causality

comprehensively. First, the mechanistic-physiological aspect; asking how a biological process takes place. Second, the adaptive-functional aspect; asking about the significant adaptive value of a biological process to the organism. Third, the historical aspect, asking what was the evolutionary course that drove the biological process in question⁹¹. The second figure is the Austrian Konrad Lorenz, who shared the Nobel prize with Tinbergen and von Frisch. Lorenz is considered one of the leading figures who enormously contributed to, if not founded, modern ethology, *i.e.*, the study of animal behavior⁹⁵⁻⁹⁷. He specified three essential questions to understand biological causation, especially animal behavior: First, what is the survival value of a behavior. Second, how does this behavior fall into the animal's natural activity. Finally, how did this behavior evolve⁹¹.

Going back to Tinbergen's four questions. Tinbergen investigated four aspects of causation. First, the survival value, asking what is the adaptive significance of the trait under investigation, or in other words, what is the current *utility of the trait*? Second, *ontology*, how did the trait under investigation develop? Third, *evolution*, how did the trait evolve? Fourth, the *mechanism*, how does the trait work? However, terminologically Tinbergen used the word 'causation' to signify the molecular mechanism underlying the evolution of the trait^{90,98}. Tinbergen emphasized the need for an integrative understanding of the four questions to acknowledge biological causation thoroughly. Nonetheless, few biological systems can offer such features to be addressed⁹⁰.

For instance, studying the singing behavior of birds⁹⁰. Many studies have been conducted to understand how the birds use their songs as a showcase for attracting mates as well as a warning signal to avoid rivals (*current utility*)⁹⁰. In addition, sonograms of wild Chaffinch differ in frequency from sonograms of Chaffinch nestlings reared in isolation⁹⁰. Hence, suggesting a sensitive age for learning singing (*ontology/development*)⁹⁰. Additionally, studies on Orioles have proven that song's clicks differ between phylogenetically related lines (*evolution*)⁹⁰. Finally, in terms of the *mechanism*, different studies have identified the neural networks that underlie learning and production of songs in Zebra finches⁹⁰.

In conclusion, the work from Huxley to Tinbergen still centers around the question about the nature of the cause and its properties. However, considering causes of

biological diversity was part of a broader picture of well-structured theories explaining natural events. Probably the most widely known theory of evolution is the Darwinian one. Therefore, I will next take a short historical leap to both, pre- and post-Darwinian thinking, in order to arrive at the concept of phenotypic plasticity as a potential driver for biological diversity and evolution.

1.3. A very short leap on the history of causation behind biological diversity

“A study of the effects of genes during development is as essential for an understanding of evolution as are the study of mutation and that of selection”

-Julian Huxley, *Evolution: The Modern synthesis*

1.3.1 Pre-Darwinian thoughts

In its essence, the question behind biological diversity is a question of whether biological entities do change or not? Did they permanently exist in the same form, or did they evolve⁹⁹? Historically, this debate dates back to Ancient Greek philosophers and Indian philosophers¹⁰⁰. Pre-Socratic, Platonic, and Aristotelian theories attempt to explain the nature of biological entities and their ability to develop and change^{99–105}. For instance, the Pre-Socratic atomism view of the material world suggests that any physical entity is composed of indivisible atoms and void¹⁰⁶. However, whether these atoms can change to produce different forms of life was a matter of heavy discussion in the ancient period^{99–105}. But more importantly, the metaphysical aspect of understanding natural philosophy was a core component in the Ancient Greek period¹⁰⁷. For example, Aristotle argued that a crucial metaphysical entity that distinguishes different living organisms is the type of soul¹⁰⁷. Plants would possess a vegetative soul capable of developing and growing, while animals would possess a sensitive soul, which adds the ability of movement. Moreover, humans would possess a rational soul, which can reason¹⁰⁷. This metaphysical approach would always append a non-empirical property to physical entities under investigation. Nevertheless, these theories have evolved simultaneously with empiricism as the mainstream source of knowledge, especially in the 17th century^{106,108}.

After empiricism became a mainstream source of knowledge by the 18th century, classification of biological organisms was essential to dealing with biological causality¹⁰⁹. The most influential attempt to classify living organisms in the 18th century, was that of the Swedish Botanist Carolus Linnaeus's treatise¹⁰⁹. Linnaeus's hierarchical classification was not the first attempt to classify biological organisms; in fact, the first classification attempt dates back to Aristotle¹⁰⁹. However, unlike previous classification methodologies, Linnaeus followed a hierarchical kingdom classification of living organisms¹⁰⁹. He adopted four categorical levels (higher categories): classes, orders, genera, and species¹⁰⁹. This detailed system gives clarity and consistency that set the stage for systematic investigation of biological diversity¹⁰⁹. The genus for Linnaeus was a cornerstone and a crucial unit to classify biological diversity¹⁰⁹. Each defined organism would be given two names, a genus notion, and a species notion; in what is so-called the binomial nomenclature¹⁰⁹. Nonetheless, the modern use of genus description traces back to the French Botanist Tourenfort¹⁰⁹.

Ernst Mayr describes the 18th century as the great age of natural philosophy¹⁰⁹. Indeed, it was, besides the hierarchical classification of organisms, the Lamarckian theory of transmutationism was developed^{99,109}. This theory was later followed by the Darwinian theory of evolution by means of natural selection in the 19th century^{99,109}.

Both theories suggest an evolvability property for living organisms. On the contrary, the theory of pre-existence was the leading theory in explaining the origin of species before the Lamarckian transformation theory⁹⁹. Pre-existence theory did not imply any change of species or the transformation from one species to the other⁹⁹. Moreover, this theory dismissed the influence of the environment on living organisms, and it could not neither explain signatures of organismal geographical variation nor the existence of hybrids as the mule⁹⁹. In this theory, unexplainable natural phenomena were considered as anomalies under fixed species thought⁹⁹.

The change of thought from a fixed species concept to a changeable biological entity was affected by the French naturalists and mathematician Georges-Louis Leclerc, Comte de Buffon (1707–1788), before being entirely synthesized as the transformation theory by the French naturalist Jean Baptiste de Lamarck (1744–1829). It is believed that

Buffon was the prominent figure to pave the way for the transformation theory led by Lamarck afterwards⁹⁹.

Buffon's contribution to natural philosophy was eminent. These contributions ranged from methodological aspects, exploring embryological generation, and mainly the reconceptualization of the species concept⁹⁹. Buffon highlighted the anatomical similarities between horses and domestic donkeys. Given the similarities between quadrupeds, Buffon suggested a single historical stem that degenerates with time giving rise to diverse biological entities⁹⁹. In the theory called the "*Unity of Type*"¹¹⁰. However, it is controversial if he stated this thought to reject it later or to stand for it⁹⁹. Nevertheless, it was one of the earliest thoughts to suggest generating biological diversity from a common entity⁹⁹.

On the other hand, Lamarck was the first to develop a coherent theory of species change⁹⁹. Moreover, Lamarck has been given credit as the "creator" of a new field of scientific knowledge at the time, biology¹¹⁰. Lamarck developed his transformation theory given the vast invertebrates collection under his supervision as the chair of "Worms" in the *Muséum national d'histoire naturelle* in Paris. In his transformation theory, Lamarck suggested that organisms move from simple forms to more complex ones over time⁹⁹. Therefore transformation, biological diversity, followed an ascending pattern instead of degeneration⁹⁹.

Nevertheless, one of his most controversial suggestions was the inheritance of acquired traits⁹⁹. Lamarck suggested that subsequent generations inherit functional local adaptation of their parents to the environment; however, these adaptations cannot transform an organism from one group to the other⁹⁹. He suggested that transformation between minor groups of organisms might be due to the use and disuse of structures⁹⁹.

Historically, two other chairs in the *Muséum* also affected thoughts regarding the transformation theory. Etienne Geoffroy St. Hilaire (1772–1844), the chair of Mammals and Birds, and Georges Cuvier (1769–1832), the chair of comparative anatomy⁹⁹. Hilaire advocated for the "*Unity of Type*", suggesting that organisms had a common structural plan, including vertebrates and invertebrates, and adaptations were secondary^{99,111,112}. He suggested that functions would follow forms¹¹². On the contrary, Cuvier advocated for

*“Conditions of Existence”*¹¹¹. He suggested that forms would follow functions¹¹². He divided the animal kingdom into four phyla according to the depiction of the nervous systems^{99,112}. These four phyla represented four distinct body plans⁹⁹. He argued for the unity of type within each branch, but argued against the ability of transformation between these four groups⁹⁹.

Years after the French leadership of evolutionary thought arrives the British heritage with its two prominent figures, Charles Darwin (1809-1882) and Alfred Russel Wallace (1823-1913), generating the idea of evolution by means of natural selection⁹⁹.

Three significant concepts are advocated in the Darwinian theory of transformation (evolution): first, species have a common descendant “descent with modification”. Darwin pointed out similarities between embryonic groups of animals and suggested that modifications occur through development, concluding an adaptable organism to its surrounding¹¹¹. Second, Darwin could offer a causal factor for evolution, unlike previous theories. The causal factor was natural selection^{109,113}. Third, he argued for a Malthusian competitiveness of different populations over limited resources^{109,113–115}. While populations would grow exponentially, resources grow arithmetically, leading to a competition between populations and the survival of the most adaptable¹¹³. Finally, Darwin recognized differences in population’s traits, emphasizing their inheritance and their impact on population survival¹¹⁵.

Furthermore, in 1868, Darwin suggested a primitive thought regarding inheritance through Pangenesis¹¹⁶. Darwin suggested minute particles, gemmules, traveling from body cells towards the gonads¹¹⁶. A blending of the gemmules from the two parents results in the transmission of inherited character displayed in the offspring¹¹⁶. However, this idea has proven incorrect shortly after being suggested¹¹⁶. Moreover, it is noteworthy that Darwin was unfamiliar with Mendel and his work. Indeed, the revival of Mendelian inheritance by the three botanists Carl Correns, Hugo de Vries, and Erich von Tschermak in the early 20th century initiated the birth of modern genetics¹¹⁷. Thus, opened the door for a new school of thoughts understanding biological diversity and biological causality, the school of the Modern Synthesis.

1.3.2 Post-Darwinian evolutionary theories

As stated, the term Modern Synthesis was coined by Julian Huxley in 1942; however, modern synthesis was a movement of several scientific figures simultaneously shaping a new paradigm understanding evolution. In the early-mid 20th century, integration of mathematical and statistical approaches, represented in population genetics, into Darwinian evolution under the light of Mendelian inheritance shaped the framework of the modern synthesis¹¹⁸. Consequently, it led to studying evolution as the change in allele frequency from generation to generation¹¹⁸. Genetic mutations associated with this change are selected by natural selection, favoring phenotypic traits with the greatest potential for adaptation^{111,119}. Thus, with this paradigm, the *how* and *why* of the causes behind biological diversity is achieved^{111,119}. A main concern of the Modern Synthesis was moving from a morphological framework for studying biological diversity to incorporating heredity and genetics¹¹⁹.

In fact, the synthesis was early on influenced by two leading figures, William Bateson (1861-1926) and Thomas Hunt Morgan (1866-1945)¹¹⁹. At the time, voices opposing the school of evolutionary morphology as the main framework to study evolutionary biology were raised, arguing for a new paradigm to understand evolution¹¹⁹. For instance, William Bateson, British biologist and the father of genetics, stated in his influential book *Materials for the Study of Variation* that "the embryological method has failed"¹¹⁹. Especially when it reaches the point of identifying mechanisms behind biological diversity¹¹⁹. In addition, a huge step forward was made by Thomas Hunt Morgan in the early 20th century, when he separated genetics from embryology¹¹⁹⁻¹²¹.

Concurrently, two main directions built-up the Modern synthesis. First is the mathematical microevolution direction, and second is the naturalist macroevolution direction¹¹⁹. The first direction was led by three prominent figures, Sewall Green Wright (1889–1988), Ronald Aylmer Fisher (1890–1962), and John Burdon Sanderson Haldane (1892–1964)^{119,122}. Fisher mathematically illustrated how the interplay between mutation and selection would create population change. This illustration was enhanced and challenged by both Wright and Haldane, in what Ernst Mayr calls The 'Fisherian synthesis'.¹¹⁹ Fisher correlated the genetic variance in the population to the increase in

fitness, in what is known as 'The Fundamental Theorem of Natural Selection'¹²³⁻¹²⁵. Wright's and Haldane's contributions were not restricted to 'The Fundamental Theorem', but were extended to formalize several influential concepts, including, for example, relatedness and kinship^{119,126,127}. Eventually, the developing of these concepts led to William David Hamilton (1939-2000) suggesting the theory of inclusive fitness^{127,128}.

The other direction was led by the Ukrainian geneticist Theodosius Grygorovych Dobzhansky (1900-1975) and the aforementioned Ernst Mayr (1904-2005)¹¹⁹. Dobzhansky was Wright's student¹¹⁹. He expanded Fisher's and Wright's theories by explaining how mutation and recombination can change phenotypes in natural populations^{119,129,130}. On the other hand, Mayr led the explanation of evolutionary change from population-level to species-level in his influential work *Systematics and the Origin of Species*^{119,131,132}. Although Dobzhansky first proposed the concept of biological species in 1935, Mayr provided a conceptual framework for speciation and reproductive isolation mechanisms^{119,132,133}. In addition, two additional scientists have contributed to the formulation of the Modern Synthesis. First, George Gaylord Simpson (1902-1984) who incorporated the paleontology angle in the theory, and George Ledyard Stebbins (1906-2000) who integrated the plant biology aspect¹¹⁹.

In conclusion, the Modern Synthesis paradigm defined a few premises regarding the causes behind biological diversity: first, genetic mutation and recombination are the leading causes behind biological variation. Second, natural selection acts on the phenotypic variation produced by genetic differences to produce adaptive phenotypes, and this process can be modeled mathematically. Third, the large anatomical change across evolutionary time can be understood under a model of accumulation of small changes^{119,134}. However, in the 1960s, pioneering discoveries in molecular biology offered additional mechanistic insights on understanding the causes behind genetic diversity¹¹⁹. It was more to explore under the question "how". Subsequently, several scientists recognized the need for extending the Modern Synthesis¹¹⁹. Since the late 20th century, a new paradigm of understanding evolution has emerged, a third wave after Darwinian evolution and the Modern Synthesis¹¹⁹. The paradigm of the Extended modern synthesis¹¹⁹.

The Modern synthesis could evidently explain the genetic mechanism behind diversity, as well as the role of natural selection in creating adaptive traits¹¹⁹. However, it could not explain the origin of the structural changes¹¹⁹. Therefore, the integration of developmental genetics and developmental biology are crucial to understanding the *arrival of the fittest* after comprehending *the survival of the fittest*¹¹⁹.

Evo-devo, the field of evolutionary developmental biology, views evolution as heritable changes in organismal development¹¹⁹. This field relied on exploring mechanisms that link genes (genotypes) to structures (phenotypes) to comprehend how embryonic changes in one generation lead to evolutionary changes over generations¹³⁵.

In fact, several publications from the late 1970s emphasized the need to integrate developmental aspects into evolutionary theory¹¹⁹. First, in 1975, King and Wilson found out that chimpanzees and humans share more than 99% of their polypeptides sequence, with the state of art technique at the time^{119,136}. Therefore, the morphological differences between the two species might be driven by changes in the regulatory regions of the genes instead of gene bodies^{119,136}. Furthermore, in 1977, the American Paleontologist Stephan G Gould published his book "*Ontogeny and phylogeny*", arguing that ontogeny does not recapitulate phylogeny^{119,137}. He proposed a new framework of how same genes can produce different body plans based on their expression pattern during development¹¹⁹. Another influential essay published in the same year is Francois Jacob's "*Evolution and Tinkering*"¹¹⁹. Jacob argued that natural selection is imperfect whether it is positive or negative^{138,139}. His argument is that evolution acts as a tinker, as such, different tinkers might have different solutions for identical problems^{138,139}. Therefore, he suggests molecular tinkering, citing studies that show distantly related organisms, like flies and pigs, use similar DNA sequences to form different body structures^{138,139}. In parallel, the development of molecular techniques such as DNA sequencing techniques, along with the technical revolution that followed until the early 21st century, highlighted molecular developmental studies as an instrumental part of evolutionary theory (Evo-Devo)¹¹⁹.

In fact, there have been numerous distinguished figures associated with this school from the 1900s to the 1980s. The five most prominent scientists besides S. G. Gould

were: D'Arcy Thompson (Theory of transformation); Gavin de Beer (Heterochrony); Richard Goldschmidt (Saltation); Conrad Hal Waddington (Epigenetic landscape); and Lancelot Law Whyte (Co-adaptation)^{140,141}. Nevertheless, there is more than one spectrum with which Evo-Devo, and in turn, the Extended Evolutionary Synthesis, should be considered. On the one hand, there is the conservative comprehension of this field. This comprehension focuses on the evolution of body plans, developmental trajectory, genetic regulation and modularity, toolkit genes, and developmental constraints during evolutionary history^{119,140}. A broader approach would incorporate the epigenetic effect of the surrounding environment and its influence on adaptive phenotypes, in what some authors call Eco-Evo-Devo^{27,28,119,140,142,143}. The main argument of this version is that the environment does not only select for variation; it also constructs, shapes, and constrains variation. In principle, this version set three fundamental concepts to be explored: developmental plasticity, inclusive inheritance, and niche construction.^{27,28,119,140,142,143}

In short, Laland and colleagues define inclusive inheritance as non-genetic factors that influence phenotype inheritance. For instance, they included parental-offspring interactions and inheritance of symbionts as two non-genetic mechanisms affecting phenotype inheritance²⁸. Furthermore, they defined niche construction as the process by which living organisms change their environment through metabolites and activities, simultaneously influencing selection regimes upon themselves²⁸. In addition, a more integrative approach of Evo-Devo was suggested incorporating the evolution of the nervous system as well as the exploring the evolution of behavioral aspects^{142,144–146}. Although, the Extended Modern Synthesis is seemingly more integrative, there is yet a disagreement regarding whether the Extended version of the Modern Synthesis would significantly contribute to evolutionary theory¹⁴⁷.

To conclude, the Extended Modern Synthesis places greater emphasis on developmental pathways, environmental signals, epigenetic changes, and symbiotic effects. Nevertheless, one of the central concepts of the Extended Modern Synthesis that I have not yet discussed is developmental plasticity. What does developmental plasticity entail? Can there be more than one type of plasticity? Can it be adaptive? Can it facilitate or hinder evolution? Is it possible to initiate biological diversity or, in other words, the

evolution of novelty through plasticity? Additionally, what are the model organisms for studying developmental plasticity? A detailed discussion of these questions will follow.

1.4. On the meaning of phenotypic plasticity

“One must take into account, the organism’s capacity for adaptive plasticity. In this regard the question which will undoubtedly receive especial attention in the future is to what extent different species or forms show different degrees of individual adaptive modification”¹⁴⁸.

-Nilsson-Ehle, Evolutionary significance of phenotypic plasticity in plants

1.4.1 Universality of phenotypic plasticity

Phenotypic plasticity is the ability of a single genotype to produce two or multiple phenotypes as a response to various environmental cues^{149–152}. The two words, phenotype and genotype, were first coined by the Danish botanist Wilhelm Johannsen in 1911^{150,153,154}. However, the genotype-phenotype relationship has been studied since Mendel¹⁵⁰. In principle, the American evolutionary biologist Richard C Lewontin defined a genotype as the constitution of the genetic makeup of an organism, where a phenotype represents the developmental manifestation of this makeup in a variety of biological features¹⁵⁵. Consequently, phenotypes result from the interactions between genes and the environment in which the organism develops.^{155,156} Therefore, this definition of phenotypic plasticity raises three critical questions: first, what kind of phenotypes can display plasticity? Second, are there genetic bases for phenotypically plastic traits? Moreover, can it be adaptive? Finally, can plastic traits drive evolution?

To begin with, phenotypic changes under the environmental influence might range from morphological, physiological, behavioral to life-history traits, with differences in the degree of phenotypic reversibility^{149–152,157}. Most commonly, physiological traits are reversible in short periods. In contrast, developmentally plastic traits that follow a specific developmental trajectory are mostly irreversible^{152,157}.

Indeed, botanists long recognized phenotypic plasticity in plant studies; however, plasticity is pervasive in the animal kingdom as well^{149–152}. Furthermore, plasticity has also been demonstrated in bacteria and even in viruses, although there is some

controversy on the terminology in this context¹⁵¹. Together, under such an inclusive definition of phenotypic plasticity, many authors argue for its universality^{151,152}.

Several examples of plastic phenotypes could be found in plants^{150,152,156,158}. For instance, Mangroves display morphological plasticity in several features, including the effect of high salinity on the ability of crown displacement toward the light; this, in turn, affects tree to tree competition^{158,159}. Another example would be the response of the same inbred genotype of the annual herb *Polygonum lapathifolium* to light intensity and water availability¹⁵⁶. In animals, the pea aphid (*Acyrtosiphon pisum*) shows morphological and behavioral plasticity as a result of developmental changes¹⁶⁰. For example, upon high density and crowding, *A. pisum* animals form wings resulting in a phenotype that allows high dispersal. In contrast, under low density conditions, animals are wingless with low dispersal¹⁶⁰. Many more examples across animal phyla could be discussed, such as social insects' caste development, i.e., wasps, bees, ants, and termites^{161–167}.

Additionally, the developmentally plastic response of beetles horns^{168,169}, the nematode *C. elegans* arrest phase (dauer) formation^{170,171}, *Daphnia cucullata* defensive hamlet¹⁷², butterflies seasonal wing plasticity¹⁷³, Arctic fox (*Vulpes lagopus*) seasonal coat color variation¹⁷⁴, the variation in shell thickness of intertidal snails¹⁷⁵, and last but not least behavioral and morphological plasticity in the predatory spadefoot toads¹⁷⁶. Furthermore, it is worth noting that several of these plastic traits are coupled in many cases. For instance, upon the higher density and thus, higher resource competition, solitorious locusts display phase transition in morphological and behavioral features to the gregarious phase¹⁷⁷.

In prokaryotes, sub-population non-genetic heterogeneity of bacterial resistance to antibiotics is considered as one form of phenotypic plasticity¹⁷⁸. Another example would be the plastic response to fluctuating temperature in terms of growth speed¹⁷⁹. And finally, the switch of the lambda bacteriophage from lytic to a lysogenic cycle under the effect of toxicity or starvation is considered as one form of phenotypic plasticity¹⁸⁰.

However, there are a few notable features associated with phenotypic plasticity that, might suggest alternative methods of categorizing this phenomenon. The first category is how phenotypic variation is displayed. Indeed, phenotypic variation of a trait

might either be continuous or discrete, the latter of which results in so-called polyphenism^{149–152,181}. Mary Jane West-Eberhard, a leading figure in the plasticity field, emphasized that polyphenism would generate alternative phenotypes^{149,151,181}. Such alternative phenotypes exhibit a distinct environmental response that facilitates downstream analysis, especially if the readout is binary¹⁵¹. Finally, West-Eberhard stressed a crucial point in the definition of alternative phenotypes: she stated that alternative phenotypes may co-occur in the same life stage within the same population, however they are not expressed by the same individual¹⁸¹. While not found in all cases of plasticity, such co-occurrences are a special feature also found in the study system described in detail below and can help identifying molecular mechanisms associated with plasticity.

Another way to categorize plasticity depends on the type of response, conditional vs. stochastic. Many alternative phenotypes show a threshold response towards environmental cues, with the machinery underlying the expression of the phenotype being quantitative¹⁸². When the factor controlling the phenotype exceeds a certain threshold, the alternative phenotype(s) is expressed¹⁸². An example would be juvenile hormone titration of caste development in social insects¹⁸³. Several polyphenic traits follow conditional induction of alternative phenotypes, for example, the induction of wing formation in aphids upon crowding¹⁶⁰. In contrast, stochastic plasticity is known in microbes, often referred to as bistability or phenotypic heterogeneity, i.e., persister cell formation in *Bacillus subtilis*¹⁸⁴. Importantly, also such systems require factors that act in a concentration-dependent manner with a threshold-type response.

A final framework to categorize plastic phenotypes would be according to the adaptive value of the expressed trait¹⁵¹. Therefore, several authors distinguished two types of plasticity, adaptive and non-adaptive plasticity^{149–152,185}. It should be noted that this categorization is and has been heavily debated in the literature.

Adaptation could be defined as the movement of the population phenotype towards the best fit to the current environment¹⁸⁶. Simply put, if plasticity displays more reproductive success and survival values in the new environment for an induced phenotype, it would be considered adaptive.

However, if the phenotype moves towards a less fit direction, it is considered maladaptive^{151,185}. Adaptive plasticity is suggested to facilitate coping with spatial-temporal fluctuation of environmental conditions^{148,149,152,185,187}. In contrast, non-adaptive plasticity is mainly attributed to unreliable response to extreme conditions^{151,185}. Taken together, all of these distinctions are helpful to categorize plasticity. However, they also increase confusion. And most importantly, they do not directly address the most crucial aspect for the acceptance of plasticity research in evolutionary biology: what is the genetic basis of plasticity?

1.4.2 Genetic basis of plasticity

In 1965 the plant ecologist Anthony David Bradshaw (1926-2008) published his breakthrough paper proposing a genetic basis controlling phenotypic plasticity, thus, founding a solid base to argue for an adaptive value of plasticity^{148–152,185,188}. Unlike other evolutionary biologists before him, Bradshaw did not consider plasticity a source of measurement error in his experiments¹⁵⁰. Instead, Bradshaw could empirically show that plants respond differently to extreme conditions. Thus, he argued for the genetic control of plasticity and that natural selection could act on it to shape these responses^{148–152,185,188}.

One of his most elegant experiments was when Bradshaw detected the absence and presence of heterophylly in 19 different species of *Potamogeton* and their hybrids¹⁵⁰. Heterophylly represents the ability of plants to produce different types of leaves as a response to water availability. The astonishing result was that only hybrid plants with at least one heterophyllous parent displayed different types of leaves¹⁵⁰.

Heterophylly absence or presence represents an alternative phenotype, in the way postulated by West-Eberhard. Moreover, West-Eberhard proposed a conceptual framework for the genetic machinery underlying alternative phenotypes. This conceptual framework relies on the concept of modularity. Modularity implies the division of biological entities into smaller parts that act semi-independently, controlled by switch points and likely serving the same function¹⁴⁹. West-Eberhard suggested that modularity is a universal property of living systems and argued that such modularity could be found at any level of biological organization, from morphological phenotypes to genetic

networks¹⁴⁹. She argued further that modularity contributes to phenotypic plasticity in that the modular structure of the trait allows the generation of developmental switches¹⁴⁹. Moreover, she divided the genetic network underlying plasticity into a switch network or determinants of regulation, where genes in this network control the shift between developmental trajectories, and an execution network or determinants of form, where genes in this network control the production of the outcome¹⁴⁹. While Bradshaw and West-Eberhard provided the foundation for the importance of genetic factors in controlling developmental plasticity, most studies systems do not allow their identification. The nematode *Pristionchus pacificus* with its mouth form plasticity, which is the subject of this thesis, has allowed unprecedented evidence supporting these original claims and identifying the genetic mechanisms of plastic trait formation.

Finally, a second argument related to adaptive plasticity is the cost of plasticity. Several authors have conceptually suggested that one major constraint for the evolution of adaptive plasticity is the cost of plasticity^{150,152,187,189}. However, two main issues are associated with this argument, resulting in very controversial discussion. First, there is tremendous inconsistency in the definition of 'cost of plasticity' in the literature. For instance, in DeWitt et al. 1998, there are five types of 'cost of plasticity', including the cost of maintenance and cost of production¹⁸⁹. In contrast, the exact cost of production is often defined as a 'cost of phenotype', and it is separated from the cost of plasticity definition in Murren et al. 2015¹⁸⁷. In Murren, the cost of phenotype is defined as the 'energetic tradeoff utilized for the production of a phenotype'. In comparison, the cost of plasticity is the fitness price incurred by a plastic genotype compared to a less plastic genotype¹⁸⁷. The second issue represents the mixed results regarding the empirical evidence of plasticity costs. For instance, a meta-analysis on 27 costs of plasticity showed that the costs detected in these studies is relatively minute, if they were identified at all¹⁹⁰. Moreover, another study showed that geographically separated genotypes of the same species, the common frog *Rana temporaria*, vary in the presence and absence of the plasticity costs¹⁹¹. Thus, much remains to be done in order to provide solid empirical evidence for the costs of plasticity.

1.4.3 Phenotypic plasticity as a driver for evolutionary novelties

Plasticity was also suggested to be a driving force for the evolution of novelty^{149,151,157,174,192–195}. As mentioned in the previous section (post-Darwinian evolutionary theories), Evo-Devo and Eco-Evo-Devo; investigate the *origin* of the fittest, not only the *survival* of the fittest. In this context, one theory that suggests how novel traits originate in a relative phylogenetic context, starting from environmental induction, is the flexible stem hypothesis, or plasticity first evolution^{149,151,152,194,196}. However, to grasp this thought in an appropriate manner, a brief historical context is needed.

In brief, plasticity was first described by the American psychologist James Baldwin (1861-1934), who was one of the earliest advocates for the effect of the environment upon selection and, therefore, evolution^{150–152,192}. In 1896 Baldwin argued upon environmental change, selection favors flexibly responding organisms^{151,152,192,197}. These flexible learned behaviors in the new environment would allow flexible organisms to survive and reproduce; thus, with time, it increases the chance of these traits to become congenital (genetically fixed or genetically accommodated)^{151,152,192,197}. However, this phenomenon was not called plasticity; instead, it was named Baldwin effect¹⁵¹. Years later, specifically in 1909¹⁹⁸, the German zoologist Richard Woltereck (1877–1944) conducted the first plasticity experiment on different water flea animals (*Daphnia*)^{151,199}. Woltereck examined head size change as a response to different nutritional levels; therefore, he could draw “phenotype curves,” which he called the norms of reactions^{151,199}.

Afterwards, and in parallel, two scientific figures extended Baldwin's accommodation theory, first the Russian evolutionary biologist Ivan Ivanovich Schmalhausen (1884-1963) and the British geneticists and developmental biologist Conrad Hal Waddington (1905-1975)^{151,152,199}. In his book *Factors of Evolution: The Theory of Stabilizing Selection*²⁰⁰, Schmalhausen formulated the theory of stabilizing selection^{151,152,199}. He argued that, for an environmentally induced trait, stabilizing selection would lead to transforming the phenotypic response to a genotypic response that is inherited across generations, notably if it is adaptive^{151,152,199}.

On the other hand, Waddington's main relevant legacies are Waddington's epigenetic landscape and the theory of genetic assimilation^{149,151,152,157}. Waddington's

epigenetic landscape is a metaphor describing the robustness of developmental phenotypes against perturbations^{149,151,152,157,201}. He depicted the development of a phenotype as valleys (developmental trajectories) where a downhill rolling ball (phenotype) moves toward its final destination through time to reach the "end state"^{149,151,152,157,192}. Waddington illustrated the epigenetic landscape in his book *The Strategy of the Genes*, published in 1957²⁰¹. He argued that the depth of the pathway represents how robust the phenotype is towards perturbations; according to Waddington, all developmental reactions are, in general, canalized²⁰¹⁻²⁰³. The more canalized a phenotype is, the less flexible it will be^{202,203}.

Waddington depicted genes as pegs underneath the epigenetic landscape; these pegs will shape the valleys through guy-wires representing the signaling output of the genes, or "the chemical tendencies, which the genes produce"^{201,204}. Waddington suggested that when the route of a ball is disturbed, a property of the system is to buffer disturbance and return the ball to the specified trajectory. Notably, this return is not necessarily to the same point and time at which the perturbation happened. Rather, the ball returns to the route at any point before reaching its' final fate, a property he called 'homeorhesis'²⁰¹.

Waddington argued that when an environmentally inducible trait shows an adaptive value, the developmental response under this trait might become canalized as it is favored by natural selection, in a process he called 'genetic assimilation'²⁰⁵. Thus, genetic assimilation is a specific case of canalization²⁰⁵. Indeed, Waddington has combined his theoretical framework with experimental evidence, where he tested for the effect of heat shock and ether vapor in inducing *crossveinless* wings and *bithorax* phenocopies in *Drosophila*, respectively. He could show that these phenotypes remain expressed after the environmental stimuli were removed^{192,205}. However, more recent experiments showed that Waddington's results were not based on genetic assimilation. Instead, they either resulted from impairing buffering heat-shock proteins that maintain normal development or instead exposing cryptic genetic variation (CGV), representing unexpressed genes that get activated under abnormal conditions^{192,205,206}.

Finally, the last two figures are Anthony David Bradshaw, who, as discussed previously, proposed the concept of the genetic control for polyphenic traits. And Mary

Jane West-Eberhard, who has vigorously and successfully advocated for the universality of plasticity, especially alternative phenotypes. She pointed out the pervasiveness of plastic phenotypes and argued for the significant role of adaptive plasticity in evolutionary theory^{149,151,181,193,207}. Moreover, she proposed a seven-step model for the evolution of adaptive novelty by plastic response where phenotypes are leaders and genes are followers¹⁴⁹.

First, trait origin; when a distinct developmental variant is produced due to an environmental stimulus or a mutational change. Second, phenotypic accommodation; the functioning of the phenotype is subject to adjustment through the response to environmental conditions. Third, the recurrence of the initial factor that induced the alternative developmental phenotype, which in turn will form a sub-population that is expressing the novel trait. Fourth, genetic accommodation, where the gene frequency of the variant changes due to selection on the regulation or the form of the novel trait. Fifth, persistence of the alternative novel trait in the population due to its adaptive value. Sixth, modification implies the evolution of new developmental branches (genetic modifiers) that are subordinate to the original switch that constitutes the novel trait. And finally, genetic fixation of the novel alternative trait through, as Waddington described, genetic assimilation¹⁴⁹. A detailed discussion of this approach follows in the discussion section at the end of this thesis.

In summary, phenotypic plasticity has proven its universality, adaptive value, and theoretically, it has been suggested as a source of evolution of novelty. Various model systems have been used to reach the current image of the role of plasticity in evolution. One of these models is the nematode *Pristionchus pacificus*.

1.5. *Pristionchus pacificus*: a model for phenotypic plasticity

"In short, if all the matter in the universe except the nematodes were swept away, our world would still be dimly recognisable, and if, as disembodied spirits, we could then investigate it we should find its mountains, hills, vales, rivers, lakes, and oceans represented by a film of nematodes"²⁰⁸

Nathan A. Cobb, Nematodes and their relationships

1.5.1 *Pristionchus pacificus* as a model organism for studying plasticity.

The roundworm nematode *Pristionchus pacificus* provides an integrative approach to investigate the role of plasticity in evolutionary theory. Six main features define the advantage of using *P. pacificus* as a model organism for investigating plasticity.

First, the undemanding maintenance and the availability of genetic manipulations. *P. pacificus* has a short generation time of about four days at 20° C²⁰⁹. *P. pacificus* feeds on various bacterial sources. However, it is easily maintained in the lab by feeding on *E. coli* culture²⁰⁹. Additionally, *P. pacificus* animals are hermaphrodites, which facilitate genetic studies as the reproduction of mothers produces genetically identical (isogenic) offspring²⁰⁹. Moreover, various genetic engineering methods, such as directed mutagenesis and transgenesis are readily available to investigate causal genetic elements behind plasticity^{210,211}. Finally, the whole genome of *P. pacificus* is fully sequenced, with almost 29,000 genes annotated²¹².

Second is the nature of the morphological plasticity. *P. pacificus* animals exhibit developmental plasticity in their mouth-form phenotype²¹³. *P. pacificus* worms can either develop a Eurystomatous (Eu) wide-mouth accommodating a hooked-like dorsal tooth and a similarly shaped sub-ventral one²¹³. Alternatively, it develops a Stenostomatous (St) narrower mouth-form, with only a thin-flint-shaped dorsal tooth²¹³. Notably, the mouth-form decision is irreversible²¹⁴. Significantly, this distinct binary read-out assisted in obtaining reliable results on the level of response. However, while worms display a discrete binary phenotype, either Eu or St, different *P. pacificus* natural isolate (isogenic strains or populations) show continuous mouth-form ratios. Thus, some populations exhibit a biased Eu mouth-form ratio, whereas others exhibit a biased St mouth-form ratio, or an unbiased ratio²¹⁴. Moreover, it has been shown that mouth-form displays a dosage-dependent response to the steroid hormone dafachronic acid, in other words, a threshold

response²¹³. Furthermore, the switch between both phenotypes accommodates both conditional and stochastic responses²¹⁵. For example, growing worms under different temperature values, crowding and starvation, or different bacterial diets have shown conditional-response on the mouth-form level^{213,216,217}. However, the exact mouth-form ratio of these isogenic animals slightly varies between replicates, even under laboratory conditions, arguing for a stochastic response that might imply a bet-hedging strategy²¹⁵.

Third, the genetic network underlying the mouth-form switch was under an immense body of investigations. Thus, as West-Eberhard argued for the modular property of the genetic network underlying the switch, several molecular players controlling the switch network, the execution network, and the environmental perception network were identified. For instance, introducing molecular lesions to the sulfatase encoding gene *eud-1*, results in a complete switch towards the St morph²¹⁴. Therefore, the gene *eud-1* was proposed to be the main switch regulator²¹⁴. Later, after *eud-1* was identified, a transcription factor of the nuclear hormone receptor family, *nhr-40*, was also shown to be part of the genetic switch network^{218,219}.

Furthermore, in the perception network, upstream to the switch network perceiving the environmental signal, molecular players related to bacterial diet sensation, temperature, and pheromones were identified^{213,216,217}. Lastly, for the execution network, Mucin-type protein DPY-6 has been shown to exhibit a role in mouth-form structural formation²²⁰, besides a group of genes coding for Astacin (metalloprotease) proteins, Chitinases and Chitinases like proteins, which were indicated to be involved in regulating mouth-form based on genetic investigations²¹⁹. Additionally, chromatin state profiling of the *P. pacificus* genome was conducted, identifying a chromatin remodeler (histone acetyltransferases) affecting mouth-form phenotype^{221,222}. These molecular details make *P. pacificus* one of the unique systems exhibiting alternative phenotypes, with a decent understanding of the molecular machinery underlying the switch.

The fourth feature is the coupling of morphological plasticity with behavioral plasticity. Eu worms display the ability to predate on other worms, while St worms exhibit a bacterivorous behavior²²³. Astonishingly, a self-recognition system was identified by Lightfoot and colleagues showing that *P. pacificus* avoided predation upon self

progeny²²³. Furthermore, Lightfoot and colleagues have shown that a disruption in the small peptide *self-1* would lead to progeny predation²²³. Additionally, it has been shown that worms with Eu predatory mouth-form are more likely to survive under harsh conditions of food depletion by feeding on other nematodes²²⁴. However, it was also shown that Eu animals incur a cost regarding developmental speed, because St worms grow faster than Eu worms²²⁵.

Fifth, is the ecological relevance of mouth-form plasticity. The life cycle of *P. pacificus* encompasses four juvenile stages and an adult stage²⁰⁹. However, under extremely harsh conditions, such as crowding and starvation, *P. pacificus* worms develop into an alternative dispersal stage instead of the third juvenile stage, named dauer¹⁵¹. Dauer larvae encompass stronger cuticles and help worms to survive harsh conditions¹⁵¹. Moreover, *P. pacificus* worms live in necromenic association with scarab beetles¹⁵¹. Upon beetle death, worms develop and feed on the microbial population on the carcass¹⁵¹. Upon food depletion, nematodes enter dauer until sensing food again, either after dispersal or after bacterial populations grow back on the beetle carcass in a boom-and-bust dynamics, as recently observed²²⁶. Also, recent work has indicated a significant role of mouth-form plasticity in resource competition on the dead carcasses²²⁷.

1.5.2 Natural variants approach to understand the evolutionary “why” and the mechanistic” how” of mouth-form phenotypic plasticity

Finally, and most importantly for the thesis to follow, a vast collection of *P. pacificus* natural isolates and *Prisitonchus* species is available. Over the years, almost 1,500 *P. pacificus* natural isolates and 49 different *Prisitonchus* species were collected^{151,228,229}. These resources make evolutionary relevant studies in the context of phylogeny and relatedness possible. It is important to note that most of the genetic and molecular work was performed on one strain of *P. pacificus*, the reference strain California PS312. Additionally, most of the observed natural isolates show an Eu-biased mouth-form ratio, especially under laboratory conditions²¹⁴. However, St-biased and unbiased isolates have been detected as well²¹⁴.

Notably, two modes of reproduction were observed at the species level: first, androdioecy, where the population is mostly hermaphrodites with spontaneous male occurrence. Second, dioecy, where populations are composed of females and males^{228,230}. Interestingly, androdioecy evolved at least seven times independently in the genus *Pristionchus*, forming eight different androdioecious species and 41 female and male species²²⁸. Investigating natural variation at the species level and between species is crucial in the puzzle of understanding the evolutionary significance of mouth-form plasticity, morphologically and behaviorally. Taken together, the specific features and the available resources of *P. pacificus* and other *Pristionchus* species make them a prime study system to investigate various research questions in the context of developmental plasticity.

2. Thesis aims

The overall goal of this thesis was to investigate the connection between morphological and behavioral plasticity in *P. pacificus* by exploring “*how*” and “*why*” mouth-form phenotypes evolved in natural isolates. This has been done both within a species and between species. To achieve this, I conducted multiple lines of research simultaneously:

1) I performed quantitative trait locus (QTL) mapping of Recombinant Inbred Lines (RILS) generated by crossing a biased *pacificus* Eu natural isolate to a biased St one. After identification of QTLs, I aimed for a molecular understanding of mouth-form plasticity in nature by CRISPR Cas-9 directed mutagenesis and RNA expression analysis (the *how* question).

2) I conducted a phylogenetic analysis of mouth-form bias across *Pristionchus* species. With an equal contribution of a postdoctoral colleague, we investigated the correlation between mouth-form bias, modes of reproduction, and relatedness, both the behavioral and morphological levels (the *why* question).

3) I explored the adaptive value of mouth-form morphology and the associated behavior. I examined the cost of phenotype and the cost of plasticity in different *P. pacificus* natural isolates through obtaining empirical fecundity, developmental speed, mouth-form ratio, killing, and self-recognition data (the *why* question).

4) Given the diverse genomic, bioinformatic, genetic and epigenetic investigations of the laboratory, I participated in various studies to enhance skills in several of the abovementioned methodologies. Towards that, I was involved in a research study investigating the functions of genes adjacent to the switch gene *eud-1*. Finally, I participated in studies introducing a new environmental condition affecting the mouth-form decision, liquid culture, and I helped create a community-curated version of the *P. pacificus* genome to facilitate genome annotation.

3. Results

3.1. The genetics of phenotypic plasticity in nematode feeding structures

Sommer RJ, **Dardiry M**, Lenuzzi M, Namdeo S, Renahan T, Sieriebriennikov B, Werner MS.

Open biology. 2017 Mar 15;7(3):160332., doi.org/10.1098/rsob.160332

3.1.1. Synopsis

This review highlights the molecular advantages of using *P. pacificus* in investigating the role of plasticity as a facilitator of morphological diversity and novelty. First, it summarizes the historical studies and conceptual frameworks defining phenotypic plasticity. Then the authors discuss genetic and epigenetic regulators of mouth-form plasticity known at the time. Two switch genes are discussed in details, *eud-1* and *nhr-40*. Mutant phenotype of the sulfatase encoding-gene, *eud-1*, shows all-St worms, while mutants of the nuclear hormone receptor, *nhr-40*, display all-Eu mouth-form. In contrast, overexpression lines of both genes exhibit the opposite phenotype to their mutants. Moreover, experiments have shown that *the eud-1* effect is dosage-dependent, and both switch genes, *eud-1*, and *nhr-40*, display haploinsufficiency. Furthermore, two genes encoding for histone-modifying enzymes, *mbd-2* and *lsy-12*, were found to be acting through *eud-1*, thus changing the mouth-form ratio when mutated. Therefore, the epigenetic regulation of the switch suggests a venue for incorporating environmental signals into the switch mechanism. Finally, the review discusses the micro and macro-evolutionary levels implemented in investigating mouth-form plasticity. Providing a striking example of how plasticity increased morphological diversification in the fig-associated *Pristionchus* species.

3.1.2. Own contribution

I participated in the group discussions regarding the conceptualization of this review. I estimate my contribution at 5%.

3.2. Environmental influence on *Pristionchus pacificus* mouth form through different culture methods

Werner MS, Sieriebriennikov B, Loschko T, Namdeo S, Lenuzzi M, **Dardiry M**, Renahan T, Sharma DR, Sommer RJ.

Scientific reports. 2017 Aug 3;7(1):1-2, doi.org/10.1038/s41598-017-07455-7

3.2.1. Synopsis

In this paper, the authors introduced a novel environmental condition that affects mouth-form plastic response in *P. pacificus*, growing worms in liquid culture (novel at the time of publication). The authors manipulated culture conditions to create a gradient of mouth-form responses ranging from almost 10% to 99% Eu in the wild-type *P. pacificus* isolate. This was achieved by manipulating a combination of medium components, e.g., T, H, and S-medium, as well as NGG or NGM; culture state; e.g., liquid or solid, and rotation speed in the case of liquid culture. Notably, *E. coli*, the standard food source under laboratory conditions, was used in all of these conditions. Furthermore, two conditions were used for the downstream analysis; the standard agar solid medium NGM condition and liquid culture S-medium, 180 rpm. These two conditions displayed the two extreme sides of the response: solid condition 99% Eu, and liquid condition 10% Eu. Furthermore, the genetic switch components, *eud-1* and *nhr-40*, were proven to act downstream to liquid culture effect. Indeed, RT-qPCR experiments displayed a reduction in *eud-1* expression as a response to worms growing in the liquid culture. Moreover, *nhr-40*, monomorphic Eu null mutants, did not respond to the liquid culture condition. Finally, the effect of the liquid culture was tested on the macroevolutionary level. The result indicated a species-specific response to the liquid culture condition.

3.2.2. Own contribution

I participated in the performing RT-qPCR experiments for various genes needed in this study. I estimate my contribution at 5%.

3.3. A developmental switch generating phenotypic plasticity is part of a conserved multi-gene locus

Sieriebriennikov B, **Dardiry M***, Prabh N*, Witte H, Roeseler W, Kieninger MR, Rödelsperger C, Sommer RJ.

Cell Reports. 2018 Jun 5;23(10):2835-43, doi.org/10.1016/j.celrep.2018.05.008

3.3.1. Synopsis

This study demonstrated the involvement of a multi-gene locus in regulating the mouth-form switch in *P. pacificus*. On the *P. pacificus* X chromosome, the sulfatase encoding *eud-1* occurs in a region of approximately 30kb containing four genes in an inverted tandem arrangement. The switch gene *eud-1* and its paralog *sul-2.2.1* are in the middle of this locus, with an almost 7kb intergenic region driving the expression of these two genes. Interestingly, two α -N-acetylglucosaminidase (*nag*) encoding paralogous exist in head-to-head orientation to the two sulfatase encoding genes. Knock-out mutants showed the involvement of these four genes in the mouth-form phenotype. For instance, *eud-1* switches the phenotype to 100% St under an Eu-inducing condition. In comparison, *sul-2.2.1* had a minor insignificant effect on the mouth-form shifting the ratio towards the same direction. In addition, the overexpression of *sul-2.2.1* in a *eud-1* mutant background led to a partial rescue. Therefore, indicating a minor role of *sul-2.2.1* in mouth-form regulation. In contrast, a double mutant in *nag-1* and *nag-2* resulted in a complete switch to Eu in the St-inducing condition. However, the quadruple mutant line displayed a *eud-1* phenotype. Furthermore, reporter lines showed a non-overlapping expression for *eud-1* and the two *nags*. The three genes are expressed in different head sensory neurons as well as in interneurons. In addition, phylogenetic sequence analysis of the multi-gene locus showed the conservation of the locus synteny throughout the *Pristionchus* genus. Finally, CRISPR Cas-9 mutants and phylogenetic analysis suggest gene conversion as a driving force behind sequence divergence between paralogous in the multi-gene locus. Thus, this study provides evidence for the involvement of a physically linked locus in regulating polyphenic switches.

3.3.2. Own contribution

I was involved in generating rescue lines and gene expression reporter lines. I also prepared DNA sequencing libraries and assisted in phenotyping mutants. I estimate my contribution at 20%.

3.4. Adult influence on juvenile phenotypes by stage-specific pheromone production

Werner MS*, Claaßen MH*, Renahan T*, **Dardiry M**, Sommer RJ.

Iscience. 2018 Dec 21; 10:123-34, doi.org/10.1016/j.isci.2018.11.027

3.4.1. Synopsis

In this article, the authors investigated the effect of intergenerational communication between different age/stage classes of *P. pacificus* on mouth-form plasticity. The authors developed a novel vital dye methodology for tracking mixed populations of *P. pacificus* nematodes. Different stages of two *P. pacificus* populations could be distinctly observed using a purple and a green dye that lasts for 3-5 days. However, first, high densities of adults within the same population have been shown to increase the Eu (predatory) mouth-form ratio within the developing juveniles/dauers on the same plate. In contrast, the effect of crowding on mouth-form was not observed when high densities of juveniles/dauers were applied. Therefore, identifying adult-specific density-dependent effects on mouth-form. Furthermore, this effect has proven to be conserved when using a mixed culture of two different *P. pacificus* populations. These results were further investigated by examining genetic mutants deficient in producing ascarosides pheromones, *daf-22* mutants, as a potential source for intergenerational communication. Another approach was also used by examining the secretion profiles of different nematode stages using high-performance liquid chromatography-mass spectrometry, suggesting the involvement of di-ascaroside#1 in inducing the Eu mouth-form phenotype in the developing worms. Thus, the authors could identify a significant role of age classes in intergenerational communication, where adult worms release pheromones to warn the developing worms inducing the predatory mouth-form to cope with the future competition.

3.4.2. Own contribution

I participated in the ecological conceptualization of intergenerational communication in *P. pacificus*. I estimate my contribution at 10%.

3.5. Crowdsourcing and the feasibility of manual gene annotation: a pilot study in the nematode *Pristionchus pacificus*

Rödelsperger C, Athanasouli M, Lenuzzi M, Theska T, Sun S, **Dardiry M**, Wighard S, Hu W, Sharma DR, Han Z.

Scientific Reports. 2019 Dec 11;9(1):1-9, doi.org/10.1038/s41598-019-55359-5

3.5.1. Synopsis

This paper applied a manual curation framework to enhance the 1:1 *P. pacificus* to *C. elegans* ortholog annotation in the *pacificus* genome. The authors first showed that the quality of different nematodes' genomes varies in terms of completeness, gene annotation level, and genome assembly. Notably, the *C. elegans* genome displays one of the highest scores in all quality measurements. Then, the authors combined information from the 1:1 *C. elegans* and *P. pacificus* orthologs, in addition to the Iso-seq and RNA-seq data from *P. pacificus*, to manually curate *pacificus* genes misannotation. This methodology identified 526 missing genes and thousands of hidden orthologous due to artificial gene fusion in the previous annotation of the *pacificus* genome. The community-based curation methodology increased the number of annotated genes from 25,517 to 28,036. Moreover, it raised the 1:1 ortholog completeness level from 86% to 97%. Thus, such a community-based manual curation has significantly improved gene annotation in *P. pacificus*, facilitating more precise downstream analyses.

3.5.2. Own contribution

I participated in manual curation of *P. pacificus* genes' annotation with my colleagues. I estimate my contribution at 10%.

3.6. Sex or cannibalism: Polyphenism and kin recognition control social action strategies in nematodes

Dardiry M*, Lightfoot JW*, Kalirad A, Giaimo S, Eberhardt G, Witte H, Wilecki M, Rödelsperger C, Traulsen A, Sommer RJ.

Science Advances. 2021 Aug 25;7(35):eabg8042, doi: 10.1126/sciadv.abg8042

3.6.1. Synopsis

In this article, the authors show that mouth-form plasticity, morphologically and behaviorally, besides kin-recognition shape the evolution of competitive or cooperative strategies in the genus *Pristionchus*. Surprisingly, phylogenetic analysis of 29 *Pristionchus* species shows a significant association of mouth-form bias and mode of reproduction. *Pristionchus* species can follow either a hermaphroditic or a gonochoristic reproduction mode, i.e., reproducing through obligatory mating between males and females. Remarkably, 6 out of 7 hermaphroditic species showed an Eu-predatory bias in their populations' mouth-form ratio. In contrast, 20 out of 22 gonochoristic species showed a St-microbivorous bias in their female populations' mouth-form ratio. Furthermore, killing assays on three different *P. uniformis* female-male natural isolates and their hybrids showed that gonochoristic species display the microbivores bias to promote mating and avoid parent-offspring conflict. On the contrary, 85% of the killing assays on 36 hermaphroditic *P. pacificus* co-occurring natural isolates showed competitive behavior, either by mutual or one-directional killing. Further genomic investigations on the 36 natural isolates revealed the involvement of whole-genome relatedness in the process of kin-recognition. The authors extended their experimental evidence with a mathematical modeling approach. With this approach, the authors simulated the interactions of three different *P. pacificus* natural isolates while manipulating kin-recognition and mouth-form bias parameters. The theoretical analysis supported an extremely high degree of genome relatedness for the natural isolates' coexistence. In conclusion, with such an integrative approach combining experiments and theory, while several examples of animal polyphenism and kin-recognition were provided, the authors argue for a crucial role of

polyphenism and kin-recognition in shaping social action strategies from nematodes to vertebrates.

3.6.2. Own contribution

I majorly contributed to the experimental part and participated in the logical framework of the mathematical work. estimate my contribution at 40%.

3.7. Experimental and theoretical support for costs of plasticity and phenotype in a nematode cannibalistic trait.

Dardiry M, Piskobulu V*, Kalirad A*, Sommer RJ.

Submitted.

3.7.1. Synopsis

In this article, the authors investigated the cost of phenotype and the cost of plasticity regarding mouth-form alternative switches in *P. pacificus*. First, the authors set the definition of both types of costs. They define the cost of phenotype as the fitness tradeoff incurred by an organism to develop an energetically costly phenotype. While the cost of plasticity is defined as the fitness reduction incurred by a more plastic organism compared to a less plastic one. The authors experimentally tested if the Eu mouth-form would exhibit a phenotype cost in terms of lower overall fecundity values compared to the St phenotype. To perform such a test, the authors used seven *P. pacificus* natural isolates where the mean mouth-form ratio in the population would roughly display an equal value for both mouth-forms, i.e., unbiased isolates. All comparisons showed a lower overall fecundity average in the Eu animals compared to the St animals, with four out of seven comparisons showing strong and/or partial support. The authors performed the same analysis again, however, this time between two Eu-biased isolates against two St-biased isolates. Indeed, the Eu-biased isolates have displayed a significant reduction in their fecundities compared to the St-biased isolates. The cost of plasticity was examined by comparing the reaction norms on three *P. pacificus* isolates in two different bacterial food sources. Profoundly, the more plastic isolate exhibited the highest cost in terms of fecundity reduction. Furthermore, four main empirical measures were performed in the two bacterial food sources: mouth-form ratio, fecundity, developmental speed, and killing rate. These empirical measurements were then implemented in a stage-structured mathematical model simulating ecologically relevant scenarios. Mathematical simulations have revealed a significant influence of the spatial structure of the environment on the dynamics of the Eu-biased vs. the St-biased populations in a resource-competition setup. In conclusion, the authors took an integrative approach combining experimental data and

mathematical simulation to understand the costs behind the evolution of mouth-form switch bias.

3.7.2. Own contribution

I majorly contributed to the experimental part and participated in the logical framework of the mathematical part. estimate my contribution at 60%.

3.8. Cost of adaptive plasticity and spatial heterogeneity in *Pristionchus pacificus*: a computational perspective

Kalirad A, **Dardiry M**, Sommer RJ.

Ready for submission.

3.8.1. Synopsis

In this article, the authors expand their previous modeling approach to simulate more parameters testing costs of plasticity and phenotypes. The authors used the experimentally-derived data to simulate four different conditions representing *P. pacificus* ecologically relevant scenarios. The extension of the previous model includes three main directions. First, using a two-dimensional stepping stone model where worm dispersal is not restricted into one direction as the previous model. In contrast, the second and third extensions represent manipulation of the parameters for dispersal rate and functional response. Functional response describes the dynamics of predation in the model. It describes the number of preys consumed by the predator as a function of prey density, providing a prey handling time parameter that can broaden the spectrum of the model. The simulations of the four scenarios resulted in the dominance of the less-plastic Eu-biased isolate in most scenarios. However, with high migration rates between food patches and low handling time, in the condition where the cost of phenotype is manifested, a clear dominance of the more-plastic isolate is obtained. Thus, under this extended model, both dispersal rate and handling time affect the dynamics of the population; however, the spatial structure of the environment remains the most influential parameter on the behavior of the model.

3.8.2. Own contribution

I participated in the logical framework of the mathematical part. estimate my contribution at 40%.

3.9. Dissecting the genetic architecture underlying mouth dimorphism in *P. pacificus* identifies *cis*-regulatory variations in a multi-gene locus.

Dardiry M, Lightfoot JW, Rödelberger C, Witte H, Eberhardt G, Sommer RJ.

In preparation.

3.9.1. Synopsis

In this article, the authors identified the genetic architecture underlying mouth-form response evolution in *P. pacificus* natural isolates. The authors first generated hybrid F1 animals by crossing an Eu-biased isolate to an St-biased isolate, both of which are genetically closely related as of previous investigations. These hybrid animals were used to generate Recombinant Inbred Lines (RILs), screened for mouth-form ratio, and utilized in a Quantitative Trait Loci (QTL) analysis. QTL mapping revealed the involvement of one major locus underlying the variation in the mouth–form threshold response. Notably, the regulatory region of *eud-1* in the multi-gene locus was a top candidate under the identified interval. RNA-seq expression analysis has shown that *eud-1* expression is 40% higher in the Eu-biased parental line than the St-biased one. Moreover, in the *eud-1* regulatory region, CRISPR Cas-9 methodology was used to introduce the genomic variants of the St-biased parent in the Eu-biased one. Such a fine-mapping approach indicated the cumulative involvement of two *eud-1*-related regulatory regions: first, a deletion in an upstream 3kb potential forkhead binding motif in the promoter/enhancer region of *eud-1*, and second, a single nucleotide polymorphism (SNP) in the *eud-1* first intron. Mutants with the deletion of the binding site and the swapped SNP in Eu-biased background showed a reduction in the mouth-form ratio similar to the St-biased parent. In addition, RT-qPCR analysis has shown a reduction in *eud-1* expression in these generated mutants. Finally, a phylogenetic analysis of the two genomic causative regions for 30 *P. pacificus* natural isolate declared diverged evolutionary mechanisms underlying mouth-form response variation across the *pacificus* clades.

3.9.2. Own contribution

I majorly participated in generating different types of data in this publication. I estimate my contribution at 80%.

4. Discussion

Since Aristotle's time, through Darwin's thoughts and Ernst Mayr's inquiries on to the West-Eberhard enterprise, the question of what causes biological diversity has served as a cornerstone to understand biological life. Ontological, logical, and epistemological frameworks have given rise to various schools of thought regarding the understanding of causality and, therefore, the understanding of biological diversity. In this thesis, I used the model organism *Pristionchus pacificus* to examine the role of phenotypic plasticity in this context of evolutionary biology.

Throughout this thesis, I have categorized my findings in line with Mayr's inquiries. The "*how-question*" would represent an inquiry of the mechanistic machinery underlying mouth-form plasticity and kin recognition. While the "*why-question*" would represent an inquiry about the adaptive value of mouth-form choice, either at the morphological level or at the behavioral level. In the end, the dichotomy between the *how* and *why* questions Mayr proposed is not strict. Conceptually, they do represent different meanings, like white and black. Nonetheless, their empirical application depicts different shades of gray.

First, on the side of the *how-driven* questions. A quantitative trait locus approach has revealed one major locus underlying the evolution of the threshold mouth-form response. Additionally, the fine mapping of this interval uncovered the involvement of two regulatory regions controlling mouth-form variation among *P. pacificus* natural isolates. The regulatory variants occur within a multi-gene locus (supergene). This locus includes two sulfatases, the switch gene *eud-1* and its paralog *sul.2.2.1*, besides two N-acetylglucosaminidases (*nag*) in an inverted tandem arrangement. Notably, the knock-out of these genes has proven their involvement in the mouth-form switch.

Interestingly, the effect of the regulatory variants is cumulative. For example, a combination of a deletion in a *cis*-regulatory potential forkhead binding motif in the promoter/enhancer of *eud-1*, in addition to a single nucleotide swap in the first intron of the same gene, leads to a shift in mouth-form ratio, i.e., it leads to a reduction of the Eubias in the population. These modifications were shown to affect *eud-1* expression, thus driving the change in mouth-form ratio.

The significant role of *cis*-regulation in evolutionary biology has been under a considerable body of investigations^{231–233}. In 1961 Jacob and Monod suggested that operator mutations might play an essential role in evolution^{234,235}. A decade later, Britten and Davidson found out that a considerable proportion of many eukaryotic genomes is constituted by repetitive sequences²³⁶. Therefore, they hypothesized a regulatory role for repetitive sequences and thus, a potential contribution to the origin of phenotypic novelty²³⁶. Also, King and Wilson strongly emphasized the role of *cis*-regulatory elements in driving phenotypic divergence in 1975¹³⁶. They argued that the degree of divergence in protein sequence between humans and chimpanzees could not justify the phenotypic divergence between the two species¹³⁶. Instead, they suggested *cis*-regulatory differences as a potential driver for phenotypic evolution¹³⁶. In fact, over the years, numerous studies have shown the contribution of *cis*-variation in morphological divergence and adaptive evolution^{237–239}. For instance, the variation in the enhancer region of the transcription factor *Pitx-1* has proven to be involved in local adaptation of the sticklebacks fish populations (*Gasterosteus aculeatus*)²⁴⁰. The same applies to *Drosophila* natural isolates, where *cis*-regulatory change for the *yellow* gene results in different wing pigmentation patterns²⁴¹.

However, a scarce number of studies have shown the significant role of *cis*-regulation on the level of organismal adaptive plasticity. For instance, a recently published paper has argued for *cis*-regulatory modifications underlying the adaptive dehydration response in *Arabidopsis* species²⁴². However, to our knowledge, the study performed in this thesis is one of the earliest investigations regarding *cis*-regulation for alternative plastic switches. Additionally, it was not to our surprise that an intronic variation, specifically first intron, is cumulatively involved in regulating *eud-1* expression. Indeed, *C. elegans* first intron has been shown to be involved in regulating gene expression²⁴³.

In conclusion, the investigations under the “*how*” question had identified naturally regulatory polymorphisms underlying the variation in the responses’ polyphenism within a multi-gene locus.

Few future directions might be inspired by the findings of the previously mentioned studies: first, further mechanistic investigations on the role of *eud-1* first intron in driving

eud-1 expression. Second, expanding the phylogenetic analysis to explore the genetic mechanism underlying the response variation in the other *P. pacificus* clades. Third, exploring the epigenetic, environmental regulation of the four genes in the multi-gene locus. Finally, biochemically inspecting how *eud-1* (sulfatase) plays a role in shaping the alternative switch.

Second, on the side of the *why*-driven questions. My phylogenetic analysis of *Pristionchus* species has revealed a significant association between mouth-form bias and reproductive mode. Showing that hermaphroditic species display a bias towards the Eu mouth-form, while in gonochoristic species females display a bias towards the St mouth-form. Furthermore, we have argued for the adaptive value of this mouth-form bias on the behavioral and ecological level. Indeed, experimental evidence has proven the involvement of the mouth-form bias in promoting cooperative social strategies between natural isolates of the gonochoristic species *P. uniforms* while aiding in competitive, predatory behavior between natural isolates of the hermaphroditic species *P. pacificus*. Thus, promoting reproduction and survivability in both species. Moreover, we could identify kin-recognition as a significant player shaping such social action strategies, demonstrating that the competitive, predatory behavior relies on a whole-genome relatedness system.

Nonetheless, several *P. pacificus* natural isolates display either unbiased mouth-form ratios or a St-biased phenotype. Therefore, we tested if the adaptive Eu bias in hermaphrodites would incur a cost. Indeed, the tested *P. pacificus* Eu-biased isolates exhibited a cost in fecundity and developmental speed compared to the St-biased ones. Moreover, we tested if the St-biased isolates would exhibit a plasticity cost. We obtained reaction norms of three *P. pacificus* strains by examining their plastic response towards two different bacterial diets. We also measured their fecundity and developmental speed change on the two diets as an approximation of fitness. Evidently, this cross-condition testing has shown a plasticity cost incurred by the St-biased strain regarding fecundity.

Furthermore, we performed predation assays between an Eu-biased strain and a St-biased strain. These empirical data were implemented in a stage-structured mathematical model to simulate relevant *Pristionchus* ecological scenarios. Our

mathematical approach revealed a significant effect of spatially structured environments on the population dynamics, i.e., the relative abundance of the St-biased and the Eu-biased isolates in the simulation. Incorporating simulations might represent a powerful tool for future studies on phenotypic plasticity, in particular if they are based on empirically obtained life history parameters. In principle, such studies allow testing the interaction of multiple factors independently, thereby also helping design further ecological experiments.

In principle, alternative mouth-form phenotypes in *Pristionchus* might be considered as an example of resource polyphenism. In resource polyphenism, alternative phenotypes facilitate the utilization of different food resources, including the development of cannibalistic morphologies in response to environmental stress²⁴⁴. Through cannibalism, trophic and survival advantages are obtained, such as extending energy resources or eliminating competition^{245,246}. Indeed, the predatory mouth-form of *P. pacificus* was shown to improve survival under adverse conditions²²⁴. Furthermore, it appears that *Pristionchus* worms engage in an intraguild predation behavior, as these worms can kill and feed on various nematodes, likely to ward off rival competitors for resources as well as to acquire additional nutrients^{247,248}.

Cannibal morphs of many other organisms exhibit the ability to recognize themselves and their relatives, thereby reducing the likelihood of harming offspring and kin; in other words, they display self and kin-recognition. Examples could be found across animals, including salamanders, spadefoot toad tadpoles, locusts, and rotifers²⁴⁹⁻²⁵². In addition, social action strategies, such as competition and cooperation, have also been associated with plasticity in other organisms. For instance, plasticity has been shown to assist in developing cooperative strategies in hymenopterans and termites²⁵³. On the other hand, it promotes competitiveness, as seen in spadefoot toads and rotifers^{250,252}. Thus, the results of our studies add nematodes to such systems and argues for the vital role of phenotypic plasticity influencing social action strategies from worms to vertebrates.

In conclusion, we have performed an integrative framework to understand the adaptive value of *Pristionchus* mouth-form plasticity, morphologically and behaviorally. This integrative approach combined empirical evidence, including genomic analysis and

experimental evolution, with formal logic represented in mathematical modeling; thus, comprehensively analyzing a puzzling evolutionary query. We have shown the adaptive value of mouth-form bias and in addition, have investigated the costs of phenotype and plasticity under relevant ecological ramifications.

Future directions might be inspired by the findings of the previously mentioned studies: first, it has been shown that kin-recognition was not solely restricted on sequence similarities of the self-recognition gene *self-1*. Instead, kin-recognition in *P. pacificus* correlated with the whole genome-relatedness measure. Thus, further investigations on the molecular machinery underlying kin-recognition might be a new area for investigations. Second, males occur spontaneously in many hermaphroditic populations of *P. pacificus*. However, the effect of the inter-isolate mating on morphological and behavioral plasticity is yet to be investigated. A third far-reaching perspective will be testing if the mouth-form switch is associated with other behaviors that might affect nematode fitness, e.g., different navigation strategies between St and Eu animals, given their energy source spectrum.

In general, for a bigger picture, in 2020, Ralf J. Sommer has published one of the most recent conceptual frameworks regarding genetic assimilation¹⁵¹. This model might be considered an updated model for the seven steps suggested by West-Eberhard in the introduction of this thesis¹⁴⁹. Sommer suggested that transgenerational effects might initiate genetic assimilation based on epigenetic machinery. In his model, Sommer suggests four crucial steps regarding the evolution of novelty through genetic assimilation. First, a monomorphic trait shows a plastic response to the environment either by environmental induction or genetic mutations. Second, the generation of developmental switches that regulate the expression of the alternative phenotypes. Third, further phenotypic diversification occurs for the alternative phenotypes due to their adaptive value and selection regimes, in a step named genetic accommodation. Finally, plasticity is terminated by genetic assimilation, or in other words, going back to monomorphism.

Indeed, a phylogenetic context regarding the switch between monomorphism, polymorphism, and polyphenism has been documented as well¹⁴⁹, as different attempts

were performed to understand genetic assimilation^{254,255}. However, the molecular identification of an evolutionary adaptive switch mechanism is yet an open question. In *Pristionchus*, with such resources availability, knowledge of the genetic network underlying mouth-form plasticity, and now a start to grasp the *how* and *why* behind natural variation, this model system provides a unique opportunity to tackle this hypothesis.

In conclusion, I have discussed five of the major articles in this thesis. I aimed to investigate the evolutionary significance of mouth-form plasticity, morphologically and behaviorally. The work of this thesis was centered around the natural isolates' perspective. Moreover, this perspective was led by *how*-driven questions regarding the mechanism underlying plasticity and *why*-driven questions regarding the adaptive value of plasticity. Thus, adding a brick in the *Pristionchus* assembly as a model key system exploring the role of phenotypic plasticity in evolutionary theory.

“We are drowning in information while starving for wisdom. The world henceforth will be run by synthesizers, people able to put together the right information at the right time, think critically about it, and make important choices wisely”

-Edward O. Wilson, *The unity of knowledge*²⁵⁶

5. References

1. Clarke, D. M. & Clarke, D. M. Descartes: A biography. (2006).
2. Holland, A. & O’Hear, A. On What Makes an Epistemology Evolutionary. *Proceedings of the Aristotelian Society, Supplementary Volumes* **58**, 177–217 (1984).
3. Bradie, M. & Harms, W. Evolutionary Epistemology. *The Stanford Encyclopedia of Philosophy* (2020).
4. Claeys, G. The ‘Survival of the Fittest’ and the Origins of Social Darwinism. *J. Hist. Ideas* **61**, 223–240 (2000).
5. Godfrey-Smith, P. Darwinism and cultural change. *Philos. Trans. R. Soc. Lond. B Biol. Sci.* **367**, 2160–2170 (2012).
6. Hodgson, G. M. Darwinism in economics: from analogy to ontology. *Journal of Evolutionary Economics* **12**, 259–281 (2002).
7. Crook, D. P. Darwinism — The political implications. *Hist. Eur. Ideas* **2**, 19–34 (1981).
8. Goering, S. Eugenics. *The Stanford Encyclopedia of Philosophy* (2014).
9. Kevles, D. J. *In the Name of Eugenics: Genetics and the Uses of Human Heredity*. (Harvard University Press, 1995).
10. Largent, M. A. On Daniel J. Kevles’s *In the Name of Eugenics*. *Hist. Stud. Nat. Sci.* **44**, 514–520 (2014).
11. Allen, G. E. Eugenics and Modern Biology: Critiques of Eugenics, 1910–1945. *Ann. Hum. Genet.* **75**, 314–325 (2011).
12. Aylesworth, G. Postmodernism. *The Stanford Encyclopedia of Philosophy* (2015).
13. Whitfield, J. Biological theory: Postmodern evolution? *Nature* **455**, 281–284 (2008).
14. Losee, J. *Theories of causality: from antiquity to the present*. (Routledge, 2017).
15. Kleinberg, S. A Brief History of Causality. in *Causality, Probability, and Time* 11–42 (Cambridge University Press, 2012).
16. Falcon, A. Aristotle on Causality. *The Stanford Encyclopedia of Philosophy* (2019).
17. Hulswit, M. A short history of causation. *SEED Journal (Semiotics, Evolution, Energy)* (2004).
18. Gärdenfors, P. & Lombard, M. Causal Cognition, Force Dynamics and Early Hunting Technologies. *Front. Psychol.* **9**, 87 (2018).

19. Bender, A. What Is Causal Cognition? *Front. Psychol.* **11**, 3 (2020).
20. Lombard, M. & Gärdenfors, P. Causal Cognition and Theory of Mind in Evolutionary Cognitive Archaeology. *Biol. Theory* (2021) doi:10.1007/s13752-020-00372-5.
21. Callaway, E. Is this cave painting humanity's oldest story? *Nature* (2019) doi:10.1038/d41586-019-03826-4.
22. Cresswell, M. J. Plato's theory of causality: Phaedo 95–106. *Australas. J. Philos.* **49**, 244–249 (1971).
23. Sedley, D. Platonic Causes. *Phronesis* **43**, 114–132 (1998).
24. Richardson, K. Causation in Arabic and Islamic Thought. *The Stanford Encyclopedia of Philosophy* (2020).
25. White, G. Medieval Theories of Causation. *The Stanford Encyclopedia of Philosophy* (2018).
26. Mumford, S. & Anjum, R. L. *Causation: A Very Short Introduction*. (Oxford University Press, 2013).
27. Müller, G. B. Evo–devo: extending the evolutionary synthesis. *Nat. Rev. Genet.* **8**, 943–949 (2007).
28. Laland, K. N. *et al.* The extended evolutionary synthesis: its structure, assumptions and predictions. *Proceedings of the Royal Society B: Biological Sciences* **282**, 20151019 (2015).
29. Bricker, P. Ontological Commitment. *The Stanford Encyclopedia of Philosophy* (2016).
30. Hofweber, T. Logic and Ontology. *The Stanford Encyclopedia of Philosophy* (2021).
31. Kim, J. Causation, Nomic Subsumption, and the Concept of Event. *J. Philos.* **70**, 217–236 (1973).
32. Horwich, P. *Asymmetries in Time: Problems in the Philosophy of Science*. (Bradford Books, 1987).
33. Rankin, M. L. & McCormack, T. The temporal priority principle: at what age does this develop? *Front. Psychol.* (2013).
34. Casati, R. & Varzi, A. Events. *The Stanford Encyclopedia of Philosophy* (2020).
35. Thomasson, A. Categories. *The Stanford Encyclopedia of Philosophy* (2019).
36. Orilia, F. & Paolini Paoletti, M. Properties. *The Stanford Encyclopedia of Philosophy*

- (2020).
37. Robinson, H. Substance. *The Stanford Encyclopedia of Philosophy* (2021).
 38. Morris, W. E. & Brown, C. R. David Hume. *The Stanford Encyclopedia of Philosophy* (2021).
 39. Andreas, H. & Guenther, M. Regularity and Inferential Theories of Causation. *The Stanford Encyclopedia of Philosophy* (2021).
 40. Kleinberg, S. *Causality, Probability, and Time*. (Cambridge University Press, 2012).
 41. Huemer, M. & Kovitz, B. Causation as Simultaneous and Continuous. *Philos. Q.* **53**, 556–565 (2003).
 42. Schaffer, J. The Metaphysics of Causation. *The Stanford Encyclopedia of Philosophy* (2016).
 43. Hume, D. *A Treatise of Human Nature*. (Courier Corporation, 2003).
 44. Garrett, D. The Representation of Causation and Hume's Two Definitions of 'Cause'. *Noûs* **27**, 167–190 (1993).
 45. Wetzel, L. Types and Tokens. *The Stanford Encyclopedia of Philosophy* (2018).
 46. Hitchcock, C. Probabilistic causation. (1997).
 47. Pinto, R. *Argument, inference and dialectic: Collected papers on informal logic*. (2001).
 48. Dutilh Novaes, C. Argument and Argumentation. *The Stanford Encyclopedia of Philosophy* (2021).
 49. Ferguson, K. G. Monotonicity in Practical Reasoning. *Argumentation* **17**, 335–346 (2003).
 50. Strasser, C. & Antonelli, G. A. Non-monotonic Logic. *The Stanford Encyclopedia of Philosophy* (2019).
 51. Hawthorne, J. Inductive Logic. *The Stanford Encyclopedia of Philosophy* (2021).
 52. Henderson, L. The Problem of Induction. *The Stanford Encyclopedia of Philosophy* (2020).
 53. Douven, I. Abduction. *The Stanford Encyclopedia of Philosophy* (2021).
 54. Steup, M. & Neta, R. Epistemology. *The Stanford Encyclopedia of Philosophy* (2020).
 55. Markie, P. & Folescu, M. Rationalism vs. Empiricism. *The Stanford Encyclopedia of Philosophy* (2021).

56. Kelly, T. Evidence. *The Stanford Encyclopedia of Philosophy* (2016).
57. Chalmers, A. F. *What Is This Thing Called Science?* (Hackett Publishing, 2013).
58. Kellert, S. H., Longino, H. E. & Kenneth Waters, C. *Scientific Pluralism*. (U of Minnesota Press, 2006).
59. Hepburn, B. & Andersen, H. Scientific Method. *The Stanford Encyclopedia of Philosophy* (2021).
60. Braillard, P.-A. & Malaterre, C. *Explanation in Biology: An Enquiry into the Diversity of Explanatory Patterns in the Life Sciences*. (Springer, Dordrecht, 2015).
61. Thornton, S. Karl Popper. *The Stanford Encyclopedia of Philosophy* (2021).
62. Popper, K. *The Logic of Scientific Discovery*. (Routledge, 2005).
63. Kraut, R. Plato. *The Stanford Encyclopedia of Philosophy* (2017).
64. Delacy, P. H. The Problem of Causation in Plato's Philosophy. *Class. Philol.* **34**, 97–115 (1939).
65. Greene, J. C. From Aristotle to Darwin: Reflections on Ernst Mayr's Interpretation in 'The Growth of Biological Thought'. *J. Hist. Biol.* **25**, 257–284 (1992).
66. Powers, J. Finding Ernst Mayr's Plato. *Stud. Hist. Philos. Biol. Biomed. Sci.* **44**, 714–723 (2013).
67. Shields, C. Aristotle. *The Stanford Encyclopedia of Philosophy* (2020).
68. Ross, S. Scientist: The story of a word. *Ann. Sci.* **18**, 65–85 (1962).
69. Cahan, D. *From Natural Philosophy to the Sciences: Writing the History of Nineteenth-Century Science*. (University of Chicago Press, 2003).
70. Boyd, R. N. The Logician's Dilemma: Deductive Logic, Inductive Inference and Logical Empiricism. *Erkenntnis* **22**, 197–252 (1985).
71. Klein, J. & Giglioni, G. Francis Bacon. *The Stanford Encyclopedia of Philosophy* (2020).
72. Mayr, E. *Toward a New Philosophy of Biology: Observations of an Evolutionist*. (Belknap Press of Harvard University Press, 1988).
73. Mix, L. Nested explanation in Aristotle and Mayr. *Synthese* **193**, 1817–1832 (2016).
74. Lennox, J. Aristotle's Biology. *The Stanford Encyclopedia of Philosophy* (2019).
75. Hintikka, J. & Sandu, G. - What is logic? in *Philosophy of Logic* (ed. Jacqueline, D.) 13–39 (North-Holland, 2007).

76. Roscoe, K. & Isle, M. *Aristotle: The Father of Logic*. (The Rosen Publishing Group, Inc, 2015).
77. Smith, R. Aristotle's Logic. *The Stanford Encyclopedia of Philosophy* (2020).
78. Barnes, J. Aristotle's Theory of Demonstration. *Phronesis* **14**, 123–152 (1969).
79. Kuhn, T. The Structure of Scientific Revolutions. in *Philosophy after Darwin* 176–177 (Princeton University Press, 2021).
80. Laland, K. N., Sterelny, K., Odling-Smee, J., Hoppitt, W. & Uller, T. Cause and Effect in Biology Revisited: Is Mayr's Proximate-Ultimate Dichotomy Still Useful? *Science* **334**, 1512–1516 (2011).
81. Laland, K. N., Odling-Smee, J., Hoppitt, W. & Uller, T. More on how and why: a response to commentaries. *Biol. Philos.* **28**, 793–810 (2013).
82. Haig, D. Proximate and ultimate causes: how come? and what for? *Biol. Philos.* **28**, 781–786 (2013).
83. Mayr, E. Cause and Effect in Biology. *Science* **134**, 1501–1506 (1961).
84. Toepfer, G. Teleology and its constitutive role for biology as the science of organized systems in nature. *Stud. Hist. Philos. Biol. Biomed. Sci.* **43**, 113–119 (2012).
85. de Laguna, G. A. The Role of Teleonomy in Evolution. *Philos. Sci.* **29**, 117–131 (1962).
86. Gotthelf, A. Aristotle's Conception of Final Causality. *Rev. Metaphys.* **30**, 226–254 (1976).
87. Johnson, M. R. *Aristotle on Teleology*. (Oxford: Oxford University Press, 2008).
88. Scriven, M. Explanation and Prediction in Evolutionary Theory. *Science* **130**, 477–482 (1959).
89. Tinbergen, N. On aims and methods of Ethology. *Zeitschrift für Tierpsychologie* **20**, 410–433 (1963).
90. Bateson, P. & Laland, K. N. Tinbergen's four questions: an appreciation and an update. *Trends Ecol. Evol.* **28**, 712–718 (2013).
91. Burkhardt, R. W., Jr. Tribute to Tinbergen: Putting Niko Tinbergen's 'Four Questions' in Historical Context. *Ethology* **120**, 215–223 (2014).
92. Huxley, J. & Others. Evolution. The modern synthesis. *Evolution. The Modern Synthesis*. (1942).

93. Gascoigne, R. M. Julian Huxley and biological progress. *J. Hist. Biol.* **24**, 433–455 (1991).
94. Pigliucci, M. & Müller, G. B. *Evolution ? the Extended Synthesis*. (MIT Press, 2010).
95. Smith, P. K. Ethology, sociobiology and developmental psychology: In memory of Niko Tinbergen and Konrad Lorenz. *Br. J. Dev. Psychol.* **8**, 187–200 (1990).
96. Lorenz, K. *King Solomon's ring*. (Routledge, 2003).
97. Lorenz, K. *The Foundations of Ethology*. (Springer Nature, 1981).
98. Hosken, D. J., Hunt, J. & Wedell, N. *Genes and Behaviour: Beyond Nature-Nurture*. (Wiley & Sons, Incorporated, John, 2019).
99. Sloan, P. Evolutionary Thought Before Darwin. *The Stanford Encyclopedia of Philosophy* (2019).
100. Berryman, S. Ancient Atomism. *The Stanford Encyclopedia of Philosophy* (2016).
101. Rieppel, O. Atomism, epigenesis, preformation and pre-existence: a clarification of terms and consequences. *Biol. J. Linn. Soc. Lond.* **28**, 331–341 (1986).
102. Nicholson, D. J. & Dupré, J. *Everything flows: towards a processual philosophy of biology*. (Oxford University Press, 2018).
103. Woodruff, L. L. History of Biology. *Sci. Mon.* **12**, 253–281 (1921).
104. Nordenskiöld, E. & Eyre, L. B. *The history of biology: A survey*. (2018).
105. Ainsworth, T. Form vs. Matter. *The Stanford Encyclopedia of Philosophy* (2020).
106. Chalmers, A. Atomism from the 17th to the 20th Century. *The Stanford Encyclopedia of Philosophy* (2019).
107. Bos, A. P. ARISTOTLE ON THE DIFFERENCES BETWEEN PLANTS, ANIMALS, AND HUMAN BEINGS AND ON THE ELEMENTS AS INSTRUMENTS OF THE SOUL (DE ANIMA 2.4.415b18). *Rev. Metaphys.* **63**, 821–841 (2010).
108. Martin, R. M. *Epistemology: A Beginner's Guide*. (Simon and Schuster, 2014).
109. Mayr, E. *The Growth of Biological Thought: Diversity, Evolution, and Inheritance*. (Harvard University Press, 1982).
110. Humphreys, J. Lamarck and the general theory of evolution. *J. Biol. Educ.* **30**, 295–303 (1996).
111. Gilbert, S. F. & Others. *Developmental biology*. (2000).
112. Willmore, K. E. The body plan concept and its centrality in evo-devo. *Evolution:*

- Education and Outreach* (2012).
113. Sloan, P. Darwin: From Origin of Species to Descent of Man. *The Stanford Encyclopedia of Philosophy* (2019).
 114. Vorzimmer, P. Darwin, Malthus, and the Theory of Natural Selection. *J. Hist. Ideas* **30**, 527–542 (1969).
 115. Gregory, T. R. Understanding Natural Selection: Essential Concepts and Common Misconceptions. *Evolution: Education and Outreach* **2**, 156–175 (2009).
 116. Liu, Y. A new perspective on Darwin's Pangenesis. *Biol. Rev. Camb. Philos. Soc.* **83**, 141–149 (2008).
 117. Portin, P. & Wilkins, A. The Evolving Definition of the Term 'Gene'. *Genetics* **205**, 1353–1364 (2017).
 118. Bowler, P. J. *Evolution: the history of an idea.* (1989).
 119. Gilbert, S. F. & Epel, D. *Ecological developmental biology: the environmental regulation of development, health, and evolution.* (Sinauer Associates, Incorporated Publishers, 2015).
 120. Muller, H. J. Thomas Hunt Morgan 1866-1945. *Science* **103**, 550–551 (1946).
 121. Gayon, J. From Mendel to epigenetics: History of genetics. *C. R. Biol.* **339**, 225–230 (2016).
 122. Sarkar, S. The founders of theoretical evolutionary genetics: Editor's introduction. in *Boston Studies in the Philosophy of Science* 1–22 (Springer Netherlands, 1992).
 123. Frank, S. A. & Slatkin, M. Fisher's fundamental theorem of natural selection. *Trends Ecol. Evol.* **7**, 92–95 (1992).
 124. Edwards, A. W. The fundamental theorem of natural selection. *Biol. Rev. Camb. Philos. Soc.* **69**, 443–474 (1994).
 125. Li, C. C. Fundamental theorem of natural selection. *Nature* **214**, 505–506 (1967).
 126. Wright, S. Coefficients of Inbreeding and Relationship. *Am. Nat.* **56**, 330–338 (1922).
 127. Wilson, E. O. Kin Selection as the Key to Altruism: Its Rise and Fall. *Soc. Res.* **72**, 159–166 (2005).
 128. Hamilton, W. D. The genetical evolution of social behaviour. I. *J. Theor. Biol.* **7**, 1–16 (1964).
 129. Dobzhansky, T. Genetics and the origin of species. *Copeia* **1952**, 287 (1952).

130. Lewontin, R. C. Dobzhansky's genetics and the origin of species: is it still relevant? *Genetics* **147**, 351–355 (1997).
131. Mayr, E. *Systematics and the Origin of Species, from the Viewpoint of a Zoologist*. (Harvard University Press, 1999).
132. Hey, J., Fitch, W. M. & Ayala, F. J. Systematics and the origin of species: an introduction. *Proc. Natl. Acad. Sci. U. S. A.* **102 Suppl 1**, 6515–6519 (2005).
133. Mallet, J. Group selection and the development of the biological species concept. *Philos. Trans. R. Soc. Lond. B Biol. Sci.* **365**, 1853–1863 (2010).
134. Koonin, E. V. Towards a postmodern synthesis of evolutionary biology. *Cell Cycle* **8**, 799–800 (2009).
135. Hall, B. K. Evolutionary Developmental Biology (Evo-Devo): Past, Present, and Future. *Evolution: Education and Outreach* **5**, 184–193 (2012).
136. King, M. C. & Wilson, A. C. Evolution at two levels in humans and chimpanzees. *Science* **188**, 107–116 (1975).
137. Gould, S. J. *Ontogeny and Phylogeny*. (Harvard University Press, 1985).
138. Jacob, F. Evolution and tinkering. *Science* **196**, 1161–1166 (1977).
139. Racine, V. 'Evolution and Tinkering'(1977), by Francois Jacob. *Embryo Project Encyclopedia* (2014).
140. Arthur, W. *Evolution: A Developmental Approach*. (John Wiley & Sons, 2010).
141. Tickle, C. & Urrutia, A. O. Perspectives on the history of evo-devo and the contemporary research landscape in the genomics era. *Philos. Trans. R. Soc. Lond. B Biol. Sci.* **372**, (2017).
142. Abouheif, E. *et al.* Eco-evo-devo: the time has come. *Adv. Exp. Med. Biol.* **781**, 107–125 (2014).
143. Gilbert, S. F., Bosch, T. C. G. & Ledón-Rettig, C. Eco-Evo-Devo: developmental symbiosis and developmental plasticity as evolutionary agents. *Nat. Rev. Genet.* **16**, 611–622 (2015).
144. Konstantinides, N., Degabriel, S. & Desplan, C. Neuro-evo-devo in the single cell sequencing era. *Curr Opin Syst Biol* **11**, 32–40 (2018).
145. Toth, A. L. & Robinson, G. E. Evo-devo and the evolution of social behavior: brain gene expression analyses in social insects. *Cold Spring Harb. Symp. Quant. Biol.* **74**,

- 419–426 (2009).
146. Toth, A. L. & Robinson, G. E. Evo-devo and the evolution of social behavior. *Trends Genet.* **23**, 334–341 (2007).
 147. Laland, K. *et al.* Does evolutionary theory need a rethink? *Nature* **514**, 161–164 (2014).
 148. Bradshaw, A. D. Evolutionary Significance of Phenotypic Plasticity in Plants. in *Advances in Genetics* (eds. Caspari, E. W. & Thoday, J. M.) vol. 13 115–155 (Academic Press, 1965).
 149. West-Eberhard, M. J. *Developmental Plasticity and Evolution*. (Oxford University Press, 2003).
 150. Pigliucci, M. *Phenotypic Plasticity: Beyond Nature and Nurture*. (Johns Hopkins University Press, 2001).
 151. Sommer, R. J. Phenotypic Plasticity: From Theory and Genetics to Current and Future Challenges. *Genetics* **215**, 1–13 (2020).
 152. Pfennig, D. W. *Phenotypic Plasticity & Evolution: Causes, Consequences, Controversies*. (Taylor & Francis, 2021).
 153. Johannsen, W. *Elemente der exakten Erblchkeitslehre*. (Fischer, 1909).
 154. Johannsen, W. The Genotype Conception of Heredity. *Am. Nat.* **45**, 129–159 (1911).
 155. Lewontin, R. C. Genotype and Phenotype. *International Encyclopedia of the Social & Behavioral Sciences* 6159–6162 (2001) doi:10.1016/b0-08-043076-7/03077-1.
 156. Sultan, S. E. Phenotypic plasticity for plant development, function and life history. *Trends Plant Sci.* **5**, 537–542 (2000).
 157. Pigliucci, M., Murren, C. J. & Schlichting, C. D. Phenotypic plasticity and evolution by genetic assimilation. *J. Exp. Biol.* **209**, 2362–2367 (2006).
 158. Schlichting, C. D. THE EVOLUTION OF PHENOTYPIC PLASTICITY IN PLANTS. *Annu. Rev. Ecol. Syst.* **17**, 667–693 (1986).
 159. Vovides, A. G., Berger, U. & Balke, T. Chapter 5 - Morphological plasticity and survival thresholds of mangrove plants growing in active sedimentary environments. in *Dynamic Sedimentary Environments of Mangrove Coasts* (eds. Sidik, F. & Friess, D. A.) 121–140 (Elsevier, 2021).
 160. Parker, B. J. & Brisson, J. A. A Laterally Transferred Viral Gene Modifies Aphid Wing

- Plasticity. *Curr. Biol.* **29**, 2098–2103.e5 (2019).
161. Wilson, E. O. & Hölldobler, B. Eusociality: origin and consequences. *Proc. Natl. Acad. Sci. U. S. A.* **102**, 13367–13371 (2005).
 162. Sumner, S., Pereboom, J. J. M. & Jordan, W. C. Differential gene expression and phenotypic plasticity in behavioural castes of the primitively eusocial wasp, *Polistes canadensis*. *Proc. Biol. Sci.* **273**, 19–26 (2006).
 163. Korb, J. & Hartfelder, K. Life history and development—a framework for understanding developmental plasticity in lower termites. *Biol. Rev. Camb. Philos. Soc.* **83**, 295–313 (2008).
 164. Molet, M., Wheeler, D. E. & Peeters, C. Evolution of novel mosaic castes in ants: modularity, phenotypic plasticity, and colonial buffering. *Am. Nat.* **180**, 328–341 (2012).
 165. Corona, M., Libbrecht, R. & Wheeler, D. E. Molecular mechanisms of phenotypic plasticity in social insects. *Curr Opin Insect Sci* **13**, 55–60 (2016).
 166. Abouheif, E. Ant caste evo-devo: it's not all about size. *Trends in ecology & evolution* vol. 36 668–670 (2021).
 167. Revely, L., Sumner, S. & Eggleton, P. The Plasticity and Developmental Potential of Termites. *Frontiers in Ecology and Evolution* **9**, (2021).
 168. Moczek, A. P. Horn polyphenism in the beetle *Onthophagus taurus*: larval diet quality and plasticity in parental investment determine adult body size and male horn morphology. *Behav. Ecol.* (1998).
 169. Moczek, A. P. & Others. Phenotypic plasticity and the origins of diversity: a case study on horned beetles. *Phenotypic plasticity in insects: mechanisms and consequences* 81–134 (2009).
 170. Fielenbach, N. & Antebi, A. C. *elegans* dauer formation and the molecular basis of plasticity. *Genes Dev.* **22**, 2149–2165 (2008).
 171. Diaz, S. A. & Viney, M. The evolution of plasticity of dauer larva developmental arrest in the nematode *Caenorhabditis elegans*. *Ecol. Evol.* **5**, 1343–1353 (2015).
 172. Laforsch, C. & Tollrian, R. INDUCIBLE DEFENSES IN MULTIPREDATOR ENVIRONMENTS: CYCLOMORPHOSIS IN *DAPHNIA CUCULLATA*. *Ecology* **85**, 2302–2311 (2004).

173. Gotthard, K., Nylin, S. & Wiklund, C. Seasonal Plasticity in Two Satyrine Butterflies: State-Dependent Decision Making in Relation to Daylength. *Oikos* **84**, 453–462 (1999).
174. Moczek, A. P. *et al.* The role of developmental plasticity in evolutionary innovation. *Proceedings of the Royal Society B: Biological Sciences* **278**, 2705–2713 (2011).
175. Trussell, G. C. PHENOTYPIC PLASTICITY IN AN INTERTIDAL SNAIL: THE ROLE OF A COMMON CRAB PREDATOR. *Evolution* **50**, 448–454 (1996).
176. Levis, N. A., Isdaner, A. J. & Pfennig, D. W. Morphological novelty emerges from pre-existing phenotypic plasticity. *Nature Ecology & Evolution* **2**, 1289–1297 (2018).
177. Wang, X. & Kang, L. Molecular mechanisms of phase change in locusts. *Annu. Rev. Entomol.* **59**, 225–244 (2014).
178. Rong, M. *et al.* Phenotypic Plasticity of *Staphylococcus aureus* in Liquid Medium Containing Vancomycin. *Front. Microbiol.* **10**, 809 (2019).
179. Hurtado-Bautista, E., Pérez Sánchez, L. F., Islas-Robles, A., Santoyo, G. & Olmedo-Alvarez, G. Phenotypic plasticity and evolution of thermal tolerance in bacteria from temperate and hot spring environments. *PeerJ* **9**, e11734 (2021).
180. Ptashne, M. A genetic switch: Gene control and phage. λ . (1986).
181. West-Eberhard, M. J. Alternative adaptations, speciation, and phylogeny (A Review). *Proc. Natl. Acad. Sci. U. S. A.* **83**, 1388–1392 (1986).
182. Roff, D. A. The Evolution of Threshold Traits in Animals. *Q. Rev. Biol.* **71**, 3–35 (1996).
183. Nijhout, H. F. & Wheeler, D. E. Juvenile Hormone and the Physiological Basis of Insect Polymorphisms. *Q. Rev. Biol.* **57**, 109–133 (1982).
184. Dubnau, D. & Losick, R. Bistability in bacteria. *Mol. Microbiol.* **61**, 564–572 (2006).
185. Ghalambor, C. K., McKAY, J. K., Carroll, S. P. & Reznick, D. N. Adaptive versus non-adaptive phenotypic plasticity and the potential for contemporary adaptation in new environments. *Funct. Ecol.* **21**, 394–407 (2007).
186. Orr, H. A. The genetic theory of adaptation: a brief history. *Nat. Rev. Genet.* **6**, 119–127 (2005).
187. Murren, C. J. *et al.* Constraints on the evolution of phenotypic plasticity: limits and costs of phenotype and plasticity. *Heredity* **115**, 293–301 (2015).

188. Peirson, B. R. E. Plasticity, stability, and yield: the origins of Anthony David Bradshaw's model of adaptive phenotypic plasticity. *Stud. Hist. Philos. Biol. Biomed. Sci.* **50**, 51–66 (2015).
189. DeWitt, T. J., Sih, A. & Wilson, D. S. Costs and limits of phenotypic plasticity. *Trends Ecol. Evol.* **13**, 77–81 (1998).
190. Van Buskirk, J. & Steiner, U. K. The fitness costs of developmental canalization and plasticity. *J. Evol. Biol.* **22**, 852–860 (2009).
191. Merilä, J., Laurila, A. & Lindgren, B. Variation in the degree and costs of adaptive phenotypic plasticity among *Rana temporaria* populations. *J. Evol. Biol.* **17**, 1132–1140 (2004).
192. Crispo, E. The Baldwin effect and genetic assimilation: revisiting two mechanisms of evolutionary change mediated by phenotypic plasticity. *Evolution* **61**, 2469–2479 (2007).
193. West-Eberhard, M. J. Developmental plasticity and the origin of species differences. *Proc. Natl. Acad. Sci. U. S. A.* **102 Suppl 1**, 6543–6549 (2005).
194. Schwander, T. & Leimar, O. Genes as leaders and followers in evolution. *Trends Ecol. Evol.* **26**, 143–151 (2011).
195. Levis, N. A. & Pfennig, D. W. Evaluating 'plasticity-first' evolution in nature: key criteria and empirical approaches. *Trends Ecol. Evol.* **31**, 563–574 (2016).
196. Levis, N. A. & Pfennig, D. W. Plasticity-led evolution: evaluating the key prediction of frequency-dependent adaptation. *Proc. Biol. Sci.* **286**, 20182754 (2019).
197. Baldwin, J. M. & Others. A new factor in evolution. *Diacronia* 1–13 (2018).
198. WOLTERECK & R. Weitere experimentelle Untersuchungen über Artveränderung, speziell über das Wesen quantitativer Artunterschiede bei Daphniden. *Verh. D. Tsch. Zool. Ges.* **1909**, 110–172 (1909).
199. Nicoglou, A. Phenotypic Plasticity: From Microevolution to Macroevolution. in *Handbook of Evolutionary Thinking in the Sciences* (eds. Heams, T., Huneman, P., Lecointre, G. & Silberstein, M.) 285–318 (Springer Netherlands, 2015).
200. Schmalhausen, I. I. Factors of evolution: the theory of stabilizing selection. **327**, (1949).
201. Waddington, C. H. *The strategy of the genes*. (Routledge, 2014).

202. Waddington, C. H. CANALIZATION OF DEVELOPMENT AND THE INHERITANCE OF ACQUIRED CHARACTERS. *Nature* **150**, 563 (1942).
203. Waddington, C. H. Canalization of development and genetic assimilation of acquired characters. *Nature* **183**, 1654–1655 (1959).
204. Rajagopal, J. & Stanger, B. Z. Plasticity in the Adult: How Should the Waddington Diagram Be Applied to Regenerating Tissues? *Dev. Cell* **36**, 133–137 (2016).
205. Flatt, T. The evolutionary genetics of canalization. *Q. Rev. Biol.* **80**, 287–316 (2005).
206. Gibson, G. & Dworkin, I. Uncovering cryptic genetic variation. *Nat. Rev. Genet.* **5**, 681 (2004).
207. West-Eberhard, M. J. PHENOTYPIC PLASTICITY AND THE ORIGINS OF DIVERSITY. *Annu. Rev. Ecol. Syst.* **20**, 249–278 (1989).
208. Cobb, N. A. Nematodes and their relationships. (1914).
209. Sommer, R. J. *Pristionchus pacificus: A Nematode Model for Comparative and Evolutionary Biology*. (BRILL, 2015).
210. Witte, H. *et al.* Gene inactivation using the CRISPR/Cas9 system in the nematode *Pristionchus pacificus*. *Dev. Genes Evol.* **225**, 55–62 (2015).
211. Han, Z. *et al.* Improving Transgenesis Efficiency and CRISPR-Associated Tools Through Codon Optimization and Native Intron Addition in *Pristionchus* Nematodes. *Genetics* **216**, 947–956 (2020).
212. Athanasouli, M. *et al.* Comparative genomics and community curation further improve gene annotations in the nematode *Pristionchus pacificus*. *BMC Genomics* **21**, 708 (2020).
213. Bento, G., Ogawa, A. & Sommer, R. J. Co-option of the hormone-signalling module dafachronic acid-DAF-12 in nematode evolution. *Nature* **466**, 494–497 (2010).
214. Ragsdale, E. J., Müller, M. R., Rödelberger, C. & Sommer, R. J. A developmental switch coupled to the evolution of plasticity acts through a sulfatase. *Cell* **155**, 922–933 (2013).
215. Susoy, V. & Sommer, R. J. Stochastic and conditional regulation of nematode mouth-form dimorphisms. *Frontiers in Ecology and Evolution* (2016).
216. Lenuzzi, M. *et al.* Influence of environmental temperature on mouth-form plasticity in *Pristionchus pacificus* acts through daf-11-dependent cGMP signaling. *J. Exp.*

- Zool. B Mol. Dev. Evol.* **n/a**, (2021).
217. Moreno, E., Lightfoot, J. W., Lenuzzi, M. & Sommer, R. J. Cilia drive developmental plasticity and are essential for efficient prey detection in predatory nematodes. *Proc. Biol. Sci.* **286**, 20191089 (2019).
218. Kieninger, M. R. *et al.* The Nuclear Hormone Receptor NHR-40 Acts Downstream of the Sulfatase EUD-1 as Part of a Developmental Plasticity Switch in *Pristionchus*. *Curr. Biol.* **26**, 2174–2179 (2016).
219. Sieriebriennikov, B. *et al.* Conserved nuclear hormone receptors controlling a novel plastic trait target fast-evolving genes expressed in a single cell. *PLoS Genet.* **16**, e1008687 (2020).
220. Sun, S., Theska, T., Witte, H., Ragsdale, E. J. & Sommer, R. J. The oscillating Mucin-type protein DPY-6 has a conserved role in nematode mouth and cuticle formation. *Genetics* (2021) doi:10.1093/genetics/iyab233.
221. Werner, M. S. *et al.* Young genes have distinct gene structure, epigenetic profiles, and transcriptional regulation. *Genome Res.* **28**, 1675–1687 (2018).
222. Serobyán, V. *et al.* Chromatin remodelling and antisense-mediated up-regulation of the developmental switch gene *eud-1* control predatory feeding plasticity. *Nat. Commun.* **7**, 12337 (2016).
223. Lightfoot, J. W. *et al.* Small peptide-mediated self-recognition prevents cannibalism in predatory nematodes. *Science* **364**, 86–89 (2019).
224. Serobyán, V., Ragsdale, E. J. & Sommer, R. J. Adaptive value of a predatory mouth-form in a dimorphic nematode. *Proceedings of the Royal Society B: Biological Sciences* **281**, 20141334 (2014).
225. Serobyán, V., Ragsdale, E. J., Müller, M. R. & Sommer, R. J. Feeding plasticity in the nematode *Pristionchus pacificus* is influenced by sex and social context and is linked to developmental speed. *Evol. Dev.* **15**, 161–170 (2013).
226. Renahan, T., Lo, W. S. & Werner, M. S. Nematode biphasic ‘boom and bust’ dynamics are dependent on host bacterial load while linking dauer and mouth-form polyphenisms. *Environmentalist* (2021).
227. Renahan, T. & Sommer, R. J. Nematode Interactions on Beetle Hosts Indicate a Role of Mouth-Form Plasticity in Resource Competition. *Frontiers in Ecology and*

- Evolution* **9**, 703 (2021).
228. Herrmann, M. *et al.* Two new Species of *Pristionchus* (Nematoda: Diplogastriidae) include the Gonochoristic Sister Species of *P. fissidentatus*. *J. Nematol.* **51**, 1–14 (2019).
229. Rödelsperger, C. *et al.* Single-Molecule Sequencing Reveals the Chromosome-Scale Genomic Architecture of the Nematode Model Organism *Pristionchus pacificus*. *Cell Rep.* **21**, 834–844 (2017).
230. Rödelsperger, C. *et al.* Phylotranscriptomics of *Pristionchus* Nematodes Reveals Parallel Gene Loss in Six Hermaphroditic Lineages. *Curr. Biol.* **28**, 3123–3127.e5 (2018).
231. Wittkopp, P. J., Haerum, B. K. & Clark, A. G. Evolutionary changes in cis and trans gene regulation. *Nature* **430**, 85–88 (2004).
232. Wray, G. A. The evolutionary significance of cis-regulatory mutations. *Nat. Rev. Genet.* **8**, 206–216 (2007).
233. Carroll, S. B., Grenier, J. K. & Weatherbee, S. D. *From DNA to Diversity: Molecular Genetics and the Evolution of Animal Design*. (John Wiley & Sons, 2013).
234. Monod, J. & Jacob, F. General Conclusions: Teleonomic Mechanisms in Cellular Metabolism, Growth, and Differentiation. *Cold Spring Harb. Symp. Quant. Biol.* **26**, 389–401 (1961).
235. Jacob, F. & Monod, J. Genetic regulatory mechanisms in the synthesis of proteins. *J. Mol. Biol.* **3**, 318–356 (1961).
236. Britten, R. J. & Davidson, E. H. Repetitive and non-repetitive DNA sequences and a speculation on the origins of evolutionary novelty. *Q. Rev. Biol.* **46**, 111–138 (1971).
237. Wittkopp, P. J. & Kalay, G. Cis-regulatory elements: molecular mechanisms and evolutionary processes underlying divergence. *Nat. Rev. Genet.* **13**, 59–69 (2011).
238. Gompel, N., Prud'homme, B., Wittkopp, P. J., Kassner, V. A. & Carroll, S. B. Chance caught on the wing: cis-regulatory evolution and the origin of pigment patterns in *Drosophila*. *Nature* **433**, 481–487 (2005).
239. McGregor, A. P. *et al.* Morphological evolution through multiple cis-regulatory mutations at a single gene. *Nature* **448**, 587–590 (2007).
240. Chan, Y. F. *et al.* Adaptive evolution of pelvic reduction in sticklebacks by recurrent

- deletion of a Pitx1 enhancer. *Science* **327**, 302–305 (2010).
241. Gompel, N. & Prud'homme, B. The causes of repeated genetic evolution. *Dev. Biol.* **332**, 36–47 (2009).
242. He, F. *et al.* Cis-regulatory evolution spotlights species differences in the adaptive potential of gene expression plasticity. *Nat. Commun.* **12**, 3376 (2021).
243. Fuxman Bass, J. I. *et al.* Transcription factor binding to *Caenorhabditis elegans* first introns reveals lack of redundancy with gene promoters. *Nucleic Acids Res.* **42**, 153–162 (2014).
244. Pfennig, D. W. & McGee, M. Resource polyphenism increases species richness: a test of the hypothesis. *Philos. Trans. R. Soc. Lond. B Biol. Sci.* **365**, 577–591 (2010).
245. Church, S. C. & Sherratt, T. N. The Selective Advantages of Cannibalism in a Neotropical Mosquito. *Behav. Ecol. Sociobiol.* **39**, 117–123 (1996).
246. Claessen, D., de Roos, A. M. & Persson, L. Population dynamic theory of size-dependent cannibalism. *Proc. Biol. Sci.* **271**, 333–340 (2004).
247. Quach, K. T. & Chalasani, S. H. Intraguild predation between *Pristionchus pacificus* and *Caenorhabditis elegans*: a complex interaction with the potential for aggressive behaviour. *J. Neurogenet.* **34**, 404–419 (2020).
248. Polis, G. A. & Holt, R. D. Intraguild predation: The dynamics of complex trophic interactions. *Trends Ecol. Evol.* **7**, 151–154 (1992).
249. Pfennig, D. W. & Collins, J. P. Kinship affects morphogenesis in cannibalistic salamanders. *Nature* **362**, 836–838 (1993).
250. Pfennig, D. W., Reeve, H. K. & Sherman, P. W. Kin recognition and cannibalism in spadefoot toad tadpoles. *Anim. Behav.* **46**, 87–94 (1993).
251. Guttal, V., Romanczuk, P., Simpson, S. J., Sword, G. A. & Couzin, I. D. Cannibalism can drive the evolution of behavioural phase polyphenism in locusts. *Ecol. Lett.* **15**, 1158–1166 (2012).
252. Gilbert, J. J. Sex-specific cannibalism in the rotifer *Asplanchna sieboldi*. *Science* **194**, 730–732 (1976).
253. Weitekamp, C. A., Libbrecht, R. & Keller, L. Genetics and Evolution of Social Behavior in Insects. *Annu. Rev. Genet.* **51**, 219–239 (2017).
254. Suzuki, Y. & Nijhout, H. F. Evolution of a polyphenism by genetic accommodation.

Science **311**, 650–652 (2006).

255. Vigne, P. *et al.* A single-nucleotide change underlies the genetic assimilation of a plastic trait. *Sci Adv* **7**, (2021).

256. Wilson, E. O. *Consilience: The unity of knowledge*. vol. 31 (Vintage, 1999)

6. Appendix



Cite this article: Sommer RJ, Dardiry M, Lenuzzi M, Namdeo S, Renahan T, Sieriebriennikov B, Werner MS. 2017 The genetics of phenotypic plasticity in nematode feeding structures. *Open Biol.* **7**: 160332. <http://dx.doi.org/10.1098/rsob.160332>

Received: 12 December 2016

Accepted: 10 February 2017

Subject Area:

developmental biology/genetics

Keywords:

phenotypic plasticity, *Pristionchus pacificus*, switch genes, nuclear hormone receptors, epigenetics

Author for correspondence:

Ralf J. Sommer

e-mail: ralf.sommer@tuebingen.mpg.de

The genetics of phenotypic plasticity in nematode feeding structures

Ralf J. Sommer, Mohannad Dardiry, Masa Lenuzzi, Suryesh Namdeo, Tess Renahan, Bogdan Sieriebriennikov and Michael S. Werner

Department for Integrative Evolutionary Biology, Max-Planck Institute for Developmental Biology, Spemannstrasse 37, 72076 Tübingen, Germany

RJS, 0000-0003-1503-7749

Phenotypic plasticity has been proposed as an ecological and evolutionary concept. Ecologically, it can help study how genes and the environment interact to produce robust phenotypes. Evolutionarily, as a facilitator it might contribute to phenotypic novelty and diversification. However, the discussion of phenotypic plasticity remains contentious in parts due to the absence of model systems and rigorous genetic studies. Here, we summarize recent work on the nematode *Pristionchus pacificus*, which exhibits a feeding plasticity allowing predatory or bacteriovorous feeding. We show feeding plasticity to be controlled by developmental switch genes that are themselves under epigenetic control. Phylogenetic and comparative studies support phenotypic plasticity and its role as a facilitator of morphological novelty and diversity.

1. Introduction

All organisms have to adapt to the environment and to environmental variation. Often, alternative conditions result in different expressions and values of traits, a phenomenon referred to as ‘phenotypic plasticity’. Generally, phenotypic (or developmental) plasticity is defined as the property of a given genotype to produce different phenotypes depending on distinct environmental conditions [1,2]. In addition to being an ecological concept that allows studying how organisms respond to environmental variation, phenotypic plasticity also represents an integral part of the evolutionary process. Given these ecological and evolutionary implications, it is not surprising that the concept of phenotypic plasticity has been contentious ever since its introduction at the beginning of the 20th century. For some, plasticity is the major driver and facilitator of phenotypic diversification, and, as such, of greatest importance for understanding evolution and its underlying mechanisms [1–3]. For others, phenotypic plasticity represents environmental noise and is sometimes considered to even hinder evolution because environmentally induced variation may slow down the rate of adaptive processes [4,5]. This controversy largely depends on two limitations. First, there is confusion over the different types of plasticity found in nature. Plasticity can be adaptive or non-adaptive, reversible or irreversible, conditional or stochastic, and continuous or discrete, all of which require careful evaluations of examples of plasticity for their potential evolutionary significance. Second, the absence of plasticity model systems has long hampered the elucidation of potential molecular and genetic mechanisms, the identification of which would provide a framework for theoretical considerations.

In 1965, Bradshaw made one of the most important contributions to the concept of phenotypic plasticity when he proposed that plasticity must have a genetic basis. This idea grew out of the observation that the plasticity of a trait is independent of the phenotype of the plastic trait itself [6]. However, little progress was made to identify underlying mechanisms, largely due to the absence of laboratory model systems of plasticity. Here, we summarize recent studies on phenotypic plasticity of feeding structures in the nematode *Pristionchus pacificus*. The

Table 1. History of phenotypic plasticity.

Date	Scientist(s)	Theory
1909	Woltereck	reaction norm
1913	Johannsen	genotype – phenotype distinction
1940 – 1950	Waddington Schmalhausen	canalization/assimilation
1965	Bradshaw	genetic basis of plasticity
1998 – 2003	Schlichting/Pigliucci West-Eberhard	facilitator hypothesis

advantages of this system have allowed unbiased genetic approaches that provide detailed insight into the genetic control of plasticity and a molecular framework for studying the mechanisms of plasticity and genetic–environmental interactions. A model system approach in nematodes might therefore help clarify the role of plasticity in evolution by shedding light on its molecular mechanisms and macro-evolutionary potentials. We will start with a brief historical account of phenotypic plasticity and its role for the evolution of novelty.

2. A historical account

The history of phenotypic plasticity begins at the beginning of the 20th century (table 1) [7]. In 1909, Richard Woltereck carried out the first experiments on plastic characters using the water flea *Daphnia*. He coined the term ‘reaction norm’ (or norm of reaction) to describe the relationship between the expressions of phenotypes across a range of different environments [3]. However, it was Johannsen (1911) who first distinguished between genotype and phenotype, and thereby introduced the concept of genotype–environment interaction [8]. This concept was only developed further three decades later by the Russian biologist Schmalhausen and the British developmental biologist Waddington. In particular, Waddington, using environmental perturbation of development, provided important conceptual contributions [9]. For example, he introduced the concept of genetic assimilation based on his work with the bithorax and crossveinless phenotypes in *Drosophila*. When fly pupae were exposed to heat shock, some of them developed a crossveinless phenotype. Upon artificial selection for multiple generations, this trait became fixed in some animals even without heat shock. Similarly, when flies were treated with ether vapour, some exhibited a homeotic bithorax phenotype, which again could be fixed even without ether induction after artificial selection for approximately 20 generations. Waddington argued that genetic assimilation allows the environmental response of an organism to be incorporated into the developmental programme of the organism. While it is now known that the fixation of the bithorax phenotype was based on the selection of standing genetic variation at a homeotic gene [10], at the time these findings were controversially discussed and often referred to as Lamarckian mechanisms. Given the missing genetic foundation of development and plasticity in the 1940s, it is not surprising that Waddington’s claim for an extended evolutionary synthesis found little support among neo-Darwinists [11].

The major conceptual advancement for plasticity research was in 1965 when Anthony Bradshaw proposed that phenotypic

plasticity and the ability to express alternative phenotypes must be genetically controlled [6]. Some plants develop alternative phenotypes in response to extreme environmental conditions. Using a comparative approach, Bradshaw realized that the plasticity of a trait could differ between close relatives of the same genus, independent of the trait itself. From this observation he concluded that the genetic control of a character is independent of the character’s plasticity. This remarkable conclusion represents one of the most important testimonies of the power of comparative approaches and the key foundation for modern studies of plasticity.

It is not surprising that botanists have paid detailed attention to reaction norm and plasticity for breeding purposes, and the first modern monographs that advertised the significance of phenotypic plasticity for development and evolution were written by active practitioners in this field [3]. Many examples of plasticity from animals are known as well, often in insects. The migratory locust *Schistocerca gregaria* can form two alternative phenotypes in relation to food availability. Adult *Schistocerca* are dark with large wings when food is abundant, whereas they are green with small wings when food is limited [12]. Similarly, many butterflies are known to form distinct wing patterns in the dry and rainy season in the tropics or in spring and summer in more temperate climates [13]. Perhaps the most spectacular examples of plasticity are those found in hymenopterans forming the basis for eusociality in insects and resulting in the most extreme forms of morphological and behavioural novelties. Mary-Jane West-Eberhard, after a long and active career studying social behaviours in Hymenoptera, proposed an extended evolutionary theory that links development and plasticity to evolution. Her monograph *Developmental plasticity and evolution* provides an exhaustive overview on alternative phenotypes in nature [2]. Building on the now available genetic understanding of developmental processes, she proposed plasticity to represent a major facilitator and driver for the evolution of novelty and the morphological and behavioural diversification in animals and plants.

This long path from Johannsen, Waddington and Bradshaw to current plasticity research has resulted in a strong conceptual framework for the potential significance of plasticity for evolution (table 1). However, scepticism remains, largely due to the near absence of associated genetic and molecular mechanisms of plasticity [14]. To overcome these limitations, plasticity research requires model systems that tie developmental plasticity in response to environmental perturbations to laboratory approaches. Before summarizing the recent inroads obtained in one laboratory model for phenotypic plasticity, the next paragraph will briefly summarize the different forms of plasticity.

3. Some important terminology: the different forms of plasticity

By definition, the concept of phenotypic plasticity incorporates many unrelated phenomena, which has resulted in enormous confusion and debate about its potential for evolutionary adaptations [15]. Three major distinctions are necessary to properly evaluate the potential significance of plasticity for evolution. First, phenotypic plasticity can be adaptive or non-adaptive, and only the former can contribute to adaptive evolution when organisms are faced with a new or altered environment.

In contrast, non-adaptive plasticity in response to extreme and often stressful environments is likely to result in maladaptive traits that are without evolutionary significance [15].

Second, plasticity can be continuous or discrete, the latter resulting in alternative phenotypes often referred to as polyphenisms. Such alternative phenotypes have several advantages for experimental analysis and evaluation in the field. Most importantly, alternative phenotypes can more readily be distinguished from genetic polymorphisms that can also result in phenotypic divergence. Multiple examples of polyphenisms from aerial and subterranean stem and leaf formation in water plants, insect wing and body form dimorphisms and the casts of social insects have been studied in detail to analyse the interaction between the genotype and the environment in the specification of plastic traits [2]. The binary readout of alternative phenotypes provides a major advantage of such experimental analyses.

Third, plasticity might be regulated by conditional and stochastic factors [16]. While the former is more common, additional stochastic elements of regulation are known in some examples of plasticity and such cases have several experimental advantages. Most examples of plasticity have environment *a* inducing phenotype *A* and environment *b* inducing phenotype *B*. However, organisms might form alternative phenotypes *A* and *B* in part due to stochastic factors that are independent of environmental alterations. The potential role of stochastic factors has been largely overlooked in plant and animal systems, but is well known in microbes. Phenotypic heterogeneity or bistability is known in many bacteria to result in phenotypically distinct subpopulations of cells [17,18]. Persister cell formation in *Staphylococcus aureus* and spore formation in *Bacillus subtilis* represent just a few examples of phenotypic heterogeneity that occur to a certain extent in a stochastic manner. Antibiotic resistance seen by persister cells resulted in detailed molecular and mechanistic insight into the stochastic regulation of phenotypic heterogeneity [19].

Adaptive versus non-adaptive, continuous versus discrete, and conditional versus stochastic regulation of plasticity represent important distinctions for the evaluation and significance of plastic traits in development and evolution. However, one additional factor that often complicates a proper evaluation of plasticity is the inherent difficulty to distinguish between genetic polymorphisms and polyphenisms. Genetic polymorphisms are a cornerstone of mainstream evolutionary theory for the generation of phenotypic divergence. Therefore, empirical studies on plasticity would profit from a proper distinction between polymorphisms and polyphenisms. Besides inbred lines in outbreeding species, self-fertilization in hermaphroditic organisms results in isogenic lines. Such isogenic lines can rule out contributions of genetic polymorphisms. Some plants, nematodes and other animals with a hermaphroditic mode of reproduction are therefore ideal for studies of plasticity, mimicking the isogenic advantages of bacteria with phenotypic heterogeneity.

In the following, we summarize recent insight into the genetic regulation of a mouth-form feeding plasticity in the nematode *P. pacificus*. This example of plasticity is adaptive, represents a dimorphic trait with two alternative phenotypes, and contains conditional and stochastic elements of regulation. *Pristionchus pacificus* is a hermaphroditic species with isogenic propagation, and is amenable to forward and reverse genetic analysis [20,21]. We begin with a brief summary of mouth-form polyphenism in this nematode species.

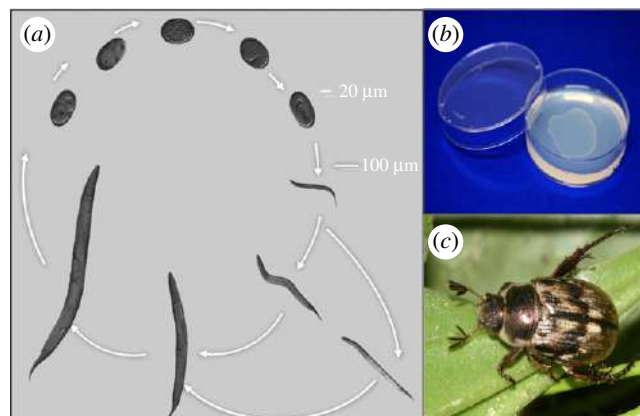


Figure 1. *Pristionchus pacificus* and growth. (a) Adult hermaphrodites lay eggs that develop through four larval stages to become adult. The first juvenile stage remains in the eggshell in *P. pacificus*. Under harsh and unfavourable conditions, worms develop into an arrested and long-lived dauer stage. (b) In the laboratory, worms are grown on agar plates with *Escherichia coli* as food source. Under these conditions, worms complete their direct life cycle in 4 days (20°C). (c) The oriental beetle *Exomala orientalis* from Japan and the United States is one of the scarab beetle hosts on which *P. pacificus* is found in the dauer larval stage.

4. Mouth-form polyphenism as a case study

The genus *Pristionchus* belongs to the nematode family Diplogastriidae, which shows entomophilic associations (figure 1) and omnivorous feeding strategies, including predation on other nematodes [22]. Usually, nematodes stay in the arrested dauer stage—a nematode-specific form of dormancy—in or on the insect vector (figure 1a). Nematode–insect associations represent a continuum between two most extreme forms, with dauer larvae of some species jumping on and off their carriers (phoresy), whereas others wait for the insect to die in order to resume development on the insect carcass (necromeny). Insect carcasses represent heterogeneous environments full of a variety of microbes. Such insect carcasses are best characterized by a boom and bust strategy of many of its inhabitants. While many nematodes, yeasts, protists and bacteria are known to proliferate on insect cadavers, few, if any, of these systems have been fully characterized, in particular with regard to species succession during decomposition.

Pristionchus pacificus and related nematodes live preferentially on scarab beetles (i.e. cockchafers, dung beetles and stag beetles; figure 1c) [23]. On living beetles, *P. pacificus* is found exclusively in the arrested dauer stage and decomposition experiments indicate that adult worms are found on the cadaver only 7 days after the beetle's death [24]. *Pristionchus* and other nematodes live on and wait for the beetle to die, resulting in enormous competition for food and survival on the carcass. It was long known that *Pristionchus* and other diplogastriid nematodes form teeth-like denticles in their mouths, which allow predatory feeding (figure 2a) [25]. Also, it was long known that many species form two alternative mouth-forms. In the case of *P. pacificus*, animals decide during larval development in an irreversible manner to adopt a eury stomatous (Eu) or a stenostomatous (St) mouth-form (figure 2a) [25]. Eu animals form two teeth with a wide buccal cavity, representing predators. In contrast, St animals have a single tooth with a narrow buccal cavity and are strict

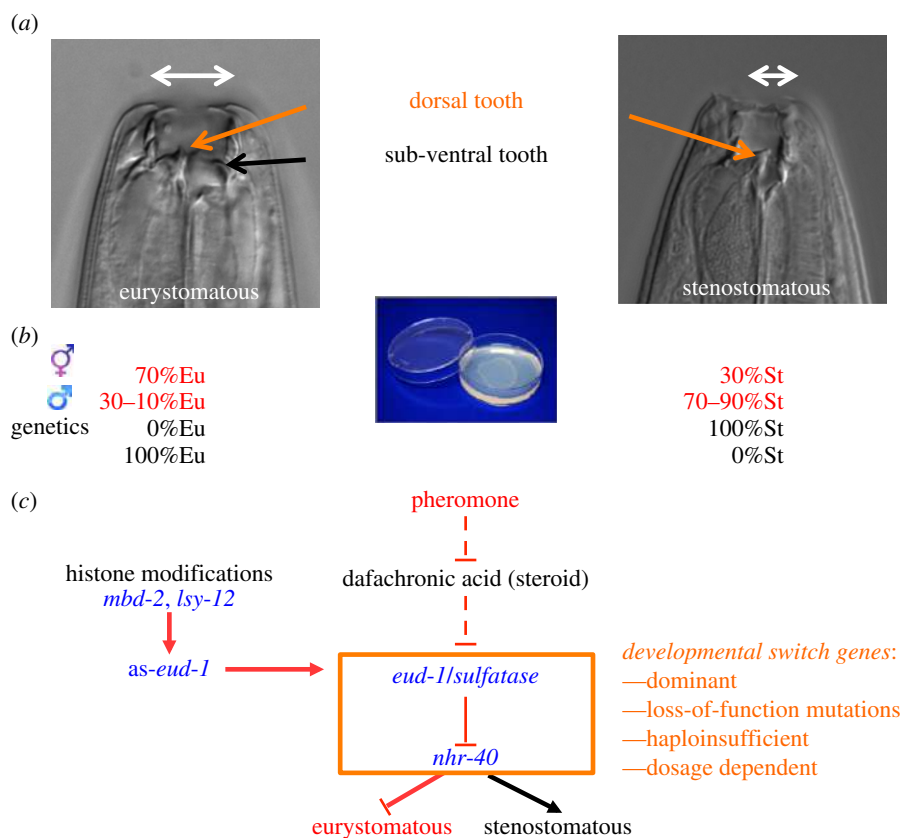


Figure 2. Genetic regulation of phenotypic plasticity of *P. pacificus* feeding structures. (a) Mouth dimorphism. During larval development, *P. pacificus* individuals make an irreversible decision to develop a eurystomatous morph with two teeth (orange and black arrows) and a broad buccal cavity (white arrow), or alternatively, a stenostomatous morph with a single dorsal tooth (orange arrow) and a narrow buccal cavity (white arrow). (b) Under fixed laboratory conditions, mouth-form plasticity shows stochastic regulation resulting in hermaphrodites having approximately 70% eurystomatous mouth-forms, whereas males have been 10–30% eurystomatous animals. In genetic screens, monomorphic mutants can be isolated that are either 100% stenostomatous or 100% eurystomatous. (c) Partial genetic network regulating mouth-form plasticity. The sulfatase-encoding *eud-1* gene and the nuclear hormone receptor are developmental switch mutations, which are dominant, *loss-of-function* and dosage dependent, resulting in all-stenostomatous or all-eurystomatous phenotypes, respectively. Small molecule signalling acts upstream of *eud-1* and involves pheromones and steroid hormone signalling, which are not a subject of this review. Histone modifications are crucial for mouth-form regulation and act through an antisense message at the *eud-1* locus (*as-eud-1*).

microbial feeders. Selection experiments have shown that the mouth-form dimorphism represents an example of phenotypic plasticity because isogenic animals can form both mouth-forms [25]. The dimorphism is discrete and adaptive with strong fitness effects preferring St and Eu animals under bacterial and predatory conditions, respectively [26,27]. Most importantly, mouth-form plasticity is regulated by conditional factors such as starvation and crowding [25], but also contains stochastic elements of regulation. Specifically, a nearly constant ratio of 70–90% Eu : 30–10% St animals is formed under fixed environmental conditions (figure 2b). It is this aspect of stochastic regulation resulting in the occurrence of both mouth-forms under standard laboratory conditions that allows manipulation of plasticity by genetic, molecular and chemical tools [16].

5. Genetics of nematode feeding plasticity

Pristionchus pacificus has been developed as a model system in evolutionary biology [20,21]. While only distantly related to *Caenorhabditis elegans*, it shares a number of features: self-fertilization, a short generation time of 4 days and monoxenic growth on *E. coli*. Adopting the functional toolkit of *C. elegans*, forward and reverse genetic tools are available in *P. pacificus*, including CRISPR-Cas9 genetic engineering and

genetic transformation [28,29]. In addition, the known beetle association allowed a vast collection of *P. pacificus* strains and genomes to be catalogued [30,31].

Given the stochastic mouth-form dimorphism of wild-type *P. pacificus* animals when grown on bacteria, mutagenesis screens for monomorphic mutants can be performed to isolate strains deficient in the formation of one particular mouth-form (figure 2b). The first such unbiased genetic screen resulted in a eurystomatous-form defective mutant, *eud-1*, which turned out to be dominant and represents a developmental switch gene (figure 2c) [32]. Mutant *eud-1* animals are all-St, resulting in the complete absence of Eu animals. In contrast, overexpression of *eud-1* in wild-type or *eud-1* mutant animals reverts this phenotype to all-Eu. These and other experiments showed that *eud-1* is haploinsufficient and dosage dependent. *eud-1* alleles are dominant, and their all-St phenotype results from reduction-of-function, but not gain-of-function mutations. Consistently, *eud-1* mutant alleles were rescued with a wild-type copy of *eud-1*, whereas overexpression of a mutant copy of the gene did not result in any phenotype, as would usually be the case for gain-of-function mutations (figure 2c) [32].

A suppressor screen for Eu animals in an all-St *eud-1* mutant background resulted in the identification of the nuclear hormone receptor *nhr-40* (figure 2c) [33]. Interestingly, *nhr-40* is also part of the developmental switch constituting similar

genetic features but with an opposite phenotype to *eud-1*: *nhr-40* mutants are all-Eu, while overexpression results in all-St lines. *nhr-40* mutants are again dominant as loss-of-function mutants and haplo-insufficient. Thus, two genes regulating mouth-form plasticity show a dominant null or reduction-of-function phenotype. This is in strong contrast to the overall pattern in nematodes. Screens for dominant mutations in *C. elegans* resulted in many gain-of-function alleles, whereas *unc-108* represents the only gene that when mutated results in a dominant null phenotype, indicating haplo-insufficient genes to be rare [34].

Together, the experiments summarized above allow four major conclusions. First, unbiased genetic analysis of *P. pacificus* feeding plasticity indicates that plasticity is indeed under genetic control. *eud-1* and *nhr-40* mutants are monomorphic, being either all-St or all-Eu. Thus, genes affect mouth-form plasticity without affecting the character state itself; in *eud-1* mutants the St mouth-form is properly formed, similar to the Eu form in *nhr-40* mutant animals. Second, both genes are part of a developmental switch with loss-of-function and overexpression, resulting in complete but opposite phenotypes. Developmental switches had long been predicted to play an important role in plasticity regulation [2], but due to the previous absence of genetic models of plasticity, little genetic evidence was obtained. Third, *eud-1* and *nhr-40* are both located on the X chromosome. *Pristionchus pacificus* has an XO karyotype in males, similar to *C. elegans* [35]. Interestingly, males have predominantly a St mouth-form [25] and *eud-1* and *nhr-40* mutant males are all-St and all-Eu, respectively. Thus, *eud-1* and *nhr-40* escape male dosage compensation, a process that is just beginning to be investigated in *P. pacificus* [36]. Finally, it is interesting to note that *eud-1* resulted from a recent duplication [32]. While *C. elegans* contains one *eud-1*/sulfatase copy located on an autosome, *P. pacificus* contains three copies, with the two recently evolved genes being located on the X chromosome. However, CRISPR/Cas9-induced mutations in the two other *eud-1*-like genes in *P. pacificus* suggest that there are no specific phenotypes associated with the knockout of both genes [37].

6. Epigenetic control of switch genes

Two common aspects of *eud-1* and *nhr-40* mutants resulting in monomorphic, plasticity-defective phenotypes are that they show no other obvious phenotypes. In contrast, an unbiased search for mouth-form defects in a collection of mutants previously isolated for their egg-laying- or vulva-defective phenotypes identified *mbd-2* and *lsy-12* mutants to resemble an all-St *eud-1*-like phenotype [38]. *mbd-2* is egg-laying-defective and encodes a member of the methyl-binding protein family that is strongly reduced in *C. elegans* but not in *P. pacificus* [39,40]. *lsy-12* encodes a conserved histone acetyltransferase, and *mbd-2* and *lsy-12* mutants were shown to result in massive histone modification defects involving multiple gene activation marks, such as H3K4me3, H3K9ac and H3K27ac [38]. Given that *mbd-2*, *lsy-12* and *eud-1* mutants have nearly identical mouth-form monomorphism, *eud-1* was itself a potential target for histone modification, and indeed *eud-1* expression is downregulated in *mbd-2* and *lsy-12* mutants. Interestingly, however, histone modification defects affect an antisense message at the *eud-1* locus, and overexpression experiments with this *as-eud-1* transcript suggest that

as-eud-1 positively regulates *eud-1* expression [38]. Together, these findings strongly suggest that the developmental switch is under epigenetic control. In principle, the epigenetic regulation of a switch mechanism is ideally suited to incorporate environmental information and environmental variation. However, information about associated mechanisms in *P. pacificus* awaits future studies, whereas several studies in insects recently already indicated the involvement of epigenetic mechanisms in gene-environmental interactions [41–43]. In conclusion, the use of forward genetic approaches in a laboratory model system provide strong evidence for the regulation of nematode feeding plasticity by developmental switch genes. Furthermore, epigenetic mechanisms including histone modifications and antisense RNA-mediated regulation might be crucial for gene–environment interactions.

7. Macro-evolutionary potentials

The genetic and epigenetic control of feeding plasticity in *P. pacificus* provides a basis to study how organisms sense and respond to the environment and to environmental variation. But is plasticity also important for evolution? Answering this question requires comparative studies that when performed in a phylogenetic context might provide insight into the significance of plasticity for evolutionary processes. Micro-evolutionary studies, by comparing many different wild isolates of *P. pacificus*, indicated strong differences in Eu:St ratios between isolates that correlated with *eud-1* expression [32]. Two recent studies have moved this analysis to the macro-evolutionary level, suggesting that phenotypic plasticity indeed facilitates rapid diversification. Susoy and co-workers studied the evolution of feeding structures in more than 90 nematode species using geometric morphometrics [44]. These species included dimorphic taxa, such as *P. pacificus*, but also monomorphic species that never evolved feeding plasticity, such as *C. elegans* (primary monomorphic), and those that had secondarily lost it (secondary monomorphic). This study found that feeding dimorphism was indeed associated with a strong increase in complexity of mouth-form structures [44]. At the same time, the subsequent assimilation of a single mouth-form phenotype (secondary monomorphism) coincided with a decrease in morphological complexity, but an increase in evolutionary rates. Thus, the gain and loss of feeding plasticity have led to increased diversity in these nematodes [8].

A second case of mouth-form plasticity increasing morphological diversification came from a striking example of fig-associated *Pristionchus* nematodes. Besides the worldwide branch of the genus that is associated with scarab beetles (currently more than 30 species), a recent study identified *Pristionchus* species, such as *P. borbonicus*, that live in association with fig wasps and figs [16]. These nematodes are extraordinarily diverse in their mouth morphology for two reasons. First, *P. borbonicus* and others form five distinct mouth-forms that occur in succession in developing fig syconia, thereby increasing the polyphenism from two to five distinct morphs. Second, the morphological diversity of these five morphs exceeds that of several higher taxa, although all five morphs are formed by the same species [16]. These findings strongly support the facilitator hypothesis, and they also indicate that ecological diversity can be maintained in the absence of genetic variation as all this diversity is seen within a single species and without associated speciation and radiation events [45].

8. Perspective

Phenotypic plasticity represents a striking phenomenon observed in organisms of all domains of life. It has been a contentious concept and was partially dismissed by mainstream evolutionary theory because many unrelated phenomena have been inappropriately mixed under the same heading. Following and extending previous attempts by Ghalambor *et al.* [15], we have tried to clarify terminology to provide necessary distinctions that will help study and evaluate plasticity, and establish its significance for evolution. Second, the use of a laboratory model system approach has provided strong evidence for the genetic control of feeding plasticity in *P. pacificus*. This genetic framework can serve as a paradigm to study in detail

how the same genotype interacts with the environment to control this plastic trait. Besides nematodes, insects and diverse plants are very important multicellular organisms for the study of phenotypic plasticity. In particular, work on butterfly wing patterns and the coloration of caterpillars, but also horn size in different beetles, provide powerful inroads in the proper evaluation of plasticity [46,47]. Together, these studies on plants, insects and nematodes will provide mechanistic insight into this fascinating biological principle and will help provide an extended framework for evolution.

Competing interests. We declare we have no competing interests.


Funding. The work described in this study was funded by the Max-Planck Society to R.J.S.

References

- Pigliucci M. 2001 *Phenotypic plasticity: beyond nature and nurture: syntheses in ecology and evolution*. Baltimore, MD: Johns Hopkins University Press.
- West-Eberhard MJ. 2003 *Developmental plasticity and evolution*. Oxford, UK: Oxford University Press.
- Schlichting CD, Pigliucci M. 1998 *Phenotypic evolution*. Sunderland, MA: Sinauer Associates.
- de Jong G. 2005 Evolution of phenotypic plasticity: patterns of plasticity and the emergence of ecotypes. *New Phytol.* **166**, 101–117. (doi:10.1111/j.1469-8137.2005.01322.x)
- Wund MA. 2012 Assessing the impacts of phenotypic plasticity on evolution. *Integr. Comp. Biol.* **52**, 5–15. (doi:10.1093/icb/ics050)
- Bradshaw AD. 1965 Evolutionary significance of phenotypic plasticity in plants. *Adv. Genet.* **13**, 115–155. (doi:10.1016/S0065-2660(08)60048-6)
- Nicoglou A. 2015 Phenotypic plasticity: from microevolution to macroevolution. In *Handbook of evolutionary thinking in the sciences* (eds T Heams, P Huneman, G Lecointre, M Silberstein), pp. 285–318. Heidelberg, Germany: Springer.
- Nijhout HF. 2015 To plasticity and back again. *Elife* **4**, e06995. (doi:10.7554/eLife.06995)
- Waddington CH. 1959 Canalisation of development and genetic assimilation of acquired characters. *Nature* **183**, 1654–1655. (doi:10.1038/1831654a0)
- Gibson G, Hogness DS. 1996 Effect of polymorphism in the *Drosophila* regulatory gene *Ultrabithorax* on homeotic stability. *Science* **271**, 200–203. (doi:10.1126/science.271.5246.200)
- Amundson R. 2005 *The changing role of the embryo in evolutionary thought*. Cambridge, UK: Cambridge University Press.
- Whitman DW, Ananthakrishnan TN. 2009 *Phenotypic plasticity in insects*. Plymouth, NH: Science Publishers.
- Nijhout HF. 1991 *The development and evolution of butterfly wing patterns*. Washington, DC: Smithsonian Institution Press.
- Laland K *et al.* 2014 Does evolutionary theory need a rethink? *Nature* **514**, 161–164. (doi:10.1038/514161a)
- Ghalambor CK, McKay JK, Carroll SP, Reznick DN. 2007 Adaptive versus non-adaptive phenotypic plasticity and the potential for contemporary adaptation in new environments. *Funct. Ecol.* **21**, 394–407. (doi:10.1111/j.1365-2435.2007.01283.x)
- Susoy V, Sommer RJ. 2016 Stochastic and conditional regulation of nematode mouth-form dimorphisms. *Front. Ecol. Evol.* **4**, 23. (doi:10.3389/fevo.2016.00023)
- Dubnau D, Losick R. 2006 Bistability in bacteria. *Mol. Microbiol.* **61**, 564–572. (doi:10.1111/j.1365-2958.2006.05249.x)
- de Jong IG, Haccou P, Kuipers OP. 2011 Bet hedging or not? A guide to proper classification of microbial survival strategies. *Bioessays* **33**, 215–223. (doi:10.1002/bies.201000127)
- Smits WK, Kuipers OP, Veening JW. 2006 Phenotypic variation in bacteria: the role of feedback regulation. *Nat. Rev. Microbiol.* **4**, 259–271. (doi:10.1038/nrmicro1381)
- Sommer RJ, McGaughan A. 2013 The nematode *Pristionchus pacificus* as a model system for integrative studies in evolutionary biology. *Mol. Ecol.* **22**, 2380–2393. (doi:10.1111/mec.12286)
- Sommer RJ. 2015 *Pristionchus pacificus: a nematode model for comparative and evolutionary biology*. Leiden, Netherlands: Brill.
- Kanzaki N, Giblin-Davis RM. 2015 Diplogastrid systematics and phylogeny. In *Pristionchus pacificus: a nematode model for comparative and evolutionary biology* (eds RJ Sommer), pp. 43–76. Leiden, Netherlands: Brill.
- Ragsdale EJ. 2015 Mouth dimorphism and the evolution of novelty and diversity. In *Pristionchus pacificus: a nematode model for comparative and evolutionary biology* (ed. RJ Sommer), pp. 301–329. Leiden, Netherlands: Brill.
- Meyer JM, Baskaran P, Quast C, Susoy V, Rödelsperger C, Glöckner FO, Sommer RJ. In press. Succession and dynamics of *Pristionchus* nematodes and their microbiome during decomposition of *Oryctes borbonicus* on La Réunion Island. *Environ. Microbiol.* (doi:10.1111/1462-2920.13697)
- Bento G, Ogawa A, Sommer RJ. 2010 Co-option of the hormone-signalling module dafachronic acid-DAF-12 in nematode evolution. *Nature* **466**, 494–497. (doi:10.1038/nature09164)
- Seroby V, Ragsdale EJ, Muller MR, Sommer RJ. 2013 Feeding plasticity in the nematode *Pristionchus pacificus* is influenced by sex and social context and is linked to developmental speed. *Evol. Dev.* **15**, 161–170. (doi:10.1111/ede.12030)
- Seroby V, Ragsdale EJ, Sommer RJ. 2014 Adaptive value of a predatory mouth-form in a dimorphic nematode. *Proc. R. Soc. B* **281**, 20141334. (doi:10.1098/rspb.2014.1334)
- Schlager B, Wang X, Braach G, Sommer RJ. 2009 Molecular cloning of a dominant roller mutant and establishment of DNA-mediated transformation in the nematode *Pristionchus pacificus*. *Genesis* **47**, 300–304. (doi:10.1002/dvg.20499)
- Witte H, Moreno E, Rödelsperger C, Kim J, Kim JS, Streit A, Sommer RJ. 2015 Gene inactivation using the CRISPR/Cas9 system in the nematode *Pristionchus pacificus*. *Dev. Genes Evol.* **225**, 55–62. (doi:10.1007/s00427-014-0486-8)
- Morgan K, McGaughan A, Villate L, Herrmann M, Witte H, Bartelmes G, Rochat J, Sommer RJ. 2012 Multi locus analysis of *Pristionchus pacificus* on La Reunion Island reveals an evolutionary history shaped by multiple introductions, constrained dispersal events and rare out-crossing. *Mol. Ecol.* **21**, 250–266. (doi:10.1111/j.1365-294X.2011.05382.x)
- Rödelsperger C, Neher RA, Weller AM, Eberhardt G, Witte H, Mayer WE, Dieterich C, Sommer RJ. 2014 Characterization of genetic diversity in the nematode *Pristionchus pacificus* from population-scale resequencing data. *Genetics* **196**, 1153–1165. (doi:10.1534/genetics.113.159855)
- Ragsdale EJ, Muller MR, Rödelsperger C, Sommer RJ. 2013 A developmental switch coupled to the evolution of plasticity acts through a sulfatase. *Cell* **155**, 922–933. (doi:10.1016/j.cell.2013.09.054)

33. Kieninger MR, Ivers NA, Rodelsperger C, Markov GV, Sommer RJ, Ragsdale EJ. 2016 The nuclear hormone receptor NHR-40 acts downstream of the sulfatase EUD-1 as part of a developmental plasticity switch in *Pristionchus*. *Curr. Biol.* **26**, 2174–2179. (doi:10.1016/j.cub.2016.06.018)
34. Park EC, Horvitz HR. 1986 Mutations with dominant effects on the behavior and morphology of the nematode *Caenorhabditis elegans*. *Genetics* **113**, 821–852.
35. Pires-daSilva A, Sommer RJ. 2004 Conservation of the global sex determination gene *tra-1* in distantly related nematodes. *Genes Dev.* **18**, 1198–1208. (doi:10.1101/gad.293504)
36. Lo TW, Pickle CS, Lin S, Ralston EJ, Gurling M, Scharfner CM, Bian Q, Doudna JA, Meyer BJ. 2013 Precise and heritable genome editing in evolutionarily diverse nematodes using TALENs and CRISPR/Cas9 to engineer insertions and deletions. *Genetics* **195**, 331–348. (doi:10.1534/genetics.113.155382)
37. Ragsdale EJ, Ivers NA. 2016 Specialization of a polyphenism switch gene following serial duplications in *Pristionchus* nematodes. *Evolution* **70**, 2155–2166. (doi:10.1111/evo.13011)
38. Serobyán V, Xiao H, Namdeo S, Rodelsperger C, Sieriebriennikov B, Witte H, Roseler W, Sommer RJ. 2016 Chromatin remodelling and antisense-mediated up-regulation of the developmental switch gene *eud-1* control predatory feeding plasticity. *Nat. Commun.* **7**, 12337. (doi:10.1038/ncomms12337)
39. Gutierrez A, Sommer RJ. 2004 Evolution of *dnmt-2* and *mbd-2*-like genes in the free-living nematodes *Pristionchus pacificus*, *Caenorhabditis elegans* and *Caenorhabditis briggsae*. *Nucleic Acids Res.* **32**, 6388–6396. (doi:10.1093/nar/gkh982)
40. Gutierrez A, Sommer RJ. 2007 Functional diversification of the nematode *mbd2/3* gene between *Pristionchus pacificus* and *Caenorhabditis elegans*. *BMC Genet.* **8**, 57. (doi:10.1186/1471-2156-8-57)
41. Simola DF *et al.* 2016 Epigenetic re(programming) of caste-specific behavior in the ant *Camponotus floridanus*. *Science* **351**, 37–39. (doi:10.1126/science.aac6633)
42. Gibert JM, Mouchel-Vielh E, De Castro S, Peronnet F. 2016 Phenotypic plasticity through transcriptional regulation of the evolutionary hotspot gene *tan* in *Drosophila melanogaster*. *PLoS Genet.* **12**, e1006218. (doi:10.1371/journal.pgen.1006218)
43. Kucharski R, Maleszka J, Foret S, Maleszka R. 2008 Nutritional control of reproductive status in honeybees via DNA methylation. *Science* **319**, 1827–1830. (doi:10.1126/science.1153069)
44. Susoy V, Ragsdale EJ, Kanzaki N, Sommer RJ. 2015 Rapid diversification associated with a macroevolutionary pulse of developmental plasticity. *Elife* **4**, e05463. (doi:10.7554/eLife.05463)
45. Phillips PC. 2016 Evolution: five heads are better than one. *Curr. Biol.* **26**, R283–R285. (doi:10.1016/j.cub.2016.02.048)
46. Emlen DJ, Hunt J, Simmons LW. 2005 Evolution of sexual dimorphism and male dimorphism in the expression of beetle horns: phylogenetic evidence for modularity, evolutionary lability, and constraint. *Am. Nat.* **166**(Suppl. 4), S42–S68. (doi:10.1086/444599)
47. Moczek AP, Sultan S, Foster S, Ledon-Rettig C, Dworkin I, Nijhout HF, Abouheif E, Pfennig DW. 2011 The role of developmental plasticity in evolutionary innovation. *Proc. R. Soc. B* **278**, 2705–2713. (doi:10.1098/rspb.2011.0971)

SCIENTIFIC REPORTS



OPEN

Environmental influence on *Pristionchus pacificus* mouth form through different culture methods

Michael S. Werner, Bogdan Sieriebriennikov, Tobias Loschko, Suryesh Namdeo, Masa Lenuzzi, Mohannad Dardiry, Tess Renahan, Devansh Raj Sharma & Ralf J. Sommer

Environmental cues can impact development to elicit distinct phenotypes in the adult. The consequences of phenotypic plasticity can have profound effects on morphology, life cycle, and behavior to increase the fitness of the organism. The molecular mechanisms governing these interactions are beginning to be elucidated in a few cases, such as social insects. Nevertheless, there is a paucity of systems that are amenable to rigorous experimentation, preventing both detailed mechanistic insight and the establishment of a generalizable conceptual framework. The mouth dimorphism of the model nematode *Pristionchus pacificus* offers the rare opportunity to examine the genetics, genomics, and epigenetics of environmental influence on developmental plasticity. Yet there are currently no easily tunable environmental factors that affect mouth-form ratios and are scalable to large cultures required for molecular biology. Here we present a suite of culture conditions to toggle the mouth-form phenotype of *P. pacificus*. The effects are reversible, do not require the costly or labor-intensive synthesis of chemicals, and proceed through the same pathways previously examined from forward genetic screens. Different species of *Pristionchus* exhibit different responses to culture conditions, demonstrating unique gene-environment interactions, and providing an opportunity to study environmental influence on a macroevolutionary scale.

Phenotypes can be dramatically influenced by environmental conditions experienced during development, a phenomenon referred to as developmental plasticity^{1–3}. Examples of plastic phenotypes have been studied for nearly a century, including differences in morphology⁴, sex and caste determination^{5–7}, and innate immunity⁸. However, despite long-held interest in the field, and decade's worth of progress linking genotype to phenotype, relatively little is known about the mechanisms connecting environment to phenotype. To study the mechanisms of environmental influence on phenotype, easily tunable methods to induce phenotypic changes and model organisms amenable to molecular biology techniques are required. For example, temperature and diet have been utilized to explore plasticity in insects and nematodes^{9–14}, some of which have revealed fundamental principles of dynamic gene regulation. In particular, investigating life cycle plasticity in *C. elegans* contributed to our understanding of nutrition and endocrine signaling^{15–18}, and the discovery of regulatory RNAs¹⁹. However, the number of case studies remains small, and heuristic insight of ecologically relevant phenotypes within an evolutionary framework is still lacking.

The model organism *P. pacificus* exhibits an environmentally sensitive developmental switch of its feeding structures²⁰. In the wild *P. pacificus* exists in a dormant state (dauer) on beetles. When beetles die *Pristionchus* exits the dauer state to feed on decomposition bacteria, and proceeds to reproductive maturity^{21,22} (Fig. 1A). While developing under crowded conditions a “wide-mouthed” eurystomatous (Eu) morph with two teeth is built, which allows adults to prey on other nematodes (Fig. 1B). Alternatively, a “narrow-mouthed” stenostomatous (St) morph with one tooth relegates diet exclusively to microorganisms (Fig. 1C). While Eu animals can exploit additional food sources²³ and attack and kill competitors²⁴, St animals mature slightly faster²⁵, creating a tradeoff of strategies depending on the environment perceived during development. Under monoxenic growth conditions in the laboratory using *Escherichia coli* OP50 bacteria as a food source on NGM-agar plates, 70–90% of the reference *P. pacificus* strain PS312 develop the Eu morph. Metabolic studies have elucidated compounds that affect this mouth-form decision. For example, the steroid hormone dafachronic acid shifts mouth-form frequencies to St²⁰. Conversely, the pheromone dasc#1 shifts the frequency to Eu²⁶. Recent mutant screens

Department of Evolutionary Biology, Max Planck Institute for Developmental Biology, 72076, Tübingen, Germany. Correspondence and requests for materials should be addressed to R.J.S. (email: ralf.sommer@tuebingen.mpg.de)

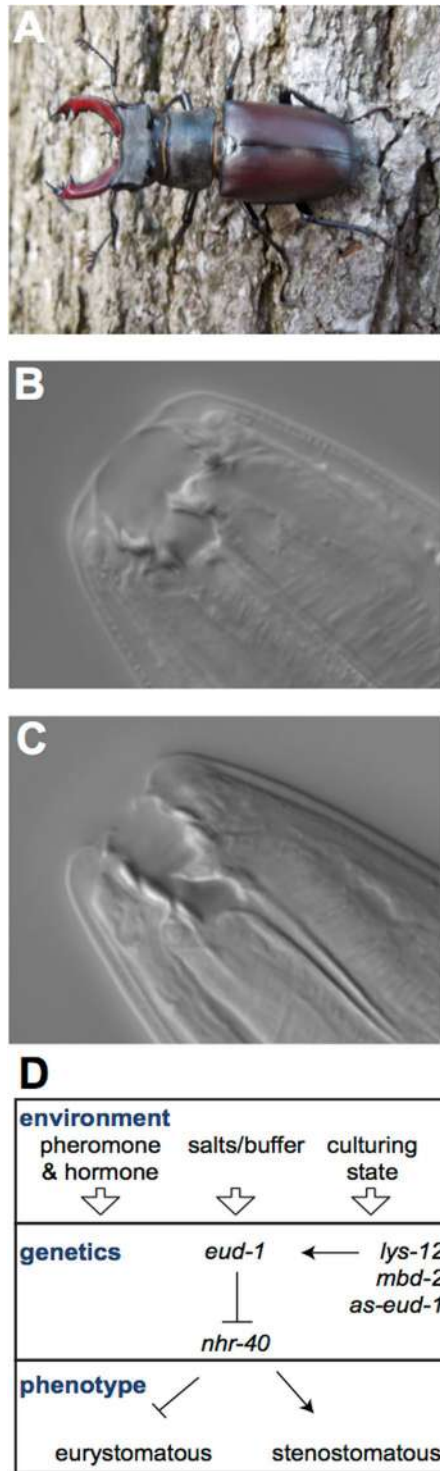


Figure 1. Life cycle and phenotypic plasticity of *Pristionchus pacificus*. (A) *P. pacificus* exist in a necromenic relationship with host beetles (i.e. shown here *Lucanus cervus*), and upon decomposition of the beetles the worms exit the dormant (dauer) state. Photo taken by M Herrmann and R Sommer. Depending on environmental conditions experienced during this period, adults develop either (B) a wide-mouth “eurystomatous” (Eu) morph with an additional tooth allowing them to prey on other nematodes, or (C) a microbivorous narrow mouth “stenostomatous” (St) morph. (D) Diagram integrating the environment into known gene-phenotype interactions of the *P. pacificus* mouth-form pathway.

have established several genes in the mouth-form regulatory pathway^{27–29}. The sulfatase *eud-1* (eurystomatous defective) is a dosage-dependent “switch” gene³⁰. *eud-1* mutants are 100% St, while overexpression of a *eud-1*

transgene confers 100% Eu²⁷. The nuclear-hormone-receptor *Ppa-nhr-40* was identified as a suppressor of *eud-1*, and regulates downstream genes²⁸. *C. elegans* homologs of the epigenetic enzymes acetyltransferase *lsy-12* and methyl-binding protein *mbd-2* have also been identified to control mouth-form plasticity, and are attractive factors for channeling environmental cues to changes in gene regulation. Both mutants led to global losses of activating-histone modifications, and decreased expression of *eud-1*²⁹.

Identification of these switch genes affords the opportunity to track regulatory mechanisms that respond to environmental cues^{31,32}. Unfortunately, the application of small molecules to affect mouth-form ratios in large enough quantities for biochemical fractionation or epigenetic profiling (e.g. ChIP) is impractical given the labor and expense of chemical synthesis or purification. Moreover, it is difficult to obtain consistent mouth-form ratios with pharmacological compounds as they are in constant competition with endogenous hormones and pheromones²⁰. Finally, while crowding/starvation can also induce the Eu morph, it is technically challenging to compare different population densities, or to synchronize starved vs. un-starved larvae. To adequately study environmental effects on phenotypic plasticity, cheap, consistent, and simple methods are needed that can tune mouth-form ratios in synchronized populations. Here, we establish a set of culture conditions to affect environmental influence on mouth form. These methods are fast, reproducible, and only require the differential application of buffer, and culturing state (solid vs. liquid). Intriguingly, different species of *Pristionchus* exhibit different response regimes, suggesting evolutionary divergence of gene-environment interactions.

Results

Liquid culture affects *Pristionchus pacificus* mouth-form. In order to accumulate large amounts of biological material for molecular and biochemical experiments we grew the laboratory California strain (PS312) of *P. pacificus* in liquid culture. To our surprise, this culture condition reversed the mouth-form phenotype from preferentially Eu to preferentially St. To better examine this observation we screened mouth-forms of adults representing a parental generation (P), and obtained³³ and split eggs evenly to either agar plates or liquid culture, and screened adults of the next generation (G1) (Fig. 2A). Reproducibly, this simple difference in culturing method led to a dramatic shift in mouth-form ratio (> 95% Eu on agar compared to ~10% Eu in liquid culture, $p < 0.001$, paired *t*-test) (Fig. 2B). Importantly, *P. pacificus* developed at similar rates in agar and liquid culture, allowing facile comparisons between conditions (Fig. 2C), and arguing against nutritional deprivation inducing the mouth-form shift. St animals have a slightly faster development than Eu animals when grown on agar²⁵, however we found developmental speed to be indistinguishable between morphs in liquid culture (Supplementary Fig. 1). The different environmental conditions present distinct energy requirements (e.g. swimming and feeding on motile bacteria in 3-dimensional liquid culture) that might offset potential tradeoffs in resource allocation.

Next, we investigated whether the change in mouth-form ratio induced by liquid culture was capable of being inherited. The mouth-form ratio of adults was consistent with the culture method they developed in regardless of the culture method of the parental generation, suggesting the effect is not transgenerational (Fig. 2D). These results also demonstrate the immediate and robust nature of this plasticity, and similar experiments coupled to mutagenesis may be useful for identifying genes involved in the ability to sense and respond to changing environments.

Buffer components and culture state affect mouth form. To investigate the potential influence of culture conditions on mouth form we examined differences in buffer composition, and solid vs. liquid culturing state. In our previous experiments we had used standard liquid culture protocols for *C. elegans*³³, which utilize S media (S), whereas we normally grow *P. pacificus* on Nematode Growth Media (NGM) agar plates³³. To assess the contribution of the chemical composition of the medium, as opposed to solid vs. liquid environments (hereafter referred to as ‘culture state’), we performed reciprocal culture experiments. Nematodes that were grown on either S-agar or NGM-liquid exhibited intermediate mouth-form ratios ($51 \pm 5\%$ Eu and $38 \pm 13\%$ Eu, respectively, $p < 0.001$ relative to solid or liquid states of the same medium, paired *t*-test) (Table 1d,h,i,p), revealing a growth-medium composition effect. However, as these mouth-form ratios were in-between the extremes of NGM-agar and S-liquid, it also suggests other environmental factors are operating.

S medium contains phosphate (50 mM) and sulfate (14 mM) - both of which have previously been shown to affect mouth-form ratios at 120 mM²⁷. To test whether this concentration of phosphate was causing the S-medium effect we made alternative formulations by replacing phosphate with 50 mM Tris (“T-Medium”) or Hepes (“H-Medium”), pH 7.5. Liquid culture in T- and H-medium yielded reproducibly higher Eu ratios ($35 \pm 8\%$ and $28 \pm 10\%$, respectively, $p < 0.05$, paired *t*-test) (Table 1d-f), demonstrating a specific, albeit subtle contribution from phosphate. Furthermore, *P. pacificus* grown in axenic (without bacteria)³⁴, M9³³, or PBS (which does not contain sulfate) -based liquid cultures were all highly St (Table 1a-c). Although nematode survival rate was poor in PBS, and development was slowed in axenic culture (9–10 days for sexual maturation, rather than 3–4).

Rotation speed of liquid culture affects mouth form. Further exploration of liquid culture methodology revealed that decreasing the rotation per minute (rpm) also affected mouth-form ratios. Previous experiments that led to high St ratios had been performed at 180 rpm, but when shifted to “slow” speeds of 70 or 50 rpm, the mouth-form ratio shifted to an intermediate Eu bias ($55 \pm 11\%$ and $66 \pm 9\%$, respectively, $p < 0.05$, *t*-test) (Table 1j,l). The simplicity of changing rpm shaking-speed to affect mouth-form ratios is an intriguing environmental perturbation as other factors like food source, buffer, and culturing state are identical. When examined without bacteria, it became evident that at slow speeds (<90 rpm) nematodes aggregated in the center of the liquid column, whereas at higher speeds they were dispersed. When combined with conditions that exhibited intermediate St ratios the effects were additive, yielding up to $87 \pm 3\%$ Eu with NGM-liquid culture (Table 1k,m,n). The higher density of nematodes at slow speeds suggests that pheromones may be responsible. Consistent with this hypothesis, we passed multiple *P. pacificus* generations from one liquid culture to another,

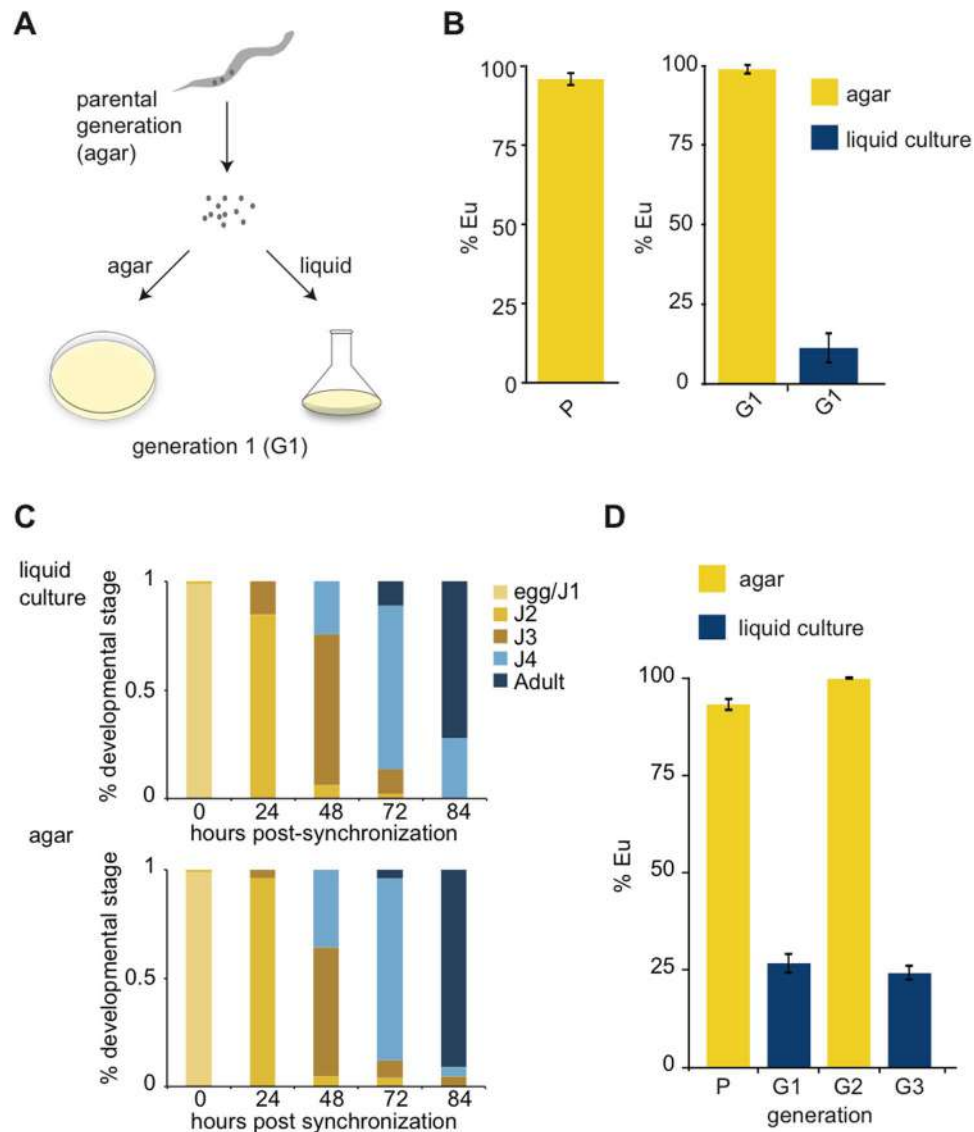


Figure 2. Different culture methods affect mouth-form phenotypic plasticity. (A) Diagram of experimental design to compare culture conditions from the same population after bleach synchronization. (B) Mouth-form ratios presented as percent eurystomatous (% Eu) from the parental generation (P) and the next generation (G1) grown in either liquid culture or agar plates, $n = 18$ biological replicates, $p < 0.05$, *students two-tailed t-test*, error bars represent SEM. (C) Developmental stages of bleach-synchronized *P. pacificus* in either agar plates or liquid culture. Bar graphs represent a typical experiment measuring >30 animals at the indicated time-points. (D) Mouth-form ratios of switching experiments between agar and liquid cultures. Nematodes were bleached between generations (P, G1, G2), and eggs-J1 larvae were passed to the next condition, $n = 3$, error bars represent SEM.

either by a 1:10 dilution, or by bleaching and washing. When passed by bleaching the next generation remained highly St ($8 \pm 4\%$). However when passed by dilution the next generation of worms exhibited intermediate Eu ratios ($51 \pm 16\%$, $p < 0.05$, *unpaired t-test*), perhaps because pheromones from the first generation were passed on to the second.

Liquid culture affects body morphology. We also observed morphological differences of body length and width between agar and liquid culture, demonstrating an additional plastic response (Supplementary Figure 2). Worms that develop in liquid culture exhibit longer, narrower bodies compared to worms that develop in agar, a phenomenon that has also been observed in *C. elegans*³³. To disentangle whether the effect on mouth form is discrete or connected to the change in body shape we grew worms in NGG culture, which is intermediate between liquid and solid states³⁵. Similar to liquid culture, adult worms grown in NGG exhibited a more slender body morphology than on agar plates ($p < 0.05$, Mann-Whitney), but they exhibited the highly Eu mouth-form ratio of worms grown in agar culture (Supplementary Fig. 2, Table 1d,o,p). While it is difficult to completely exclude the possibility that they are connected, there is no obvious correlation between the St mouth form and

	Condition	% Eu	S.E.M.
A	LC PBS, 180 rpm	7	3.2
B	LC Axenic Culture, 180 rpm	8.8	8.8
C	LC M9, 180 rpm	11.5	6.2
D	LC S-medium, 180 rpm	12.8	3.2
E	LC H-medium, 180 rpm	28	10.1
F	LC T-medium, 180 rpm	35	7.6
G	LC S-medium, 100 rpm	35.2	3
H	LC NGM, 180 rpm	37.8	12.9
I	AG S-medium	51.4	5.4
J	LC S-medium, 70 rpm	55.1	10.9
K	LC T-medium, 50 rpm	61.5	16.9
L	LC S-medium, 50 rpm	65.9	9
M	LC H-medium, 50 rpm	70.6	15
N	LC NGM, 50 rpm	87.3	3.3
O	NGG	97.1	2.5
P	AG NGM	98.7	0.7

Table 1. Buffer/ions and physical culture state affect mouth-form phenotype. A panel of culturing methods covers phenotypic ratios from ~10–99% Eu. LC = liquid culture, AG = agar, T and H medium = S-medium with phosphate replaced with 50 mM Tris or HEPES, pH 7.5, respectively, NGG = NGM with agar replaced with Gelrite/Gelzan CM (Sigma)³⁵. $N \geq 3$ biological replicates per condition, and standard error mean (SEM) is presented in the last column. Mouth-form phenotypes were assessed 4–5 days after bleach-synchronization (see Methods).

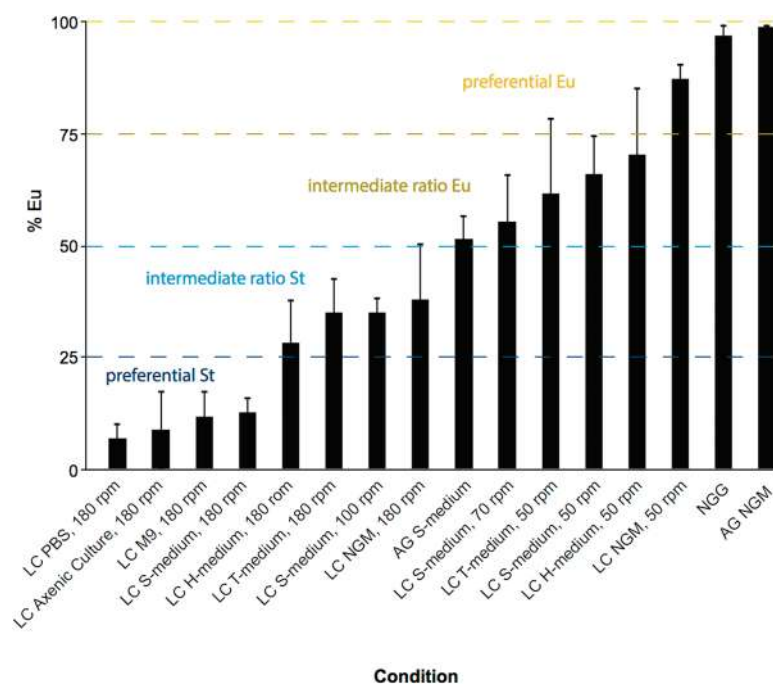


Figure 3. Comprehensive evaluation of culture method on mouth-form ratio in *P. pacificus*. Same data as in Table 1, but presented according to gradation of effect on mouth-form phenotype, from low to high % eurytomatous. LC = liquid culture, AG = agar, T and H medium = S-medium with phosphate replaced with 50 mM Tris or HEPES, pH 7.5, respectively, NGG = NGM with agar replaced with Gelrite/Gelzan CM (Sigma)³⁵. Error bars represent standard error mean (SEM) for different biological replicates ($n \geq 3$, Methods).

slender morphology observed in liquid culture. Therefore, it seems these two instances of phenotypic plasticity are under distinct regulation.

Collectively, we have established a broad range of culturing methods that allow the acquisition of almost any mouth-form ratio from an isogenic strain (Fig. 3). A variety of liquid culture conditions, including buffers without phosphates or sulfates, exhibited an effect on mouth form, suggesting an unknown environmental effect that is perhaps specific to solid or liquid states.

Liquid culture acts upstream of known switch genes. Next, we sought to place the environmental effects of liquid culture relative to known genetic and environmental factors. First, we examined whether liquid culture had an effect on mutants that are 100% Eu on agar plates^{27,28}. Animals from a *eud-1* overexpression line and *Ppa-nhr-40* mutant line remained 100% Eu in liquid culture, arguing that these genes act downstream of the environmental effect of liquid culture (Fig. 4A). Next, we assessed whether the *dasc#1* pheromone was capable of inducing the Eu mouth-form in liquid culture, as it does on agar. *dasc#1* experiments demonstrate a large variability in phenotypic ratio (Fig. 4B), however they typically exhibited a higher Eu proportion than control worms without *dasc#1* treatment ($p=0.068$, paired *t*-test). This intermediate and variable effect suggests that liquid culture and the *dasc#1* pheromone act in parallel and antagonistically to each other. Finally, we also compared the expression of four genes in different culturing conditions that are up- or down-regulated in *eud-1* mutants (100% St) vs. wild-type (70–100% Eu)²⁷. There was a strong correspondence between *eud-1* vs. wild-type RNA-seq data, and liquid vs. agar culture RT-qPCR (Fig. 4C,D). These results provide further evidence that the environmental effect of liquid culture is upstream of *eud-1*, and that this method is suitable for studying genetic pathways that have been determined through mutational experiments^{27–29}.

Liquid culture effect is dependent on genetic background. Finally, we explored whether there was a macro-evolutionary difference in responses to culture conditions. We chose four *Pristionchus* species that flank *P. pacificus* phylogenetically; three are highly Eu on agar (>95%), and one is highly St (>95%) (Fig. 5A,B). Remarkably, each species exhibited distinct phenotypic responses to liquid culture. For example, *P. maupasi* was highly Eu in both conditions, while *P. entomophagus* shifted to almost 100% St (Fig. 5C) in liquid culture. Meanwhile *P. mayeri* was St in both culture conditions. Taken together, these data show a genetic basis to environmental effects on phenotypic plasticity, which can be exploited for evolutionary, genetic, and molecular exploration of plasticity mechanisms. Whether these differences in response reflect adaptive changes to different environments, or are a result of drift remains to be seen in future investigations.

Discussion

We describe multiple methods for the culture of preferentially St (<25% Eu), intermediate St (25–50% Eu), intermediate Eu (50–75% Eu), and preferentially Eu (>75% Eu) *P. pacificus* (Fig. 3, Methods). Growth rates are similar between conditions, allowing the generation of developmentally synchronized populations. The effects are immediate, and immediately reversible when switching between liquid and agar, suggesting they are not transgenerational. Importantly, the genetic pathways towards building each respective mouth form are consistent with pathways established from prior forward genetics^{27,28}. Finally, the environmental response is unique in four species of *Pristionchus* tested, arguing that evolution has acted, passively or actively, on gene-environment interactions. The ability to toggle between mouth forms with simple culturing conditions provides powerful new tools to study the genetic and molecular mechanisms of phenotypic plasticity.

Perturbation of environmental factors such as salt concentration^{15,36–38}, pathogen^{8,39–42}, temperature^{7,10,13,43–45}, and diet^{46,47} have been exploited for decades to study adaptive responses. More recent genome-wide profiling of epigenetic information carriers has revealed potential mechanisms for communicating stimuli to changes in gene expression. So called ‘poised’ or ‘permissive’ chromatin states can respond to external signals, leading to changes in transcription that ultimately affect tissue differentiation^{48–55}. The time is now ripe to test whether similar processes affect phenotypic plasticity, a critical link between ecology and molecular mechanism that has just begun to be explored^{56–60}.

Our panel of *P. pacificus* culture conditions saturates the mouth-form frequency space (Fig. 3). The ability to shift ratios by rpm shaking-speed provides perhaps the cleanest method because of its simplicity. In shaking speeds greater than 90 rpm nematodes are dispersed, while below 90 rpm they are concentrated in the center of the liquid vortex. Since different buffer formulations also affected mouth-form ratios, and the combination with slow rpm yielded an additive effect, it seems that alterations in the abundance, diffusion, and local concentration of pheromones and ions (i.e. phosphate and sulfate) contribute to the observed differences between liquid and agar culture conditions. However, we note that densely packed nematodes at slow rpm (much denser than on a plate) in NGM-liquid media are still insufficient to recapitulate the >95% Eu phenotype seen on NGM-agar plates. While it remains possible that these are the only contributing factors, we speculate an additional unknown factor is extant related to bacterial density, metabolism, or the liquid environment itself.

Whether liquid culture is a direct stimulator of the St mouth form is currently unknown. Field observations and competition experiments are required to (1) assess if *Pristionchus* experiences wet-enough conditions in the wild to mimic liquid culture conditions as with other lotic, lentic or marine nematodes^{61–63}, and (2) determine whether the St mouth form provides an advantage in this environment. Both *C. elegans* and *P. pacificus* exhibit a slender morphology in liquid culture, suggesting a conserved plastic response to this environment. It is conceivable that a liquid culture-dependent signaling pathway related to mouth form also exists, although it could be mediated indirectly through other factors. Seemingly unrelated stimuli are capable of inducing the same developmental pathway by eventually descending on a downstream switch or ‘evocator’^{64–66}. Regardless of the ultimate environmental factor, our analysis of gene expression in liquid culture reflects patterns observed in constitutive St mutants, suggesting that similar downstream pathways are utilized (Fig. 1D). Importantly however, we did not observe faster St development in liquid culture as has been observed on agar, and which is predicted to be the tradeoff advantage of the St morph²⁵. It is formally possible that we did not have enough temporal resolution to identify the small but significant differences previously observed (55 hours for St and 61 hours for Eu). It is also worth noting that laboratory culture conditions are highly artificial, and it is perhaps not surprising that they could affect ecological strategies. Nevertheless, our results suggest that caution should be taken when studying *P. pacificus* ecology across different environments, as it may be context dependent. Going forward, it will be

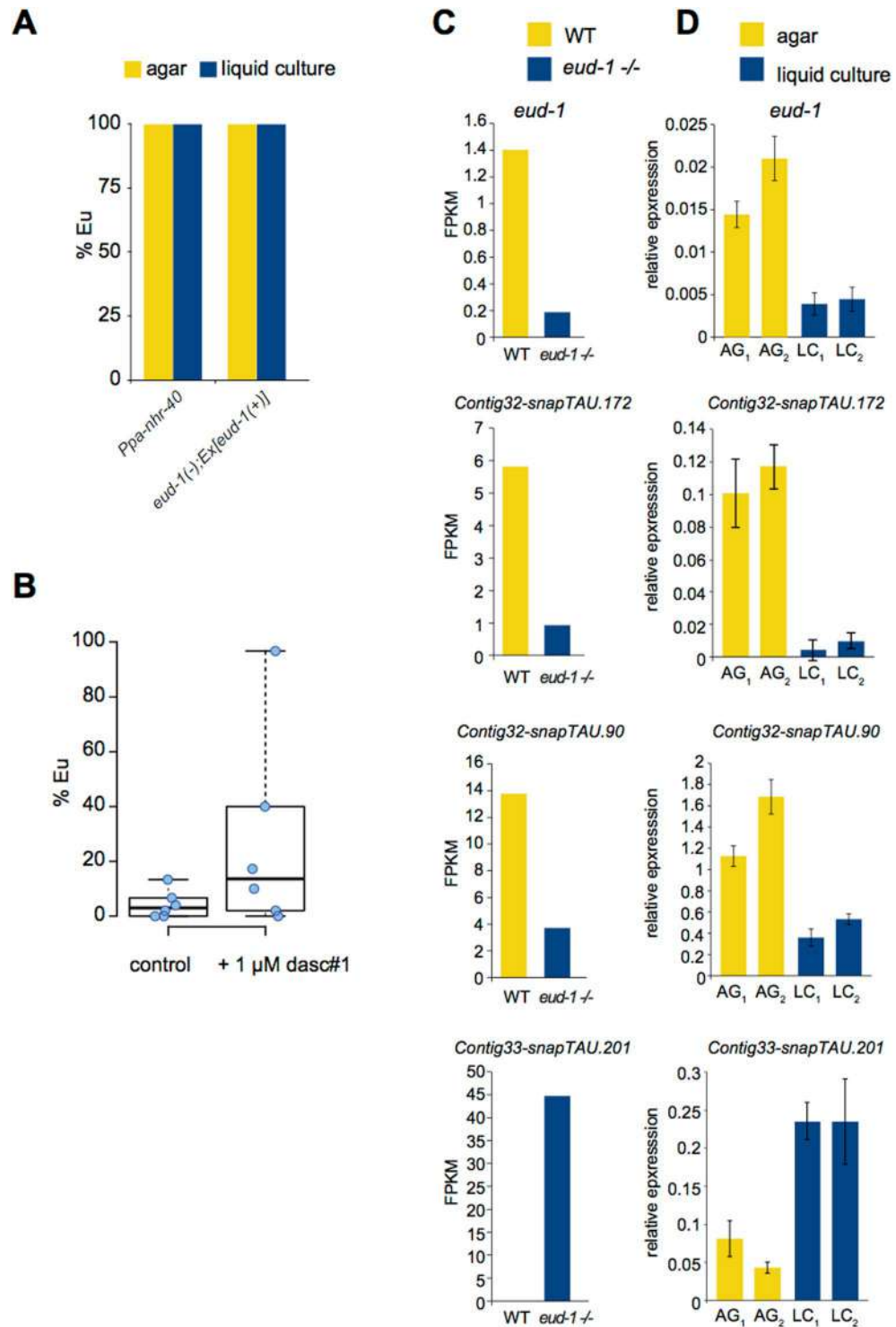


Figure 4. The environmental effect of liquid culture is upstream of known genetic components and induces similar pathways. **(A)** Mouth-form ratios of *eud-1* overexpression²⁷ and a *Ppa-nhr-40*²⁸ mutant in liquid culture reveals no effects, suggesting these genes are downstream, $n = 3$ biological replicates. **(B)** Addition of 1 μ M dasc#1 exhibits a variable response that appears to induce Eu, although it is not statistically significant ($p = 0.068$). **(C)** Expression analysis of four genes by RNA-seq from *eud-1* mutants (the average of 4 homozygous mutant alleles is represented)²⁷ (100% St) compared to the RS2333 California strain (70–100% Eu), y-axis = fpkm (relative expression). **(D)** Reverse transcription-quantitative PCR (RT-qPCR) of *P. pacificus* PS312 grown in liquid culture/S-medium (LC) vs. NGM-agar plates (AG) for the two biological replicates displayed, with four technical replicates each. The y-axis represents $2^{\Delta Ct}$ (relative expression) compared to the housekeeping gene *Ppa-Y45F10D.4* (iron binding protein)⁶⁹, error bars represent standard deviation of $n = 4$ technical replicates.

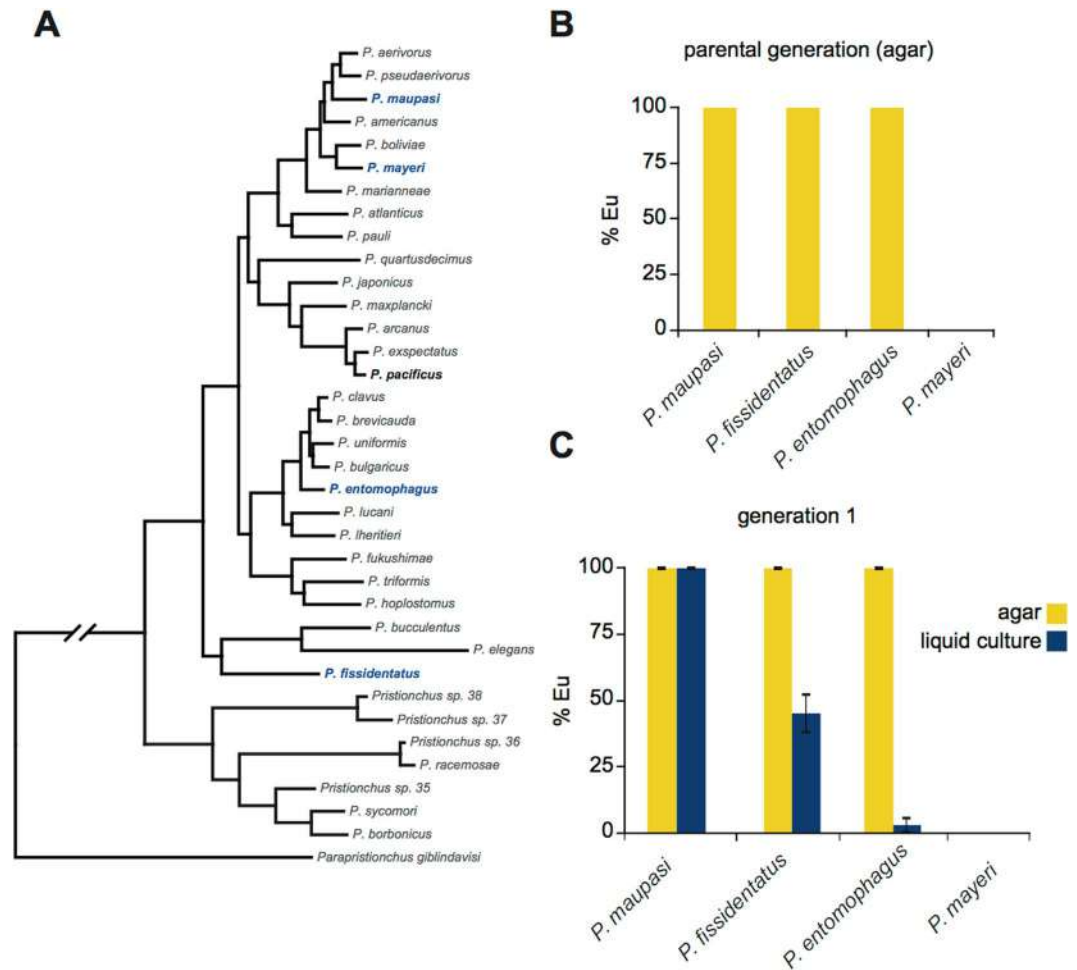


Figure 5. Macro-evolutionary view of liquid culture environmental influence. **(A)** Phylogeny of *Pristionchus* species⁷⁰ highlighting *P. pacificus* (bold), *P. fissidentatus*, *P. mayeri*, and *P. entomophagus* (blue). **(B)** Mouth-form ratio of parental generations ($n = 3$) of indicated species on NGM-agar after three consecutive healthy generations on OP50. **(C)** Mouth-form ratios of indicated species in either NGM-agar or liquid culture/S-medium ($n = 3$), error bars represent SEM.

informative to assess if the developmental speed of different species correlates with their response to liquid culture, and the aqueous content in which they are found in nature.

Which culture method is utilized will depend on the purpose of the experiment. Exploiting intermediate ratio conditions may be useful to study genes or other environmental factors predicated to effect mouth form but in an unknown direction (Eu or St). For experiments that require the greatest separation in mouth-form frequencies we recommend S-medium at 180 rpm (St) vs. NGM agar plates (Eu). We also frequently observed a modest degree of variation, which is expected for a stochastic phenotypic trait⁶⁷. As such, every measurement utilizing these culturing methods should be performed side-by-side with control samples. It is our hope that these methods will be a contribution to the study of environmental effects on *P. pacificus* mouth form, and phenotypic plasticity in general.

Methods

Strains and species. For all *P. pacificus* experiments the California strain PS312 was used, except comparisons to RNA-seq data, which used a more grown-out version of the same strain (RS2333). For experiments with different species (Fig. 5) *P. maupasi*, *P. fissidentatus*, and *P. mayeri* were compared to *P. pacificus*. Epistasis experiments (Fig. 4A) were performed with *Ppa-nhr-40(tu505)* and *eud-1(tu445);tuEx[eud-1(+)]*.

Culture methods. Five young adult *Pristionchus* nematodes were passed every 4–6 days on 10 ml NGM-agar, 60 mm plates at 20 °C seeded with 300 μ l of overnight cultures of *Escherichia coli* OP50 (grown in LB at 37 °C) and covered with parafilm to avoid experiencing starvation for three consecutive generations³³. The mouth-form phenotype of 4th generation adults represents the parental (P) generation (Fig. 2A,C, and D). Prior to all subsequent phenotyping experiments adults were synchronized by washing off of plates with M9 using plastic Pasteur pipettes into 15 ml conical tubes, and adding 30% final volume NaOH/bleach (0.5 ml NaOH, 1 ml bleach/3.5 ml washed worms) for 9 minutes with gentle agitation every few minutes. Carcasses were filtered through a 120 μ m

nylon net (Millipore) fixed between two rubber gaskets in a plastic funnel, washed by applying 3 ml M9 drop-wise on the filter, then pelleted $500 \times g$, 1 minute, room temperature. Eggs-J1 were washed by gentle re-suspension in 3 ml M9, and re-centrifuged $500 \times g$, 1 minute, room temperature. It is important not to wash worms with S-medium before or directly after bleach because it will start to precipitate. M9 wash was removed by pipette, and then eggs-J1s were ready for re-suspension in the appropriate buffer depending on the experiment.

For the majority of experiments, eggs-J1 larvae were re-suspended in $100 \mu\text{l}$ M9 \times the number of test conditions (i.e. $200 \mu\text{l}$ for comparing one agar vs. one liquid culture condition). For re-culturing on agar, eggs-J1 were pipetted in the center of the OP50 lawn on 60 mm agar plates (NGM or S-medium), then the plate was tilted in 360° to spread and dry the eggs. Afterwards the plates were stored at 20° and adults were phenotyped 4–5 days later (see below for details of phenotyping). For culturing in liquid formats, $100 \mu\text{l}$ of eggs-J1 were pipetted into 10 ml of medium in 50 ml-volume autoclaved Erlenmeyer flasks. To prepare monoxenic liquid cultures the amount of OP50 *E. coli* was empirically determined. For all liquid cultures described (except axenic culture) 100 ml of overnight OP50 *E. coli* (grown in LB) to an optical density (OD_{600}) of 0.5, was pelleted 30 minutes, 4°C at $3,000 \times g$ in an SLA-3000 rotor and re-suspended in 10 ml filter-sterilized ($0.22 \mu\text{m}$, Millipore) S-medium³³ unless otherwise noted (e.g. M9 or PBS, Fig. 2). The concentration of bacteria is a critical parameter. The procedure described above led to healthy cultures of *P. pacificus* at the normal developmental rate observed on agar plates (3–4 days²¹), while adding less (50 ml or 10 ml) OP50 led to slower rates, or even the inability to develop beyond the J2 larval stage when significantly less was added. Liquid cultures were incubated 180 rpm, $20\text{--}22^\circ\text{C}$ unless otherwise noted for “slow” rpm experiments (50 and 70 rpm).

For experiments with “H” or “T” medium, S-medium was prepared as before³³ except that phosphates were replaced with 50 mM of HEPES or Tris, pH 7.5, respectively. Axenic culture was prepared according to Samuel *et al.*³⁴ with the exception that flavin-mononucleotide was replaced with riboflavin (Sigma) at the same amount, and cultures were shaken at 180 rpm instead of 70. As previously noted³⁴ with *C. elegans*, *P. pacificus* also develops slower in axenic culture, reaching maturity (adults) at 9–10 days after adding eggs. Culture in NGG was performed similar to Muschiol and Traunspurger 2007³⁵. In short, 3 ml of NGM was prepared with agar replaced with Gelrite/Gelzan CM (Sigma) at 0.75 g/L and seeded with $300 \mu\text{l}$ of OP50 and bleached eggs, then incubated at 20°C .

To collect nematodes from liquid cultures for tracking developmental stages or mouth-form phenotyping we developed a filtering method using removable $5 \mu\text{m}$ filters (Millipore) combined with the Sterifil aseptic system (47 mm, Millipore). Filters are applied to the Sterifil apparatus and a small amount of M9 is added and vacuumed through to ensure a tight and continuous seal. Then liquid cultures are decanted into the funnel and slowly vacuumed. All *P. pacificus* developmental stages are large enough to be blocked by the $5 \mu\text{m}$ filter, while bacteria pass through. However when attempting to isolate J2s we recommend applying $2 \times 5 \mu\text{m}$ filters. After all liquid has passed through the filter, nematodes were washed with ~ 25 ml of M9 by decanting directly on to the filter and applying vacuum pressure. Then the funnel was removed, and forceps were used to transfer the filter to an open 50 ml conical tube in a curved shape to fit into the opening. Nematodes were then washed from the filter by repeatedly applying the same 1 ml of M9 over the filter. Then this 1 ml was transferred to 1.5 ml microcentrifuge tube, and incubated at room temperature for 5 minutes to allow adults to swim to the bottom. Adults were pelleted by a quick (2–3 seconds) centrifugation, and the supernatant was removed. If juveniles are desired, the tube, now free of bacteria after filtering, can also be centrifuged at max speed >5 minutes to pellet. Nematode pellets were then phenotyped, or flash-frozen in liquid N2 and stored -80°C for subsequent processing (e.g. RT-qPCR).

Developmental rate determination. Worms were grown in liquid culture after bleach synchronization then filtered through a $20 \mu\text{m}$ filter 2 hours post bleach to isolate synchronous J2 animals, and then returned to liquid culture. Individual aliquots from the same flasks were monitored at regular intervals, and mouth-forms of adults were recorded at the J4-adult transition ($n = 2$). Flasks were rotated at 50 rpm to obtain large quantities of both St and Eu animals. Although not shown, several J4 were present at the earlier time points of 59 and 62 hours, which verified that we were observing the J4-adult transition.

Mouth-form phenotyping. For phenotyping nematodes grown on agar plates or NGG³⁵, adults were selected with a wire pick and transferred to $3\text{--}5 \mu\text{l}$ of M9 spotted on 4% agar pads (containing 10 mM sodium azide) on a standard microscope slide, then covered with a cover slip. For nematodes grown in liquid culture, after gently pelleting adults, they were re-suspended in the remaining M9 and $3\text{--}5 \mu\text{l}$ were directly pipetted onto the agar pad. When comparing mouth-forms of different conditions, we often performed ‘blind’ comparisons by writing the identity of the sample (i.e. “agar” or “liquid”) on the slide, and then using laboratory tape to cover the identity, and blindly selecting a slide before placing it in the microscope holder. After counting, the identity of the sample was revealed by removing the tape. Phenotyping was performed at $40\text{--}100\times/1.4$ oil objective on a Differential Interference Contrast (DIC) microscope (Zeiss) according to buccal landmarks previously described²⁰. In short, Eu were determined by the presence of a wide-mouth, a hooked dorsal tooth, and an additional subventral tooth. Conversely St animals were determined by a narrow-mouth, flint-like dorsal tooth, and absence of a subventral tooth (Fig. 1B,C). The number of biological replicates (n) was ≥ 3 for all conditions, and as high as 18 for liquid culture/S-medium, with each replicate including ≥ 50 animals with the exception that PBS and NGM-liquid cultures yielded significantly fewer animals, and included ≥ 20 animals per replicate. Mouth-forms were assessed 4–5 days after bleach-synchronization. Error bars represent standard error means (SEM), and statistical significance was assessed by *paired 2-tailed t-tests* unless otherwise indicated in the text.

dasc#1 experiments. dasc#1 was added at $1 \mu\text{M}$ final concentration according to previous methods³⁶ to eggs-J1 larvae in liquid culture. Mouth-forms were phenotyped as described above after 4 days and compared to

control liquid cultures without dasc#1. The p-value was determined by a 1-tailed, paired *t*-test for $n = 6$ biological replicates.

Morphology measurements. Length and width measurements were performed on synchronized adult animals four days after bleaching. Measurements were made of 12 animals grown on agar, 13 grown on NGG, and 10 in liquid culture using the ImageJ plug-in WormSizer⁶⁸. Box plots in Supplementary Figure 2 show quartile edges (25% and 75%) of the distribution and medians (black bars), made in R {boxplot(shape=Condition, data = worm_sizes, horizontal = TRUE, notch = FALSE)}.

Expression analysis. RNA-seq data was obtained from Ragsdale, Müller *et al.*²⁷, and average fpkms from 4 mutant alleles of *eud-1* vs. one wild-type California RS2333 were plotted. For RT-qPCR, RNA was first extracted from either 1 agar plate or 1 liquid culture of synchronized young adults (4 days post-bleaching) of the California strain PS312 (same as RS2333 but an earlier frozen stock) by Trizole extraction followed by purification with Zymo RNA-Clean & Concentrator-25 columns following manufacturers instructions from Zymo. 500–1,000 ng of purified RNA was converted to cDNA using SuperScript II (Invitrogen) for 1 hour with Oligo(dT)₁₈ primer in 20 µl reactions, and then heat-inactivated with 40 µl of 150 mM KOH/20 mM Tris-base for 10 minutes at 99 °C followed by 40 µl of 150 mM HCl, and 100 µl of TE. 4 µl of cDNA was used for each technical replicate in 10 µl qPCR reactions with 1x LightCycler[®] 480 SYBR Green I Master Mix (Roche) and 0.25 µM of each primer on a Light-Cycler 480, 384 well format. All primer sets were validated for single amplicon production with Tm melt-curve analysis, and efficiency with a 5-log titration of cDNA. Relative expression ($2^{\Delta\Delta Ct}$) was measured relative to *Ppa-Y45F10D.4* (iron binding protein)⁶⁹ for each gene.

Data availability. All data generated or analyzed during this study are included in this article and its Supplementary Information files.

References

- West-Eberhard, M. J. Developmental Plasticity and Evolution. (2003).
- Bradshaw, A. D. Evolutionary Significance of Phenotypic Plasticity in Plants. *Adv. in Genetics* **13**, 115–155 (1965).
- Gauze, G. F. *Problems of evolution*. **37**, part 2 (1947).
- Huxley, J. Problems of relative growth. (1932).
- Weaver, N. Rearing Honeybee Larvae on Royal Jelly in the Laboratory. *Bee World* (1955).
- Charnov, E. L. & Bull, J. When is sex environmentally determined? *Nature* **266**, 828–830 (1977).
- Ferguson, M. W. & Joanen, T. Temperature of egg incubation determines sex in Alligator mississippiensis. *Nature* **296**, 850–853 (1982).
- Palacios, M. G., Sparkman, A. M. & Bronikowski, A. M. Developmental plasticity of immune defence in two life-history ecotypes of the garter snake, *Thamnophis elegans* - a common-environment experiment. *J Anim Ecol* **80**, 431–437 (2011).
- Waddington, C. H. Genetic Assimilation of an Acquired Character. *Evolution* **7**, 118 (1953).
- Gibert, J.-M., Peronnet, F. & Schlötterer, C. Phenotypic Plasticity in *Drosophila* Pigmentation Caused by Temperature Sensitivity of a Chromatin Regulator Network. *PLoS Genet* **3**, e30 (2007).
- Golden, J. W. & Riddle, D. L. The *Caenorhabditis elegans* dauer larva: Developmental effects of pheromone, food, and temperature. *Developmental Biology* **102**, 368–378 (1984).
- Sikkink, K. L., Reynolds, R. M. & Ituarte, C. M. Rapid evolution of phenotypic plasticity and shifting thresholds of genetic assimilation in the nematode *Caenorhabditis remanei*. *G3*: (2014).
- Powsner, L. The effects of temperature on the durations of the developmental stages of *Drosophila melanogaster*. *Physiological Zoology* (1935).
- Brakefield, P. M., Gates, J., Keys, D. & Kesbeke, F. Development, plasticity and evolution of butterfly eyespot patterns. *Nature* (1996).
- Fielenbach, N. & Antebi, A. C. *elegans* dauer formation and the molecular basis of plasticity. *Genes & Development* **22**, 2149–2165 (2008).
- Riddle, D. L., Swanson, M. M. & Albert, P. S. Interacting genes in nematode dauer larva formation. *Nature* **290**, 668–671 (1981).
- Albert, P. S. & Riddle, D. L. Mutants of *Caenorhabditis elegans* that form dauer-like larvae. *Developmental Biology* **126**, 270–293 (1988).
- Gottlieb, S. & Ruvkun, G. *daf-2*, *daf-16* and *daf-23*: genetically interacting genes controlling Dauer formation in *Caenorhabditis elegans*. *Genetics* **137**, 107–120 (1994).
- Lee, R. C., Feinbaum, R. L. & Ambros, V. The *C. elegans* heterochronic gene *lin-4* encodes small RNAs with antisense complementarity to *lin-14*. **75**, 843–854 (1993).
- Bento, G., Ogawa, A. & Sommer, R. J. Co-option of the hormone-signalling module dafachronic acid–DAF-12 in nematode evolution. *Nature* **466**, 494–497 (2010).
- Sommer, R. J. & McGaughan, A. The nematode *Pristionchus pacificus* as a model system for integrative studies in evolutionary biology. *Molecular Ecology* **22**, 2380–2393 (2013).
- Meyer, J. M. *et al.* Succession and dynamics of *Pristionchus* nematodes and their microbiome during decomposition of *Oryctes borbonicus* on La Réunion Island. *Environmental Microbiology* **19**, 1476–1489 (2017).
- Seroby, V., Ragsdale, E. J. & Sommer, R. J. Adaptive value of a predatory mouth-form in a dimorphic nematode. *Proceedings of the Royal Society of London B: Biological Sciences* **281**, 20141334–989 (2014).
- Wilecki, M., Lightfoot, J. W., Susoy, V. & Sommer, R. J. Predatory feeding behaviour in *Pristionchus* nematodes is dependent on phenotypic plasticity and induced by serotonin. *J. Exp. Biol.* **218**, 1306–1313 (2015).
- Seroby, V., Ragsdale, E. J., Müller, M. R. & Sommer, R. J. Feeding plasticity in the nematode *Pristionchus pacificus* is influenced by sex and social context and is linked to developmental speed. *Evolution & Development* **15**, 161–170 (2013).
- Bose, N. *et al.* Complex Small-Molecule Architectures Regulate Phenotypic Plasticity in a Nematode. *Angewandte Chemie International Edition* **51**, 12438–12443 (2012).
- Ragsdale, E. J., Müller, M. R., Rödelberger, C. & Sommer, R. J. A Developmental Switch Coupled to the Evolution of Plasticity Acts through a Sulfatase. **155**, 922–933 (2013).
- Kieninger, M. R. *et al.* The Nuclear Hormone Receptor NHR-40 Acts Downstream of the Sulfatase EUD-1 as Part of a Developmental Plasticity Switch in *Pristionchus*. *Curr. Biol.* (2016).
- Seroby, V. *et al.* Chromatin remodelling and antisense-mediated up-regulation of the developmental switch gene *eud-1* control predatory feeding plasticity. *Nat Commun* **7**, 12337 (2016).
- Mather, K. & De Winton, D. Adaptation and counter-adaptation of the breeding system in *Primula*. *Annals of Botany* (1941).
- Sommer, R. J. *et al.* The genetics of phenotypic plasticity in nematode feeding structures. *Open Biology* **7**, 160332–118 (2017).

32. Serobyán, V. & Sommer, R. J. Developmental systems of plasticity and trans-generational epigenetic inheritance in nematodes. *Current Opinion in Genetics & Development* **45**, 51–57 (2017).
33. Stiernagle, T. *Maintenance of C. elegans*, WormBook, ed. The *C. elegans Research Community*. (WormBook, 2006).
34. Samuel, T. K., Sinclair, J. W., Pinter, K. L. & Hamza, I. Culturing *Caenorhabditis elegans* in Axenic Liquid Media and Creation of Transgenic Worms by Microparticle Bombardment. *Journal of Visualized Experiments: JoVE* e51796 (2014).
35. Muschiol, D. & Traunspurger, W. Life cycle and calculation of the intrinsic rate of natural increase of two bacterivorous nematodes from chemoautotrophic Movile Cave, Romania. *Nematology* **9**, 271–284 (2007).
36. Barberon, M. *et al.* Adaptation of Root Function by Nutrient-Induced Plasticity of Endodermal Differentiation. *Cell* **164**, 447–459 (2016).
37. Abbruzzese, G. *et al.* Leaf morphological plasticity and stomatal conductance in three *Populus alba* L. genotypes subjected to salt stress. *Environmental and Experimental Botany* **66**, 381–388 (2009).
38. Wang, Y. *et al.* Salt-induced plasticity of root hair development is caused by ion disequilibrium in *Arabidopsis thaliana*. *J Plant Res* **121**, 87–96 (2008).
39. Touchon, J. C. T. C., Gomez-Mestre, I. G.-M. & Warkentin, K. M. W. M. Hatching plasticity in two temperate anurans: responses to a pathogen and predation cues. *Canadian Journal of Zoology* **84**, 556–563 (2006).
40. Hong, J. K. & Hwang, B. K. Induction by pathogen, salt and drought of a basic class II chitinase mRNA and its *in situ* localization in pepper (*Capsicum annuum*). *Physiologia Plantarum* **114**, 549–558 (2002).
41. Pulendran, B., Palucka, K. & Banchereau, J. Sensing Pathogens and Tuning Immune Responses. *Science* **293**, 253–256 (2001).
42. Huang, Q. *et al.* The Plasticity of Dendritic Cell Responses to Pathogens and Their Components. *Science* **294**, 870–875 (2001).
43. Plunkett, C. R. Temperature as a tool of research in phenogenetics: methods and results (1932).
44. Woodward, D. E. & Murray, J. D. On the Effect of Temperature-Dependent Sex Determination on Sex Ratio and Survivorship in Crocodylians. *Proceedings of the Royal Society of London B: Biological Sciences* **252**, 149–155 (1993).
45. Manenti, T., Loeschcke, V., Moghadam, N. N. & Sørensen, J. G. Phenotypic plasticity is not affected by experimental evolution in constant, predictable or unpredictable fluctuating thermal environments. *Journal of Evolutionary Biology* **28**, 2078–2087 (2015).
46. Brzek, P., Kohl, K., Caviédes-Vidal, E. & Karasov, W. H. Developmental adjustments of house sparrow (*Passer domesticus*) nestlings to diet composition. *J. Exp. Biol.* **212**, 1284–1293 (2009).
47. Watson, E., MacNeil, L. T., Arda, H. E., Zhu, L. J. & Walhout, A. J. M. Integration of Metabolic and Gene Regulatory Networks Modulates the *C. elegans* Dietary Response. *Cell* **153**, 253–266 (2013).
48. Bernstein, B. E. *et al.* A Bivalent Chromatin Structure Marks Key Developmental Genes in Embryonic. *Stem Cells*. **125**, 315–326 (2006).
49. Rougvie, A. E. & Lis, J. T. Postinitiation transcriptional control in *Drosophila melanogaster*. *Mol. Cell. Biol.* **10**, 6041–6045 (1990).
50. Rada-Iglesias, A. *et al.* A unique chromatin signature uncovers early developmental enhancers in humans. *Nature* **470**, 279–283 (2011).
51. Zentner, G. E., Tesar, P. J. & Scacheri, P. C. Epigenetic signatures distinguish multiple classes of enhancers with distinct cellular functions. *Genome Res.* **21**, 1273–1283 (2011).
52. Maxwell, C. S. *et al.* Pol II Docking and Pausing at Growth and Stress Genes in *C. elegans*. *Cell Rep* **6**, 455–466 (2014).
53. Gaertner, B. *et al.* Poised RNA Polymerase II Changes over Developmental Time and Prepares Genes for Future Expression. *Cell Rep* **2**, 1670–1683 (2012).
54. Ernst, J. *et al.* Mapping and analysis of chromatin state dynamics in nine human cell types. *Nature* **473**, 43–49 (2011).
55. Hsu, H. T. *et al.* Recruitment of RNA polymerase II by the pioneer transcription factor PHA-4. *Science* **384**, 1372–1376 (2015).
56. Ozawa, T. *et al.* Histone deacetylases control module-specific phenotypic plasticity in beetle weapons. *Proc. Natl. Acad. Sci. USA* **113**, 15042–15047 (2016).
57. Kucharski, R., Maleszka, J., Foret, S. & Maleszka, R. Nutritional Control of Reproductive Status in Honeybees via DNA Methylation. *Science* **319**, 1827–1830 (2008).
58. Simola, D. F. *et al.* Epigenetic (re)programming of caste-specific behavior in the ant *Camponotus floridanus*. *Science* **351**, aac6633–aac6633 (2016).
59. Kooke, R. *et al.* Epigenetic basis of morphological variation and phenotypic plasticity in *Arabidopsis thaliana*. *Plant Cell* **27**, 337–348 (2015).
60. Zhang, Y. Y., Fischer, M., Colot, V. & Bossdorf, O. Epigenetic variation creates potential for evolution of plant phenotypic plasticity. *New Phytologist* **197**, 314–322 (2013).
61. Traunspurger, W. The biology and ecology of lotic nematodes. *Freshwater Biology* **44**, 29–45 (2000).
62. Tietjen, J. H. & Lee, J. J. Life history and feeding habits of the marine nematode, *Chromadora macrolaimoides steiner*. *Oecologia* **12**, 303–314 (1973).
63. Herman, P. M. J. & Vranken, G. Studies of the life-history and energetics of marine and brackish-water nematodes. *Oecologia* **77**, 457–463 (1988).
64. Waddington, C. H. *Organisers and Genes* by C. H. Waddington. (The University Press, 1940).
65. Waddington, C. H. Canalization of development and the inheritance of acquired characters. *Nature* (1942).
66. Baeuerle, P. A. & Baltimore, D. I κ B: a specific inhibitor of the NF- κ B transcription factor. *Science* (1988).
67. Susoy, V. & Sommer, R. J. Stochastic and Conditional Regulation of Nematode Mouth-Form Dimorphisms. *Front. Ecol. Evol.* **4**, 6706 (2016).
68. Moore, B. T., Jordan, J. M. & Baugh, L. R. WormSizer: high-throughput analysis of nematode size and shape. *PLoS ONE* **8**, e57142 (2013).
69. Schuster, L. N. & Sommer, R. J. Expressional and functional variation of horizontally acquired cellulases in the nematode *Pristionchus pacificus*. *Gene* **506**, 274–282 (2012).
70. Susoy, V. *et al.* Large-scale diversification without genetic isolation in nematode symbionts of figs. *Science Advances* **2**, e1501031–e1501031 (2016).

Acknowledgements

We are thankful to current members of the Sommer laboratory for thoughtful critique of experiments, results, and interpretations, and Dr. Matthias Herrmann for assistance with the photo in Figure 1A. This study was funded by the Max Planck Society.

Author Contributions

M.S.W., B.S. and R.J.S. conceived and designed the experiments. M.S.W. and T.L. performed mouth-form experiments with help from B.S. in making axenic culture, RNA-seq analysis (also with assistance from S.N.), and rpm experiments. M.S.W., B.S., S.N., M.L., M.D., T.R. and D.R.S. all contributed to RT-qPCR experiments. M.S.W. wrote the manuscript with edits and assistance from R.J.S., and with contribution and approval from all other authors.

Additional Information

Supplementary information accompanies this paper at doi:[10.1038/s41598-017-07455-7](https://doi.org/10.1038/s41598-017-07455-7)

Competing Interests: The authors declare that they have no competing interests.

Publisher's note: Springer Nature remains neutral with regard to jurisdictional claims in published maps and institutional affiliations.



Open Access This article is licensed under a Creative Commons Attribution 4.0 International License, which permits use, sharing, adaptation, distribution and reproduction in any medium or format, as long as you give appropriate credit to the original author(s) and the source, provide a link to the Creative Commons license, and indicate if changes were made. The images or other third party material in this article are included in the article's Creative Commons license, unless indicated otherwise in a credit line to the material. If material is not included in the article's Creative Commons license and your intended use is not permitted by statutory regulation or exceeds the permitted use, you will need to obtain permission directly from the copyright holder. To view a copy of this license, visit <http://creativecommons.org/licenses/by/4.0/>.

© The Author(s) 2017

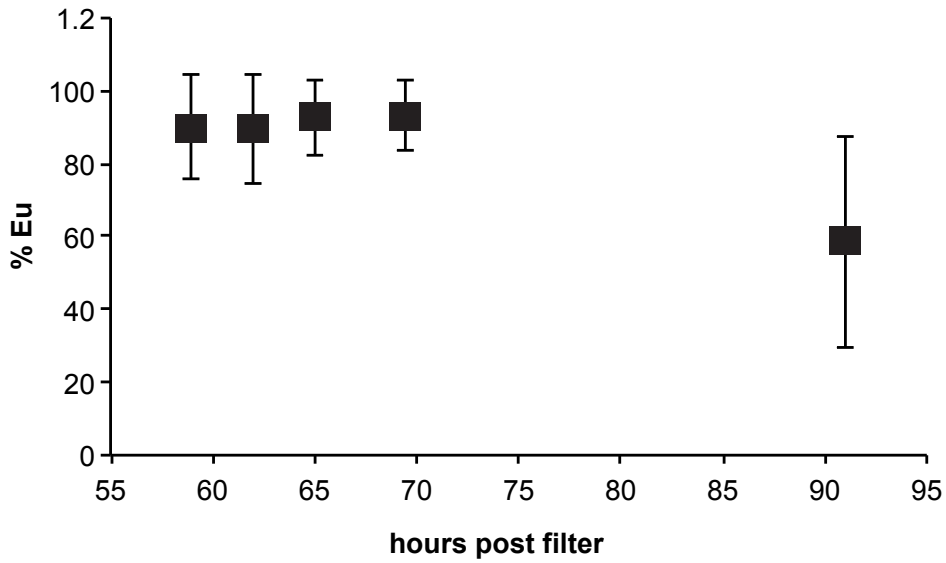
Supplementary Information

Environmental influence on *Pristionchus pacificus* mouth form through different culture methods

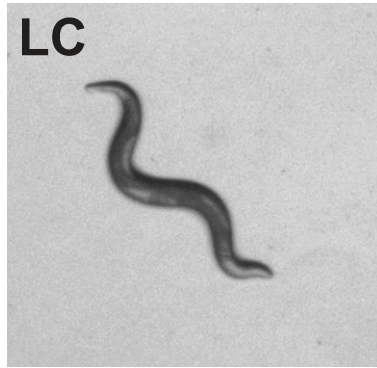
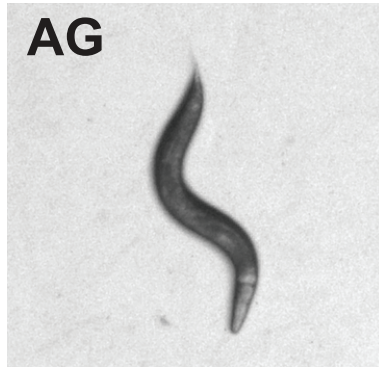
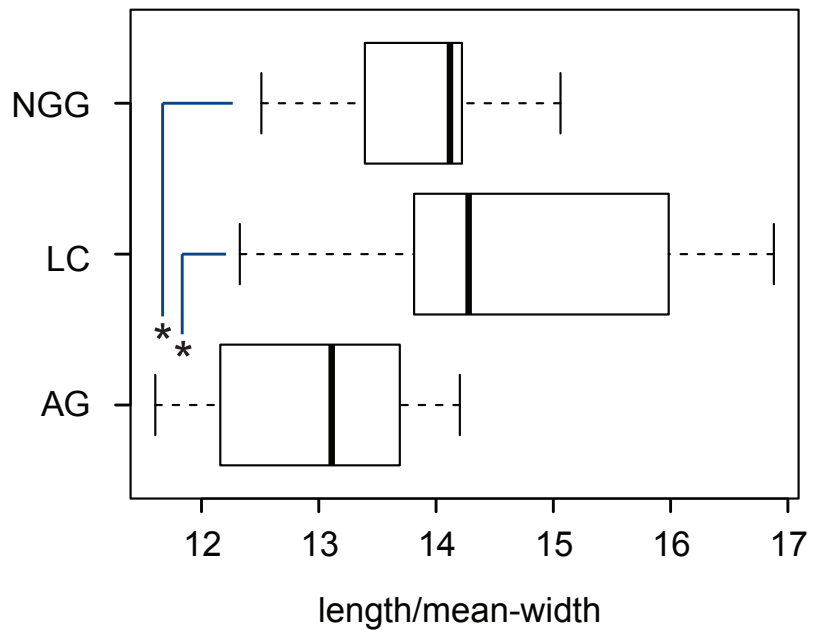
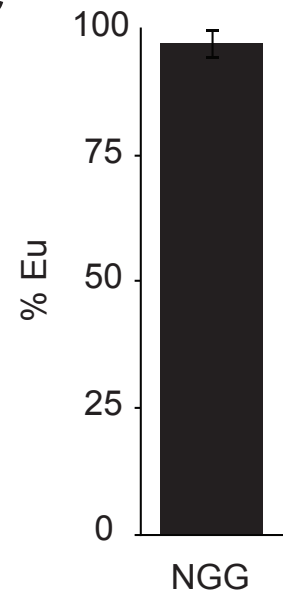
Michael S. Werner, Bogdan Sieriebriennikov, Tobias Loschko, Suryesh Namdeo,
Masa Lenuzzi, Mohannad Dardiry, Tess Renahan, Devansh Raj Sharma and
Ralf J. Sommer*

¹Department of Evolutionary Biology, Max Planck Institute for Developmental
Biology, 72076 Tübingen, Germany

*Correspondence: ralf.sommer@tuebingen.mpg.de



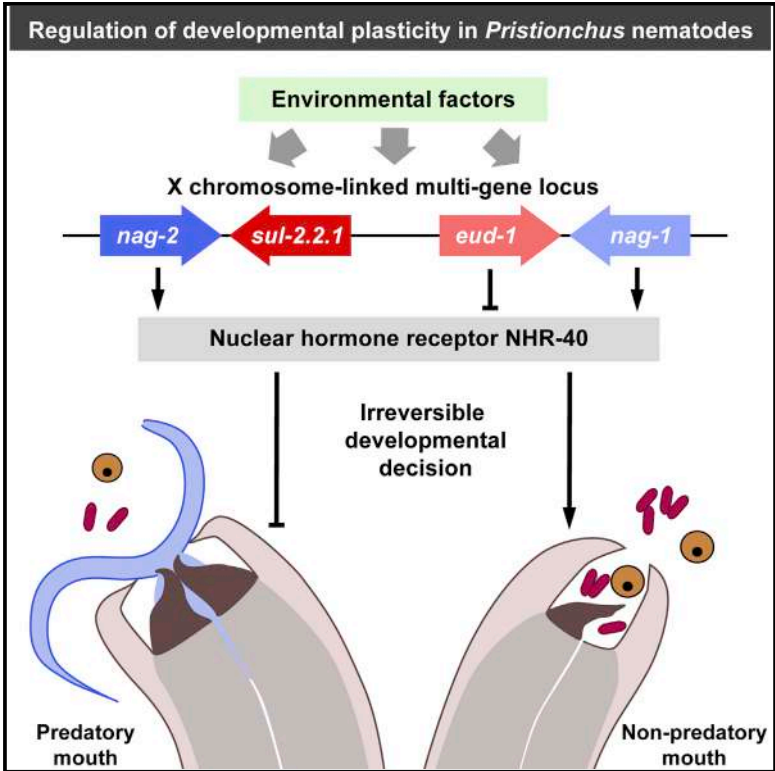
Supplementary Figure 1. Growth rate of morphs in liquid culture. Percent Eu of adult hermaphrodites grown in liquid at the J4-adult transition (59-70 hours post filter), and at 91 hours, a time point at which we normally collect and phenotype animals (n = 2). Worms were incubated at 22° C in S-Medium with 50 rpm shaking to induce sufficient numbers of both, St and Eu animals, allowing statistical significance testing ($p > 0.05$ between any two time-points arguing against slower development of Eu animals, two-tailed t-test).

A**B****C**

Supplementary Figure 2. Slender morphology does not correlate with mouth-form. (A) Images of *P. pacificus* grown in liquid culture and NGG display more slender morphology than on agar plates, quantified in (B). Measurements of adults from the same synchronized population were made with Wormsizer⁶⁸, n = 12 (agar), 13 (NGG), and 10 (liquid culture = 'LC'). Statistical significance was measured with a nonparametric Mann-Whitney U test in R. (C) Same as in Figure 2, mouth-form ratio of adult PS312 grown in NGG, n = 3.

A Developmental Switch Generating Phenotypic Plasticity Is Part of a Conserved Multi-gene Locus

Graphical Abstract



Authors

Bogdan Sieriebriennikov, Neel Prabh, Mohannad Dardiry, ..., Manuela R. Kieninger, Christian Rödelsperger, Ralf J. Sommer

Correspondence

ralf.sommer@tuebingen.mpg.de

In Brief

The clonally reproducing roundworm *Pristionchus pacificus* can develop either as a toothed predator or as a narrow-mouthed microbe feeder depending on environmental conditions. Sieriebriennikov et al. show that the switch gene controlling this developmental decision is physically linked with two other genes having opposing influence on the same phenotype.

Highlights

- The *eud-1* switch induces the development of predatory morphology in *P. pacificus*
- *nag-1* and *nag-2* surround *eud-1* and have opposite effects on the same phenotype
- The locus architecture is conserved in *Pristionchus*, but not in other dimorphic genera
- Gene conversion counteracts divergence between paralogs within the locus



A Developmental Switch Generating Phenotypic Plasticity Is Part of a Conserved Multi-gene Locus

Bogdan Sieriebriennikov,¹ Neel Prabh,^{1,2} Mohannad Dardiry,^{1,2} Hanh Witte,¹ Waltraud Röseler,¹ Manuela R. Kieninger,^{1,3} Christian Rödelberger,¹ and Ralf J. Sommer^{1,4,*}

¹Department for Integrative Evolutionary Biology, Max Planck Institute for Developmental Biology, Max-Planck-Ring 9, 72076 Tübingen, Germany

²These authors contributed equally

³Present address: Wellcome Trust/Cancer Research UK Gurdon Institute, University of Cambridge, Cambridge CB2 1QN, England, UK

⁴Lead Contact

*Correspondence: ralf.sommer@tuebingen.mpg.de

<https://doi.org/10.1016/j.celrep.2018.05.008>

SUMMARY

Switching between alternative complex phenotypes is often regulated by “supergenes,” polymorphic clusters of linked genes such as in butterfly mimicry. In contrast, phenotypic plasticity results in alternative complex phenotypes controlled by environmental influences rather than polymorphisms. Here, we show that the developmental switch gene regulating predatory versus non-predatory mouth-form plasticity in the nematode *Pristionchus pacificus* is part of a multi-gene locus containing two sulfatases and two α -N-acetylglucosaminidases (*nag*). We provide functional characterization of all four genes, using CRISPR-Cas9-based reverse genetics, and show that *nag* genes and the previously identified *eud-1*/sulfatase have opposing influences. Members of the multi-gene locus show non-overlapping neuronal expression and epistatic relationships. The locus architecture is conserved in the entire genus *Pristionchus*. Interestingly, divergence between paralogs is counteracted by gene conversion, as inferred from phylogenies and genotypes of CRISPR-Cas9-induced mutants. Thus, we found that physical linkage accompanies regulatory linkage between switch genes controlling plasticity in *P. pacificus*.

INTRODUCTION

Many animals and plants exhibit complex traits that occur as discrete alternative morphs. In general, two mechanisms are known to underlie the formation of alternative phenotypes: genetic polymorphism and plasticity (polyphenism). Examples of adaptive alternative phenotypes are butterfly wing patterns involved in mimicking unsavory species, long- and short-styled flowers in primroses shaped to promote cross-fertilization, and single-queen versus multiple-queen

colonies in fire ants (Charlesworth, 2015; Schwander et al., 2014). These phenotypes are inherited as single genetic polymorphisms—a phenomenon referred to as “supergenes”—which presumably contain multiple physically linked genes associated with the phenotype (Joron et al., 2011; Kim et al., 2017; Kunte et al., 2014; Li et al., 2016; Wang et al., 2013). While the identities of the causal genes are, in some cases, yet to be determined, the evolutionary turnover of supergene loci is believed to be rapid. For example, in *Papilio* butterflies, the *doublesex* haplotype associated with the mimetic morph is restricted to three species, and its origin dates back to 2 million years ago, while mimicry in other species of the same genus is controlled by different loci (Timmermans et al., 2014; Zhang et al., 2017).

Physical linkage of functionally related genes is not restricted to examples traditionally considered within the supergene concept. For example, the major histocompatibility complex (MHC) in chordates and the Y chromosome also contain functionally related genes specifying alternative phenotypes (Edwards and Hedrick, 1998; Schwander et al., 2014). Studies on these loci and other loci that contain linked genes but are not associated with alternative phenotypes, such as clusters of tandem duplicates and imprinted clusters, revealed that physical proximity facilitates coordinated regulation of gene expression (Hallast et al., 2005; Trowsdale, 2002; Zakharova et al., 2009). Arguably, concerted transcription of the linked genes is also important for loci associated with complex traits, with an additional advantage of facilitating co-adaptation between the genes through the reduction of recombination.

Complex alternative phenotypes may also develop under environmental influence rather than polymorphisms. This phenomenon is known as developmental or phenotypic plasticity, with the genes responsible for both phenotypes present in the same organism (West-Eberhard, 2003). Additionally, genomes of species that exhibit plasticity contain a set of regulatory genes that switch between the developmental trajectories upon perception of relevant environmental inputs. Conceptually, plasticity and genetic polymorphism represent different mechanisms of generating alternative phenotypes. However, the differences and similarities remain largely unexplored,



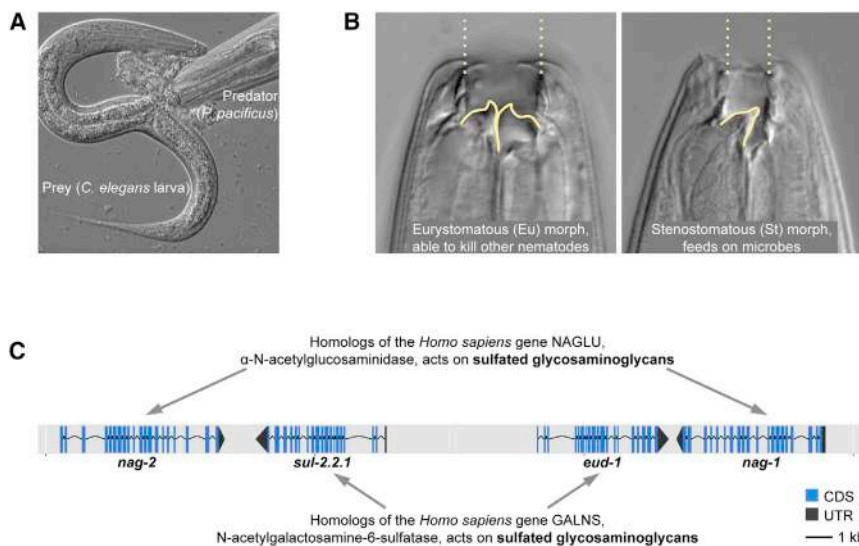


Figure 1. Developmental Plasticity of Predatory Morphology in *Pristionchus pacificus*

(A) Adult *P. pacificus* devouring a larva of *Caenorhabditis elegans*.

(B) Mouths of eury stomatous (Eu) and stenostomatous (St) morphs. The omnivorous Eu morph has a wide mouth with two teeth, whereas the microbivorous St morph has a narrow mouth with a dorsal tooth only.

(C) Genomic locus containing the previously identified developmental switch gene *eud-1* consists of two pairs of duplicated genes in an inverse tandem arrangement. Both pairs encode proteins that potentially have sulfated glycosaminoglycans as their substrate.

because knowledge about the mechanisms and evolution of plastic traits is scarce.

Nonetheless, recent findings provided first insight into the mechanisms associated with developmental plasticity (Projecto-Garcia et al., 2017). Studies on plasticity between predatory and microbe-feeding morphs in the nematode *Pristionchus pacificus* identified the sulfatase-encoding gene *eud-1* as a developmental switch and also implicated the chromatin modifiers *lxy-12* and *mbd-2* and the nuclear hormone receptor *nhr-40* in the same pathway (Figures 1A, 1B, and 2D) (Kieninger et al., 2016; Ragsdale et al., 2013; Seroby et al., 2016). While wild-type populations show a mixture of two morphs (Bento et al., 2010), mutations in *eud-1* lead to the absence of “wide-mouthed” eury stomatous (Eu) animals, which have two hooked teeth and are facultative predators (Wilecki et al., 2015). Instead, all animals in the mutant lines develop into “narrow-mouthed” stenostomatous (St) morphs, which have one flint-like tooth and only feed on microbes (Figure 1B). These phenotypes and additional genetic experiments indicated that *eud-1* acts as a developmental switch (Ragsdale et al., 2013), confirming long-standing theoretical predictions that plasticity requires developmental reprogramming and new input by developmental switch genes (West-Eberhard, 2003, 2005). Also, the functional characterization of *eud-1* revealed that it operates in phenotypically divergent populations of *P. pacificus* and in the closely related species *P. expectatus*, with which *P. pacificus* can form viable but sterile hybrids (Ragsdale et al., 2013). Thus, the *eud-1* switch gene is an important regulator of mouth-form plasticity and its evolution.

Here, we expand the investigation of *eud-1* to the neighboring genomic regions. Interestingly, *eud-1* belongs to an inverted tandem duplication containing two sulfatase and two α-N-acetylglucosaminidase (*nag*)-encoding genes. The main finding of this study is that the *nag-1* and *nag-2* genes have an opposing effect on the morph frequencies in comparison to *eud-1*. Thus, plasticity in *P. pacificus* is controlled by a set of genes that display

tional and evolutionary implications of physical linkage between the genes it contains.

RESULTS

The Switch Gene *eud-1* and Its Tandem Paralog Are Surrounded by a Pair of NAGLU Genes

eud-1 is located on the left arm of the X chromosome of *P. pacificus*. It belongs to an ~30-kb region that contains four genes in an inverted tandem configuration (Figure 1C). Specifically, *eud-1* and its paralog *sul-2.2.1* are in the center of this cluster in a head-to-head orientation, and they are separated by an ~7-kb intergenic region that contains a promoter driving the expression of *eud-1* (Ragsdale et al., 2013). Both genes are homologous to the *Caenorhabditis elegans* gene *sul-2* and to the human gene GALNS coding for an N-acetylgalactosamine-6-sulfatase. *Cel-sul-2* is a single autosomal gene, whereas *P. pacificus* has three *sul-2*-like genes, one on the same autosome as in *C. elegans* and the X chromosome *eud-1* and *sul-2.2.1* genes, which most likely result from lineage-specific duplication and translocation events (Ragsdale et al., 2013).

Interestingly, the two neighboring genes of *eud-1* and *sul-2.2.1* are also inverted duplicates, homologous to an uncharacterized *C. elegans* autosomal gene *K09E4.4* and the human gene NAGLU encoding an α-N-acetylglucosaminidase. In humans, both GALNS and NAGLU have sulfated glycosaminoglycans as their substrates, and mutations in these genes cause different types of mucopolysaccharidosis, a disorder characterized by disrupted formation of extracellular matrix (Beesley et al., 2005; Rivera-Colón et al., 2012). This offers the possibility that the homologs of GALNS and NAGLU in *P. pacificus* play a role in similar biochemical pathways. This potential relationship and the peculiar genomic arrangement of the locus prompted us to test the function of the NAGLU homologs in *P. pacificus*, which we named *nag-1* and *nag-2*.

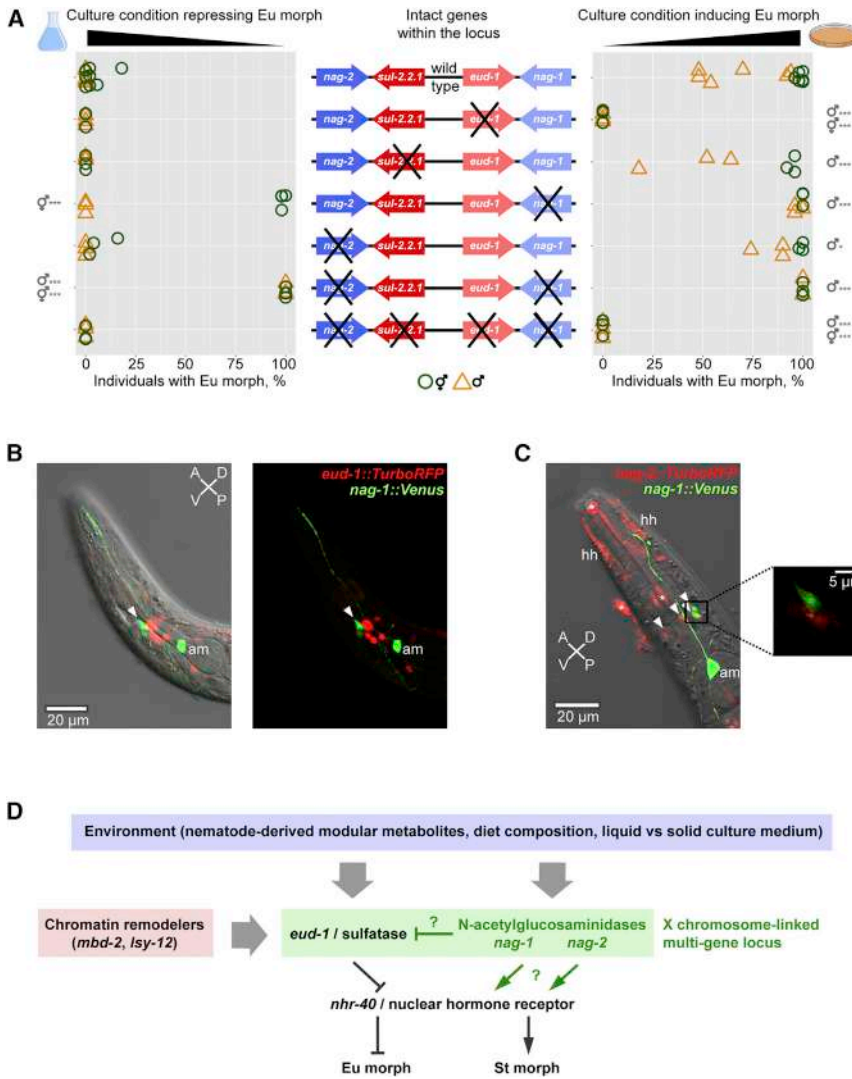


Figure 2. *eud-1* Locus Organization, Functions, and Expression of Individual Genes

(A) Morph frequencies in wild-type and mutant lines in both sexes and two culture conditions. Triangles represent males, and circles represent hermaphrodites. The cartoon illustrates the genotype of every examined line. Arrows represent genes, and arrowheads point toward the 3' ends. Crosses indicate inactivated genes. Strains from top to bottom: PS312 wild-type, *eud-1(tu445)*, *sul-2.2.1(iub2)*, *nag-1(tu1137)*, *nag-2(tu1138)*, *nag-1(tu1142)*, *nag-2(tu1143)*, and *tuDf1[nag-1 sul-2.2.1 eud-1 nag-2]*. **p* < 0.05; ****p* < 0.001; all the comparisons are to wild-type, and only statistically significant comparisons are shown.

(B) *nag-1* and *eud-1* do not co-localize. Head region of an animal carrying *nag-1* and *eud-1* reporters. Left: overlay of a differential interference contrast (DIC) image, maximum-intensity Z-projection of the Venus channel, and sum-of-slices projection of the TurboRFP channel. Right: the same without DIC.

(C) *nag-1* and *nag-2* do not co-localize. Head of an animal carrying *nag-1* and *nag-2* reporters. Main frame: overlay of a DIC image, maximum-intensity Z-projection of the Venus channel, and maximum-intensity projection of the TurboRFP channel. Inset: overlay of Venus and TurboRFP channels in the same plane.

In (B) and (C), arrowheads indicate cell bodies of labial sensilla. am, amphid neuron; hh, head hypodermis; A, anterior end; P, posterior end; D, dorsal side; V, ventral side. In (C), asterisks indicate auto-fluorescent regions.

(D) Updated model of the regulation of mouth-form plasticity.

See also Figures S1 and S2.

nag-1 and *nag-2* Regulate the Same Phenotype as *eud-1*

To study the function of *nag-1* and *nag-2* in *P. pacificus*, we knocked out both genes using CRISPR-Cas9 technology (Witte et al., 2015). We isolated *nag-1(tu1137)* and *nag-2(tu1138)* single mutants and a double-knockout line *nag-1(tu1142) nag-2(tu1143)* (Figure S1A). Additionally, we obtained a line with a deletion *tuDf1[nag-1 sul-2.2.1 eud-1 nag-2]* that affects all four genes in the locus (Figure S1B). In the absence of an *a priori* expectation as to whether the knockout phenotype of the *nag* genes will be Eu constitutive (Euc) or Eu deficient (Eud), mouth form was assessed under two culture conditions (Figure 2A). One of them (liquid S-medium) is Eu repressing for wild-type worms (Werner et al., 2017), thus facilitating identification of the Euc phenotype. Another condition (agar plates with nematode growth medium) is Eu inducing, which aids detection of the Eud phenotype. For the same reason, we phenotyped both sexes, as wild-type males are more prone to becoming St than wild-type hermaphrodites on agar plates (Seroby et al., 2013). Knockout of *nag-1* resulted in a partially penetrant Euc

phenotype, observable in hermaphrodites in liquid culture and in males on agar plates (Figure 2A). Mutation in its paralog, *nag-2*, also resulted in a Euc phenotype, although it was weaker and only manifested in a slight shift toward Eu in males on agar plates. When *nag-1* and *nag-2* were inactivated, the Euc phenotype became completely penetrant and evident in both sexes and in both culture conditions, demonstrating additive action of the two paralogous genes (Figure 2A). As the *nag-1 nag-2* phenotype is opposite that of *eud-1*, we scored mouth-form frequency in the line where all four genes were deleted. The quadruple mutant had a completely penetrant Eud phenotype identical to that of the *eud-1* single knockout, demonstrating that *eud-1* is epistatic over *nag-1* and *nag-2* (Figures 2A and 2D). These experiments indicate that, first, both *nag* genes and *eud-1* control the same developmentally plastic trait and, second, *nag-1* and *nag-2* have opposing effects on mouth-form frequencies to *eud-1*, because they promote the formation of St morphs. Given the clustering of these genes and the X chromosome position, which reduces recombination in nematodes with their XO sex determination system (Pires-daSilva and Sommer, 2004), these findings demonstrate that the multi-gene locus controlling developmental plasticity in *P. pacificus* has at

least some supergene characteristics. Therefore, we continued to study the development, expression, and evolution of this multi-gene locus.

The *eud-1* Paralog *sul-2.2.1* Has Only a Minor Role in Mouth-Form Specification

Since both the *nag-1* and *nag-2* mutants had mouth-form defects, we re-analyzed the already existing *sul-2.2.1* mutant. Previous studies had not found any significant effect of *sul-2.2.1* on mouth-form plasticity, but these experiments were only performed in hermaphrodites and in one culture condition (Ragsdale and Ivers, 2016). We observed only a weak but significant shift toward St morphs in males on agar plates (Figure 2A). Similarly, when we overexpressed both genes in a *eud-1* mutant background, we observed a much stronger rescue with *eud-1* compared to *sul-2.2.1* (Figure S2B). Thus, *nag-1*, *nag-2*, and *eud-1* play major roles in the regulation of mouth-form plasticity, whereas *sul-2.2.1* appears to have only a minor contribution.

nag-1, *nag-2*, and *eud-1* Are Expressed in Different Sensory Neurons and Interneurons

Next, we investigated in which tissues *nag-1* and *nag-2* are expressed and whether they co-localize with each other and with *eud-1*, which is expressed in several head neurons (Ragsdale et al., 2013). We created transcriptional reporter constructs for both genes and generated transgenic animals. *nag-1* was expressed in 1 pair of head neurons, with the wiring pattern and cell body position resembling those of amphid neurons in *C. elegans* (Altun and Hall, 2017), and in 1–3 pairs of head neurons bearing semblance to labial sensilla (Figures 2B, 2C, and S2C). *nag-2* localized to 1–3 pairs of different labial sensilla but also to hypodermal cells at the head tip (Figure 2C; Figures S2D and S2E). Importantly, *nag-1* and *nag-2* did not co-localize (Figure 2C), which is consistent with their additive contributions to the phenotype suggesting that the paralogs underwent sub-functionalization. Also, *nag-1* and *eud-1* were expressed in different cells (Figure 2B), which, taken together with *eud-1* being epistatic to *nag-1*, indicates that *eud-1* is expressed in downstream interneurons and/or in sensory neurons perceiving an environmental input that can override the input perceived through cells expressing *nag-1*. Thus, the multi-gene locus regulating plasticity in *P. pacificus* consists of genes that are expressed in non-overlapping sensory and interneurons.

Synteny in the Locus Is Preserved throughout the Genus *Pristionchus*

To examine the evolution of the multi-gene locus, we investigated the architecture of the *eud-1* locus in seven other species of *Pristionchus*, which represent the taxonomic distribution of the genus (N.P. W.R., H.W., G. Eberhardt, R.J.S., C.R., unpublished data) and all of which exhibit mouth-form plasticity. Performing a BLASTP search for homologs of *nag-1* and *eud-1* in the selected genomes, we found at least two homologs of *nag-1* and at least three homologs of *eud-1* in every species (Data S1). A pair of sulfatase genes and a pair of *nag* genes always adjoined each other, and their order and orientation were conserved across all tested species of *Pristionchus* (Figure 3A). Similarly, homologs of *C. elegans* *dpy-23* and *F40E10.6*, which

are adjacent to *nag-2* and *nag-1* in *P. pacificus*, respectively, were found to surround the plasticity locus in all *Pristionchus* species (Figure 3A). Importantly, *dpy-23* and *F40E10.6* are not part of the locus regulating plasticity, as knockout mutants of these genes do not have mouth-form-defective phenotypes (Table S1). Thus, genes constituting the plasticity multi-gene locus in *P. pacificus* are syntenic throughout the genus *Pristionchus*, which represents an evolutionary diversification of more than 30 species (Ragsdale et al., 2015).

The Locus Architecture Is Different in Other Dimorphic Genera

Having established that the locus architecture is preserved in *Pristionchus* spp., we inspected the genomes of two more dimorphic species of the same family: a close relative, *Micoletzky japonica* (N.P. et al., unpublished data), and a basal species, *Allodiplogaster sudhausi*, sequenced in this study. We found that *M. japonica* had three NAGLU homologs in the same locus and that the sulfatase genes were exterior to a pair of NAGLU homologs, opposite to what is found in *Pristionchus* (Figure 3A; Data S1). In contrast, all NAGLU homologs and all sulfatase genes were on different contigs and never adjoined each other in *A. sudhausi*, although contigs were large enough and contained several BLAST hits with other *Pristionchus* genes in the neighboring regions (Figures 3A and S3A; Data S1). These findings result in several conclusions. First, synteny within the locus is restricted to the *Pristionchus* genus, implying that its architecture, as observed in *P. pacificus*, has evolved at the base of or in the genus. Second, a tandem arrangement is also found in *M. japonica*, while the order and orientation of genes are different. Finally, the clustering of *eud-1* and *nag-1* homologs is absent in the basal *A. sudhausi*, indicating that the physical linkage between NAGLU homologs and sulfatases is not essential for mouth-form plasticity and may have evolved after the origin of plasticity or, alternatively, has been lost in *A. sudhausi*.

Evolutionary History of Paralogs in the Locus Is Shaped by Gene Conversion

To investigate the evolutionary forces acting on the individual genes, we reconstructed maximum-likelihood phylogenies for all sulfatase and NAGLU homologs within the syntenic block (Figure 3B; Figures S3B and S3C). Interestingly, neither the NAGLU nor the sulfatase gene tree recapitulated the species tree, the latter of which is shown in Figure 3A. Specifically, paralogs clustered with each other in the basal clades, whereas orthologous clusters were formed only in the terminal clades, albeit of different depths in the sulfatase and the NAGLU tree (Figure 3B; Figures S3B and S3C). For example, EUD-1 and SUL-2.2.1, of the closely related species *P. pacificus*, *P. exspectatus*, and *P. arcanus*, recapitulate the species phylogeny. In contrast, in all the more basal species (*P. maxplancki*, *P. japonicus*, *P. fissidentatus*, *P. mayeri*, and *P. entomophagus*), the two paralogous sequences of each species group together. Similarly, NAG-1 and NAG-2 sequences of *P. mayeri* and *P. fissidentatus* group together (Figure S3C). Given the conserved structure of the *Pristionchus* plasticity multi-gene locus, these patterns are unlikely to result from independent gene duplications. Therefore, we explored an alternative mechanism—namely, the involvement of gene conversion.

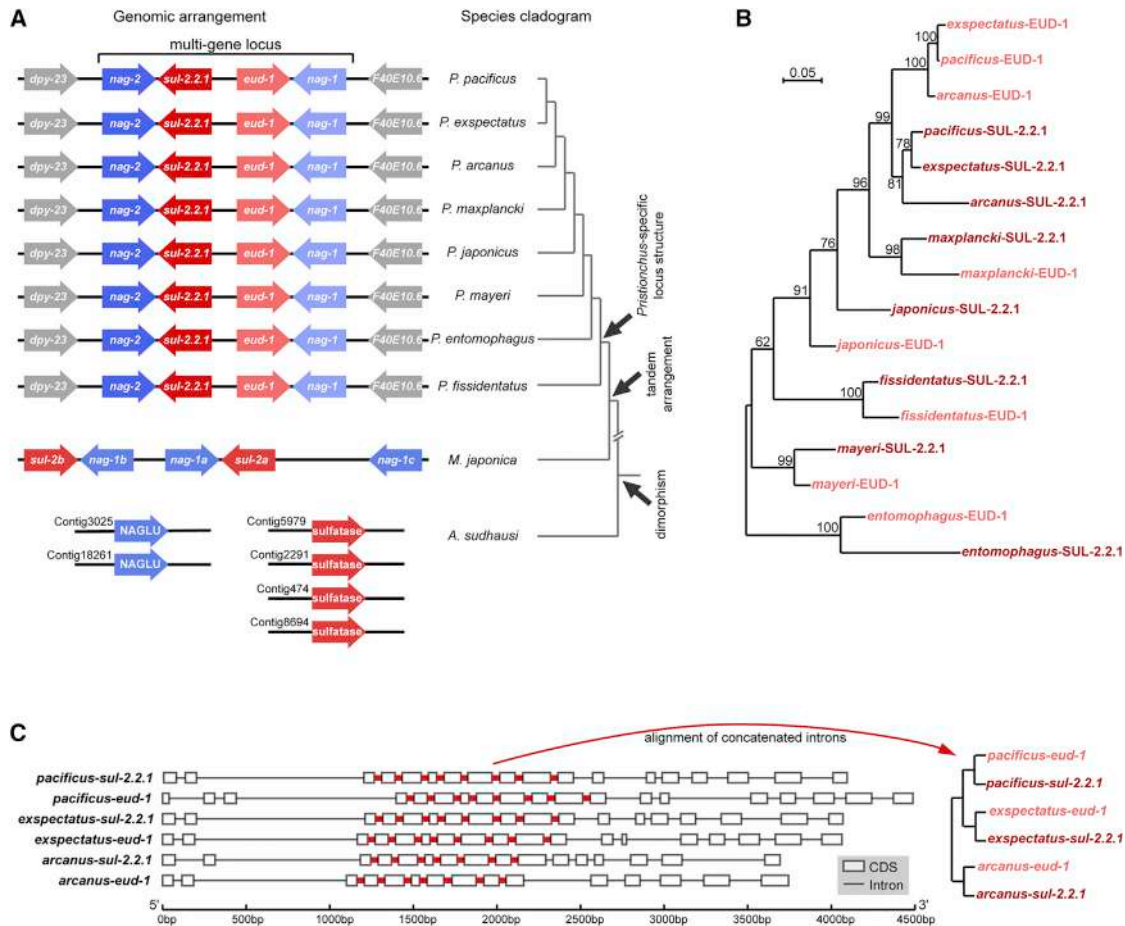


Figure 3. Evolution of the Multi-gene Locus in the Family Diplogastriidae

(A) Cartoon representation of the syntenic arrangement of the genes in the locus in eight species of *Pristionchus*; a closely related species, *Micoletzky japonica*; and a basal but already dimorphic species, *Allodiplogaster sudhausi*. Colored arrows represent gene predictions, and tips point toward the 3' ends. Gene predictions connected with a black line are located in the same scaffold and adjoin each other. In *Pristionchus* spp., gene names are assigned based on proximity to homologs of the *C. elegans* genes *dpy-23* and *F40E10.6*.

(B) Maximum-likelihood tree of amino acid sequences of EUD-1 homologs in the genus *Pristionchus*. Numbers indicate values of bootstrap support.

(C) Exon-intron structure of *eud-1* and *sul-2.2.1* in *P. pacificus*, *P. expectatus*, and *P. arcanus*. Introns that align in all six sequences are indicated in red. On the right, a cladogram built from the intron alignment.

See also Figure S3 and Table S1.

For this, we scrutinized the nucleotide sequences of sulfatases in *P. pacificus*, *P. expectatus*, and *P. arcanus*, those species in which sulfatase homologs still formed orthologous clusters (Figure 3C). Given that species-specific codon bias may lead to convergence of coding sequences, we focused on intronic sequences instead. We aligned the intronic regions and removed all unreliable columns. The resultant alignment broke down into two blocks: a region where introns of either one or the other orthologous group were aligned and a region where all sequences were aligned but variants at the informative sites matched between paralogs (Figure S4). These two regions yielded conflicting phylogenetic trees in which, correspondingly, either orthologs or paralogs clustered together (Figure 3C; Figure S4). Thus, we observe not only that the two gene pairs in the locus, i.e., sulfatases and the NAGLU homologs, show incongruence between their tree topologies but also that even

the different parts of the two sulfatases genes show contrasting phylogenetic signals. Considering that we have established that the locus synteny originated in the common ancestor of the *Pristionchus* nematodes, we propose that gene conversion is the most likely mechanism that can explain the complex phylogeny we observe at this locus. Gene conversion has been inferred in other gene families, including opsin genes in fish and humans (Cortesi et al., 2015; Zhao et al., 1998), but direct experimental support for gene conversion is generally scarce (Lynch, 2007).

Experimental Demonstration of Gene Conversion between *nag-1* and *nag-2*

Strikingly, we obtained what seems a direct evidence for gene conversion between *nag-1* and *nag-2* under experimental, laboratory conditions. After CRISPR-Cas9-induced double-strand

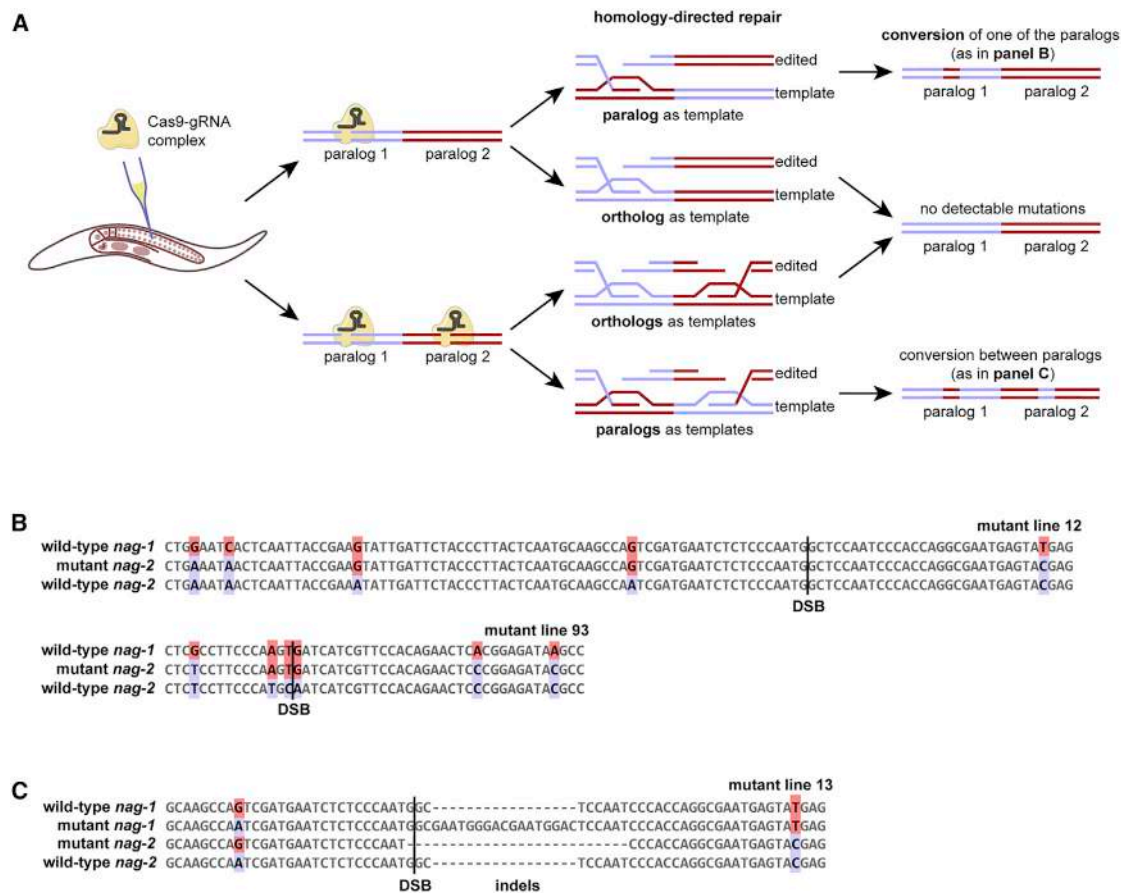


Figure 4. Gene Conversion between Paralogs in the Multi-gene Locus

(A) Hypothetical mechanism of gene conversion that occurred in CRISPR-Cas9-induced mutants and resulted in sequence similarity patterns shown in (B) and (C). In all drawn scenarios, sister chromatids are used as repair templates; however, intra-chromatid conversion may also be possible.

(B and C) Alignment of wild-type and mutant *nag-1* and *nag-2* sequences that underwent gene conversion in either one (B) or both paralogs (C) following CRISPR-Cas9-induced double-strand breaks (DSBs). Colored nucleotides mark informative sites.

See also Figure S4.

break (DSB), we found three independent mutants, in which some informative positions were exchanged between *nag-1* and *nag-2* (Figure 4). Specifically, in two experiments, we targeted exon 5 of both *nag-1* and *nag-2* (Figure S1A) and genotyped a total of 192 F1 progeny of injected animals, 18 of which carried molecular lesions in one or both genes. Interestingly, two mutant lines had genotypes that were best explained by gene conversion (Figure 4). We then repeated an experiment with a different guide RNA (gRNA) targeting exon 4 of *nag-2* (Figure S1A). Here, we genotyped 96 F1 animals and isolated 8 mutants, one of which had a genotype that is consistent with gene conversion (Figures 4A and 4B). Thus, we observed gene conversion at the multi-gene locus under experimental conditions with a relatively high frequency (3 out of 26 mutants in 288 tested animals). Even though CRISPR-Cas9-mediated DSB-induction is clearly not part of normal cell physiology, the fact that the paralogs of affected genes could be used as repair templates demonstrates the propensity of paralogous sequences in the locus to be interconverted.

DISCUSSION

This study has established that the predatory mouth-form dimorphism in *P. pacificus* is controlled by a multi-gene locus, which includes the switch gene *eud-1*. The region contains two pairs of duplicated genes in an inverted tandem configuration. The paralogs *nag-1* and *nag-2*, which code for α -N-acetylglucosaminidases, additively promote the microbivorous St morph, while the *eud-1*/sulfatase promotes the omnivorous Eu morph. The deletion of the complete locus shows that *eud-1* is epistatic over *nag-1* and *nag-2*. We show that *nag* genes and *eud-1* are all expressed in neurons, suggesting their role in environmental perception, a hallmark of developmental plasticity. We speculate that the opposing effects of *eud-1* and the *nag* genes and their non-overlapping expression are linked to the perception of disparate environmental input, which may have necessitated their coadaptation maintained by physical linkage. Additionally, such genomic organization may facilitate coordinated expression during the time window when the developmental decision is taken.

The multi-gene locus controlling plasticity in *P. pacificus* has multiple similarities to, but also important differences from, other gene clusters that regulate complex traits, which include, but are not limited to, supergenes. We compared our system to other known examples with regard to its relationship with alternative phenotypes, its physical size, and its evolutionary history and reached five major conclusions. First, the multi-gene locus characterized in this study regulates developmental plasticity, in contrast to supergenes and other clusters of linked genes, which represent genetic polymorphisms specifying alternative phenotypes. This demonstrates that the concept of coordinated expression and evolution of structural genes associated with polymorphic phenotypes can be extended to signaling genes associated with plastic phenotypes.

Second, we compared the size of the plasticity multi-gene locus in *P. pacificus* with those of similar loci in other organisms. While the smallest known supergene contains one coding sequence with several associated non-coding genetic elements, and the largest known MHC complex contains several thousand genes (Delarbre et al., 1992; Nishikawa et al., 2015), the plasticity locus in *P. pacificus* consists of four enzyme-encoding genes, three of which are functionally important for dimorphism. Thus, according to the current knowledge, the size of the plasticity multi-gene locus in *P. pacificus* is at the lower end of the range typically found in other known clusters of functionally related genes.

The third conclusion of our study is that the architecture of the *eud-1* locus has been conserved over millions of years and a diversification of more than 30 species. In contrast, traits controlled by supergenes are believed to have multiple origins, and the evolution of supergenes is thought to be rapid, based on comparisons between species of butterflies and ants in well-resolved phylogenetic context (Joron et al., 2011; Purcell et al., 2014; Timmermans et al., 2014; Zhang et al., 2017). Similarly, the number of MHC clusters and their exact gene composition are highly variable between and within different species of primates (Adams and Parham, 2001; Norman et al., 2017). In *Pristionchus*, all eight species with recently sequenced genomes—which cover the complete phylogeny of the genus and were collected in different geographic locations, in different years, and from different host beetles—have the same locus architecture.

Fourth, our outgroup comparison allows insight into the long-term evolutionary stability of the locus organization and its correlation with the trait it controls. Phylogenetic reconstructions in Diplogastridae, the family to which the genus *Pristionchus* belongs, date the evolution of the dimorphism and mouth-form plasticity to the last common ancestor of the entire family (Susoy et al., 2015). The genus *Allodiplogaster* is one of the basal taxa, and sequencing and genome analysis in *A. sudhausi* revealed the absence of clustering of *eud-1* and *nag-1* homologs in this species. These results indicate that the evolution of the trait—alternative mouth forms and plasticity—and the structure of the locus are uncoupled. It is possible that such patterns simply reflect structural turnover in these genomes, and selection for linkage is not always sufficiently strong to counteract it. Alternatively, mouth-form control may be subject to developmental systems drift in Diplogastri-

dae, whereby different loci may control predatory plasticity in *Pristionchus* and in *Allodiplogaster*.

The final conclusion from our study is to provide sequence-based and experimental support for the involvement of gene conversion in shaping the architecture of the plasticity locus in *P. pacificus* and for limiting the divergence of linked genes. Gene conversion was previously observed between paralogs in segmentally duplicated clusters (Hallast et al., 2005; Sharon et al., 1999), in MHC loci in vertebrates (Chen et al., 2007; Goebel et al., 2017), and between odorant-binding proteins in the fire ant supergene (Pracana et al., 2017). Similarly, we inferred from phylogenies that gene conversion has occurred within both pairs of paralogs in the *Pristionchus* multi-gene locus. At the same time, however, the additive phenotypic effects and the non-overlapping expression of *nag-1* and *nag-2*, as well as the drastic difference in the phenotypic contribution between *eud-1* and *sul-2.2.1*, clearly demonstrate that both pairs of paralogs have functionally diverged. Thus, evolution of individual genes is likely shaped by a balance between gene conversion and divergence.

Generally, it is thought that gene conversion constraints divergence and contributes to the neo- or sub-functionalization after gene duplication by preventing newly formed paralogs from pseudogenization (Cortesi et al., 2015; Lynch et al., 2001; Walsh, 1987). Similarly, gene conversion between paralogs can disrupt chromosome structure by enabling non-homologous crossovers (Connallon and Clark, 2010). Such an event may have created the different arrangements of NAGLU and sulfatase homologs in *Pristionchus* and *Micoletzkyia*. However, direct evidence for gene conversion is generally scarce, largely due to limited functional tools that would permit the visualization of gene conversion in action. Despite this, in our CRISPR-Cas9 experiments targeting *nag-1* and *nag-2*, we observed molecular lesions that can best be explained by gene conversion. While CRISPR-Cas9-mediated DSB induction represents an un-physiological perturbation, the very fact that paralogs can be used as repair templates demonstrates the propensity of paralogous sequences in the multi-gene locus regulating plasticity to be interconverted.

Taken together, our study shows that physical linkage of functionally related genes occurs between signaling genes associated with phenotypic plasticity. Future investigations will focus on two questions. First, comparisons between wild isolates of *P. pacificus* are necessary to explore the haplotype composition and patterns of selection in the region. It is possible that genetic polymorphisms in the plasticity locus exist and that they correspond to different frequencies of the alternative phenotypes. Second, studying chromatin states and genetic regulatory elements in the locus will elucidate how transcription from the multi-gene locus is regulated.

STAR★METHODS

Detailed methods are provided in the online version of this paper and include the following:

- KEY RESOURCES TABLE
- CONTACT FOR REAGENT AND RESOURCE SHARING
- EXPERIMENTAL MODEL AND SUBJECT DETAILS
- METHOD DETAILS

- CRISPR-Cas9 mutagenesis
- Mouth form phenotyping
- Genetic rescue of *eud-1* mutants
- Co-localization experiments
- Whole-genome sequencing
- Phylogenetic reconstructions
- **QUANTIFICATION AND STATISTICAL ANALYSIS**
- **DATA AND SOFTWARE AVAILABILITY**

SUPPLEMENTAL INFORMATION

Supplemental Information includes four figures, one table, and one data file and can be found with this article online at <https://doi.org/10.1016/j.celrep.2018.05.008>.

ACKNOWLEDGMENTS

We would like to thank Drs. Hernán Burbano and Talia Karasov for discussion. We are also grateful to Drs. Michael Werner, James Lightfoot, Adrian Streit, and Ms. Tess Renahan for giving their comments on the manuscript. The *sul-2.2.1* mutant line was kindly provided by Dr. Erik Ragsdale. The work was funded by the Max Planck Society.

AUTHOR CONTRIBUTIONS

Conceptualization, B.S., N.P., M.R.K., and R.J.S.; Methodology, B.S., N.P., M.D., C.R., M.R.K., and R.J.S.; Formal Analysis, B.S. and N.P.; Investigation, B.S., N.P., M.D., H.W., and W.R.; Resources, H.W. and W.R.; Writing – Original Draft, B.S. and R.J.S.; Writing – Review & Editing, B.S., N.P., M.D., and R.J.S.; Visualization, B.S. and N.P.; Supervision, C.R. and R.J.S.

DECLARATION OF INTERESTS

The authors declare no competing interests.

Received: February 6, 2018

Revised: April 4, 2018

Accepted: May 2, 2018

Published: June 5, 2018

REFERENCES

- Adams, E.J., and Parham, P. (2001). Species-specific evolution of *MHC* class I genes in the higher primates. *Immunol. Rev.* *183*, 41–64.
- Altun, Z.F., and Hall, D.H. (2017). Handbook of *C. elegans* anatomy. In *WormAtlas*. <http://www.wormatlas.org/hermaphrodite/hermaphroditehomepage.htm>.
- Beesley, C.E., Jackson, M., Young, E.P., Vellodi, A., and Winchester, B.G. (2005). Molecular defects in Sanfilippo syndrome type B (mucopolysaccharidosis IIIB). *J. Inher. Metab. Dis.* *28*, 759–767.
- Bento, G., Ogawa, A., and Sommer, R.J. (2010). Co-option of the hormone-signalling module dafachronic acid-DAF-12 in nematode evolution. *Nature* *466*, 494–497.
- Charlesworth, D. (2015). The status of supergenes in the 21st century: recombination suppression in Batesian mimicry and sex chromosomes and other complex adaptations. *Evol. Appl.* *9*, 74–90.
- Chen, J.-M., Cooper, D.N., Chuzhanova, N., Férec, C., and Patrinos, G.P. (2007). Gene conversion: mechanisms, evolution and human disease. *Nat. Rev. Genet.* *8*, 762–775.
- Connallon, T., and Clark, A.G. (2010). Gene duplication, gene conversion and the evolution of the Y chromosome. *Genetics* *186*, 277–286.
- Cortesi, F., Musilová, Z., Stieb, S.M., Hart, N.S., Siebeck, U.E., Malmström, M., Tørresen, O.K., Jentoft, S., Cheney, K.L., Marshall, N.J., et al. (2015). Ancestral duplications and highly dynamic opsin gene evolution in percomorph fishes. *Proc. Natl. Acad. Sci. USA* *112*, 1493–1498.
- Cribari-Neto, F., and Zeileis, A. (2010). Beta regression in R. *J. Stat. Softw.* *34*, 1–24.
- Delarbre, C., Jaulin, C., Kourilsky, P., and Gachelin, G. (1992). Evolution of the major histocompatibility complex: a hundred-fold amplification of MHC class I genes in the African pigmy mouse *Nannomys setulosus*. *Immunogenetics* *37*, 29–38.
- Edwards, S.V., and Hedrick, P.W. (1998). Evolution and ecology of MHC molecules: from genomics to sexual selection. *Trends Ecol. Evol.* *13*, 305–311.
- Goebel, J., Promerová, M., Bonadonna, F., McCoy, K.D., Serbielle, C., Strandh, M., Yannic, G., Burri, R., and Fumagalli, L. (2017). 100 million years of multigene family evolution: origin and evolution of the avian MHC class IIB. *BMC Genomics* *18*, 460.
- Hallast, P., Nagirnjaja, L., Margus, T., and Laan, M. (2005). Segmental duplications and gene conversion: Human luteinizing hormone/chorionic gonadotropin beta gene cluster. *Genome Res.* *15*, 1535–1546.
- Joron, M., Frezal, L., Jones, R.T., Chamberlain, N.L., Lee, S.F., Haag, C.R., Whibley, A., Becuwe, M., Baxter, S.W., Ferguson, L., et al. (2011). Chromosomal rearrangements maintain a polymorphic supergene controlling butterfly mimicry. *Nature* *477*, 203–206.
- Katoh, K., and Standley, D.M. (2013). MAFFT multiple sequence alignment software version 7: improvements in performance and usability. *Mol. Biol. Evol.* *30*, 772–780.
- Kieninger, M.R., Ivers, N.A., Rödelsperger, C., Markov, G.V., Sommer, R.J., and Ragsdale, E.J. (2016). The nuclear hormone receptor NHR-40 acts downstream of the sulfatase EUD-1 as part of a developmental plasticity switch in *Pristionchus*. *Curr. Biol.* *26*, 2174–2179.
- Kim, K.-W., Bennison, C., Hemmings, N., Brookes, L., Hurley, L.L., Griffith, S.C., Burke, T., Birkhead, T.R., and Slate, J. (2017). A sex-linked supergene controls sperm morphology and swimming speed in a songbird. *Nat. Ecol. Evol.* *1*, 1168–1176.
- Kunte, K., Zhang, W., Tenger-Trolander, A., Palmer, D.H., Martin, A., Reed, R.D., Mullen, S.P., and Kronforst, M.R. (2014). *doublesex* is a mimicry supergene. *Nature* *507*, 229–232.
- Langmead, B., and Salzberg, S.L. (2012). Fast gapped-read alignment with Bowtie 2. *Nat. Methods* *9*, 357–359.
- Lenth, R. (2016). Least-squares means: the R package lsmeans. *J. Stat. Softw.* *69*, 1–33.
- Li, J., Cocker, J.M., Wright, J., Webster, M.A., McMullan, M., Dyer, S., Swarbreck, D., Caccamo, M., Oosterhout, C.V., and Gilmartin, P.M. (2016). Genetic architecture and evolution of the S locus supergene in *Primula vulgaris*. *Nat. Plants* *2*, 16188.
- Lynch, M. (2007). *The Origins of Genome Architecture* (Sinauer Associates).
- Lynch, M., O’Hely, M., Walsh, B., and Force, A. (2001). The probability of preservation of a newly arisen gene duplicate. *Genetics* *159*, 1789–1804.
- Nishikawa, H., Iijima, T., Kajitani, R., Yamaguchi, J., Ando, T., Suzuki, Y., Sugano, S., Fujiyama, A., Kosugi, S., Hirakawa, H., et al. (2015). A genetic mechanism for female-limited Batesian mimicry in *Papilio* butterfly. *Nat. Genet.* *47*, 405–409.
- Norman, P.J., Norberg, S.J., Guethlein, L.A., Nemat-Gorgani, N., Royce, T., Wroblewski, E.E., Dunn, T., Mann, T., Alicata, C., Hollenbach, J.A., et al. (2017). Sequences of 95 human *MHC* haplotypes reveal extreme coding variation in genes other than highly polymorphic *HLA class I* and *II*. *Genome Res.* *27*, 813–823.
- Pires-daSilva, A., and Sommer, R.J. (2004). Conservation of the global sex determination gene *tra-1* in distantly related nematodes. *Genes Dev.* *18*, 1198–1208.
- Pracana, R., Levantis, I., Martínez-Ruiz, C., Stolle, E., Priyam, A., and Wurm, Y. (2017). Fire ant social chromosomes: Differences in number, sequence and expression of odorant binding proteins. *Evol. Lett.* *1*, 199–210.

- Projecto-Garcia, J., Biddle, J.F., and Ragsdale, E.J. (2017). Decoding the architecture and origins of mechanisms for developmental polyphenism. *Curr. Opin. Genet. Dev.* *47*, 1–8.
- Purcell, J., Brelsford, A., Wurm, Y., Perrin, N., and Chapuisat, M. (2014). Convergent genetic architecture underlies social organization in ants. *Curr. Biol.* *24*, 2728–2732.
- Ragsdale, E.J., and Ivers, N.A. (2016). Specialization of a polyphenism switch gene following serial duplications in *Pristionchus* nematodes. *Evolution* *70*, 2155–2166.
- Ragsdale, E.J., Müller, M.R., Rödelberger, C., and Sommer, R.J. (2013). A developmental switch coupled to the evolution of plasticity acts through a sulfatase. *Cell* *155*, 922–933.
- Ragsdale, E.J., Kanzaki, N., and Herrmann, M. (2015). Taxonomy and natural history: the genus *Pristionchus*. In *Pristionchus Pacificus: A Nematode Model for Comparative and Evolutionary Biology*, R.J. Sommer, ed. (BRILL), pp. 77–120.
- Rivera-Colón, Y., Schutsky, E.K., Kita, A.Z., and Garman, S.C. (2012). The structure of human GALNS reveals the molecular basis for mucopolysaccharidosis IV A. *J. Mol. Biol.* *423*, 736–751.
- Rödelberger, C., Meyer, J.M., Prabh, N., Lanz, C., Bemm, F., and Sommer, R.J. (2017). Single-molecule sequencing reveals the chromosome-scale genomic architecture of the nematode model organism *Pristionchus pacificus*. *Cell Rep.* *21*, 834–844.
- Schindelin, J., Arganda-Carreras, I., Frise, E., Kaynig, V., Longair, M., Pietzsch, T., Preibisch, S., Rueden, C., Saalfeld, S., Schmid, B., et al. (2012). Fiji: an open-source platform for biological-image analysis. *Nat. Methods* *9*, 676–682.
- Schlager, B., Wang, X., Braach, G., and Sommer, R.J. (2009). Molecular cloning of a dominant roller mutant and establishment of DNA-mediated transformation in the nematode *Pristionchus pacificus*. *Genesis* *47*, 300–304.
- Schwander, T., Libbrecht, R., and Keller, L. (2014). Supergenes and complex phenotypes. *Curr. Biol.* *24*, R288–R294.
- Sela, I., Ashkenazy, H., Katoh, K., and Pupko, T. (2015). GUIDANCE2: accurate detection of unreliable alignment regions accounting for the uncertainty of multiple parameters. *Nucleic Acids Res.* *43* (W1), W7–W14.
- Seroby, V., Ragsdale, E.J., Müller, M.R., and Sommer, R.J. (2013). Feeding plasticity in the nematode *Pristionchus pacificus* is influenced by sex and social context and is linked to developmental speed. *Evol. Dev.* *15*, 161–170.
- Seroby, V., Xiao, H., Namdeo, S., Rödelberger, C., Sieriebriennikov, B., Witte, H., Röseler, W., and Sommer, R.J. (2016). Chromatin remodelling and antisense-mediated up-regulation of the developmental switch gene *eud-1* control predatory feeding plasticity. *Nat. Commun.* *7*, 12337.
- Sharon, D., Glusman, G., Pilpel, Y., Khen, M., Gruetzner, F., Haaf, T., and Lancet, D. (1999). Primate evolution of an olfactory receptor cluster: diversification by gene conversion and recent emergence of pseudogenes. *Genomics* *67*, 24–36.
- Smithson, M., and Verkuilen, J. (2006). A better lemon squeezer? Maximum-likelihood regression with beta-distributed dependent variables. *Psychol. Methods* *11*, 54–71.
- Stamatakis, A. (2014). RAxML version 8: a tool for phylogenetic analysis and post-analysis of large phylogenies. *Bioinformatics* *30*, 1312–1313.
- Stiernagle, T. (2016). Maintenance of *C. elegans*. *WormBook*, 1–11.
- Susoy, V., Ragsdale, E.J., Kanzaki, N., and Sommer, R.J. (2015). Rapid diversification associated with a macroevolutionary pulse of developmental plasticity. *eLife* *4*, e05463.
- Timmermans, M.J.T.N., Baxter, S.W., Clark, R., Heckel, D.G., Vogel, H., Collins, S., Papanicolaou, A., Fukova, I., Joron, M., Thompson, M.J., et al. (2014). Comparative genomics of the mimicry switch in *Papilio dardanus*. *Proc. Biol. Sci.* *281*, 20140465.
- Trowsdale, J. (2002). The gentle art of gene arrangement: the meaning of gene clusters. *Genome Biol.* *3*, comment2002.1–comment2002.5.
- Walsh, J.B. (1987). Sequence-dependent gene conversion: can duplicated genes diverge fast enough to escape conversion? *Genetics* *117*, 543–557.
- Wang, J., Wurm, Y., Nipitwattanaphon, M., Riba-Grognuz, O., Huang, Y.-C., Shoemaker, D., and Keller, L. (2013). A Y-like social chromosome causes alternative colony organization in fire ants. *Nature* *493*, 664–668.
- Werner, M.S., Sieriebriennikov, B., Loschko, T., Namdeo, S., Lenuzzi, M., Dardiry, M., Renahan, T., Sharma, D.R., and Sommer, R.J. (2017). Environmental influence on *Pristionchus pacificus* mouth form through different culture methods. *Sci. Rep.* *7*, 7207.
- West-Eberhard, M.J. (2003). *Developmental Plasticity and Evolution* (Oxford University Press).
- West-Eberhard, M.J. (2005). Developmental plasticity and the origin of species differences. *Proc. Natl. Acad. Sci. USA* *102* (Suppl 1), 6543–6549.
- Wilecki, M., Lightfoot, J.W., Susoy, V., and Sommer, R.J. (2015). Predatory feeding behaviour in *Pristionchus* nematodes is dependent on phenotypic plasticity and induced by serotonin. *J. Exp. Biol.* *218*, 1306–1313.
- Witte, H., Moreno, E., Rödelberger, C., Kim, J., Kim, J.S., Streit, A., and Sommer, R.J. (2015). Gene inactivation using the CRISPR/Cas9 system in the nematode *Pristionchus pacificus*. *Dev. Genes Evol.* *225*, 55–62.
- Zakharova, I.S., Shevchenko, A.I., and Zakian, S.M. (2009). Monoallelic gene expression in mammals. *Chromosoma* *118*, 279–290.
- Zhang, W., Westerman, E., Nitzany, E., Palmer, S., and Kronforst, M.R. (2017). Tracing the origin and evolution of supergene mimicry in butterflies. *Nat. Commun.* *8*, 1269.
- Zhao, Z., Hewett-Emmett, D., and Li, W.H. (1998). Frequent gene conversion between human red and green opsin genes. *J. Mol. Evol.* *46*, 494–496.

STAR★METHODS

KEY RESOURCES TABLE

REAGENT or RESOURCE	SOURCE	IDENTIFIER
Bacterial and Virus Strains		
<i>Escherichia coli</i> : Strain OP50	<i>Caenorhabditis</i> genetics center	RRID:WB-STRAIN:OP50
Chemicals, Peptides, and Recombinant Proteins		
Alt-R CRISPR-Cas9 tracrRNA	Integrated DNA Technologies	Cat#1072534
EnGen Cas9 NLS, <i>S. pyogenes</i>	New England Biolabs	Cat#M0646M
Deposited Data		
Whole-genome sequences of <i>Allodiplogaster sudhausi</i>	This paper	ENA: ERS2028649
Whole-genome sequences of <i>Allodiplogaster sudhausi</i>	This paper	ENA: ERS2028650
Experimental Models: Organisms/Strains		
<i>Pristionchus pacificus</i> : strain PS312	Stock of Dep. IV, MPI Developmental Biology Tuebingen	RRID:WB-STRAIN:PS312
<i>Pristionchus pacificus</i> : strain RS2561: <i>eud-1(tu445)</i>	Ragsdale et al., 2013	N/A
<i>Pristionchus pacificus</i> : strain EJR1033: <i>sul-2.2.1(iub2)</i>	Ragsdale and Ivers, 2016	N/A
<i>Pristionchus pacificus</i> : strain RS3191: <i>nag-1(tu1137)</i>	This paper	N/A
<i>Pristionchus pacificus</i> : strain RS3192: <i>nag-2(tu1138)</i>	This paper	N/A
<i>Pristionchus pacificus</i> : strain RS3195: <i>nag-1(tu1142)</i> <i>nag-2(tu1143)</i>	This paper	N/A
<i>Pristionchus pacificus</i> : strain RS3198: <i>tuDf1[nag-1</i> <i>sul-2.2.1 eud-1 nag-2]</i>	This paper	N/A
<i>Pristionchus pacificus</i> : strain RS2653: <i>tuEx177</i> <i>[eud-1p::TurboRFP::rpl-23utr]</i>	Ragsdale et al., 2013	N/A
<i>Pristionchus pacificus</i> : strain RS3250: <i>tuEx275</i> <i>[nag-1p::Venus::rpl-23utr]</i>	This paper	N/A
<i>Pristionchus pacificus</i> : strain RS3381: <i>tuEx280</i> <i>[nag-2p::TurboRFP::rpl-23utr]</i>	This paper	N/A
<i>Pristionchus pacificus</i> : strain RS3200: <i>eud-1(tu445)</i> ; <i>tuEx271[eud-1p::eud-1(+):cds::rpl-23utr]</i>	This paper	N/A
<i>Pristionchus pacificus</i> : strain RS3201: <i>eud-1(tu445)</i> ; <i>tuEx272[eud-1p::eud-1(+):cds::rpl-23utr]</i>	This paper	N/A
<i>Pristionchus pacificus</i> : strain RS3268: <i>eud-1(tu445)</i> ; <i>tuEx276[eud-1p::sul-2.2.1cds::rpl-23utr]</i>	This paper	N/A
<i>Pristionchus pacificus</i> : strain RS3272: <i>eud-1(tu445)</i> ; <i>tuEx278[eud-1p::sul-2.2.1cds::rpl-23utr]</i>	This paper	N/A
<i>Allodiplogaster sudhausi</i> : strain SB413	Stock of Dep. IV, MPI Developmental Biology Tuebingen	N/A
Oligonucleotides		
sgRNA target sequence: exon 5 of <i>nag-1</i> and <i>nag-2</i> : CCTGGTGGGATTGGAGCCAT	This paper	N/A
crRNA target sequence: exon 4 of <i>nag-2</i> : TCTGTGGAACGATGATTGCA	This paper	N/A
crRNA target sequence: <i>dpy-23</i> : CAACGACAAATTGACGTTAG	This paper	N/A
crRNA target sequence: <i>F40E10.6</i> : AGGGTGAGCAGAGACATGAT	This paper	N/A
Recombinant DNA		
Plasmid: pUC19- <i>egl-20p::TurboRFP::rpl-23utr</i>	Schlager et al., 2009	N/A
Plasmid: pUC19- <i>eud-1p::eud-1cds::rpl-23utr</i>	This paper	N/A

(Continued on next page)

Continued

REAGENT or RESOURCE	SOURCE	IDENTIFIER
Plasmid: pUC19- <i>eud-1p::sul-2.2.1cds::rpl-23utr</i>	This paper	N/A
Plasmid: pUC19- <i>nag-1p::Venus::rpl-23utr</i>	This paper	N/A
Plasmid: pUC19- <i>nag-2p::TurboRFP::rpl-23utr</i>	This paper	N/A
Software and Algorithms		
Bowtie 2	Langmead and Salzberg, 2012	N/A
FIJI	Schindelin et al., 2012	RRID:SCR_002285
DISCOVAR <i>de novo</i>	https://software.broadinstitute.org/software/discovar/blog/	N/A
MAFFT	Katoh and Standley, 2013	RRID:SCR_011811
GUIDANCE2	Sela et al., 2015	N/A
RAXML	Stamatakis, 2014	RRID:SCR_006086
R	http://www.r-project.org/	RRID:SCR_001905

CONTACT FOR REAGENT AND RESOURCE SHARING

Further information and requests for resources and reagents should be directed to and will be fulfilled by the Lead Contact, Ralf J. Sommer (ralf.sommer@tuebingen.mpg.de).

EXPERIMENTAL MODEL AND SUBJECT DETAILS

Stock cultures of *P. pacificus* wild-type strain PS312, all the mutant and transgenic strains used in this study and *A. sudhausi* SB413 were maintained following standard protocols for *C. elegans* (Stiernagle, 2016). Specifically, worms were kept at room temperature (20–25°C) on 6 cm plates with nematode growth medium (NGM) consisting of 1.7% agar, 3 g/L NaCl, 2.5 g/L tryptone, 1 mM CaCl₂, 1 mM MgSO₄, 5 mg/L cholesterol and 25 mM KPO₄ buffer (diluted from a 1 M stock solution of 108.3 g/L KH₂PO₄ and 35.6 g/L K₂HPO₄ with pH adjusted to 6.0). *Escherichia coli* OP50 was used as the food source. Bacteria were grown overnight at 37°C in L Broth consisting of 10 g/L tryptone, 5 g/L yeast extract and 5 g/L NaCl with pH adjusted to 7.0. Bacterial lawns were grown from 250–400 uL of the overnight culture on NGM agar plates at room temperature, and nematodes were transferred to the lawns. For maintenance, *P. pacificus* cultures were propagated clonally by passing self-fertilizing hermaphrodites only. For the experiments where presence of males was required, males spontaneously formed in stock cultures were allowed to breed and thus increase the male proportion in the population. These mixed-sex cultures were propagated by passing multiple animals of both sexes and different developmental stages to new plates.

METHOD DETAILS**CRISPR-Cas9 mutagenesis**

Procedure for CRISPR-Cas9 mutagenesis was based on the existing protocol for *P. pacificus* (Witte et al., 2015) and included several modifications described below. Single guide RNA (sgRNA) obtained from Toolgen was used to target exon 5 in *nag-1* and *nag-2*, whereas the rest of the loci were targeted using hybridized target-specific CRISPR RNAs (crRNAs) and universal *trans*-activating CRISPR RNA (tracrRNA) obtained from Integrated DNA Technologies (Alt-R product line). To hybridize crRNA and tracrRNA, 10 uL of the 100 uM stock of each molecule were combined, denatured at 95°C for 5 min and allowed to cool down and anneal at room temperature for 5 min. 5 uL of the hybridization product or 2 uL of 3 ug/uL sgRNA was combined with 2 uL of 20 uM Cas9 protein (New England Biolabs) and incubated at room temperature for 5 min. The mixture was diluted with Tris-EDTA buffer to the total volume of 25 uL and injected in the gonad rachis in 1 day old hermaphrodites. The sgRNA and all the crRNAs were designed to target 20 bp upstream of protospacer adjacent motifs (PAMs) marked in Figure S1A. Molecular lesions were detected in F1 progeny by high-resolution melting curve analysis of PCR amplicons using LightCycler 480 High Resolution Melting Master on a LightCycler 480 Instrument II (Roche). Presence of mutations in candidate amplicons was verified by Sanger sequencing. To detect large rearrangements that affected multiple genes in the locus (Figure S1B), genomic DNA was extracted from worms, for which no PCR amplicon containing the sgRNA or crRNA target site could be obtained. Next generation sequencing libraries were prepared using TruSeq DNA PCR-Free Low Throughput Library Prep Kit and sequenced on a HiSeq 3000 machine (Illumina). Reads were mapped to the El Paco assembly of the *P. pacificus* genome (Rödelsperger et al., 2017) using Bowtie 2 (Langmead and Salzberg, 2012). Consequently, read coverage in the locus of interest was visually inspected to detect any deviations from the pattern in the surrounding regions.

Mouth form phenotyping

Phenotyping was done in two culture conditions. Culturing *P. pacificus* on NGM agar plates (as stock cultures are maintained, see above) induces the Eu morph and thus enables identification of Eu-deficient (Eud) phenotype, whereas culturing the worms in liquid S-medium represses the Eu morph and facilitates identification of the Eu-constitutive (Euc) mutant phenotype (Werner et al., 2017). S-medium consists of 5.85 g/L NaCl, 1 g/L K₂HPO₄, 6 g/L KH₂PO₄, 5 mg/L cholesterol, 3 mM CaCl₂, 3 mM MgSO₄, 18.6 mg/L disodium EDTA, 6.9 mg/L FeSO₄·7H₂O, 2 mg/L MnCl₂·4H₂O, 2.9 mg/L ZnSO₄·7H₂O, 0.25 mg/L CuSO₄·5H₂O and 10 mM Potassium citrate buffer (diluted from a 1 M stock solution of 20 g/L citric acid monohydrate and 293.5 g/L tri-potassium citrate monohydrate with pH adjusted to 6.0) (Stiernagle, 2016). Liquid cultures were started with nematode eggs extracted by bleaching animals collected from stock cultures (Stiernagle, 2016; Werner et al., 2017). For this, worms were washed from plates with water and incubated for 10 min in a mixture of household bleach at 1:5 final dilution and NaOH at the final concentration of 0.5 M. Extracted eggs were pelleted down, washed with water and added to 10 mL of S-medium that contained re-suspended *E. coli* OP50 in the amount corresponding to 100 mL of an overnight bacterial culture (see above) with OD₆₀₀ of 0.5. Flasks with liquid cultures were incubated on a shaking platform at 180 rpm. Only adults were phenotyped for mouth form. Animals were immobilized on agar pads containing 0.3% NaN₃ and examined using differential interference contrast (DIC) microscopy. The Eu morph was distinguished from the St morph based on the presence of the right ventrosublateral tooth, the shape of the dorsal tooth and the width of the mouth (buccal cavity).

Genetic rescue of *eud-1* mutants

Constructs for the genetic rescue of *eud-1(tu445)* mutants were made by fusing 2 kb of sequence upstream of the first ATG codon of the *eud-1* gene with wild-type coding DNA sequence (CDS) of either *eud-1* or *sul-2.2.1* and 3' untranslated region (UTR) of a ribosomal gene *rpl-23* (Data S1; Figure S2A). Previously published CDS sequence of *eud-1* was used (Ragsdale et al., 2013) and CDS sequence of *sul-2.2.1* was identified based on the available gene prediction (Rödelsperger et al., 2017) and verified with rapid amplification of cDNA ends (RACE). Synthetic gBlocks fragments containing the CDS sequences were obtained from Integrated DNA Technologies. pUC19-based plasmids carrying the rescue constructs were assembled using NEBuilder HiFi DNA Assembly Master Mix (New England Biolabs). For transformation, complex arrays were made by digesting the rescue construct, a tail-specific transformation marker (*egl-20p::TurboRFP*) and *eud-1* mutant genomic DNA with the restriction enzyme FastDigest PstI (Thermo Fisher Scientific), followed by a clean-up using Wizard SV Gel and PCR Clean-Up System (Promega), and mixing the digested components. Final concentrations in the mix were 10 ng/uL for each plasmid and 60 ng/uL for gDNA. Transformation arrays were injected in the gonad rachis in 1 day old hermaphrodites (Schlager et al., 2009). F1 progeny were examined under a fluorescent dissecting microscope and animals expressing transformation marker were isolated and allowed to self-fertilize.

Co-localization experiments

Reporter constructs for *nag-1* and *nag-2* were made by cloning a sequence upstream of the first ATG codon of the respective gene (5.1 kb for *nag-1* and 3.9 kb for *nag-2*) into a pUC19-based plasmid containing a fluorescent protein (Venus for *nag-1* and TurboRFP for *nag-2*) and the 3' UTR of the ribosomal gene *rpl-23* (Data S1). Cloning was done using NEBuilder HiFi DNA Assembly Master Mix (New England Biolabs). Complex arrays were prepared and transgenic lines were created as described above for the *eud-1* rescue experiments with the exception that wild-type gDNA was used in the transformation arrays instead of mutant gDNA. To establish co-localization of expression of different genes, animals carrying the *tuEx275[nag-1p::Venus]* reporter were crossed either with *tuEx280[nag-2p::TurboRFP]* or with previously available *tuEx177[eud-1p::TurboRFP]*, and F1 progeny were microscopically examined. For crossing, small bacterial lawns were grown from 10–50 uL of bacterial culture. Up to six adult males of one strain were transferred to a plate containing one or two hermaphrodites of the other strain. Hermaphrodites used for mating were visually older and had no visible eggs inside the uteri, which indicated that most of self-produced sperm had been used and thus the probability of self-fertilization was reduced. Mating success was verified by observing sex ratio in the progeny. Cross progeny were immobilized on agar pads containing 0.3% NaN₃ and imaged using a Leica TCS SP8 confocal microscope. Post-processing of images was done using FIJI [version 1.0] (Schindelin et al., 2012). The main figures contain expression patterns in the head region. Additionally, *nag-1* was expressed in the oviduct and *nag-2* was expressed in the vulva and, occasionally, in pharyngeal gland cells (Figure S2C–E).

Whole-genome sequencing

A. sudhausi worms from nutrient depleted plates were rinsed with M9 buffer (3 g/L KH₂PO₄, 6 g/L Na₂HPO₄, 5 g/L NaCl, 1 mM MgSO₄) and the worm pellet was collected by centrifugation at 1300 rpm for 3 minutes at 4°C. The pellet was immediately frozen by pouring liquid nitrogen onto it and then ground to a fine powder using mortar and pestle. The powder was transferred to the lysis buffer from Genomic DNA Buffer Set (QIAGEN) and Genomic-tip 100/G columns (QIAGEN) were used for DNA extraction as per the manufacturer's protocol. We used Qubit 2.0 Fluorometer (Thermo Fisher Scientific) and NanoDrop ND 1000 spectrometer (Peqlab) for DNA quality and quantity determination.

Library preparation for the whole genome sequencing was done with TruSeq DNA PCR-Free Library Prep kit following the manufacturer's protocol and the prepared libraries were run on Illumina MiSeq. The initial assembly was generated with DISCOVAR *de novo* assembler (<https://software.broadinstitute.org/software/discovar/blog/>). Then, we checked for *E. coli* contamination by BLASTN searches against the NCBI nt database and removed contaminated contigs after manual inspection to create the final assembly.

Phylogenetic reconstructions

Multiple sequence alignments were created by MAFFT (version 7.271) (Katoch and Standley, 2013) and unreliable alignment positions were identified and removed through GUIDANCE2 (version 2.02) (Sela et al., 2015). After manual inspection, each alignment was passed to RAxML (version 8.2.4) (Stamatakis, 2014) for making maximum likelihood trees with 100 bootstrap replicates.

QUANTIFICATION AND STATISTICAL ANALYSIS

Morph frequencies were compared by fitting beta regression using the R package betareg (Cribari-Neto and Zeileis, 2010). Since morph ratios in some strains included the extremes 0 and 1, we followed the guidelines outlined by Smithson and Verkuilen and applied a $(y*(n-1)+0.5)/n$ transformation, where y is the response variable and n is the sample size (Smithson and Verkuilen, 2006). Post hoc pairwise comparison was done using the R package lsmeans with false discovery rate correction of the p values (Lenth, 2016). All p values < 0.05 are summarized with asterisks in corresponding figures. For strains carrying mutations in *nag-2*, *sul-2.2.1*, *eud-1*, *nag-1* or in any combination of these genes, at least three biological replicates with at least 50 individuals per replicate were counted for each sex. For strains in which genes outside of the supergene were altered, only one biological replicate was collected and only hermaphrodites were phenotyped. For transgenic *eud-1* rescue lines, at least three biological replicates with at least 30 transgenic individuals per replicate were counted and only hermaphrodites were phenotyped.

DATA AND SOFTWARE AVAILABILITY

The whole-genome sequencing data for *A. sudhausi* are deposited in the European Nucleotide Archive at <https://www.ebi.ac.uk/ena> with sample accession numbers ENA: ERS2028649 and ERS2028650.

FASTA files containing all the gene predictions used in this study are provided in the supplemental file [Data S1](#).

Cell Reports, Volume 23

Supplemental Information

A Developmental Switch

Generating Phenotypic Plasticity

Is Part of a Conserved Multi-gene Locus

Bogdan Sieriebriennikov, Neel Prabh, Mohannad Dardiry, Hanh Witte, Waltraud Röseler, Manuela R. Kieninger, Christian Rödelsperger, and Ralf J. Sommer

Supplemental information

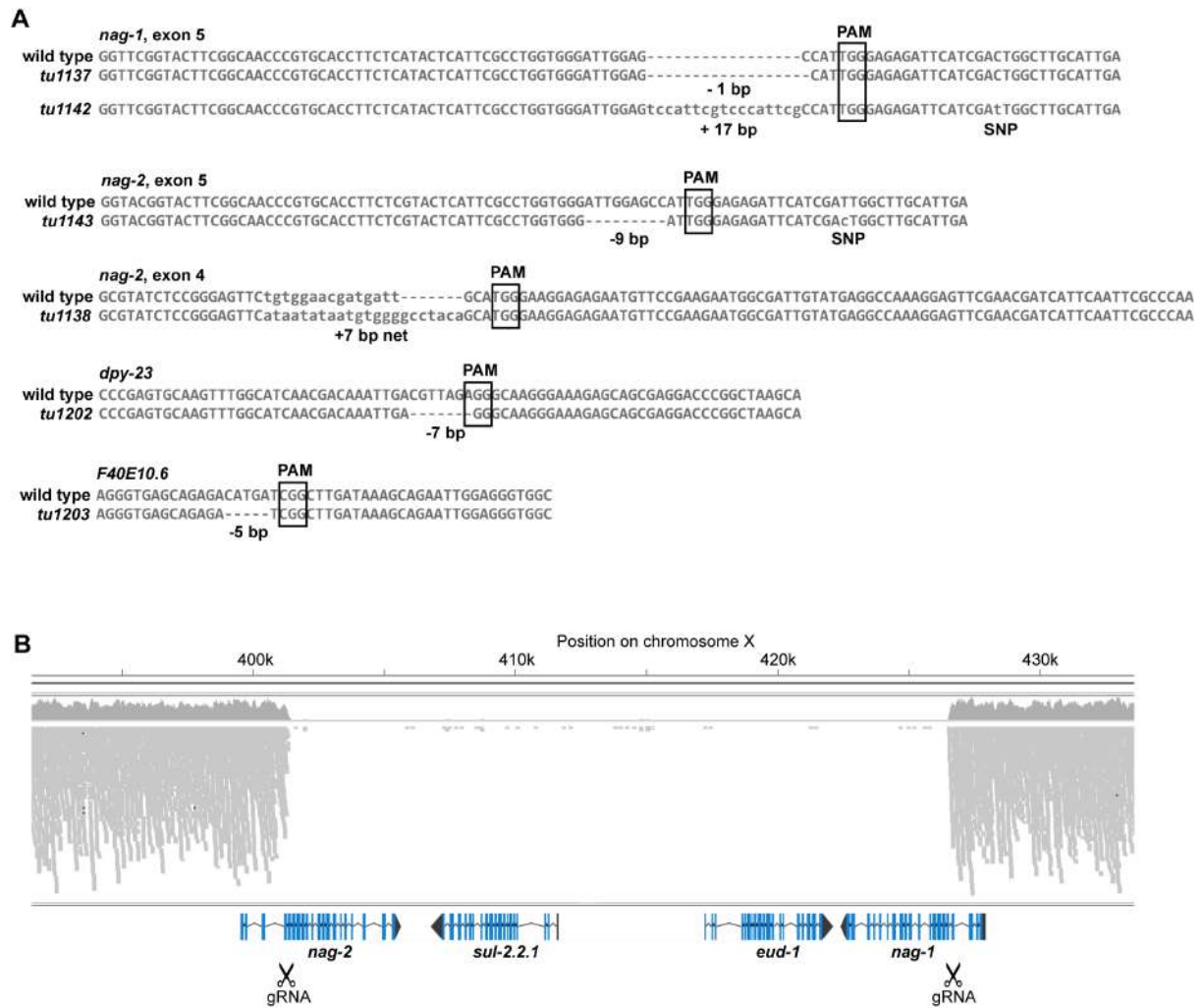


Figure S1. Molecular lesions in CRISPR/Cas9 mutants. Related to Figure 2. (A) Alignment of wild type and *nag-1* and *nag-2* mutant sequences. PAM = protospacer adjacent motif. All sgRNA/crRNAs were designed to target 20 bp upstream of PAMs. SNP = single nucleotide polymorphism. (B) Whole-genome resequencing reads mapping to the plasticity multi-gene locus in the quadruple mutant *tuDf1[nag-1 sul-2.2.1 eud-1 nag-2]*.

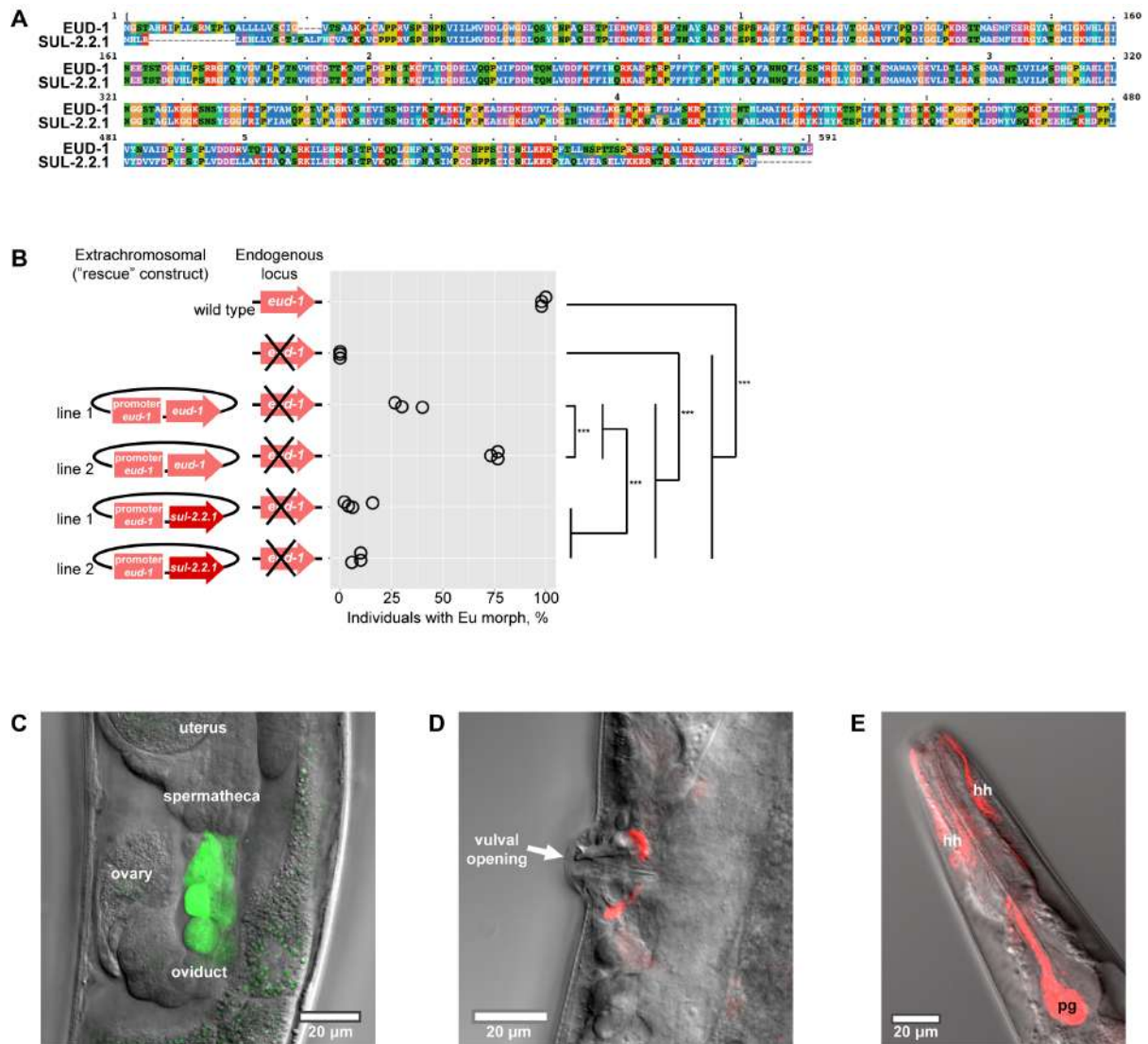


Figure S2. Rescue experiments with sulfatase CDS and expression patterns of *nag* genes. Related to Figure 2. (A) Alignment of amino acid sequences of EUD-1 and SUL-2.2.1 in *P. pacificus*. (B) Overexpression of *sul-2.2.1* can only partially rescue the *eud-1* mutant phenotype. Shown are morph frequencies in wild type PS312 hermaphrodites, the *eud-1*(*tu445*) mutant and the ‘rescue’ lines (top to bottom) *eud-1*(*tu445*);*tuEx271*[*eud-1p*::*eud-1*(+)], *eud-1*(*tu445*);*tuEx272*[*eud-1p*::*eud-1*(+)], *eud-1*(*tu445*);*tuEx278*[*eud-1p*::*sul-2.2.1*(+)] and *eud-1*(*tu445*);*tuEx276*[*eud-1p*::*sul-2.2.1*(+)]. *** = $p < 0.001$. (C) Fragment of the reproductive system in a *P. pacificus* hermaphrodite of the *tuEx275*[*nag-1p*::*Venus*] reporter line. Overlay of DIC image and standard deviation Z-projection of the Venus channel. (D) Vulva region of a hermaphrodite carrying the *tuEx280*[*nag-2p*::*TurboRFP*] reporter. Overlay of DIC image and standard deviation Z-projection of the TurboRFP channel. (E) Head region of an animal of the *tuEx280*[*nag-2p*::*TurboRFP*] reporter line. Overlay of DIC image and maximal intensity Z-projection of the TurboRFP channel. hh = head hypodermis, pg = pharyngeal gland.

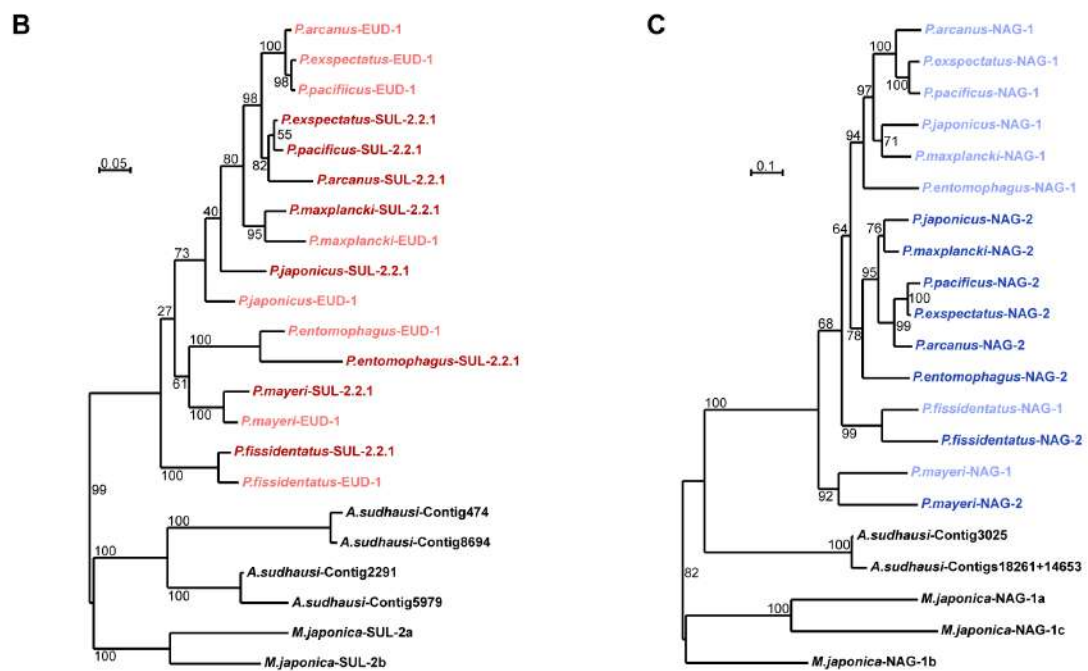
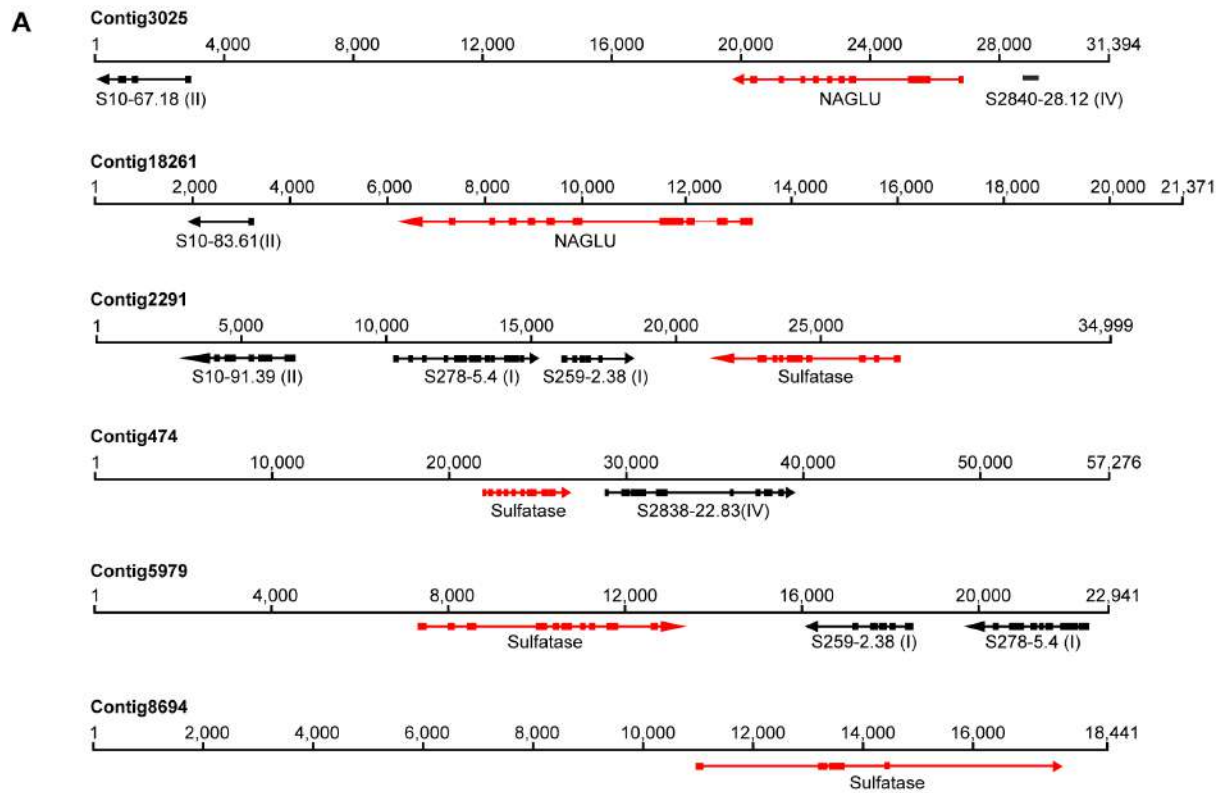


Figure S3. Genomic location of EUD-1 and NAG-1 homologs in newly sequenced *A. sudhausi* and maximum likelihood tree of EUD-1 and NAG-1 homologs in all studied genomes. Related to Figure 3. (A) Contigs of the *A. sudhausi* genome containing EUD-1 and NAG-1 homologs. Neighboring *P. pacificus* homologs are labelled with their chromosome numbers in parenthesis. The scale bar indicates the base position

on each contig. **(B)** Maximum likelihood tree of amino acid sequences of EUD-1 homologs in all studied genomes. **(C)** Maximum likelihood tree of amino acid sequences of NAG-1 homologs in all studied genomes. In B and C, numbers show values of bootstrap support. Only genes shown in Fig. 3A are included.

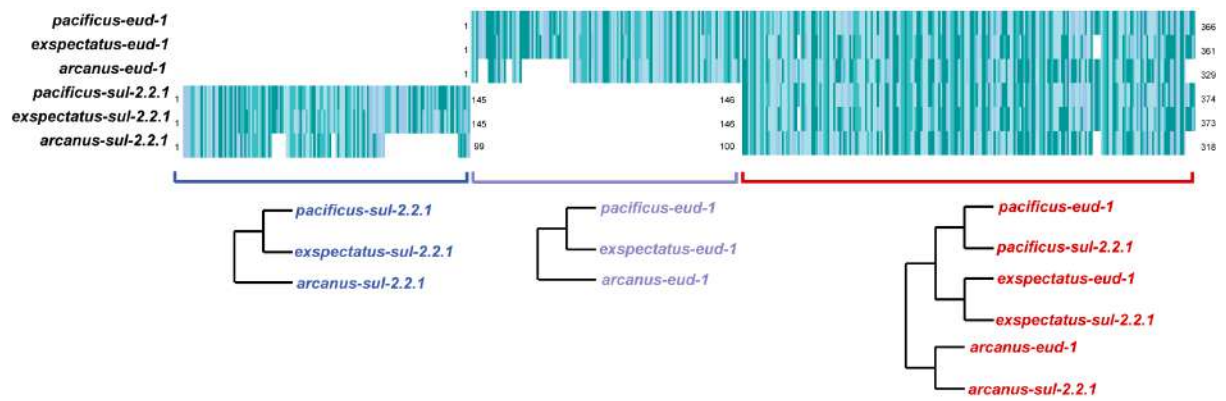


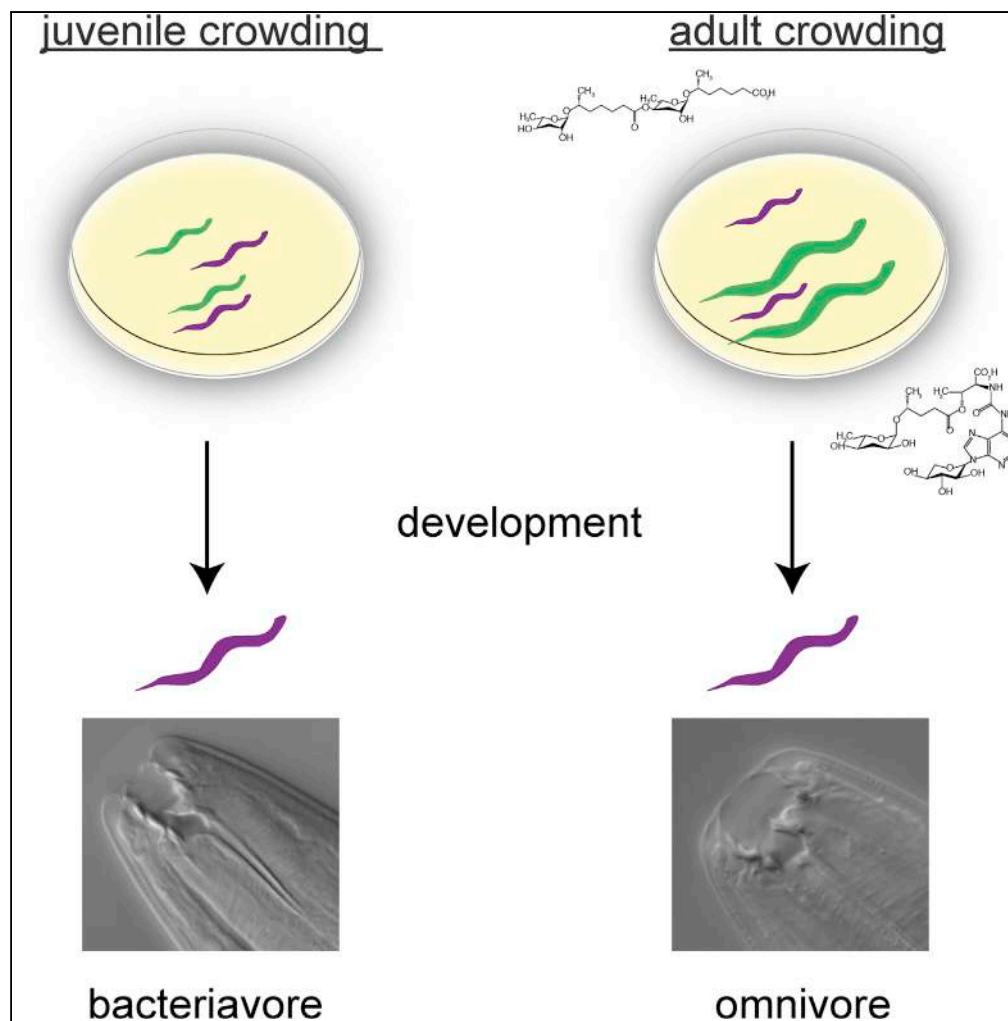
Figure S4. Visual representation of the reliable columns extracted from the alignment of intronic region of *eud-1* and *sul-2.2.1*, and cladograms generated from different parts of the alignment. Related to Figures 3 and 4. Each column is color-coded by the corresponding nucleotide composition for each gene. Absence of color indicates gap at the given alignment position for the given gene. Unrooted tree placed below the alignments were generated based on the parts of the alignment directly above them.

Table S1. Phenotypes of strains with CRISPR/Cas9-induced mutations in genes adjacent to the multi-gene locus in *P. pacificus*. Related to Figure 3.

Culture condition	Strain	Eu	St
Liquid culture	Wild-type PS312	1	49
Liquid culture	<i>dpy-23(tu1202)</i>	2	48
Liquid culture	<i>F40E10.6(tu1203)</i>	1	49
Agar plates	Wild-type PS312	50	0
Agar plates	<i>dpy-23(tu1202)</i>	50	0
Agar plates	<i>F40E10.6(tu1203)</i>	50	0

Article

Adult Influence on Juvenile Phenotypes by Stage-Specific Pheromone Production



Michael S. Werner,
 Marc H. Claaßen,
 Tess Renahan,
 Mohannad Dardiry, Ralf J.
 Sommer

ralf.sommer@tuebingen.mpg.de

HIGHLIGHTS

Novel vital dye method for tracking mixed nematode populations

Adult, but not juvenile, crowding induces the omnivorous morph in *P. pacificus*

Omnivorous morph-inducing pheromones are produced late in development

Age class is an important component of density-dependent phenotypic plasticity

Werner et al., iScience 10,
 123–134
 December 21, 2018 © 2018
 The Author(s).
<https://doi.org/10.1016/j.isci.2018.11.027>

Article

Adult Influence on Juvenile Phenotypes by Stage-Specific Pheromone Production

Michael S. Werner,^{1,2} Marc H. Claaßen,^{1,2} Tess Renahan,^{1,2} Mohannad Dardiry,¹ and Ralf J. Sommer^{1,3,*}

SUMMARY

Many animal and plant species respond to population density by phenotypic plasticity. To investigate if specific age classes and/or cross-generational signaling affect density-dependent plasticity, we developed a dye-based method to differentiate co-existing nematode populations. We applied this method to *Pristionchus pacificus*, which develops a predatory mouth form to exploit alternative resources and kill competitors in response to high population densities. Remarkably, adult, but not juvenile, crowding induces the predatory morph in other juveniles. High-performance liquid chromatography-mass spectrometry of secreted metabolites combined with genetic mutants traced this result to the production of stage-specific pheromones. In particular, the *P. pacificus*-specific di-ascaroside#1 that induces the predatory morph is induced in the last juvenile stage and young adults, even though mouth forms are no longer plastic in adults. Cross-generational signaling between adults and juveniles may serve as an indication of rapidly increasing population size, arguing that age classes are an important component of phenotypic plasticity.

INTRODUCTION

Population density is an important ecological parameter, with higher densities corresponding to increased competition for resources (Hastings, 2013). In addition to density-dependent selection (MacArthur, 1962; Travis et al., 2013), which operates on evolutionary timescales, some organisms can respond dynamically to population density through phenotypic plasticity. For example, plants can sense crowding by detecting the ratio of red (chlorophyll absorbing) to far red (non-absorbing) light, and respond by producing higher shoots (Dudley and Schmitt, 2015). Locusts undergo solitary to swarm (i.e., gregarious) transition as a result of increased physical contact (Pener and Simpson, 2009; Simpson et al., 2001). Intriguingly, population density can also have cross-generational effects, defined here as the density of one age group affecting the phenotypes of another. For example, adult crowding of the desert locust *Schistocerca gregaria* (Maeno and Tanaka, 2008; Simpson and Miller, 2007) and migratory locust *Locusta migratoria* (Chen et al., 2015; Ben Hamouda et al., 2011) also influences the egg size, number, and morphology of their progeny, high population densities of red squirrels elicit hormonal regulation in mothers to influence faster-developing offspring (Dantzer et al., 2013), and crowding in aphids can induce winged progeny from flightless parents (Sloggett and Weisser, 2002; Sutherland, 1969). In many species, population density and cross-generational signaling are communicated by pheromones; however, the precise nature, mechanisms of induction, age specificity, and exact ecological role are not well understood.

Nematodes are a powerful model system to investigate the mechanisms of density-dependent plasticity because many small molecule pheromones that affect plastic phenotypes have been characterized (Butcher, 2017; Butcher et al., 2007; von Reuss et al., 2012). For example, in the model organism *Caenorhabditis elegans*, high population densities induce entry into a stress-resistant dormant “dauer” stage (Fielenbach and Antebi, 2008). The decision to enter dauer was revealed to be regulated by a family of small molecule nematode-derived modular metabolites (NDMMs) called ascarosides that act as pheromones (Butcher et al., 2007, 2008; Jeong et al., 2005). Ascarosides consist of an ascarylose sugar with a fatty acid side chain and modular head and terminal groups (Figure 1A). The level and composition of ascarosides were later shown to be dependent on sex (Chasnov et al., 2007; Izrayelit et al., 2012) and development (Kaplan et al., 2011), although it is thought that early larval development into dauer can be induced by pheromones from all developmental stages (Golden and Riddle, 1982). Subsequent studies revealed that specific NDMMs also regulate other life history traits, such as mating (Chasnov et al., 2007; Izrayelit et al., 2012), social behavior (Srinivasan et al., 2012), and developmental speed (Ludewig et al., 2017). Although NDMMs are broadly conserved (Choe et al., 2012; Dong et al., 2018; Markov et al., 2016), inter- and intraspecific competition have driven the evolution of distinct response regimes (different levels of sensitivity to the

¹Department of Evolutionary Biology, Max Planck Institute for Developmental Biology, Tübingen 72076, Germany

²These authors contributed equally

³Lead Contact

*Correspondence: ralf.sommer@tuebingen.mpg.de

<https://doi.org/10.1016/j.isci.2018.11.027>



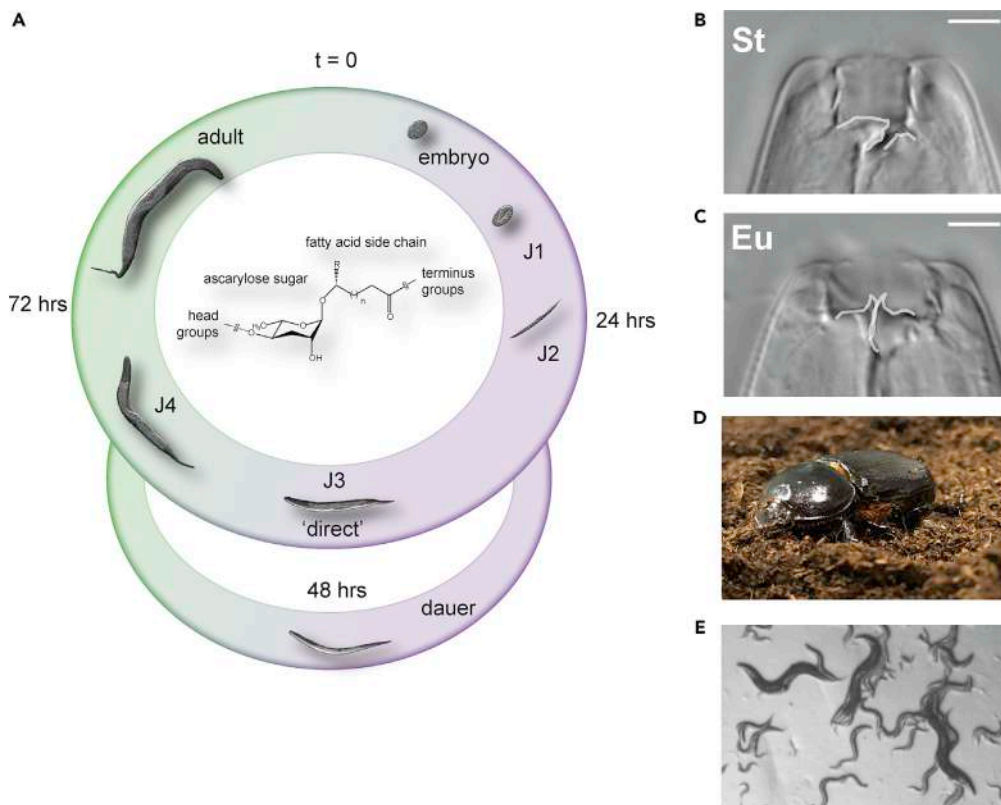


Figure 1. Life Cycle and Developmental Plasticity of the Model Nematode *Pristionchus pacificus*

(A) The life cycle of *P. pacificus* consists of four juvenile stages (J1–J4) until sexual maturation (adult hermaphrodites). Like many nematodes *P. pacificus* can enter a long-living “dormant” dauer state that is resistant to harsh environmental conditions. The decision to continue through the direct life cycle or enter dauer is regulated by small-molecule-excreted ascarosides (chemical structure adapted from [Butcher, 2017](#)).

(B and C) (B) *P. pacificus* can also adopt one of two possible feeding structures; either a microbivorous narrow mouth (stenostomatous, St) or (C) an omnivorous wide mouth (eurystomatous, Eu) with an extra tooth that can be utilized to kill and eat other nematodes or fungi. White lines indicate the presence of an extra tooth (right side) in the Eu morph or its absence in the St morph, and the dorsal tooth (left side), which is narrow and elongated (flint-like) in St and hook like in Eu. Scale bar, 5 μ M. (D) *P. pacificus* is often found in a necromenic association with beetles (e.g., shown here *Oryctes borbonicus*, photo taken by Tess Renahan) in the dauer state and resumes the free-living life cycle upon beetle death to feed on the ensuing microbial bloom. (E) RSC017 mixed-staged worms on agar plates.

same pheromone, or sensitivity to different pheromones) for the same phenotypes ([Bose et al., 2014](#); [Choe et al., 2012](#); [Diaz et al., 2014](#); [Falcke et al., 2018](#); [Greene et al., 2016](#)). In addition, distinct plastic phenotypes have evolved that are regulated by more complex ascaroside structures ([Bose et al., 2012](#)).

In *Pristionchus pacificus*, a soil-associated nematode that is reliably found on scarab beetles ([Figure 1A](#)) ([Herrmann et al., 2006, 2007](#); [Sommer and McGaughan, 2013](#)), an ascaroside dimer (dasc#1) that is not found in *C. elegans* regulates the development of a predatory mouth form ([Bento et al., 2010](#); [Bose et al., 2012](#); [Sommer et al., 2017](#)). Mouth-form plasticity represents an example of a morphological novelty that results in predatory behavior to exploit additional resources and kill competitors. Specifically, adult *P. pacificus* exhibit either a narrow stenostomatous (St) mouth ([Figure 1B](#)), which is restricted to bacterial feeding, or a wide eurystomatous (Eu) mouth with an extra denticle ([Figure 1C](#)), which allows for feeding on bacteria and fungi ([Sanghi et al., 2016](#)), and predation on other nematodes ([Wilecki et al., 2015](#)). This type of phenotypic plasticity is distinct between direct, non-arrested development and indirect (dauer) development because the mouth form decision results in two alternative life history strategies in the adult (for review, see [Sommer & Mayer, 2015](#)). Recent studies in *P. pacificus* have begun to investigate the dynamics and succession of nematodes on decomposing beetle carcasses to better understand the ecological significance of mouth-form plasticity ([Meyer et al., 2017](#)). These studies revealed that on a carcass

(Figure 1D), *P. pacificus* exits the dauer diapause to feed on microbes, and then re-enters dauer after food sources have been exhausted, displaying a “boom-and-bust” ecology (Meyer et al., 2017; Sommer and McLaughran, 2013). Presumably different stages of this succession comprise different ratios of juveniles and adults, and recognizing the age structure of a population as a juvenile could provide predictive value for adulthood. However, it is unknown whether the mouth-form decision is sensitive to crowding by different age classes (example of crowding by different age groups, Figure 1E). More broadly, whereas age classes are known to be important for population growth and density-dependent selection (Hastings, 2013; Charlesworth, 1994; 1972), their role in phenotypic plasticity has thus far been largely unexplored.

Although nematodes have many experimental advantages, including easy laboratory culture and advanced genetic, genomic, and the aforementioned chemical tools, their small size has made investigations at the organismal level and in experimental ecology challenging. For example, no *in vivo* methodologies are currently available to label distinct populations without the need for transgenics, which is only available in select model organisms such as *C. elegans*, *P. pacificus*, and some of their relatives. Here, we combine a novel dye-staining method with the first developmental pheromone profiling in *P. pacificus* to study the potential effects of age on density-dependent plasticity. This vital dye method allows tracking adults with juveniles, or juveniles with juveniles, and can be applied to any nematode system that can be cultured under laboratory conditions. In contrast to dauer, we found that mouth form is strongly affected by cross-generational signaling. Specifically, only adult crowding induces the predatory morph, which is controlled by stage-specific pheromones.

RESULTS

A Vital Dye Method for Labeling Nematode Populations

To directly test if different age groups of *P. pacificus* influence mouth form, we required two synchronized populations to co-habit the same space, yet still be able to identify worms from different age groups. To do so, we developed a dye-staining methodology to robustly differentiate between nematode populations. After trying several vital dyes, we identified that neutral red (Thomas and Lana, 2008) and CellTracker Green BODIPY (Thermo) stain nematode intestines brightly and specifically to their respective channels (Figures 2A–2E and S1, Transparent Methods). These dyes stained all nematodes tested including *C. elegans* (Figure S2) and dauer larvae (Figures S3A and S3B). Both dyes lasted more than 3 days and neutral red >5 days (Figures S3C–S3G), allowing long-term tracking of mixed nematode populations. Importantly, neither neutral red nor CellTracker Green staining affected viability, developmental rate, or the formation of specific morphological structures, such as *P. pacificus* mouth form (Figure S4). Thus, neutral red and CellTracker Green allow specific labeling of worm populations to study age-dependent effects on phenotypes.

Adult but Not Juvenile Crowding Induces the Predatory Mouth Form in *P. pacificus*

To assess potential intra- or inter-generational influence on *P. pacificus* mouth form, we stained 200 juveniles stage 2 (J2s) of the highly St strain RSC017 (Figure 3A) with neutral red and added an increasing number of CellTracker Green-stained RSC017 adults or juveniles (J2s or J3/4s) (Figure 2F). After 3 days, we phenotyped red animals that had developed into adults. Almost half (48%) of the population developed an Eu mouth form with 500 adult animals, compared with less than 4% with 500 J2 or J3/4 juveniles ($n > 100$ from 2–5 independent biological replicates; for display, summed percentages are shown in Figures 3B–3D). We performed a direct statistical comparison between crowded plates and controls (no added crowding animals) for every number and stage of crowding. After multiple testing corrections, only 200 and 500 adult-crowded plates yielded significant differences compared with control (un-crowded) plates (Bonferroni-corrected $p = 6.9 \times 10^{-3}$ and $<2.2 \times 10^{-16}$, respectively, Fisher's exact test on Eu counts). To ascertain if there is a general difference between juvenile or adult crowding, we performed a binomial regression on replicate Eu count data, with stage (J2–J4 versus adults) and number of crowding animals included as fixed effects (Transparent Methods, Table S1). Indeed, we observed a significant difference between adult and juvenile crowding and the incidence of Eu morphs ($p = 1.32 \times 10^{-2}$).

We were also curious if dauers, which have a thickened cuticle and represent a distinct stage in the boom-and-bust life cycle of nematodes, could still respond to adults. Indeed, the same trend that was observed with juveniles was seen with dauers; only 200 and 500 adults significantly induced the Eu mouth form, albeit to a more muted extent (Figures 3E and 3F) (Bonferroni-corrected $p = 2.4 \times 10^{-2}$ and 7.3×10^{-5} , respectively; Fisher's exact test; and binomial regression between dauer and adult crowding $p = 2.96 \times 10^{-3}$).

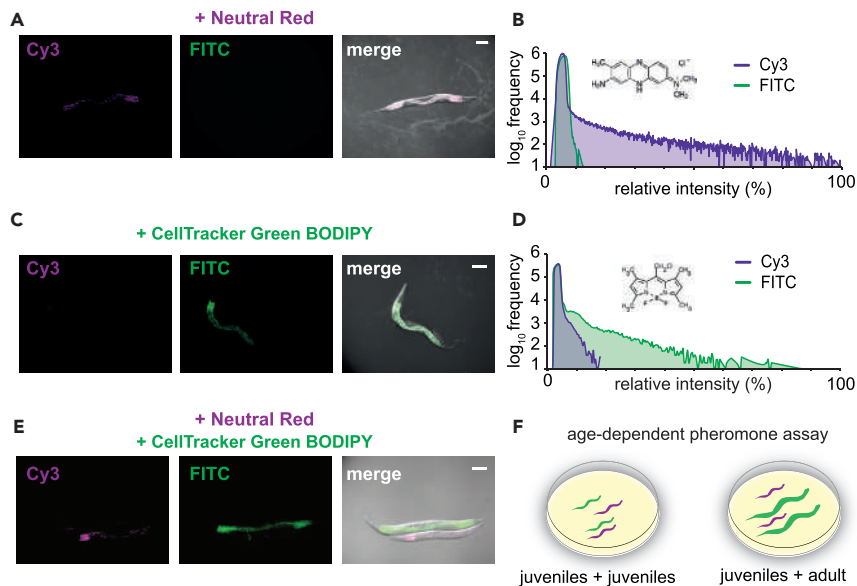


Figure 2. Vital Dye Method in Nematodes Allows Mixing Different Populations Together

(A) Neutral Red-stained adults (0.005% for 3 hours) imaged with Cy3 and FITC excitations and filters, and merged with DIC.

(B) An example of the relative intensities of fluorescence displayed as a histogram with the chemical structure of Neutral Red.

(C) CellTracker Green BODIPY (Thermo)-stained adults (50 μ M for 3 hours) imaged with Cy3 and FITC excitations and filters, and merged with DIC.

(D) An example of the relative intensities of fluorescence displayed as a histogram with the chemical structure of CellTracker Green BODIPY.

(E) Combined worms from Neutral Red and CellTracker Green BODIPY staining on the same slide, merged with DIC.

(F) Age-dependent functional pheromone assay: experimental juveniles were stained with neutral red and challenged with CellTracker Green BODIPY-stained juveniles or adults on standard condition Nematode Growth Media (NGM) agar plates seeded with 300 μ L OP50 *E. coli*. Three days later, only red-positive and green-negative adults were phenotyped.

With a total of 200 dauers and 500 adults, 25.7% of dauers became Eu, whereas only 1.8% of dauers become Eu on a plate containing 700 dauers (and no adults) (Figure 3F). Collectively, these data indicate that adult crowding specifically induces the Eu mouth form. However, it should be noted that because of the difficulty in obtaining a pure J4 culture from RSC017s, we cannot rule out that crowding by large numbers of J4s could also induce the Eu morph.

Even though we did not detect a mouth-form switch in large populations of J2s or dauers, and food was still visible on plates containing the most animals (500 “crowders”), we could not completely rule out the possible effect of food availability on mouth form. As a proxy for starvation, we conducted assays with greatly increased numbers of juveniles from 1,000 to 10,000 that would rapidly deplete bacterial food. We noticed a stark cliff in the fraction of animals that reach adulthood at 4,000–5,000 juveniles, arguing that food is a limiting resource at this population density (Figure 3G). Importantly, however, in these plates we still did not see a shift in mouth form (Figure 3H) ($p = 0.99$, binomial regression, Table S1). With an overwhelming 10,000 worms on a plate, 5.8% were Eu, compared with 48% in the presence of only 500 adults. Although longer-term starvation may have an impact on mouth form, under our experimental conditions it appears to be negligible.

Late-Stage Secretions Induce the Eu Mouth Form

As the mouth-form decision in *P. pacificus* can be influenced by NDMMs (Bose et al., 2012), we wondered if the difference in Eu induction between adults and juveniles resulted from differences in secreted pheromones. To test this hypothesis, we added secretions from 24- and 72-hr cultures of RSC017 and the laboratory strain RS2333 (which is highly Eu) to RSC017 juveniles. We found that the 72-hr (late juvenile stage

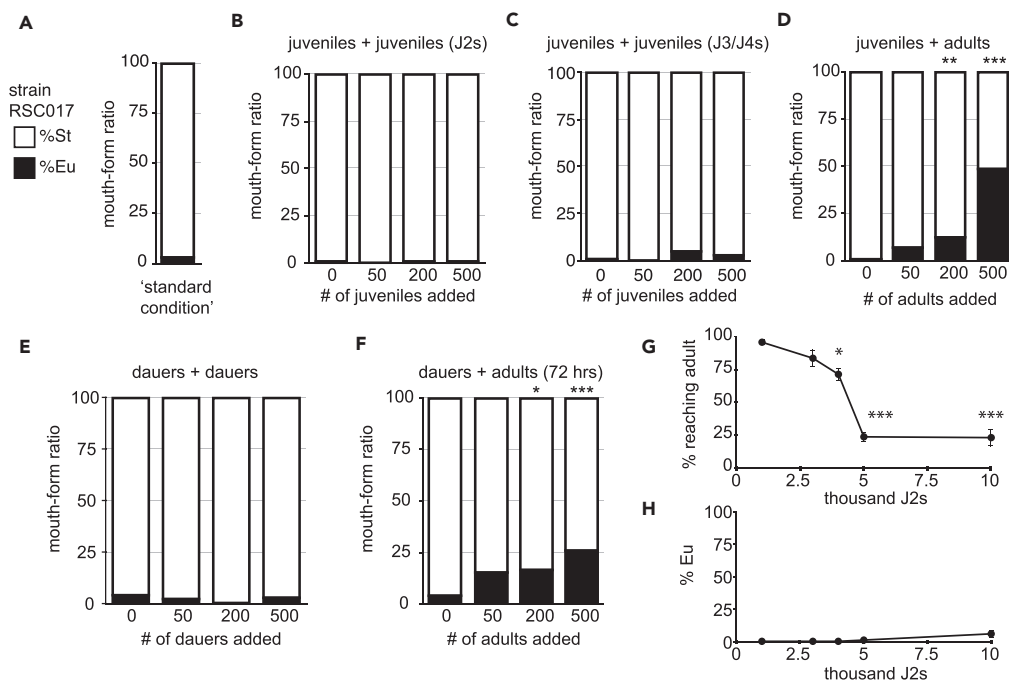


Figure 3. Vital Dye Method Demonstrates Adult-Specific Density Effect on Mouth Form

(A–F) (A) The wild isolate RSC017 grown in standard conditions (5 young adults passed to fresh plates, progeny phenotyped 4 days later) are highly stenostomatous (<10%, $n = 102$). Mouth form ratios of neutral red-stained J2s (B–D) and dauers (E and F), with increasing number of CellTracker Green-stained competitors (total number of animals $n > 100$ per experiment, with 3–5 independent biological replicates for J2 and adult crowding, and 2 for J3/J4s). Overall significance between strain and age was determined by a binomial linear regression (see [Transparent Methods](#)), and pairwise comparisons were assessed by Fisher’s exact test on summed Eu counts (** $p < 0.001$, ** $p < 0.01$, * $p < 0.05$). Mouth forms were phenotyped at 40–100 \times on a Zeiss Axio Imager 2 light microscope.

(G and H) (G) Percent reaching adulthood and percent Eu of those that reached adulthood (H) after increasing numbers of J2s were added to standard 6-cm Nematode Growth Media (NGM) agar plates with 300 μ L OP50 *E. coli* bacteria ($n = 2$ biological replicates, with total $n > 200$ for percent reaching adulthood, and total $n > 100$ for mouth form). Significance was determined by a binomial regression; Error bars represent standard deviation of the two biological replicates).

4/adult, [Figure S4H](#); [Werner et al., 2017](#)) secretions from both strains led to a significant increase in the Eu morph relative to the 24-hr (early juvenile J2) secretions ($p = 5.27 \times 10^{-6}$, 1.33×10^{-3} , respectively, Fisher’s exact test on Eu counts relative to S-medium controls, $n = 2$ –4 biological replicates; for display, summed percentages are shown in [Figure 4](#)). To confirm that the effect was caused by ascaroside pheromones, we exposed RSC017 juveniles to supernatant from a *P. pacificus* *daf-22.1*;*daf-22.2* double mutant, which exhibits virtually no ascaroside production in both *C. elegans* and *P. pacificus* ([Golden and Riddle, 1985](#); [Markov et al., 2016](#)). Again, early juvenile secretion had no impact on Eu frequency, but in contrast to wild-type supernatants, we observed no significant increase in Eu frequency with the 72-hr secretions ($p = 0.8324$, Fisher’s exact test, [Figure 4](#)). Thus, late-stage NDMMs induce development of the Eu mouth form.

Developmental-Staged NDMM Profiles Reveal Age-Specific Synthesis of *dasc#1*

Next, we investigated whether the different effects of early and late pheromones are ones of dosage, or of identity. To determine the potential age-specific differences in pheromones, we profiled *P. pacificus* NDMM levels in two strains and at three time points throughout development with high-performance liquid chromatography-mass spectrometry ([Figures 5A](#), [5B](#), and [S5](#)). We performed a linear regression with the area under the curve of each NDMM chromatogram ([Figure S5A](#)) as the response variable. Stage and strain were modeled as fixed effects, and because we performed separate regression analyses for each pheromone, we adjusted the resulting p values for multiple testing using false discovery rate (FDR) (see [Table S2](#) for p and FDR values between stage and strain). We observed that among developmental stages there were significant differences in the levels of *ascr#9*, *ascr#12*, *npar#1*, and *dasc#1*, and that *dasc#1*,

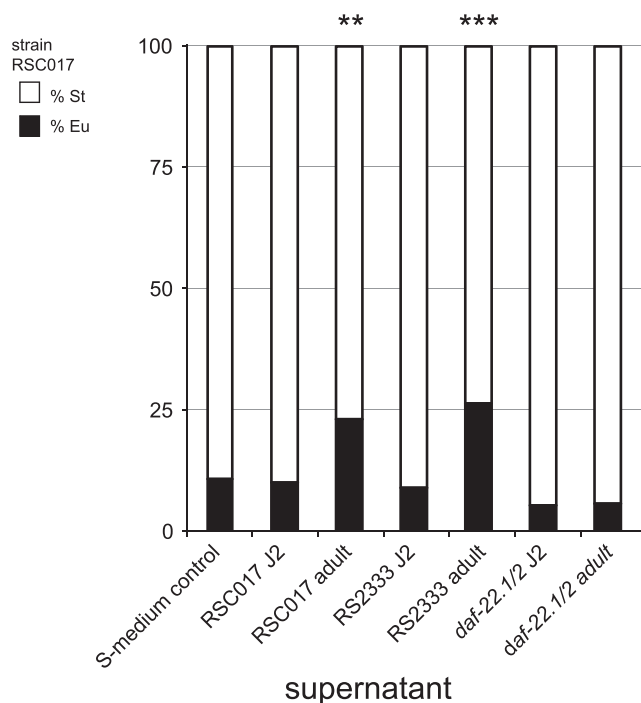


Figure 4. Late-Stage Secretions Induce Predatory Morph in Juveniles

Highly St strain RSC017 juveniles were exposed to 24- and 72-hr supernatants of its own strain, and to the 24- and 72-hr supernatants of the highly Eu strain RS2333. Mouth form was phenotyped 3 days later. Worms exposed to 24-hr secretions remained highly St, whereas worms exposed to 72-hr secretions had a small but significant increase in Eu morphs ($p < 0.05$, Fisher's exact test). Supernatants from the double mutant *daf-22.1/2*, which has deficient ascaroside pheromone production (Golden and Riddle, 1985; Markov et al., 2016), did not elicit increases in Eu from either 24- or 72-hr supernatants. Worms exposed to the S-media control also remained highly St. $n = 4$ independent biological replicates for RS2333 and *daf-22.1/2* secretions, and $n = 2$ independent biological replicates for RSC017 secretions, with an average count of 55 animals per replicate. For display, total Eu and St counts are presented as percentages (** $p < 0.01$, *** $p < 0.001$).

ubas#1, and *ubas#2* are affected by both stage and strain ($FDR < 0.05$). Interestingly, *dasc#1* is the most potent known Eu-inducing pheromone when tested as a single synthesized compound, whereas *npar#1* is both an Eu- and a dauer-inducing pheromone (Bose et al., 2012). Closer inspection revealed *dasc#1*, *npar#1*, and *ascr#9* increase throughout development in both strains, and *dasc#1* peaks at 72 hr in RS2333 (Figures 5C and 5D and 5F–5I, $p < 0.05$, Student's two-tailed t test between 72 and 24 hr for each NDMM in both strains, and 72 and 48 hr for *dasc#1* in RS2333, Table S3). Intriguingly, the trajectory of *dasc#1* appeared “binary/off-on” in both strains; in some replicates *dasc#1* levels were undetectable, whereas others were high and virtually no replicates exhibited intermediate levels (Figures 5F and 5G). In fact, our statistical model for *dasc#1* fits better if we assume cubic rather than linear growth (model difference Akaike information criterion, $\Delta AIC = 3.958$). In contrast, *ascr#9*, which was also statistically increased but does not affect known plastic phenotypes (Bose et al., 2012), displayed a more gradual increase in both strains (Figures 5E, 5J, and 5K), and the model fits better with linear growth ($AIC_{linear} - AIC_{cubic} = -1.208$). Meanwhile, the induction pattern of *npar#1* appears particular to each strain, although our linear model did not detect significant strain effects. Thus the kinetics of induction appears to be NDMM specific, which may be related to their roles in phenotypic plasticity.

We were interested to know if there was a transcriptional signal that would correlate with the increase in NDMMs throughout development. An analysis of previously published RNA sequencing data (Baskaran et al., 2015) reveals an ~5-fold increase in transcription of the thiolase *Ppa-daf-22.1* (Figure S6A) between J2 and J4/adults, the most downstream enzyme in the β -oxidation pathway of ascaroside synthesis. However, this enzyme is responsible for the last step in synthesizing many NDMMs in addition to *dasc#1*, *npar#1*, and *ascr#9*, so other enzymes must also be involved, and identifying them is an area of active research.

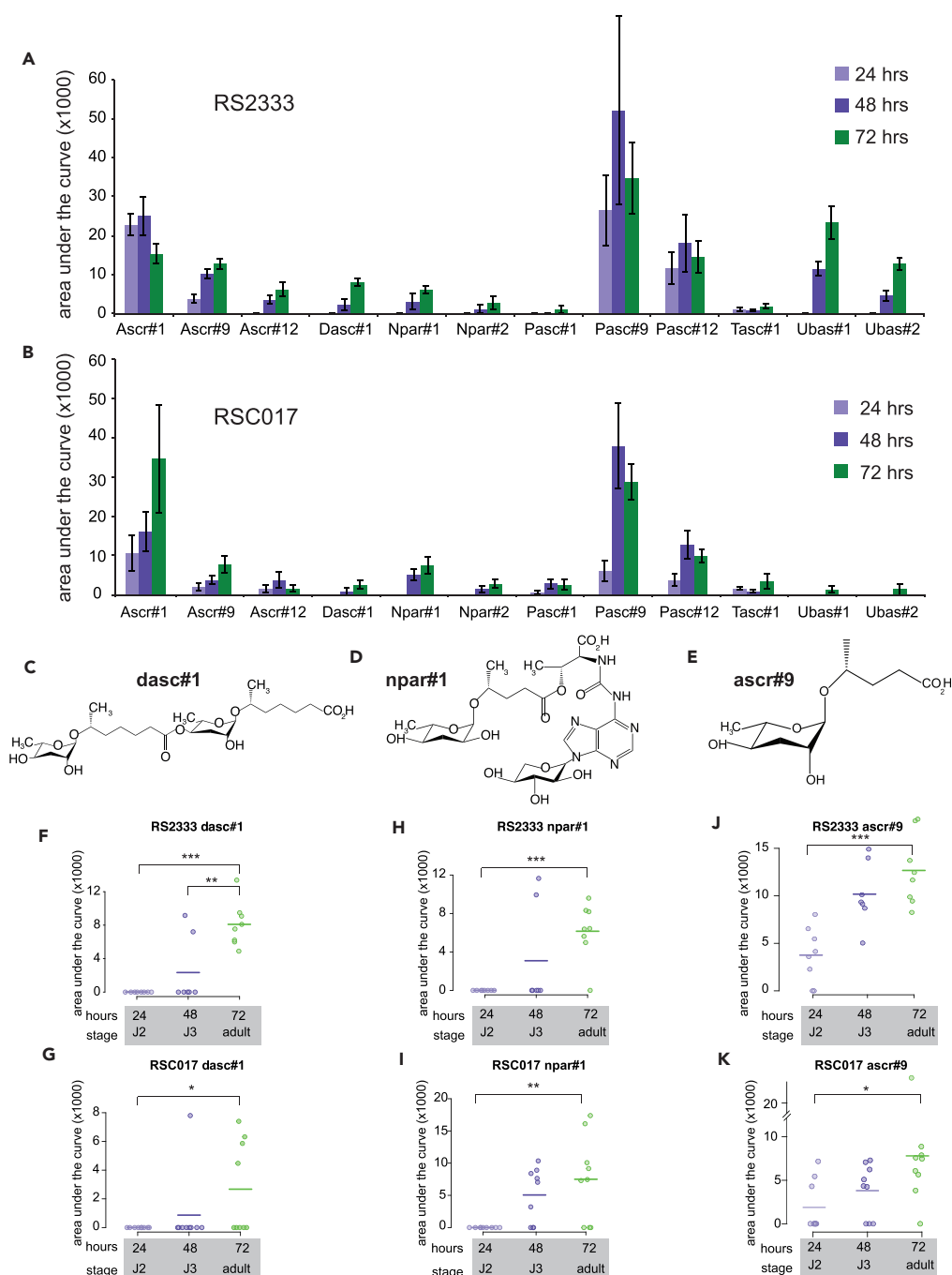


Figure 5. Time-Resolved Nematode-Derived Modular Metabolites (NDMMs) in *Pristionchus pacificus*

(A and B) (A) Time-resolved secretion profile of nematode-derived modular metabolites from the wild-type laboratory strain RS2333 and (B) wild isolate RSC017. In both strains, at 24 hr cultures represent predominantly J2 stage worms, at 48 hr a mix of J2–J4, and at 72 hr predominantly adults in RSC017 (90%, Figure S4H) and a mix of J4/adults in RS2333 (Werner et al., 2017). Data are presented as the mean of 8 (RS2333) and 9 (RSC017) biological replicates, and error bars represent the standard error of mean (SEM).

(C–E) Chemical structures of age-specific NDMMs (C) dasc#1, (D) npar#1, and (E) ascr#9, as described in the Small Molecule Identifier Database (<http://www.smid-db.org/>), produced in ChemDraw.

(F–K) Time-resolved abundance of (F and G) dasc#1, (H and I) npar#1, and (J and K) ascr#9 NDMMs in RS2333 and RSC017.

Each data point represents a biological replicate, and for comparison with (A and B) lines represent mean abundance. p values calculated by a 2-tailed Student's t test (***p < 0.001, **p < 0.01, *p < 0.05).

In principle, the increase in abundance of *dasc#1*, *npar#1*, and *ascr#9* throughout development could be a result of a concomitant increase in body mass. We used WormSizer (Moore et al., 2013) to measure the size of RSC017 animals from each time point and then normalized NDMM abundances by volume. We found a 1.1-fold difference in body volume between 24- and 48-hr samples, and a 1.3-fold difference between 24- and 72-hr samples. However, normalizing by these factors did not affect the significance of *dasc#1*, *npar#1*, or *ascr#9* between time points (Tables S3 and S4; Figures S6B–S6D). We also suspect that size is not the only factor because no other compounds significantly increased throughout development in our linear model. Finally, we profiled the endo-metabolome of eggs and found appreciable amounts of *ascr#1*, #9, and #12 and *pasc#9*, but little to no traces of other ascaroside derivatives (Figure S5C), suggesting age-specific synthesis, rather than release from ascarosides already present in eggs/J1. Together, these results suggest that the observed increase in *ascr#9*, *npar#1*, and *dasc#1* over time corresponds to age-specific production. The observation that *dasc#1* is produced specifically during the juvenile-to-adult transition is especially intriguing because adults are no longer able to switch mouth forms, hinting at cross-generational signaling.

DISCUSSION

Here, we introduce a novel dye-based method that allowed us to assess cross-generational influence on mouth form. Our results demonstrate that adult crowding induces the Eu predatory morph, and that this effect is, at least partially, a result of age-specific pheromones. In doing so, we provide the first multi-stage time series of pheromone production in *P. pacificus*, which shows that *dasc#1* exhibits a surprising switch-like induction pattern. Collectively, our results suggest that adults represent a “critical age group” with respect to phenotypic plasticity. The fact that adults also represent the critical age group with respect to population density (Charlesworth, 1972) may explain their outsized contribution to induction of the Eu morph. The presence of adults may indicate rapidly decreasing bacterial resources, and thus developing the Eu morph will allow worms to exploit additional resources and kill competitors.

Our developmental profiling revealed an increase in two NDMMs that affect plastic phenotypes. Given that J4s can produce *dasc#1/npar#1*, we believe the lack of effect of the J3/J4 stage compared with adults in our mixed-culture assay simply reflects the more consistently present and higher amounts of *dasc#1/npar#1* produced at 72 hr and experienced for longer periods of time. The observation that this trend occurs regardless of body size implies that these molecules are programmed for stage-specific production. The “off-on” induction kinetics might reflect a population-level feedback loop, wherein the production of excess pheromones is based on a threshold level of previously produced pheromones. The variability observed at 48 hr for *dasc#1/npar#1* might reflect biological variability in developmental timing and/or technical variation in staging. It is also worth noting that although *npar#1* is the major dauer-inducing pheromone in *P. pacificus* (Bose et al., 2012), we did not observe dauer juveniles in any of our dye-crowding assays. Thus, it seems that mouth-form phenotype is the first-level plastic response to population density. Presumably higher concentrations are required for dauer induction, reflecting a calculated response strategy depending on the level of crowding or duration of starvation. Interestingly, the effect of 72-hr supernatants was noticeably less (23%–26% Eu) than the physical presence of adult worms (up to 48% with only 500 adults). It is difficult to compare pheromone concentrations between experiments, but presumably worms in the vital dye assay experienced a greater local concentration as they were in direct contact with each other for longer periods of time, and were also older than the 72-hr supernatant assayed in our pheromone profiling. However, it is also formally possible that other factors, like increased physical contact, can induce the Eu morph.

The maximum levels of Eu reached in our mixed culture experiment was ~50% with 500 adults, begging the question if this could be pushed further by using greater levels of crowding. However, this proved technically difficult due to food constraints with excess worms. Adding more food (OP50 LB) began to decrease the integrity of the agar, which made recovering animals for phenotyping difficult. Importantly, adults do not seem capable of eating other adults, which might otherwise push the Eu frequency even higher as a defense strategy. We also suspect that there are unknown trade-offs between the Eu and St mouth forms, which may manifest in a “ceiling” of the Eu frequency even under more crowded conditions.

Among the many environmental influences on mouth form (Werner et al., 2017), population density and starvation are perhaps the most ecologically relevant. However, teasing apart these two factors has

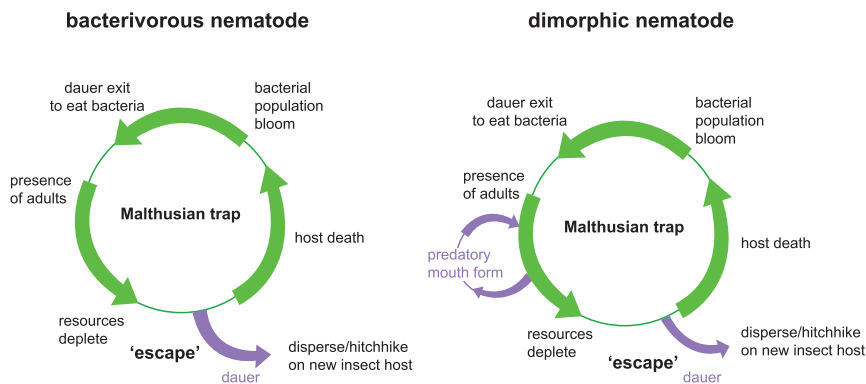


Figure 6. Conceptual Model of the Role of Critical Age Classes in Mouth-Form Phenotypic Plasticity

Conceptual life cycle models of monomorphic or dimorphic mouth-form nematodes. In an isolated niche such as a decaying insect carcass, at some point microbial food supplies will run out, leading to a Malthusian catastrophe. Nematodes escape this trap by entering the dauer state and dispersing, and re-starting the cycle. Dimorphic nematodes may sense the impending “catastrophe” earlier by recognizing an abundance of adults in the population, and switching to the Eu morph to exploit new resources and kill competitors. By analogy to economic models, the mouth-form switch is a technological innovation to temporarily escape a Malthusian resource trap.

been a challenge (Bento et al., 2010). Here, we demonstrate that whereas a strong shift is observed with age-specific pheromones, no such effect was seen under limited resource conditions. Thus, age-specific crowding is sufficient to induce the Eu mouth form. Nevertheless, this does not preclude that long-term starvation could also have an effect. Determining the relative contributions of these factors to mouth form will be important to better understand the sophisticated ecological response strategies of *P. pacificus*, nematodes, and phenotypic plasticity in general.

Why do adults and not juveniles affect mouth form? For now we can only speculate, but given that St animals develop slightly faster (Seroby et al., 2013), there may be a “race” to sexual maturation in emergent populations at low densities. However, as the nematode population increases, there will likely be a commensurate decrease in bacterial populations. When faced with competition from other nematodes, *P. pacificus* has a particular advantage in developing the Eu morph; their expanded dietary range includes other nematode competitors. Indeed, when nematode prey is the only available food source, animals with the Eu morph have longer lifespans and more progeny than animals with the St morph (Seroby et al., 2014). When resources become depleted as the population size increases, *C. elegans* and other monomorphic nematodes may enter dauer and disperse (Frézal and Félix, 2015). However, in St-biased dimorphic strains of *P. pacificus*, juveniles may switch to the Eu morph in response to adults as a first-level indication of rapidly increasing population size (Figure 6). Then, after prolonged starvation and crowding, worms will presumably enter dauer. By analogy to economic models of population growth (Malthus, 1826; Trewavas, 2002) mouth-form plasticity is a “technological innovation” to temporarily escape a Malthusian resource trap.

The evolution of dimorphic mouth forms is one among myriad nematode ecological strategies. For example, entomopathogenic nematodes release their symbiont bacteria in insect hosts to establish their preferred food source, and the bacteria can release antibiotics to kill off competing bacteria and fungi (Griffin, 2012). Some free-living species, like those of the genus *Oscheius*, may refrain from combat and stealthily feed and reproduce amid warring entomopathogenic species (Campos-Herrera, 2015a). Interspecific killing also occurs in gonochoristic species, in which both mated and virgin males are killed, implying fighting not just for mates but for resources as well (O’Callaghan et al., 2014; Zenner et al., 2014). Different reproductive strategies also exist, and hermaphroditic species have an advantage over gonochoristic species when colonizing a new niche, such as an insect carcass (Campos-Herrera, 2015b). Meanwhile, insect hosts and colonizing nematodes have their own distinct pheromone-based attraction and toxicity (Cinkornpumin et al., 2014; Renahan and Hong, 2017). Finally, the renaissance of *C. elegans* sampling from around the world (Cook et al., 2017; Evans et al., 2016; Félix et al., 2013; Petersen et al., 2014; Pouillet and Braendle, 2015) is rapidly building a resource of wild isolates that will almost certainly have different and fascinating ecologies. We hope our method for labeling and then combining different

nematode populations on the same plate will aid in studies to identify these strategies. Perhaps the time is also ripe to complement these studies with more sophisticated ecological modeling that can lead to testable hypotheses.

Although beyond the scope of this manuscript, the cross-generational communication we observed could in principle reflect an intended signal from adults to juveniles, i.e., kin selection (Bourke, 2014). However, we favor a more simplistic view that juveniles have evolved to recognize late-stage metabolites. Regardless of these interpretations, our results argue that age classes are a critical factor in density-dependent plasticity, as has been theorized in density-dependent selection (Charlesworth, 1994).

Limitations of the Study

Given the ubiquity of certain traits in reproductive adults and their contribution to population growth, we suspect similar results will be found in other systems. However, it may depend on the phenotype and system being studied. For example, the population dynamics of this nematode (fast hermaphroditic reproduction) may be sufficiently different from other species such that our findings have limited generalizability. In addition, our method of staining different populations, although fast and easy, is particular to nematodes. Finally, to what extent our ecological interpretations exist in nature remains to be determined.

METHODS

All methods can be found in the accompanying [Transparent Methods supplemental file](#).

SUPPLEMENTAL INFORMATION

Supplemental Information includes Transparent Methods, six figures, and four tables and can be found with this article online at <https://doi.org/10.1016/j.isci.2018.11.027>.

ACKNOWLEDGMENTS

We would like to thank all members of the Sommer lab, Dr. Talia Karasov, Dr. Hernan Burbano, and Moises Exposito-Alonso for guidance with statistical analysis, and Dr. Adrian Striet (Max Planck Institute) and Dr. Cameron Weadick (University of Sussex) for thoughtful critique and discussion. The work was funded by the Max Planck Society.

AUTHOR CONTRIBUTIONS

M.S.W. and R.J.S. conceived of the project. M.H.C. conducted pheromone profiling with help from M.S.W. and T.R. M.S.W. and T.R. designed and conducted dye-labeling experiments. T.R. and M.H.C. performed supernatant experiments. M.D. and M.S.W. considered ecological implications. M.S.W. and T.R. wrote the manuscript with input and edits from all authors.

DECLARATION OF INTERESTS

The authors declare no competing interests.

Received: August 15, 2018

Revised: November 15, 2018

Accepted: November 15, 2018

Published: December 21, 2018

REFERENCES

- Baskaran, P., Rödelsperger, C., Prabh, N., Serobyayn, V., Markov, G.V., Hirsekorn, A., and Dieterich, C. (2015). Ancient gene duplications have shaped developmental stage-specific expression in *Pristionchus pacificus*. *BMC Evol. Biol.* 15, 185.
- Ben Hamouda, A., Tenaka, S., Ben Hamouda, M.H., and Bouain, A. (2011). Density-dependent phenotypic plasticity in body coloration and morphometry and its transgenerational changes in the migratory locust, *Locusta migratoria*. *J. Entomol. Nematol.* 3, 105–116.
- Bento, G., Ogawa, A., and Sommer, R.J. (2010). Co-option of the hormone-signalling module dafachronic acid–DAF-12 in nematode evolution. *Nature* 466, 494–497.
- Bose, N., Meyer, J.M., Yim, J.J., Mayer, M.G., Markov, G.V., Ogawa, A., Schroeder, F.C., and Sommer, R.J. (2014). Natural variation in dauer pheromone production and sensing supports intraspecific competition in nematodes. *Curr. Biol.* 24, 1536–1541.
- Bose, N., Ogawa, A., von Reuss, S.H., Yim, J.J., Ragsdale, E.J., Sommer, R.J., and Schroeder, F.C. (2012). Complex small-molecule architectures regulate phenotypic plasticity in a nematode. *Angew. Chem. Int. Ed.* 51, 12438–12443.

- Bourke, A.F.G. (2014). Hamilton's rule and the causes of social evolution. *Philos. Trans. R. Soc. Lond. B Biol. Sci.* 369, 20130362.
- Butcher, R.A. (2017). Small-molecule pheromones and hormones controlling nematode development. *Nat. Chem. Biol.* 13, 577–586.
- Butcher, R.A., Fujita, M., Schroeder, F.C., and Clardy, J. (2007). Small-molecule pheromones that control dauer development in *Caenorhabditis elegans*. *Nat. Chem. Biol.* 3, 420–422.
- Butcher, R.A., Ragains, J.R., Kim, E., and Clardy, J. (2008). A potent dauer pheromone component in *Caenorhabditis elegans* that acts synergistically with other components. *Proc. Natl. Acad. Sci. U S A* 105, 14288–14292.
- Campos-Herrera, R. (2015a). Traditional and molecular detection methods reveal intense interguild competition and other multitrophic interactions associated with native entomopathogenic nematodes in Swiss tillage soils. *Plant Soil* 389, 237–255.
- Campos-Herrera, R. (2015b). *Nematode Pathogenesis of Insects and Other Pests* (Springer).
- Charlesworth, B. (1994). *Evolution in Age-Structured Populations* (Cambridge Univ. Press).
- Charlesworth, B. (1972). Selection in populations with overlapping generations. III. Conditions for genetic equilibrium. *Theor. Popul. Biol.* 3, 377–395.
- Chasnov, J.R., So, W.K., Chan, C.M., and Chow, K.L. (2007). The species, sex, and stage specificity of a *Caenorhabditis* sex pheromone. *Proc. Natl. Acad. Sci. U S A* 104, 6730–6735.
- Chen, B., Li, S., Ren, Q., Tong, X., Zhang, X., and Kang, L. (2015). Paternal epigenetic effects of population density on locust phase-related characteristics associated with heat-shock protein expression. *Mol. Ecol.* 24, 851–862.
- Choe, A., von Reuss, S.H., Kogan, D., Gasser, R.B., Platzer, E.G., Schroeder, F.C., and Sternberg, P.W. (2012). Ascaroside signaling is widely conserved among nematodes. *Curr. Biol.* 22, 772–780.
- Cinkornpumin, J.K., Wisidagama, D.R., Rapoport, V., Go, J.L., Dieterich, C., Wang, X., Sommer, R.J., and Hong, R.L. (2014). A host beetle pheromone regulates development and behavior in the nematode *Pristionchus pacificus*. *Elife* 3, e03229.
- Cook, D.E., Zdraljic, S., Roberts, J.P., and Andersen, E.C. (2017). CeNDR, the *Caenorhabditis elegans* natural diversity resource. *Nucleic Acids Res.* 45, D650–D657.
- Dantzer, B., Newman, A.E.M., Boonstra, R., Palme, R., Boutin, S., Humphries, M.M., and McAdam, A.G. (2013). Density triggers maternal hormones that increase adaptive offspring growth in a wild mammal. *Science* 340, 1215–1217.
- Diaz, S.A., Brunet, V., Lloyd-Jones, G.C., Spinner, W., Wharam, B., and Viney, M. (2014). Diverse and potentially manipulative signalling with ascarosides in the model nematode *C. elegans*. *BMC Evol. Biol.* 14, 46.
- Dong, C., Reilly, D.K., Bergame, C., Dolke, F., Srinivasan, J., and von Reuss, S.H. (2018). Comparative ascaroside profiling of *Caenorhabditis* exometabolomes reveals species-specific (ω) and ($\omega - 2$)-hydroxylation downstream of peroxisomal β -oxidation. *J. Org. Chem.* 83, 7109–7120.
- Dudley, S.A., and Schmitt, J. (2015). Testing the adaptive plasticity hypothesis: density-dependent selection on manipulated stem length in *impatiens capensis*. *Am. Nat.* 147, 445–465.
- Evans, K.S., Zhao, Y., Brady, S.C., Long, L., McGrath, P.T., and Andersen, E.C. (2016). Correlations of genotype with climate parameters suggest *Caenorhabditis elegans* niche adaptations. *G3 (Bethesda)* 7, 289–298.
- Falcke, J.M., Bose, N., Artyukhin, A.B., Rödelsperger, C., Markov, G.V., Yim, J.J., Grimm, D., Claassen, M.H., Panda, O., Baccile, J.A., et al. (2018). Linking genomic and metabolomic natural variation uncovers nematode pheromone biosynthesis. *Cell Chem. Biol.* 25, 787–796.e12.
- Félix, M.-A., Jovelín, R., Ferrari, C., Han, S., Cho, Y.R., Andersen, E.C., Cutter, A.D., and Braendle, C. (2013). Species richness, distribution and genetic diversity of *Caenorhabditis* nematodes in a remote tropical rainforest. *BMC Evol. Biol.* 13, 10.
- Fielenbach, N., and Antebi, A. (2008). *C. elegans* dauer formation and the molecular basis of plasticity. *Genes Dev.* 22, 2149–2165.
- Frézal, L., and Félix, M.-A. (2015). The natural history of model organisms: *C. elegans* outside the Petri dish. *Elife* 4, e05849.
- Golden, J.W., and Riddle, D.L. (1982). A pheromone influences larval development in the nematode *Caenorhabditis elegans*. *Science* 218, 578–580.
- Golden, J.W., and Riddle, D.L. (1985). A gene affecting production of the *Caenorhabditis elegans* dauer-inducing pheromone. *Mol. Gen. Genet.* 198, 534–536.
- Greene, J.S., Brown, M., Dobosiewicz, M., Ishida, I.G., Macosko, E.Z., Zhang, X., Butcher, R.A., Cline, D.J., McGrath, P.T., and Bargmann, C.I. (2016). Balancing selection shapes density-dependent foraging behaviour. *Nature* 539, 254–258.
- Griffin, C.T. (2012). Perspectives on the behavior of entomopathogenic nematodes from dispersal to reproduction: traits contributing to nematode fitness and biocontrol efficacy. *J. Nematol.* 44, 177–184.
- Hastings, A. (2013). *Population Biology: Concepts and Models* (Springer).
- Herrmann, M., Mayer, W.E., and Sommer, R.J. (2006). Nematodes of the genus *Pristionchus* are closely associated with scarab beetles and the Colorado potato beetle in Western Europe. *Zoology* 109, 96–108.
- Herrmann, M., Mayer, W.E., Hong, R.L., Kienle, S., Minasaki, R., and Sommer, R.J. (2007). The nematode *Pristionchus pacificus* (Nematoda: Diplogastridae) is associated with the oriental beetle *exomala orientalis* (Coleoptera: Scarabaeidae) in Japan. *Zoolog. Sci.* 24, 883–889.
- Izrayelit, Y., Srinivasan, J., Campbell, S.L., Jo, Y., Reuss, von, S.H., Genoff, M.C., Sternberg, P.W., and Schroeder, F.C. (2012). Targeted metabolomics reveals a male pheromone and sex-specific ascaroside biosynthesis in *Caenorhabditis elegans*. *ACS Chem. Biol.* 7, 1321–1325.
- Jeong, P.-Y., Jung, M., Yim, Y.-H., Kim, H., Park, M., Hong, E., Lee, W., Kim, Y.H., Kim, K., and Paik, Y.-K. (2005). Chemical structure and biological activity of the *Caenorhabditis elegans* dauer-inducing pheromone. *Nature* 433, 541–545.
- Kaplan, F., Srinivasan, J., Mahanti, P., Ajredini, R., Durak, O., Nimalendran, R., Sternberg, P.W., Teal, P.E.A., Schroeder, F.C., Edison, A.S., et al. (2011). Ascaroside expression in *Caenorhabditis elegans* is strongly dependent on diet and developmental stage. *PLoS One* 6, e17804.
- Ludwig, A.H., Gimond, C., Judkins, J.C., Thornton, S., Pulido, D.C., Micikas, R.J., Döring, F., Antebi, A., Braendle, C., and Schroeder, F.C. (2017). Larval crowding accelerates *C. elegans* development and reduces lifespan. *PLoS Genet.* 13, e1006717.
- MacArthur, R.H. (1962). Some generalized theorems of natural selection. *Proc. Natl. Acad. Sci. U S A* 48, 1893–1897.
- Maeno, K., and Tanaka, S. (2008). Maternal effects on progeny size, number and body color in the desert locust, *Schistocerca gregaria*: density- and reproductive cycle-dependent variation. *J. Insect Physiol.* 54, 1072–1080.
- Malthus, T.R. (1826). *An Essay on the Principle of Population* (Cambridge University Press).
- Markov, G.V., Meyer, J.M., Panda, O., Artyukhin, A.B., Claassen, M., Witte, H., Schroeder, F.C., and Sommer, R.J. (2016). Functional conservation and divergence of daf-22 paralogs in *Pristionchus pacificus* Dauer development. *Mol. Biol. Evol.* 33, 2506–2514.
- Meyer, J.M., Baskaran, P., Quast, C., Susoy, V., Rödelsperger, C., Glöckner, F.O., and Sommer, R.J. (2017). Succession and dynamics of *Pristionchus* nematodes and their microbiome during decomposition of *Oryctes borbonicus* on La Réunion Island. *Environ. Microbiol.* 19, 1476–1489.
- Moore, B.T., Jordan, J.M., and Baugh, L.R. (2013). WormSizer: high-throughput analysis of nematode size and shape. *PLoS One* 8, e57142.
- O'Callaghan, K.M., Zenner, A.N.R.L., Hartley, C.J., and Griffin, C.T. (2014). Interference competition in entomopathogenic nematodes: male *Steinernema* kill members of their own and other species. *Int. J. Parasitol.* 44, 1009–1017.
- Pener, M.P., and Simpson, S.J. (2009). Locust phase polyphenism: an update. *Adv. Insect Physiol.* 36, 196–201.
- Petersen, C., Dirksen, P., Prahl, S., Strathmann, E.A., and Schulenburg, H. (2014). The prevalence of *Caenorhabditis elegans* across 1.5 years in

selected North German locations: the importance of substrate type, abiotic parameters, and *Caenorhabditis* competitors. *BMC Ecol.* 14, 4.

Pouillet, N., and Braendle, C. (2015). Sampling and isolation of *C. elegans* from the natural habitat. *Methods Mol. Biol.* 1327, 221–229.

Renahan, T., and Hong, R.L. (2017). A species-specific nematocide that results in terminal embryogenesis. *J. Exp. Biol.* 220, 3238–3247.

Sanghvi, G.V., Baskaran, P., Röseler, W., Sieriebriennikov, B., Rödelsperger, C., and Sommer, R.J. (2016). Life history responses and gene expression profiles of the nematode *Pristionchus pacificus* cultured on *Cryptococcus* yeasts. *PLoS One* 11, e0164881.

Seroby, V., Ragsdale, E.J., and Sommer, R.J. (2014). Adaptive value of a predatory mouth-form in a dimorphic nematode. *Proc. R. Soc. Lond. B Biol. Sci.* 281, 20141334–20141989.

Seroby, V., Ragsdale, E.J., Müller, M.R., and Sommer, R.J. (2013). Feeding plasticity in the nematode *Pristionchus pacificus* influenced by sex and social context and is linked to developmental speed. *Evol. Dev.* 15, 161–170.

Simpson, S.J., Despland, E., Hägele, B.F., and Dodgson, T. (2001). Gregarious behavior in desert locusts is evoked by touching their back legs. *Proc. Natl. Acad. Sci. U S A* 98, 3895–3897.

Simpson, S.J., and Miller, G.A. (2007). Maternal effects on phase characteristics in the desert locust, *Schistocerca gregaria*: a review of current understanding. *J. Insect Physiol.* 53, 869–876.

Sloggett, J.J., and Weisser, W.W. (2002). Parasitoids induce production of the dispersal morph of the pea aphid, *Acyrtosiphon pisum*. *Oikos* 98 (2), 323–333.

Sommer, R.J., and Mayer, M.G. (2015). Toward a synthesis of developmental biology with evolutionary theory and ecology. *Annu. Rev. Cell Dev. Biol.* 31, 453–471.

Sommer, R.J., and McLaughran, A. (2013). The nematode *Pristionchus pacificus* as a model system for integrative studies in evolutionary biology. *Mol. Ecol.* 22, 2380–2393.

Sommer, R.J., Dardiry, M., Lenuzzi, M., Namdeo, S., Renahan, T., Sieriebriennikov, B., and Werner, M.S. (2017). The genetics of phenotypic plasticity in nematode feeding structures. *Open Biol.* 7, <https://doi.org/10.1098/rsob.160332>.

Srinivasan, J., von Reuss, S.H., Bose, N., Zaslaver, A., Mahanti, P., Ho, M.C., O'Doherty, O.G., Edison, A.S., Sternberg, P.W., and Schroeder, F.C. (2012). A modular library of small molecule signals regulates social behaviors in *Caenorhabditis elegans*. *PLoS Biol.* 10, e1001237.

Sutherland, O.R.W. (1969). The role of crowding in the production of winged forms by two strains of the pea aphid, *Acyrtosiphon pisum*. *J. Insect Physiol.* 15, 1385–1410.

Thomas, M.C., and Lana, P.D.C. (2008). Evaluation of vital stains for free-living marine nematodes. *Braz. J. Oceanogr.* 56, 249–251.

Travis, J., Leips, J., and Rodd, F.H. (2013). Evolution in population parameters: density-dependent selection or density-dependent fitness? *Am. Nat.* 181, S9–S20.

Trewavas, A. (2002). Malthus foiled again and again. *Nature* 418, 668–670.

von Reuss, S.H., Bose, N., Srinivasan, J., Yim, J.J., Judkins, J.C., Sternberg, P.W., and Schroeder, F.C. (2012). Comparative metabolomics reveals biogenesis of ascarosides, a modular library of small-molecule signals in *C. elegans*. *J. Am. Chem. Soc.* 134, 1817–1824.

Werner, M.S., Sieriebriennikov, B., Loschko, T., Namdeo, S., Lenuzzi, M., Dardiry, M., Renahan, T., Sharma, D.R., and Sommer, R.J. (2017). Environmental influence on *Pristionchus pacificus* mouth form through different culture methods. *Sci. Rep.* 7, 7207.

Wilecki, M., Lightfoot, J.W., Susoy, V., and Sommer, R.J. (2015). Predatory feeding behaviour in *Pristionchus* nematodes is dependent on phenotypic plasticity and induced by serotonin. *J. Exp. Biol.* 218, 1306–1313.

Zenner, A.N.R.L., O'Callaghan, K.M., and Griffin, C.T. (2014). Lethal fighting in nematodes is dependent on developmental pathway: male-male fighting in the entomopathogenic nematode *Steinernema longicaudum*. *PLoS One* 9, e89385.

ISCI, Volume 10

Supplemental Information

**Adult Influence on Juvenile Phenotypes
by Stage-Specific Pheromone Production**

Michael S. Werner, Marc H. Claßen, Tess Renahan, Mohannad Dardiry, and Ralf J. Sommer

1
2
3
4
5
6
7
8
9
10
11
12
13
14
15
16
17
18
19
20
21
22
23
24

Supplemental Information

Transparent Methods

Nematode strains and husbandry

P. pacificus Wild-type RS2333 (California) and RSC017 (La Réunion) strains were kept on 6 cm nematode growth media (NGM) plates seeded with OP50 and kept at 20°C. RSC017 is highly St and does not predate on other nematodes, and thus was used for biological assays instead of the highly Eu, predatory RS2333. To induce dauer, mixed-stage plates with little to no OP50 were washed with M9 and the resulting worm pellets were used in a modified 'White Trap' method. Worm pellets were placed on killed *Tenebrio molitor* grubs and dispersing dauers were collected in surrounding MilliQ water. Age of dauers ranged from one week to one month.

Dye staining

A stock solution of Neutral Red was prepared by dissolving 0.5 mg in 10 ml 5% acetic acid and stored at -20°C. Working solutions were prepared by 100x dilution in M9, aliquoted, stored at -20°C, and thawed directly before use. Working solutions were kept for approximately 1 month. Stock solutions of 10 mM CellTracker Green BODIPY were made in DMSO and stored at -20°C. J2s were prepared from 20-40 x 6 cm plates 6 days after passaging 5 worms to each plate on 300 µl OP50. Worms were washed from plates with M9 into a conical tube, and then filtered through 2 x 20 µM filters (Millipore) placed between rubber gaskets. The flow-through contained mostly J2 and some J3, which were pelleted by centrifugation, 8 seconds on a table-top eppendorf centrifuge 5424, reaching approximately 10,000 x g. The older/larger adult worms

25 remained on the filters, and were washed into a 50 ml conical tube with ~2 ml M9. Adults were
26 then isolated by transferring worms to a 15 ml conical, and allowing them to swim/sink to the
27 bottom of the tube. Adults reach the bottom faster than younger stages do, and after 3-5 rounds
28 of removing supernatant and re-suspending in 2-3 ml M9, the pellet contains almost exclusively
29 adults, which were re-suspended in 1 ml M9/50 μ M Green BODIPY (Thermo Fisher). The J2
30 pellet was either directly re-suspended in 1 ml Neutral Red working solution, or in 1 ml M9 and
31 split to two tubes, re-centrifuged, and re-suspended in 1 ml working solution Neutral Red
32 (0.005% in M9) or 1 ml M9/50 μ M Green BODIPY (Thermo Fisher). For the intermediate time
33 point juveniles (J3s and some J4s), J2s isolated from 20 μ M filtering were placed back on agar
34 plates containing 300 μ l OP50 bacterial food and grown for another 24 hours, and then washed
35 from plates in M9 and re-filtered through 5 μ M filters, then re-suspended in 1 ml 50 μ M Green
36 BODIPY (Thermo Fisher). Each tube was rotated for 3 hours in the dark at 20°C, then washed
37 by centrifugation as before, and re-suspended in 1 ml M9. This was repeated 3-4x until the dye
38 was no longer visible in the worm pellet. Then, the concentration of worms per microliter was
39 determined by aliquoting 2 μ l onto a glass coverslip in 5 technical replicates, and counted under
40 a dissecting microscope. Finally the appropriate number of animals was added to 6 cm plates
41 that had been previously seeded with 300 μ l OP50, and incubated at 20°C. After 3 days, 100%
42 of worms exhibited Neutral Red staining ($n=50$, Supplementary Figure 3). Dauers and J2s
43 recovered after Neutral Red staining developed at the same developmental speed (3-4 days)
44 and with the same mouth-form ratio as control worms recovered side-by-side (100% St for both,
45 Supplementary Figure 4, $n=30$). Dauers and J2s stained with CellTracker Green BODIPY (50
46 μ M) (Thermo) were similar, although less efficiently stained compared to Neutral Red. On day 4,
47 90% retained intestinal fluorescence (Supplementary Figure 3), and brightness decreased with
48 the number of days. J2s in +/- 50 μ M CellTracker Green BODIPY also developed at equivalent
49 rates and mouth-form ratios (Supplementary Figure 4). Lower than 25 μ M did not yield strongly

50 fluorescent worms after three hours. CellTracker Blue CMAC (Thermo Fisher) was also used at
51 50 μ M and imaged 3 days post-staining for *P. pacificus*, and one day post-staining for *C.*
52 *elegans*. However, due to the higher fluorescent background in the blue light spectrum in both
53 *P. pacificus* and *C. elegans*, we performed all experiments using only Neutral Red and
54 CellTracker Green BODIPY.

55

56 **Microscopy**

57 All images were taken on a Zeiss Axio Imager 2 with an Axiocam 506 mono, and processed
58 using Zen2 pro software. Image brightness and contrast were enhanced in ImageJ with a
59 minimum displayed value of 10 and maximum of 100 for all images in Figure 2, and
60 Supplementary Figures 1 and 2, and a minimum of 21 and maximum of 117 for Supplementary
61 Figure 3. The following exposure times were used for all images: Cy3 (peak emission = 561,
62 exposure = 80 ms), FITC (peak emission = 519, exposure = 150 ms), Dapi (peak emission =
63 465, exposure = 80 ms), DIC (exposure = 80-140 ms).

64

65 **Mixed culture experiments and statistical analysis**

66 We performed the mixed culture experiments presented in Figure 3 with a minimum total
67 number of counts $n > 100$, from three to five independent biological replicates for J2/24 hr,
68 dauer, and adult competitor experiments, and two for the intermediate (J3/4) juvenile
69 experiment (median counts per replicate for J2/24 hr=29, dauers=27, and adults=21, and avg.
70 J3/4 counts was 75). J2 or dauers were stained with Neutral Red, then added to green-stained
71 J2, dauer, J3/4, or adult populations as described in the 'Dye Staining' method section, on 6 cm
72 plates with 300 μ l OP50 and incubated at 20°C. To ensure consistent bacterial food supply, we
73 added 1 ml more overnight OP50-LB to each plate on the following day, then air-dried under a
74 chemical fume hood for 1 hour, then returned the plates to 20°C. On days three to four, we

75 phenotyped 'red' adults that exhibited no 'green' staining. To assess whether the age of the
76 'green' surrounding population affects the mouth form of the dependent variable 'red' J2s we
77 performed a binomial regression on Eu counts (i.e. "successes") weighted by the number of
78 counts per replicate, and the stage (juveniles vs. adults) and number added as a fixed effects,
79 using a generalized linear model from the standard statistical package in R:

```
80 glm(formula=cbind(Eu,total)~'stage_added' * '#_added', data='J2/Da', family="binomial")
```

81 See Supplementary Table S1 for a table containing the resulting p values. The AIC for our
82 models (85.52 for juveniles and 72.32 for dauers) was substantially lower than the null
83 hypothesis (220.16 for J2s and 147.29 for dauers), arguing a reasonable fit. For pair-wise
84 comparisons of the effect of age for a given number of added animals, we performed a post-hoc
85 Fisher's exact test on a contingency table containing the summed counts ($n > 100$) of Eu and St
86 observations against control plates (no added crowding animals). For display, we converted Eu
87 counts into percent of total in Figure 3, with the p values for the number of animals added
88 indicated over the relevant column (Significance codes: 0 '****' 0.001, '**' 0.01, '*' 0.05).

89

90 **Measuring the effect of food depletion on mouth form**

91 To verify that starvation was not a factor in our mixed culture experiments, we added increasing
92 number of J2s to standard 6 cm plates with 300 μ l OP50 to rapidly consume bacterial food, and
93 measured both the amount of animals that reached adulthood, and the percent Eu in each
94 population for two biological replicates. To assess the affects of added J2s to each dependent
95 variable we performed a binomial regression with count data weighted by the total number of
96 counts for each replicate:

```
97 glm(formula = cbind(reached_adult, total)~thousand_J2s, data=data_2, family="binomial")
```

98 p values indicate a significant difference in percent reaching adult as a function of J2s added,
99 but not in percent Eu (Table S1 bottom frame).

100

101 **Supernatant collection and assays**

102 Strains RS2333, RSC017, and RS2333-*daf-22.1;22.2* were raised in 10 ml liquid culture as in
103 the time-resolved NDMM collections (see below). For each time point, 9 ml of the supernatant
104 was lyophilized overnight, extracted again overnight with 90% ethanol (diluted in Millipore water)
105 while being stirred, and centrifuged (4000 x g, 10 min, 4°C). The solvent was evaporated and
106 the solid re-dissolved with 1 ml Millipore water. This clear extract was then directly used for the
107 assays. One ml of the supernatant was cleaned for HPLC-MS analysis for quality control, as
108 described in HPLC-MS sample preparation below. For the assays, RSC017 was synchronized
109 by bleaching (Werner et al., 2017) and added to plates seeded with 300 µl OP50. The
110 supernatants were added to the RSC017 J2s in two 500 µl increments (for a total of 1 ml
111 supernatant) and dried for 30 minutes in a sterile hood after each addition. Plates were kept at
112 20°C and adult mouth forms were screened three days later. To determine significance a Fisher
113 Exact test was performed on summed count data relative to S-medium control contingency
114 tables, and the data are presented for representation as percentages in Figure 4.

115

116 **HPLC-MS sample preparation for exo-metabolome and time resolved analysis**

117 To collect staged pheromone profiles, we seeded 35 x 6 cm plates with 5 worms each, and
118 bleached 5-6 days later when gravid to collect eggs/J1s. These were then added to 6 x 10 ml
119 flasks with OP50 as described in Werner et al., 2017 (Werner et al., 2017). Then at 24, 48, or 72
120 hr time intervals, supernatants were obtained by centrifugation (>4,000 x g, 4°C for 10 minutes).
121 1 ml supernatant was adsorbed onto a SPE-C8 cartridge (Thermo Scientific Hypersep C8 100
122 mg/1ml), conditioned with 1 ml MeOH followed by 2 ml Millipore water. The adsorbed material
123 was then washed with 200 µl water and subsequently eluted with 200 µl MeOH. This extract
124 was then measured directly via HPLC-qTof MS (Bruker ImpactII).

125

126 **HPLC-MS measurement**

127 20 µl extract was injected into a Thermo UltiMate 3000 HPLC equipped with a Sigma-Aldrich
128 Ascentis Express C18 2.7 µm 10 mm x 4.6 mm column at 20°C with a flow of 500 µl/min. All MS
129 measurements have been performed in negative ion mode and molecules are detected as [M-
130 H]⁻ ions. The solvent gradient started with 5% acetonitrile (ACN)/ 95% water (both containing
131 0.1% formic acid) for 2 minutes. After this equilibration step, the ACN proportion was increased
132 to 65% over 8 min, then to 100% ACN in 1.2 minutes followed by a hold step for 8.8 minutes.
133 Afterwards, the system was flushed to 5% ACN with 2 minutes equilibration for a total of 22
134 minutes. For calibration, a sodium formate cluster building solution was automatically injected in
135 the first 2 minutes of each run. Data analysis was performed with TASQ version 1.0 from Bruker
136 Daltonics. Extracted ion chromatograms for each well-known compound with a mass width of
137 0.1 m/z and time slices of 0.5 minutes around the expected retention time were produced after
138 calibrating and baseline correction. Assignment errors were corrected with the provided MRSQ
139 value, and areas under the curve were calculated from the integral of each peak.

140

141 **Statistical analysis of NDMMs**

142 NDMM levels were compared simultaneously against strains and developmental stages by a
143 linear model in R: `lm('NDMM' ~ 'developmental stage' * 'strain', data='data.frame')`). In essence,
144 the linear model regressed the abundance of NDMMs against stage and strain as fixed effects.
145 *P* values between stages and strains were adjusted for multiple testing by a false discovery rate
146 correction (FDR). The level of fit between linear vs. exponential growth was determined by the
147 Akaike information criterion (AIC). The lowest AIC for iterations of different exponents
148 ($n=1,2,3,\dots$) was used for comparison to the simple linear model. While significant in both cases,
149 for consistency we present the original *p* values from the original linear model in Table S2.

150 **Supplemental Figure Legends**

151

152 **Figure S1, related to Figure 2. Vital dye staining of *Pristionchus pacificus*.**

153 (A) Control *P. pacificus* imaged with Cy3, FITC, and DAPI filters, and a merge with Differential
154 Interference Contrast (DIC). Histogram on the right represents quantification of intensity with
155 each filter. (B) Same as (A) but stained with 0.005% Neutral Red, (C), 50 μ M CellTracker Green
156 BODIPY (Thermo Fisher), or (D) 50 μ M CellTracker Blue CMAC Dye (Thermo Fisher). J2s were
157 stained (see Transparent Methods), and ensuing adult animals were imaged 3 days later on a
158 Zeiss Axio Imager 2 with an AxioCam 506 mono, and processed using Zen2 pro software.
159 Image brightness and contrast were enhanced in ImageJ for display, with a minimum displayed
160 value of 10 and maximum of 100 for all images. Note that while Neutral Red and CellTracker
161 Green staining are bright and specific to their respective channels, CellTracker Blue is
162 indistinguishable from background fluorescence.

163

164 **Figure S2, related to Figure 2. Vital dye staining of *Caenorhabditis elegans*.**

165 (A-D) Same as Supplementary Figure 1, but with *C. elegans*.

166

167 **Figure S3, related to Figure 2. Vital dye staining of *P. pacificus* dauers, and duration of**

168 **staining.** (A) Control *P. pacificus* dauer imaged with DIC, Cy3, and FITC filters. (B) Dauers
169 stained with either 0.005% Neutral Red or 50 μ M CellTracker Green BODIPY and imaged
170 immediately after staining with DIC, Cy3, and FITC filters and merged with DIC. Images were
171 taken using Zeiss Axio Imager 2 with an AxioCam 506 mono, processed using Zen2pro
172 software, and adjusted in ImageJ, with a display value minimum of 21 and maximum of 117.

173 (C-G) 50 μ M CellTracker Green BODIPY and 0.005% Neutral Red-stained J2s were imaged
174 every day for five days. Percent of individuals retaining the dyes are shown in panels next to
175 each microscope image for each day. Both stains are seen in all organisms for three days;
176 Neutral Red (NR) persists for at least five, while the number of Green BODIPY (GB) –stained
177 worms drops on day four. All images are merged with DIC, n=31 GB, 63 NR day 1, 68 GB, 56
178 NR day 2, 50 GB, 50 NR day 3, 50 GB, 50 NR day 4, 50 GB, 50 NR day 5.

179

180 **Figure S4, related to Figure 2. Vital dye staining does not affect *P. pacificus* mouth form**
181 **or development.**

182 (A) Neutral Red and CellTracker Green BODIPY-stained J2s reach adulthood at the same
183 rate as unstained J2s (3 days). (B) All of the J2s stained retain the dye in adulthood in the
184 intestine. (C) Neither dye affects mouth form; both unstained and stained worms remain
185 100% St (n=30). (D-F) Same as for (A-C) except with dauers instead of J2s, and only with
186 Neutral Red. (G) Developmental rate of J2 unstained, Neutral Red-stained (NR), and
187 CellTracker Green BODIPY-stained (GB) RSC017 every 12 hours post-J2 staining. Two
188 biological replicates, n=60. To see if there were significant differences between stained
189 and un-stained, a Fisher's Exact test was performed on summed counts of each stage (all
190 $p>0.05$) (H) Staging of RSC017 worms from liquid culture at the relevant time points, 24
191 hrs, 48 hrs, and 72 hrs. Error bars represent standard error of the mean for 3 biological
192 replicates, n>100 animals counted per replicate.

193

194 **Table S1, related to Figure 3. Table of binomial regression *p* values for crowding assays.**

195 Significance *p* values from binomial regression of vital-dye method for age and number added,
196 and from binomial regression of number-reaching-adult and Eu counts, for each number of
197 individuals added relative to 1,000 individuals added (see Transparent Methods for details).

198

199 **Figure S5, related to Figure 5. Pheromone profiling quality control.**

200 (A) Extracted ion traces (width 0.1 m/z) of 11 of the 12 NDMMs used in this publication from a
201 seven-day mixed-stage sample, double peak of 247.12 m/z indicate isomeric structures
202 (Part#9/Ascr#9). (B) Example of an averaged spectrum over a calibration segment; sodium-
203 formate cluster building solution was used to ensure high mass accuracy in each run. (C)
204 Comparison of an endometabolome sample from a seven- day mixed-stage cultured compared
205 to the endometabolome of eggs, produced by using bleached eggs from 80 x 60 mm plates.

206

207 **Table S2, related to Figure 5. Table of linear regression p values with FDR corrections for**
208 **strain and stage comparison of NDMM levels.** FDR-corrected and uncorrected p values from
209 linear regression of *P. pacificus* NDMMs (alternating grey background between NDMMs for
210 clarity). Red values indicate FDR<0.05.

211

212 **Table S3, related to Figure 5. P values from pairwise comparison of dasc#1, npar#1, and**
213 **ascr#9 throughout development.** Significance assessed with a two-tailed student's t -test. Top
214 table indicates comparison of raw pheromone levels experienced by worms, and the bottom
215 table indicates comparison of volume-normalized pheromone levels (normalized data from
216 WormSizer (Moore et al., 2013), Fig. S6B-D).

217

218 **Figure S6, related to Figure 5. Enzyme that synthesizes NDMMs is transcriptionally**
219 **regulated during development, and volume normalization of pheromones.** (A) Comparison
220 of *daf-22.1* (FPKM) by RNA-seq through different stages of development, data from Baskaran et
221 al., 2015 (Baskaran et al., 2015). A two-sided students t -test was performed between 56-68

222 hours (J4-adults) and 22 hours (J2s) (Significance codes: 0 '***' 0.001, '**' 0.01, '*' 0.05). (B)
223 Representative images of worms raised in liquid culture at 24 hrs, 48 hrs, and 72 hrs. (C)
224 Comparison of worm volumes (picoLiters) for 24 hrs, 48hrs, and 72 hrs, using WormSizer
225 (Moore et al., 2013). (D) Time-resolved NDMM levels of RSC017 normalized by worm volume
226 (upper graph) and unnormalized (lower graph, also shown in Figure 5B). Data is presented as
227 the mean of nine biological replicates and error bars represent standard error of the mean
228 (SEM). In the upper graph, levels were normalized to worm volume based on the data shown in
229 (C).

230

231 **Table S4, related to Figure 5. Raw and volume-normalized data of RSC017 pheromones,**
232 **in absolute value of area under the curve.** Normalization of 48 hr and 72 hr time point
233 abundances relative to 24 hrs. Average volumes obtained by WormSizer (Moore et al.,
234 2013)(Figure S6B-C).

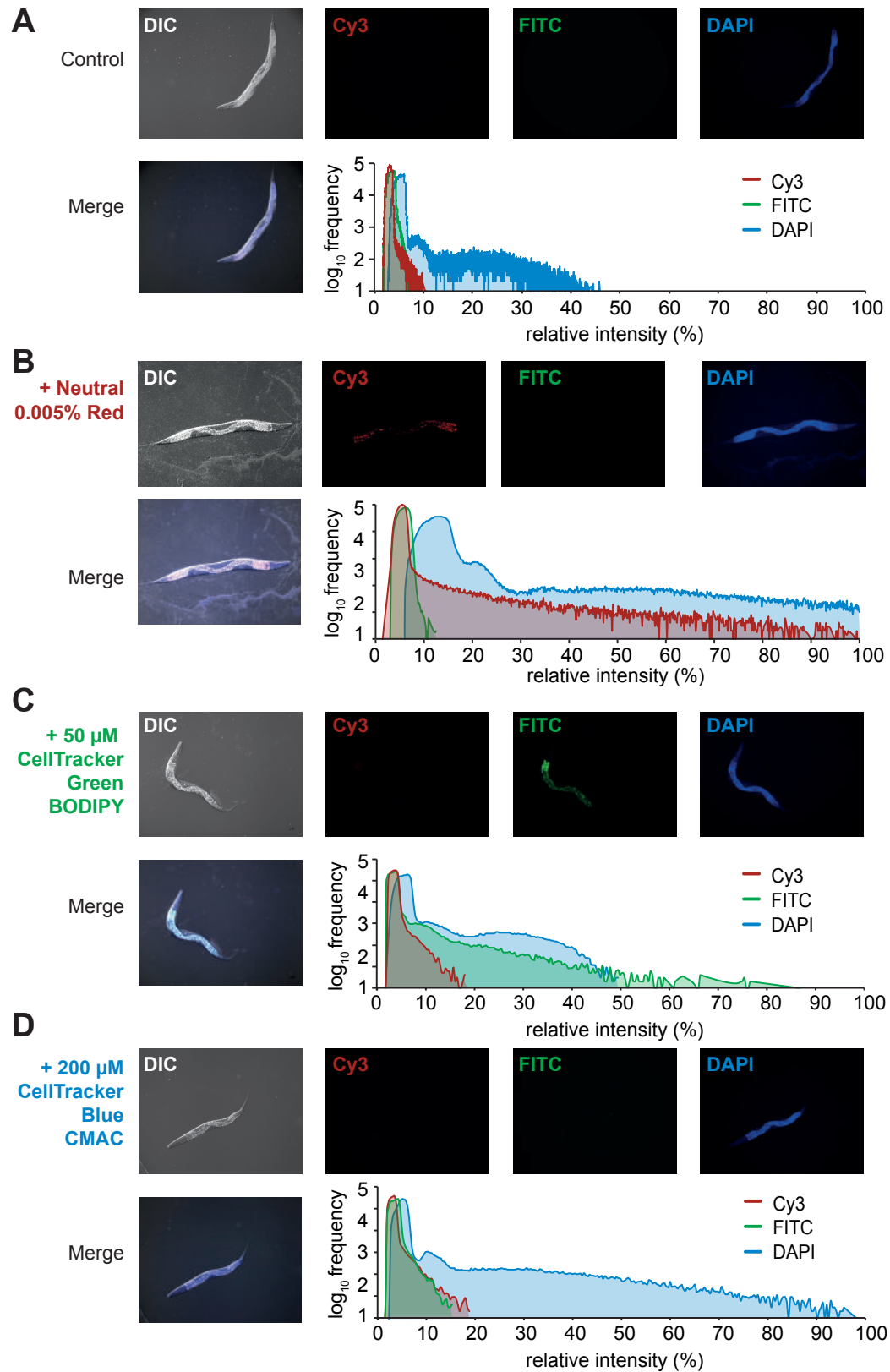


Figure S1, related to Figure 2. Vital dye staining of *Pristionchus pacificus*.

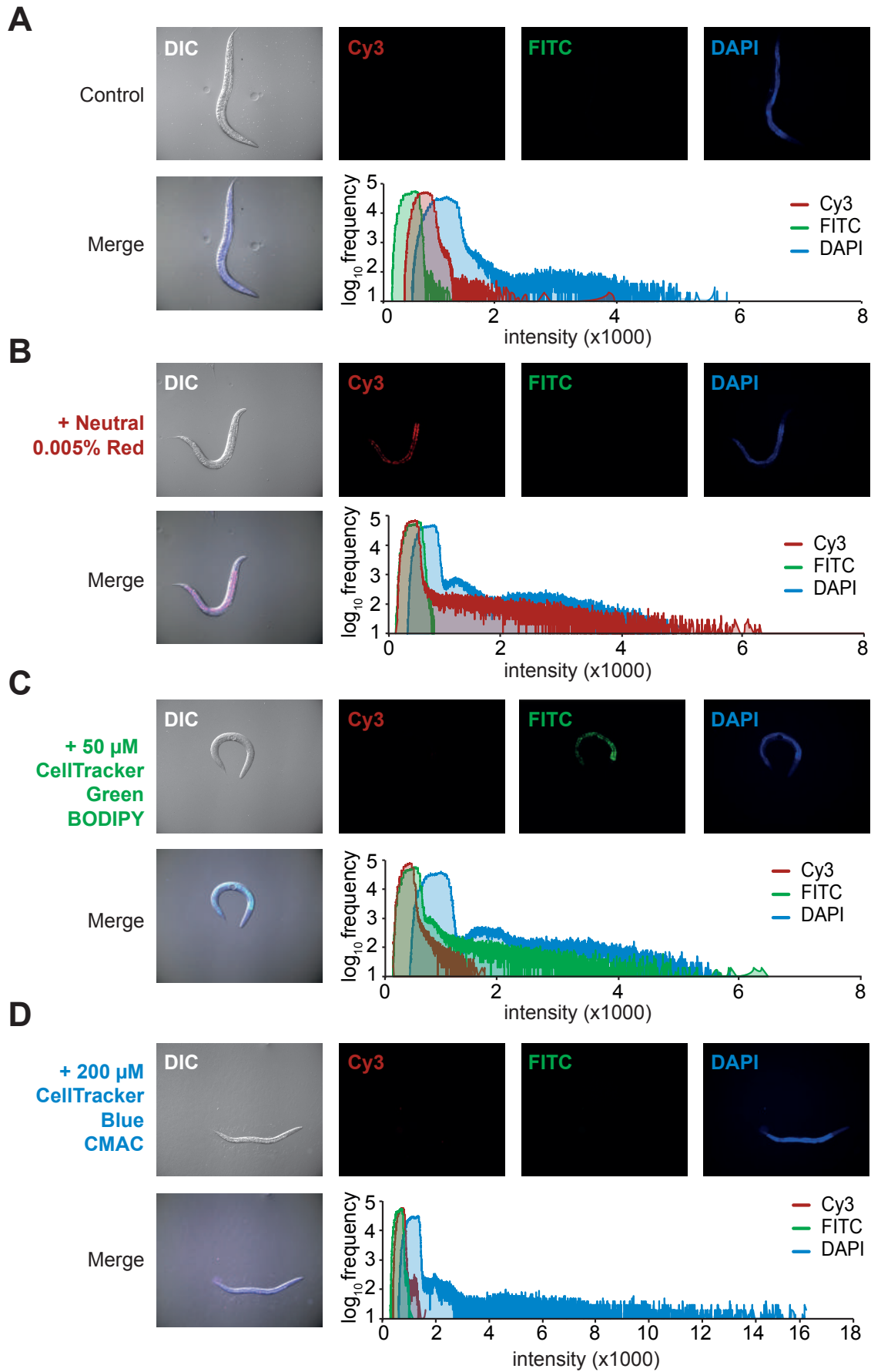


Figure S2, related to Figure 2. Vital dye staining of *Caenorhabditis elegans*.

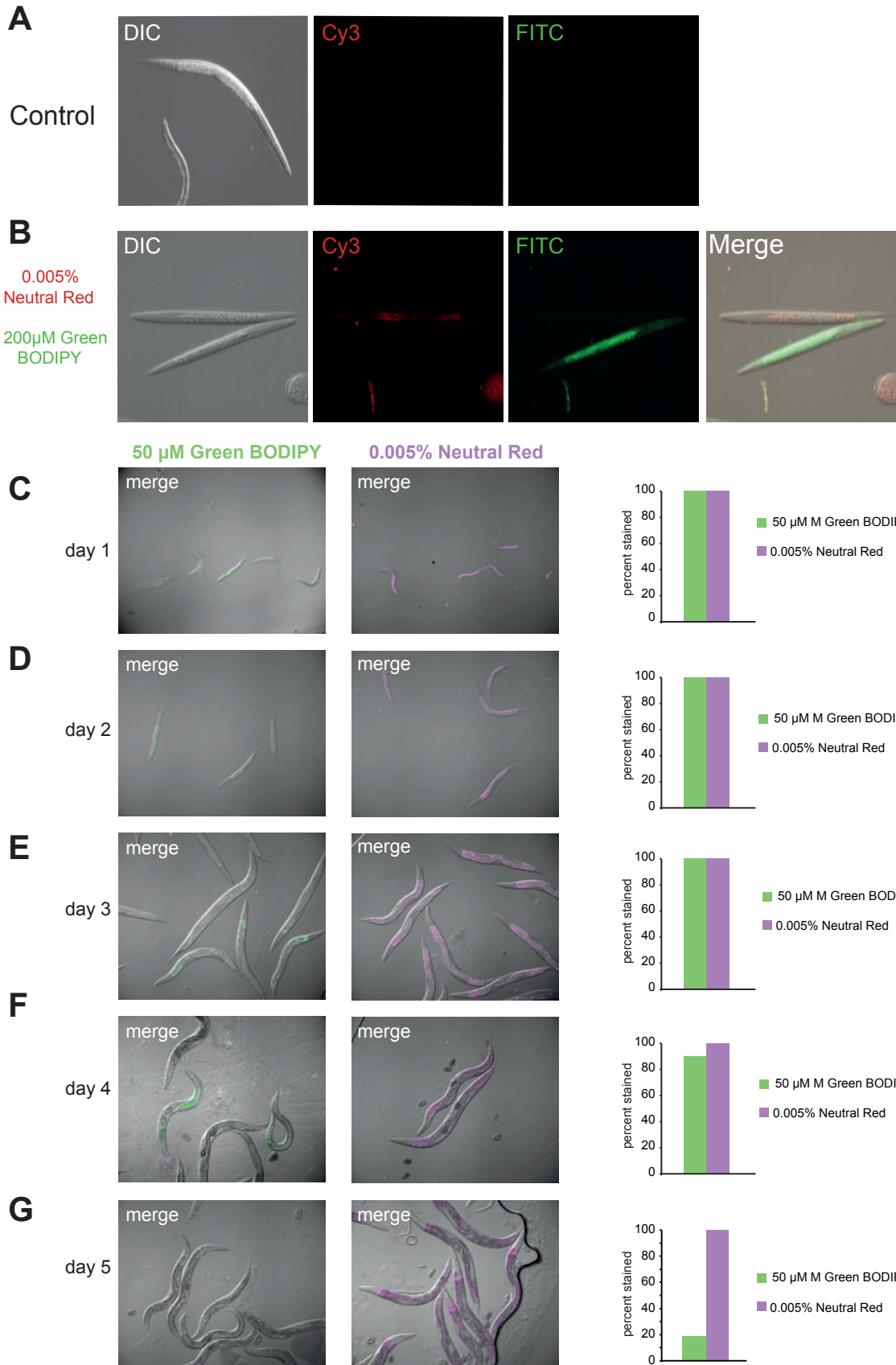


Figure S3, related to Figure 2. Vital dye staining of *Pristionchus pacificus* dauers, and duration of staining.

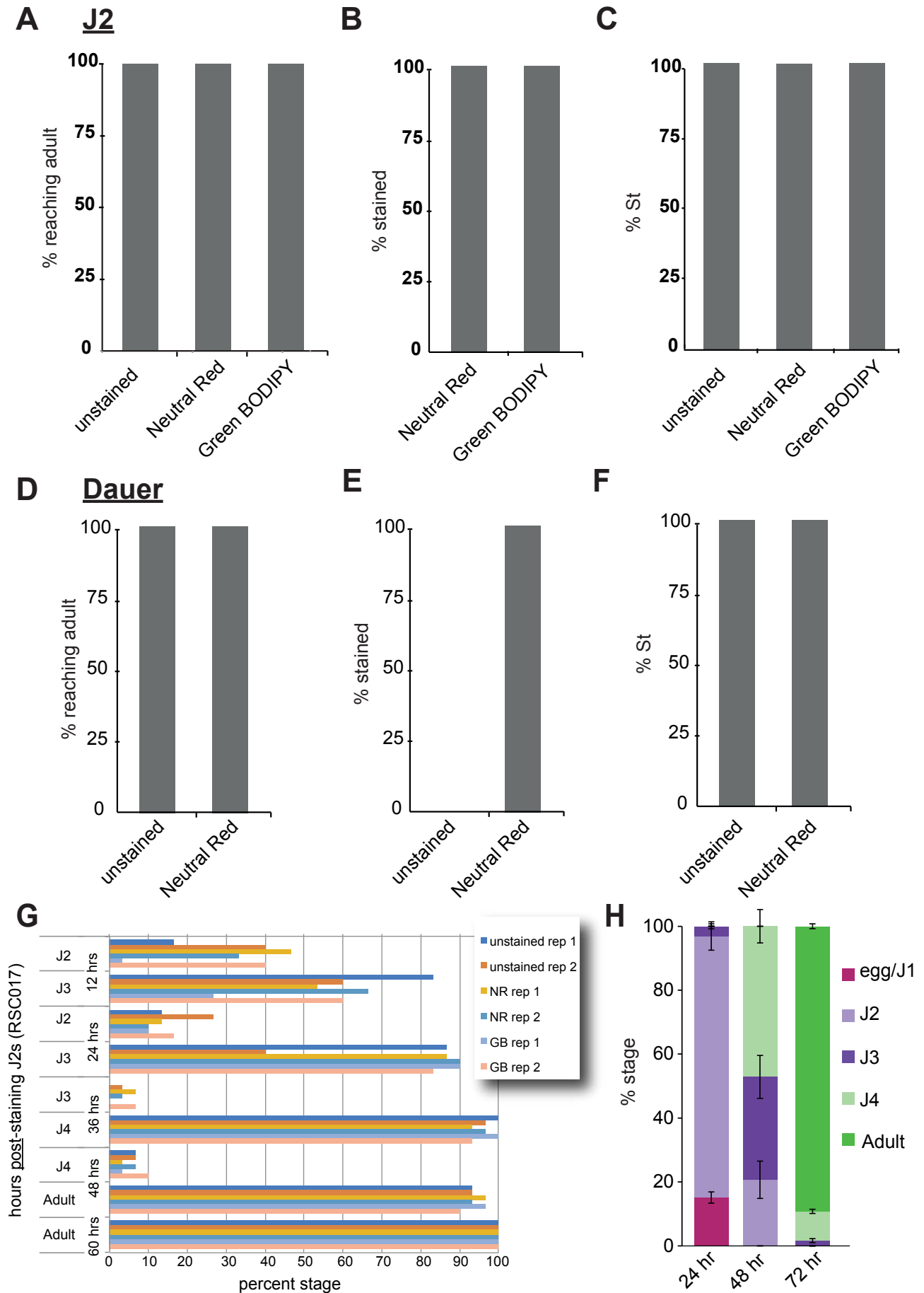


Figure S4, related to Figure 2. Vital dye staining does not affect *P. pacificus* mouth form or development.

**effect of population age on mouth
form of developing juveniles**

binomial regression	<i>p</i> value red-stained J2s	<i>p</i> value red-stain dauers
stage added (adults vs. juveniles)	0.0132	0.002955
number added	4.28e-13	0.000404

**effect of number of peers on development and mouth form
(proxy for potential starvation effects on mouth form)**

binomial regression	<i>p</i> value for development (relative to 1,000)	<i>p</i> value for Eu (relative to 1,000)
3,000 J2s added	0.3408	1.0
4,000 J2s added	0.0424	1.0
5,000 J2s added	6.06E-14	0.99
10,000 J2s added	4.09E-14	0.99

Table S1, related to Figure 3. Table of binomial regression *p* values for vital-dye method and excess crowding.

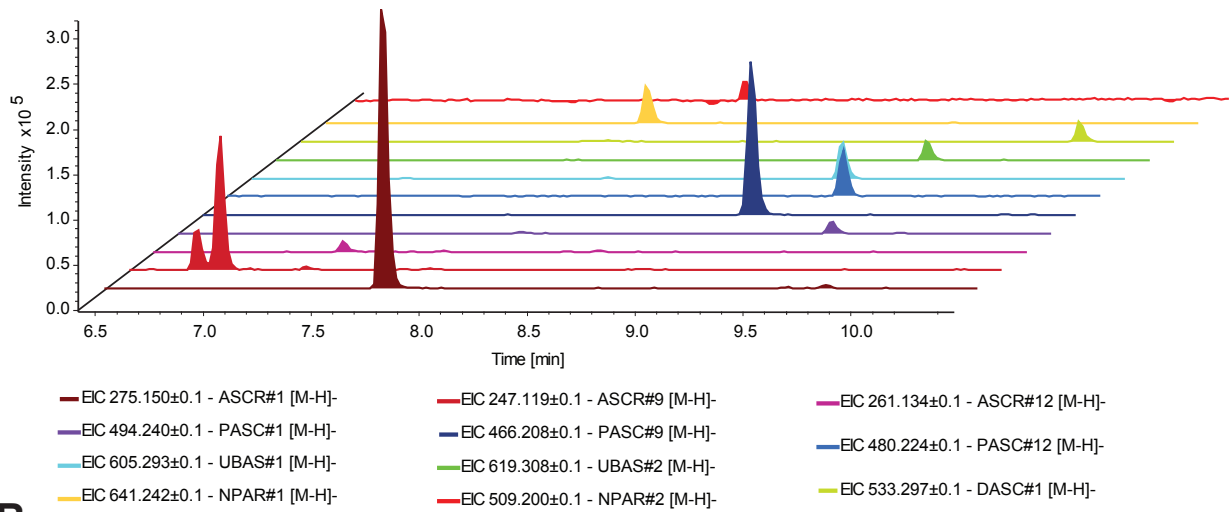
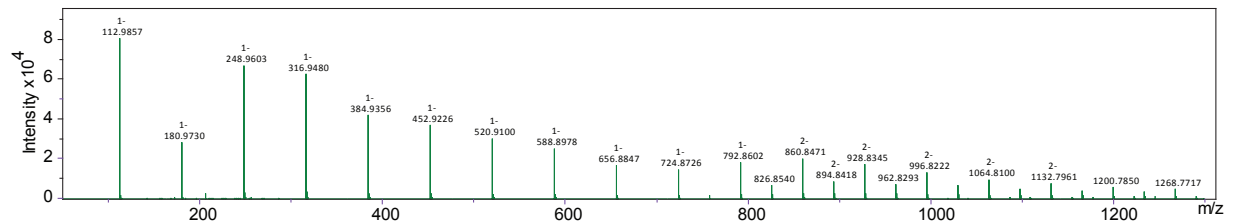
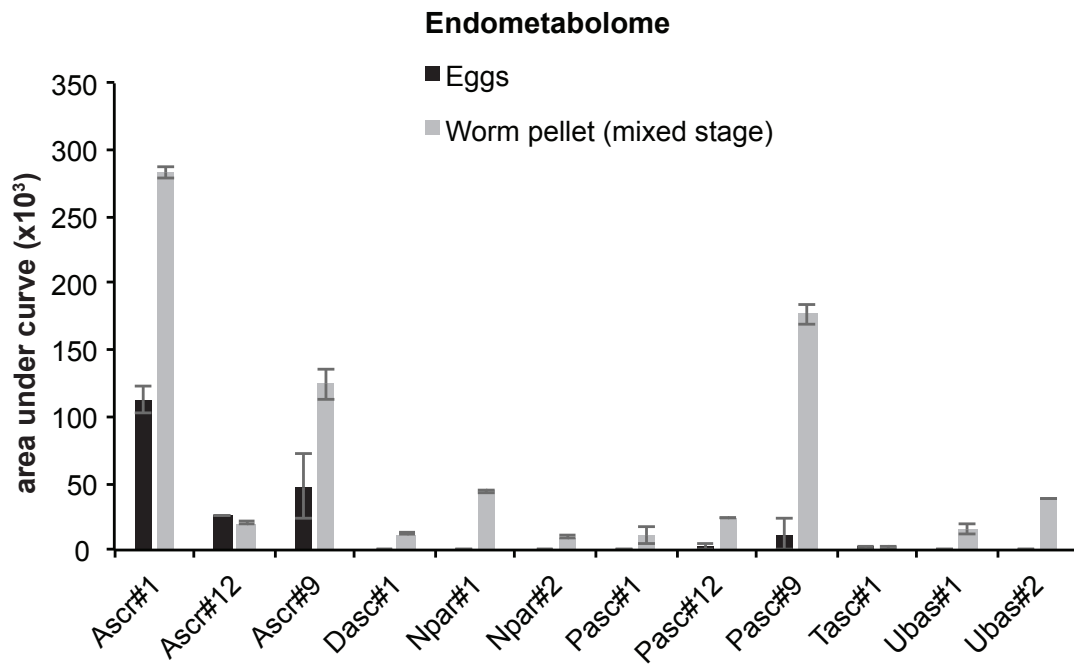
A**B****C**

Figure S5, related to Figure 5. Pheromone profiling quality control

NDMM comparison	pvalue	fdr corrected
ascr1_stage	0.4733	0.774490909
ascr1_strain	0.0429	0.110314286
ascr1_stage:strain	0.031	0.085846154
ascr9_stage	3.79E-05	0.0002274
ascr9_strain	0.651	0.778064516
ascr9_stage:strain	0.272	0.50148
ascr12_stage	0.0029	0.01404
ascr12_strain	0.0897	0.201825
ascr12_stage:strain	0.0302	0.085846154
dasc1_stage	9.62E-08	8.66E-07
dasc1_strain	0.11363	0.240628235
dasc1_stage:strain	0.00351	0.01404
npar1_stage	0.0033	0.01404
npar1_strain	0.9426	0.984
npar1_stage:strain	0.6355	0.778064516
npar2_stage	0.0516	0.12384
npar_2strain	0.984	0.984
npar2_stage:strain	0.9716	0.984
pasc1_stage	0.449	0.769714286
pasc1_strain	0.753	0.847125
pasc1_stage:strain	0.564	0.778064516
pasc9_stage	0.616	0.778064516
pasc9_strain	0.267	0.50148
pasc9_stage:strain	0.523	0.778064516
pasc12_stage	0.6122	0.778064516
pasc12_strain	0.2786	0.50148
pasc12_stage:strain	0.67	0.778064516
tasc1_stage	0.522	0.778064516
tasc1_strain	0.862	0.940363636
tasc1_stage:strain	0.57	0.778064516
ubas1_stage	3.13E-12	1.13E-10
ubas1_strain	0.00538	0.019368
ubas1_stage:strain	6.69E-08	8.03E-07
ubas2_stage	1.34E-11	2.41E-10
ubas2_strain	0.00711	0.023269091
ubas2_stage:strain	6.18E-07	4.45E-06

Table S2, related to Figure 5. Table of linear regression *p* values with *FDR* correction for strain and stage comparison of NDMM levels.

RS2333	dasc#1	npar#1	ascr#9
72 hrs compared to 24 hrs	5.75E-07	3.47E-05	1.03E-04
72 hrs compared to 48 hrs	5.71E-03	1.76E-01	1.97E-01
RSC017	dasc#1	npar#1	ascr#9
72 hrs compared to 24 hrs	2.55E-02	3.66E-03	2.03E-02
72 hrs compared to 48 hrs	2.12E-01	3.66E-01	1.04E-01

Volume normalized

RS2333	dasc#1	npar#1	ascr#9
72 hrs compared to 24 hrs	5.75E-07	3.47E-05	1.02E-03
72 hrs compared to 48 hrs	1.44E-02	2.92E-01	6.21E-01
RSC017	dasc#1	npar#1	ascr#9
72 hrs compared to 24 hrs	2.55E-02	3.66E-03	4.34E-02
72 hrs compared to 48 hrs	2.71E-01	5.46E-01	1.70E-01

Table S3, related to Figure 5. P values from pairwise comparison of dasc#1, npar#1, and ascr#9 throughout development.

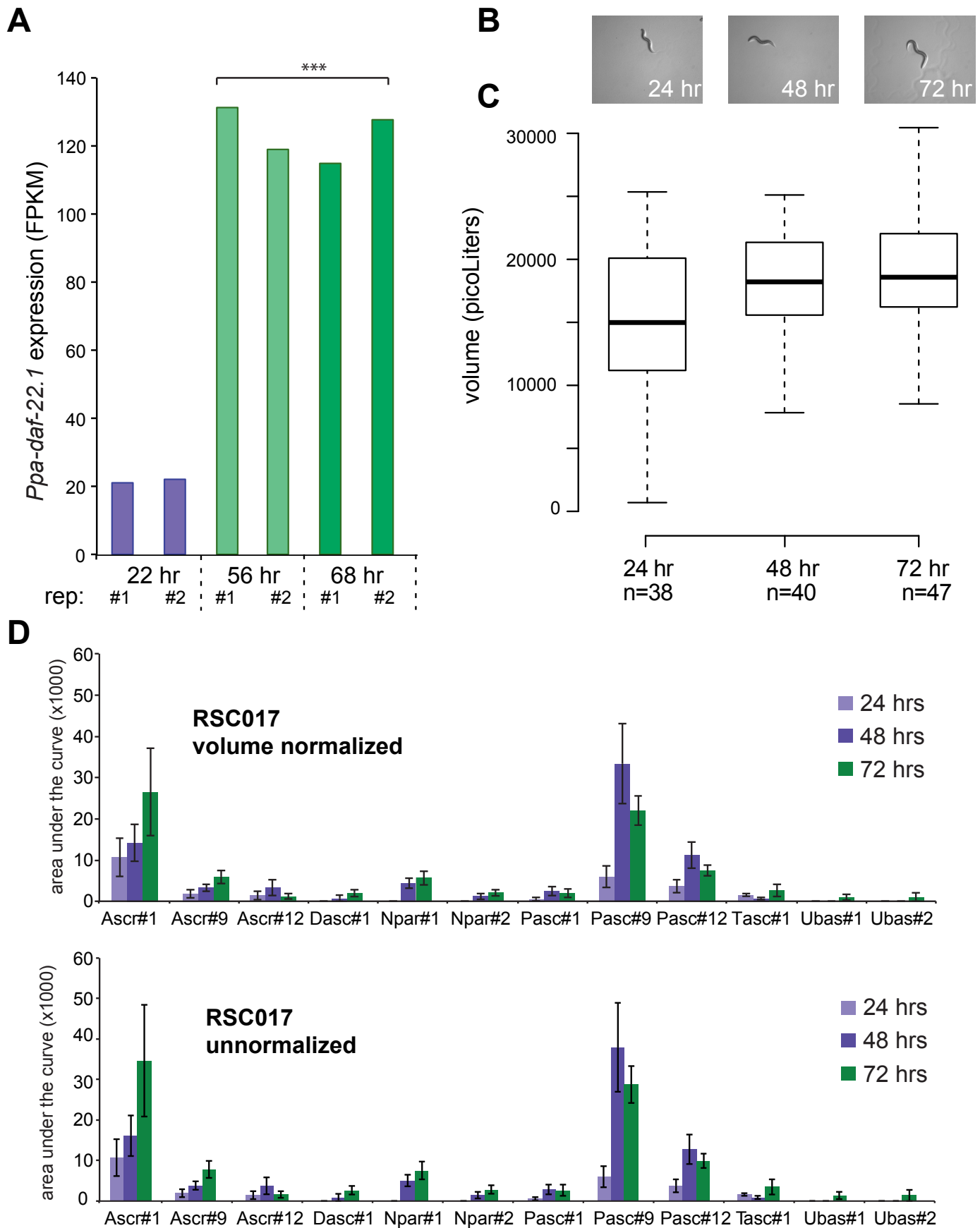


Figure S6, related to Figure 5. Enzyme that synthesize NDMMs is transcriptionally regulated during development, and volume normalization of pheromones.

STAGE	DASC1	NPAR1	Pasc9	Ascr1	Ascr12	Ascr9	Npar2	Pasc1	Pasc12	Tasc1	Ubas1	Ubas2
24	0	0	0	0	0	0	0	0	0	1610	0	0
24	0	0	0	4489	0	0	0	0	0	1214	0	0
24	0	0	0	0	0	0	0	0	0	1769	0	0
24	0	0	0	22265	0	4301	0	0	0	1169.5	0	0
24	0	0	0	28319.5	0	5450	0	0	0	1871.5	0	0
24	0	0	7193.5	35197.5	8299.5	7177	0	0	9476	3918	0	0
24	0	0	16048.5	3929.5	5028.5	0	0	0	8318	969.5	0	0
24	0	0	19293.5	2386.5	0	0	0	1657.5	11094	999	0	0
24	0	0	11623.5	0	0	0	0	3667.5	4799.5	949.5	0	0
48	7800	8901	111298	7866	0	4250	6050	8486	35583.5	2827	0	0
48	0	8393	54479	7660	0	7077	5605	6699	19222.5	1047.5	0	0
48	0	10347	32381.5	11133	0	4339	0	6513	11901.5	2324	0	0
48	0	0	13819	34084	16659.5	5087	0	0	5916	1217	0	0
48	0	0	6893	40108	12167	7298	0	0	0	0	0	0
48	0	0	6766	32972	5415	6235.5	0	0	0	0	0	0
48	0	7635.5	56471.5	6725	0	0	1522	3957	17663.5	400.5	0	0
48	0	7036	29685.5	4781	0	0	0	0	13964.5	0	0	0
48	0	3205.5	29656	0	0	0	0	0	10977	0	0	0
72	0	16111.5	45664.5	9007	0	7593.5	5065	10394.5	17614.5	2243	0	12581
72	6321	9157.5	36161.5	7275	0	5649	5062	8322	13492	562.5	0	0
72	4475.5	17381	51388	7354.5	0	7472	7192	5269.5	12932	1192	0	0
72	7400.5	10075	25671	93903	6060	22877	6485	0	8342	12416	6377.5	0
72	0	0	9248.5	61584	3670.5	7879	0	0	0	14621	0	0
72	5861	0	13904	107297	4907.5	8875	0	0	5734	0	5697.5	0
72	0	0	20159.5	12767.5	0	0	0	0	9426	0	0	0
72	0	7294.5	28800	6249	0	3823	0	0	7802	544	0	0
72	0	7454.5	28094	6695.5	0	6082	1696.5	0	13884.5	201	0	0

RSC017 pheromone levels

STAGE	DASC1	NPAR1	Pasc9	Ascr1	Ascr12	Ascr9	Npar2	Pasc1	Pasc12	Tasc1	Ubas1	Ubas2
24	0	0	0	0	0	0	0	0	0	1610	0	0
24	0	0	0	4489	0	0	0	0	0	1214	0	0
24	0	0	0	0	0	0	0	0	0	1769	0	0
24	0	0	0	22265	0	4301	0	0	0	1169.5	0	0
24	0	0	0	28319.5	0	5450	0	0	0	1871.5	0	0
24	0	0	7193.5	35197.5	8299.5	7177	0	0	9476	3918	0	0
24	0	0	16048.5	3929.5	5028.5	0	0	0	8318	969.5	0	0
24	0	0	19293.5	2386.5	0	0	0	1657.5	11094	999	0	0
24	0	0	11623.5	0	0	0	0	3667.5	4799.5	949.5	0	0
48	6859.790284	7828.076066	97882.17167	6917.834663	0	3737.706244	5320.734771	7463.100045	31294.27533	2486.234248	0	0
48	0	7381.310238	47912.11729	6736.665843	0	6223.940492	4929.374941	5891.504502	16905.42548	921.2346567	0	0
48	0	9099.77565	28478.24347	9791.03144	0	3815.97821	0	5727.924887	10466.89667	2043.86572	0	0
48	0	0	12153.26179	29975.52462	14651.36875	4473.81451	0	0	5202.887092	1070.303176	0	0
48	0	0	6062.119798	35273.39342	10700.39338	6418.301217	0	0	0	0	0	0
48	0	0	5950.428341	28997.56477	4762.277486	5483.874656	0	0	0	0	0	0
48	0	6715.119066	49664.44193	5914.370469	0	0	1338.538566	3480.024379	15534.34688	352.2238473	0	0
48	0	6187.88262	26107.21852	4204.69966	0	0	0	0	12281.22326	0	0	0
48	0	2819.109969	26081.27444	0	0	0	0	0	9653.835634	0	0	0
72	0	12340.85154	34977.427	6899.050356	0	5816.358263	3879.61475	7961.827348	13492.09753	1718.060392	0	9636.610695
72	4841.667292	7014.328149	27698.45781	5572.398284	0	4326.938544	3877.316854	6374.364057	10334.40517	430.8555374	0	0
72	3428.078147	13313.24461	39361.42997	5633.292533	0	5723.293467	5508.823155	4036.254674	9905.46455	913.0307566	0	0
72	5668.526941	7717.101403	19663.09778	71926.44894	4641.750323	17522.99045	4967.285618	0	6389.683365	9510.226404	4884.944337	0
72	0	0	7084.031	47171.21318	2811.476	6035.041385	0	0	0	11199.18011	0	0
72	4489.323208	0	10649.98292	82185.7895	3758.9752	6797.942923	0	0	4392.045603	0	4364.087865	0
72	0	0	15441.47948	9779.463242	0	0	0	0	7219.989859	0	0	0
72	0	5587.334609	22059.80351	4786.517783	0	2928.285723	0	0	5976.062049	416.6851775	0	0
72	0	5709.889073	21519.03194	5128.521334	0	4658.601562	1299.460301	0	10635.04659	153.9590454	0	0

RSC017 volume normalized pheromone levels

Table S4, related to Figure 5. Raw and normalized data of RSC017 pheromones, in absolute value of area under the curve.

OPEN

Crowdsourcing and the feasibility of manual gene annotation: A pilot study in the nematode *Pristionchus pacificus*

Christian Rödelberger*, Marina Athanasouli, Maša Lenuzzi, Tobias Theska, Shuai Sun, Mohannad Dardiry, Sara Wighard, Wen Hu, Devansh Raj Sharma & Ziduan Han

Nematodes such as *Caenorhabditis elegans* are powerful systems to study basically all aspects of biology. Their species richness together with tremendous genetic knowledge from *C. elegans* facilitate the evolutionary study of biological functions using reverse genetics. However, the ability to identify orthologs of candidate genes in other species can be hampered by erroneous gene annotations. To improve gene annotation in the nematode model organism *Pristionchus pacificus*, we performed a genome-wide screen for *C. elegans* genes with potentially incorrectly annotated *P. pacificus* orthologs. We initiated a community-based project to manually inspect more than two thousand candidate loci and to propose new gene models based on recently generated Iso-seq and RNA-seq data. In most cases, misannotation of *C. elegans* orthologs was due to artificially fused gene predictions and completely missing gene models. The community-based curation raised the gene count from 25,517 to 28,036 and increased the single copy ortholog completeness level from 86% to 97%. This pilot study demonstrates how even small-scale crowdsourcing can drastically improve gene annotations. In future, similar approaches can be used for other species, gene sets, and even larger communities thus making manual annotation of large parts of the genome feasible.

How well can biological knowledge be transferred across species? Are biological functions carried out by the same genes in different organisms? How fast do regulatory networks diverge? In order to address these fundamental questions, more than 20 years ago, the nematode *Pristionchus pacificus* has been introduced as a so-called “satellite” model organism to one of the most successful animal model systems, *Caenorhabditis elegans*^{1,2}. Since then, several comparative studies in developmental and ecological contexts have highlighted the importance of developmental system drift as a concept in evolution³ and have demonstrated that the divergence between *Pristionchus* and *Caenorhabditis* was accompanied by extensive chemical^{4–6}, genic^{7–9}, and morphological^{10–12} innovations. The establishment of multiple genetic^{13,14} and genomic tools and resources^{15,16} by Sommer and colleagues motivated an increasing number of independent groups to adapt *P. pacificus* as a model system for comparative studies at a mechanistic level^{17–21}. However, reverse genetic approaches based on candidate genes with known functions in *C. elegans*^{22,23} have been hampered not only by the huge amount of lineage-specific duplications^{23–26}, but also by missing and incorrect gene annotations. Traditionally, protein-coding genes are annotated by gene prediction algorithms that model general sequence features of transcription and translation start and end sites, as well as splicing signals^{27–29}. This can be complemented with evidence based approaches using transcriptomic and protein homology data^{30,31}. While automated annotation pipelines perform reasonably well to be useful for genetic screens^{32–34} and evolutionary genomic analyses^{35–37}, their outcomes by far do not meet the standards of the gene annotations from classical model organisms such as *C. elegans*, *Drosophila melanogaster*, and *Mus musculus* that have been curated over decades by a large research community³⁸. In order to make the *P. pacificus* system more tractable for researchers without extensive genomic and phylogenetic expertise, we need to minimize the discrepancy in gene annotation quality between *C. elegans* and *P. pacificus*. To this end, we employed an integrative approach using comparative genomic and transcriptomic data combined with crowdsourcing to improve the *P. pacificus* annotations of *C. elegans* homologs and orthologs. First, we carry out a comparative assessment of 22

Max Planck Institute for Developmental Biology, Department for Integrative Evolutionary Biology, Max-Planck-Ring 9, 72076, Tübingen, Germany. *email: christian.roedelberger@tuebingen.mpg.de

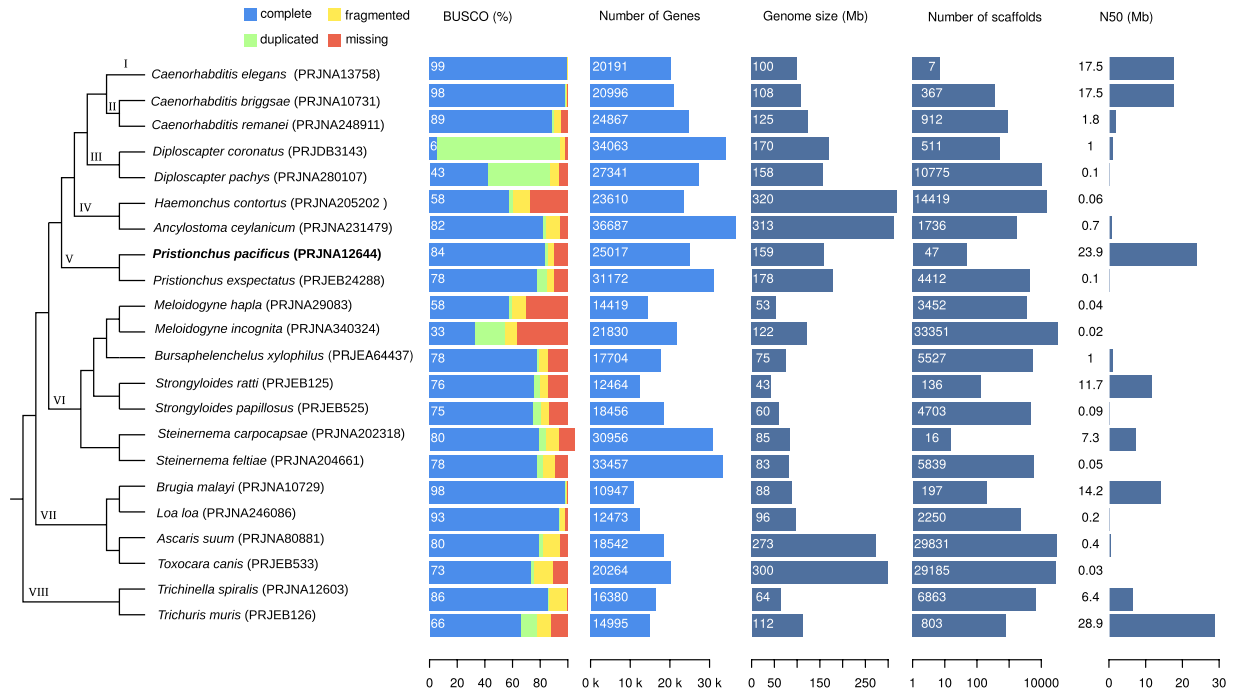


Figure 1. Comparative assessment of nematode genome quality. Genomic data for 22 nematode species was obtained from WormBase ParaSite (release WBPS13) and evaluated based on completeness level of gene annotations and genome assembly contiguity. The barplots show the results of a benchmarking of single copy orthologs (BUSCO⁴⁰) analysis, the number of genes, genome sizes, number of scaffolds, and the N50 measure of assembly contiguity. The genome and annotations of *P. pacificus* exhibit an overall comparatively high quality. The schematic phylogeny is based on phylogenomic analysis of 108 nematodes³⁹, Roman numerals indicate phylostrata that are used for further analysis.

nematode genomes and demonstrate that *P. pacificus* has one of the best available nematode genomes. Second, we perform a genomewide screen for *C. elegans* genes where homologs and orthologs are not or incorrectly annotated in the *P. pacificus* genome. Third, a community-based manual curation of suspicious gene models reveals thousands of hidden orthologs and missing homologs. This pilot study can be extended to even larger gene sets and communities possibly employing citizen scientists, which would raise the quality of gene annotations to the next level³⁸.

Results

The quality of nematode draft genomes is highly heterogeneous. To obtain a general overview of the current status of nematode genome quality, we analyzed assemblies and gene annotations of 22 species (Fig. 1). The species were arbitrarily selected to span the diversity of the nematode phylum³⁹. We will further use this taxon sampling to perform an analysis of gene age, i.e. phylostratigraphic analysis where each phylostratum is defined by at least two outgroup species to minimize the effect of species-specific gene loss. Nematode genomes range in size between 43 and 320 Mb and contain between 11 and 37 thousand annotated protein-coding genes (Fig. 1). Analyses of assembly features and gene annotations indicate a wide range of qualitative variability. Some genomes are assembled and scaffolded to the level of chromosomes with high degrees of contiguity (the N50 value which is a measure of genome assembly contiguity is up to 29 Mb) whereas others are largely fragmented into up to 33 thousand scaffolds with N50 values below 0.1 Mb (Fig. 1). Similarly, analyses of completeness levels based on benchmarking universal single copy orthologs (BUSCO⁴⁰) reveal substantial amount of either missing or duplicated genes and it is not totally clear to what extent these differences are of biological or technical nature⁴¹. In the case of *Diploscapter coronatus*, the apparent high fraction of duplicated genes could either be explained by hybridization of two divergent lineages or a whole genome duplication⁴². The genome of *P. pacificus*, which was generated by assembly from single-molecule, long-read sequencing data and scaffolding with the help of a genetic linkage map¹⁵, shows one of the highest levels of contiguity (47 scaffolds, N50 = 24 Mb). Gene annotations were generated by the MAKER2 pipeline^{30,31} which combined gene prediction algorithms, transcriptome data, and protein homology data from other *Pristionchus* species^{11,15,43}. The completeness level of gene annotations (BUSCO completeness: 84%) is in the upper range when compared to most other nematode genomes (median 78%, interquartile range (IQR): 68–85%, Fig. 1). This demonstrates the relatively high quality of the current *P. pacificus* assembly and gene annotations.

Complementary genome and transcriptomes reveal potentially missing gene models. The completeness analysis as implemented in the software BUSCO⁴⁰ can also be applied to the raw genome assembly of *P. pacificus*. This yielded a combined completeness value of 93% (complete single copy and duplicates) as

Data set	BUSCO (%)				Ref
	Complete Single Copy (+Duplicates)	Duplicate	Fragmented	Missing	
Genome assembly (El Paco assembly)	91.6 (92.9)	1.3	3.1	4.0	¹⁵
El Paco annotation v1/WS268	84.0 (85.8)	1.8	4.3	9.9	¹⁵
<i>de novo</i> transcriptome assembly	59.1 (97.1)	38.0	2.6	0.3	¹⁶
Iso-Seq assembly	48.0 (73.3)	25.3	10.9	15.8	⁴⁴
El Paco annotation v2	95.4 (97.1)	1.7	2.0	0.9	this study

Table 1. Completeness analysis of different *P. pacificus* data set. The high level of duplicates in the two transcriptomic data sets is due to the presence of isoforms.

compared to 86% for the *P. pacificus* gene annotations and indicates towards the presence of incorrectly annotated or missing *C. elegans* orthologs in the genome of *P. pacificus*. Moreover, the fact that a recent *de novo* transcriptome assembly that was based on a strand-specific RNA-seq data set exhibited an even higher combined completeness level of 97% (Table 1) demonstrates even further room for improvement¹⁶. Finally, single-molecule, long-read transcriptome sequencing data were recently generated for *P. pacificus* which allows a much more accurate definition of gene structures from reference alignments of single reads⁴⁴. However, neither transcriptomic data set was available when the existing gene annotations (version: El Paco annotation v1/WormBase release: WS268) were generated and they could still be used for further improvement.

To systematically identify potentially missing genes in the *P. pacificus* genome, we searched for *C. elegans* genes lacking homologs in the current *P. pacificus* gene annotations (BLASTP e-value < 10⁻⁵) but having a matching open reading frame in the *de novo* transcriptome assembly (Fig. 2a). While 12,504 (62%) *C. elegans* genes had BLASTP hits in both data sets, 634 (3%) *C. elegans* genes showed only BLASTP hits against the current gene annotations suggesting that these genes are properly annotated but are expressed so weakly that they were not captured in the transcriptome assembly of mixed-stage cultures⁴⁵. Similarly, we identified 526 (3%) *C. elegans* genes that were only found in the transcriptome assembly and therefore represent candidates for missing gene annotations.

Community-based curation identifies missing genes in the *P. pacificus* genome. In order to improve the existing gene annotations, we chose to manually inspect and classify all 526 missing gene candidates in the *P. pacificus* genome browser (<http://www.pristionchus.org>). Thereby, we recruited and trained colleagues as community annotators, who would be capable to classify a genomic locus and to propose a correction to the existing gene models (see *Methods*). Lists of missing gene candidates were shared in online spreadsheets and documents, which allowed multiple annotators to inspect and correct candidate loci in parallel. 119 (25%) of the 486 non-redundant *P. pacificus* loci were classified as missing genes in predicted UTRs of annotated genes (Fig. 2b). We would speculate that this is caused by the fact that nematode genomes are compact and UTR regions can frequently overlap⁴⁵. This can cause artificial fusion of transcripts during the assembly of RNA-seq data. Consequently, only the largest ORF of such a gene is annotated as protein-coding and the rest is classified as 3' and 5' UTR. Alternatively, this problem could arise when a fused gene prediction from the sister species is used as homology information but MAKER2 fails to generate a complete gene model out of it. The *C. elegans* gene C29H12.2 is one example of a missing gene model residing in the UTR of a *P. pacificus* *rars-2* homolog (Fig. 2c). The corresponding *P. pacificus* locus is spanned by two assembled transcripts that are homologous two C29H12.2 and *rars-2*, respectively. Both transcripts are also well supported by Iso-seq data and exhibit different expression levels^{44,46}. In such a case, we would propose a replacement of the old *P. pacificus* gene model by the two distinct transcripts.

After manual inspection of all 526 missing gene candidates, 201 (41%) of the 486 non-redundant *P. pacificus* loci were classified as missing genes (Fig. 2b). Presumably this kind of error could arise when the gene annotation pipeline is mostly dependent on gene prediction algorithms which fail to predict all genes in gene dense regions (e.g. operon structures) as the intergenic distances might span only a few hundred nucleotides, which could be too small for triggering the initiation of a new gene model. The *C. elegans* gene *apn-1* is one example of a missed gene model in a gene dense region (Fig. 2d). Given that the *P. pacificus* homolog of *apn-1* has good transcriptomic support, the correction in this case would simply add the transcript to the existing gene models. Other instances of missing homologs are due to borderline cases in the BLASTP searches where one search resulted in an e-value slightly below the e-value threshold (10⁻⁵) and the result of the other BLASTP search was slightly above the threshold. In total, we encountered 87 of such cases which we termed 'weak similarity' (Fig. 2b). For such cases no correction was proposed. In summary, we compiled corrections for 280 *P. pacificus* genes which were replaced by 714 new gene models. All these changes were submitted to WormBase and were incorporated in the release WS272.

Artificial gene fusions mask thousands of hidden orthologs. A small number of *C. elegans* genes with missing homologs in the current gene annotations (version: El Paco v1/WS268) of *P. pacificus* were classified as located in fused gene models (Fig. 2b). One potential explanation could be that an artificially fused gene prediction from the sister species is taken as homology data to annotate the orthologous locus in *P. pacificus*, but small errors cause parts of the gene model to be either incompletely or incorrectly annotated in *P. pacificus* resulting in a loss of detectable homology (Fig. 2c). Even if the homolog of a *C. elegans* gene is incorporated in the correct ORF within an artificially fused gene model, this could still cause a loss of one-to-one orthology as the

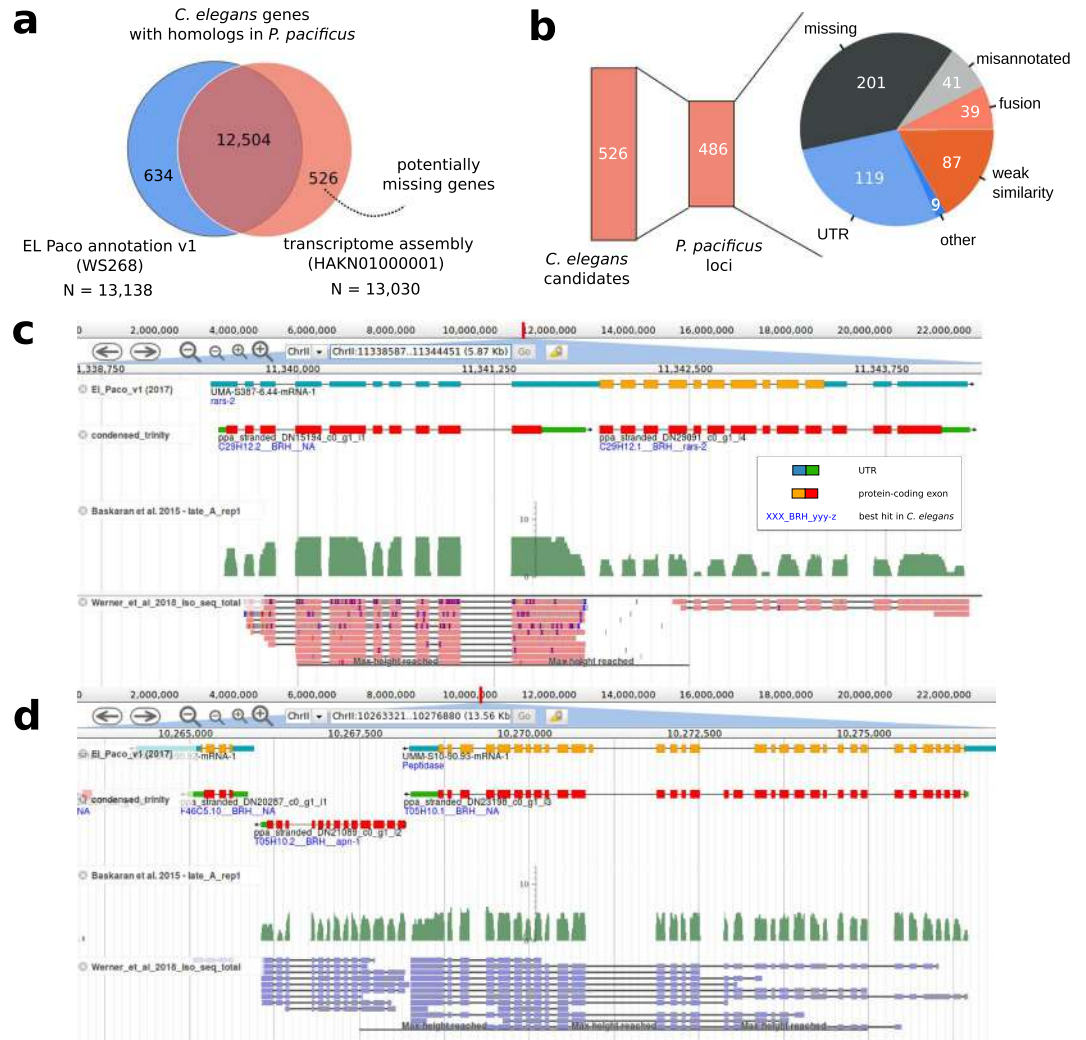


Figure 2. Identification of missing genes. **(a)** 526 potentially missing genes were identified based on *C. elegans* genes with homologs in the transcriptome assembly but not in current gene annotations. **(b)** The 526 missing gene candidates were located in 486 *P. pacificus* loci that were classified based on community annotators. **(c)** The genome browser screenshot shows a homolog of *C. elegans* C29H12.2 which is located in the annotated 5'UTR of a *P. pacificus* gene. This locus harbors two *P. pacificus* transcripts with different expression levels and well supported as non-overlapping transcripts based on RNA-seq and Iso-seq data. **(d)** A homolog of *apn-1* is completely missing from current gene annotations.

corresponding *P. pacificus* gene can only be identified as one-to-one ortholog of a single *C. elegans* gene. Thus, we performed a second screen for *C. elegans* genes that had a predicted one-to-one ortholog (best-reciprocal hit) in the transcriptome assembly but not in current gene annotations (Fig. 3a). In total, 6075 (93%) of *C. elegans* genes with a predicted one-to-one ortholog (based on best-reciprocal hits) in current gene annotations, also had a predicted one-to-one ortholog against the *de novo* transcriptome assembly (Fig. 3a). Nevertheless, we found 2075 *C. elegans* genes that only had predicted one-to-one orthologs in the *de novo* transcriptome assembly but not in the current set of gene annotations (version: El Paco v1/WS268). Community-based classification and curation of the 1281 corresponding *P. pacificus* loci classified 912 (71%) cases as artificial gene fusions (Fig. 3b). One such an example is the *C. elegans* gene D1053.3. Its putative ortholog is fused with the *P. pacificus* *mbv-12* ortholog (Fig. 3c). Apart from being orthologous to two different *C. elegans* genes, both *P. pacificus* genes are supported as non-overlapping transcripts by RNA-seq and Iso-seq, and are expressed at different levels. This confirmed the interpretation of an artificially fused annotation. The proposed correction in this case would be a replacement of the old gene model by the two non-overlapping transcripts. In total, we updated 1241 *P. pacificus* gene models and replaced them with 3305 new models. These updates were submitted to WormBase and will be released following curation. The new *P. pacificus* gene annotation (version: El Paco v2) with 28,036 gene models is also available on <http://www.pristionchus.org/download>. The results of the BUSCO analysis (Complete and Single Copy: 95.4%, Duplicated:

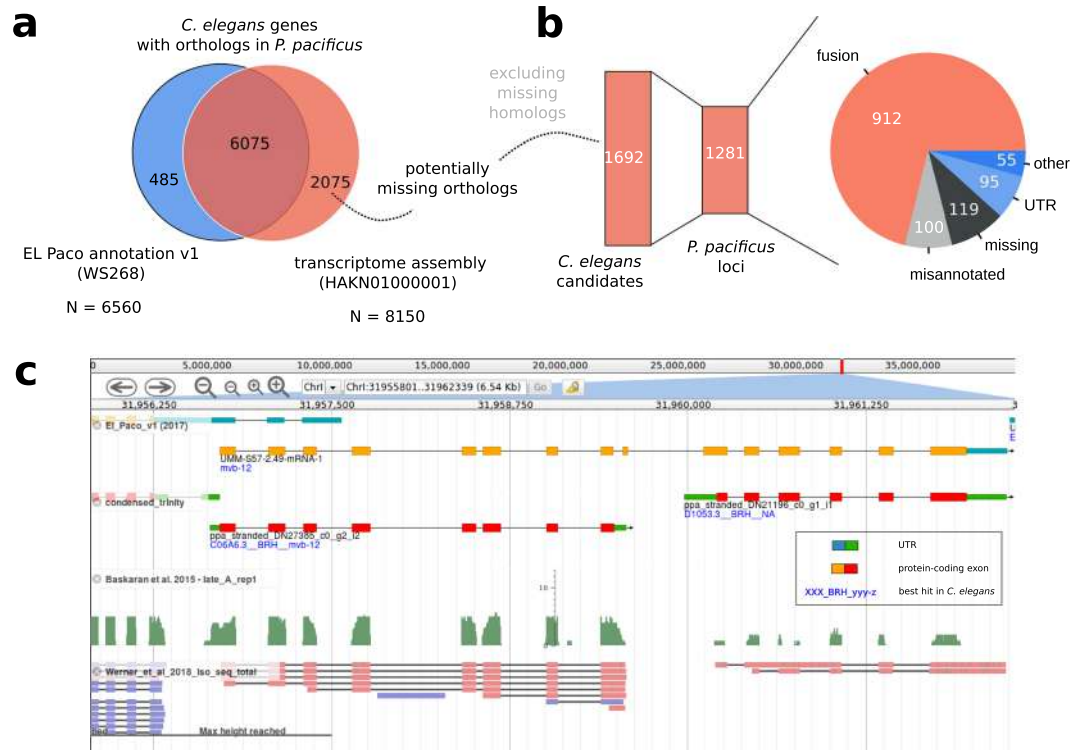


Figure 3. Community-based curation of hidden orthologs. (a) We identified 2075 putative *C. elegans* one-to-one orthologs that were specific to the *P. pacificus* transcriptome assembly. (b) Community-based curation classified most of the corresponding gene loci as artificial gene fusions. (c) Non-overlapping transcripts corresponding to *P. pacificus* orthologs of *mvb-12* and D1053.3 are artificially fused in a current gene model. This prohibits the detection of a one-to-one ortholog of D1053.3 based on a genome-wide approach such as best reciprocal hits.

1.7%, Fragmented: 2.0%, Missing: 0.9%) indicate that the new annotation represents a substantial improvement over the previous annotations¹⁵ (Table 1).

Improved gene annotations facilitate the establishment of a catalog of *C. elegans* homologs and orthologs in the *P. pacificus* genome. Since our primary focus was to improve the annotation of *C. elegans* orthologs in the *P. pacificus* genome, we wanted to use the updated gene annotation to generate a catalog of predicted orthologs between *C. elegans* and *P. pacificus*. As the identification of orthologs typically requires sufficient genomic and phylogenetic knowledge to retrieve relevant protein data sets and to perform reconstruction of gene trees^{24,45,46}, a genome-wide catalog of orthologs would be highly useful as a starting point for researchers without sufficient expertise. Previous comparisons between *C. elegans* and *P. pacificus* identified putative one-to-one orthologs for roughly 6000–8000 genes^{44,46}. To further characterize *C. elegans* genes without orthologs in *P. pacificus*, we additionally carried out a phylostratigraphic analysis⁴⁷ to estimate their relative age. Basically, phylostratigraphy uses absence-presence patterns of a gene to map its origin to an internal branch in a species tree⁴⁷. Our analysis revealed that 5258 (26%) of *C. elegans* genes do not have BLAST hits in *Pristionchus* or more distantly related species (Phylostrata I–IV, Supplemental Table 1). This strongly suggests that they are younger than the common ancestor between *C. elegans* and *P. pacificus* and consequently have no orthologs. Next, we applied two different approaches to predict orthologs between *C. elegans* and *P. pacificus*: best reciprocal hits and Markov clustering as implemented in the software orthAgo⁴⁸. Computation of best reciprocal hits is a standard approach for predicting one-to-one orthologs across species^{49,50}. In order to capture more complex orthology relationships (e.g. many-to-many), more general approaches such as Markov clustering have been widely applied^{48,51}. Based on best reciprocal hits, we identified 8348 predicted one-to-one orthologs between both species (Supplemental Table 1) whereas the orthAgo pipeline identified 7643 orthologous clusters, of which only 3345 corresponded to one-to-one orthologs. The large majority (98%) of these predicted one-to-one orthologs was also identified as best reciprocal hits and in 3260 (99%) cases, the same *P. pacificus* gene was predicted as one-to-one ortholog. The large discrepancy between the total number of best reciprocal hits and one-to-one orthologs defined by orthAgo could be explained by the fact that best reciprocal hits do not take inparalogs into account⁴⁹. However, only 1049 (21%) of *C. elegans* genes that were not identified as one-to-one orthologs by orthAgo could be explained by the presence of lineage-specific inparalogs, suggesting that orthAgo with default settings might be too conservative for this analysis. This is further supported by the reanalysis of 57 one-to-one orthologous pairs that were previously confirmed by phylogenetic analysis⁴⁶. While 53 of the previously confirmed one-to-one orthologs were captured as best reciprocal hits, only 33 were also identified

by orthoAgogue. Taken together, the improved gene annotation facilitated the prediction of substantially more one-to-one orthologs (Fig. 3a, Supplemental Table 1). This resource can be taken as a starting point to identify candidate genes in *P. pacificus*.

Discussion

With *C. elegans*, *C. briggsae*, and *P. pacificus*, three genetically tractable and free living nematode model organisms have been well established and can be used to study the evolution of gene function at various time-scales^{2,3,52}. For example, recent reverse genetic approaches in *P. pacificus* have revealed functional divergence of genes with known roles in *C. elegans* dauer formation^{22,23,53}. In addition, mutant screens in *P. pacificus* for social behaviours have uncovered multiple orthologous *C. elegans* genes for which a behavioral phenotype had been overlooked previously^{33,54}. Together with complementary studies of the functional importance of novel genes^{7,32,55}, this makes nematodes an extremely powerful system to study genome evolution and gene function at a mechanistic level.

In order to facilitate fruitful functional studies across multiple model organisms, it is crucial to generate genomic resources (e.g. assemblies, annotations) and experimental genetic toolkits (e.g. forward and reverse genetics) of comparable quality. The chromosome-scale assembly of the *P. pacificus* genome¹⁵ was a major step towards making this species more tractable for other groups. In our study, we aimed to minimize the discrepancy between automatically generated gene annotations for *P. pacificus* and heavily curated annotations for *C. elegans*. To this end, we incorporated recently generated Iso-seq and RNA-seq data into current gene annotations by manual curation of suspicious candidate loci that were identified by comparative genomic analysis. While application of alternative annotation pipelines can generate overall better gene annotations^{29,41}, they cannot guarantee that gene annotations will only improve. In certain cases, new annotation pipelines will also cause new errors. In contrast, during manual inspection, each community curator has the choice to not propose any change of gene models in case of uncertainty. Thus, manual inspection should only lead to removal of errors and thus improve annotation quality without introducing biases elsewhere. While manual annotation is an incredibly tedious task that is probably not scalable to complete genomes³⁸, we minimized the workload by focusing on a small gene set of *C. elegans* orthologs, recruiting colleagues as community curators, and restricting the task just to the selection of alternative gene models that were generated from transcriptomic data^{16,44} or previous rounds of gene prediction^{56,57}. In our opinion, the most crucial aspect of this community project is a good training of new annotators. We achieved this by personal training sessions between experienced and new annotators and the possibility to always discuss cases of uncertainty with other curators. For larger projects, initial training could be achieved by comprehensive online tutorials and communication via email, but this will likely be less efficient. In the case of the *P. pacificus* gene annotations, our study raised the gene count from 25,517 to 28,036 and increased the single copy ortholog completeness level from 86% to 97%. In the *P. pacificus* genome, the greatest source of error was the artificial fusion of neighboring genes. This type of error might be more prevalent in nematodes where genomes are compact⁹ and genes frequently overlap^{37,45}. Consequently, manual annotation of restricted gene sets has been proposed and applied previously to circumvent this problem⁵⁸. Given that nematode genomes tend to be pretty compact (Fig. 1), we anticipate that misannotation due to overlapping gene models should be much less pronounced in large vertebrate or plant genomes. Nevertheless, it would be interesting to apply similar screens for gene annotation artifacts to other systems and eventually this could reveal some incorrect annotations in the genomes of classical model organisms.

While this study was restricted to *P. pacificus* genes with putative orthologs in *C. elegans*, we cannot reliably estimate the fraction of erroneous gene models across the whole genome. Our results would suggest that the fraction of missing genes is around one percent (Fig. 2a,b) and the amount of gene models affected by artificial fusions may be up to 15% (Fig. 3a). However, as the *P. pacificus* genome has a higher gene density and a higher concentration of old genes at the chromosome centers^{8,15}, we hypothesize that errors due to artificial gene fusions should be much less pronounced at chromosome arms. To test this, an unbiased quantification of error rates across genomic segments would be needed. In future, we also plan to focus on large gene families and lineage-specific orphan genes⁵⁵ that were not explicit subjects of this study. Artificial fusions in these classes of genes could be identified by screens for unexpectedly long gene models or unusual protein domain content. For orphan genes abundant RNA-seq studies of different developmental stages^{22,46}, tissues^{10,46}, environmental conditions⁵⁹, sexes¹⁶, and genetic backgrounds^{60,61} could be used to detect non-overlapping transcripts that exhibit anticorrelated expression within a single locus. Thus, while our study has demonstrated that community-based curation of gene annotations is feasible and can lead to substantial improvements, continued effort is needed to lift its quality to a level that would be similar to classical model organisms.

Methods

Comparative assessment of nematode genomes. We downloaded 22 nematode genomes and corresponding protein sequences from WormBase ParaSite (release WBPS13). For *Steinernema carpocapsae*, the latest version at WBPS14 was used. In case of multiple isoforms, we selected the longest isoform for further analysis. We ran BUSCO (version 3.0.1) in protein mode (option: -m prot) against the nematode_odb9 data set (N = 982 genes) to evaluate the completeness level of available protein sequences.

Genome browser integration of transcriptomic resources. To allow community annotators to propose alternative gene models, we integrated recent raw read alignments and reference guided transcript assemblies of Iso-seq data⁴⁴ and a *de novo* assembly of strand-specific RNA-seq data¹⁶ into our genome browser (implemented in jbrowse⁶²) on our webserver (<http://www.pristionchus.org>). Genomic coordinates for the *de novo* transcriptome assembly were generated by alignment to the *P. pacificus* reference genome (version El Paco) with the program exonerate⁶³ (version: 2.2.0, options: -m est2genome - dncwordlen 20 - maxintron 20000). To reduce the complexity of this data set, a condensed version of the *de novo* transcriptome assembly (selection of the isoform with the longest ORF as single representative isoform per gene, minimum peptide length of 60 amino acids, removal of single exon transcripts) with annotated best-reciprocal hits and best hits (BLASTP, e-value < 10⁻⁵) in

C. elegans was also incorporated into our jbrowse instance. In addition, predicted protein sequences of previous versions of *P. pacificus* annotations (Hybrid1⁵⁶ and TAU2011⁵⁷) were mapped against the *P. pacificus* assembly by exonerate (version: 2.2.0, options: -m protein2genome -dwordlen 20 -maxintron 20000). All data sets are available under the gene annotation track of the El Paco reference assembly in our genome browser. To evaluate the quality of the two recent transcriptome assemblies, we ran BUSCO (version 3.0.1, options -m trans) against the nematode_odb9 data set (N = 982 genes) for completeness assessment (Table 1).

Identification of missing and fused gene models in current gene annotations. We ran bidirectional BLASTP (e-value < 10⁻⁵) searches between *C. elegans* (version: WS260, longest isoform per gene) and two different *P. pacificus* data sets: the annotated proteins (version: El Paco v1, WS268) and the *de novo* transcriptome assembly¹⁶. For the *de novo* transcriptome, we reduced the redundancy resulting from different isoforms by selecting the longest ORFs per gene. Based on the different BLASTP searches, we first screened for *C. elegans* proteins with BLASTP hits against ORFs in the *de novo* transcriptome assembly but not against the currently annotated proteins. This yielded 526 candidate genes. In a second phase, we screened for *C. elegans* proteins with putative orthologs, defined by best-reciprocal BLASTP relationships, in the *de novo* transcriptome assembly but not in the annotated proteins, resulting in 2075 candidate genes.

Community-based manual curation of candidate loci. All *C. elegans* genes together with their candidate homologs and orthologs in the *P. pacificus de novo* transcriptome assembly were stored in a shared online spreadsheet. Community annotators were trained to find the corresponding locus in the genome browser by entering the transcript identifier and to manually inspect the surrounding regions that were defined by the encompassing *P. pacificus* gene model. The candidate locus was then classified as untranslated region (UTR) (the query transcript overlapped exons that were annotated as UTR), missing gene (the query transcript did not overlap any annotated exon), gene fusion (the query transcript did overlap protein-coding exons and homology was detected by BLASTP), misannotation (the query transcript did overlap protein-coding exons but no BLASTP hit was found due incorrect reading frame annotation or minimal overlap) or inconclusive. After classification, a correction was proposed that either added new genes (identifiers could be selected from the *de novo* assembled transcripts, Iso-seq assemblies, or previous versions of gene annotations) or replaced an existing gene model by one or more new genes. In such a case the objective was to lose as little annotated coding sequence as possible. Thus, new genes were selected from the above mentioned data set in order to cover as much coding sequence of the initial gene model as possible. If parts of the old gene model were not covered, BLAST searches against *C. elegans* and other *Pristionchus* species were used to split the old gene model into several parts with sequence matches to distinct *C. elegans* genes, or to extract partial protein sequences of the old gene model that were not covered. Such protein sequence stretches were given a pseudo identifier and were stored in a shared online document. All these sequences were later automatically reannotated by mapping them against the reference genome with the help of exonerate. In case that an existing gene model was replaced by multiple new gene models, we additionally selected one of the new gene models to inherit the WormBase identifier of the old gene model to allow WormBase to record the history of a given gene model. Usually, either the most conserved or the longest new gene model was chosen. Due to the fact that a single artificially fused gene could cause missing homologs and orthologs for multiple *C. elegans* genes, some loci were curated multiple times. We randomly picked some of these cases to compare the classifications and the corresponding corrections from multiple curators, which turned out to be largely consistent. In case of redundant curations, one out of many possible curations for a given locus was chosen based on the following criteria: preference towards higher number of new models, experience of the curator (number of curated loci), and transcriptional evidence over gene prediction.

Phylostratigraphy and orthology predictions. Outgroup data sets were defined by concatenating all protein sequence data from different species in the ladder-like phylogeny leading to *C. elegans* (Fig. 1). More precisely, we pooled all data from species in an induced subtree defined by branches with roman numbers in Fig. 1. We then ran a BLASTP search (e-value < 0.001) of *C. elegans* proteins (longest isoform per gene) against each of the outgroup data sets. Starting from the *C. elegans* genes with homologs in the most distant outgroup set (VIII), we iteratively defined phylostrata by comparison with the next, more closely related outgroup set. The results of this analysis are summarized in Supplemental Table 1. *C. elegans* specific genes are assigned to phylostratum I, whereas genes that are present in the most divergent outgroups are assigned to phylostratum VIII. Orthologs were defined after performing all pairwise BLASTP searches including self-searches (e-value < 10⁻⁵) between *C. elegans* and *P. pacificus* and extracting best reciprocal hits from the BLAST output files. Simultaneously, the program orthAgogue was run with default setting on the same input files⁴⁸.

Data availability

The strand-specific *de novo* transcriptome was submitted to the European Nucleotide Archive under the accession HAKN01000001¹⁶ and the Iso-seq data was submitted to the European Nucleotide Archive under the accessions ERX2315712 and ERX2315713⁴⁴. All data sets are also available at <http://www.pristionchus.org/download>. The initial set of *P. pacificus* gene annotations corresponds to WormBase WS268. Corrections from this study were submitted to WormBase and will be released following curation.

Received: 1 October 2019; Accepted: 20 November 2019;

Published online: 11 December 2019

References

- Sommer, R. J., Carta, L. K., Kim, S.-Y. & Sternberg, P. W. Morphological, genetic and molecular description of *Pristionchus pacificus* sp. n. (Nematoda: Neodiplogastridae). *Fundam. Appl. Nematol.* **19**, 511–521 (1996).
- Sternberg, P. W. Why *Caenorhabditis elegans* is great and *Pristionchus pacificus* might be better. In *Pristionchus pacificus* (ed. Sommer, R. J.) **11**, 1–17 (BRILL).
- Sommer, R. J. Evolution of regulatory networks: nematode vulva induction as an example of developmental systems drift. *Adv. Exp. Med. Biol.* **751**, 79–91 (2012).
- Bose, N. *et al.* Complex small-molecule architectures regulate phenotypic plasticity in a nematode. *Angew. Chem. Int. Ed Engl.* **51**, 12438–12443 (2012).
- Yim, J. J., Bose, N., Meyer, J. M., Sommer, R. J. & Schroeder, F. C. Nematode signaling molecules derived from multimodular assembly of primary metabolic building blocks. *Org. Lett.* **17**, 1648–1651 (2015).
- Falcke, J. M. *et al.* Linking genomic and metabolomic natural variation uncovers nematode pheromone biosynthesis. *Cell Chem Biol* **25**, 787–796.e12 (2018).
- Mayer, M. G., Rödelsperger, C., Witte, H., Riebesell, M. & Sommer, R. J. The orphan gene *dauerless* regulates dauer development and intraspecific competition in nematodes by copy number variation. *PLoS Genet.* **11**, e1005146 (2015).
- Prabh, N. *et al.* Deep taxon sampling reveals the evolutionary dynamics of novel gene families in *Pristionchus* nematodes. *Genome Res.* **28**, 1664–1674 (2018).
- Rödelsperger, C., Streit, A. & Sommer, R. J. Structure, function and evolution of the nematode genome. In: *eLS*. John Wiley & Sons, Ltd: Chichester, <https://doi.org/10.1002/9780470015902.a0024603> (2013).
- Lightfoot, J. W., Chauhan, V. M., Aylott, J. W. & Rödelsperger, C. Comparative transcriptomics of the nematode gut identifies global shifts in feeding mode and pathogen susceptibility. *BMC Res. Notes* **9**, 142 (2016).
- Susoy, V. *et al.* Large-scale diversification without genetic isolation in nematode symbionts of figs. *Sci Adv* **2**, e1501031 (2016).
- Bumbarger, D. J., Riebesell, M., Rödelsperger, C. & Sommer, R. J. System-wide rewiring underlies behavioral differences in predatory and bacterial-feeding nematodes. *Cell* **152**, 109–119 (2013).
- Witte, H. *et al.* Gene inactivation using the CRISPR/Cas9 system in the nematode *Pristionchus pacificus*. *Dev. Genes Evol.* **225**, 55–62 (2015).
- Srinivasan, J. *et al.* A bacterial artificial chromosome-based genetic linkage map of the nematode *Pristionchus pacificus*. *Genetics* **162**, 129–134 (2002).
- Rödelsperger, C. *et al.* Single-molecule sequencing reveals the chromosome-scale genomic architecture of the nematode model organism *Pristionchus pacificus*. *Cell Rep.* **21**, 834–844 (2017).
- Rödelsperger, C. *et al.* Phylotranscriptomics of *Pristionchus* nematodes reveals parallel gene loss in six hermaphroditic lineages. *Curr. Biol.* **28**, 3123–3127.e5 (2018).
- Namai, S. & Sugimoto, A. Transgenesis by microparticle bombardment for live imaging of fluorescent proteins in *Pristionchus pacificus* germline and early embryos. *Dev. Genes Evol.* **228**, 75–82 (2018).
- Lo, T.-W. *et al.* Precise and heritable genome editing in evolutionarily diverse nematodes using TALENs and CRISPR/Cas9 to engineer insertions and deletions. *Genetics* **195**, 331–348 (2013).
- Bui, L. T. & Ragsdale, E. J. Multiple plasticity regulators reveal targets specifying an induced predatory form in nematodes. *Mol. Biol. Evol.* <https://doi.org/10.1093/molbev/msz171> (2019).
- Ishita, Y., Chihara, T. & Okumura, M. Serotonergic modulation of feeding behavior in *Caenorhabditis elegans* and other related nematodes. *Neurosci. Res.* <https://doi.org/10.1016/j.neures.2019.04.006> (2019).
- Liu, Z. *et al.* Predator-secreted sulfolipids induce defensive responses in *C. elegans*. *Nature Communications* **9** (2018).
- Moreno, E. *et al.* DAF-19/RFX controls ciliogenesis and influences oxygen-induced social behaviors in *Pristionchus pacificus*. *Evol. Dev.* **20**, 233–243 (2018).
- Markov, G. V. *et al.* Functional conservation and divergence of *daf-22* paralogs in *Pristionchus pacificus* dauer development. *Mol. Biol. Evol.* **33**, 2506–2514 (2016).
- Markov, G. V., Baskaran, P. & Sommer, R. J. The same or not the same: lineage-specific gene expansions and homology relationships in multigene families in nematodes. *J. Mol. Evol.* **80**, 18–36 (2015).
- Namdeo, S. *et al.* Two independent sulfation processes regulate mouth-form plasticity in the nematode. *Development* **145** (2018).
- Rödelsperger, C. Comparative genomics of gene loss and gain in *Caenorhabditis* and Other Nematodes. In *Methods in Molecular Biology* 419–432 (2018).
- Korf, I. Gene finding in novel genomes. *BMC Bioinformatics* **5**, 59 (2004).
- Stanke, M. *et al.* AUGUSTUS: ab initio prediction of alternative transcripts. *Nucleic Acids Res.* **34**, W435–9 (2006).
- Hoff, K. J., Lomsadze, A., Borodovsky, M. & Stanke, M. Whole-genome annotation with BRAKER. *Methods Mol. Biol.* **1962**, 65–95 (2019).
- Cantarel, B. L. *et al.* MAKER: an easy-to-use annotation pipeline designed for emerging model organism genomes. *Genome Res.* **18**, 188–196 (2008).
- Holt, C. & Yandell, M. MAKER2: an annotation pipeline and genome-database management tool for second-generation genome projects. *BMC Bioinformatics* **12**, 491 (2011).
- Lightfoot, J. W. *et al.* Small peptide-mediated self-recognition prevents cannibalism in predatory nematodes. *Science* **364**, 86–89 (2019).
- Moreno, E. *et al.* Regulation of hyperoxia-induced social behaviour in *Pristionchus pacificus* nematodes requires a novel cilia-mediated environmental input. *Sci. Rep.* **7**, 17550 (2017).
- Kieninger, M. R. *et al.* The nuclear hormone receptor NHR-40 acts downstream of the sulfatase EUD-1 as part of a developmental plasticity switch in *Pristionchus*. *Curr. Biol.* **26**, 2174–2179 (2016).
- Baskaran, P. & Rödelsperger, C. Microevolution of duplications and deletions and their impact on gene expression in the Nematode *Pristionchus pacificus*. *PLoS One* **10**, e0131136 (2015).
- Weller, A. M., Rödelsperger, C., Eberhardt, G., Molnar, R. I. & Sommer, R. J. Opposing forces of A/T-biased mutations and G/C-biased gene conversions shape the genome of the nematode *Pristionchus pacificus*. *Genetics* **196**, 1145–1152 (2014).
- Prabh, N. & Rödelsperger, C. Divergence, and mixed origin contribute to the emergence of orphan genes in nematodes. *G3* **9**, 2277–2286 (2019).
- Salzberg, S. L. Next-generation genome annotation: we still struggle to get it right. *Genome Biol.* **20**, 92 (2019).
- Smythe, A. B., Holovachov, O. & Kocot, K. M. Improved phylogenomic sampling of free-living nematodes enhances resolution of higher-level nematode phylogeny. *BMC Evolutionary Biology* **19** (2019).
- Simão, F. A., Waterhouse, R. M., Ioannidis, P., Kriventseva, E. V. & Zdobnov, E. M. BUSCO: assessing genome assembly and annotation completeness with single-copy orthologs. *Bioinformatics* **31**, 3210–3212 (2015).
- McLean, F., Berger, D., Laetsch, D. R., Schwartz, H. T. & Blaxter, M. Improving the annotation of the *Heterorhabditis bacteriophora* genome. *Gigascience* **7** (2018).
- Hiraki, H. *et al.* Genome analysis of *Diploscapter coronatus*: insights into molecular peculiarities of a nematode with parthenogenetic reproduction. *BMC Genomics* **18**, 478 (2017).
- Rödelsperger, C. *et al.* Characterization of genetic diversity in the nematode *Pristionchus pacificus* from population-scale resequencing data. *Genetics* **196**, 1153–1165 (2014).

44. Werner, M. S. *et al.* Young genes have distinct gene structure, epigenetic profiles, and transcriptional regulation. *Genome Res.* **28**, 1675–1687 (2018).
45. Rödelsperger, C., Menden, K., Seroby, V., Witte, H. & Baskaran, P. First insights into the nature and evolution of antisense transcription in nematodes. *BMC Evol. Biol.* **16**, 165 (2016).
46. Baskaran, P. *et al.* Ancient gene duplications have shaped developmental stage-specific expression in *Pristionchus pacificus*. *BMC Evol. Biol.* **15**, 185 (2015).
47. Domazet-Loso, T., Brajković, J. & Tautz, D. A phylostratigraphy approach to uncover the genomic history of major adaptations in metazoan lineages. *Trends Genet.* **23**, 533–539 (2007).
48. Ekseth, O. K., Kuiper, M. & Mironov, V. orthAgogue: an agile tool for the rapid prediction of orthology relations. *Bioinformatics* **30**, 734–736 (2014).
49. Remm, M., Storm, C. E. & Sonnhammer, E. L. Automatic clustering of orthologs and in-paralogs from pairwise species comparisons. *J. Mol. Biol.* **314**, 1041–1052 (2001).
50. Tatusov, R. L. A Genomic Perspective on Protein Families. *Science* **278**, 631–637 (1997).
51. Li, L., Stoeckert, C. J. Jr & Roos, D. S. OrthoMCL: identification of ortholog groups for eukaryotic genomes. *Genome Res.* **13**, 2178–2189 (2003).
52. Verster, A. J., Ramani, A. K., McKay, S. J. & Fraser, A. G. Comparative RNAi Screens in *C. elegans* and *C. briggsae* Reveal the Impact of Developmental System Drift on Gene Function. *PLoS Genetics* **10**, e1004077 (2014).
53. Sieriebriennikov, B., Markov, G. V., Witte, H. & Sommer, R. J. The Role of DAF-21/Hsp90 in Mouth-Form Plasticity in *Pristionchus pacificus*. *Mol. Biol. Evol.* **34**, 1644–1653 (2017).
54. Moreno, E. & Sommer, R. J. A cilia-mediated environmental input induces solitary behaviour in *Caenorhabditis elegans* and *Pristionchus pacificus* nematodes. *Nematology* **20**, 201–209 (2018).
55. Prabh, N. & Rödelsperger, C. Are orphan genes protein-coding, prediction artifacts, or non-coding RNAs? *BMC Bioinformatics* **17**, 226 (2016).
56. Borchert, N. *et al.* Proteogenomics of *Pristionchus pacificus* reveals distinct proteome structure of nematode models. *Genome Res.* **20**, 837–846 (2010).
57. Sinha, A., Sommer, R. J. & Dieterich, C. Divergent gene expression in the conserved dauer stage of the nematodes *Pristionchus pacificus* and *Caenorhabditis elegans*. *BMC Genomics* **13**, 254 (2012).
58. Stoltzfus, J. D., Minot, S., Berriman, M., Nolan, T. J. & Lok, J. B. RNAseq analysis of the parasitic nematode *Strongyloides stercoralis* reveals divergent regulation of canonical dauer pathways. *PLoS Negl. Trop. Dis.* **6**, e1854 (2012).
59. Sanghvi, G. V. *et al.* Life history responses and gene expression profiles of the nematode *Pristionchus pacificus* cultured on *Cryptococcus* yeasts. *PLoS One* **11**, e0164881 (2016).
60. Seroby, V. *et al.* Chromatin remodelling and antisense-mediated up-regulation of the developmental switch gene *eud-1* control predatory feeding plasticity. *Nat. Commun.* **7**, 12337 (2016).
61. Moreno, E., McGaughan, A., Rödelsperger, C., Zimmer, M. & Sommer, R. J. Oxygen-induced social behaviours in *Pristionchus pacificus* have a distinct evolutionary history and genetic regulation from *Caenorhabditis elegans*. *Proc. Biol. Sci.* **283**, 20152263 (2016).
62. Buels, R. *et al.* JBrowse: a dynamic web platform for genome visualization and analysis. *Genome Biol.* **17**, 66 (2016).
63. Slater, G. S. C. & Birney, E. Automated generation of heuristics for biological sequence comparison. *BMC Bioinformatics* **6**, 31 (2005).

Acknowledgements

The authors would like to thank the complete *Pristionchus* community for their long-term interest in studying *P. pacificus* and thus motivating this work. Further thanks to Bogdan Sieriebriennikov for providing additional manual curations and to all members of the Sommer lab for general discussions. Finally, special thanks to Michael Paulini for incorporating the updated gene models into WormBase. This work was funded by the Max Planck Society.

Author contributions

Conceptualization, C.R.; Investigation, C.R., M.A., M.L., T.T., S.S., M.D., S.W., W.H., D.R.S. and Z.H.; Writing – Original Draft, C.R.; Writing – Review & Editing, C.R., M.A., M.L., T.T., S.S., M.D., S.W., W.H., D.R.S. and Z.H.; Supervision, C.R.

Competing interests

The authors declare no competing interests.

Additional information

Supplementary information is available for this paper at <https://doi.org/10.1038/s41598-019-55359-5>.

Correspondence and requests for materials should be addressed to C.R.

Reprints and permissions information is available at www.nature.com/reprints.

Publisher's note Springer Nature remains neutral with regard to jurisdictional claims in published maps and institutional affiliations.



Open Access This article is licensed under a Creative Commons Attribution 4.0 International License, which permits use, sharing, adaptation, distribution and reproduction in any medium or format, as long as you give appropriate credit to the original author(s) and the source, provide a link to the Creative Commons license, and indicate if changes were made. The images or other third party material in this article are included in the article's Creative Commons license, unless indicated otherwise in a credit line to the material. If material is not included in the article's Creative Commons license and your intended use is not permitted by statutory regulation or exceeds the permitted use, you will need to obtain permission directly from the copyright holder. To view a copy of this license, visit <http://creativecommons.org/licenses/by/4.0/>.

© The Author(s) 2019

NEUROSCIENCE

Sex or cannibalism: Polyphenism and kin recognition control social action strategies in nematodes

James W. Lightfoot^{1,2†}, Mohannad Dardiry^{1,3†}, Ata Kalirad¹, Stefano Giaimo⁴, Gabi Eberhardt¹, Hanh Witte¹, Martin Wilecki¹, Christian Rödelsperger¹, Arne Traulsen⁴, Ralf J. Sommer^{1*}

Resource polyphenisms, where single genotypes produce alternative feeding strategies in response to changing environments, are thought to be facilitators of evolutionary novelty. However, understanding the interplay between environment, morphology, and behavior and its significance is complex. We explore a radiation of *Pristionchus* nematodes with discrete polyphenic mouth forms and associated microbivorous versus cannibalistic traits. Notably, comparing 29 *Pristionchus* species reveals that reproductive mode strongly correlates with mouth-form plasticity. Male-female species exhibit the microbivorous morph and avoid parent-offspring conflict as indicated by genetic hybrids. In contrast, hermaphroditic species display cannibalistic morphs encouraging competition. Testing predation between 36 co-occurring strains of the hermaphrodite *P. pacificus* showed that killing inversely correlates with genomic relatedness. These empirical data together with theory reveal that polyphenism (plasticity), kin recognition, and relatedness are three major factors that shape cannibalistic behaviors. Thus, developmental plasticity influences cooperative versus competitive social action strategies in diverse animals.

INTRODUCTION

Resource polyphenisms are plastic traits facilitating the exploitation of alternative resources in response to environmental pressures on an organism. These polyphenic traits can have a profound influence on an organism's morphology, ecology, physiology, and behavior, and they have been observed among diverse taxa (1–4). Examples of resource polyphenisms can be seen in alternative feeding morphs, where distinct feeding structures and, subsequently, different feeding strategies are found between discrete morphs. One of the most dramatic examples of alternate feeding strategies are predatory versus nonpredatory and even cannibalistic versus noncannibalistic forms, resulting in diverse diets and the induction of aggressive behaviors (5–9). Furthermore, some cannibal morphs display recognition of self and relatives, therefore reducing the risk of harming progeny and kin (5–10). However, understanding the complex network of influences acting on the developmental decision behind cannibalistic versus noncannibalistic polyphenisms is difficult, as it requires a combination of ecological insights together with genetic, molecular, and, frequently, behavioral analysis, which is not readily available in many species.

In diplogastrid nematodes of the genus *Pristionchus*, a polyphenic trait exists in which one of two alternative mouth morphs develop. This irreversible developmental decision results in the formation of either the *stenostomatous* (St) morph, where animals have a single tooth with a narrow mouth cavity, or, alternatively, the *eurystomatous* (Eu) morph, whereby the animal is wide mouthed with two teeth (Fig. 1A) (11, 12). Coinciding with these morphological distinctions, behavioral differences between these morphs are evident: While the St mouth form feeds on bacteria, the Eu morph is omnivorous and

capable of supplementing its bacterial diet by predated on the larvae of other nematode species, including feeding on conspecifics (Fig. 1B) (13). In addition, this predatory biting behavior also serves to repel potential competitors from their location, as while adult nematode cuticles are sufficient to prevent penetration and death, attacks do provoke an avoidance behavior in the recipient, which can cause their dispersal from the limited nutrient sources (14). The formation of the Eu morph is associated with an adaptive cost in the form of an increase in developmental time (15, 16). In one species, *P. pacificus*, a wide range of molecular and genetic tools are available (17–20). As such, the mouth-form decision and the associated predatory behaviors have been extensively studied and are dependent on genetic and environmental factors (21–27). Furthermore, alongside the predatory behaviors, a self-recognition system exists based on the small peptide signal *self-1*, which promotes the killing and cannibalism of progeny of intraspecific competitors but not of self-progeny (28). We investigated a radiation of 29 *Pristionchus* species and unexpectedly found that mouth-form preference shows a strong correlation with reproductive mode. Empirical and theoretical evidence indicates the interaction of several major factors—plasticity, kin recognition, and relatedness—that determine the most appropriate social action strategy in individual species.

RESULTS

Mouth form correlates with reproductive mode

Previous studies on mouth-form plasticity and predation in *Pristionchus* have focused nearly exclusively on the hermaphrodite *P. pacificus*; however, this organism is only one species in a well-described phylogeny thus far encompassing around 50 species (29). Furthermore, within the genus *Pristionchus*, two different modes of reproduction are observed, gonochorism and hermaphroditism. The ancestral gonochoristic reproductive mode is most common and requires obligate mating between females and males. In contrast, hermaphroditic species are capable of self-fertilizing and propagating without a mating partner; however, this severely limits their genetic diversity and results in highly related populations (30). In *Pristionchus*,

¹Max Planck Institute for Developmental Biology, Max-Planck Ring 9, 72076 Tübingen, Germany. ²Max Planck Research Group Self-Recognition and Cannibalism, Center of Advanced European Studies and Research (CAESAR), Ludwig-Erhard-Allee 2, Bonn 53175, Germany. ³Department of Genetics, Faculty of Agriculture, Cairo University, 12613 Giza, Egypt. ⁴Max Planck Institute for Evolutionary Biology, August-Thienemann-Str. 2, 24306 Plön, Germany.

*Corresponding author. Email: ralf.sommer@tuebingen.mpg.de

†These authors contributed equally to this work.

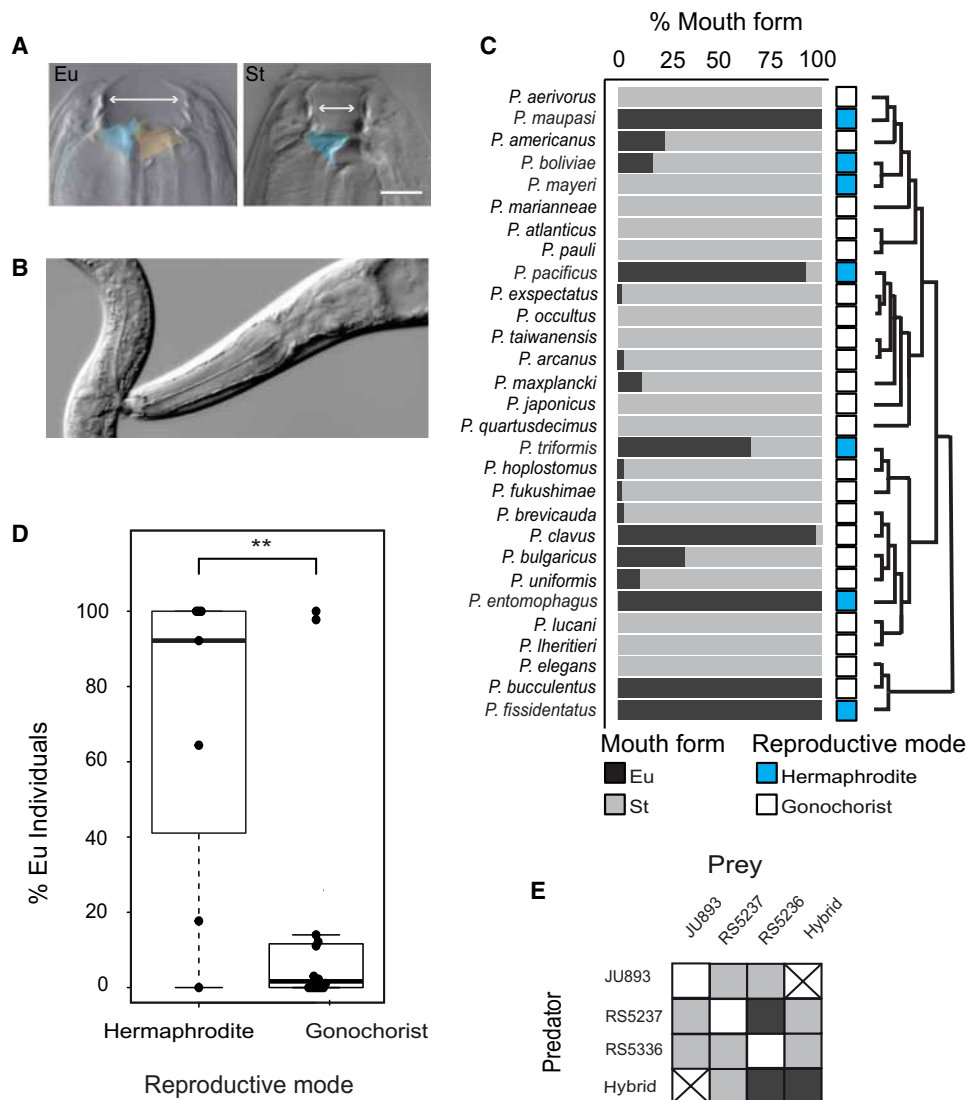


Fig. 1. Plasticity and reproductive mode correlate in *Pristionchus* nematodes. (A) *Pristionchus* mouth-form dimorphism. *P. pacificus* predatory eury stomatous form (Eu), which has a larger mouth opening and two teeth compared to the nonpredatory stenostomatous form (St), which has a narrow mouth opening and a single tooth. Scale bar, 5 μ m. (B) Killing behavior with a *P. pacificus* predator killing a *C. elegans* larva. (C) % Eu mouth-form frequency in 29 distinct *Pristionchus* species including phylogeny and their associated reproductive modes. Comparisons were made between hermaphrodites and females from gonochoristic species. Mouth-form frequency is the mean value of three independent replicates, each consisting of 30 animals. Note that, in many species, no Eu animals were detected. (D) Groupings of all species sharing reproductive strategy with mouth form associated with reproductive mode. $**P < 0.01$, showing significant association between reproductive mode and mouth-form preference. (E) Predator-prey killing grid among diverse *P. uniformis* strains from the United States (RS5237), Germany (RS5236), and France (JU893), and a hybrid strain generated by mating RS5237 and RS5236. Assays were conducted using rare Eu *P. uniformis* predators. All strains display a within-strain self-recognition system and between-strain killing. Color intensity represents killing efficiency with high (>30 corpses) shown in black, medium (one to 30 corpses) in gray, or low (0 corpses) in white. Data are the mean of three standard corpse assays. Crossed boxes indicated not tested.

this mating type has evolved at least seven times independently with eight known hermaphroditic species (29, 31). As mating between conspecific females and males is necessary in gonochoristic species, how the reproductive mode may influence the mouth-form decision and its associated predatory behaviors is currently unknown.

Therefore, we first analyzed the mouth-form abundance across the *Pristionchus* phylogenetic clade by investigating 29 different species (Fig. 1C and table S1). Notably, mouth-form preference shows a strong association with reproductive mode [$P = 0.0043$, analysis of variance (ANOVA)], while no phylogenetic signal was detected

($P = 0.637$ and 0.769 ; for C_{mean} and Moran's I index, respectively) (Fig. 1D). The majority of gonochoristic species adopt the nonpredatory St morph (20 of 22 tested species). In contrast, hermaphroditic species appear to be affiliated with the predatory Eu morph in five of seven analyzed species. This mouth-form association is robustly maintained under diverse environmental conditions including different temperatures and diets (fig. S1). In the gonochoristic Eu species (*P. bucculentus* and *P. clavus*), limited available strains make it difficult to confirm whether these mouth-form associations are consistent throughout these species, whereas in the hermaphroditic

St-associated species (*P. mayeri* and *P. boliviae*), all available strains are St. Thus, our observations support a vision of parallel evolution of mouth-form fate and reproductive mode that may imply an adaptive value for such associations (32). Therefore, reproductive mode represents a previously neglected factor that influences the expression of cannibalistic behaviors in *Pristionchus* nematodes.

Mouth form promotes gonochoristic mating

Why would the gonochoristic reproductive mode associate with the nonpredatory St morph? We reasoned that the St bias might prevent fatal cannibalistic encounters between genetically distinct individuals in which the opportunity to mate is paramount. To test this hypothesis, we selected *P. uniformis* in which a multitude of genetically diverse natural isolates are available. All 13 analyzed *P. uniformis* strains confirmed a consistently strong St mouth-form association (fig. S2 and table S2), and reciprocal mating experiments among three *P. uniformis* strains from the United States, France, and Germany produced viable and fertile F2 progeny, validating the potential for these strains to be mating partners (fig. S3, A and B).

To test whether the nonpredatory St mouth form will facilitate mating and prevent killing between conspecifics, we selected rare Eu animals from these three strains and analyzed killing interactions (fig. S4). No killing was detected when predators were tested against prey of the same strain, indicating robust self-recognition (Fig. 1E). In contrast, cannibalism was observed between conspecifics with predators from all strains killing prey of all other genotypes. Moreover, when cross progeny between two different strains were tested in a reciprocal predator-prey setup, it showed mutual killing (Fig. 1E and table S3). Specifically, both parental predators killed their hybrid prey progeny, and similarly, hybrid predators killed prey of both parental lines. Last, hybrid predators killed their siblings in predator-prey assays. Together, these results indicate that the adoption of the nonpredatory St mouth form in gonochoristic species may be an adaptive strategy that avoids the killing of potential mating partners and therefore facilitates mating. In addition, full siblings can be quite divergent in gonochoristic species, and thus the adoption of the nonpredatory morph will guarantee not to consume your sisters or brothers. In summary, through the establishment of an St mouth form in gonochoristic nematodes, they circumvent cannibalistic tendencies, which may repel potential mates (14) and kill hybrid larvae and thus avoid parent-offspring conflict.

Predatory traits in hermaphrodites promote competition

Hermaphroditic species are frequently affiliated with the predatory Eu morph, the opposite of that observed in gonochoristic species. As hermaphrodites do not require a mating partner, we hypothesized that it may be advantageous to adopt a predatory strategy by killing rivals and removing competitors, an example of intraguild predation (33, 34). This could be particularly relevant, as reproduction via selfing minimizes genetic diversity and maintains close genetic relatedness with their offspring, which are not cannibalized by parents due to a self-recognition system (28). However, little is known about the ecological relevance of predation and cannibalism, as previous studies in *P. pacificus* focused exclusively on geographically diverse strains. To investigate the ecological significance of cannibalism, we used *P. pacificus* isolates from the small island La Réunion in the Indian Ocean (Fig. 2A), which, despite its age of only 2 to 3 million years, harbors a huge diversity of genetic lineages (35). We used 36 strains from three island populations at Trois Bassins, Grand Etang (GE),

and Nez de Boeuf, which frequently co-occur with a specific beetle species (Fig. 2B and table S1). These 36 strains were randomly chosen from a previous genomic meta-analysis of 264 La Réunion-based strains, and some of them are extremely closely related as indicated by their nucleotide diversity of $\pi < 0.001$ (36). Furthermore, genome analysis confirmed that these strains propagate exclusively by selfing with no heterozygosity observed in their genomes. We first analyzed the mouth-form ratios in these wild isolates for evidence of a particular morph. In all but two of these strains, the predatory Eu mouth form was the prevalent morph, potentially promoting competition and killing between strains (Fig. 2, C to E).

To test this hypothesis, we assessed the potential for killing and cannibalism between naturally co-occurring isolates. We set up pairwise killing assays between all 12 strains from each location to explore ecologically relevant predatory interactions, which revealed three distinct behaviors (Fig. 2, F to H, and fig. S4). First, we observed mutual cannibalism whereby strains kill one another with varying degrees of efficiency (63.1%). Second, we found multiple examples of one-directional killing, i.e., strain RSC066 from GE cannibalizes the strains RSC033, RSA054, and RS5407 but is not cannibalized in return. In total, we found that 24.3% of the strains displayed one-directional killing. Last, we detected examples of reciprocal recognition with some strains avoiding predatory behaviors altogether (12.6%). Notably, differing degrees of cannibalism were also observed between strains. Specifically, some strains exhibit extreme predation with more than 400 successful killing events in standardized corpse assays, whereas other strains show infrequent killing (table S4). Together, these results indicate that, in the hermaphroditic *P. pacificus*, the Eu morph is strongly favored and promotes competition between most, though not all, ecologically relevant conspecifics.

Genomic relatedness mediates killing strategies

Consequently, we wanted to understand the mechanism(s) behind the killing decision. Two theoretical assumptions could explain the observed behaviors. A single gene or allele(s) thereof could allow the recognition of other carriers, preventing cannibalism and resulting in a so-called “green beard effect” (37–41). Alternatively, the overall relatedness of strains might influence cannibalistic behaviors as originally proposed in kin selection theory by Hamilton (37, 42). To distinguish between these possibilities, we first assessed whether the previously identified component of the self-recognition signal *self-1* acts as a green beard. *self-1* encodes for a secreted small peptide and contains a hypervariable C-terminal domain in which single amino acid alterations result in killing (28). If cannibalism were solely dependent on *self-1*, the competitive interactions between the La Réunion-based strains should strictly correlate with the SELF-1 sequence in the hypervariable domain. Therefore, we identified *self-1* from RNA sequencing (RNA-seq) data and generated profiles of their hypervariable domains for the majority of the 36 strains (Fig. 2, F to H). At all three locations, some strains shared an identical SELF-1 hypervariable domain (29 of 198 pairwise comparisons). We observed killing between 20 of these 29 strains. Thus, *self-1* alone is insufficient to predict killing outcome and is not a green beard.

Next, we analyzed whether the overall genomic relatedness is a predictor of the killing versus cooperation decision among strains (Fig. 2, I to K). Genome-wide relatedness between pairs was determined from the number of single-nucleotide polymorphisms (SNPs) as identified from RNA-seq data and was scaled relative to the population average. In this analysis, positive values indicate that strain

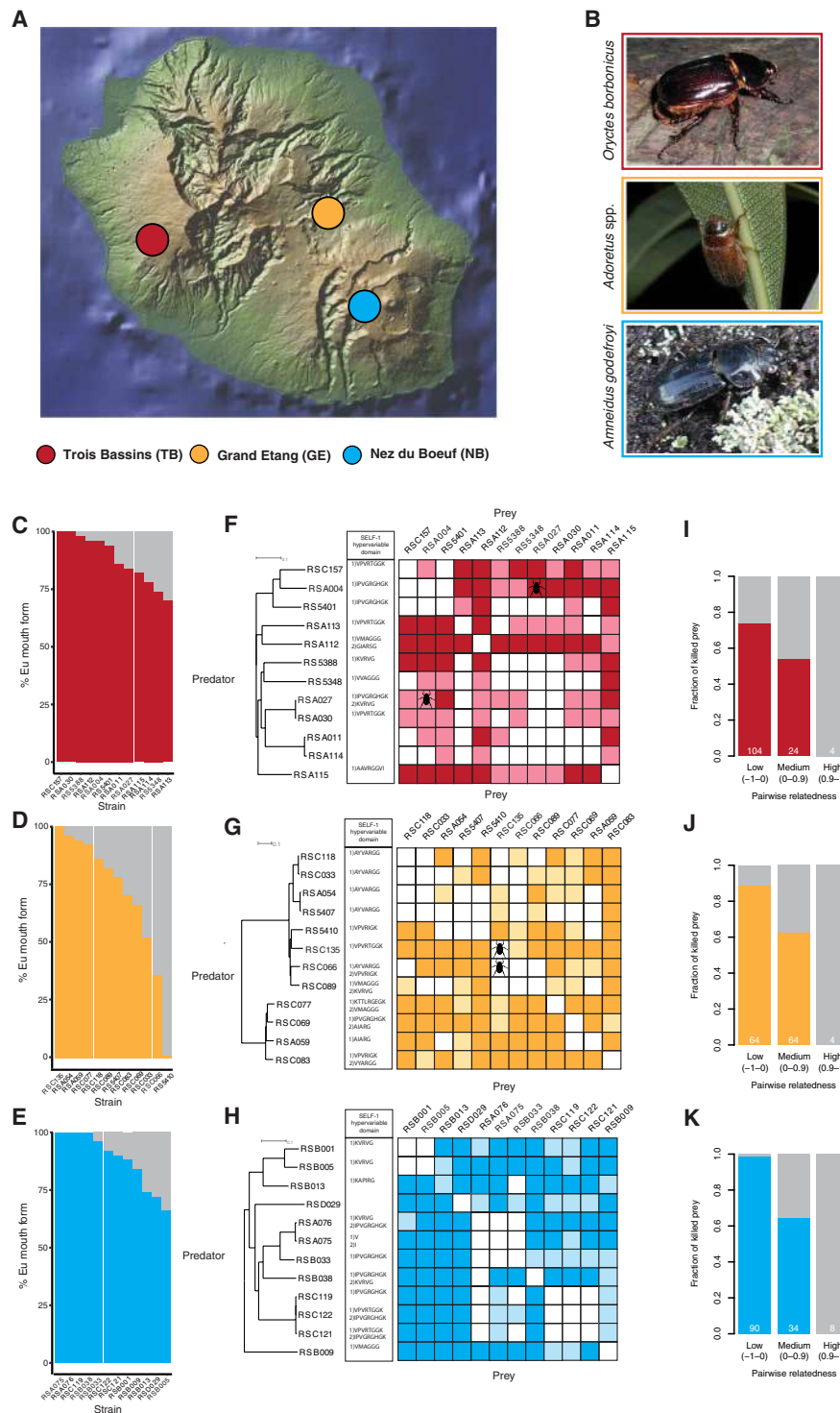


Fig. 2. Cannibalism is abundant in *P. pacificus*. (A) Strains from the hermaphroditic *P. pacificus*, isolated from three locations on La Réunion island. (B) *P. pacificus* from the three locations have distinct beetle associations. (C to E) Mouth-form decision is strongly biased toward the predatory Eu morph in the majority of wild isolates ($n = 50$ animals for each strain). (F to H) Predator-prey killing grids between strains at each location. Color intensity represents killing interactions resulting from the mean of two standard corpse assays, corresponding to either high (>30 corpses), medium (1 to 30 corpses), or low (0 corpses) killing frequencies. Strain phylogeny, SELF-1 copy number, and hypervariable sequences are also included. A beetle symbol represents pairs of strains isolated from the same beetle host. (I to K) Quantification of the fraction of killing interactions categorized according to the degree of relatedness between strains, calculated by the number of SNPs from RNA-seq data scaled relative to the population average. Numbers in each column indicate the total numbers of pairs in each category. The degree of relatedness between pairs is scored according to the thresholds, low (-1.0 to 0.0), medium (0.0 to 0.9), and high (0.9 to 1.0). Photo credit: Matthias Herrmann, MPI Developmental Biology, Germany; Jacques Rochat, Micropoda, France.

pairs are more closely related than the population average, while negative values indicate that pairs are more distantly related, as originally suggested by Hamilton's theoretical studies and their subsequent developments (see Materials and Methods) (37, 39, 42). We found that extremely closely related strains with an r value above 0.9 do not kill one another. In contrast, pairs of strains that are more distantly related than the population average are likely to kill each other ($P < 0.05$ across three populations, Fisher's exact test). Thus, strains, which are more closely related, frequently avoid cannibalistic behaviors, while more distantly related strains instead compete and kill one another. Furthermore, as killing correlates with the degree of genetic dissimilarity, this suggests multiple important genetic regions associated with nematode identity across the genome and demonstrates the ability of these nematodes to distinguish kin from non-kin with remarkable precision (Fig. 2, I to K). Thus, genomic relatedness informs the cannibalistic decision and overall interaction strategy.

Modeling cannibalistic strategies

Last, we modeled the costs and benefits of cannibalism and mouth-form plasticity in age-structured populations propagating by selfing, which represents the derived trait in *Pristionchus* evolution, by using two age classes of the Eu and St morphs, juveniles and adults (Fig. 3, A and B). Reproduction is biased toward one of the morphs. Adult population size is regulated by adult competition, and Eu adults can prey on all juveniles. When individuals of different strains x and y interact, predation depends on (i) population structure determined by the probability of encounter, (ii) their overall relatedness, and (iii) their ability for self-recognition (Fig. 3A). This approach allowed us to explore the circumstances that would result in the adoption of the Eu morph and its associated cannibalistic behavior.

First, we modeled under which conditions two strains would be able to coexist by modifying their degree of relatedness (r) and the encounter probability (b) (Fig. 3, C and D). Only under extremes of relatedness ($r = 0.99$ or 0.95) or in the absence of any encounter ($b = 0$) can x and y coexist for 100 steps. In contrast, if x and y are less related ($r < 0.9$), one strain will ultimately dominate. When strains are not interacting ($b = 0$), the St morph will surpass the Eu form, although both coexist. However, the Eu form will outcompete the St morph, with increased encounters and limited relatedness. These findings robustly corroborate our empirical data in the hermaphroditic *P. pacificus*. Second, a strong self-recognition system is required for the prevalence of the Eu morph and essential for population growth in general (fig. S5). Third, we used modeling to overcome the experimental limitations of the pairwise cannibalism assays. When modeling the interactions between three strains, we found that two highly related strains x and z more rapidly outcompeted a less related strain y (Fig. 3E). The coexistence of x and z may hint at a cooperative strategy between potential kin, allowing closely related strains to flourish while rapidly removing possible competitors. However, this initial "cooperation" will ultimately result in competitive interactions between x and z . Furthermore, the fixed genomic relatedness difference of 0.2 and 0.1 between strains x and z relative to y results in notably different population trajectories (Fig. 3E and fig. S6). These results are consistent with the empirical findings observed on La Réunion (Fig. 2). Together, therefore, modeling approaches indicate which conditions, in particular, overall genetic relatedness and self-recognition systems, are necessary to drive the prevalence of the predatory Eu morph and have likely facilitated the coexistence of cannibalistic forms.

DISCUSSION

Here, we integrate genome-level understanding of relatedness in a social action strategy and demonstrate through both empirical data and modeling that polyphenism (plasticity), kin recognition, and genomic relatedness shape cannibalistic behaviors. The unexpected association between mouth-form plasticity and reproductive mode during *Pristionchus* evolution suggests strong selection, resulting in the best action strategy to increase reproductive success (39). This includes the evolution of cooperative strategies in gonochoristic species while enhancing selfish actions in hermaphroditic ones. The correlation of phenotypically plastic traits and social interaction strategies may be a frequently observed principle, as it also has a role in inducing cooperative strategies in hymenopterans and termites (43) while also promoting competitive behaviors, as seen in salamanders, spadefoot toads, and rotifers (5, 6, 9, 10). It is important to note that while the mouth-form fate observed in *Pristionchus* is consistently associated with reproductive mode, the ability to form the alternative mouth form is still maintained in most populations. Therefore, the alternative mouth form must be beneficial under certain environmental conditions and may be a bet-hedging strategy. Correspondingly, two gonochoristic and two hermaphroditic species show the opposite mouth-form association. It is possible that these species are in transition toward the canonically associated morph or these isolates are not representative of their species as a whole. Alternatively, they may be under different evolutionary pressures, maintaining the opposing mouth-form strategy, despite the accompanying impediments. As St animals still feed on the carcasses of other nematodes under laboratory conditions (13), a scavenging strategy is one potential system, which we have not yet investigated in the wild and which may facilitate the adoption of the alternative morph. Furthermore, a recent analysis of the decaying beetle environment on which many of these nematodes are associated revealed intense competition for resources such as food availability that resulted in biphasic boom and bust nematode population dynamics (44). Therefore, Eu gonochoristic species may exploit a specific element of these ecological dynamics, despite the cost to mating chance.

Cannibalism in *Pristionchus* is part of a complex intraguild predation behavior, as these worms can kill and feed on various nematodes, likely as a means to both remove rivals competing for the same resources and acquire extra nutrients (33, 34). In addition, they are capable of repelling adult potential competitors from their territory through the avoidance response generated from a predatory bite on an adult cuticle (14). While previous studies revealed cannibalism behaviors between geographically distant strains but not on self-progeny due to a self-recognition system (28), we have now been able to demonstrate that this behavior is ecologically relevant and depends on more than just the previously identified self-recognition component *self-1*. Furthermore, the self-identification mechanism extends to more than just self-progeny, as it also includes close kin. The complexity of the mechanism is also likely to expand beyond a single gene involving components across the whole genome. Thus, in the predatory genus *Pristionchus*, the evolution of plasticity, genomic relatedness, and self-recognition systems enable the existence of cannibalistic behaviors. Therefore, we propose developmental plasticity as a general principle that influences cooperative versus competitive social action strategies in different animal systems from nematodes to vertebrates.

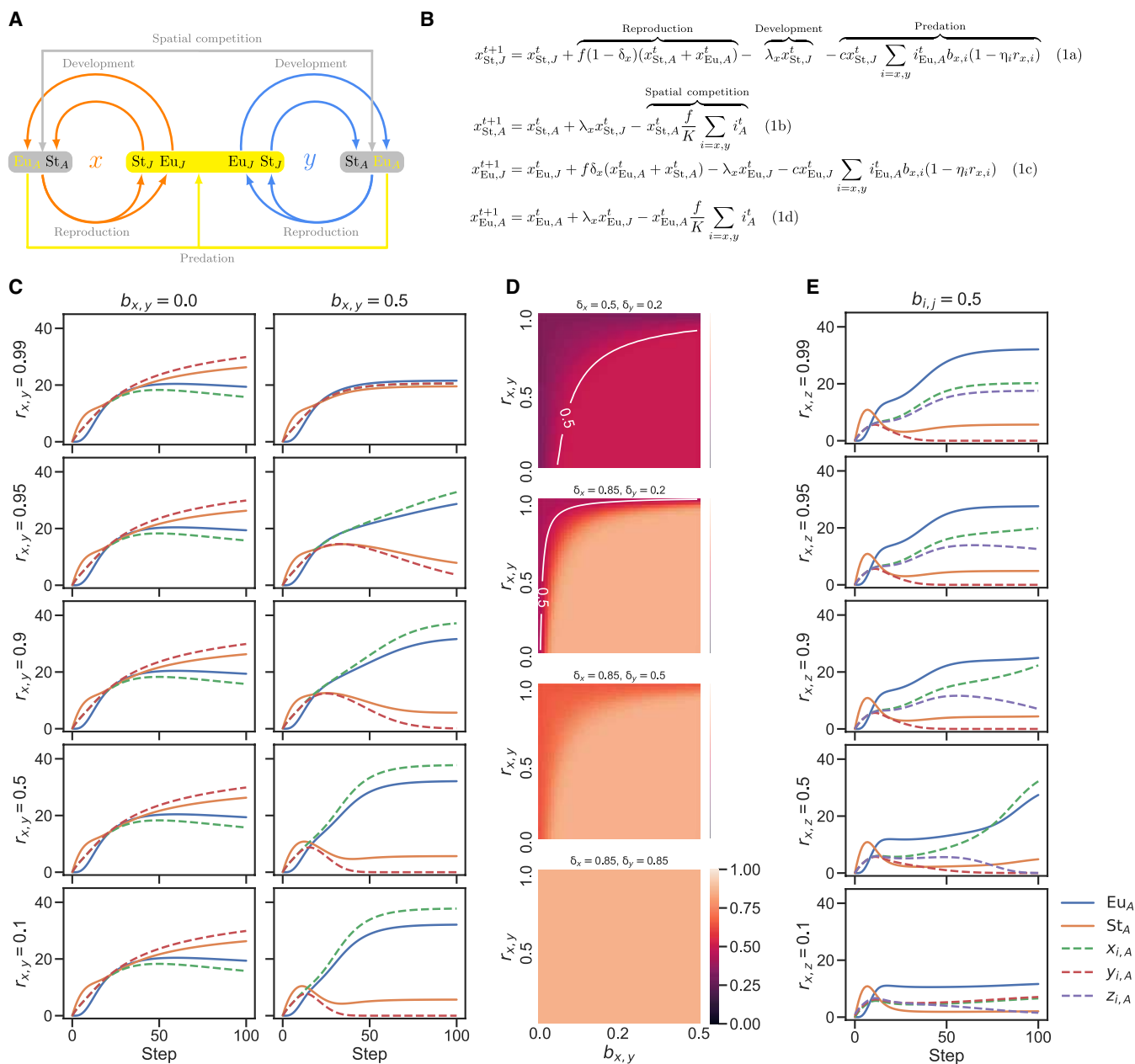


Fig. 3. Predation of hermaphrodites fits a selfing model of cannibalism. (A) Diagram of variables used throughout the model. (B) Dynamical equations solved for generating models. Genotype x dynamics follows four equations, 1a to 1d, with carrying capacity (K) and cost of predation (c). Genotype i adults will produce Eu juveniles with probability δ_i and St juveniles with probability $1 - \delta_i$. At each step, fraction λ develop into adults with adults producing f offspring. A fraction ($b_{i,j}$) of predatory encounters between juveniles of genotype j and Eu adults of genotype i is realized. The propensity of Eu adults to prey on juveniles decreases with increasing genomic relatedness (r), where $r_{i,j} = r_{j,i}$ and two individuals of the same genotype are fully related ($r_{i,i} = 1$). Predation depends on the genotype-dependent ability for kin recognition (η_i). Dynamics of genotypes y and z follow the same equations. (C) If genotypes do not interact ($b = 0.0$), the St -biased strain (y , $\delta_y = 0.2$) outnumbers the Eu -biased strain (x , $\delta_x = 0.85$). With high probability of encounter ($b = 0.5$), the St -biased genotype y can only coexist with genotype x if genetic relatedness is high and there is kin recognition. (D) Heatmaps representing the frequency of Eu adults after 100 steps under different combinations of r and b . The majority of conditions result in a strong Eu bias. The white contour line indicates when 50% of adults are of Eu after 100 steps. (E) Three-genotype selfing model, given $\delta_x = \delta_y = \delta_z = 0.85$. The coexistence of x , y , and z under high encounter ($b = 0.5$) is determined by pairwise relatedness ($r_{xy} = 0.2$, $r_{yz} = 0.1$). x and z outcompete y , reinforcing the role of relatedness. Results of (C), (D), and (E) are obtained by numerically solving Eqs. 1a to 1d for two and three-genotype cases. In all models, the initial number of juveniles of the St morph for each strain was 10, with other types set at 0 ($K = 50$, $\lambda = 0.1$, $\eta = 0.99$, $c = 0.1$, and $f = 0.6$).

MATERIALS AND METHODS**Nematode and bacterial strains**

A list of all nematode species and strains can be found in table S1. Wild *P. pacificus* isolates from specific field sites on La Réunion were always frozen and stored within the first 10 generations after isolation to minimize domestication and thereby facilitate the investigation of interactions between ecologically relevant populations.

Nematode culture conditions

All nematode species and strains were grown under standard nematode growth conditions on nematode growth media (NGM) plates seeded with *Escherichia coli* OP50 and maintained at 20°C.

Mouth-form phenotyping

Mouth-form phenotyping was performed as previously reported (27). In brief, synchronized adults were placed onto a Discovery stereomicroscope with high magnification ($\times 150$). The Eu mouth form was determined by the presence of a wide mouth with two teeth, whereas the St forms were determined by a narrow mouth and a single tooth. Animals with the Eu mouth type were picked for predation assays.

Mouth form–reproductive mode statistical analysis

An association between mouth-form preference and reproductive mode was determined by fitting beta regression model using the R package *betareg* (45). Mouth-form ratios of some species represent 0 and 1 values. Thereby, we applied a $(y^*(n - 1) + 0.5)/n$ transformation, where y is the response variable and n is the sample size (46). ANOVA test was run on the model using R package *car* (47). Phylogenetic analysis was performed on a modified Newick version of the *Pristionchus* phylogeny in Rödelsperger *et al.* (29). Phylogenetic signal was analyzed using R package *phylosignal* (48), based on the method of autocorrelation while using mouth-form ratios as a continuous trait.

Predation assays: Corpse assays

Corpse assays facilitated rapid quantification of predatory behavior and were conducted as previously described (15, 25). Briefly, to generate substantial quantities of larvae for use as prey, *Pristionchus* strains were maintained on *E. coli* OP50 bacteria until freshly starved, resulting in an abundance of young larvae. These plates were washed with M9 buffer, passed through two Millipore 20- μ m filters and centrifuged at 377g to form a concentrated larval pellet of juvenile animals. Excess buffer was removed, and 1 μ l of worm pellet was deposited onto a 6-cm NGM-unseeded assay plates. This resulted in roughly 3000 prey larvae on each assay plate. Assay plates were left for a minimum of 1 hour to allow larvae to distribute evenly over the plate. Young adult *Pristionchus* predators were screened for the required mouth form and transferred to empty NGM plates for 30 min to remove any excess bacteria from their bodies. Subsequently, 20 *Pristionchus* predators were added to assay plates and allowed to feed for 24 hours before removal, and the plates were scored for the presence of corpses.

Population genomic analysis and relatedness

Raw RNA-seq reads were aligned to the *P. pacificus* reference genome (version El Paco) by the TopHat2 software (version 2.0.14, default settings) (49). Variable positions that were previously identified on the basis of population-scale whole-genome sequencing (20, 36)

were called in the RNA-seq alignments with the samtools mpileup (version 0.1.18, default options) and bcftools view (version 0.1.17-dev, -cg options) programs (50). Between 10,000 and 70,000 single-nucleotide variant (SNP) positions with homozygous calls in either all samples or samples of a given population (variant quality score ≥ 20) were concatenated into pseudoalignments. These alignments were taken to calculate a neighbor-joining tree (51), representing the genome-wide phylogenetic relationships, and to calculate a percentage identity matrix that was further used to compute genome-wide relatedness. Percentage identity values were normalized by subtracting the population mean identity value. Genome-wide relatedness r was then obtained by dividing the normalized identity with the maximum absolute normalized identity value so that genetically identical pairs of strains have an $r = 1$, whereas the average $r = 0$ and pairs that are more distant than the average have an $r < 0$.

RNA-seq for identification of *self-1*

RNA-seq transcriptome data for all 36 *P. pacificus* strains were generated by first washing worms from three well-grown plates for each strain. These were pelleted down before resuspending in 1 ml of TRIzol. RNA was phenol-chloroform-extracted and cleaned using the RNA Clean & Concentrator Kits (Zymo Research) according to the manufacturer's guidelines. RNA was subsequently prepared using TruSeq RNA Sample Preparation Kit v2 (Illumina Inc.) according to the manufacturer's guidelines from 1 μ g of total RNA in each sample. Libraries were quantified using a combination of Qubit and BioAnalyzer (Agilent Technologies) and normalized to 2.5 nM. Samples were subsequently sequenced as 150-base pair paired-end reads on multiplexed lanes of an Illumina HiSeq3000 (Illumina Inc.). RNA-seq data have been deposited at the European Nucleotide Archive under the study accession PRJEB41213. The *self-1* locus could be assembled in 33 of 36 strains by the Trinity software (version 2.2.0) (52). Several strains have multiple copies of the *self-1* locus as previously described (28). On the basis of the classification of assembled sequences into genes and isoforms by the Trinity assembler, copy number was determined as the number of Trinity genes with *self-1* homologs (as identified by TBLASTN searches).

Map generation

The La Reunion island map was generated using the software GeoMapApp (53).

Modeling

In our discrete-time model, the population consists of two stages, juveniles (J) and adults (A); two morphs, predatory (Eu) and non-predatory (St); and $n \geq 2$ genotypes. At each time step, a fraction λ of all juveniles in the population develop into adults, and the remaining fraction $1 - \lambda$ persist in the juvenile stage, while every adult produces f new juveniles. Morphs are genetically determined at birth: For an adult of genotype i , a fraction δ_i of the produced juveniles f is of the Eu morph, while the remaining fraction $1 - \delta_i$ is of the St morph. Resource competition between adults due to limited environmental carrying capacity K leads to adult mortality in proportion to total adult densities. The only cause of death for juveniles is predation. Preys (juveniles) and predators (Eu adults) meet in proportion to their densities. For a juvenile of genotype j and a Eu adult of genotype i , the risk of predation upon an encounter is $b_{j,i}$. The propensity of an Eu adult to actually prey decreases with increasing genomic relatedness (r) with the encountered juvenile, where $r_{i,j} = r_{j,i}$

and two individuals from the same genotype are fully related, i.e., $r_{i,i} = 1$. The adult predation propensity also depends on the genotype-dependent ability in kin recognition (η_i). We assume equal recognition abilities for all genotypes ($\eta_i = \eta_j$ for any two genotypes i and j). The parameter c sets the genotype-independent overall frequency of predator-prey interactions, and it can be interpreted as the cost of predation.

In the simplest scenario, there are only two genotypes x and y . On the basis of the aforementioned life cycle, the dynamics of the subpopulation of genotype x is

$$x_{St,j}^{t+1} = x_{St,j}^t + \overbrace{f(1 - \delta_x)(x_{St,A}^t + x_{Eu,A}^t)}^{\text{Reproduction}} - \overbrace{\lambda x_{St,j}^t}_{\text{Development}} - \overbrace{c x_{St,j}^t \sum_{i=x,y} i_{Eu,A}^t b_{x,i}(1 - \eta_i r_{x,i})}_{\text{Predation}} \quad (1a)$$

$$x_{St,A}^{t+1} = x_{St,A}^t + \lambda x_{St,j}^t - \overbrace{x_{St,A}^t \sum_{i=x,y} i_A^t}_{\text{Spatial competition}} \quad (1b)$$

$$x_{Eu,j}^{t+1} = x_{Eu,j}^t + f \delta_x (x_{St,A}^t + x_{Eu,A}^t) - \lambda x_{Eu,j}^t - c x_{Eu,j}^t \sum_{i=x,y} i_{Eu,A}^t b_{x,i}(1 - \eta_i r_{x,i}) \quad (1c)$$

$$x_{Eu,A}^{t+1} = x_{Eu,A}^t + \lambda x_{Eu,j}^t - \overbrace{x_{Eu,A}^t \sum_{i=x,y} i_A^t}_{\text{Spatial competition}} \quad (1d)$$

The dynamics of the subpopulation of genotype y are analogous to Eqs. 1a to 1d. In the n genotype case, the subpopulation of genotype j is described by dynamical equations as in Eqs. 1a to 1d, with the only difference that both the predation term and the spatial competition term are generalized. A software used to numerically solve the recursive equations of our model was written in Python 2.7 and is available at https://github.com/Kalirad/asexual_plastic_model.

SUPPLEMENTARY MATERIALS

Supplementary material for this article is available at <http://advances.sciencemag.org/cgi/content/full/7/35/eabg8042/DC1>

REFERENCES AND NOTES

- D. W. Pfennig, M. McGee, Resource polyphenism increases species richness: A test of the hypothesis. *Philos. Trans. R. Soc. Lond. B Biol. Sci.* **365**, 577–591 (2010).
- M. J. West-Eberhard, Developmental plasticity and the origin of species differences. *Proc. Natl. Acad. Sci. U.S.A.* **102**, 6543–6549 (2005).
- M. J. West-Eberhard, *Developmental Plasticity and Evolution* (Oxford Univ. Press, 2003).
- H. F. Nijhout, Development and evolution of adaptive polyphenisms. *Evol. Dev.* **5**, 9–18 (2003).
- D. W. Pfennig, J. P. Collins, Kinship affects morphogenesis in cannibalistic salamanders. *Nature* **362**, 836–838 (1993).
- D. W. Pfennig, H. K. Reeve, P. W. Sherman, Kin recognition and cannibalism in spadefoot toad tadpoles. *Anim. Behav.* **46**, 87–94 (1993).
- R. K. Vijendravarma, S. Narasimha, T. J. Kawecki, Predatory cannibalism in *Drosophila melanogaster* larvae. *Nat. Commun.* **4**, 1789 (2013).
- V. Guttal, P. Romanczuk, S. J. Simpson, G. A. Sword, I. D. Couzin, Cannibalism can drive the evolution of behavioural phase polyphenism in locusts. *Ecol. Lett.* **15**, 1158–1166 (2012).
- D. W. Pfennig, P. W. Sherman, J. P. Collins, Kin recognition and cannibalism in polyphenic salamanders. *Behav. Ecol.* **5**, 225–232 (1994).
- J. Gilbert, Sex-specific cannibalism in the rotifer *Asplanchna sieboldi*. *Science* **194**, 730–732 (1976).
- G. Bento, A. Ogawa, R. J. Sommer, Co-option of the hormone-signalling module daftachronic acid-DAF-12 in nematode evolution. *Nature* **466**, 494–497 (2010).
- V. Susoy, E. J. Ragsdale, N. Kanzaki, R. J. Sommer, Rapid diversification associated with a macroevolutionary pulse of developmental plasticity. *eLife* **4**, e05463 (2015).
- M. Wilecki, J. W. Lightfoot, V. Susoy, R. J. Sommer, Predatory feeding behaviour in *Pristionchus* nematodes is dependent on phenotypic plasticity and induced by serotonin. *J. Exp. Biol.* **218**, 1306–1313 (2015).
- K. T. Quach, S. H. Chalasani, Distinct foraging strategies generated by single-action behavioural flexibility. *bioRxiv*, 2021.03.09.434602 (2021).
- V. Serobyanyan, E. J. Ragsdale, M. R. Müller, R. J. Sommer, Feeding plasticity in the nematode *Pristionchus pacificus* is influenced by sex and social context and is linked to developmental speed. *Evol. Dev.* **15**, 161–170 (2013).
- V. Serobyanyan, E. J. Ragsdale, R. J. Sommer, Adaptive value of a predatory mouth-form in a dimorphic nematode. *Proc. Biol. Sci.* **281**, 20141334 (2014).
- C. Dieterich, S. W. Clifton, L. N. Schuster, A. Chinwalla, K. Delehaunty, I. Dinkelacker, L. Fulton, R. Fulton, J. Godfrey, P. Minx, M. Mitreva, W. Roeseler, H. Tian, H. Witte, S. P. Yang, R. K. Wilson, R. J. Sommer, The *Pristionchus pacificus* genome provides a unique perspective on nematode lifestyle and parasitism. *Nat. Genet.* **40**, 1193–1198 (2008).
- H. Witte, E. Moreno, C. Rödelberger, J. Kim, J.-S. Kim, A. Streit, R. J. Sommer, Gene inactivation using the CRISPR/Cas9 system in the nematode *Pristionchus pacificus*. *Dev. Genes Evol.* **225**, 55–62 (2014).
- Z. Han, W. S. Lo, J. W. Lightfoot, H. Witte, S. Sun, R. J. Sommer, Improving transgenesis efficiency and CRISPR-associated tools through codon optimization and native intron addition in *Pristionchus* nematodes. *Genetics* **216**, 947–956 (2020).
- C. Rödelberger, J. M. Meyer, N. Prabh, C. Lanz, F. Bemm, R. J. Sommer, Single-molecule sequencing reveals the chromosome-scale genomic architecture of the nematode model organism *Pristionchus pacificus*. *Cell Rep.* **21**, 834–844 (2017).
- B. Sieriebriennikov, N. Prabh, M. Dardiry, H. Witte, W. Röseler, M. R. Kieninger, C. Rödelberger, R. J. Sommer, A developmental switch generating phenotypic plasticity is part of a conserved multi-gene locus. *Cell Rep.* **23**, 2835–2843.e4 (2018).
- M. S. Werner, B. Sieriebriennikov, T. Loschko, S. Namdeo, M. Lenuzzi, M. Dardiry, T. Renahan, D. R. Sharma, R. J. Sommer, Environmental influence on *Pristionchus pacificus* mouth form through different culture methods. *Sci. Rep.* **7**, 7207 (2017).
- B. Sieriebriennikov, S. Sun, J. W. Lightfoot, H. Witte, E. Moreno, C. Rödelberger, R. J. Sommer, Conserved nuclear hormone receptors controlling a novel plastic trait target fast-evolving genes expressed in a single cell. *PLoS Genet.* **16**, e1008687 (2020).
- E. Moreno, J. W. Lightfoot, M. Lenuzzi, R. J. Sommer, Cilia drive developmental plasticity and are essential for efficient prey detection in predatory nematodes. *Proc. R. Soc. B* **286**, 20191089 (2019).
- N. Akduman, J. W. Lightfoot, W. Röseler, H. Witte, W. S. Lo, C. Rödelberger, R. J. Sommer, Bacterial vitamin B12 production enhances nematode predatory behavior. *ISME J.* **14**, 1494–1507 (2020).
- M. Okumura, M. Wilecki, R. J. Sommer, Serotonin drives predatory feeding behavior via synchronous feeding rhythms in the nematode *Pristionchus pacificus*. *G3* **7**, 3745–3755 (2017).
- E. J. Ragsdale, M. R. Müller, C. Rödelberger, R. J. Sommer, A developmental switch coupled to the evolution of plasticity acts through a sulfatase. *Cell* **155**, 922–933 (2013).
- J. W. Lightfoot, M. Wilecki, C. Rödelberger, E. Moreno, V. Susoy, H. Witte, R. J. Sommer, Small peptide-mediated self-recognition prevents cannibalism in predatory nematodes. *Science* **364**, 86–89 (2019).
- C. Rödelberger, W. Röseler, N. Prabh, K. Yoshida, C. Weiler, M. Herrmann, R. J. Sommer, Phylotranscriptomics of *Pristionchus* nematodes reveals parallel gene loss in six hermaphroditic lineages. *Curr. Biol.* **28**, 3123–3127.e5 (2018).
- C. G. Thomas, G. C. Woodruff, E. S. Haag, Causes and consequences of the evolution of reproductive mode in *Caenorhabditis* nematodes. *Trends Genet.* **28**, 213–220 (2012).
- C. J. Weadick, R. J. Sommer, Mating system transitions drive life span evolution in *Pristionchus* nematodes. *Am. Nat.* **187**, 517–531 (2016).
- N. Gompel, B. Prud'homme, The causes of repeated genetic evolution. *Dev. Biol.* **332**, 36–47 (2009).
- K. T. Quach, S. H. Chalasani, Intraguild predation between *Pristionchus pacificus* and *Caenorhabditis elegans*: A complex interaction with the potential for aggressive behaviour. *J. Neurogenet.* **40**, 404–419 (2020).
- G. A. Polis, R. D. Holt, Intraguild predation: The dynamics of complex trophic interactions. *Trends Ecol. Evol.* **7**, 151–154 (1992).
- K. Morgan, A. M. Gaughran, L. Villate, M. Herrmann, H. Witte, G. Bartelmes, J. Rochat, R. J. Sommer, Multi locus analysis of *Pristionchus pacificus* on La Réunion Island reveals an evolutionary history shaped by multiple introductions, constrained dispersal events and rare out-crossing. *Mol. Ecol.* **21**, 250–266 (2012).
- A. McGaughran, C. Rödelberger, D. G. Grimm, J. M. Meyer, E. Moreno, K. Morgan, M. Leaver, V. Serobyanyan, B. Rakitsch, K. M. Borgwardt, R. J. Sommer, Genomic profiles of diversification and genotype-phenotype association in island nematode lineages. *Mol. Biol. Evol.* **33**, 2257–2272 (2016).

37. W. D. Hamilton, The genetical evolution of social behaviour. I. *J. Theor. Biol.* **7**, 1–16 (1964).
38. S. Smukalla, M. Caldara, N. Pochet, A. Beauvais, S. Guadagnini, C. Yan, M. D. Vinces, A. Jansen, M. C. Prevost, J. P. Latgé, G. R. Fink, K. R. Foster, K. J. Verstrepen, FLO1 is a variable green beard gene that drives biofilm-like cooperation in budding yeast. *Cell* **135**, 726–737 (2008).
39. S. A. West, A. Gardner, Altruism, spite, and greenbeards. *Science* **327**, 1341–1344 (2010).
40. D. C. Queller, E. Ponte, S. Bozzaro, J. E. Strassmann, Single-gene greenbeard effects in the social amoeba *Dictyostelium discoideum*. *Science* **299**, 105–106 (2003).
41. L. Keller, K. G. Ross, Selfish genes: A green beard in the red fire ant. *Nature* **394**, 573–575 (1998).
42. W. D. Hamilton, Selfish and spiteful behaviour in an evolutionary model. *Nature* **228**, 1218–1220 (1970).
43. C. A. Weitekamp, R. Libbrecht, L. Keller, Genetics and evolution of social behavior in insects. *Annu. Rev. Genet.* **51**, 219–239 (2017).
44. T. Renahan, W.-S. Lo, M. S. Werner, J. Rochat, M. Herrmann, R. J. Sommer, Nematode biphasic “boom and bust” dynamics are dependent on host bacterial load while linking dauer and mouth-form polyphenisms. *Environ. Microbiol.* 10.1111/1462-2920.15438 (2021).
45. F. Cribari-Neto, A. Zeileis, Beta Regression in R. *J. Stat. Softw.* **34**, 10.18637/jss.v034.i02 (2010).
46. M. Smithson, J. Verkuilen, *Fuzzy Set Theory: Applications in the Social Sciences* (SAGE, 2006).
47. J. Fox, S. Weisberg, *R Companion to Applied Regression, Third edition* (SAGE, 2019).
48. F. Keck, F. Rimet, A. Bouchez, A. Franc, phylosignal: An R package to measure, test, and explore the phylogenetic signal. *Ecol. Evol.* **6**, 2774–2780 (2016).
49. D. Kim, G. Perte, C. Trapnell, H. Pimentel, R. Kelley, S. L. Salzberg, TopHat2: Accurate alignment of transcriptomes in the presence of insertions, deletions and gene fusions. *Genome Biol.* **14**, R36 (2013).
50. H. Li, B. Handsaker, A. Wysoker, T. Fennell, J. Ruan, N. Homer, G. Marth, G. Abecasis, R. Durbin; 1000 Genome Project Data Processing Subgroup, The Sequence Alignment/Map format and SAMtools. *Bioinformatics* **25**, 2078–2079 (2009).
51. K. P. Schliep, phangorn: Phylogenetic analysis in R. *Bioinformatics* **27**, 592–593 (2011).
52. M. G. Grabherr, B. J. Haas, M. Yassour, J. Z. Levin, D. A. Thompson, I. Amit, X. Adiconis, L. Fan, R. Raychowdhury, Q. Zeng, Z. Chen, E. Mauceli, N. Hacohen, A. Gnirke, N. Rhind, F. di Palma, B. W. Birren, C. Nusbaum, K. Lindblad-Toh, N. Friedman, A. Regev, Full-length transcriptome assembly from RNA-Seq data without a reference genome. *Nat. Biotechnol.* **29**, 644–652 (2011).
53. W. B. F. Ryan, S. M. Carbotte, J. O. Coplan, S. O'Hara, A. Melkonian, R. Arko, R. A. Weissel, V. Ferrini, A. Goodwillie, F. Nitsche, Global multi-resolution topography synthesis. *Geochem. Geophys. Geosyst.* **10**, Q03014 (2009).

Acknowledgments: We thank B. Sieriebriennikov for the mouth-form image; M. Herrmann, J. Rochat, and the La Réunion field team for species and strain isolation; K. Yoshida for support in the statistical analysis; and L. Keller (Lausanne) and P. Rainey (Plön) for discussions. We thank members of the Sommer Lab for discussion and T. Renahan for carefully reading the manuscript. **Funding:** This work was funded by the Max Planck Society. **Author contributions:** J.W.L. and M.D. performed all lab experiments with assistance from G.E., H.W., and M.W. Bioinformatic data analysis was performed by C.R. Modeling was carried out by M.D., A.K., S.G., and A.T. All experiments were designed by J.W.L., M.D., and R.J.S. **Competing interests:** The authors declare that they have no competing interests. **Data and materials availability:** All data needed to evaluate the conclusions in the paper are present in the paper and/or the Supplementary Materials. RNA-seq data have been deposited at the European Nucleotide Archive under the study accession PRJEB41213.

Submitted 28 January 2021

Accepted 1 July 2021

Published 25 August 2021

10.1126/sciadv.abg8042

Citation: J. W. Lightfoot, M. Dardiry, A. Kalirad, S. Giaimo, G. Eberhardt, H. Witte, M. Wilecki, C. Rödelsperger, A. Traulsen, R. J. Sommer, Sex or cannibalism: Polyphenism and kin recognition control social action strategies in nematodes. *Sci. Adv.* **7**, eabg8042 (2021).

Sex or cannibalism: Polyphenism and kin recognition control social action strategies in nematodes

James W. LightfootMohannad DardiryAta KaliradStefano GiaimoGabi EberhardtHanh WitteMartin WileckiChristian RödelspergerArne TraulsenRalf J. Sommer

Sci. Adv., 7 (35), eabg8042. • DOI: 10.1126/sciadv.abg8042

View the article online

<https://www.science.org/doi/10.1126/sciadv.abg8042>

Permissions

<https://www.science.org/help/reprints-and-permissions>

Use of think article is subject to the [Terms of service](#)

Science Advances (ISSN) is published by the American Association for the Advancement of Science. 1200 New York Avenue NW, Washington, DC 20005. The title *Science Advances* is a registered trademark of AAAS.

Copyright © 2021 The Authors, some rights reserved; exclusive licensee American Association for the Advancement of Science. No claim to original U.S. Government Works. Distributed under a Creative Commons Attribution NonCommercial License 4.0 (CC BY-NC).

Supplementary Materials for

Sex or cannibalism: Polyphenism and kin recognition control social action strategies in nematodes

James W. Lightfoot, Mohannad Dardiry, Ata Kalirad, Stefano Giaimo, Gabi Eberhardt, Hanh Witte, Martin Wilecki, Christian Rödelsperger, Arne Traulsen, Ralf J. Sommer*

*Corresponding author. Email: ralf.sommer@tuebingen.mpg.de

Published 25 August 2021, *Sci. Adv.* **7**, eabg8042 (2021)

DOI: [10.1126/sciadv.abg8042](https://doi.org/10.1126/sciadv.abg8042)

This PDF file includes:

Figs. S1 to S6
Tables S1 to S4

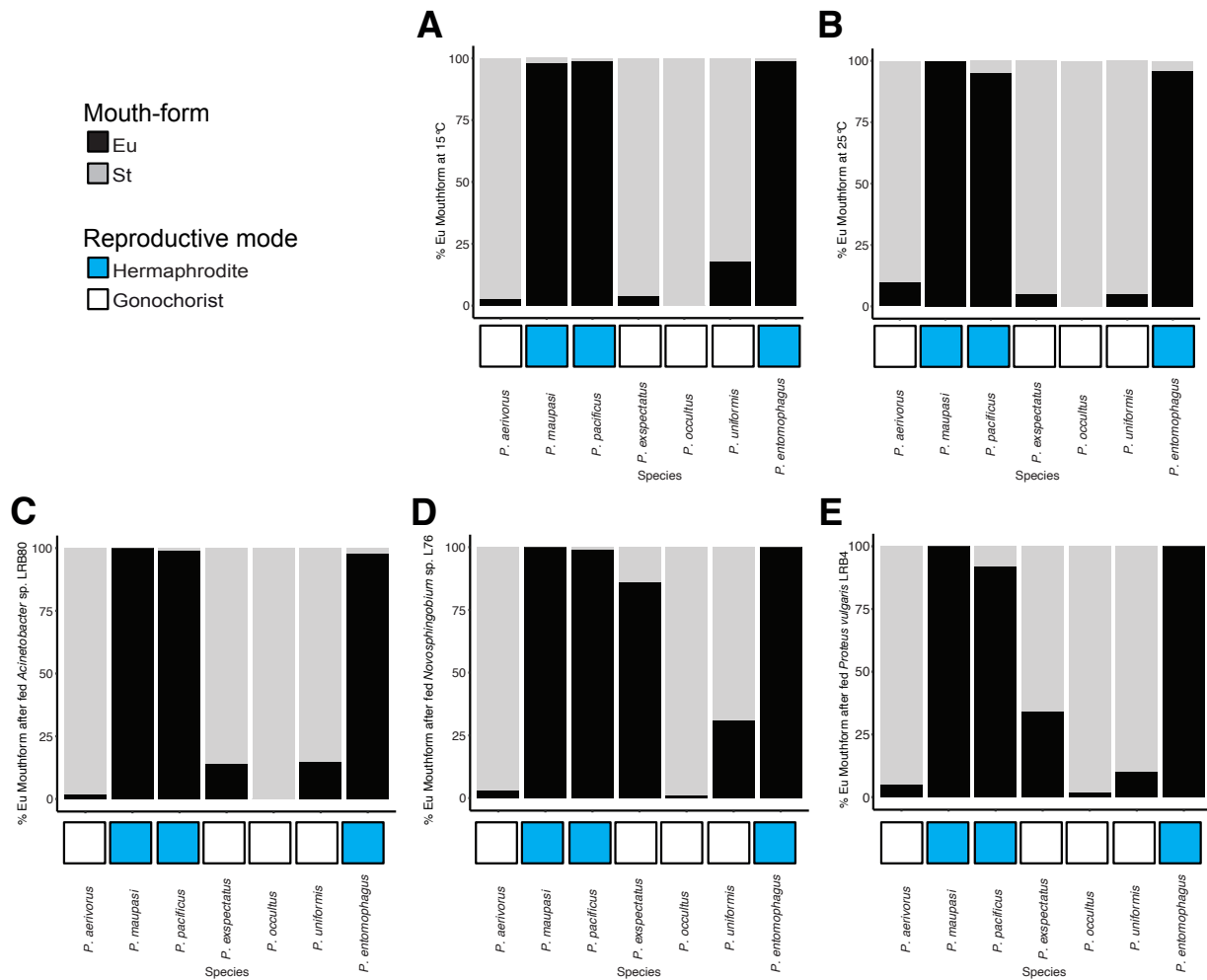


Fig. S1. Mouth form preference is robust and consistent under different environmental conditions. (A) Mouth form preference is maintained across species representing both gonochoristic and hermaphroditic modes of reproduction at difference temperatures including lower temperature conditions of 15°C and (B) higher temperatures of 25°C. (C) Mouth form preference is maintained across species representing both gonochoristic and hermaphroditic modes of reproduction when fed on different bacterial diets including *Acinetobacter* sp, (D) *Novosphingobium* and (E) *Proteus vulgaris*. For each species, mouth form was scored from either 100 hermaphrodites or alternatively 100 females from the gonochoristic species.

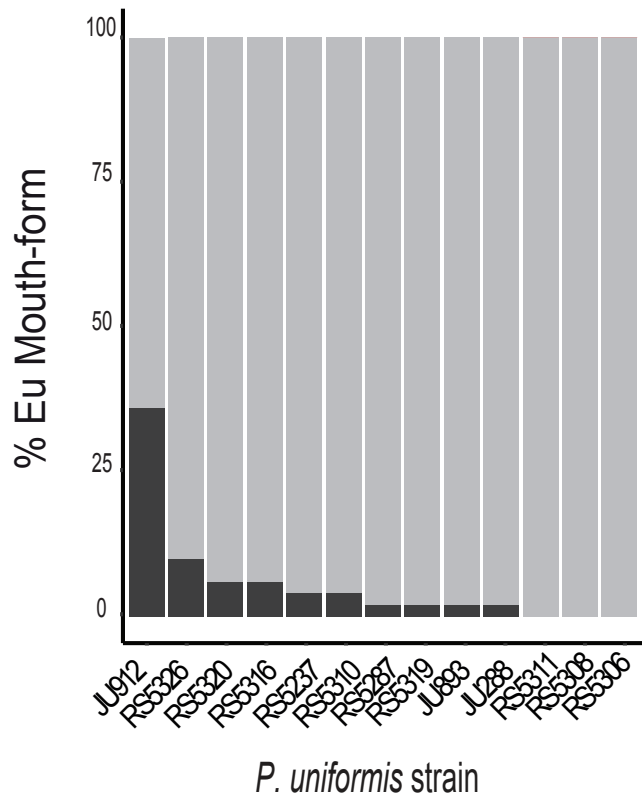
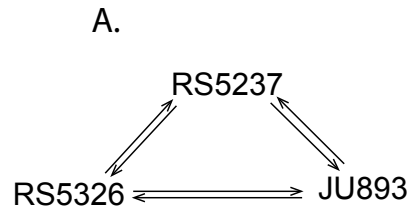


Fig. S2. *P. uniformis* mouth-form frequency. The adoption of the non-predatory St mouth form in *P. uniformis* is consistent across the majority of isolated strains. Mouth-form frequency was quantified by assessing 50 animals of each strain.



B.

	RS5237 x RS5326	RS5237 x JU892	JU892 x RS5326	JU892 x RS237	RS5326 x RS5237	RS5326 x JU892
Replicate 1	122	160	230	153	82	91
Replicate 2	160	105	235	127	40	20
Replicate 3	170	190	120	189	116	71
Replicate 4	220	130	210	50	110	54

Fig. S3. *P. uniformis* between strain mating. (A) Mating experiments between three *P. uniformis* strains from different geographic locations utilized in corpse assays. All strains were tested with one another four times and all mated successfully. (B) All mating experiments resulted in viable progeny. Table show number of viable progeny from each between strain mating replicate.

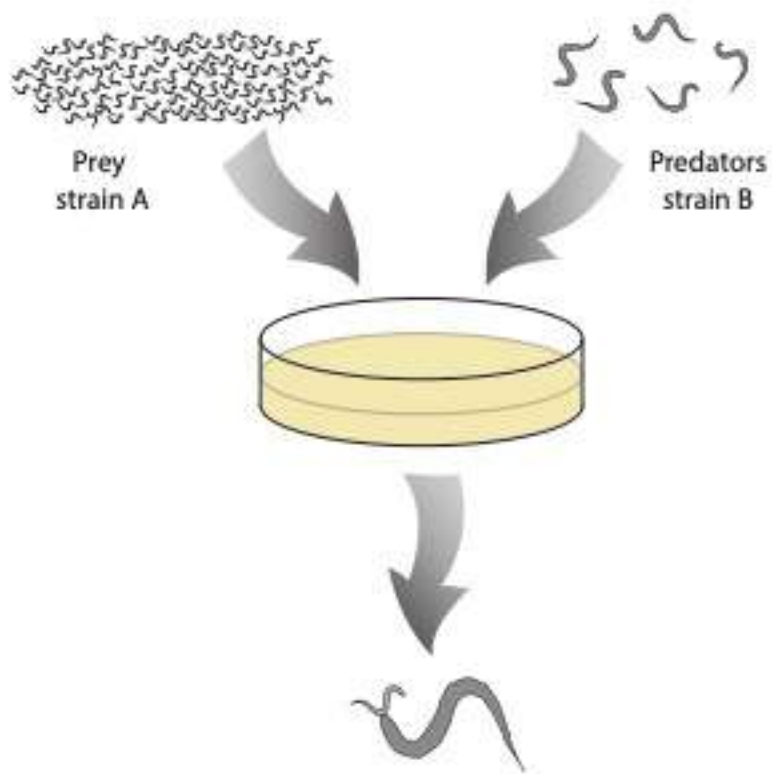


Fig. S4. Predation assays. Cartoon schematic of the corpse assays used for assessing pairwise killing interactions. Larvae of one strain were isolated and placed onto an assay plate as prey along with 20 adults of a different strain as potential predators. After 24 hours the predators were removed and the number of corpses left on the assay plate were scored.

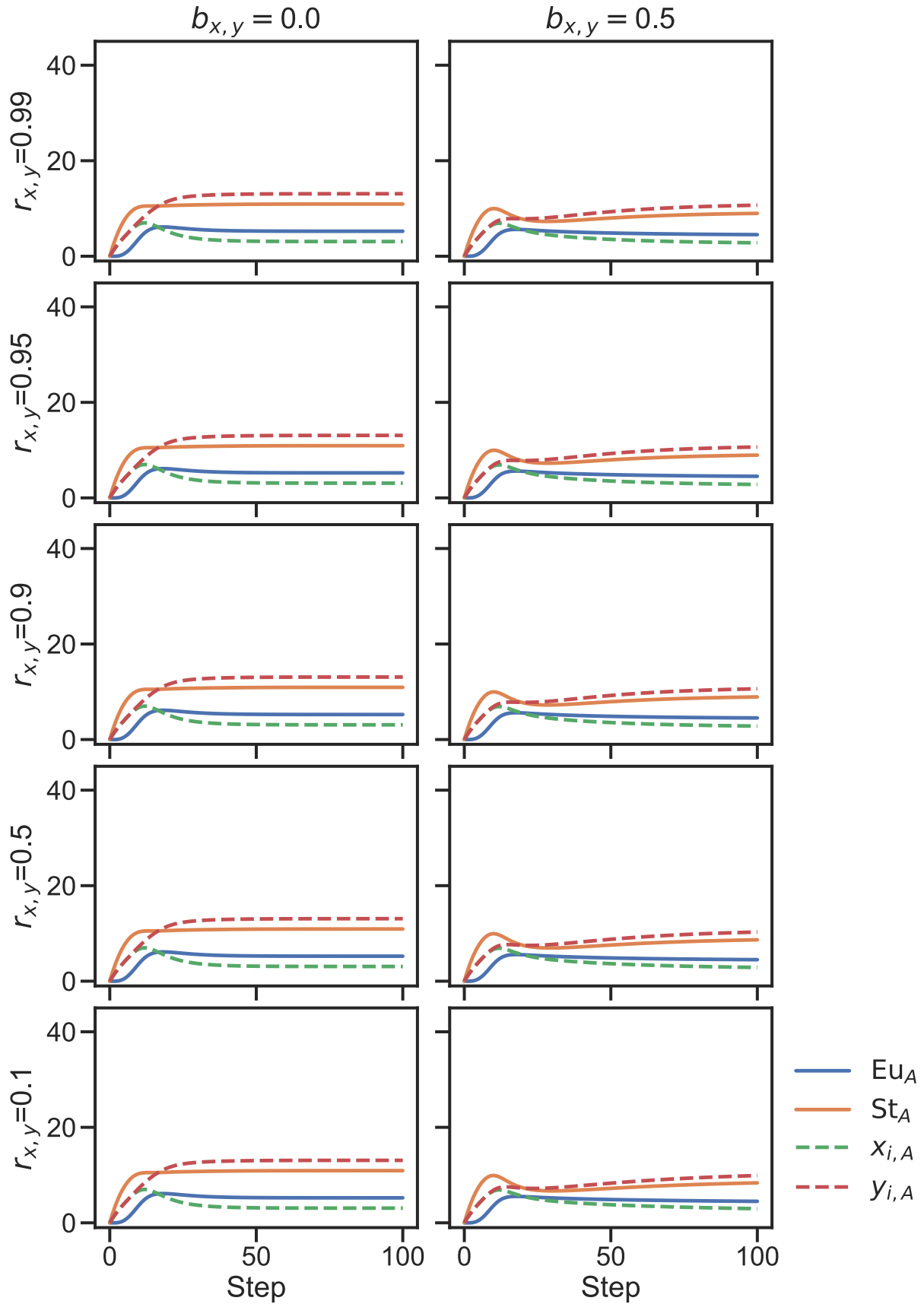


Fig. S5. Self-recognition system is fundamental for the adoption of the Eu morph. With a poorly-operating self-recognition system ($\eta = 0.2$), the effects of the genetic relatedness and the encounter probability between the St-biased strain ($y, \delta_y = 0.2$) and the Eu-biased strain ($x, \delta_x = 0.85$) on their dynamics are largely nullified, since the Eu adults indiscriminately prey upon the juveniles of their own genotype, as well as the juveniles of the other genotype. Results were obtained by numerically solving the two-genotype version of Eq.S1. The initial numbers of juveniles of the St morph for each strain were 10, with other types set at zero. ($K = 50, \lambda = 0.1, c = 0.1, f = 0.6$)

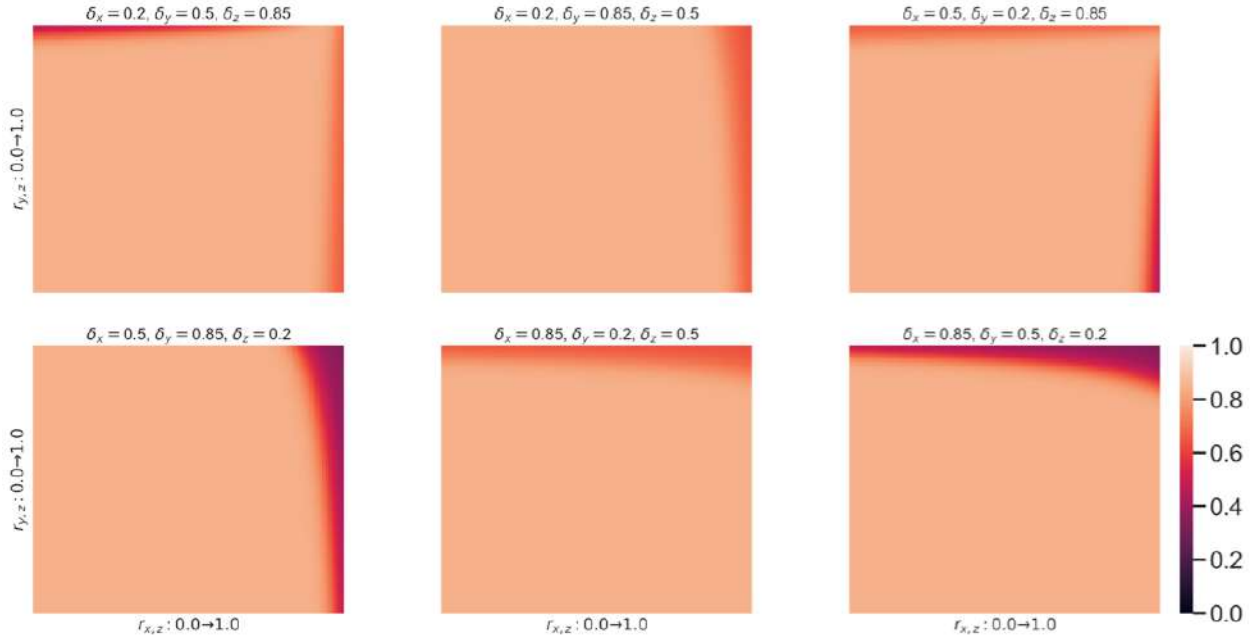


Fig. S6. The effect of genetic relatedness on the frequency of Eu morphs in the three-genotype asexual model. The heat maps represent the frequency of the adults of Eu morph after 100 steps under different combinations of r_{xz} and r_{yz} for the three-genotype case with different combinations of developmental bias for each genotype. All outcomes result in a high Eu frequency. The results are obtained by numerically solving the three-genotype version of Eq.S1. The initial numbers of juveniles of St morph for each strain were 10, with other types set at zero ($K = 50, \lambda = 0.1, \eta = 0.99, c = 0.1, f = 0.6, r_{xy} = 0.1, b = 0.5$).

Species	Strain designation	Location Isolated
<i>P. pacificus</i>	RSC157	La Reunion - Trois Basin
<i>P. pacificus</i>	RS5401	La Reunion - Trois Basin
<i>P. pacificus</i>	RSA113	La Reunion - Trois Basin
<i>P. pacificus</i>	RSA112	La Reunion - Trois Basin
<i>P. pacificus</i>	RS5388	La Reunion - Trois Basin
<i>P. pacificus</i>	RS5348	La Reunion - Trois Basin
<i>P. pacificus</i>	RSA027	La Reunion - Trois Basin
<i>P. pacificus</i>	RSA030	La Reunion - Trois Basin
<i>P. pacificus</i>	RSA011	La Reunion - Trois Basin
<i>P. pacificus</i>	RSA114	La Reunion - Trois Basin
<i>P. pacificus</i>	RSA115	La Reunion - Trois Basin
<i>P. pacificus</i>	RSC118	La Reunion - Grand Etang
<i>P. pacificus</i>	RSC033	La Reunion - Grand Etang
<i>P. pacificus</i>	RSA054	La Reunion - Grand Etang
<i>P. pacificus</i>	RS5407	La Reunion - Grand Etang
<i>P. pacificus</i>	RS5410	La Reunion - Grand Etang
<i>P. pacificus</i>	RSC135	La Reunion - Grand Etang
<i>P. pacificus</i>	RSC066	La Reunion - Grand Etang
<i>P. pacificus</i>	RSC089	La Reunion - Grand Etang
<i>P. pacificus</i>	RSC077	La Reunion - Grand Etang
<i>P. pacificus</i>	RSC069	La Reunion - Grand Etang
<i>P. pacificus</i>	RSA059	La Reunion - Grand Etang
<i>P. pacificus</i>	RSC083	La Reunion - Grand Etang
<i>P. pacificus</i>	RSB001	La Reunion - Nez du Boeuf
<i>P. pacificus</i>	RSB005	La Reunion - Nez du Boeuf
<i>P. pacificus</i>	RSB013	La Reunion - Nez du Boeuf
<i>P. pacificus</i>	RSD029	La Reunion - Nez du Boeuf
<i>P. pacificus</i>	RSA076	La Reunion - Nez du Boeuf
<i>P. pacificus</i>	RSA075	La Reunion - Nez du Boeuf
<i>P. pacificus</i>	RSB033	La Reunion - Nez du Boeuf
<i>P. pacificus</i>	RSB038	La Reunion - Nez du Boeuf
<i>P. pacificus</i>	RSC119	La Reunion - Nez du Boeuf
<i>P. pacificus</i>	RSC122	La Reunion - Nez du Boeuf
<i>P. pacificus</i>	RSC121	La Reunion - Nez du Boeuf
<i>P. pacificus</i>	RSB009	La Reunion - Nez du Boeuf
<i>P. uniformis</i>	RS5237	USA
<i>P. uniformis</i>	RS5326	Germany
<i>P. uniformis</i>	JU893	France
<i>P. uniformis</i>	JU912	France
<i>P. uniformis</i>	JU288	France
<i>P. uniformis</i>	RS5320	USA
<i>P. uniformis</i>	RS5306	USA
<i>P. uniformis</i>	RS5311	USA
<i>P. uniformis</i>	RS5310	USA
<i>P. uniformis</i>	RS5287	Germany
<i>P. uniformis</i>	RS5316	Germany
<i>P. uniformis</i>	RS5308	Germany
<i>P. uniformis</i>	RS5319	Germany
<i>P. aerivorus</i>	RS5106	American clade
<i>P. maupasi</i>	RS0143	American clade
<i>P. americanus</i>	RS5140	American clade
<i>P. boliviae</i>	RS 5262	American clade
<i>P. mayeri</i>	RS5460	American clade
<i>P. marianneae</i>	RS5108	American clade
<i>P. atlanticus</i>	CZ3975	American clade
<i>P. pauli</i>	RS5130	American clade
<i>P. pacificus</i>	PS312	Asian clade
<i>P. expectatus</i>	RS5522	Asian clade
<i>P. occultus</i>	RS5811	Asian clade
<i>P. taiwanesis</i>	RS5797	Asian clade
<i>P. arcanus</i>	RS5527	Asian clade
<i>P. maxplancki</i>	RS5594	Asian clade
<i>P. japonicus</i>	SB393	Asian clade
<i>P. quartusdecimus</i>	RS5230	Asian clade
<i>P. triformis</i>	RS5233	European clade
<i>P. hoplostomus</i>	JU1090	European clade
<i>P. Fukushimae</i>	RS5595	European clade
<i>P. brevicauda</i>	RS5231	European clade
<i>P. clavus</i>	RS5284	European clade
<i>P. bulgaricus</i>	RS5283	European clade
<i>P. uniformis</i>	RS5326	European clade
<i>P. entomophagus</i>	RS0144	European clade
<i>P. lucani</i>	RS5050	European clade
<i>P. lheritieri</i>	SB245	European clade
<i>P. elegans</i>	RS5698	Asian clade
<i>P. bucculentus</i>	RS5596	Asian clade
<i>P. fissidentatus</i>	RS5133	Asian clade

Table S1. List of all species and strains utilized.

Species	Strain designation	Location Isolated	Eurystomatous animals	Total number of animals checked
<i>P. uniformis</i>	JU912	France	19	52
<i>P. uniformis</i>	RS5326	Germany	5	50
<i>P. uniformis</i>	RS5320	USA	3	52
<i>P. uniformis</i>	RS5316	Germany	3	52
<i>P. uniformis</i>	RS5237	USA	2	52
<i>P. uniformis</i>	RS5310	USA	2	52
<i>P. uniformis</i>	RS5287	Germany	1	50
<i>P. uniformis</i>	RS5319	Germany	1	50
<i>P. uniformis</i>	JU893	France	1	50
<i>P. uniformis</i>	JU288	France	1	50
<i>P. uniformis</i>	RS5311	USA	0	51
<i>P. uniformis</i>	RS5308	Germany	0	51
<i>P. uniformis</i>	RS5306	USA	0	50

Table S2. Raw data of all *P. uniformis* mouth form frequencies.

Predator	Prey			
	JU893	RS5237	RS5326	Hybrid
JU893	0/2/1/0*	5/7/4	5/4/6	NA
RS5237	6/14/21	0/0/0	9/4/15	13/11/9
RS5326	80/60/56	12/20/16	0/0/0	25/24/31
Hybrid	NA	42/38/30	22/23/15	42/36/52

Table S3. Raw data of all *P. uniformis* pairwise killing assays. Three replicates were conducted for each pairwise interaction. Generating any Eu animals in strain JU893 was difficult and required abnormal degrees of starvation.

Predator	Prey											
	RSC157	RSA004	R55401	RSA113	RSA112	R55388	R55348	RSA027	RSA030	RSA011	RSA114	RSA115
RSC157	0/0	0/5	0/0	29/132	59/27	4 / 5	73/186	55/7	0/58	24/51	14/17	43/7
RSA004	0/0	0/0	0/0	30/83	98/120	3 / 19	24/32	101/118	22/54	22/41	67/178	36/33
R55401	0/0	0/0	0/0	0/5	100/81	0/0	0/0	0/0	0/0	0/11	0/0	40/26
RSA113	101/96	77/71	55/72	0/0	41/47	0/0	0/10	1/0	0/1	0/9	0/0	31/ 5
RSA112	55/ 42	98/144	220/246	88/123	0/0	76/86	131/112	65/85	51/11	39/81	47/63	44/13
R55388	56/81	132/102	33/31	0/0	115/109	0/0	0/0	0/0	0/0	0/2	0/1	44/23
R55348	0/0	11 / 13	0/1	0/0	28/30	0/0	0/0	0/0	0/0	0/0	0/0	50/68
RSA027	0/16	5 / 3	21/40	0/0	29/18	04 / 09	0/2	0/0	0/0	0/31	0/1	35/28
RSA030	0/1	0/2	2 / 9	0/0	21/16	0/0	0/2	0/0	0/0	0/32	0/8	17 / 4
RSA011	0/0	19/24	0/1	0/0	31/44	0/2	0/0	0/0	0/0	0/0	0/0	32/33
RSA114	0/0	0/0	0/17	0/0	0/58	0/0	0/0	0/0	0/0	0/0	0/0	44/3
RSA115	292/348	340/303	46/39	66/81	63/52	43/2	19/21	34/11	22 / 11	60/109	29/38	0/0

Predator	prey											
	RSC118	RSC033	RSA054	R55407	R55410	RSC135	RSC066	RSC089	RSC077	RSC069	RSA059	RSC083
RSC118	0/0	0/0	55/29	0/0	122/267	0/0	0/12	0/0	50/17	21/14	33/41	56/141
RSC033	0/0	0/0	0/0	0/1	62/84	0/0	0/0	0/14	0/3	0/6	57/104	103/174
RSA054	0/0	0/0	0/14	0/0	0/0	0/3	0/0	55/6	0/18	0/9	0/0	37/55
R55407	0/0	0/0	0/0	0/0	0/0	6/0	0/0	20/18	0/0	0/0	0/0	89/81
R55410	189/227	203/177	0/0	0/0	0/0	49/76	022/ 12	201/330	163/198	15/21	0/0	98/140
RSC135	104/134	382/299	144/100	369/256	290/395	0/0	3/0	350/406	192/136	188/180	178/256	184/148
RSC066	0/0	44/116	126/117	194/139	400/460	0/0	0/0	0/0	177/363	11/ 6	3 / 8	253/377
RSC089	1/0	0/0	0/0	13 / 8	122/309	0/0	0/0	0/0	29 / 07	0/5	0/0	83/73
RSC077	207/101	198/210	109/42	41/3	149/190	10/10	50/ 88	111/72	0/0	31/66	51/ 55	165/185
RSC069	200/372	199/262	173/166	313/276	333/401	07 / 16	250/299	379/404	32/66	0/0	150/140	29/22
RSA059	254/333	188/241	0/0	03/ 02	29/77	40/42	291/312	145/132	59/43	0/0	0/0	120/147
RSC083	189/146	35/19	21/54	33/14	289/441	105/123	153/132	300/349	36/42	128/110	159/180	0/0

Predator	Prey											
	RSB001	RSB005	RSB013	RSD029	RSA076	RSA075	RSB033	RSB038	RSC119	RSC122	RSC121	RSB009
RSB001	0/0	0/0	93/144	29/36	33/12	55/90	39/63	192/232	0/3	0/1	42/66	37/31
RSB005	0/0	0/0	37/10	31/39	41/33	160/185	142/181	78/107	288/330	15/13	98/119	40/34
RSB013	64/81	177/123	8/0	321/381	37/46	217/257	0/0	88/59	287/280	77/111	418/420	30/26
RSD029	61/55	316/277	201/124	0/0	19/26	180/169	0/3	199/320	13/23	4/0	20/16	39/34
RSA076	39/6	455/388	188/210	500/436	0/0	0/0	0/0	342/287	119/166	29/44	88/146	47/91
RSA075	104/172	262/233	155/279	220/159	0/0	0/0	0/0	281/231	67/51	21/16	80/58	44/60
RSB033	44/32	131/177	37/53	253/313	0/0	0/0	0/0	33/27	0/1	0/2	0/1	33/8
RSB038	297/198	407/419	60/49	226/286	0/0	53/42	29/33	0/0	170/228	43/31	70/93	10/1
RSC119	45/33	366/315	114/172	70/100	0/0	0/6	0/0	29/47	0/0	0/0	0/0	22/7
RSC122	288/213	341/277	44/79	265/241	0/0	0/5	0/3	34/64	0/0	0/0	0/0	8/5
RSC121	363/296	351/314	41/39	355/384	0/0	0/4	0/0	300/356	0/0	0/0	0/0	10/13
RSB009	80/82	247/215	27/32	98/162	107/189	76/130	66/92	289/256	21/16	29/17	150/170	0/0

Table S4. Raw data of all *P. pacificus* pairwise killing assays. Two replicates were conducted for each pairwise interaction. Grid 1 in Red data is Trois Basin, Grid 2 in Yellow is Grand Etang and Grid 3 in Blue is Nez de Boeuf.

1 **Title**

2

3

4 **Experimental and theoretical support for costs of plasticity and phenotype in a nematode**
5 **cannibalistic trait.**

6

7

8

9 **Mohannad Dardiry, Veysi Piskobulu[#], Ata Kalirad[#] & Ralf J. Sommer***

10

11

12 Max Planck Institute for Developmental Biology; Department for Integrative Evolutionary
13 Biology, Max Planck Ring 9, 72076 Tübingen, Germany

14

15

16 [#]These two authors contributed equally

17

18 *Corresponding author at: ralf.sommer@tuebingen.mpg.de

19

20 ORCID numbers:

21

22 MD: <https://orcid.org/0000-0002-9860-6590>

23 AK: <https://orcid.org/0000-0002-9500-3903>

24 VP: <https://orcid.org/0000-0003-4330-789X>

25 RJS: <https://orcid.org/0000-0003-1503-7749>

26

27

28

29

30

31

32

33 **Abstract**

34
35 Developmental plasticity is the ability of a genotype to express multiple phenotypes under different
36 environmental conditions and has been shown to facilitate the evolution of novel traits. However,
37 while associated costs of both plasticity and phenotype have been theoretically predicted,
38 empirically such costs remain poorly documented and little understood. Here, we use a plasticity
39 model system, hermaphroditic nematode *Pristionchus pacificus*, to experimentally measure these
40 costs in wild isolates under controlled laboratory conditions. *P. pacificus* can develop either a
41 bacterial feeding or predatory mouth morph in response to different external stimuli, with natural
42 variation of mouth-morph ratios between strains. We first demonstrated the cost of phenotype by
43 analyzing fecundity and developmental speed in relation to mouth morphs across the *P. pacificus*
44 phylogenetic tree. Then, we exposed three *P. pacificus* strains to two distinct microbial diets that
45 induce strain-specific mouth-form ratios. Our results indicate that a highly-plastic strain does
46 shoulder a cost of plasticity, *i.e.*, the diet-induced predatory mouth morph is associated with
47 reduced fecundity and slower developmental speed. In contrast, a non-plastic strain suffers from
48 the cost of phenotype in unfavorable conditions, but shows increased fitness and higher
49 developmental speed under favorable conditions. Furthermore, we computationally illustrate the
50 consequences of the costs of plasticity and phenotype on the population dynamics in spatially-
51 homogeneous and spatially-structured populations using empirically-derived life history
52 parameters for modeling. This study provides comprehensive support for the costs of plasticity
53 and phenotype based on empirical and modeling approaches.

54
55 **Keywords:** Cost of plasticity- Cost of phenotype- cannibalism- adaptive plasticity- Markov
56 population models.

57
58 **Introduction**

59
60 Changing and fluctuating environments are a hallmark of all ecosystems, affecting the life and
61 evolution of all organisms [1,2]. The ability of an organism to respond to changing environments
62 by expressing alternative phenotypes can, in theory, facilitate adaptation, as it makes various trait
63 optima across time and space in a given environment accessible to a genotype without the need for

64 genetic change [2–4]. Indeed, many case studies in plants, insects, vertebrates, and nematodes have
65 indicated the importance of phenotypic plasticity for promoting adaptations across environments
66 and for the evolution of novelty [3,5,6]. We refer to this type of phenotypic plasticity that facilitates
67 adaptation “adaptive plasticity”. However, it is important to emphasize that not all examples of
68 phenotypic plasticity are adaptive and conceptually, an organism cannot be infinitely plastic to
69 cope with any environment [7]. Additionally, plastic genotypes can vary in their degree of
70 plasticity across different conditions [8,9]. Such assumptions imply the existence of constraints on
71 the evolution of adaptive plasticity, and a huge and growing body of research has been dedicated
72 to identify such hypothetical constraints [2,7,10–13]. Theoretically, several factors can hinder the
73 evolution of adaptive plasticity; namely, limited genetic variation, weak selection, and the
74 unreliability of environmental signals [2,9,11]. Most importantly, however, it has been argued that
75 fitness costs will limit the evolution of plastic phenotypes [7]. Such arguments are largely
76 theoretically based, and detecting the cost of adaptive plasticity remains a formidable challenge.
77 Here, we use the plasticity model system, the nematode *Pristionchus pacificus* (Fig. 1), to obtain
78 experimental evidence for plasticity-associated costs.

79

80 In general, to understand the costs associated with adaptive plasticity, one first has to consider the
81 potential trade-off in a non-plastic genotype: assuming that the non-plastic genotype expresses a
82 phenotype adapted to environment II, the same phenotype could be less suited in environment I,
83 resulting in a fitness reduction (Fig. 2a). This fitness trade-off has been referred to as *cost of*
84 *phenotype* by several authors [7,13]. In contrast, a genotype expressing a plastic phenotype
85 induced only by environment II can have lower fitness than a less-plastic or non-plastic genotype
86 in that environment (Fig. 2a). This hypothetical fitness trade-off associated with a plastic
87 genotyped was referred to as *cost of plasticity* [7,13]. Understandably, the terms ‘cost of
88 phenotype’ and ‘costs of plasticity’ are, by virtue of their definitions, ripe for confusion [2,10]. A
89 comprehensive analysis of these constraints would adequately improve our understanding of the
90 role of plasticity in adaptive evolution. However, empirical studies on the costs of phenotype and
91 plasticity remain scarce. This has been largely due to two reasons: Firstly, in the wild, conditions
92 can often not be properly controlled and the effect of various factors not be delineated. Secondly,
93 laboratory experiments are time consuming and, in particular, large organisms cannot be easily

94 investigated. To study the constraints of plasticity, we make use of natural isolates of nematodes
95 that, given their small size and rapid reproduction, can be examined under laboratory conditions.
96

97 The nematode *P. pacificus* is an established model system for studying phenotypic plasticity
98 [14,15]. The developmentally plastic mouth of *P. pacificus* can exhibit two distinct forms; the
99 eurystomatous (Eu) morph with a wide stoma and hooked-like teeth, or the stenostomatous (St)
100 morph with a narrow stoma and a single tooth (Fig.1a)[16]. *P. pacificus* is a hermaphroditic
101 nematode and the use of isogenic cultures has facilitated the elucidation of genetic and epigenetic
102 mechanisms underlying this irreversible switch. Specifically, the sulfatase-encoding *eud-1* gene
103 was identified as the key developmental switch that is regulated by various environmental factors
104 and epigenetic mechanisms, and directs a downstream gene regulatory network consisting of more
105 than 20 identified proteins including structural components of mouth formation [17–23].
106 Importantly, worms respond to surrounding environmental cues to adopt their mouth form in a
107 strain-specific manner and various environmental stimuli, including temperature, culturing
108 condition, crowding and diet have been shown to influence mouth-morph ratios [24–26].
109 Principally, three major features assist in studying *P. pacificus* mouth-form plasticity. First, the
110 vast collection of naturally occurring wild isolates with hundreds of *P. pacificus* strains being
111 sequenced, resulting in a highly resolved phylogeny of diverse populations (Fig.1b) [27].
112 Interestingly, culturing these isolates on the laboratory bacterium *E. coli* displays a range of mouth-
113 morph ratios, *i.e.*, some strains are Eu-biased, others are St-biased, while some express
114 intermediate mouth-form ratios (see below) [17]. Second, morphological mouth-form plasticity is
115 coupled to behavioral plasticity. Specifically, the Eu form enables predation and cannibalism on
116 other nematodes, while such animals can still feed on bacteria. In contrast, the St form obligates
117 worms to feed on bacteria (Fig.1c) [28]. This extension of morphological plasticity to behavior is
118 thought to be involved in intraguild predation, *i.e.*, the elimination of resource competitors via rival
119 killing and the expansion of nutrition [29]. Finally, the natural habitat of *P. pacificus* and its
120 relatives has been intensively studied. *P. pacificus* is a soil nematode that is reliably found in
121 association with scarab beetles with recent studies describing the dynamics and succession of
122 nematodes on the beetle carcass after the insect's death (Fig.1d)[30]. These experiments revealed
123 a vital response of mouth-form acquisition in response to the presence of competing nematodes on
124 the insect carcass indicating the ecological significance of adaptive plasticity [31].

125

126 It should be noted that, switching between the Eu and St mouth forms is a specific example of
127 phenotypic plasticity, where the plastic phenotype of an individual can assume one of two
128 alternative mouth morphs, an irreversible decision that occurs during the development of *P.*
129 *pacificus* via a bi-stable developmental genetic switch [19]. The bias of the developmental switch
130 determines the ratio of mouth morphs with substantial natural variation between populations of *P.*
131 *pacificus* [17]. In this respect, mouth-form plasticity in *P. pacificus* is more akin to the switch
132 between lytic and lysogenic cycles in bacteriophage λ [32] than wing pattern polyphenism in
133 butterflies that is seasonally controlled [33]. Importantly, the relative simplicity of mouth-morph
134 plasticity in *P. pacificus* - binary readout, isogenic husbandry of genetically diverse strains and
135 strain-specific bi-stability - makes it ideal to study different facets of phenotypic plasticity beyond
136 the identification of associated genetic and epigenetic mechanisms.

137

138 Here, we took advantage of these features to perform a systematic analysis of mouth morphs and
139 their associated costs. The cost of plasticity and cost of phenotype can, theoretically, be measured
140 by comparing the fitness of individuals of the same strain with an identical genetic background but
141 opposite phenotypes, or a pair of *P. pacificus* strains, one plastic and one non-plastic, in two
142 different environments (Fig. 2a). Such theoretical expectation relies on a set of assumptions, chief
143 amongst them is the notion that a trait is adapted to a given environment. While establishing an
144 adaptive value for a given trait is a non-trivial issue, we attempt to solve this and related issues by
145 experimentally measuring the costs of phenotype and plasticity under laboratory conditions, using
146 fecundity and developmental speed as fitness parameters in strains sampled across the *P. pacificus*
147 phylogenetic tree. Subsequently, we focused on the response of three *P. pacificus* strains, with
148 varying levels of plasticity, to two different bacterial diets. We extended our empirical findings
149 via simulating ecologically relevant scenarios in spatially-homogeneous and spatially-structured
150 populations using empirically-derived life history parameters. Our study provides comprehensive
151 support for the costs of plasticity and phenotype based on empirical and computational approaches.

152 **Results**

153 **Within and between strain comparisons reveal a cost of phenotype**

154 First, we measured the cost of phenotype by studying whether the formation of the predatory mouth
155 morph negatively affects fecundity. We took advantage of the extensive collection of *P. pacificus*
156 natural isolates and selected seven strains with intermediate mouth-morph ratios from across the
157 *P. pacificus* phylogeny (Fig.1b)[27,34]. The ratios of these strains were considered intermediate
158 since they were neither predominantly expressing the predatory (Eu) nor predominantly expressing
159 the non-predatory (St) morph on the standard laboratory food source *E. coli* (Fig. 2b, *SI Appendix*;
160 Table. S4). It should be noted that “intermediate” in this context does not imply an exact 50-50
161 chance of expressing either of the mouth morphs. Instead, it merely indicates that both alternative
162 morphs can be easily found in a lab grown culture. Therefore, these strains allow testing whether
163 there is a cost of phenotype within the same genetic background and by obtaining animals of both
164 morphs on the same petri dish. To measure the cost of phenotype, we selected overall individual
165 fecundity as primary fitness parameter to capture reproductive capacity of *P. pacificus*
166 hermaphrodites via selfing [35–37]. Testing for daily fecundity showed that the majority of
167 progeny were laid within a window of 62 hours after maturation (nearly 91%) in an overall window
168 of appr. 158 hours of total egg-laying (*SI Appendix*; Fig. S1a& Table. S2). Consequently, the
169 number of eggs laid in this window provide a reasonable estimate of the life-time fecundity. In
170 these intra-genotype comparisons, we found a tendency of St animals to have more progeny than
171 Eu worms. Specifically, the estimated differences in the mean value of fecundity between St and
172 Eu animals based on the data showed strong and/or partial support in four out of seven comparisons
173 (Fig. 2c, *SI Appendix*; Table S1; Table S6). These findings suggest that the production of the
174 predatory mouth morph can incur a cost in the form of fewer progeny. This observation is in
175 concert with a previously reported slower rate of development conceived by nematodes exhibiting
176 the predatory morph in comparison to non-predatory worms [38].

177 Second, we measured fecundity and developmental speed in *P. pacificus* natural isolates that show
178 a biased mouth-morph choice, *i.e.*, strains that would produce an abundance of St or Eu mouth
179 morphs on the standard laboratory food source *E. coli* (Fig. 2d, *SI Appendix*; Table S4). We
180 selected two pairs of closely-related strains from the diverged clades B and C of *P. pacificus* from
181 La Réunion island [39]. We found that in both pairs the St-biased strains produce more overall

182 progeny than the Eu-biased strains (Fig. 2e, *SI Appendix*; Table S1; Table S7). Specifically, giving
183 the same time window of the first 62 hours, the St-biased strains had a 21% and 17% higher
184 fecundity in clades B and C, respectively (*SI Appendix*; Fig. S2b& Table. S2), which in turn may
185 affect population dynamics and resource competition in the wild. Similarly, the St-biased strains
186 showed a higher developmental speed than the Eu-biased strains (Fig. 2f, *SI Appendix*; Table. S3).
187 For example, 75 hours after egg-laying, nearly 60% of the St-biased strain RSC011 reached
188 adulthood; whereas only 27% of the Eu-biased strain RSA076 reached the same stage. Note that
189 inter-clade comparisons show considerable differences in these isolates' developmental speed,
190 which is due to the genetic background. Together, both, our pairwise comparisons of total eggs
191 laid by Eu and St individuals in intermediate strains, and the pairwise comparisons of fecundity
192 and developmental speed in four biased strains from two different *P. pacificus* clades clearly
193 illustrate the cost of producing the Eu phenotype.

194 **Across-conditions testing indicates a cost of plasticity**

195 Next, we wanted to determine if a cost of mouth-form plasticity exists in *P. pacificus*. Such a cost
196 of plasticity would be eminent when testing a less plastic genotype relative to a more plastic
197 genotype under different conditions [4,7,12,13]. Therefore, we performed a cross condition test by
198 conducting experiments on two distinct food sources, the standard *E. coli* condition used in the
199 previous section, and a *Novosphingobium* diet. The bacterial species *Novosphingobium* was found
200 to be naturally associated with *P. pacificus* and was proven to increase intraguild predation in the
201 *P. pacificus* reference strain PS312 from California [40,41]. However, it was never studied in non-
202 domesticated wild isolates of *P. pacificus*. Therefore, we used three strains with different mouth-
203 morph ratios on *E. coli*, and grew them on *Novosphingobium*; the highly St-biased strain RSC017,
204 the intermediate strain RSC019, and the highly Eu-biased strain RS5405. Indeed, RSC017 and
205 RSC019 showed a substantial increase of the Eu morph of 84% and 40% on *Novosphingobium*,
206 respectively, indicating strong plasticity. In contrast, the Eu-biased strain RS5405 remained highly
207 Eu in the new condition (Fig. 3a, *SI Appendix*; Table. S4). Thus, we established two distinct food
208 conditions that differentially affect plasticity levels of the three isolates.

209 Theoretically, the cost of plasticity would be displayed in the strain that exhibits the largest change
210 in mouth-morph ratio upon altering food conditions. Accordingly, we would expect to detect the

211 highest effect on fitness in the most plastic strain, and vice versa. Indeed, we found that RSC017
212 has the lowest fecundity and the slowest developmental speed on *Novosphingobium* when
213 compared to the less-plastic strains (Fig. 3b-c, *SI Appendix*; Table. S1,3, Table S8). Thus, a strain
214 that plastically responds to a dietary change with the formation of the Eu mouth morph exhibits
215 reduced fitness under these novel conditions indicating a cost of plasticity. In contrast, RS5405
216 exhibits the highest levels of fecundity and developmental speed on *Novosphingobium* (Fig. 3b-c,
217 *SI Appendix*; Table. S1,3). Thus, a strain that is preferentially Eu under both food conditions
218 exhibits increased fitness when exposed to this new diet. Consistent with these observations,
219 RSC019 exhibits intermediate mouth morph ratios in all measurements compared to other strains
220 on *Novosphingobium*; (Fig. 3b-c, *SI Appendix*; Table. S1,3). Taken together, these findings
221 indicate a cost of mouth-morph plasticity in response to dietary induction. In conclusion, we
222 observe a cost of phenotype, as well as, a cost of plasticity in mouth-form plasticity of *P. pacificus*,
223 which raises the fascinating question: which cost plays a larger role in shaping the population
224 dynamics and, consequently, the evolution of mouth-morph ratios?

225 **The cost of phenotype maximizes the benefits of plasticity**

226 To investigate how the cost of plasticity and the cost of phenotype would manifest in the wild, we
227 constructed a stage-classified model to simulate population dynamics of the St-biased strain
228 RSC017 and the Eu-biased strain RS5405; on both tested food sources (Fig. 4a). For modeling,
229 we used the fecundity measurements from the lab and scaled the developmental rates of the model
230 based on the laboratory estimates of developmental speed of *P. pacificus* (see **Materials and**
231 **Methods**). First, we tested population dynamics of the selected strains in separation, *i.e.*, without
232 interactions or competition. Surprisingly, the change from *E. coli* to *Novosphingobium* has only a
233 minor effect on the final population size of RSC017 (Fig. 4b). The reduction in fecundity on
234 *Novosphingobium* relative to *E. coli* is presumably compensated by the increase in developmental
235 speed on *Novosphingobium*. To test the hypothesis that faster developmental speed was indeed
236 compensating for the cost of plasticity (*i.e.*, lower fecundity), we simulated the dynamics of
237 RSC017 by assuming no change in developmental speed. Indeed, the results of this simulation
238 confirmed this expectation (Fig S6). In contrast, in RS5405 the increase in fecundity and
239 developmental speed on *Novosphingobium* results in a higher frequency of all developmental
240 stages compared to its dynamic on *E. coli* (Fig. 4c). Importantly, the between strains cost of

241 phenotype is clearly displayed when comparing RS5405 and RSC017 frequencies on *E. coli* (Fig.
242 4b-c). Thus, comparing both populations' trajectories without involving interactions reveals that
243 the cost of phenotype has a larger effect on the population dynamics than the cost of plasticity.

244 **The cost of plasticity manifests in a competition setup**

245 In nature, *P. pacificus* does not occur in isolation, rather it competes with other nematodes over
246 resources. Additionally, giving the coupling between morphological and behavioral plasticity, Eu
247 worms are able to predate while St worms are not. Testing the costs of plasticity and phenotype in
248 a competition setup might shed light on the evolution of the predatory mouth morph. Therefore,
249 we first tested if predation rate positively correlates with the proportion of predatory individuals
250 in wild isolates. To avoid the compounding effect of relatedness on predation [59], we selected *C.*
251 *elegans* as prey for *P. pacificus* predators. Indeed, testing nine *P. pacificus* wild isolates with
252 different mouth morph bias, shows that morphological and behavioral plasticity positively
253 correlate (*SI Appendix*; Fig. S3). Second, we measured predation rates of the two oppositely biased
254 strains RSC017 and RS5405 against one another by testing predation rates over the two food
255 sources *E. coli* and *Novosphingobium* (Fig. 4d). On an *E. coli* diet, RS5405 predation rates were
256 far higher than RSC017 predation rates; giving their opposite mouth morph bias.

257 Next, we used the experimentally obtained predation values for each food source to simulate the
258 effect of interactions between strains on their dynamics in a spatially-homogeneous population
259 (see **Materials and Methods**, *SI Appendix*; Fig. S4). Specifically, we used these estimates to
260 simulate the interactions between the two isolates in a population with an equal number of RSC017
261 and RS5405 young adults at the start of the simulation. Notably, simulated populations were
262 completely dominated by RS5405 for both food conditions. In addition, rapid elimination of
263 RSC017 averts the formation of its dauer larvae, as J2 animals of this strain were completely
264 eradicated by RS5405 predators (Fig. 4e, f). Thus, the cost of plasticity greatly affects the dynamics
265 of RSC017 in a spatially-homogenous population.

266 **Spatial structure significantly affects population dynamics**

267 While modeling the interaction of RSC017 and RS5405 in a population without any spatial
268 structure is informative, a more realistic scenario would involve dispersal from different

269 populations upon the depletion of food on the beetle carcass, and competition over the nutrient-
270 rich carcasses in the vicinity. Exploring such scenarios in the lab would be a tremendous
271 undertaking. Therefore, we extended our model to construct a source and sink version of the
272 stepping-stone migration scenario to illustrate the costs of plasticity and phenotype on the
273 dynamics of in a structured population (Fig. 5a). We constructed a simple structured population
274 by arranging n localities in one dimension. Each simulation starts with 50 young adults (YAs) of
275 RSC017 in the first locality and 50 YAs of RS5405 in the n^{th} locality, with reset of localities being
276 empty. All the localities contain a fixed amount of resource and dauer larvae migrate with a fixed
277 rate from a food-poor locality to a neighboring food-rich locality (Fig. 5a). The simulation
278 concludes when all the food in every locality has been depleted.

279 This modeling approach results in three major findings. First, on *E. coli*, higher fecundity of
280 RSC017 allows adults of this isolate to completely dominate the structured population even in the
281 face of predation (Fig. 5b, *SI Appendix*; Fig. S5a). Although the predation rate of RS5405 is higher,
282 even dauer larvae of RSC017 continue to fully dominate the structured population (Fig. 5c). These
283 results support a considerable cost of phenotype for RS5405 in the spatially-structured population.
284 In addition, in a scenario without predatory interactions, the frequency of RSC017 decreases only
285 marginally (Fig 5b vs. d, c vs. e). This finding results from the change in the number of migratory
286 dauer larvae of the predatory strain RS5405 (*SI Appendix*; Fig. S5a,b). Most importantly, the pace
287 in which the RSC017 population grows, results in exceptionally high numbers of RSC017
288 predators that outcompete RS5405 in the presence of interaction. Thus, the cost of phenotype
289 substantially influences RS5405 abundance, in particular in the presence of interactions.

290 Second, on *Novosphingobium*, higher fecundity and faster developmental speed of RS5405 turns
291 this isolate into a formidable adversary for RSC017. Therefore, the frequencies of RSC017 adults
292 and dauer larvae are extremely reduced in the structured population (Fig. 5b, c). However, when
293 interactions are limited, in contrast to *E. coli*, the frequencies would slightly increase (Fig 5b vs.
294 d, c vs. e). This is due to RS5405 profiting from a higher growth rate and higher predation on
295 *Novosphingobium*, but only higher growth when interactions are eliminated (*SI Appendix*; Fig.
296 S5c,d). Thus, the cost of plasticity would greatly affect RSC017 abundance when competing with
297 a predator under this condition.

298 **Initial food source also affects population dynamics**

299 Finally, to capture how significantly the costs of plasticity and phenotype would affect the
300 dynamics of structured populations, we simulated two scenarios where each isolate would start
301 with a favorable food source; *E. coli* for RSC017, and *Novosphingobium* for RS5405; or the
302 unfavorable food source; *Novosphingobium* for RSC017, and *E. coli* for RS5405 (Fig. 5b-e). A
303 pair of food sources were labeled “favorable” or “unfavorable” for a strain given the relative
304 fecundity of the strain on each source. Interestingly, the results indicate that the initial condition
305 in which each population starts dramatically affects which strain would ultimately dominate the
306 structured population. When the conditions are favorable for both strains, the cost of plasticity of
307 RSC017 is greater than the cost of phenotype of PS5405. In contrast, the relationship between the
308 costs reverses under conditions that are unfavorable to both strains. Thus, the interaction of the
309 cost of phenotype and the cost of plasticity is context dependent. Together, these simulations reveal
310 that spatial structure and initial food sources could affect the population dynamics with different
311 consequences for the costs of plasticity and phenotypes on the two isolates. However, such
312 projections about the population dynamics of these strains of *P. pacificus* should be taken with
313 caution, as many aspects of *P. pacificus* population dynamics and its dispersal patterns in the wild
314 remains poorly understood.

315 **Discussion**

316
317 Resource polyphenism is one example of developmental plasticity where alternative phenotypes
318 facilitate utilizing different food resources, including developing cannibalistic morphs as a
319 response to environmental stress [42]. Cannibalism provides trophic and survival advantages by
320 either extending energy resources or eliminating competition [43,44]. Evidently, the predatory
321 mouth form in *P. pacificus* has proven to boost survivorship under severe conditions [45], and
322 reduce competition on the basis of genomic relatedness [34]. Nevertheless, various *P. pacificus*
323 natural isolates are either predominantly non-predatory, *i.e.*, St-biased, or intermediate. Here, we
324 could demonstrate the cost sustained by the production of the predatory phenotype (the Eu moth
325 morph). In isolation, the fitness payoff incurred by the Eu-biased population makes it inferior to
326 the St-biased strain (Fig. 4b,c). Strikingly, our computational model indicates this cost of
327 phenotype to be more detrimental when both isolates are interacting in a spatially-homogenous

328 population. The effect of growth rate, developmental speed and predation are highly context
329 dependent, as shown by our simulations under different starting conditions, resulting in the
330 different of population dynamics and a different dominance pattern due to the costs of plasticity
331 and phenotype (*SI Appendix*; Fig. S5). Together, our results suggest a four-pronged explanatory
332 framework, combining cost of plasticity, cost of phenotype, environmental influence, and
333 population structure, each playing a crucial role in adaptive plasticity.

334

335 Conceptually, the cost of plasticity has been suggested as a major factor hindering the evolution
336 of adaptive plasticity. However, it has been challenging to experimentally detect these costs,
337 especially in metazoans. For instance, the predator-induced spine of *Daphnia pulex* was reported
338 to show mild support for both the costs of production and maintenance [46]. Similarly, in the
339 Scandinavian frog, *Rana temporaria*, the costs of metamorphic size were shown to exhibit a
340 plasticity cost in southern populations, whereas northern populations displayed no such costs [47].
341 Moreover, a meta-analysis of 27 studies on the cost of plasticity, of which only seven were on
342 animals, has concluded that costs of plasticity are mostly low if existing at all [48]. However, the
343 same authors suggested that these costs may influence adaptive evolution under stressful
344 conditions. Additionally, meta-analysis on aquatic gastropods argued for further empirical
345 investigations to better quantify the energetic costs of plasticity of shell formation [49]. A more
346 recent study on the cannibalistic cane toads, signifies favoring canalized defenses over plasticity,
347 providing the high cost of plasticity rather than the cost of phenotype [50]. Together, this diversity
348 of findings indicates the need for establishing a comprehensive empirical framework to address
349 both theoretical and conceptual asserts. Our results in *P. pacificus*, likely benefited from the binary
350 and easily distinguishable state of the polyphenic trait, Eu vs. St mouth morph, and the isogeneic
351 nature of all tested strains, which together facilitate empirical measurements of fitness
352 components, *i.e.*, fecundity and developmental speed, of each morph in the laboratory.
353 Additionally, accounting for two fitness components assisted in the transition from abstract
354 measures to simulating a range of ecologically relevant scenarios. Thus, our study complements
355 previous knowledge with a systematic analysis of defined costs in an evolutionary adaptive trait.

356

357

358

359 **Limits of this study**

360

361 While this study provides comprehensive insight into adaptive plasticity, several questions remain
362 to be answered. For example, measuring predation dynamics and migration rates on beetle
363 carcasses can increase the accuracy of modeling approaches. Also, predator consumption might
364 differ as a functional response to prey density, giving search and handling time, besides foraging
365 efficiency and predation risks [51–55]. Additionally, in nature, nematode mobility is not restricted
366 to a one-dimensional dispersal. Thus, such parameters merits further empirical and theoretical
367 analyses. Finally, a key question that was hardly identified in other plastic systems is the molecular
368 machinery underlying the production and maintenance of plasticity [4,7]. In *P. pacificus*, the
369 readily available molecular techniques permit such potential investigations. In conclusion, this
370 study integrates empirical and theoretical approaches to emphasize how different types of costs
371 influence the evolution of adaptive plasticity, while setting the stage for further investigations.

372

373 **Figures captions**

374

375 **Fig. 1: Mouth-form plasticity in *P. pacificus*:** (a) Mouth-morph dimorphism in *P. pacificus*. The
376 bacterivorous St morph possesses a single tooth with a narrow buccal cavity, whereas the
377 predatory Eu morph displays two teeth with a broad buccal cavity. (b) *P. pacificus* phylogenetic
378 tree representing the genomic relationship between 323 *P. pacificus* wild isolates. The three major
379 clades of *P. pacificus* are all represented in this study. Note that clades A, B, and C have
380 approximately 1% inter-clade genomic divergence. (Adopted from Rödelsperger et al., 2017). (c)
381 *P. pacificus* adult preying on a *C. elegans* worm. (d) *P. pacificus* life cycle including four juvenile
382 stages before reaching adulthood. In stressful conditions; e.g., food depletion, juvenile worms
383 develop into the alternatively dauer stage, which also represents the dispersal stage. Upon suitable
384 conditions, worms exit the dauer stage and resume normal development.

385 **Fig. 2: Within and between strain costs of phenotype in *P. pacificus*:** (a) The cost of plasticity
386 and the cost of phenotype in our model can be illustrated by a hypothetical scenario: The plastic
387 strain A switches from St mouth form to Eu when grown in environment II, but this plastic

388 response to environment II is accompanied by a reduction in fitness, α , which is the cost of
389 plasticity. Strain B is non-plastic and facultatively expresses the Eu morph in environments I and
390 II, but its phenotype is an adaptation to environment II, while in environment I the same phenotype
391 is accompanied by a reduction in fitness, β , which is the cost of phenotype. It is evident that costs
392 of phenotype and plasticity are, by definition, exclusively meaningful in comparative studies in
393 environments, which can be described as adaptive and non-adaptive with regards to a given trait.

394 (b) Mouth-morph ratio of seven intermediate *P. pacificus* genotypes used in this study. The
395 number of worms assayed for each strain (n) is indicated above each of the 95% highest density
396 interval (HDI) bar the mean percentage of Eu mouth morph for each strain. (c) Overall fecundity
397 of the same seven intermediate strains. On average 51 and 47, Eu and St mothers per strain were
398 scored, respectively. Bars indicate the 95%HDI for the mean estimated using Kruschke's BEST
399 method (see **Materials and Methods**). The top panel indicates the 95% HDI for the estimated
400 difference in means for each pairwise comparison. We used [-5,5] interval as our region of
401 practical equivalence (ROPE), *i.e.*, differences of means within this interval are practically equal
402 to no difference. Two comparisons, RSC019 and RSC033, are outside the ROPE, *i.e.*, means in
403 these comparisons are different; two other comparisons, RSA622 and RSA645, partially overlap
404 with the ROPE, and the rest of the comparisons include the ROPE, implying no difference. The
405 same ROPE is used for all the subsequent analyses. (d) Mouth-morph ratio of four biased *P.*
406 *pacificus* wild isolates representing clades B and C, respectively. For each strain, mouth-morph
407 ratios were scored for three biological replicates with a total number of 150 worms per strain. (e)
408 Overall fecundity of the same biased strains. Both St-biased strains showed credibly higher overall
409 fecundity than the Eu-biased strains. The top panel indicates the 95% HDI for the estimated
410 difference in means for each pairwise comparison using Kruschke's BEST method. The 95% HDI
411 for the estimated difference in means in two comparisons does not overlap with the ROPE,
412 indicating difference, while the rest of comparisons only partially overlap with the ROPE. (f)
413 Developmental speed for the biased strains from the two clades. For RSC011, 263; RSA076, 232;
414 RSC017, 320; and RS5405, 306 individuals were staged. Worms were staged according to the
415 following developmental stages: E= eggs; J2, J3, J4 = juvenile stages; YA= young adults with no
416 eggs inside the uterus; BA= breeding adults with eggs inside the uterus. In (a) and (d), the 95%HDI
417 for each strain was estimated using a Bayesian approach to estimate the probability of expressing
418 the Eu mouth morph based on the observations (see **Material and Methods**).

419 **Fig. 3: Cost of plasticity across conditions: (a)** Mouth-morph ratios on *E. coli* and
420 *Novosphingobium* for three *P. pacificus* strains, representing biased and intermediate mouth-
421 morph ratios. A total of 150 animals were used to score the mouth-morph ratio for each strain per
422 condition, indicating three biological replicates. The 95%HDI of means for each strain was
423 estimated using the Bayesian approach, described in details in **Material and Methods**. **(b)** Overall
424 fecundity of the three strains on both food conditions. The top panel indicates the 95% HDI for
425 the estimated difference in means for each pairwise comparison. In all three pairwise comparisons,
426 the 95% HDI for the estimated difference in means does not overlap with the ROPE, indicating
427 credible differences between each pair. We used [-5,5] interval as our region of practical
428 equivalence (ROPE), *i.e.*, differences of means within this interval are practically equal to no
429 difference. The pairwise comparisons are based on Kruschke's BEST method (see **Materials and**
430 **Methods**). Comparable numbers of mothers were used: RSC017(*E. coli*=40,
431 *Novosphingobium*=47); RSC019 (*E. coli*=48, *Novosphingobium*=45); RS5405(*E. coli*=40,
432 *Novosphingobium*=43) **(c)**. Developmental speed for the three genotypes on both conditions.
433 Individual worms were staged 75 hours after mothers were killed; for RSC017(*E. coli*=320,
434 *Novosphingobium*=301); RSC019 (*E. coli*=265, *Novosphingobium*=331); RS5405(*E. coli*=306,
435 *Novosphingobium*=489) individuals were staged. Worms were staged according to the following
436 developmental stages: E= eggs; J2, J3, J4 = juvenile stages; YA= young adults with no eggs inside
437 the uterus; BA= breeding adults with eggs inside the uterus.

438 **Fig. 4: Costs of phenotype and plasticity in a spatially-homogeneous population: (a)** Life cycle
439 of *P. pacificus* as a Markov chain (E: egg, J2-4: juvenile stages, D: dauer, YA: young adult, BA_{*i*}:
440 breeding adult of the day *i*, OA: old adult). Note that J1 larvae in *P. pacificus* remain in the egg
441 shell and are considered part of E in our model. Solid arrows represent the transition between
442 different developmental stages. Egg-laying by BA adults is indicated by a dotted arrow. Five
443 different breeding adults are included in the model (BA₁ to BA₅). **(b-c)** Population dynamics of
444 RSC017 and RS5405 on *E. coli* and *Novosphingobium*. Note that the end point of 1000 steps
445 represent an arbitrary endpoint, which roughly corresponds to 10 generations. Food will be gone
446 long before this end point, as evident by the production of dauer larvae. Simulations based on
447 empirical data demonstrate the differential response of the strains on both food conditions. The
448 number of adults and dauer larvae for RSC017 in *E. coli* relative to their counts on

449 *Novosphingobium* are 1.05 and 1.09, respectively. For RS5405, the number of adults and dauer
450 larvae in *E. coli* relative to their counts on *Novosphingobium* are 2.28 and 0.82, reflecting the faster
451 YA to BA₁ and higher fecundity of RS5405 on *Novosphingobium*. Note that J is the sum of all
452 juvenile stages. Upon the depletion of food, juvenile stages and eggs stop transitioning into the
453 next developmental stage, except for J₂, which develops into dauer larvae. **(d)** Standard with-strain
454 corpse assay. Each dot represents a mean of five replicates, and error bars represent standard
455 deviation. For each replicate, 20 adult predators were added to ≈ 3000 J₂ prey, and corpses were
456 screened after 24 hours. **(e-f)** Simulation of the effect of with-strain predation on population
457 dynamics in a spatially-homogeneous population. Using predation rate estimates from the corpse
458 assay, we simulated the interaction of RSC017 and RS5405 on *E. coli* and *Novosphingobium*. In
459 both conditions, the non-plastic strain RS5405 drives RSC017 into extinction. Simulations in (b),
460 (c) start with 50 YAs of a strain. The initial food supply, $S_0 = 10^{12}$. On *E. coli*, for both strains, γ_E
461 $= 0.0415$, $\gamma_{J_2} = 0.055$, $\gamma_{J_3} = 0.085$, $\gamma_{J_4} = 0.07$, $\gamma_{YA} = 0.1$, $\gamma_{Bi} = 0.0415$, $\sigma_{OA} = 0.995$ (see Materials
462 and Methods for more information). On *Novosphingobium*, $\gamma_{YA} = 0.13$ for RSC107 and $\gamma_{YA} = 0.4$
463 for RS5405 to account for the change in the developmental speed observed in the experiment. The
464 same transition probabilities and survival are used for the rest of the simulations. Simulations in
465 (e) and (f) start with 50 YAs of each strain. Predation rates: on *E. coli*, $\eta_{RSC017} = 1.7 \times 10^{-4}$ and
466 $\eta_{RS5405} = 3.3 \times 10^{-4}$; on *Novosphingobium*, $\eta_{RSC017} = 6.4 \times 10^{-5}$ and $\eta_{RS5405} = 4.7 \times 10^{-4}$. The
467 same predation rates are used in the subsequent simulations.

468

469 **Fig. 5: Costs of phenotype and plasticity in a spatially-structured population: (a)** A structured
470 population, consisting of 12 localities are arranged in a line. Each simulation starts with 50 YAs
471 of RSC017 on the first locality and 50 YAs of RS5405 on the 12th locality. At each step, ω dauer
472 larvae migrate from population i to j if j has more food than i . **(b-c)** The frequency of RSC017
473 adults (YA, BA _{i} , OA) (b) and dauer larvae (c) across 12 localities with interaction (i.e., predation)
474 after 1000 steps. As previously noted, the end point of 1000 steps represent an arbitrary endpoint,
475 which roughly corresponds to 10 generations. Food will be gone long before as evident by the
476 production of dauer larvae. **(d-e)** The frequency of RSC017 adults (YA, BA _{i} , OA) (d) and dauer
477 larvae (e) across 12 localities assuming no interaction between the two strains. In this scenario,
478 the frequency of RSC017 in the metapopulation is a function of developmental speed and
479 fecundity only. At the start of the simulation, for each strain in localities 1 and 12, $n_E = n_{J_2} = n_{J_3} =$

480 $n_{J4} = n_{BA} = n_{OA} = 0$, and $n_{YA} = 50$. while $m = 0.1$. The initial food supply, $S_0 = 10^{12}$ in the entire
481 metapopulation.

482

483 **Materials and Methods**

484 **Bacterial & nematodes strain culture and maintenance**

485 The two bacteria used as food source under monoxenic conditions were the standard *E. coli* lab
486 strain OP50 and the naturally *Pristionchus*-associated *Novosphingobium* sp. L76 [40]. OP50 was
487 grown overnight at 37°C in Lysogeny broth medium (LB) without shaking, while
488 *Novosphingobium* sp. L76 was grown overnight at 30°C in LB at 157 rpm. On the following day,
489 6-cm nematode growth medium (NGM) Petri-dishes were seeded with 300µl of *E. coli* OP50 or
490 *Novosphingobium* and left for overnight incubation [22]. Nematodes were reared on the seeded
491 NGM plates at 20°C. Three adults were passed to new plates every 5 days for *E. coli*, and every 4
492 days for *Novosphingobium*; giving the difference in developmental speed.

493 **Mouth form phenotyping**

494 Mouth-form scoring was performed on a ZEISS SteREO Discovery.V20 microscope, PlanApo S
495 1.5x objective with eyepiece PL 10x/23 Br.foc. Mouth-form phenotype was identified according
496 to the mouth width and the shape of the dorsal tooth of young adults as previously reported [16].
497 For all experiments, three replicates were scored at 20°C on 300µl of the relevant food. The total
498 number of worms scored per strain is as follows: Intra-strain analysis (RS5348= 138, RS1113= 243,
499 RSA662= 289, RSA645= 211, RSC019= 150, RSC033= 157, RSD029= 188). In all other analyses,
500 i.e., inter-strain analysis, plasticity cost, and predation assays, we used 150 animals per strain.

501 **Overall and daily self-fecundity measure**

502 Maintenance cultures were first bleached to obtain synchronized eggs before starting an
503 experiment. Bleaching protocol was performed as previously reported in [56]. Upon
504 synchronization, J4 larvae were individually isolated on separate plates spotted with 20µl of the
505 relevant bacteria. The next day, when worms are young adults, the mouth form was scored to
506 ensure its consistency with the maintenance culture. For four consecutive days, single worms were

507 transferred to fresh plates every 24 hours. Starting from day 5, worms were kept on the same plate
508 for two more days and then killed. This provides a daily readout for the first four days and a day 5
509 readout representing the last three days combined. This experimental design was performed given
510 that approximately 90% of the worm's self-progeny is produced within the first three days of
511 adulthood. To obtain fecundity counts, all plates were counted for viable progeny after five days
512 from transferring the mother, thus acquiring both daily and overall self-fecundity. Plates were kept
513 at 20°C across all steps of the experimental design (*SI Appendix*; Fig. S1a).

514

515 **Developmental speed measure**

516 From maintenance cultures, J4 animals were isolated to avoid any outcrossing of the
517 hermaphrodite worms with spontaneous males in the population. After 24 hours, these worms are
518 developed into breeding adults. Afterwards, 10 breeding adults were placed on a fresh plate with
519 100µl of the respective food source. Plates were incubated for two hours in order to obtain eggs
520 before the mothers were removed. Note that *P. pacificus* lays its eggs in the 2 or 4-cell stage,
521 resulting in at least 40-50 highly synchronized egg clutches. After 75 hours, worms were observed
522 to determine the developmental stage of the progeny. For each strain, and accordingly for each
523 food condition; 40 – 50 mothers were isolated representing 4-5 biological replicates. Between 232
524 to 489 progenies were staged for each experiment. Plates were kept at 20°C across all steps of the
525 experimental design (*SI Appendix*; Fig. S1b). The time point of 75hrs was chosen to capture the
526 transition rate from juvenile stages to adulthood [57,58].

527

528 **Predation assays: corpse assay**

529 Two types of predation assays were performed in this study; inter-specific and intra-specific
530 predation assays. In the inter-specific predation assays, young adult *P. pacificus* predators, prey
531 on *C. elegans* L1 larvae; while in the intra-specific predation assays, young adult predators of a
532 particular *P. pacificus* strain prey on *P. pacificus* J2 larvae of the other strain.

533

534 Corpse assays were performed to quantify both inter as well as intra-specific predation rates. All
535 assays were conducted as previously described in [59]. In short, for the inter-specific corpse assay,
536 freshly starved *C. elegans* plates were washed with M9 buffer to collect L1 larvae, passed through
537 two Millipore 20µm filters to remove other developmental stages, and followed by centrifugation

538 at 377g/2min to obtain a concentrated larval pellet. One μl of the L1 wash was added onto an
 539 empty 6cm (NGM) plate, which represents roughly 3000 larval prey. The *C. elegans* larvae were
 540 given at least 1hour window to proportionally spread across the plate. For predators, five *P.*
 541 *pacificus* young adults were blindly picked (independent of mouth-form) from *E. coli* OP50
 542 maintenance cultures. This procedure reflects the predation rates of a population in relevance to
 543 mouth-form ratio. Predators were first kept for 10-15 min on an empty plate to reduce body-
 544 attached bacteria and were then added to assay plates. The number of corpses was scored after 2
 545 hours with three biological replicates conducted for each assay. For intra-specific predation, we
 546 increased the number of predators from 5 to 20 and the assay time from 2 hours to 24 hours as
 547 previously reported in[59]. In addition, predators were grown on the relevant food source before
 548 being blindly picked; i.e., *E. coli* or *Novosphingobium*. For the intra-specific setup, five biological
 549 replicates were conducted per assay (*SI Appendix*; Fig. S1c).

550 Model

551 To model the dynamics of *P. pacificus* in different environments based on our laboratory data, we
 552 envisioned the development of a worm as a finite-state Markov chain (Fig. 4a). The Markov chain
 553 is used to construct a stage-structured population model (for more on this approach to modelling
 554 population dynamics, see[60,61]). The projection matrix for this chain is:

$$\mathbf{A}_{B,S} = \begin{bmatrix}
 \text{E} & \text{J2} & \text{D} & \text{J3} & \text{J4} & \text{YA} & \text{BA}_1 & \dots & \text{BA}_5 & \text{OA} \\
 1 - \gamma_E & 0 & 0 & 0 & 0 & 0 & F_1 & \dots & F_5 & 0 \\
 \gamma_E & (1 - \gamma_{J2})(1 - \gamma_{J2}^*) & 0 & 0 & 0 & 0 & 0 & \dots & 0 & 0 \\
 0 & \gamma_{J2}^* & 1 - \gamma_D & 0 & 0 & 0 & 0 & \dots & 0 & 0 \\
 0 & \gamma_{J2} & 0 & 1 - \gamma_{J3} & 0 & 0 & 0 & \dots & 0 & 0 \\
 0 & 0 & \gamma_D & \gamma_{J3} & 1 - \gamma_{J4} & 0 & 0 & \dots & 0 & 0 \\
 0 & 0 & 0 & 0 & \gamma_{J4} & 1 - \gamma_{YA} & 0 & \dots & 0 & 0 \\
 0 & 0 & 0 & 0 & 0 & \gamma_{YA} & 1 - \gamma_{BA_1} & \dots & 0 & 0 \\
 \vdots & \vdots & \vdots & \vdots & \vdots & \vdots & \vdots & \dots & \vdots & \vdots \\
 0 & 0 & 0 & 0 & 0 & 0 & 0 & \dots & 1 - \gamma_{BA_5} & 0 \\
 0 & 0 & 0 & 0 & 0 & 0 & 0 & \dots & \gamma_{BA_5} & \delta_{OA}
 \end{bmatrix} ,$$

555 where γ_i is the probability of transition from developmental stage i into the next developmental
 556 stage. In the case of J2, γ_{J2} and γ_{J2}^* are the probabilities for $J2 \rightarrow J3$ and $J2 \rightarrow D$, respectively.
 557 Note that as long as food is available ($S_t > 0$), $J2 \rightarrow D$ transition has a zero probability. We assume
 558 that all individuals in each stage survive and develop into the next stage, except for old adults
 559 (OA), which have a survival probability, δ_{OA} . In the absence of food, the transition probabilities
 560 of all the juvenile stages, as well as the eggs, are zero, while the transition probability for $J2 \rightarrow D$
 561

562 is no longer zero ($\gamma_{J2}^* = 0.1$). The five breeding adult stages (BA₁ to BA₅) each have their own
 563 respective per capita fecundity, F_i , for a given bacterial diet (B), based on the daily self-fecundity
 564 experiment. For a given *P. pacificus* strain, the transition probabilities and fecundities in the
 565 projection matrix depend on the experimentally-informed estimates. The transition probabilities
 566 and fecundities for RSC017 and RS5405 are listed in **Table 3**.
 567

Transition probabilities			
	<i>E. coli</i>	<i>Novosphingobium</i>	Starvation
E > J2	0.0415	0.0415	0
J2 > dauer	0	0	0.1
J2 > J3	0.055	0.055	0
J3 > J4	0.085	0.085	0
Dauer > J4	0.1	0.1	0
J4 > YA	0.07	0.07	0
YA > BA _i	0.1	0.13* , 0.4**	0
BA _i > BA _{i+1}	0.0415	0.0415	0.0415
Fecundities			
	<i>E. coli</i>	<i>Novosphingobium</i>	
BA ₁	22.65*, 19.8**	11.66*, 16.88**	
BA ₂	68.45*, 60.3**	62.53*, 80.77**	
BA ₃	57.05*, 43.02**	47.13*, 77.7**	
BA ₄	33.4*, 19.9**	13.94*, 16.28**	
BA ₅	4.97*, 6.6**	0.72*, 1.4**	

568 **Table 3: Parameters used in the model.** The fecundity values are based on the average daily
 569 number of eggs laid by a given strain on a given food source. RSC017 specific values is indicated
 570 by * and RS5405 specific values is indicated by **.

571
 572 The transition probabilities between different stages are set such that the occupancy time for each
 573 of the Markov states in our life cycle, *i.e.*, the average time spent over an individuals' life in that
 574 state, would correspond to the developmental speed of *P. pacificus* in hours. The mean occupancy

575 time is obtained by calculating the fundamental matrix (\mathbf{N}) for transition matrix \mathbf{U} , where $\mathbf{N} =$
576 $(\mathbf{I} - \mathbf{U})^{-1}$ (Caswell, 2019). We used a reduced form of our projection matrix that excluded the
577 dauer stage to calculate the fundamental matrix. On *E. coli*, we assume no difference in
578 developmental speed between RSC017 and RS5405. The first column of the fundamental matrix
579 for these strains on OP50 is [24.1, 18.2, 11.8, 14.3, 10, 24, 24, 24, 24, 24, 200], implying that an egg
580 spends on average 24.1 hours in the egg stage, 18.2 in J2, 11.8 in J3, 14.3 in J4, 10 in YA, 24 in
581 each of the five breeding adult stages, and 200 hours (roughly 8.5 days) in the old adult stage
582 before dying. These values are in line with the laboratory measurements of developmental
583 speed [57, 58]. We adjusted the probability of YA \rightarrow BA₁ such that the duration of YA stage on
584 *Novosphigobium* would reduce to ≈ 8 and ≈ 6 hours for RSC017 and RS5405, respectively.

585

586 **Consumption**

587 Resource consumption is included in the model by assuming fixed consumption rates for each
588 developmental stage. Given food source S_t , if there exist m developmental stages in the population
589 at t and n_i individuals belong to developmental stage i , the amount of available food in the next
590 step will be:

$$591 \quad S_{t+1} = S_t - \sum_{i=1}^m \rho_i n_i \quad , \quad (1)$$

591

592 where ρ_i is the per capita consumption rate for developmental stage i .

593

594 **Predation**

595 If a population consists of two strains, i and j , the number of surviving J2 individuals of strain i at
596 time $t + 1$ is:

$$597 \quad V_i(t + 1) = V_i(t) - \eta_{ji} P_j(t) V_i(t) \quad , \quad (2)$$

597

598 where η_{ji} is the rate at which adults from strain j kill J2s of strain i , $P_j(t)$ is the
599 number of predatory adults of strain j in the population at time t , and $V_i(t)$ is the number of J2s of
600 strain i . For the highly plastic strain, RSC017, the expected number of predatory adults equals the
601 number of RSC017 adults in the population multiplied by the probability of developing the
602 predatory mouth form on a given bacterial diet.

603

604 **Population dynamic**

605 Assume $\mathbf{n}_i(t)$ to be a 12×1 array, where each entry represents the count of each developmental
606 stage of strain i in a population at time t . The expected composition of the population at time $t + 1$
607 would be:

$$\mathbf{n}_i(t + 1) = \mathbf{A}_t \mathbf{n}_i(t) - \mathbf{K}_i(t) - \mathbf{E}_i(t) \quad , \quad (3)$$

608

609 where $K_i(t)$ is the number of J2 individuals of strain i that were killed at time t and $E_i(t)$ is the
610 number of dauer larvae that emigrated from the population at time t .

611

612 **Structured population in one dimension**

613 In order to investigate the effect of dispersal on the population dynamics, we constructed a one-
614 dimensional structured population that consisted of n localities arranged in a line. At each step, a
615 proportion ω of the dauer larvae from a locality emigrates to its neighboring locality if the
616 neighboring locality has more available food, resulting in a one-way dispersal pattern from a
617 source to a sink. Throughout the model, $n = 12$ and $\omega = 0.1$.

618

619 **Estimating the predation parameter**

620 To estimate the predation parameter for η_{ji} , we fitted the solution to the difference equation 2,

$$\mathbf{V}_i(t) = \mathbf{V}_i(0) \left(\mathbf{1} - \boldsymbol{\eta}_{ji} \mathbf{P}_j(t) \right)^t \quad (4)$$

621

622 to our empirical data from killing assays. Each killing assay starts with ≈ 3000 J2 worms of strain
623 i ($V_i(0) = 3000$) and 20 adults of strain j . The number of corpses is counted after 24 hours.

624 Assuming a fixed killing rate over the duration of the killing assay, we estimated the η_{ji} that would
625 result in the number of corpses observed in our assay.

626

627 **Statistical analyses**

628 To analyze the experimental data, instead of taking the Frequentist approach, we opted for
629 Bayesian alternatives. To calculate the probability of developing the Eu mouth morph, we assumed

630 the number of observed Eu worms in a sample of n worms follows the likelihood function
631 $y \sim \text{Bernoulli}(\theta)$, where, as our prior, we assume θ is drawn from a beta distribution with $\alpha =$
632 $\beta = 1$, which corresponds to a uniform distribution. For our Bayesian estimation for comparing
633 two groups, equivalent to t-test, for two samples, a and b, we follow Kruschke's BEST approach
634 [62,63]: we define likelihood functions, $y_i^a \sim \mathcal{T}(\nu, \mu_a, \sigma_a)$ and $y_i^b \sim \mathcal{T}(\nu, \mu_b, \sigma_b)$. As our prior, we
635 assume that the mean of each sample is from a normal distribution, with the mean and twice the
636 standard deviation of a pooled sample. For the standard deviation, we assume a wide uniform prior,
637 $\text{Unifrom}(1,300)$. Following Kruschke, we use $\nu = 30$; at higher values of ν , the t-distribution
638 converges to the normal distribution. Such an approach is preferable to the standard t-test, since it
639 compares means and standard deviations between to the two groups. The mean and the 95%
640 highest density interval of our estimates of the parameters of interests, difference in means and
641 difference in standard deviations of two groups, as well as the effects size are reported. This
642 approach lacks the simple and, somewhat deceptive, clarity of Null hypothesis significance testing,
643 but the Bayesian approach is more scientifically appealing, and it enables side-stepping the many
644 issues with p-value [64]. All statistical analyses were conducted with PyMC3 in Python 3.7.1,
645 using the No-U-Turn Sampler. In every analysis, we used effective sample size of $\geq 10,000$ for
646 stable estimates of HDIs and ensured that all the 4 MCMC chain had converged, i.e., $\hat{R} = 1$ [65].
647 The code used to analyze the data with PyMC3.9.3 are included in Jupiter notebooks and are
648 accessible on our Github repository associated with this manuscript. The detailed results of the
649 BEST approach can be found in Tables S6-S8.

650

651

652 **Data availability**

653 The software used to run all simulations and conduct all the data analysis was written in Python
654 3.7.1. For reproducibility, the code and the raw experimental data are available at
655 (https://github.com/Kalirad/cost_of_plasticity).

656

657 **Acknowledgments**

658

659 We thank Dr. Matthias Herrmann and Metta Riebesell for *P. pacificus* life cycle images; Dr. James
660 Lightfoot for the predation image; the La Réunion field team for strains isolation; Drs. Kohta
661 Yoshida and Christian Rödelsperger, and all members of the Sommer lab for discussions.

662

663 **Supplementary figures captions**

664

665 **Fig. S1: Schematic representation of the experimental setup:** (a) Daily and overall fecundity
666 measurement. *P. pacificus* animals were transferred on a daily basis. The overall self-progeny was
667 counted as the sum of the seven days. (b) Developmental speed measurement. *P. pacificus* cultures
668 were initiated by isolating J4 animals from the maintenance culture. Mothers were kept at the same
669 plate for 2 hours, which results in the production of synchronized eggs. After 75 hours, worms
670 were observed to determine the developmental stage of the progeny. (c) *P. pacificus* standardized
671 corpse assay. Either *P. pacificus* or *C. elegans* larvae were collected as prey. Prey larvae and
672 predator adults were added to assay plates. Time upon corpse scoring and specifications of the
673 experiment varies according to the interaction type, *i.e.*, intra or inter-specific perdition setup.
674 (Adopted from Lightfoot et al, 2019).

675

676 **Fig. S2: Daily self-fecundity:** (a-c) Daily count for four intermediate *P. pacificus* wild isolates on
677 *E. coli* (a), two pairs of biased *P. pacificus* wild isolates on *E. coli* (b), and three selected *P.*
678 *pacificus* wild isolates on *Novosphingobium* (c), respectively.

679

680 **Fig. S3: Inter-specific predation assay:** A negative-binomial model was fitted to the observed
681 relationship between the mouth-form ratio and the number of corpses counted in the experimental
682 corpse assay. The negative-binomial model was fitted using PyMC3 and the credible estimate for
683 $\beta 0 = 2.19$ ($1.81 \geq 95\%HDI \leq 2.56$) and $\beta 1 = 1.41$ ($1 \geq 95\%HDI \leq 1.82$). 95% HDP region indicates
684 the highest posterior density. The orange dots are the mean estimate sampled from the posterior
685 predictive distribution.

686

687 **Fig. S4: Estimating predation rates from experimental data:** The dotted lines indicated the
688 number of corpses observed after 24 hours of the experimental corpse assay. The solid lines
689 indicate $V_i(t) = V_i(0) \left(1 - \eta_{ji} P_j(t)\right)^t$ with a given killing rate, η_{ji} , that generates the same
690 number of corpses as the killing assay for a given strain on a bacterial diet. η_{ji} was obtained by
691 solving the equation for $t = 24$.

692

693 **Fig. S5: The effect of interaction on the pattern of dauer larvae dispersal:** We measured the
694 total number of RSC017 and RS5405 dauer larvae that migrated from each of the 12 localities to
695 a neighboring locality in the one-dimensional stepping stone model during the simulation shown
696 in Fig 5. The first locality (1) was the starting locality for RSC017, and the last locality (12) was
697 the starting locality for RS5405. The number of migrating dauer larvae for source locality (i) is
698 the total number of dauer larvae dispersed from (i) to locality ($i+1$), provided that ($i+1$) contained
699 food. (a-b) are the dynamics on *E. coli*, while (c-d) are the dynamics on *Novosphingobium*.

700

701 **Fig. S6: The interplay between developmental speed and fecundity in RSC017:** To test our
702 hypothesis that faster developmental speed was indeed compensating for the cost of plasticity,
703 (i.e., lower fecundity), we simulated the dynamics of RSC017 by assuming no change in
704 developmental speed. The difference in the steady-state counts of A and D stages on *E. coli* versus
705 *Novosphingobium* compared to Fig. 4b supports this hypothesis.

706

707 **References**

708

- 709 1. Sæther B-E, Engen S. The concept of fitness in fluctuating environments. *Trends Ecol Evol.*
710 2015;30: 273–281.
- 711 2. Pfennig DW. *Phenotypic Plasticity & Evolution: Causes, Consequences, Controversies.*
712 Taylor & Francis; 2021.
- 713 3. West-Eberhard MJ. *Developmental Plasticity and Evolution.* Oxford University Press; 2003.
- 714 4. Pigliucci M. *Phenotypic Plasticity: Beyond Nature and Nurture.* Johns Hopkins University
715 Press; 2001.
- 716 5. Moczek AP, Sultan S, Foster S, Ledón-Rettig C, Dworkin I, Nijhout HF, et al. The role of
717 developmental plasticity in evolutionary innovation. *Proc Biol Sci.* 2011;278: 2705–2713.
- 718 6. Sommer RJ. Phenotypic Plasticity: From Theory and Genetics to Current and Future
719 Challenges. *Genetics.* 2020;215: 1–13.
- 720 7. Murren CJ, Auld JR, Callahan H, Ghalambor CK, Handelsman CA, Heskell MA, et al.
721 Constraints on the evolution of phenotypic plasticity: limits and costs of phenotype and
722 plasticity. *Heredity.* 2015;115: 293–301.

- 723 8. Scheiner SM. Genetics and Evolution of Phenotypic Plasticity. *Annu Rev Ecol Syst.*
724 1993;24: 35–68.
- 725 9. Schlichting C, Pigliucci M. *Phenotypic Evolution: A Reaction Norm Perspective.* Sinauer;
726 1998.
- 727 10. Auld JR, Agrawal AA, Relyea RA. Re-evaluating the costs and limits of adaptive
728 phenotypic plasticity. *Proceedings of the Royal Society B: Biological Sciences.* 2010;277:
729 503–511.
- 730 11. Snell-Rood EC, Van Dyken JD, Cruickshank T, Wade MJ, Moczek AP. Toward a
731 population genetic framework of developmental evolution: the costs, limits, and consequences
732 of phenotypic plasticity. *Bioessays.* 2010;32: 71–81.
- 733 12. Dewitt TJ, Sih A, Wilson DS. Costs and limits of phenotypic plasticity. *Trends Ecol Evol.*
734 1998;13: 77–81.
- 735 13. Callahan HS, Maughan H, Steiner UK. Phenotypic plasticity, costs of phenotypes, and
736 costs of plasticity: toward an integrative view. *Ann N Y Acad Sci.* 2008;1133: 44–66.
- 737 14. Sommer RJ, McGaughan A. The nematode *Pristionchus pacificus* as a model system for
738 integrative studies in evolutionary biology. *Mol Ecol.* 2013;22: 2380–2393.
- 739 15. Sommer RJ, Dardiry M, Lenuzzi M, Namdeo S, Renahan T, Sieriebriennikov B, et al. The
740 genetics of phenotypic plasticity in nematode feeding structures. *Open Biol.* 2017;7.
741 doi:10.1098/rsob.160332
- 742 16. Bento G, Ogawa A, Sommer RJ. Co-option of the hormone-signalling module dafachronic
743 acid-DAF-12 in nematode evolution. *Nature.* 2010;466: 494–497.
- 744 17. Ragsdale EJ, Müller MR, Rödelsperger C, Sommer RJ. A developmental switch coupled
745 to the evolution of plasticity acts through a sulfatase. *Cell.* 2013;155: 922–933.
- 746 18. Kieninger MR, Ivers NA, Rödelsperger C, Markov GV, Sommer RJ, Ragsdale EJ. The
747 Nuclear Hormone Receptor NHR-40 Acts Downstream of the Sulfatase EUD-1 as Part of a
748 Developmental Plasticity Switch in *Pristionchus*. *Curr Biol.* 2016;26: 2174–2179.
- 749 19. Sieriebriennikov B, Prabh N, Dardiry M, Witte H, Röseler W, Kieninger MR, et al. A
750 Developmental Switch Generating Phenotypic Plasticity Is Part of a Conserved Multi-gene
751 Locus. *Cell Rep.* 2018;23: 2835-2843.e4.
- 752 20. Bui LT, Ivers NA, Ragsdale EJ. A sulfotransferase dosage-dependently regulates
753 mouthpart polyphenism in the nematode *Pristionchus pacificus*. *Nat Commun.* 2018;9: 1–10.

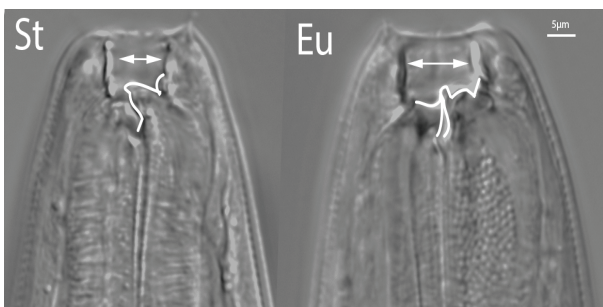
- 754 21. Namdeo S, Moreno E, Rödelsperger C, Baskaran P, Witte H, Sommer RJ. Two independent
755 sulfation processes regulate mouth-form plasticity in the nematode *Pristionchus pacificus*.
756 *Development*. 2018;145. doi:10.1242/dev.166272
- 757 22. Sieriebriennikov B, Sun S, Lightfoot JW, Witte H, Moreno E, Rödelsperger C, et al.
758 Conserved nuclear hormone receptors controlling a novel plastic trait target fast-evolving
759 genes expressed in a single cell. *PLoS Genet*. 2020;16: e1008687.
- 760 23. Sun S, Theska T, Witte H, Ragsdale EJ, Sommer RJ. The oscillating Mucin-type protein
761 DPY-6 has a conserved role in nematode mouth and cuticle formation. *Genetics*. 2021.
762 doi:10.1093/genetics/iyab233
- 763 24. Lenuzzi M, Witte H, Riebesell M, Rödelsperger C, Hong RL, Sommer RJ. Influence of
764 environmental temperature on mouth-form plasticity in *Pristionchus pacificus* acts through
765 *daf-11*-dependent cGMP signaling. *J Exp Zool B Mol Dev Evol*. 2021;n/a.
766 doi:10.1002/jez.b.23094
- 767 25. Werner MS, Sieriebriennikov B, Loschko T, Namdeo S, Lenuzzi M, Dardiry M, et al.
768 Environmental influence on *Pristionchus pacificus* mouth form through different culture
769 methods. *Sci Rep*. 2017;7: 7207.
- 770 26. Werner MS, Claaßen MH, Renahan T, Dardiry M, Sommer RJ. Adult Influence on Juvenile
771 Phenotypes by Stage-Specific Pheromone Production. *iScience*. 2018;10: 123–134.
- 772 27. Rödelsperger C, Meyer JM, Prabh N, Lanz C, Bemm F, Sommer RJ. Single-Molecule
773 Sequencing Reveals the Chromosome-Scale Genomic Architecture of the Nematode Model
774 Organism *Pristionchus pacificus*. *Cell Rep*. 2017;21: 834–844.
- 775 28. Wilecki M, Lightfoot JW, Susoy V, Sommer RJ. Predatory feeding behaviour in
776 *Pristionchus* nematodes is dependent on phenotypic plasticity and induced by serotonin. *J Exp*
777 *Biol*. 2015;218: 1306–1313.
- 778 29. Quach KT, Chalasani SH. Intraguild predation between *Pristionchus pacificus* and
779 *Caenorhabditis elegans*: a complex interaction with the potential for aggressive behaviour. *J*
780 *Neurogenet*. 2020;34: 404–419.
- 781 30. Renahan T, Lo WS, Werner MS. Nematode biphasic 'boom and bust' dynamics are
782 dependent on host bacterial load while linking dauer and mouth-form polyphenisms.
783 *Environmentalist*. 2021. Available: [https://sfamjournals.onlinelibrary.wiley.com/doi/abs/10.11](https://sfamjournals.onlinelibrary.wiley.com/doi/abs/10.1111/1462-2920.15438)
784 [11/1462-2920.15438](https://sfamjournals.onlinelibrary.wiley.com/doi/abs/10.1111/1462-2920.15438)

- 785 31. Renahan T, Sommer RJ. Nematode Interactions on Beetle Hosts Indicate a Role of Mouth-
786 Form Plasticity in Resource Competition. *Frontiers in Ecology and Evolution*. 2021;9: 703.
- 787 32. Ptashne M. A genetic switch: Gene control and phage. *lambda*. 1986. Available:
788 <https://www.osti.gov/biblio/5413898>
- 789 33. Nijhout HF. Developmental Perspectives on Evolution of Butterfly Mimicry. *Bioscience*.
790 1994;44: 148–157.
- 791 34. Lightfoot JW, Dardiry M, Kalirad A, Giaimo S, Eberhardt G, Witte H, et al. Sex or
792 cannibalism: Polyphenism and kin recognition control social action strategies in nematodes.
793 *Sci Adv*. 2021;7. doi:10.1126/sciadv. abg8042
- 794 35. Haldane JBS. The Effect of Variation of Fitness. *Am Nat*. 1937;71: 337–349.
- 795 36. Crow JF, Kimura M, Others. An introduction to population genetics theory. An
796 introduction to population genetics theory. 1970. Available:
797 <https://www.cabdirect.org/cabdirect/abstract/19710105376>
- 798 37. Orr HA. Fitness and its role in evolutionary genetics. *Nat Rev Genet*. 2009;10: 531–539.
- 799 38. Seroby V, Ragsdale EJ, Müller MR, Sommer RJ. Feeding plasticity in the nematode
800 *Pristionchus pacificus* is influenced by sex and social context and is linked to developmental
801 speed. *Evol Dev*. 2013;15: 161–170.
- 802 39. Rödelsperger C, Neher RA, Weller AM, Eberhardt G, Witte H, Mayer WE, et al.
803 Characterization of genetic diversity in the nematode *Pristionchus pacificus* from population-
804 scale resequencing data. *Genetics*. 2014;196: 1153–1165.
- 805 40. Akduman N, Rödelsperger C, Sommer RJ. Culture-based analysis of *Pristionchus*-
806 associated microbiota from beetles and figs for studying nematode-bacterial interactions. *PLoS*
807 *One*. 2018;13: e0198018.
- 808 41. Akduman N, Lightfoot JW, Röseler W, Witte H, Lo W-S, Rödelsperger C, et al. Bacterial
809 vitamin B12 production enhances nematode predatory behavior. *ISME J*. 2020;14: 1494–1507.
- 810 42. Pfennig DW, McGee M. Resource polyphenism increases species richness: a test of the
811 hypothesis. *Philos Trans R Soc Lond B Biol Sci*. 2010;365: 577–591.
- 812 43. Church SC, Sherratt TN. The Selective Advantages of Cannibalism in a Neotropical
813 Mosquito. *Behav Ecol Sociobiol*. 1996;39: 117–123.
- 814 44. Claessen D, de Roos AM, Persson L. Population dynamic theory of size-dependent
815 cannibalism. *Proc Biol Sci*. 2004;271: 333–340.

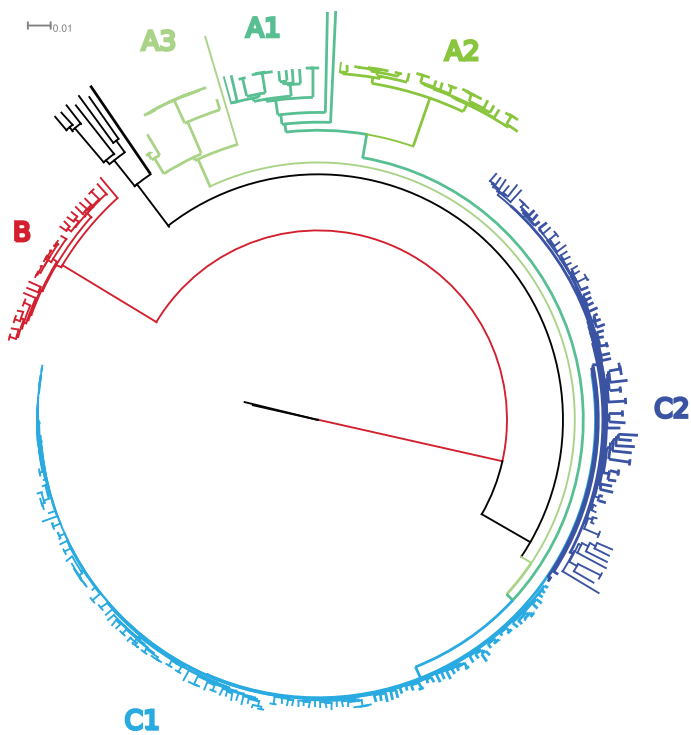
- 816 45. Serobyán V, Ragsdale EJ, Sommer RJ. Adaptive value of a predatory mouth-form in a
817 dimorphic nematode. *Proceedings of the Royal Society B: Biological Sciences*. 2014;281:
818 20141334.
- 819 46. Scheiner SM, Berrigan D. The genetics of phenotypic plasticity. VIII. The cost of plasticity
820 in *Daphnia pulex*. *Evolution*. 1998;52: 368–378.
- 821 47. Merilä J, Laurila A, Lindgren B. Variation in the degree and costs of adaptive phenotypic
822 plasticity among *Rana temporaria* populations. *J Evol Biol*. 2004;17: 1132–1140.
- 823 48. Van Buskirk J, Steiner UK. The fitness costs of developmental canalization and plasticity.
824 *J Evol Biol*. 2009;22: 852–860.
- 825 49. Bourdeau PE, Butlin RK, Brönmark C, Edgell TC, Hoverman JT, Hollander J. What can
826 aquatic gastropods tell us about phenotypic plasticity? A review and meta-analysis. *Heredity* .
827 2015;115: 312–321.
- 828 50. DeVore JL, Crossland MR, Shine R. Trade-offs affect the adaptive value of plasticity:
829 stronger cannibal-induced defenses incur greater costs in toad larvae. *Ecol Monogr*. 2021;91:
830 e01426.
- 831 51. Holling CS. Some Characteristics of Simple Types of Predation and Parasitism¹. *Can*
832 *Entomol*. 1959;91: 385–398.
- 833 52. Holling CS. The Components of Predation as Revealed by a Study of Small-Mammal
834 Predation of the European Pine Sawfly¹. *Can Entomol*. 1959;91: 293–320.
- 835 53. Solomon ME. The Natural Control of Animal Populations. *J Anim Ecol*. 1949;18: 1–35.
- 836 54. Lima SL, Valone TJ, Caraco T. Foraging-efficiency-predation-risk trade-off in the grey
837 squirrel. *Anim Behav*. 1985;33: 155–165.
- 838 55. Sentis A, Hemptinne JL, Brodeur J. How functional response and productivity modulate
839 intraguild predation. *Ecosphere*. 2013;4: art46.
- 840 56. Stiernagle T. Maintenance of *C. elegans*. *WormBook*. 2006; 1–11.
- 841 57. Sun S, Rödelsperger C, Sommer RJ. Single worm transcriptomics identifies a
842 developmental core network of oscillating genes with deep conservation across nematodes.
843 *Genome Res*. 2021;31: 1590–1601.
- 844 58. Sommer RJ. *Pristionchus pacificus*: A Nematode Model for Comparative and Evolutionary
845 Biology. BRILL; 2015.

- 846 59. Lightfoot JW, Wilecki M, Rödelsperger C, Moreno E, Susoy V, Witte H, et al. Small
847 peptide-mediated self-recognition prevents cannibalism in predatory nematodes. *Science*.
848 2019;364: 86–89.
- 849 60. Caswell H. *Sensitivity Analysis: Matrix Methods in Demography and Ecology*. Springer,
850 Cham; 2019.
- 851 61. Keyfitz, Nathan. *Applied mathematical demography*. New York: Wiley; 1977.
- 852 62. Kruschke JK. Bayesian estimation supersedes the t test. *J Exp Psychol Gen*. 2013;142:
853 573–603.
- 854 63. Kruschke J. *Doing Bayesian Data Analysis: A Tutorial with R, JAGS, and Stan*. Academic
855 Press; 2014.
- 856 64. Wasserstein RL, Lazar NA. The ASA Statement on p-Values: Context, Process, and
857 Purpose. *Am Stat*. 2016;70: 129–133.
- 858 65. Kruschke JK. Bayesian Analysis Reporting Guidelines. *Nat Hum Behav*. 2021;5: 1282–
859 1291.
- 860

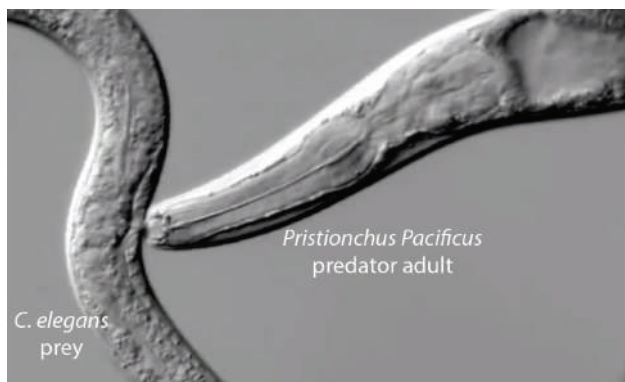
a



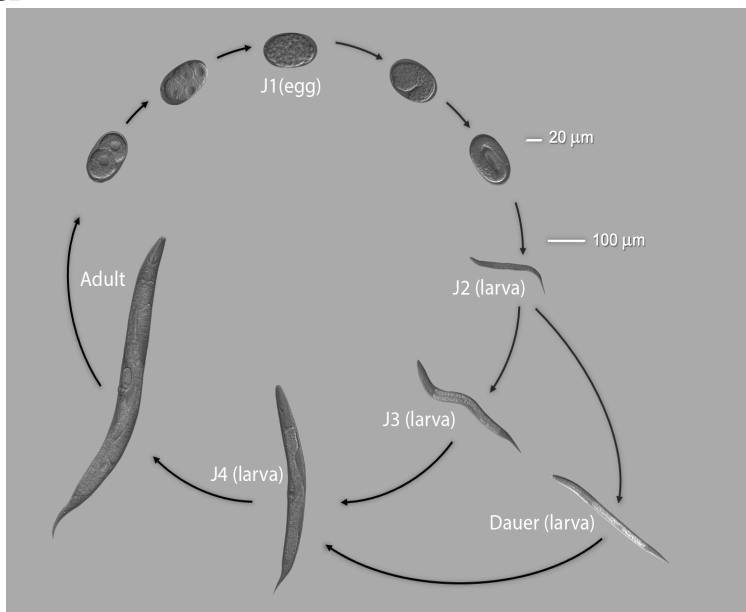
b



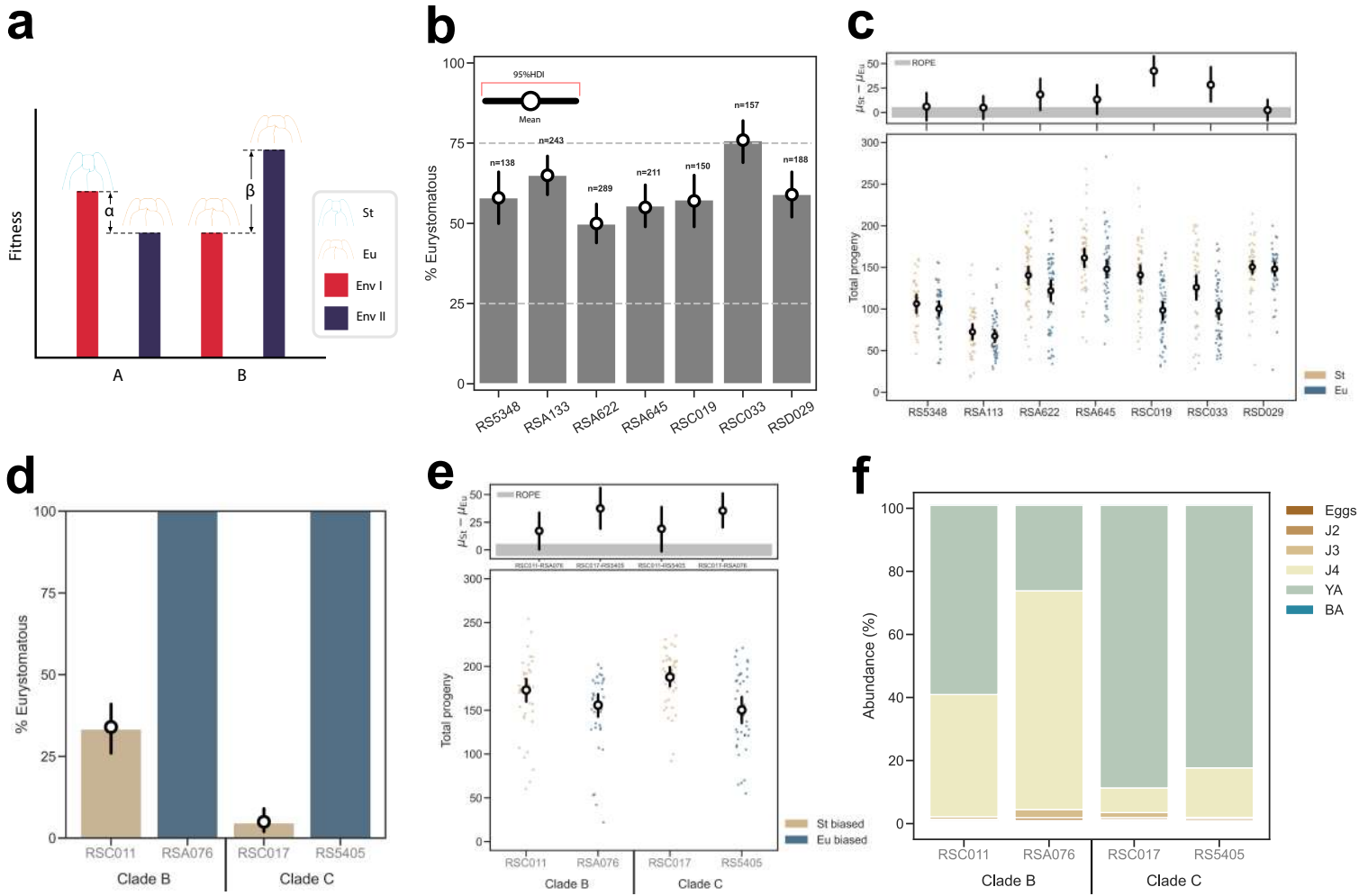
c



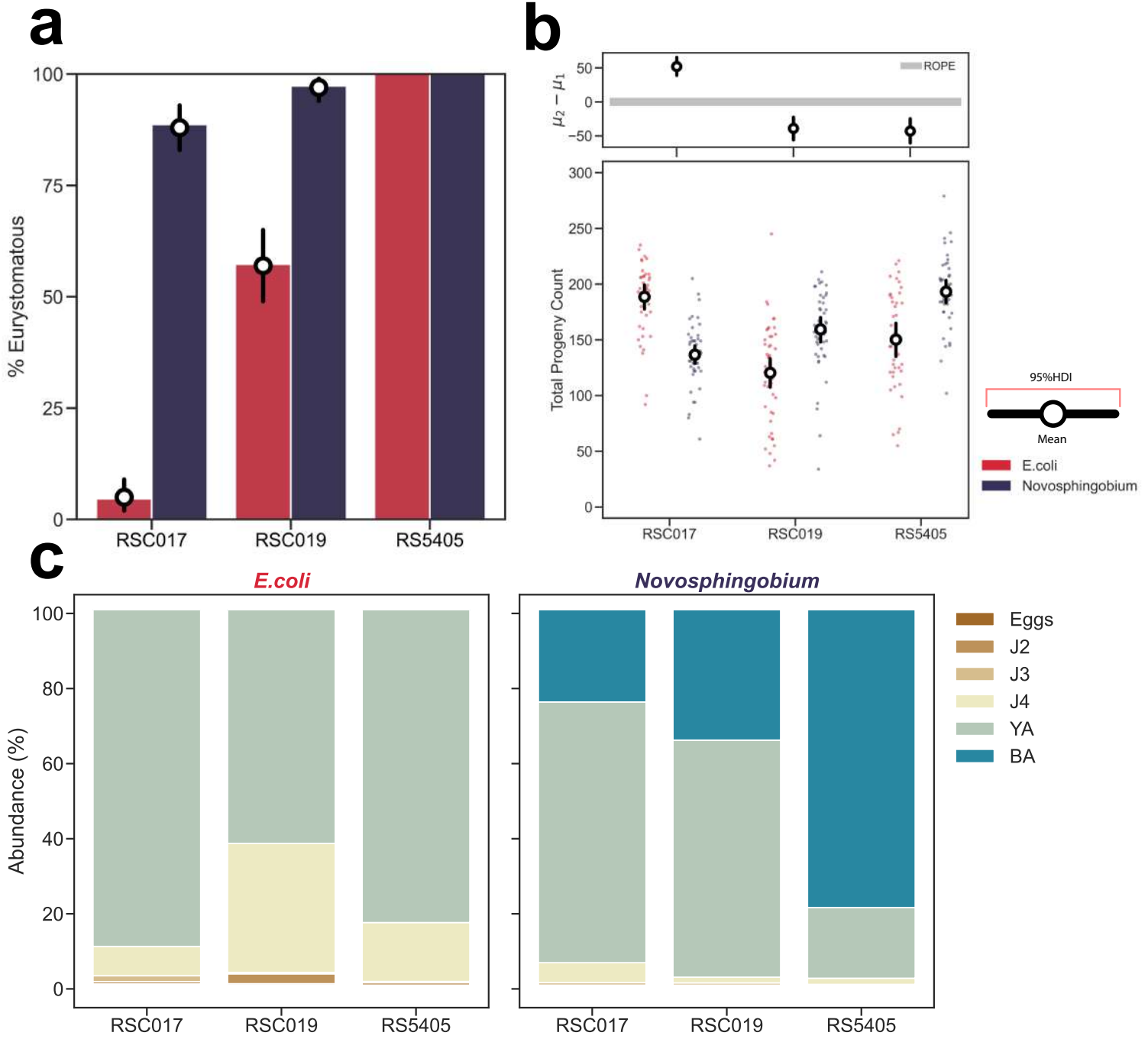
d



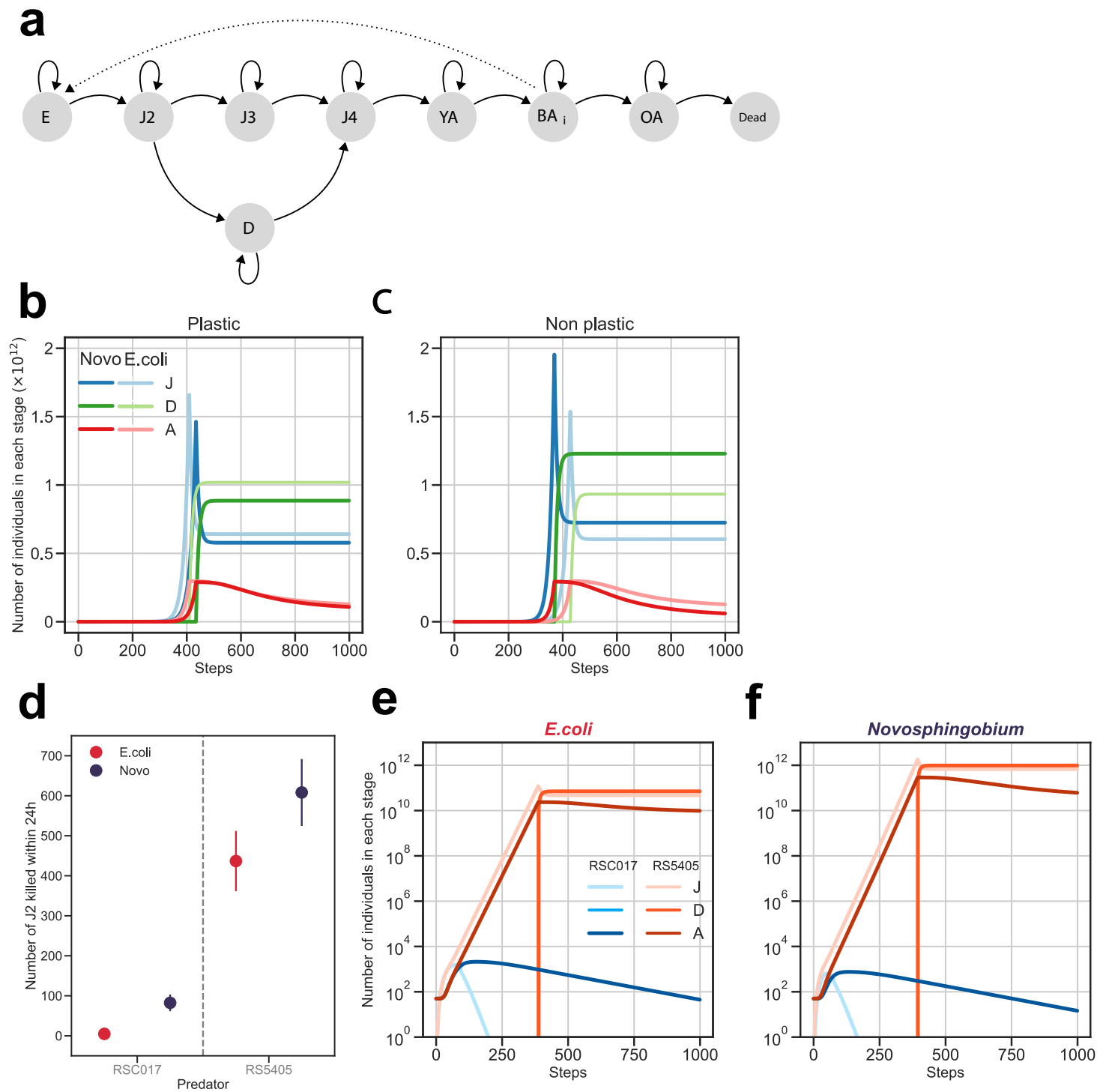
(Figure 1)



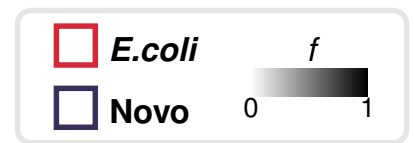
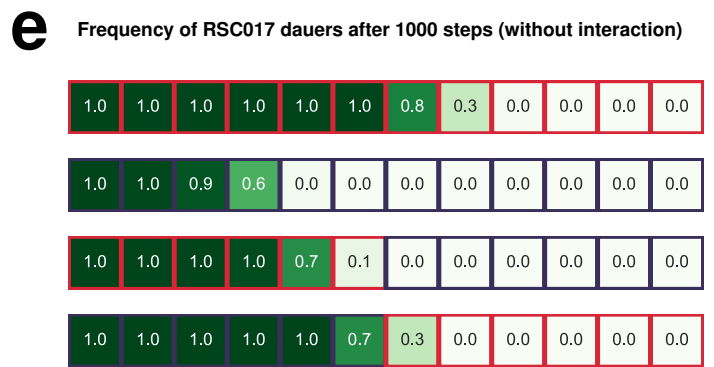
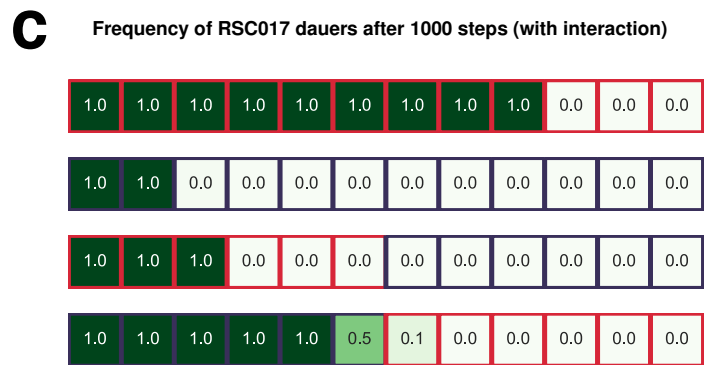
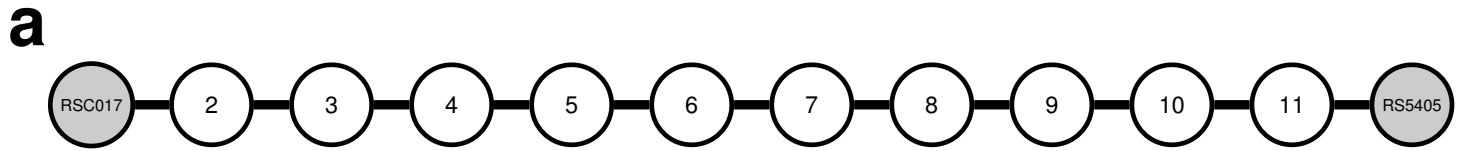
(Figure 2)



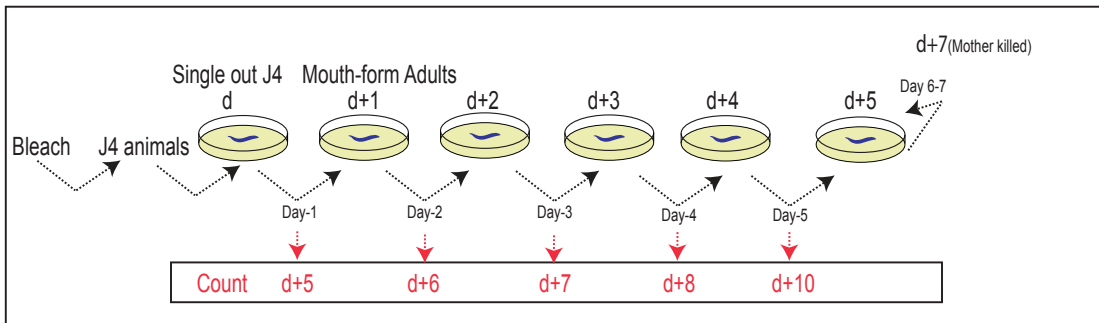
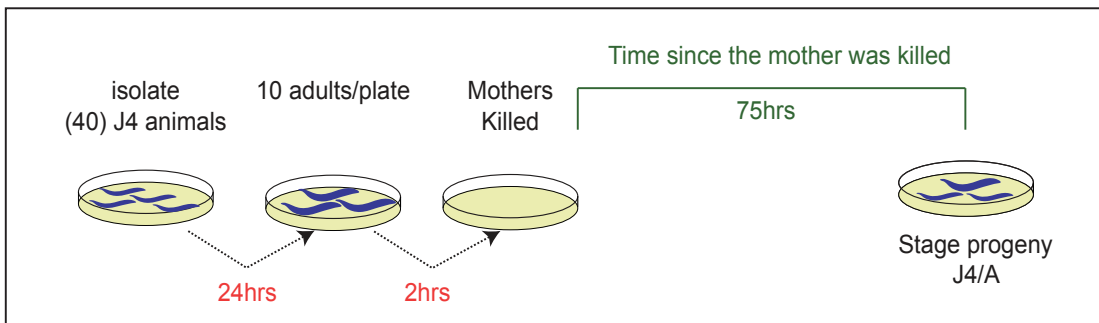
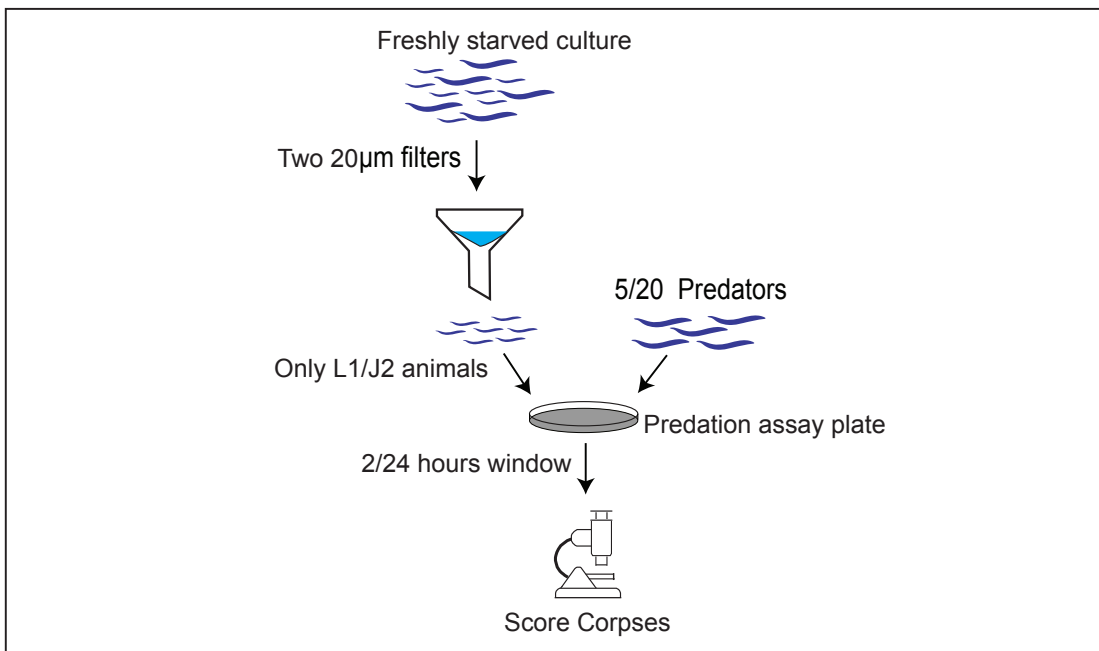
(Figure 3)



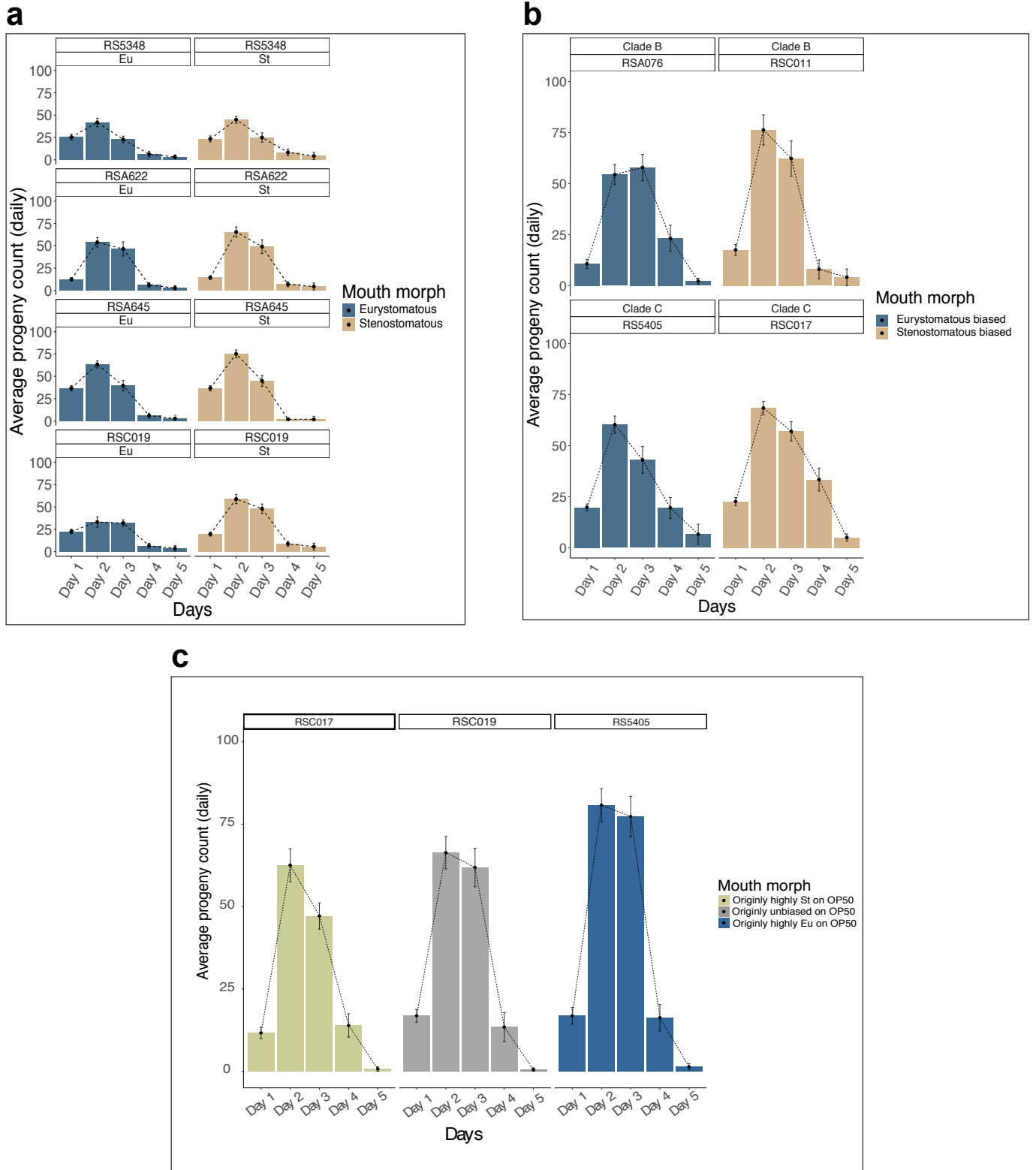
(Figure 4)



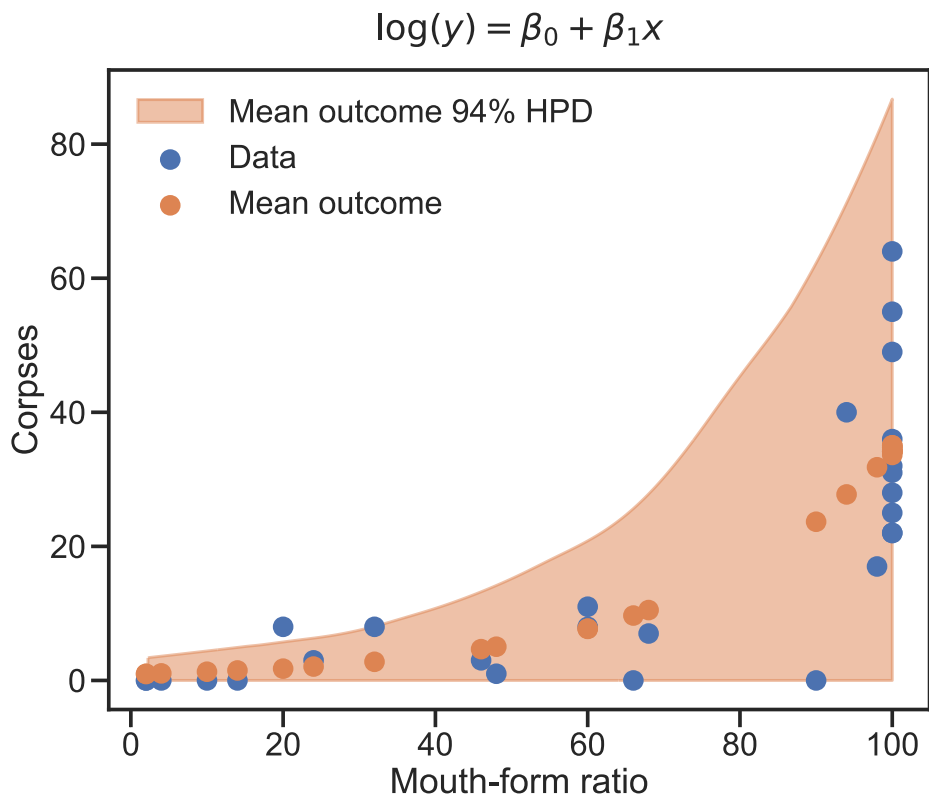
(Figure 5)

a**b****c**

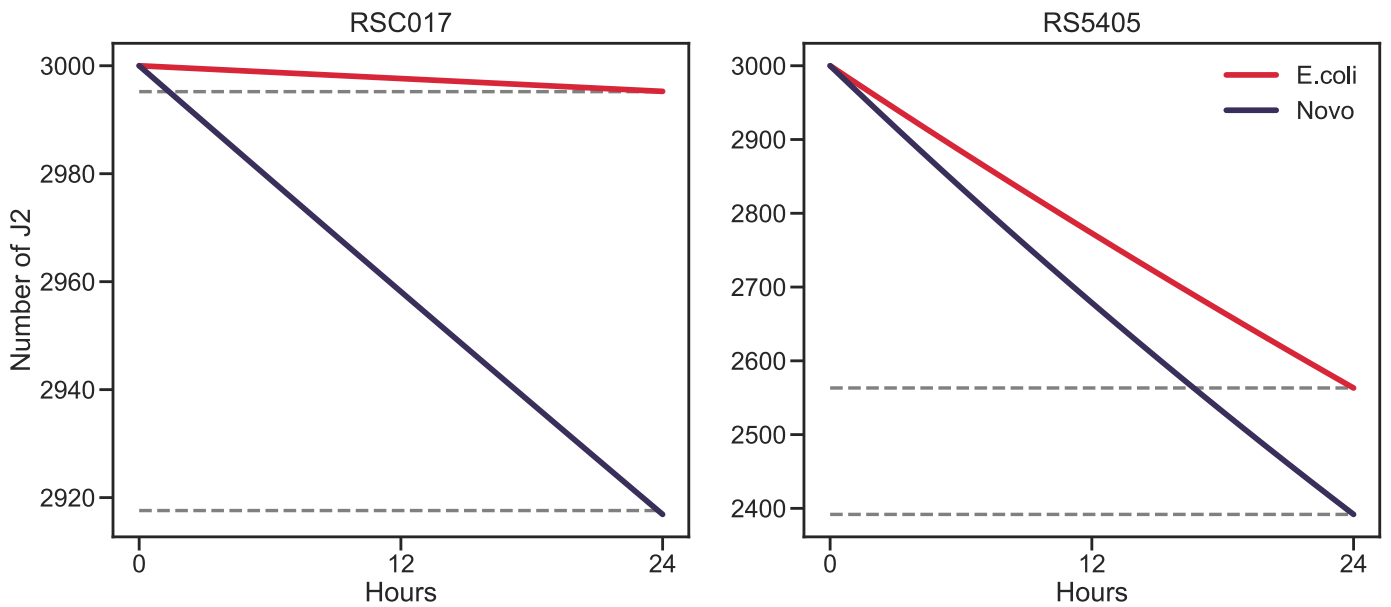
(Supplementary Figure 1)



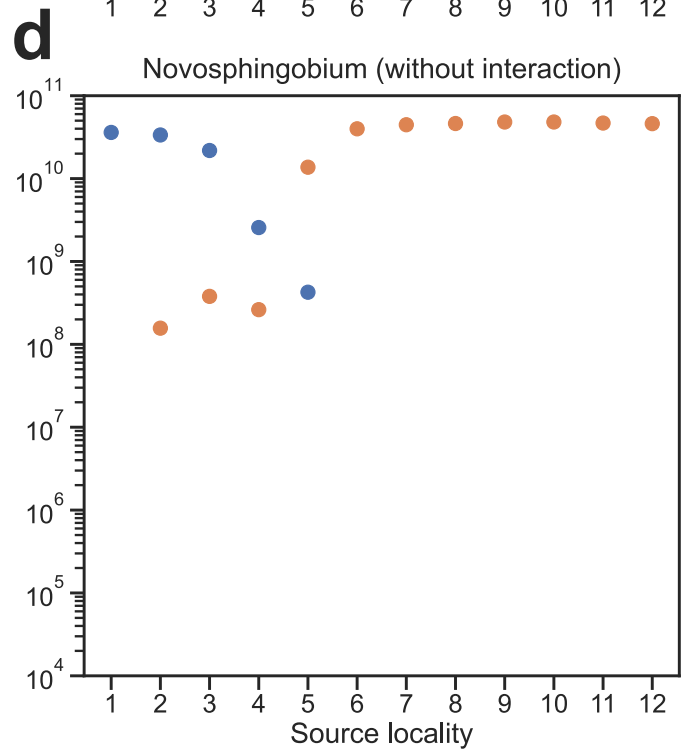
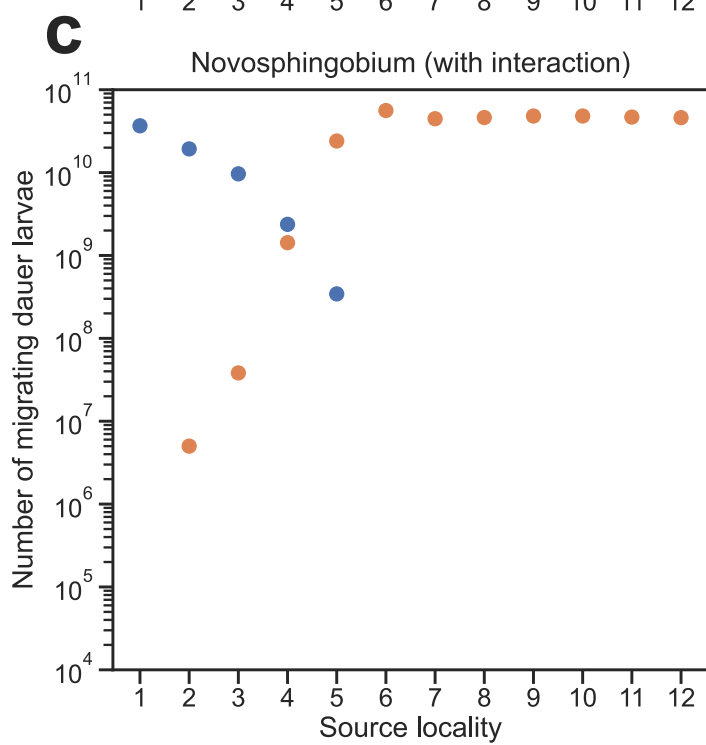
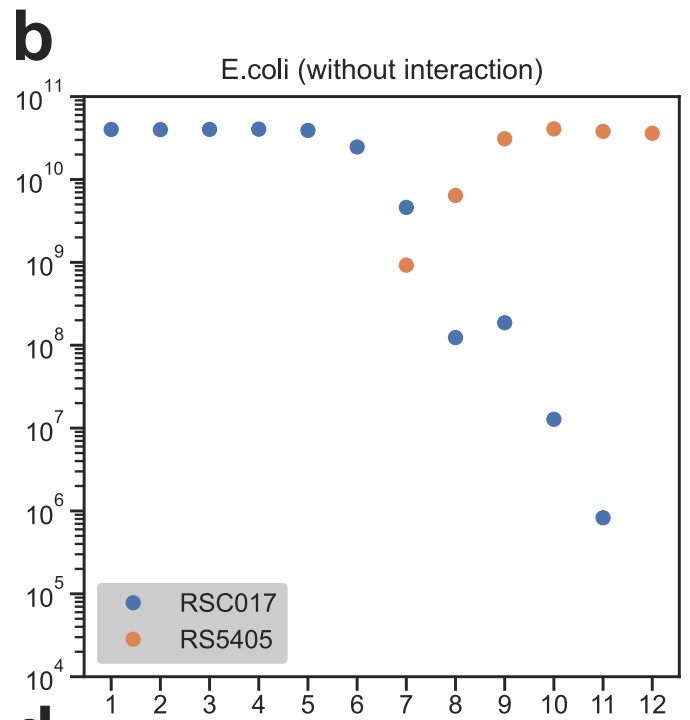
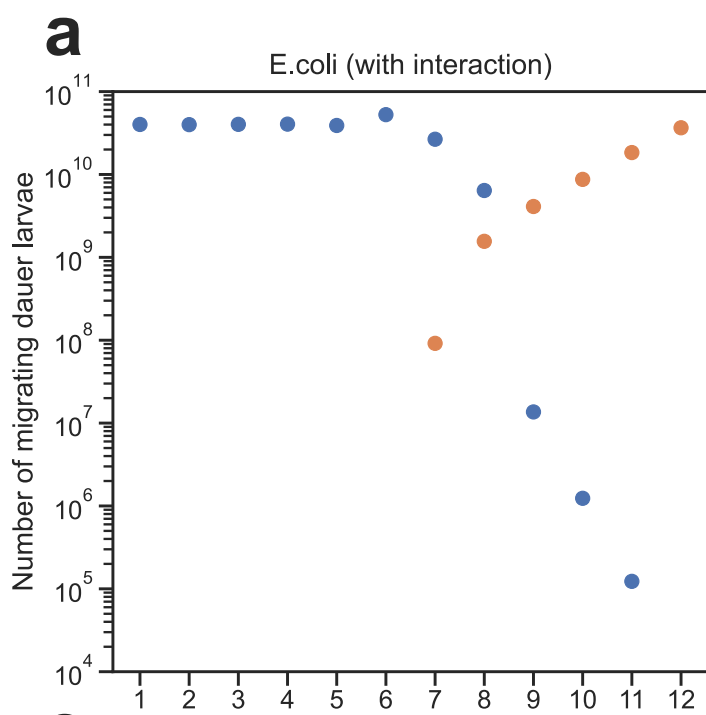
(Supplementary Figure 2)



(Supplementary Figure 3)

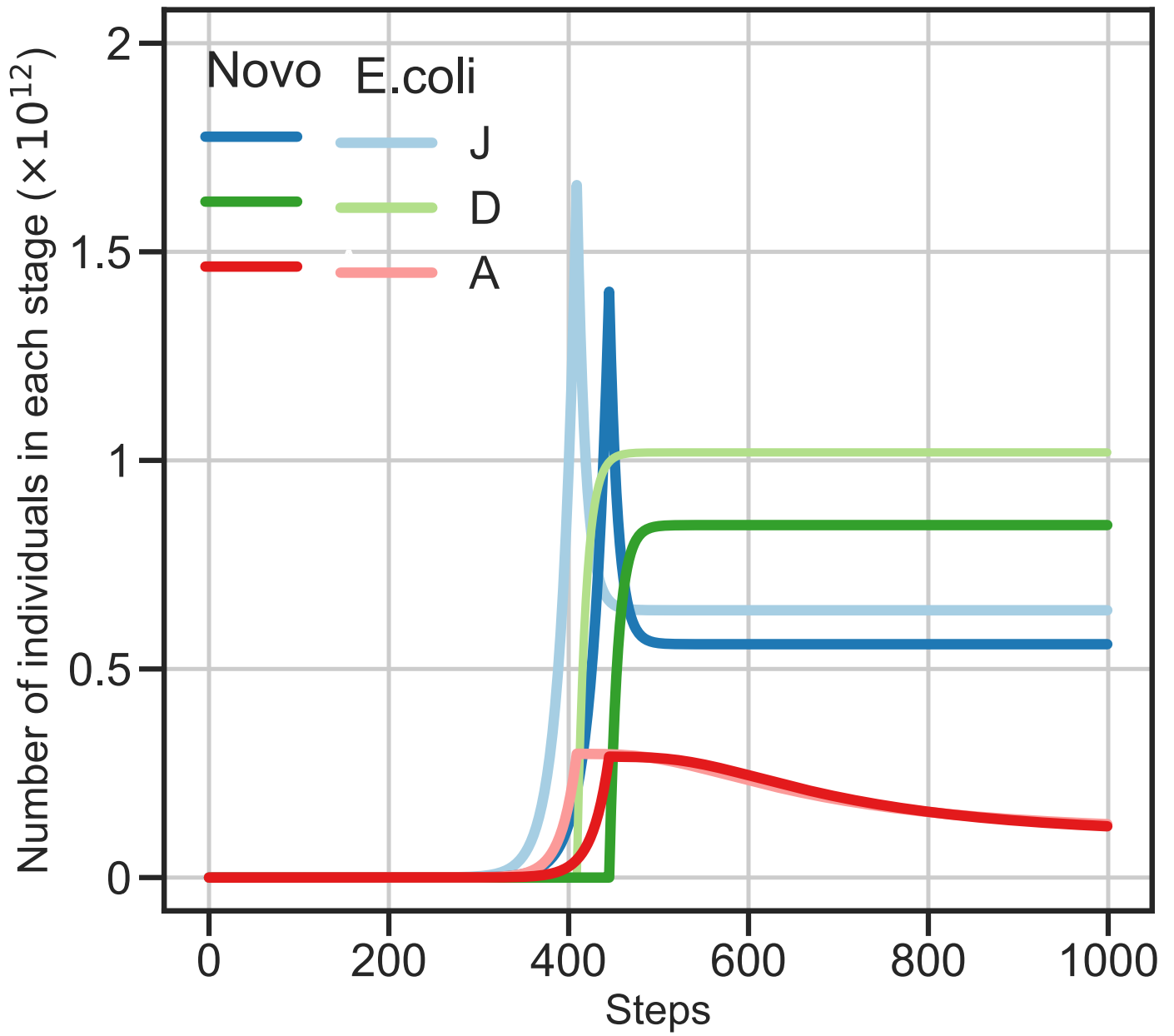


(Supplementary Figure 4)



(Supplementary Figure 5)

RSC017



(Supplementary Figure 6)

Strain	Location/clade	Number of Eu individuals	Number of St individuals	Overall fecundity mean Eu	Overall fecundity mean St	Standard deviation Eu	Standard deviation St	Experimental setup	Condition		
RSS348	La Reunion, Trois Bassins (TB)/C	44	33	99,75	105,9399939	29,03576383	30,79259184	intra-genotype cost of phenotype	<i>E. coli</i>		
RSAL13	La Reunion, Trois Bassins (TB)/C	54	41	68,18518519	72,92682927	25,92738341	29,5375949	intra-genotype cost of phenotype	<i>E. coli</i>		
RSAB22	Mauritius, Sugarcane Institute (MU)/C	50	49	121,5833333	140,0169492	45,12216625	40,81180188	intra-genotype cost of phenotype	<i>E. coli</i>		
RSAB45	Mauritius, Lakaz Chamarel Med.pla (MU)/A	55	54	148,6363636	160,8333333	38,48056924	40,74344489	intra-genotype cost of phenotype	<i>E. coli</i>		
RSC019	La Reunion, Colorado (CO)/C	54	53	98,2037037	140,8490566	36,15030448	39,83330797	intra-genotype cost of phenotype	<i>E. coli</i>		
RSC033	La Reunion, Grand Etang Lake-3 (GE)/C	54	47	97,92592593	125,5744681	36,31302685	48,02433472	intra-genotype cost of phenotype	<i>E. coli</i>		
RSD029	La Reunion, Nez de Boeuf (NB)/B	46	54	143,3478261	146,7407407	31,13784221	32,59363906	intra-genotype cost of phenotype	<i>E. coli</i>		
Strain	Location/clade	Number of Eu individuals	Number of St individuals	Overall fecundity mean Eu	Overall fecundity mean St	Overall fecundity Eu+St	Standard deviation Eu	Standard deviation St	Standard deviation Eu+St	Experimental setup	Condition
RSC011	La Reunion, Coteau Kerveguen (CK)/B	9	32	173,2222222	166,75	168,1707317	36,04087186	45,10131963	42,93710659	inter-genotype cost of plasticity	<i>E. coli</i>
RS4076	La Reunion, Nez de Boeuf (NB)/B	40	0	148,3	0	148,3	42,70002702	0	42,70002702	inter-genotype cost of plasticity	<i>E. coli</i>
RSS405	La Reunion, Trois Bassins (TB)/C	40	0	149,625	0	149,625	45,37348571	0	45,37348571	inter-genotype cost of plasticity	<i>E. coli</i>
RSC017	La Reunion, Colorado (CO)/C	0	40	0	186,525	186,525	0	33,05394775	33,05394775	inter-genotype cost of plasticity	<i>E. coli</i>
Strain	Location/clade	Number of Eu individuals	Number of St individuals	Overall fecundity mean Eu	Overall fecundity mean St	Overall fecundity Eu+St	Standard deviation Eu	Standard deviation St	Standard deviation Eu+St	Experimental setup	Condition
RSS4054	La Reunion, Trois Bassins (TB)/C	43	0	193,0465116	0	193,0465116	33,0273721	0	33,0273721	Cost of phenotype	<i>Novosphingobium</i>
RSC017	La Reunion, Colorado (CO)/C	47	0	136,2553191	0	136,2553191	27,9887152	0	27,9887152	Cost of phenotype	<i>Novosphingobium</i>
RSC019	La Reunion, Colorado (CO)/C	45	0	157,3777778	0	157,3777778	37,0321046	0	37,0321046	Cost of phenotype	<i>Novosphingobium</i>

(Table Supplementary 1)

Strain	Mean progeny count	Days	Standard deviation	Number of individuals	Condition	Percentage	Animals mouth form	Expirmental setup
RS5348	25,31818182	Day 1	11,19961	44	<i>E. coli</i>	25,3816371	Eu	intra-genotype cost of phenotype
RS5348	41,90909091	Day 2	15,71522	44	<i>E. coli</i>	42,0141262	Eu	intra-genotype cost of phenotype
RS5348	22,79545455	Day 3	12,53011	44	<i>E. coli</i>	22,852586	Eu	intra-genotype cost of phenotype
RS5348	6,431818182	Day 4	10,78414	44	<i>E. coli</i>	6,44793803	Eu	intra-genotype cost of phenotype
RS5348	3,29545	Day 5	7,79558	44	<i>E. coli</i>	3,30370927	Eu	intra-genotype cost of phenotype
RS5348	23,42424242	Day 1	9,87747	33	<i>E. coli</i>	22,1110036	St	intra-genotype cost of phenotype
RS5348	44,9393	Day 2	11,41528	33	<i>E. coli</i>	42,4198574	St	intra-genotype cost of phenotype
RS5348	24,93939394	Day 3	15,51801	33	<i>E. coli</i>	23,5412108	St	intra-genotype cost of phenotype
RS5348	8,363636364	Day 4	11,01368	33	<i>E. coli</i>	7,89474384	St	intra-genotype cost of phenotype
RS5348	4,272727273	Day 5	11,39976	33	<i>E. coli</i>	4,03318435	St	intra-genotype cost of phenotype
RSA645	36,83636364	Day 1	11,11349	55	<i>E. coli</i>	24,7828746	Eu	intra-genotype cost of phenotype
RSA645	63,34545455	Day 2	14,95081	55	<i>E. coli</i>	42,617737	Eu	intra-genotype cost of phenotype
RSA645	39,54545455	Day 3	22,02593	55	<i>E. coli</i>	26,6055046	Eu	intra-genotype cost of phenotype
RSA645	6,036363636	Day 4	10,45619	55	<i>E. coli</i>	4,06116208	Eu	intra-genotype cost of phenotype
RSA645	2,872727273	Day 5	14,02650	55	<i>E. coli</i>	1,93272171	Eu	intra-genotype cost of phenotype
RSA645	36,74074074	Day 1	10,71621	54	<i>E. coli</i>	22,8439839	St	intra-genotype cost of phenotype
RSA645	75,22222222	Day 2	16,58104	54	<i>E. coli</i>	46,7702936	St	intra-genotype cost of phenotype
RSA645	44,92592593	Day 3	22,62979	54	<i>E. coli</i>	27,9332182	St	intra-genotype cost of phenotype
RSA645	2,018518519	Day 4	5,06371	54	<i>E. coli</i>	1,25503742	St	intra-genotype cost of phenotype
RSA645	1,925925926	Day 5	12,64143	54	<i>E. coli</i>	1,1974669	St	intra-genotype cost of phenotype
RSA622	12,4	Day 1	6,99927	50	<i>E. coli</i>	10,1987663	Eu	intra-genotype cost of phenotype
RSA622	53,86666667	Day 2	18,98391	50	<i>E. coli</i>	44,304318	Eu	intra-genotype cost of phenotype
RSA622	46,46666667	Day 3	28,50600	50	<i>E. coli</i>	38,2179575	Eu	intra-genotype cost of phenotype
RSA622	6	Day 4	9,42949	50	<i>E. coli</i>	4,93488691	Eu	intra-genotype cost of phenotype
RSA622	2,85	Day 5	9,37329	50	<i>E. coli</i>	2,34407128	Eu	intra-genotype cost of phenotype
RSA622	14,37288136	Day 1	7,74351	49	<i>E. coli</i>	10,2651011	St	intra-genotype cost of phenotype
RSA622	65,42372881	Day 2	20,17271	49	<i>E. coli</i>	46,725578	St	intra-genotype cost of phenotype
RSA622	48,96610169	Day 3	27,42071	49	<i>E. coli</i>	34,9715531	St	intra-genotype cost of phenotype
RSA622	6,898305085	Day 4	10,12626	49	<i>E. coli</i>	4,92676431	St	intra-genotype cost of phenotype
RSA622	4,355932203	Day 5	14,28860	49	<i>E. coli</i>	3,11100351	St	intra-genotype cost of phenotype
RSC019	22,61111111	Day 1	9,51546	54	<i>E. coli</i>	23,024703	Eu	intra-genotype cost of phenotype
RSC019	33,18518519	Day 2	22,06515	54	<i>E. coli</i>	33,7921931	Eu	intra-genotype cost of phenotype
RSC019	32,01851852	Day 3	13,87340	54	<i>E. coli</i>	32,6041863	Eu	intra-genotype cost of phenotype
RSC019	6,611111111	Day 4	9,97434	54	<i>E. coli</i>	6,73203847	Eu	intra-genotype cost of phenotype
RSC019	3,777777778	Day 5	11,58344	54	<i>E. coli</i>	3,84687913	Eu	intra-genotype cost of phenotype
RSC019	19,52830189	Day 1	7,97015	53	<i>E. coli</i>	13,8647019	St	intra-genotype cost of phenotype
RSC019	58,88679245	Day 2	19,53071	53	<i>E. coli</i>	41,8084394	St	intra-genotype cost of phenotype
RSC019	48,05660377	Day 3	19,27475	53	<i>E. coli</i>	34,119223	St	intra-genotype cost of phenotype
RSC019	8,773584906	Day 4	9,97434	53	<i>E. coli</i>	6,22906899	St	intra-genotype cost of phenotype
RSC019	5,603773585	Day 5	14,41999	53	<i>E. coli</i>	3,97856664	St	intra-genotype cost of phenotype
RSC011	17,53658537	Day 1	8,553062495	41	<i>E. coli</i>	10,4278463	highly st	inter-genotype cost of plasticity
RSC011	76,24390244	Day 2	23,9629923	41	<i>E. coli</i>	45,3372009	highly st	inter-genotype cost of plasticity
RSC011	62,26829268	Day 3	27,51064081	41	<i>E. coli</i>	37,026831	highly st	inter-genotype cost of plasticity
RSC011	8	Day 4	14,91978552	41	<i>E. coli</i>	4,75707034	highly st	inter-genotype cost of plasticity
RSC011	4,12195122	Day 5	13,14000594	41	<i>E. coli</i>	2,45105149	highly st	inter-genotype cost of plasticity
RSA076	10,675	Day 1	7,230233886	40	<i>E. coli</i>	7,1982468	highly Eu	inter-genotype cost of plasticity
RSA076	54,375	Day 2	16,02031963	40	<i>E. coli</i>	36,6655428	highly Eu	inter-genotype cost of plasticity
RSA076	57,875	Day 3	21,06624728	40	<i>E. coli</i>	39,0256237	highly Eu	inter-genotype cost of plasticity
RSA076	23,2	Day 4	20,65491808	40	<i>E. coli</i>	15,6439649	highly Eu	inter-genotype cost of plasticity
RSA076	2,175	Day 5	4,684330125	40	<i>E. coli</i>	1,46662171	highly Eu	inter-genotype cost of plasticity
RSC017	22,65	Day 1	6,290204024	40	<i>E. coli</i>	12,1431444	highly st	inter-genotype cost of plasticity
RSC017	68,45	Day 2	10,19684797	40	<i>E. coli</i>	36,6974936	highly st	inter-genotype cost of plasticity
RSC017	57,05	Day 3	15,19606899	40	<i>E. coli</i>	30,5857124	highly st	inter-genotype cost of plasticity
RSC017	33,4	Day 4	18,09348941	40	<i>E. coli</i>	17,9064469	highly st	inter-genotype cost of plasticity
RSC017	4,975	Day 5	5,757882	40	<i>E. coli</i>	2,66720279	highly st	inter-genotype cost of plasticity
RS5405	19,8	Day 1	5,302152441	40	<i>E. coli</i>	13,2696386	highly Eu	inter-genotype cost of plasticity
RS5405	60,3	Day 2	13,61597855	40	<i>E. coli</i>	40,4120813	highly Eu	inter-genotype cost of plasticity
RS5405	43,025	Day 3	18,94457165	40	<i>E. coli</i>	28,8346567	highly Eu	inter-genotype cost of plasticity
RS5405	19,4878049	Day 4	16,20667795	40	<i>E. coli</i>	13,0604105	highly Eu	inter-genotype cost of plasticity
RS5405	6,6	Day 5	4,684330125	40	<i>E. coli</i>	4,42321288	highly Eu	inter-genotype cost of plasticity
RSC017	11,67391304	Day 1	6,09208721	47	<i>Novosphingobium</i>	8,58419751	on <i>E. coli</i> highly St	cost of plasticity
RSC017	62,53191489	Day 2	17,5261929	47	<i>Novosphingobium</i>	45,9816949	on <i>E. coli</i> highly St	cost of plasticity
RSC017	47,12765957	Day 3	13,86835155	47	<i>Novosphingobium</i>	34,6544588	on <i>E. coli</i> highly St	cost of plasticity
RSC017	13,93617021	Day 4	12,39460657	47	<i>Novosphingobium</i>	10,2477068	on <i>E. coli</i> highly St	cost of plasticity
RSC017	0,723404255	Day 5	2,337800226	47	<i>Novosphingobium</i>	0,53194203	on <i>E. coli</i> highly St	cost of plasticity
RSC019	16,86666667	Day 1	6,652408996	45	<i>Novosphingobium</i>	10,6020394	on <i>E. coli</i> unbiased	cost of plasticity
RSC019	66,35555556	Day 2	16,87541993	45	<i>Novosphingobium</i>	41,709736	on <i>E. coli</i> unbiased	cost of plasticity
RSC019	61,86666667	Day 3	20,0086345	45	<i>Novosphingobium</i>	38,8881129	on <i>E. coli</i> unbiased	cost of plasticity
RSC019	13,44444444	Day 4	15,10953275	45	<i>Novosphingobium</i>	8,45090096	on <i>E. coli</i> unbiased	cost of plasticity
RSC019	0,555555556	Day 5	1,778093406	45	<i>Novosphingobium</i>	0,34921078	on <i>E. coli</i> unbiased	cost of plasticity
RS5405	16,88372093	Day 1	8,555752742	43	<i>Novosphingobium</i>	8,76315975	on <i>E. coli</i> highly Eu	cost of plasticity
RS5405	80,76744186	Day 2	16,65595448	43	<i>Novosphingobium</i>	41,9207353	on <i>E. coli</i> highly Eu	cost of plasticity
RS5405	77,34146341	Day 3	20,45382126	43	<i>Novosphingobium</i>	40,1425493	on <i>E. coli</i> highly Eu	cost of plasticity
RS5405	16,27906977	Day 4	13,30471735	43	<i>Novosphingobium</i>	8,44932759	on <i>E. coli</i> highly Eu	cost of plasticity
RS5405	1,395348837	Day 5	3,193293082	43	<i>Novosphingobium</i>	0,72422808	on <i>E. coli</i> highly Eu	cost of plasticity

(Table Supplementary 2)

Strain	Total count	J1(eggs)	J2	J3	J4	Young Adult (YA)	Adult with eggs(BA)	Number of Mothers	%J1(eggs)	%J2	%J3	%J4	%YA	%BA	Condition
RSC017	70	0	1	0	8	61	0	9	0	1,428571	0	11,42857	87,14286	0	<i>E. coli</i>
RSC017	72	0	0	3	6	63	0	9	0	0	4,166667	8,333333	87,5	0	<i>E. coli</i>
RSC017	66	1	1	1	8	55	0	10	1,515152	1,515152	1,515152	12,12121	83,33333	0	<i>E. coli</i>
RSC017	62	0	0	1	0	61	0	9	0	0	1,612903	0	98,3871	0	<i>E. coli</i>
RSC017	50	0	0	0	3	47	0	10	0	0	0	6	94	0	<i>E. coli</i>
RS5405	69	0	0	0	13	56	0	10	0	0	0	18,84058	81,15942	0	<i>E. coli</i>
RS5405	51	0	0	0	10	41	0	10	0	0	0	19,60784	80,39216	0	<i>E. coli</i>
RS5405	71	0	1	0	12	58	0	10	0	1,408451	0	16,90141	81,69014	0	<i>E. coli</i>
RS5405	56	0	1	0	7	48	0	10	0	1,785714	0	12,5	85,71429	0	<i>E. coli</i>
RS5405	59	0	0	1	6	52	0	10	0	0	1,694915	10,16949	88,13559	0	<i>E. coli</i>
RSC019	54	0	0	0	28	26	0	10	0	0	0	51,85185	48,14815	0	<i>E. coli</i>
RSC019	59	0	3	0	16	40	0	10	0	5,084746	0	27,11864	67,79661	0	<i>E. coli</i>
RSC019	47	0	1	1	23	22	0	10	0	2,12766	2,12766	48,93617	46,80851	0	<i>E. coli</i>
RSC019	53	0	2	0	9	42	0	10	0	3,773585	0	16,98113	79,24528	0	<i>E. coli</i>
RSC019	52	1	1	0	15	35	0	10	1,923077	1,923077	0	28,84615	67,30769	0	<i>E. coli</i>
RSC011	68	0	0	1	31	36	0	10	0	0	1,470588	45,58824	52,94118	0	<i>E. coli</i>
RSC011	98	0	1	1	33	63	0	9	0	1,020408	1,020408	33,67347	64,28571	0	<i>E. coli</i>
RSC011	41	0	0	0	21	20	0	10	0	0	0	51,21951	48,78049	0	<i>E. coli</i>
RSC011	56	0	0	0	17	39	0	9	0	0	0	30,35714	69,64286	0	<i>E. coli</i>
RSA076	50	0	1	1	38	10	0	10	0	2	2	76	20	0	<i>E. coli</i>
RSA076	59	0	1	4	44	10	0	9	0	1,694915	6,779661	74,57627	16,94915	0	<i>E. coli</i>
RSA076	70	0	0	1	53	16	0	9	0	0	1,428571	75,71429	22,85714	0	<i>E. coli</i>
RSA076	53	0	0	0	26	27	0	9	0	0	0	49,0566	50,9434	0	<i>E. coli</i>
RSC017	72	0	0	0	5	55	12	10	0	0	0	6,944444	76,38889	16,66667	<i>Novosphingobium</i>
RSC017	87	0	0	0	2	67	18	10	0	0	0	2,298851	77,01149	20,68966	<i>Novosphingobium</i>
RSC017	65	0	0	0	6	40	19	9	0	0	0	9,230769	61,53846	29,23077	<i>Novosphingobium</i>
RSC017	77	0	0	2	3	47	25	10	0	0	2,597403	3,896104	61,03896	32,46753	<i>Novosphingobium</i>
RS5405	124	0	0	0	3	46	75	10	0	0	0	2,419355	37,09677	60,48387	<i>Novosphingobium</i>
RS5405	131	0	0	1	1	21	108	10	0	0	0,763359	0,763359	16,03053	82,44275	<i>Novosphingobium</i>
RS5405	126	0	0	0	0	13	113	10	0	0	0	10,31746	89,68254		<i>Novosphingobium</i>
RS5405	108	0	0	0	4	12	92	10	0	0	0	3,703704	11,11111	85,18519	<i>Novosphingobium</i>
RSC019	86	0	0	0	0	72	14	10	0	0	0	0	83,72093	16,27907	<i>Novosphingobium</i>
RSC019	73	0	0	0	2	46	25	10	0	0	0	2,739726	63,0137	34,24658	<i>Novosphingobium</i>
RSC019	83	0	0	2	3	43	35	10	0	0	2,409639	3,614458	51,80723	42,16867	<i>Novosphingobium</i>
RSC019	89	0	0	0	0	48	41	10	0	0	0	0	53,93258	46,06742	<i>Novosphingobium</i>

(Table Supplementary 3)

Strain	Condition	Number of Eu animals	Total number of animals counted	%Eu	Experimental setup
RSA133	<i>E. coli</i>	28	47	59,57447	intra-genotype cost of phenotype
RSA133	<i>E. coli</i>	63	93	67,74194	intra-genotype cost of phenotype
RSA133	<i>E. coli</i>	67	103	65,04854	intra-genotype cost of phenotype
RSD029	<i>E. coli</i>	33	47	70,21277	intra-genotype cost of phenotype
RSD029	<i>E. coli</i>	38	71	53,52113	intra-genotype cost of phenotype
RSD029	<i>E. coli</i>	40	70	57,14286	intra-genotype cost of phenotype
RSC033	<i>E. coli</i>	32	45	71,11111	intra-genotype cost of phenotype
RSC033	<i>E. coli</i>	47	58	81,03448	intra-genotype cost of phenotype
RSC033	<i>E. coli</i>	40	54	74,07407	intra-genotype cost of phenotype
RSC019	<i>E. coli</i>	33	50	66	intra-genotype cost of phenotype
RSC019	<i>E. coli</i>	30	50	60	intra-genotype cost of phenotype
RSC019	<i>E. coli</i>	23	50	46	intra-genotype cost of phenotype
RS5348	<i>E. coli</i>	30	53	56,60377	intra-genotype cost of phenotype
RS5348	<i>E. coli</i>	20	35	57,14286	intra-genotype cost of phenotype
RS5348	<i>E. coli</i>	30	50	60	intra-genotype cost of phenotype
RSA645	<i>E. coli</i>	57	111	51,35135	intra-genotype cost of phenotype
RSA645	<i>E. coli</i>	34	50	68	intra-genotype cost of phenotype
RSA645	<i>E. coli</i>	26	50	52	intra-genotype cost of phenotype
RSA622	<i>E. coli</i>	32	116	27,58621	intra-genotype cost of phenotype
RSA622	<i>E. coli</i>	96	143	67,13287	intra-genotype cost of phenotype
RSA622	<i>E. coli</i>	16	30	53,33333	intra-genotype cost of phenotype
RSC017	<i>E. coli</i>	1	50	2	inter-genotype cost of plasticity
RSC017	<i>E. coli</i>	5	50	10	inter-genotype cost of plasticity
RSC017	<i>E. coli</i>	1	50	2	inter-genotype cost of plasticity
RS5405	<i>E. coli</i>	50	50	100	inter-genotype cost of plasticity
RS5405	<i>E. coli</i>	50	50	100	inter-genotype cost of plasticity
RS5405	<i>E. coli</i>	50	50	100	inter-genotype cost of plasticity
RSC011	<i>E. coli</i>	10	50	20	inter-genotype cost of plasticity
RSC011	<i>E. coli</i>	16	50	32	inter-genotype cost of plasticity
RSC011	<i>E. coli</i>	24	50	48	inter-genotype cost of plasticity
RSA076	<i>E. coli</i>	50	50	100	inter-genotype cost of plasticity
RSA076	<i>E. coli</i>	50	50	100	inter-genotype cost of plasticity
RSA076	<i>E. coli</i>	50	50	100	inter-genotype cost of plasticity
RSA619	<i>E. coli</i>	49	50	98	Predation assay
RSA619	<i>E. coli</i>	50	50	100	Predation assay
RSA619	<i>E. coli</i>	47	50	94	Predation assay
RSA639	<i>E. coli</i>	50	50	100	Predation assay
RSA639	<i>E. coli</i>	50	50	100	Predation assay
RSA639	<i>E. coli</i>	50	50	100	Predation assay
RSA635	<i>E. coli</i>	45	50	90	Predation assay
RSA635	<i>E. coli</i>	34	50	68	Predation assay
RSA635	<i>E. coli</i>	30	50	60	Predation assay
RS5200	<i>E. coli</i>	7	50	14	Predation assay
RS5200	<i>E. coli</i>	12	50	24	Predation assay
RS5200	<i>E. coli</i>	2	50	4	Predation assay
RSC019	<i>Novosphingobium</i>	49	50	98	cost of plasticity
RSC019	<i>Novosphingobium</i>	49	50	98	cost of plasticity
RSC019	<i>Novosphingobium</i>	48	50	96	cost of plasticity
RSC017	<i>Novosphingobium</i>	44	50	88	cost of plasticity
RSC017	<i>Novosphingobium</i>	47	50	94	cost of plasticity
RSC017	<i>Novosphingobium</i>	42	50	84	cost of plasticity
RS5405	<i>Novosphingobium</i>	50	50	100	cost of plasticity
RS5405	<i>Novosphingobium</i>	50	50	100	cost of plasticity
RS5405	<i>Novosphingobium</i>	50	50	100	cost of plasticity

(Table Supplementary 4)

Prey	Predator	Corpses	Condition	Experimental setup
<i>C. elegans</i> (N2)	<i>P. Pacificus</i> (RSA076)	28	<i>E. coli</i>	inter-specific assay
<i>C. elegans</i> (N2)	<i>P. Pacificus</i> (RSA076)	31	<i>E. coli</i>	inter-specific assay
<i>C. elegans</i> (N2)	<i>P. Pacificus</i> (RSA076)	49	<i>E. coli</i>	inter-specific assay
<i>C. elegans</i> (N2)	<i>P. Pacificus</i> (RSC011)	8	<i>E. coli</i>	inter-specific assay
<i>C. elegans</i> (N2)	<i>P. Pacificus</i> (RSC011)	8	<i>E. coli</i>	inter-specific assay
<i>C. elegans</i> (N2)	<i>P. Pacificus</i> (RSC011)	1	<i>E. coli</i>	inter-specific assay
<i>C. elegans</i> (N2)	<i>P. Pacificus</i> (RS5405)	32	<i>E. coli</i>	inter-specific assay
<i>C. elegans</i> (N2)	<i>P. Pacificus</i> (RS5405)	36	<i>E. coli</i>	inter-specific assay
<i>C. elegans</i> (N2)	<i>P. Pacificus</i> (RS5405)	25	<i>E. coli</i>	inter-specific assay
<i>C. elegans</i> (N2)	<i>P. Pacificus</i> (RSC017)	0	<i>E. coli</i>	inter-specific assay
<i>C. elegans</i> (N2)	<i>P. Pacificus</i> (RSC017)	0	<i>E. coli</i>	inter-specific assay
<i>C. elegans</i> (N2)	<i>P. Pacificus</i> (RSC017)	0	<i>E. coli</i>	inter-specific assay
<i>C. elegans</i> (N2)	<i>P. Pacificus</i> (RSC019)	0	<i>E. coli</i>	inter-specific assay
<i>C. elegans</i> (N2)	<i>P. Pacificus</i> (RSC019)	11	<i>E. coli</i>	inter-specific assay
<i>C. elegans</i> (N2)	<i>P. Pacificus</i> (RSC019)	3	<i>E. coli</i>	inter-specific assay
<i>C. elegans</i> (N2)	<i>P. Pacificus</i> (RSA639)	55	<i>E. coli</i>	inter-specific assay
<i>C. elegans</i> (N2)	<i>P. Pacificus</i> (RSA639)	64	<i>E. coli</i>	inter-specific assay
<i>C. elegans</i> (N2)	<i>P. Pacificus</i> (RSA639)	22	<i>E. coli</i>	inter-specific assay
<i>C. elegans</i> (N2)	<i>P. Pacificus</i> (RS5200)	0	<i>E. coli</i>	inter-specific assay
<i>C. elegans</i> (N2)	<i>P. Pacificus</i> (RS5200)	3	<i>E. coli</i>	inter-specific assay
<i>C. elegans</i> (N2)	<i>P. Pacificus</i> (RS5200)	0	<i>E. coli</i>	inter-specific assay
<i>C. elegans</i> (N2)	<i>P. Pacificus</i> (RSA635)	0	<i>E. coli</i>	inter-specific assay
<i>C. elegans</i> (N2)	<i>P. Pacificus</i> (RSA635)	7	<i>E. coli</i>	inter-specific assay
<i>C. elegans</i> (N2)	<i>P. Pacificus</i> (RSA635)	8	<i>E. coli</i>	inter-specific assay
<i>C. elegans</i> (N2)	<i>P. Pacificus</i> (RSA619)	17	<i>E. coli</i>	inter-specific assay
<i>C. elegans</i> (N2)	<i>P. Pacificus</i> (RSA619)	22	<i>E. coli</i>	inter-specific assay
<i>C. elegans</i> (N2)	<i>P. Pacificus</i> (RSA619)	40	<i>E. coli</i>	inter-specific assay
RSC017	RSC017	0	<i>E. coli</i>	intra-specific assay
RSC017	RSC017	0	<i>E. coli</i>	intra-specific assay
RSC017	RSC017	0	<i>E. coli</i>	intra-specific assay
RSC017	RSC017	0	<i>E. coli</i>	intra-specific assay
RSC017	RS5405	443	<i>E. coli</i>	intra-specific assay
RSC017	RS5405	539	<i>E. coli</i>	intra-specific assay
RSC017	RS5405	340	<i>E. coli</i>	intra-specific assay
RSC017	RS5405	496	<i>E. coli</i>	intra-specific assay
RSC017	RS5405	366	<i>E. coli</i>	intra-specific assay
RS5405	RSC017	7	<i>E. coli</i>	intra-specific assay
RS5405	RSC017	4	<i>E. coli</i>	intra-specific assay
RS5405	RSC017	10	<i>E. coli</i>	intra-specific assay
RS5405	RSC017	0	<i>E. coli</i>	intra-specific assay
RS5405	RSC017	3	<i>E. coli</i>	intra-specific assay
RS5405	RS5405	0	<i>E. coli</i>	intra-specific assay
RS5405	RS5405	0	<i>E. coli</i>	intra-specific assay
RS5405	RS5405	0	<i>E. coli</i>	intra-specific assay
RS5405	RS5405	0	<i>E. coli</i>	intra-specific assay
RS5405	RS5405	0	<i>E. coli</i>	intra-specific assay
RS5405	RS5405	1	<i>E. coli</i>	intra-specific assay
RSC017	RSC017	0	<i>Novosphingobium</i>	intra-specific assay
RSC017	RSC017	0	<i>Novosphingobium</i>	intra-specific assay
RSC017	RSC017	0	<i>Novosphingobium</i>	intra-specific assay
RSC017	RSC017	0	<i>Novosphingobium</i>	intra-specific assay
RSC017	RSC017	0	<i>Novosphingobium</i>	intra-specific assay
RSC017	RS5405	587	<i>Novosphingobium</i>	intra-specific assay
RSC017	RS5405	691	<i>Novosphingobium</i>	intra-specific assay
RSC017	RS5405	720	<i>Novosphingobium</i>	intra-specific assay
RSC017	RS5405	530	<i>Novosphingobium</i>	intra-specific assay
RSC017	RS5405	513	<i>Novosphingobium</i>	intra-specific assay
RS5405	RSC017	102	<i>Novosphingobium</i>	intra-specific assay
RS5405	RSC017	90	<i>Novosphingobium</i>	intra-specific assay
RS5405	RSC017	42	<i>Novosphingobium</i>	intra-specific assay
RS5405	RSC017	87	<i>Novosphingobium</i>	intra-specific assay
RS5405	RSC017	91	<i>Novosphingobium</i>	intra-specific assay
RS5405	RS5405	0	<i>Novosphingobium</i>	intra-specific assay
RS5405	RS5405	0	<i>Novosphingobium</i>	intra-specific assay
RS5405	RS5405	0	<i>Novosphingobium</i>	intra-specific assay
RS5405	RS5405	0	<i>Novosphingobium</i>	intra-specific assay
RS5405	RS5405	0	<i>Novosphingobium</i>	intra-specific assay
RS5405	RS5405	0	<i>Novosphingobium</i>	intra-specific assay

(Table Supplementary 5)

		mean	sd	hdi_2.5%	hdi_97.5%	mcse_mean	mcse_sd	ess_mean	ess_sd	ess_bulk	ess_tail	r_hat
RS5348	group1_mean	106.35	5.54	95.36	117.27	0.03	0.02	44288.58	44288.58	44459.22	29104.65	1.0
	group2_mean	100.24	4.55	91.47	109.22	0.02	0.01	52011.46	51888.25	52073.74	31707.78	1.0
	group1_std	28.79	3.49	22.40	35.90	0.02	0.01	40484.90	40044.28	40107.94	29067.03	1.0
	group2_std	30.94	4.21	23.41	39.55	0.02	0.01	46105.51	43578.48	48035.44	29783.35	1.0
	ν _minus_one	39.55	30.60	2.45	100.24	0.15	0.12	40548.75	34484.50	38321.99	29693.67	1.0
	difference of means	6.10	7.16	-8.09	20.04	0.03	0.03	47002.57	32385.34	47019.65	31337.94	1.0
	difference of stds	-2.15	5.34	-12.93	8.16	0.02	0.02	47861.82	24887.63	48419.06	30915.78	1.0
	effect size	0.20	0.24	-0.26	0.67	0.00	0.00	48479.04	33778.71	48479.04	32474.91	1.0
	RSA113	group1_mean	72.43	4.71	63.33	81.79	0.02	0.02	38494.22	38338.84	38625.12	29630.08
group2_mean		67.47	3.73	60.26	74.88	0.02	0.01	35369.72	35122.37	35454.78	29608.96	1.0
group1_std		25.04	2.96	19.45	31.09	0.02	0.01	31425.22	31425.22	30631.53	23335.99	1.0
group2_std		28.73	3.79	21.65	36.37	0.02	0.01	36190.61	36190.61	35353.63	26825.76	1.0
ν _minus_one		30.29	27.80	1.58	85.69	0.16	0.12	31626.48	29183.47	26499.70	22546.26	1.0
difference of means		4.96	5.99	-6.71	16.77	0.03	0.02	38678.71	29701.85	38709.34	30238.24	1.0
difference of stds		-3.69	4.54	-12.89	4.85	0.02	0.02	50760.35	31125.47	51249.34	30618.26	1.0
effect size		0.18	0.22	-0.24	0.63	0.00	0.00	38403.69	29573.92	38385.19	30436.70	1.0
RSA622		group1_mean	140.37	5.49	129.50	151.01	0.02	0.02	53904.73	53863.07	54013.50	31536.61
	group2_mean	122.04	6.06	110.26	134.06	0.03	0.02	58497.36	58301.66	58554.71	30948.75	1.0
	group1_std	45.27	4.45	37.00	54.15	0.02	0.01	47137.68	45665.99	48520.77	31873.18	1.0
	group2_std	40.73	4.15	33.05	49.16	0.02	0.01	50387.56	48675.23	51706.14	30854.68	1.0
	ν _minus_one	47.21	33.10	4.63	112.85	0.16	0.12	45293.25	35808.20	50484.83	30000.31	1.0
	difference of means	18.33	8.21	2.48	34.48	0.03	0.03	56920.94	49831.68	56926.73	32492.54	1.0
	difference of stds	4.54	6.00	-7.28	16.38	0.03	0.02	52755.12	31794.16	53112.82	31238.64	1.0
	effect size	0.43	0.19	0.06	0.81	0.00	0.00	57735.40	51414.98	57704.25	32517.12	1.0
	RSA645	group1_mean	161.32	5.51	150.61	172.23	0.03	0.02	29696.94	29695.99	29727.32	27777.68
group2_mean		148.03	5.07	138.15	158.13	0.03	0.02	33176.32	33172.21	33210.03	28720.70	1.0
group1_std		34.82	4.74	25.39	43.98	0.03	0.02	20351.06	20351.06	19906.60	15117.07	1.0
group2_std		37.28	5.16	27.08	47.63	0.04	0.03	20961.56	20961.56	20823.39	15012.76	1.0
ν _minus_one		19.10	21.76	0.68	62.98	0.14	0.10	24942.00	24942.00	16744.65	15051.39	1.0
difference of means		13.29	7.52	-1.45	28.13	0.04	0.03	30697.45	29006.35	30708.63	28439.65	1.0
difference of stds		-2.46	5.80	-13.42	9.28	0.03	0.03	44305.30	24135.03	44477.83	30354.09	1.0
effect size		0.37	0.22	-0.06	0.79	0.00	0.00	26926.55	24017.49	27090.24	24570.85	1.0
RSC019		group1_mean	141.00	5.67	130.12	152.28	0.03	0.02	50926.85	50814.60	51097.71	32148.50
	group2_mean	98.42	5.19	87.89	108.29	0.02	0.01	61677.20	61401.01	61936.33	31875.30	1.0
	group1_std	36.45	3.83	29.50	44.20	0.02	0.01	47860.74	46007.86	49607.05	32207.17	1.0
	group2_std	39.51	4.37	31.21	48.15	0.02	0.01	46458.58	45334.95	47074.59	30847.29	1.0
	ν _minus_one	43.53	32.06	3.20	106.10	0.16	0.12	41438.60	34412.42	43317.58	30879.68	1.0
	difference of means	42.58	7.71	27.33	57.55	0.03	0.02	55793.15	54133.14	55808.36	33027.60	1.0
	difference of stds	-3.06	5.73	-14.29	8.30	0.03	0.02	51630.58	27138.29	51822.58	31195.47	1.0
	effect size	1.12	0.22	0.71	1.57	0.00	0.00	53821.11	53231.61	53714.18	32412.45	1.0
	RSC033	group1_mean	126.02	7.35	111.40	140.26	0.03	0.02	49886.01	49757.38	49939.36	31496.47
group2_mean		97.68	5.18	87.51	107.80	0.02	0.02	56855.55	56855.55	56953.60	32201.96	1.0
group1_std		36.52	3.84	29.23	44.06	0.02	0.01	48872.02	47041.67	50632.76	32242.19	1.0
group2_std		48.48	5.43	38.49	59.32	0.02	0.02	50161.88	47803.66	52465.20	31056.12	1.0
ν _minus_one		47.32	33.00	4.31	112.04	0.15	0.12	45438.58	34962.37	52086.13	30450.19	1.0
difference of means		28.34	9.00	11.31	46.58	0.04	0.03	51251.75	48144.35	51301.57	32921.36	1.0
difference of stds		-11.97	6.61	-24.87	1.11	0.03	0.02	52766.04	41823.87	53399.79	31224.45	1.0
effect size		0.66	0.21	0.24	1.08	0.00	0.00	51295.43	49900.73	51222.00	32243.60	1.0
RSD029		group1_mean	150.47	3.86	142.66	157.81	0.02	0.02	26840.09	26840.09	27461.50	25228.92
	group2_mean	148.00	4.01	140.03	155.70	0.02	0.02	26725.97	26725.97	26946.35	24328.41	1.0
	group1_std	22.01	4.20	14.13	30.23	0.03	0.02	21833.11	21833.11	21714.85	24084.62	1.0
	group2_std	23.59	4.42	15.33	32.34	0.03	0.02	20004.84	20004.84	19970.91	24013.22	1.0
	ν _minus_one	4.07	5.98	0.23	10.89	0.05	0.03	17423.34	17423.34	18718.25	18563.22	1.0
	difference of means	2.47	5.38	-8.12	13.04	0.03	0.03	30095.83	22559.26	30149.17	25893.37	1.0
	difference of stds	-1.58	4.60	-10.67	7.46	0.02	0.02	43416.62	23634.96	43374.54	30787.33	1.0
	effect size	0.11	0.24	-0.34	0.59	0.00	0.00	30840.64	23145.28	30856.97	27514.64	1.0

(Table Supplementary 6)

			mean	sd	hdi_2.5%	hdi_97.5%	mcse_mean	mcse_sd	ess_mean	ess_sd	ess_bulk	ess_tail	r_hat
RSC011	RSA076	group1_mean	173.11	6.60	159.80	185.68	0.05	0.03	20055.49	20055.49	20307.51	20799.06	1.0
		group2_mean	155.91	6.49	142.80	168.20	0.05	0.04	17058.45	17058.45	17493.96	19034.09	1.0
		group1_std	31.45	7.53	18.36	46.26	0.07	0.05	12754.75	12754.75	12672.96	17474.07	1.0
		group2_std	34.38	7.33	20.79	48.86	0.06	0.04	13767.41	13767.41	13532.92	16649.57	1.0
		ν _minus_one	8.20	14.79	0.05	34.74	0.12	0.08	16354.65	16354.65	11972.32	18171.42	1.0
		difference of means	17.20	8.49	0.42	33.67	0.05	0.04	26719.07	24856.96	26764.59	23583.41	1.0
		difference of stds	-2.93	7.24	-17.42	11.20	0.04	0.03	33344.50	21506.83	33410.45	26520.92	1.0
		effect size	0.54	0.28	0.00	1.08	0.00	0.00	23262.27	21803.22	23383.43	23893.89	1.0
		RSC017	RS5405	group1_mean	187.83	5.50	177.48	199.00	0.03	0.02	47392.11	47378.63	47586.81
group2_mean	150.31			7.62	135.37	165.16	0.04	0.03	42081.11	41894.70	42248.44	29312.61	1.0
group1_std	45.66			5.78	35.00	57.12	0.03	0.02	38915.14	37575.96	40104.00	29175.40	1.0
group2_std	32.20			4.34	24.20	41.10	0.02	0.02	35056.14	35056.14	34412.62	25372.71	1.0
ν _minus_one	35.59			29.43	1.88	93.97	0.16	0.11	35502.55	33664.83	31016.51	24524.15	1.0
difference of means	37.52			9.37	19.23	56.05	0.04	0.03	46285.23	44490.64	46385.14	31252.22	1.0
difference of stds	13.46			7.06	0.05	27.66	0.03	0.03	43853.56	36052.82	44634.26	30176.78	1.0
effect size	0.96			0.26	0.44	1.44	0.00	0.00	42294.03	41242.60	42318.11	31393.10	1.0
RSC011	RS5405			group1_mean	169.51	6.90	155.66	182.67	0.03	0.02	40465.22	40465.22	40583.91
		group2_mean	150.30	7.55	135.60	165.28	0.03	0.02	48130.69	47929.46	48267.64	29891.28	1.0
		group1_std	45.59	5.74	34.96	57.04	0.03	0.02	38202.31	37327.33	38795.11	29926.13	1.0
		group2_std	41.75	5.71	30.84	53.37	0.03	0.02	31156.75	31156.75	30539.75	20989.48	1.0
		ν _minus_one	35.52	29.67	1.85	94.59	0.16	0.11	36030.15	34366.06	29709.41	22856.79	1.0
		difference of means	19.21	10.20	-1.17	38.88	0.05	0.04	45381.95	41240.13	45437.15	30700.41	1.0
		difference of stds	3.85	7.81	-11.31	19.54	0.04	0.03	44107.74	26317.30	44324.06	30590.77	1.0
		effect size	0.44	0.24	-0.02	0.91	0.00	0.00	42592.21	39285.06	42523.00	30975.96	1.0
		RSC017	RSA076	group1_mean	190.62	5.57	179.83	201.50	0.04	0.03	20170.80	20170.80	20191.90
group2_mean	155.19			6.61	141.84	167.54	0.05	0.03	18740.82	18740.82	19094.64	22424.67	1.0
group1_std	32.92			7.41	19.17	47.02	0.06	0.04	14327.45	14327.45	13994.00	17528.73	1.0
group2_std	27.97			5.20	17.79	37.89	0.04	0.03	16279.51	16279.51	15866.95	14238.72	1.0
ν _minus_one	10.19			16.65	0.07	41.27	0.12	0.09	18361.16	18361.16	12963.22	19656.19	1.0
difference of means	35.44			7.80	20.43	51.10	0.05	0.03	27442.44	26584.28	27506.64	26097.59	1.0
difference of stds	4.95			6.76	-8.40	18.32	0.04	0.03	28478.22	27589.53	28333.95	24675.94	1.0
effect size	1.19			0.33	0.56	1.84	0.00	0.00	18013.75	16708.00	18856.68	18107.95	1.0

(Table Supplementary 7)

			mean	sd	hdi_2.5%	hdi_97.5%	mcse_mean	mcse_sd	ess_mean	ess_sd	ess_bulk	ess_tail	r_hat
RSC017		group1_mean	136.68	4.03	128.76	144.61	0.02	0.02	30134.98	30089.30	30142.38	28043.68	1.0
		group2_mean	188.76	5.49	177.72	199.24	0.03	0.02	26691.97	26671.53	26679.34	27794.28	1.0
		group1_std	30.74	4.76	21.44	40.23	0.03	0.02	21145.26	21145.26	20600.88	16254.60	1.0
		group2_std	25.78	3.84	18.27	33.49	0.03	0.02	18301.01	18301.01	18205.07	14843.09	1.0
		ν _minus_one	22.33	24.57	0.54	72.34	0.16	0.11	23904.73	23904.73	15621.20	15418.15	1.0
		difference of means	-52.08	6.75	-65.89	-39.28	0.04	0.03	28356.32	28356.32	28331.43	27488.67	1.0
		difference of stds	4.96	5.19	-5.36	15.01	0.03	0.02	42592.26	31112.81	42895.42	30491.32	1.0
		effect size	-1.85	0.38	-2.63	-1.14	0.00	0.00	15278.14	14008.37	16916.90	15006.72	1.0
		RSC019		group1_mean	159.43	5.56	148.20	170.08	0.03	0.02	35074.09	35074.09	35326.07
group2_mean	120.43			6.53	107.60	133.11	0.03	0.02	34973.10	34922.50	35048.27	29085.70	1.0
group1_std	42.05			5.25	32.24	52.69	0.03	0.02	29378.54	29378.54	28916.58	23523.62	1.0
group2_std	34.03			4.91	24.37	43.64	0.03	0.02	23215.59	23215.59	22619.31	19544.81	1.0
ν _minus_one	24.41			25.24	0.87	74.82	0.16	0.11	25448.29	25448.29	19098.29	21041.60	1.0
difference of means	38.99			8.48	22.60	55.81	0.04	0.03	36163.81	36163.81	36196.96	30852.16	1.0
difference of stds	8.02			6.48	-4.88	20.75	0.03	0.03	42905.59	31911.02	43313.34	29541.96	1.0
effect size	1.03			0.25	0.56	1.54	0.00	0.00	28231.13	28231.13	28293.33	27728.87	1.0
RS5405				group1_mean	193.22	5.12	183.27	203.41	0.02	0.02	47608.73	47608.73	47716.57
		group2_mean	150.31	7.58	135.20	164.92	0.03	0.02	47988.22	47905.57	48091.29	29946.84	1.0
		group1_std	45.62	5.73	35.16	57.26	0.03	0.02	39810.10	38774.98	40479.30	30143.67	1.0
		group2_std	32.10	4.14	24.46	40.66	0.02	0.02	30237.53	30237.53	29904.20	24384.60	1.0
		ν _minus_one	35.76	29.71	1.76	95.44	0.16	0.12	35205.23	32927.22	32069.09	25974.07	1.0
		difference of means	42.91	9.15	24.64	60.53	0.04	0.03	47872.99	46705.32	47882.70	31455.53	1.0
		difference of stds	13.53	6.86	0.43	27.28	0.03	0.03	43146.27	37519.75	43490.71	31025.20	1.0
		effect size	1.09	0.25	0.59	1.58	0.00	0.00	46283.55	45517.30	46213.44	30409.33	1.0

(Table Supplementary 8)

Cost of adaptive plasticity and spatial heterogeneity in *Pristionchus pacificus*: a computational prospective

Ata Kalirad¹, Mohannad Dardiry¹, Ralf J. Sommer^{1,*}

1 Department for Integrative Evolutionary Biology, Max Planck Institute for Biology Tübingen, 72076 Tübingen, Germany

* ralf.sommer@tuebingen.mpg.de

Abstract

Phenotypic (developmental) plasticity, the ability of a single genotype to produce distinct phenotypes under different environmental conditions, has become a leading concept in contemporary ecology and evolutionary biology, with the most extreme examples being the formation of alternative phenotypes or polyphenisms. However, several aspects associated with phenotypic plasticity in general, and polyphenisms in particular, remain controversial, such as the existence of associated costs. While already predicted by some of the pioneers of plasticity research, i.e. Schmalhausen and Bradshaw, experimental and theoretical approaches have provided limited support for the costs of plasticity for various reasons. In experimental studies, one common restriction is the measurement of all relevant parameters over long time periods. Similarly, theoretical studies rarely use modelling approaches that incorporate specific experimentally-derived fitness parameters. As a result, the existences of the costs of plasticity remain a matter of debate. Here, we provide an integrative approach to understand the cost of adaptive plasticity and its ecological ramifications, by combining laboratory data from the nematode model system *Pristionchus pacificus* with a modified stage-structured matrix population model. We take advantage of the available laboratory measurements of two different isogenic strains grown on two distinct food sources and simulate their population dynamics in a two-dimensional metapopulation. Comparing a plastic and a non-plastic strain, this system allows us to explore how the effect of dispersal and competition influence the ecological projections of the costs of adaptive plasticity.

Whether a theory is true, or new, or intellectually significant, depends on its meaning; and the meaning of a theory [...] is a function of the meanings of the words in which the theory is formulated.

Karl Popper [35]

INTRODUCTION

The expression of alternative phenotypes by a single genotype in different environments, i.e., phenotypic plasticity or polyphenism, remains a topic of great interest and

1

2

3

discussion in both ecology and evolution [40, 53, 61]. A plastic organism capable of assuming the form and function fitted to multiple environments could have an sizeable advantage in competition against genetically hard-wired competitors. However, such adaptive plasticity, given the hypothetical machinery behind it, should intuitively incur a cost. This possible cost did not escape the pioneers of the study of plasticity; for example, Bradshaw verbally argued that a case of adaptive plasticity could be selected against if the plastic trait were too costly [5]. This hypothetical cost of adaptive plasticity, has ever since been analyzed, elaborated upon, and reviewed in the literature (e.g., see [2, 13, 16, 30, 33]).

It should be noted that, curiously, the term “cost of plasticity” is sometimes used in reference to the aforementioned hypothesis, for example see [2, 8], even though the purported fitness trade-off can only be attributed to plasticity when it is adaptive. While this rather minute ambiguity reflects the extensive interchangeable usage of “plasticity” and “adaptive plasticity” in the literature, it should be avoided, since, as pointed out by Bradshaw, “the concept of plasticity does not also have any implications concerning the adaptive value of the changes occurring [...]” [5].

There have been many attempts to measure the cost of adaptive plasticity in nature (e.g., [24, 46, 48]). The general design of such studies involves finding a plastic trait that can be plausibly characterized as adaptive with regards to a given environmental condition, and measuring a component of fitness, e.g., fecundity, size, etc., across two or more conditions, one being the condition to which the plastic response is adapted. While such studies should, in principle, demonstrate the cost of plasticity, they have provided mixed evidence; a meta-analysis of 27 studies of the cost of adaptive plasticity concluded that the costs measured in these studies are quite infinitesimal, if present at all [50]. Surprisingly, while *Daphnia* is sometimes used as a visual aide to illustrate the cost of adaptive plasticity (e.g., [34]), the induction of the defensive spine in *Daphnia pulex*, in response to a predator (*Chaoborus americanus*), was shown to have negligible cost in spite of a forgiving statistical approach [39].

On the theoretical front, attempts have been made to provide concrete theoretical predictions with regards to the effect of the cost of adaptive plasticity. In one of the earliest examples, Van Tienderen [51] analyzed the cost of adaptive plasticity in an arbitrary quantitative trait with a Gaussian cost function. While his model predicts scenarios in which the plastic genotype could coexist with the specialist one, the results are dependent on the initial condition and the selection regime, among others. In a more recent study, Doret *et al.* [28] use a modified Gillespie algorithm to simulate a model of gene network to investigate the cost of adaptive plasticity. They distinguished between two possible mechanisms for the plastic response to the environmental change: environmental signal and performance signal, the latter being an endogenous signal that indicates how well the organism is functioning in a given environment. They concluded that being plastic is only costly when the developmental system relies on the environmental signal. This result is intriguing, but, since Doret *et al.* measured cost via the robustness of the development, any attempt to relate their results to the experimental measurements of the cost of adaptive plasticity, in which a component of fitness is measured, should proceed with a modicum of caution.

The experimental and theoretical approaches mentioned above have contributed to an extensive body of work on adaptive plasticity. However, given the paucity of support for costs of plasticity in the wild and the nature of the theoretical works on this topic, the existence of such costs remains a matter of debate. One could shed more light on

this phenomenon by melding relevant experimental data on the differential response to environmental fluctuations with a modelling approach. Specifically, modelling of the population dynamics to extrapolate from experimental snapshots observed in the wild or the laboratory, can provide computational predictions of the ecological consequences of adaptive plastic responses and their purported costs. Here, we provide an example of this integrative approach to understand the cost of adaptive plasticity and its ecological ramifications, by combining laboratory data from the nematode *Pristionchus pacificus* with a modified stage-structured matrix population model.

P. pacificus is a well-established model to study phenotypic plasticity [47]. The mouth form of this hermaphroditic nematode can assume two alternative states: a wide eury stomatous (Eu) form with two teeth, which enables the nematode to prey upon other nematodes, and a narrow bacterivorous stenostomatous (St) form with a single tooth (Fig 1)a. *P. pacificus* and its relatives are soil nematodes that are most reliably found in association with scarab beetles [18,21]. These nematodes stay in the arrested dauer larval stage as long as the adult beetle is alive and flourish on the beetle cadaver in the soil once the beetle has died [29,38]. Mouth-form plasticity and intraguild predation are important life history traits in the short-lived and competitive ecosystem of the decaying beetle [38]. The state of the mouth form can be influenced by a variety of stimuli, including temperature, culture methods, pheromones, and bacterial diet [3,26,59,60]. In addition to change in mouth form due to environmental cues, different wild isolates of *P. pacificus* exhibit a range of mouth-form ratios under laboratory condition [37]. Given that the molecular machinery regulating mouth-form plasticity in *P. pacificus* has been identified [6,23,31,44,45], this study system has the prospect of merging experimental and theoretical approaches of plasticity research and associated boundary conditions, such as the costs of adaptive plasticity.

In this study, we take advantage of the available laboratory measurements of two different isogenic strains of *P. pacificus* grown on two different two food sources, *Escherichia coli* and *Novosphingobium* sp. L76 (previously published in [12]). The plastic strain (RSC017) predominantly assumes the St mouth form on *E. coli*, but almost entirely switches to the Eu mouth form on *Novosphingobium*. In contrast, the non-plastic strain (RS5405) develops the Eu mouth form on both conditions. Using the experimentally-estimated parameters for developmental speed, fecundity, and predation, we simulate the population dynamics of these two strains on a lattice. We explore how the effect of dispersal and the choice of the predation model influence the ecological projections concerning the cost of adaptive plasticity in competition between the plastic and the non-plastic strains.

MATERIALS AND METHODS

To simulate the population dynamics of the interaction between the plastic and the non-plastic strains of *P. pacificus*, we use a modified version of a stage-structured matrix population model used in [12]. In this model, we envision the life cycle of *P. pacificus* as a absorbing finite-state Markov chain (for more on modelling life cycles as a Markov chain, see [9,22]). In the presence of food, the *P. pacificus* life cycle starts transitions through egg, J1, J2, J3, J4, young adult (YA), and adult stages. In our model, for the sake of simplicity, we combine egg and the non-motile J1 stage into one stage, E.

The available laboratory measurements on the plastic and the non-plastic strains includes the counts of the number of eggs laid by the hermaphrodite during the first five days of adulthood. To incorporate these data in our model, we divided the adult stage

into five breeding stages (BA₁ - BA₅) and a post-breeding old adult stage (OA). The fecundity for each breeding stage is the mean number eggs laid by the stage in the laboratory for a given strain on a given bacterial diet.

The dynamics of the population is determined by a transition matrix, \mathbf{U} . In \mathbf{U} , entry i, i indicates the probability that stage i survives and does not develop into the next stage and entry i, j is the probability of stage transition from state i to state j . The transition probabilities for all the stages in the model on the two different bacterial diets, and during starvation, are outlined in Table 1. Given the absence of laboratory measurements on the survival probability of preadult stages, we assume unity survival probability (σ) for all the preadult stages. Based on the experimental studies, the median lifespan in *P. pacificus* after maturation is 37 days, with maximum lifespan of 48 days [56]. However, the lifespan of *P. pacificus* was measured by allowing individual worms to grow in isolation, and survival was assessed by prodding the worm and observing its movement, or lack thereof, in response. Such lifespan analyses (e.g., [57, 58]) illustrate the upper bounds of life expectancy in *P. pacificus*, but do not provide data on the realized lifespan of *P. pacificus* adults in competition with other stages or younger adults. In the absence of such data, we assign an arbitrary survival probability to the adults ($\sigma = 0.995$) to ensure that they will die after a reasonable number of steps in our projections. The average number of steps an individual spends in any stage in a life cycle can be calculated by generating the fundamental matrix for the transition matrix for that life cycle, i.e., $\mathbf{N} = (\mathbf{I} - \mathbf{U})^{-1}$, where \mathbf{I} is an identity matrix [9]. The first column in \mathbf{N} , vector \mathcal{T} , represents the occupancy time in the Markov chain for an individual that starts from the E stage. For example, given the transition probabilities for the two strains on *E. coli*, vector \mathcal{T} , excluding the dauer stage, would be

$$\mathcal{T} = (24.1, 18.2, 11.8, 14.3, 10, 24, 24, 24, 24, 24, 200) \quad , \quad (1)$$

which, equating each step with an hour, is in line with the experimental data from *P. pacificus* [47, 49]. The change in the developmental speed of the plastic and the non-plastic strains on *Novosphingobium* based on the previous experimental measurements [12] is reflected in the probabilities of YA \rightarrow BA₁ in the model.

The fecundity of the plastic and the non-plastic strains for each of the five breeding adult stages are based on the average number eggs laid by the non-plastic and plastic strains on *E. coli* and *Novosphingobium* [12] (Table 2). The mean number of eggs laid are used to construct the fecundity matrix \mathbf{F} :

$$\mathbf{F} = \begin{pmatrix} 0 & \dots & f_1 & \dots & f_5 & 0 \\ 0 & \dots & \dots & \dots & \dots & 0 \\ \vdots & \dots & \dots & \dots & \dots & \vdots \\ 0 & \dots & \dots & \dots & \dots & 0 \end{pmatrix} \quad , \quad (2)$$

where $f_i = P_{i \rightarrow i+1} m_s^i$, since we assume survival probability of one for all the stages, except for the old adult stage, and the mothers are hermaphrodites. m_s^i is the mean number of eggs laid by the breeding adult of stage i from strain s .

The transition from abundance to starvation (Fig 1c) is modeled via a simple consumption model. Given food source \mathcal{S}_i , if there exist m developmental stages in the population at t and n_i individuals belong to developmental stage i , the amount of available food in the next step will be:

$$\mathcal{S}_{t+1} = \mathcal{S}_t - \sum_{i=1}^m \rho_i n_i \quad , \quad (3)$$

where ρ_i is the per capita consumption rate for developmental stage i . 149

The population is represented by a vector 150

$$\mathbf{n} = (n_1, \dots, n_{12}) \quad , \quad (4)$$

where n_i represent the number of individuals that belong to stage i in the population. If the population is composed of one strain and assuming no spatial structure, the composition of the population at time $t + 1$ will be 151

$$\mathbf{n}(t + 1) = \mathbf{A}\mathbf{n}(t) \quad , \quad (5)$$

where $\mathbf{A} = \mathbf{U} + \mathbf{F}$. 152

If the population is composed of two strains, the number of J2 individuals of strain i which survive to $t + 1$ will be 153

$$V_i(t + 1) = V_i(t) - \alpha_{ji} V_i(t) P_j(t) \quad , \quad (6)$$

where α_{ji} is the rate at which adults from strain j bite J2s of strain i , $P_j(t)$ is the number of predatory adults of strain j , and $V_i(t)$ is the number of J2s of strain i . $P_j(t) = \lambda n_A^j$, where λ is the probability of having a predatory mouth form and n_A^j is the total number of adults of strain j , which includes YA, BA $_i$, and OA stages. For the non-plastic strain, $\lambda = 1$ regardless of the bacterial diet, while for the plastic strain, $\lambda = 0.02$ on *E. coli* and $\lambda = 0.9$ on *Novosphingobium*. α_{ji} for each strain on the two different bacterial diets was estimated using the killing assay data [12]. 154

To simulate the effect of spatial heterogeneity on the population dynamics, we simulate the population on 10×10 lattice, in which each of the 100 points represent a locality with \mathcal{S}_0 food of a given type. The plastic and non-plastic strains start the simulation from the four corners of the lattice (Fig 2a). In nature, upon the depletion of bacteria on the beetle carcass, *P. pacificus* dauer larvae are generated and rapidly disperse in the surrounding soil [38]. To simulate the dispersion of the dauer larvae in our model, at each step m dauer larvae disperse to all the neighboring localities with more food. We used both the von Neumann neighborhood (4 neighbors for a non-boundary locality) and the Moore neighborhood (6 neighbors for a non-boundary locality), but given similarities of our results using these two alternative neighborhood definitions, we only show the results based on the Moore neighborhood. 155

By including predation and migration, the expected composition of strain i in a given locality at time $t + 1$ would be 156

$$\mathbf{n}_i(t + 1) = \mathbf{A}_i \mathbf{n}_i(t) - \phi_i(t) - \omega_i(t) \quad , \quad (7)$$

where $\phi_i(t)$ is the number of J2 individuals of strain i that were killed and $\omega_i(t)$ is the number of dauer larvae of strain i that emigrated from the locality at time t . 157

The software used to run all simulations was written in Python 3.7 with NumPy [17] version 1.21.0. All code and data are available at https://github.com/Kalirad/lattice_projection. 158

Stage	$P_{i \rightarrow j}$		
	<i>E. coli</i>	<i>Novosphingobium</i>	Starvation
E	0.0415	0.0415	0
J2 (\rightarrow d)	0	0	0.1
J2 (\rightarrow J3)	0.055	0.055	0
J3	0.085	0.085	0
Dauer	0.1	0.1	0
J4	0.07	0.07	0
YA	0.1	0.13 (P), 0.4 (NP)	016
BA _i	0.0415	0.0415	0.0415

Table 1. The transition probabilities used in the model. The transition values that differ between the plastic (P) and the non-plastic (NP) strains are in bold.

Adult stage	<i>E. coli</i>		<i>Novosphingobium</i>	
	m_P	m_{NP}	m_P	m_{NP}
BA ₁	22.65	19.8	11.66	16.88
BA ₂	68.45	60.3	62.53	80.77
BA ₃	57.05	43.02	47.13	77.7
BA ₄	33.4	19.9	13.94	16.28
BA ₅	4.97	6.6	0.72	1.4
R_0	186.52	149.62	135.98	193.03

Table 2. The fecundity (m) of the five breeding adult stages in our model for the plastic (P) and the non-plastic (NP) strains on two different bacterial diets based on the laboratory measurements. R_0 is the rate of increase per generation, given by the leading eigenvalue of \mathbf{FN} , where \mathbf{F} is the fecundity matrix and \mathbf{N} is the fundamental matrix of a given transition matrix [11].

RESULTS

The plastic strain suffers from cost of plasticity on *Novosphingobium*

The experimental data from Dardiry *et al.* [12] indicate a negative trade-off between fecundity and plasticity, i.e., the number of eggs laid on *Novosphingobium* by the plastic strain was significantly reduced compared to the number of eggs laid on *E. coli* - this trade-off is reflected in the estimated R_0 in our model based on the experimental data (Table 2). Our projection of the number of adults and dauers of the plastic strain relative to the non-plastic strain on our 10×10 lattice reflects the severity of this trade-off for the plastic strain, where on *E. coli*, the final frequency of dauers of the plastic strain relative to all the dauers on the lattice is 0.65, while on *Novosphingobium*, this frequency is reduced to 0.06 (Fig 2 b-c). It should be noted that the dominance of the plastic strain on *E. coli* itself is not a trivial observation, since a projection in a mixed population with no spatial structure would always result in the non-plastic strain driving the plastic strain to extinction due to the fact that the non-plastic adults always develop the predatory Eu mouth form (Supp fig [to be added]).

Spatial heterogeneity of resources can affect the cost of plasticity

It is reasonable to assume that only in within the confines of the laboratory, a living organism would find itself on a single resource. A simple approach to introduce spatial resource heterogeneity to our lattice model is to divide the lattice into four equal

patches and alternatively assign *Novosphingobium* and *E. coli* to each patch. In “pattern 1”, plastic strain starts on *E. coli* patches, while in “pattern 2”, it starts the simulation on *Novosphingobium*. While the plastic strain is successful on pure *E. coli* (Fig 2 b), the higher fecundity of the plastic strain on its starting patch in “pattern 1” is not enough to counter the non-plastic strain, specifically given its faster development and its high R_0 on *Novosphingobium* (Fig 3a). Pattern 2 provides a surprisingly dynamic, where the plastic strain, starting on *Novosphingobium*, occupies almost half of the lattice, in spite of its lower R_0 on its starting patch (Fig 3b). This seemingly surprising result in pattern 2 is the result of the higher developmental speed of the plastic strain on *Novosphingobium*.

To investigate the effect of the dauer larvae dispersal in our lattice on the dynamics of the model, we measured the final frequency of the adults and the dauer larvae of the plastic strain across a wide range of dispersion rates (Fig 4). On *E. coli*, the plastic strain, with its high R_0 , dominates even more with higher dispersion (Fig 4a). On *Novosphingobium* and pattern 1, both of which are unfavorable to the plastic strain, higher dispersion leads to the eradication of the plastic strain from the lattice (Fig 4b-c). Interestingly, pattern 2 is somewhat robust to the increase in the dispersion (Fig 4d).

The effect of the functional response on the projections is affected by the spatial heterogeneity of resources

The dynamics of predation in our model, determined by Eq. 6, can be characterized as a type I functional response, where the number of prey that is consumed increases linearly as a function of the number of preys [19, 20]. More than half a century after Holling’s characterization of prey consumption, his framework is still widely used [14]. In order to explore the effect of density-dependent predation, we modified Eq. 6 into

$$V_i(t+1) = V_i(t) - \frac{\alpha_{ji}V_i(t)}{1 + \alpha_{ji}hV_i(t)}P_j(t) \quad , \quad (8)$$

where h determines the handling and ingestion time. Although our estimates of α_{ji} is based on the laboratory data from our predation assay (described in [3, 42, 52]). In this assay ≈ 3000 J2 larvae of strain i are placed in a plate with 20 adults of strain j and, after 24 hours, the number of corpses on the plate are counted. The predation rate is calculated by fitting the solution to Eq.6 to the data. Since the number of prey and predators are fixed in this assay, it is impossible to divine any concrete relationship between prey and predator densities and per capita killing rate. In addition, in spite of studies on intraguild killing in *P. pacificus* (e.g., [52, 62]), there is no data to enable us to estimate h with any level of certainty. To sidestep this issue, we investigated the behavior of our lattice model over a wide range of h . It should be noted that with very low h , Eq 8 converges to Eq 6. We did not consider type III functional response, simply because it is simply a general version of type II and it would require us to introduce more arbitrary parameters to the model.

In a lattice with *E. coli* as its source, the plastic strain dominates across a wide range of handling time and dispersion rates, specifically in low handling time regimes (Fig 5 a). The fact that low handling time in this regime is beneficial to the plastic strain indicates that its high R_0 results in more than enough predatory adults, thus preferring a higher killing rate, which type II response with low h provides. In both unfavorable regimes to the plastic strain, i.e., *Novosphingobium* and pattern 1, high h , resulting in lower predation of the plastic J2 larvae by the non-plastic adults, and low

dispersion is slightly favorable to the plastic strain 5 b-c). Interestingly, the dynamics of pattern 2 is rather robust to a wide range of handling time and dispersion rates.

DISCUSSION

While it is impossible to deny the role of adaptive plasticity in evolution [61], many issues concerning adaptive plasticity, ranging from mechanisms at the molecular level to its ecological consequences, are yet to be fully understood. The cost of adaptive plasticity is one issue that is ostensibly a logical consequence of being plastic and yet, there has been a paucity of evidence in its favor. Here, following experimental investigations by Dardiry *et al.* [12], we studied the possible ecological ramifications of the cost of adaptive plasticity in *P. pacificus*. Our results show that spatial structure (modeled as a two-dimensional lattice) and spatial heterogeneity in resource distribution can affect how the cost of adaptive plasticity manifest itself in an ecosystem.

Dardiry *et al.* [12] demonstrated a clear trade-off between plasticity and fecundity, as a major component of fitness in *P. pacificus* mouth-form plasticity. In contrast, it is surprising that there has been a dearth of evidence supporting the cost of plasticity in other experimental investigations. DeWitt *et al.* in their much-cited theoretical contribution on this topic [13], broke down the cost of plasticity into: (1) maintenance costs, (2) production costs, (3) information acquisition costs, (4) developmental instability, and (5) genetic costs. The first three categories relate to the excess energy required to maintain express and maintain a plastic trait in an individual. Developmental instability is an intrinsic cost of plasticity compared to a canalized developmental program. The last category, genetic costs, is a slightly odd addition, since any trait could suffer from linkage with deleterious loci, having negative pleiotropic effects on other genes, or epistatically affecting other loci. Also, it should be noted that at the time of that original writing, the genetic and molecular control of any plastic trait was not known. This is currently changing with model systems, such as mouth-form plasticity in *P. pacificus*, providing molecular mechanisms of phenotypic plasticity. However, while such studies provide complex gene regulatory networks, their complexity is not unusually large and they contain many pleiotropic factors that are also known from other regulatory interactions (reviewed in [4]). Thus, the growing understanding of the genetic and molecular mechanisms of plastic trait regulation do not support an unusually high genetic cost.

Also, the excess-energy costs (1 - 3) would invariably depend on the molecular machinery behind a plastic trait. But how energetically costly a plastic phenotype could be? Answering such question depends on the identity of the plastic organism of interest, as well as our understanding of the molecular machinery that generates the observed polyphenism. Even in a model as extensively studied as *P. pacificus*, and in spite of the bistability of the plastic trait, i.e., predatory versus non-predatory mouth morphs, the molecular machinery underpinning the plasticity is not fully elucidated [6, 7, 31, 43–45]. Other, well-characterized molecular circuitries behind polyphenism can be found in an extensive body of literature on “phenotypic heterogeneity” in microorganisms (reviewed in [1]). For example, LuxI/LuxR signaling in *Vibrio fischeri*, which enables quorum sensing and results in bioluminescence, is one of such circuitries [15, 32]. Given the the genes and proteins involved in LuxI/LuxR signaling, it is not clear if such a circuitry, relative to total energetic cost of the cell, would burden the organism with an excessive energy bill [10, 25, 55]. In addition, one of the main sources of non-genetic phenotypic heterogeneity are Bi-stable toggle switches [4, 41, 54], and their (relative) simplicity can hardly be an evidence for an inherent energetic cost associated with plasticity.

Importantly, the prevalence of bi-stable switches, as drivers of non-genetic phenotypic heterogeneity, and the relative simplicity of other well-characterized mechanisms found in microorganisms do not imply that the first three sources of cost of plasticity, as outlined by DeWitt *et al.*, simply do not exist. Instead, in the absence of knowledge on the genetic and molecular basis of a plastic trait, it is not warranted to automatically attach an excess energetic cost for the plastic trait under study. If a plastic trait is generated by a bi-stable switch, or a similarly simple genetic circuit, the energetic cost relative to the total energy bill of the organism, could be low enough not to affect fitness. Concerning the fourth source of cost, the developmental instability, even DeWitt *et al.* did not count it as a necessary consequence of phenotype plasticity, and a recent theoretical exploration of the relation between two seems to suggest that phenotypic plasticity is feasible without jeopardizing developmental robustness [28].

In the case of *P. pacificus* mouth-form plasticity, Dardiry and colleagues strongly imply a cost associated with being plastic in their comparison of a pair of *P. pacificus* strains [12]. However, given the behavioral nature of the plastic trait, i.e., enabling intraguild predation, establishing a trade-off in the plastic strain in isolation is not sufficient to infer the ecological consequences of this cost. The model presented here is an attempt to understand the ecological effects of the cost of plasticity in space and time. The logic behind such an approach, investigating the effect of spatial and temporal patterns on population and ecosystem dynamics, has long been advocated in ecology (e.g., [27]). *P. pacificus* provides an ideal case study for incorporating laboratory measurements with computational models to understand the realized cost of plasticity in nature. Thus, this system can be expanded in the future in multiple directions by overcoming current limitations.

Indeed, we are not oblivious to the limitations of our current approach to modeling. First, as noted in our discussion of the functional response, our characterization of the predatory interaction between the plastic and the non-plastic strains is limited to the laboratory data from our predation assay, which lacks the necessary manipulations to accurately estimate the type and the parameters of functional response in *P. pacificus*. We hope that new experimental attempts to measure predation in *P. pacificus* will enable us to rectify this issue in future models. Second, rate of dispersion of dauer larvae in *P. pacificus* is still a known unknown. In particular, we simply do not know if the rate of dispersion is different between the plastic and non-plastic strains. Future studies in the mold of the approach used by Renahan *et al.* [38] will surely shed some light on this elusive aspect of *P. pacificus* ecology. Third, one could argue that a deterministic demographic model inevitably neglects the stochastic vagaries of nature. Although this criticism can be leveled against demographic models in general (e.g., see [36]), we are sympathetic to it, but believe that even a deterministic demographic model can provide insights into the ecology of an organism. Finally, spatial heterogeneity in our model could be considered too simplistic. This is demonstrably true, but investigating the effects of spatial heterogeneity of *E. coli* and *Novosphingobium* is simply an exploration of the importance of the constitution of the ecological niche, including the biotic and the abiotic factors, on the cost of plasticity. Our goal is to follow this study by devising increasingly more sophisticated computational models to take advantage of our ability to thoroughly study *P. pacificus* in the lab and to experimentally test some of the predictions of these models. We hope that such a direct feedback between experimental measurements and modeling can produce fascinating insights into the “entangled banks” of nature.

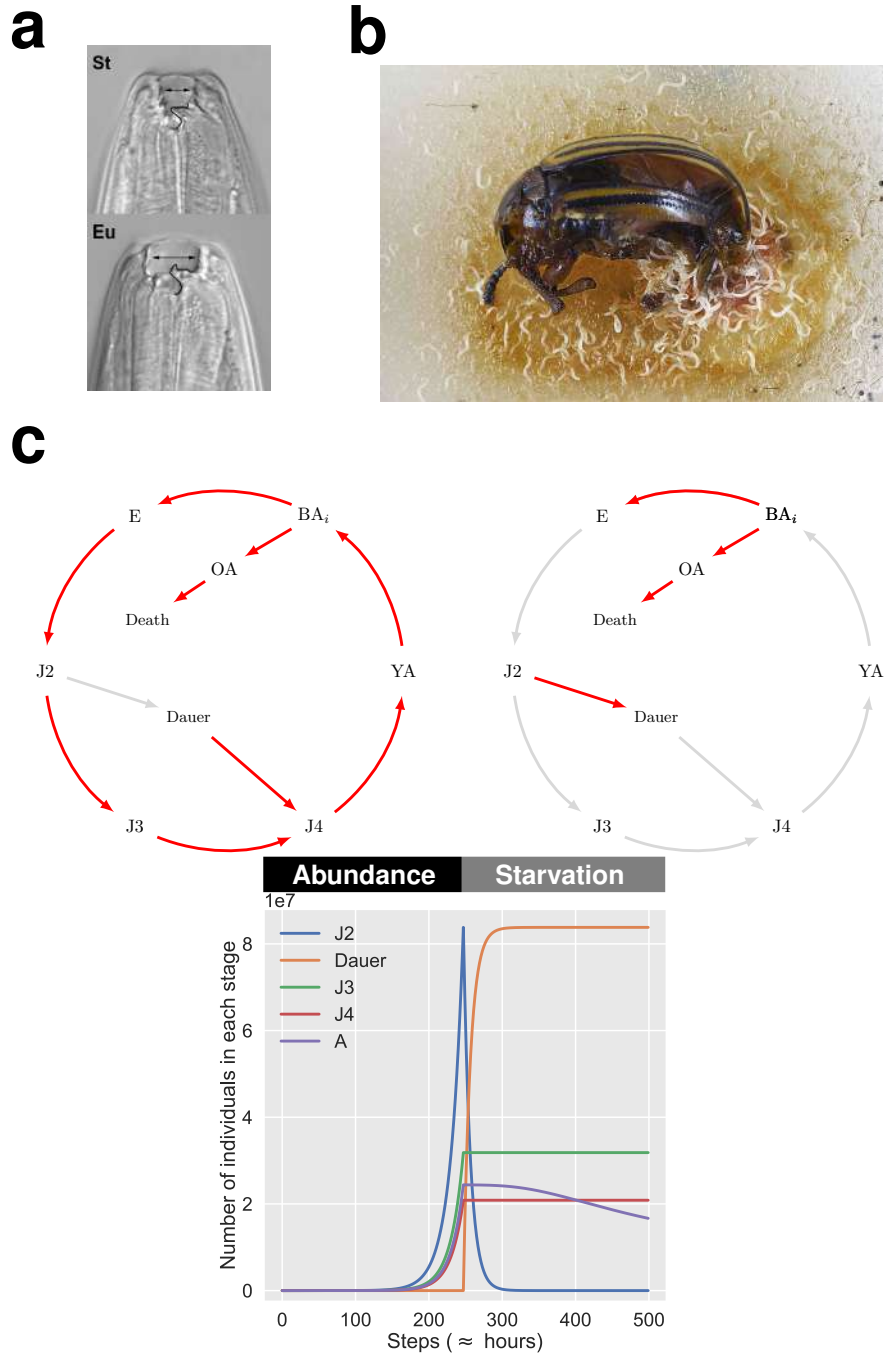


Figure 1. (a) The nematode *P. pacificus* expresses two alternative mouth forms, the eury stomatous (Eu) and the stenostomatous (St) from, in response to a variety of external stimuli. (b) In nature, *P. pacificus* can be found feeding on the bacteria decomposing the carcass of beetles, in this case *Leptinotarsa decemlineata*, a chrysomelid beetle (photo courtesy of Matthias Hermann). (c) In model, the worms follow two alternative life cycles. The red arrows indicate the possible transitions between developmental stages in each cycle. The dynamics of the model switches from the abundance life cycle to the starvation cycle upon the depletion of the food in the environment. Simulations started with 50 young adults of the plastic strain with *E. coli* as the diet. (E: egg, YA: young adult, BA_i: breeding adult of day *i*, OA: old adult. In the time series, A includes YA, B₁ - B₅, and OA. $\mathcal{S}_0 = 10^9$.)

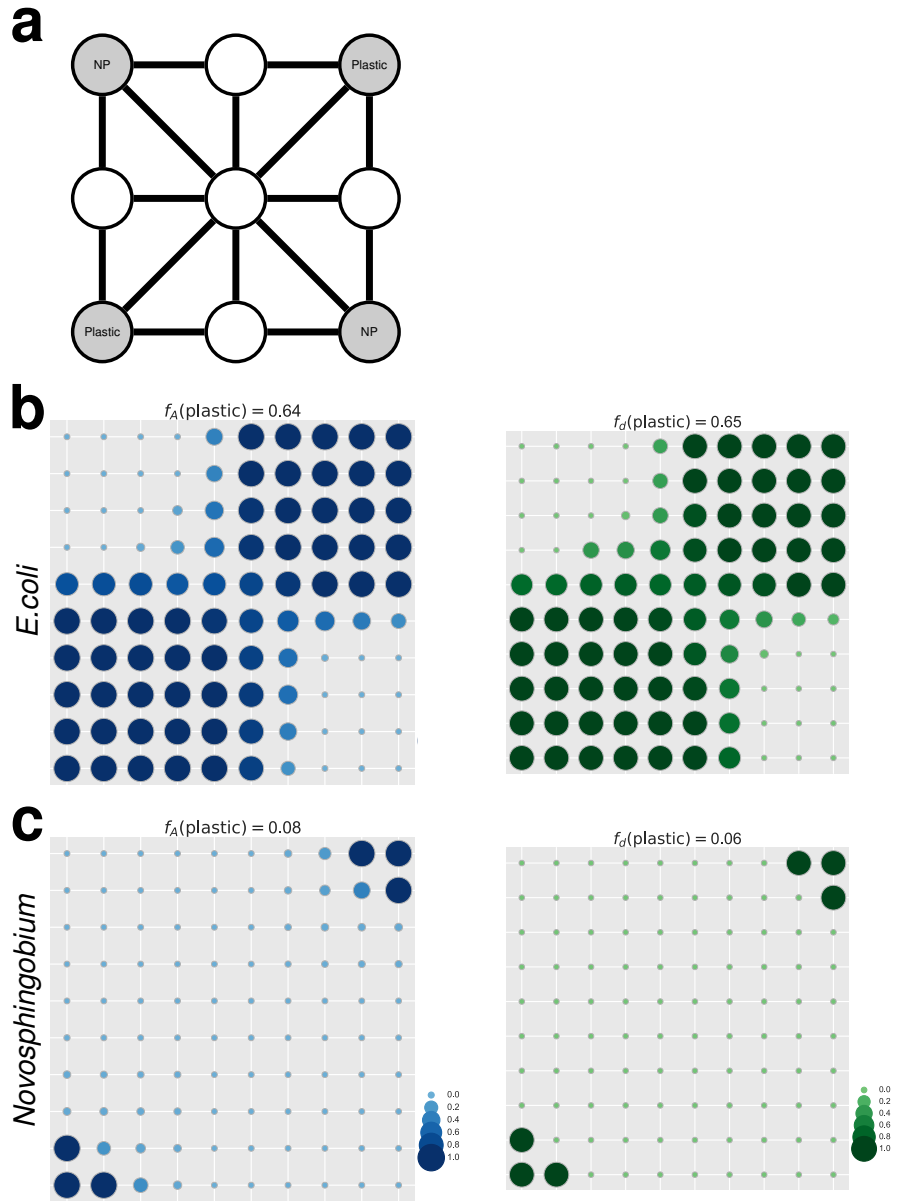


Figure 2. (a) To simulate the effect of spatial heterogeneity on the cost of plasticity, we simulate the dynamics of the population over a $n \times n$ lattice. At the start of the simulation, on each corner of the lattice, 50 young adults of the plastic or the non-plastic (NP) strain are positioned. The vertices in the lattice represent the possible dispersal paths for the dauer larvae in the lattice. In the following simulations a 10×10 lattice was used. (b) On *E. coli*, the higher fecundity of the plastic strain depletes the resource in each locality faster, enabling the strain to rapidly spread to neighboring localities. This effect is reflected in the frequency of the plastic strain adults, relative to all the adults in each population, as well as the frequency of the plastic strain dauer larvae, relative to all the dauer larvae on the lattice. (c) On *Novosphingobium*, the faster developmental speed of the non-plastic strain and its higher fecundity relative to the plastic strain, makes it a formidable competitor. Simulations were carried for 800 steps. ($m = 0.02$ and $\mathcal{S}_0 = 10^{10}$ in each locality. Predation rates: on *E. coli*, $\eta_{\text{plastic}} = 1.7 \times 10^{-4}$ and $\eta_{\text{NP}} = 3.3 \times 10^{-4}$; on *Novosphingobium*, $\eta_{\text{plastic}} = 6.4 \times 10^{-5}$ and $\eta_{\text{NP}} = 4.7 \times 10^{-4}$. Unless otherwise stated, the same parameters are used in the subsequent simulations.)

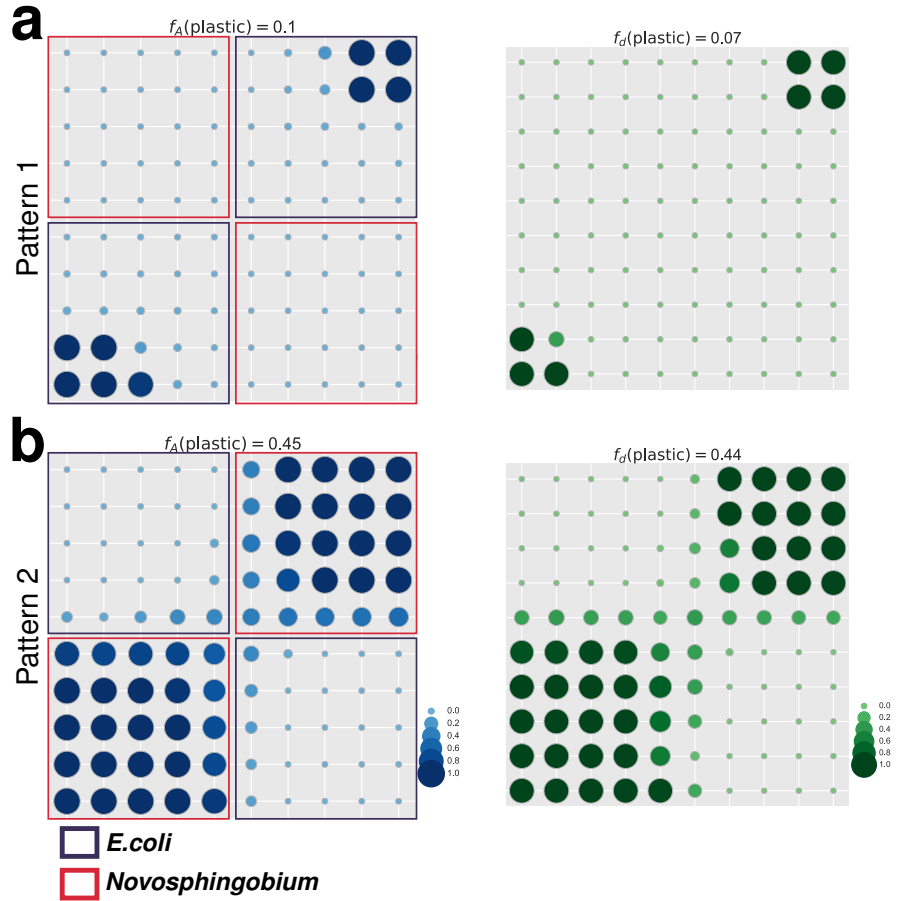


Figure 3. To explore the effect of resource heterogeneity on the population dynamics of the plastic strain on the 10×10 lattice, we divided the lattice into four patches and allocated *E. coli* and *Novosphingobium* to each patch in two different patterns. For both patterns in (a) and (b), the frequency of the plastic strain adults, as well as those of dauer larvae, in each population at the end of 800 steps of simulation are shown. In (a), the plastic strain starts on *E. coli* and the non-plastic strain starts on *Novosphingobium*. In this spatial arrangement, given the higher R_0 and faster development of the non-plastic strain on *Novosphingobium*, it dominates the lattice. (b) If the plastic strain starts on *Novosphingobium* and the non-plastic strain starts on *E. coli*, the plastic strain can compete fairly well. The ability of the plastic strain to compete successfully on pattern 2 is due to its faster development, relative to its developmental speed on *E. coli*, and in spite of its lower R_0 on *Novosphingobium*.

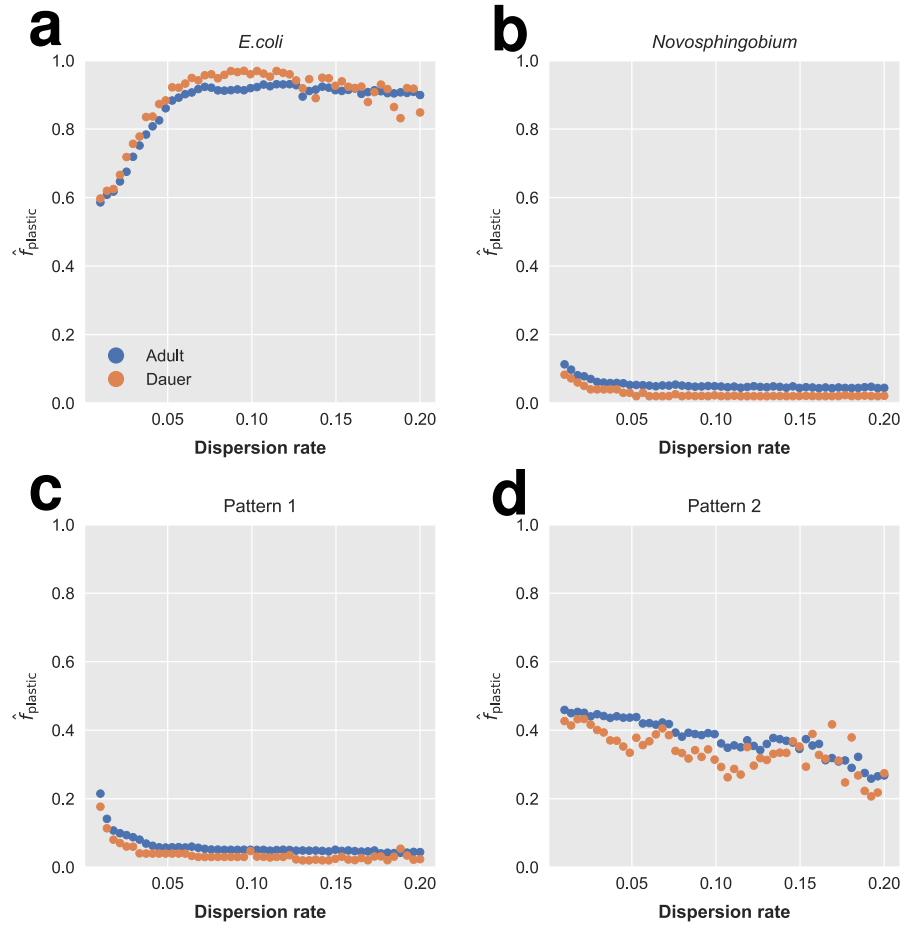


Figure 4. In order illustrate the effects of dispersal of the dauer larvae on the population dynamics of the plastic strain on the 10×10 lattice, the frequency of the plastic strain adults and dauer larvae on the lattice at the end of 800 steps are plotted as a function of the dispersion rate (m). (a) On the *E. coli* diet, which is favourable for the plastic strain, the increase in dispersal allow this strain to utterly dominate the lattice. On *Novosphingobium* and pattern 1, (b-c) which are both unfavorable to the plastic strain, the increased dispersion rate results in the elimination of the plastic strain. (d) Interestingly, the final frequencies of the plastic adults and dauer larvae on pattern 2 is somewhat robust to change in the dispersion rate.

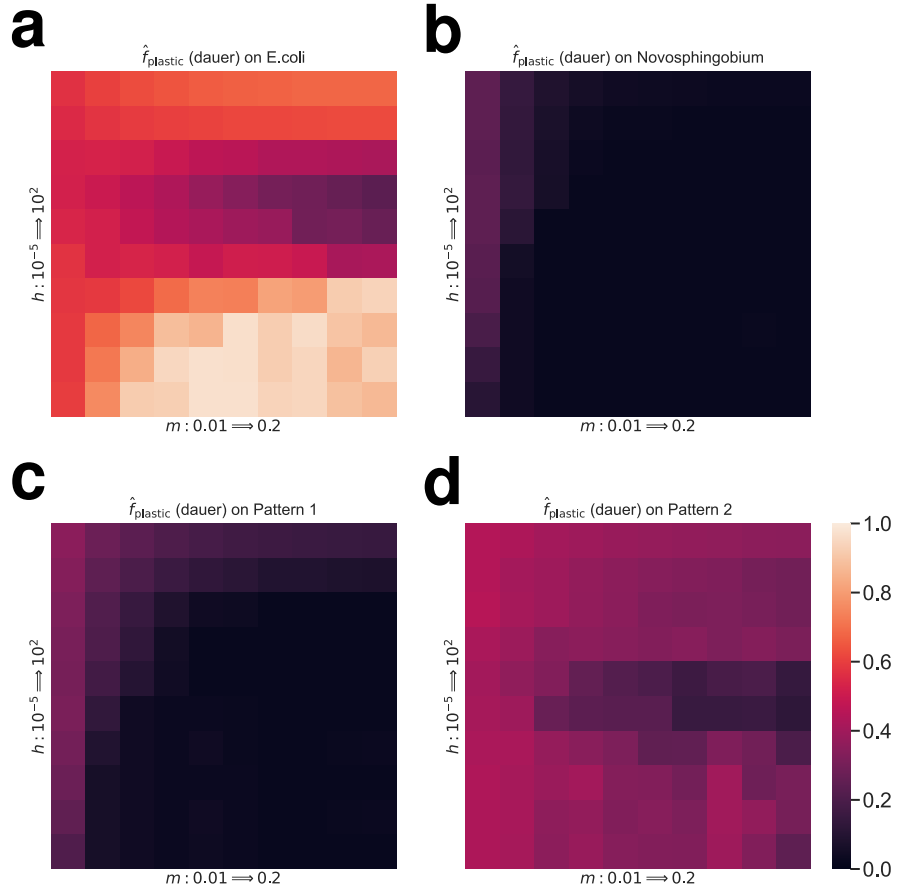


Figure 5. To illustrate the effect of the type of functional response, we looked at the effect of varying the handling time (h) in Eq.8, as well as changing the dispersion rate (m) on the population dynamics of the plastic strain on the 10×10 lattice. Each cell each of the heatmaps indicated the frequency of the dauer larvae of the plastic strain, relative to all the dauer larvae on the lattice, after 800 steps with a given combination of values for h and m . (a) On *E. coli*, the plastic strain can dominate the lattice when handling time and/or dispersion are low. The fact that low handling time favours the plastic strain indicates that given its much higher R_0 on *E. coli*, the strain benefits from predation, even though only 2% of the plastic adults develop the predatory mouth form. On *Novosphingobium* and pattern 1 (b-c), both previously shown to be unfavorable to the plastic strain, only with very high handling time, i.e., low effective predation, and low dispersal, the plastic strain dauer larvae reach non-zero frequencies on the lattice. Interestingly, pattern 2 is again somewhat robust, this time to variation in handling time and dispersion.

References

1. M. Ackermann. A functional perspective on phenotypic heterogeneity in microorganisms. *Nature Reviews Microbiology*, 13(8):497–508, 2015.
2. A. A. Agrawal. A scale-dependent framework for trade-offs, syndromes, and specialization in organismal biology. *Ecology*, 101(2):e02924, 2020.
3. N. Akduman, J. W. Lightfoot, W. Röseler, H. Witte, W.-S. Lo, C. Rödelberger, and R. J. Sommer. Bacterial vitamin b12 production enhances nematode predatory behavior. *The ISME Journal*, 14(6):1494–1507, 2020.
4. G. Balázsi, A. van Oudenaarden, and J. J. Collins. Cellular decision making and biological noise: From microbes to mammals. *Cell*, 144(6):910–925, 2011.
5. A. Bradshaw. Evolutionary significance of phenotypic plasticity in plants. volume 13 of *Advances in Genetics*, pages 115–155. Academic Press, 1965.
6. L. T. Bui, N. A. Ivers, and E. J. Ragsdale. A sulfotransferase dosage-dependently regulates mouthpart polyphenism in the nematode *Pristionchus pacificus*. *Nature Communications*, 9(1):4119, 2018.
7. L. T. Bui and E. J. Ragsdale. Multiple Plasticity Regulators Reveal Targets Specifying an Induced Predatory Form in Nematodes. *Molecular Biology and Evolution*, 36(11):2387–2399, 07 2019.
8. H. S. Callahan, H. Maughan, and U. K. Steiner. Phenotypic plasticity, costs of phenotypes, and costs of plasticity. *Annals of the New York Academy of Sciences*, 1133(1):44–66, 2008.
9. H. Caswell. *Sensitivity Analysis: Matrix Methods in Demography and Ecology*. Springer, New York, 2019.
10. L. Claudia and R. E. G. *Vibrio fischeri luxS and ains: Comparative study of two signal synthases*. *Journal of Bacteriology*, 186(12):3873–3881, 2021/12/16 2004.
11. J. Cushing and Z. Yicang. The net reproductive value and stability in matrix population models. *Natural Resource Modeling*, 8(4):297–333, 1994.
12. M. Dardiry, V. Piscobulu, A. Kalirad, and R. J. Sommer. Experimental and theoretical support for costs of plasticity and phenotype in a nematode cannibalistic trait. 2022.
13. T. J. DeWitt, A. Sih, and D. S. Wilson. Costs and limits of phenotypic plasticity. *Trends in Ecology Evolution*, 13(2):77–81, 1998.
14. R. P. Dunn and K. A. Hovel. Predator type influences the frequency of functional responses to prey in marine habitats. *Biology Letters*, 16(1):20190758, 2020.
15. A. Eberhard. Inhibition and activation of bacterial luciferase synthesis. *Journal of bacteriology*, 109(3):1101–1105, 03 1972.
16. A. Forsman. Rethinking phenotypic plasticity and its consequences for individuals, populations and species. *Heredity*, 115(4):276–284, 2015.

-
17. C. R. Harris, K. J. Millman, S. J. van der Walt, R. Gommers, P. Virtanen, D. Cournapeau, E. Wieser, J. Taylor, S. Berg, N. J. Smith, R. Kern, M. Picus, S. Hoyer, M. H. van Kerkwijk, M. Brett, A. Haldane, J. F. del Río, M. Wiebe, P. Peterson, P. Gérard-Marchant, K. Sheppard, T. Reddy, W. Weckesser, H. Abbasi, C. Gohlke, and T. E. Oliphant. Array programming with numpy. *Nature*, 585(7825):357–362, 2020.
 18. M. Herrmann, W. E. Mayer, R. L. Hong, S. Kienle, R. Minasaki, and R. J. Sommer. The Nematode *Pristionchus pacificus* (Nematoda: Diplogastridae) Is Associated with the Oriental Beetle *Exomala orientalis* (Coleoptera: Scarabaeidae) in Japan. *Zoological Science*, 24(9):883 – 889, 2007.
 19. C. S. Holling. The components of predation as revealed by a study of small-mammal predation of the european pine sawfly. *The Canadian Entomologist*, 91(5):293–320, 1959.
 20. C. S. Holling. Some characteristics of simple types of predation and parasitism. *The Canadian Entomologist*, 91(7):385–398, 1959.
 21. N. Kanzaki, M. Herrmann, C. Weiler, W. Röseler, T. Theska, J. Berger, C. Rödelsperger, and R. J. Sommer. Nine new *pristionchus* (nematoda: Diplogastridae) species from china. *Zootaxa*, 4943(1):1–66, 2021/12/07 2021.
 22. H. Keyfitz, Nathan; Caswell. *Applied mathematical demography*. Springer, New York, 2005.
 23. M. R. Kieninger, N. A. Ivers, C. Rödelsperger, G. V. Markov, R. J. Sommer, and E. J. Ragsdale. The nuclear hormone receptor *nhr-40* acts downstream of the sulfatase *eud-1* as part of a developmental plasticity switch in *Pristionchus*. *Current Biology*, 26(16):2174–2179, 2016.
 24. R. A. Krebs and M. E. Feder. Natural variation in the expression of the heat-shock protein *hsp70* in a population of *Drosophila Melanogaster* and its correlation with tolerance of ecologically relevant thermal stress. *Evolution*, 51(1):173–179, 1997.
 25. L. N. L., D. A. K., B. J. L., and S. E. V. Bright mutants of *vibrio fischeri* *es114* reveal conditions and regulators that control bioluminescence and expression of the *lux* operon. *Journal of Bacteriology*, 192(19):5103–5114, 2021/12/16 2010.
 26. M. Lenuzzi, H. Witte, M. Riebesell, C. Rödelsperger, R. L. Hong, and R. J. Sommer. Influence of environmental temperature on mouth-form plasticity in *pristionchus pacificus* acts through *daf-11*-dependent *cgmp* signaling. *Journal of Experimental Zoology Part B: Molecular and Developmental Evolution*, n/a(n/a), 2021.
 27. S. A. Levin. The problem of pattern and scale in ecology: The robert h. macarthur award lecture. *Ecology*, 73(6):1943–1967, 1992.
 28. R. Matthey-Doret, J. A. Draghi, and M. C. Whitlock. Plasticity via feedback reduces the cost of developmental instability. *Evolution Letters*, 4(6):570–580, 2020.
 29. J. M. Meyer, P. Baskaran, C. Quast, V. Susoy, C. Rödelsperger, F. O. Glöckner, and R. J. Sommer. Succession and dynamics of *pristionchus* nematodes and their microbiome during decomposition of *oryctes borbonicus* on la réunion island. *Environmental Microbiology*, 19(4):1476–1489, 2021/12/06 2017.

-
30. C. J. Murren, J. R. Auld, H. Callahan, C. K. Ghalambor, C. A. Handelsman, M. A. Heskell, J. G. Kingsolver, H. J. Maclean, J. Masel, H. Maughan, D. W. Pfennig, R. A. Relyea, S. Seiter, E. Snell-Rood, U. K. Steiner, and C. D. Schlichting. Constraints on the evolution of phenotypic plasticity: limits and costs of phenotype and plasticity. *Heredity*, 115(4):293–301, 2015.
 31. S. Namdeo, E. Moreno, C. Rödelsperger, P. Baskaran, H. Witte, and R. J. Sommer. Two independent sulfation processes regulate mouth-form plasticity in the nematode *Pristionchus pacificus*. *Development*, 145(13), 07 2018. dev166272.
 32. K. H. Neelson, T. Platt, and J. W. Hastings. Cellular control of the synthesis and activity of the bacterial luminescent system. *Journal of bacteriology*, 104(1):313–322, 10 1970.
 33. R. A. Newman. Adaptive plasticity in amphibian metamorphosis. *BioScience*, 42(9):671–678, 2021/11/26/ 1992.
 34. D. W. Pfennig. *Phenotypic Plasticity Evolution: Causes, Consequences, Controversies*. CRC Press, 2021.
 35. K. Popper. *Unended Quest*. Routledge, 1992.
 36. V. Radchuk, S. Kramer-Schadt, and V. Grimm. Transferability of mechanistic ecological models is about emergence. *Trends Ecol Evol*, 34(6):487–488, Jun 2019.
 37. E. J. Ragsdale, M. R. Müller, C. Rödelsperger, and R. J. Sommer. A developmental switch coupled to the evolution of plasticity acts through a sulfatase. *Cell*, 155(4):922–933, 2013.
 38. T. Renahan, W.-S. Lo, M. S. Werner, J. Rochat, M. Herrmann, and R. J. Sommer. Nematode biphasic ‘boom and bust’ dynamics are dependent on host bacterial load while linking dauer and mouth-form polyphenisms. *Environmental Microbiology*, 23(9):5102–5113, 2021/12/04 2021.
 39. S. M. Scheiner and D. Berrigan. The genetics of phenotypic plasticity. viii. the cost of plasticity in daphnia pulex. *Evolution*, 52(2):368–378, 2021/11/26/ 1998.
 40. I. I. Schmalhausen. *Factors of evolution: the theory of stabilizing selection*. The University of Chicago Press, 1949.
 41. R. Sekine, M. Yamamura, S. Ayukawa, K. Ishimatsu, S. Akama, M. Takinoue, M. Hagiya, and D. Kiga. Tunable synthetic phenotypic diversification on waddington’s landscape through autonomous signaling. *Proceedings of the National Academy of Sciences*, 108(44):17969–17973, 2011.
 42. V. Serobyán, E. J. Ragsdale, M. R. Müller, and R. J. Sommer. Feeding plasticity in the nematode *Pristionchus pacificus* is influenced by sex and social context and is linked to developmental speed. *Evolution & Development*, 15(3):161–170, 2013.
 43. V. Serobyán, H. Xiao, S. Namdeo, C. Rödelsperger, B. Sieriebriennikov, H. Witte, W. Röseler, and R. J. Sommer. Chromatin remodelling and antisense-mediated up-regulation of the developmental switch gene eud-1 control predatory feeding plasticity. *Nature Communications*, 7(1):12337, 2016.
 44. B. Sieriebriennikov, N. Prabh, M. Dardiry, H. Witte, W. Röseler, M. R. Kieninger, C. Rödelsperger, and R. J. Sommer. A developmental switch generating phenotypic plasticity is part of a conserved multi-gene locus. *Cell Reports*, 23(10):2835–2843.e4, 2018.

-
45. B. Sieriebriennikov, S. Sun, J. W. Lightfoot, H. Witte, E. Moreno, C. Rödelsperger, and R. J. Sommer. Conserved nuclear hormone receptors controlling a novel plastic trait target fast-evolving genes expressed in a single cell. *PLOS Genetics*, 16(4):1–27, 04 2020.
 46. M. J. Smekens and P. H. van Tienderen. Genetic variation and plasticity of *plantago coronopus* under saline conditions. *Acta Oecologica*, 22(4):187–200, 2001.
 47. R. J. Sommer and A. McGaughran. The nematode *Pristionchus pacificus* as a model system for integrative studies in evolutionary biology. *Molecular Ecology*, 22(9):2380–2393, 2013.
 48. U. K. Steiner and J. Van Buskirk. Environmental stress and the costs of whole-organism phenotypic plasticity in tadpoles. *Journal of Evolutionary Biology*, 21(1):97–103, 2008.
 49. S. Sun, C. Rödelsperger, and R. J. Sommer. Single worm transcriptomics identifies a developmental core network of oscillating genes with deep conservation across nematodes. *Genome Res*, 31(9):1590–1601, Sep 2021.
 50. J. Van Buskirk and U. K. Steiner. The fitness costs of developmental canalization and plasticity. *Journal of Evolutionary Biology*, 22(4):852–860, 2009.
 51. P. H. Van Tienderen. Evolution of generalists and specialists in spatially heterogeneous environments. *Evolution*, 45(6):1317–1331, Sep 1991.
 52. L. J. W., D. Mohannad, K. Ata, G. Stefano, E. Gabi, W. Hanh, W. Martin, R. Christian, T. Arne, and S. R. J. Sex or cannibalism: Polyphenism and kin recognition control social action strategies in nematodes. *Science Advances*, 7(35):eabg8042, 2021/12/03.
 53. C. Waddington. *The Strategy of the Genes*. Routledge, 1957.
 54. J. Wang, K. Zhang, L. Xu, and E. Wang. Quantifying the waddington landscape and biological paths for development and differentiation. *Proceedings of the National Academy of Sciences*, 108(20):8257–8262, 2011.
 55. C. M. Waters and B. L. Bassler. Quorum sensing: Cell-to-cell communication in bacteria. *Annual Review of Cell and Developmental Biology*, 21(1):319–346, 2005. PMID: 16212498.
 56. C. J. Weadick and R. J. Sommer. Mating system transitions drive life span evolution in *pristionchus* nematodes. *The American Naturalist*, 187(4):517–531, 2021/12/17 2016.
 57. C. J. Weadick and R. J. Sommer. Unexpected sex-specific post-reproductive lifespan in the free-living nematode *pristionchus exspectatus*. *Evolution & Development*, 18(5-6):297–307, 2021/12/17 2016.
 58. C. J. Weadick and R. J. Sommer. Hybrid crosses and the genetic basis of interspecific divergence in lifespan in *pristionchus* nematodes. *Journal of Evolutionary Biology*, 30(3):650–657, 2021/12/17 2017.
 59. M. S. Werner, M. H. Claaßen, T. Renahan, M. Dardiry, and R. J. Sommer. Adult influence on juvenile phenotypes by stage-specific pheromone production. *iScience*, 10:123–134, 2018.

-
60. M. S. Werner, B. Sieriebriennikov, T. Loschko, S. Namdeo, M. Lenuzzi, M. Dardiry, T. Renahan, D. R. Sharma, and R. J. Sommer. Environmental influence on *pristionchus pacificus* mouth form through different culture methods. *Scientific Reports*, 7(1):7207, 2017.
 61. M. J. West-Eberhard. *Developmental plasticity and evolution*. Oxford University Press, 2003.
 62. M. Wilecki, J. W. Lightfoot, V. Susoy, and R. J. Sommer. Predatory feeding behaviour in *Pristionchus* nematodes is dependent on phenotypic plasticity and induced by serotonin. *Journal of Experimental Biology*, 218(9):1306–1313, 05 2015.

1 Dissecting the genetic architecture underlying mouth dimorphism in *P.*
2 *pacificus* identifies *cis*-regulatory variations in a multi-gene locus.

3

4 **Mohannad Dardiry, James W Lightfoot, Christian Rödelberger, Hanh Witte, Gabi Eberhardt &**
5 **Ralf J Sommer.**

6

7

8 **1. Introduction**

9

10 The genetic network underlying mouth-form plasticity in *Pristionchus pacificus* was
11 identified using the reference laboratory strain from California PS312 (Fig. 1A) (Bento,
12 Ogawa and Sommer, 2010; Ragsdale *et al.*, 2013; Kieninger *et al.*, 2016; Serobyan *et al.*,
13 2016; Bui, Ivers and Ragsdale, 2018a; Namdeo *et al.*, 2018; Sieriebriennikov and
14 Sommer, 2018; Sieriebriennikov *et al.*, 2018; Werner, Claaßen, *et al.*, 2018; Moreno *et*
15 *al.*, 2019; Sieriebriennikov *et al.*, 2020; Sun *et al.*, 2021). However, the vast collection of
16 *P. pacificus* wild isolates gathered across the years permits rigorous exploration of the
17 evolution of the genetic architecture underlying mouth-form dimorphism in nature (Fig.
18 1B). Previous studies showed different mouth-form preferences for *P. pacificus* wild
19 isolates (Ragsdale *et al.*, 2013; Werner, Claaßen, *et al.*, 2018; Lenuzzi *et al.*, 2021).
20 Notably, on the population level, most *P. pacificus* wild isolates exhibit a bias towards the
21 eury stomatous mouth-form, whereas some wild isolates display a bias towards the
22 stenostomatous form. Interestingly, other wild isolates show no bias towards any of the
23 mouth forms, rather fluctuating between roughly equal numbers of individuals harboring
24 both mouth forms, suggesting a bet-hedging strategy for survival (Susoy and Sommer,
25 2016). This diversity in mouth-form ratios suggests a polymorphic variation behind the
26 evolution of such dimorphic responses. Thus, implementing a natural variation approach
27 can complement previous genetic studies and might shed light on the evolution of the
28 mouth-form dimorphism. Furthermore, such studies can bridge the gap in our current
29 understanding of the phenotype-genotype relationship.

30

31 **2. Recombinant inbred lines (RILs) and Quantitative trait loci (QTL) approaches**
32 **reveal the involvement of a major locus regulating mouth-form dimorphism in *P.***
33 ***pacificus* natural isolates**

34
35 *P. pacificus* is an androdioecious species (Kanzaki *et al.*, 2013), where the population
36 consists mainly of hermaphroditic animals, besides a few spontaneously occurring males.
37 This mode of reproduction allows the coexistence of both self-fertilization and inter-
38 crossing reproductive strategies within the same population. We took advantage of this
39 reproductive mode to cross different wild isolates. Specifically, we made use of the wide
40 collection of more than 1,500 *P. pacificus* wild isolates with more than 300 lines being
41 whole-genome sequenced to identify the genetic architecture underlying the variation of
42 mouth-form bias in nature (McGaughan *et al.*, 2016). First, we generated F1 hybrid
43 animals by out-crossing a preferentially eurystomatous (Eu) isolate (RSA076) to a
44 preferentially stenostomatous (St) isolate (RSC011) (Fig. 2A). Afterwards, we allowed F1
45 animals to self-fertilize for at least 12 generations. The propagation of 160 animals
46 resulted in the creation of recombinant inbred lines (RILs). These RILs have different
47 mouth-form ratios, reflecting their mosaic homozygous genetic makeup (Fig. 2B,C).
48 Subsequently, we performed a quantitative-trait-locus analysis (QTL) to statistically
49 associate the phenotypic trait under study, eurystomatous ratio, to a genomic region in
50 the sequenced RILs (Fig. 2D). Surprisingly, the QTL analysis identified only one major
51 locus on the X chromosome. This locus stretches for around 219 Kb. Notably the two
52 other narrow signals detected in the analysis were a result of translocations from the X
53 chromosome; as the genome of the distantly related reference strain PS312 was used for
54 mapping (Supplementary Fig. 1). Interestingly, this region covers the previously described
55 multi-gene switch locus, containing the *eud-1* sulfatase and its paralog *sul.2.2.1*, in
56 addition to the two α -N-acetylglucosaminidase (*nag*) coding genes; all known to be
57 involved in mouth-form dimorphism (Sieriebriennikov *et al.*, 2018) (Fig. 3A).

58
59
60

61 **3. Genetic variant analysis and stage-specific RNA sequencing support the role of**
62 ***cis*-regulatory elements in the switch gene *eud-1***

63

64 In total, 35 predicted genes were mapped under the QTL peak, with the multi-gene locus
65 being a top candidate for downstream investigation. First, between the two parental lines,
66 we performed a comparative genetic analysis of the 29 kb region spanning the multi-gene
67 locus (Fig. 3A). This variant analysis revealed 62 single nucleotide polymorphisms
68 (SNPs) with only one representing a nonsynonymous substitution. This substitution was
69 in one of the α -N-acetylglucosaminidase encoding genes, *nag-2*, changing one particular
70 codon from a predicted Phenylalanine to Isoleucine (nucleotide wise, thiamine in the Eu
71 parental line; RSA076, and adenine in the St parental line; RSC011). This gene was
72 shown to be involved in inducing the St mouth-morph in the reference strain PS312
73 (Sieriebriennikov *et al.*, 2018). Therefore, we performed a swap experiment, using
74 CRISPR/Cas-9 engineering to introduce the Eu parental nucleotide in the St RSC011
75 genetic background. We generated two independent lines carrying this substitution
76 (*tu1489*, *tu1490*), both of which did not show any change in the highly St phenotype.
77 Thus, this finding dismisses any role of this substitution in controlling mouth-form variation
78 in nature (Fig. 3B; Supplementary table 1).

79

80 In principle, many dimorphic phenotypes are assumed to follow the threshold trait model
81 (Roff, 1996). The threshold model suggests a continuous distribution of an underlying
82 factor that when exceeding a specific limit, switches the phenotype; in other words, a
83 discrete phenotype that is controlled by a continuously distributed variable (Roff, 1996,
84 1998; Charlesworth and Charlesworth, 2010; Snell-Rood *et al.*, 2018). Indeed, previous
85 studies on *P. pacificus* mouth-form have shown a dosage-dependent response to the
86 steroid hormone dafachronic acid (Bento, Ogawa and Sommer, 2010). In addition,
87 experimentally manipulating copy numbers of the sulfatase switch gene *eud-1*, and the
88 sulfotransferase coding gene *sult-1/seud-1*, proved to have dosage-dependent effects on
89 the eury stomatous mouth-form ratio (Bui, Ivers and Ragsdale, 2018b). Therefore, we
90 speculated that mouth-form dimorphism may be regulated through differential expression
91 of the switch gene *eud-1*. Accordingly, we took two complementary approaches to test

92 this hypothesis. First, we knocked out *eud-1* in both parental lines to test if the switch
93 function is conserved across *P. pacificus* clades. Indeed, we observed a complete switch
94 of the mouth form ratio to 100% St (*tu1449*, *tu1262*, *tu1263*) (Fig. 3C,D; Supplementary
95 table 1).

96
97 We also generated *sul.2.2.1*, the *eud-1* paralog, knockout mutants in the Eu parental line.
98 However, these mutants did not display a switch phenotype, and the Eu ratio in the
99 population was mildly affected (*tu1429*) (Fig. 3C; Supplementary table 1). To complement
100 the knockout approach, we performed stage-specific RNA sequencing on the two parental
101 lines. Worm pellets for RNA extraction were collected on the worms 36hrs after bleaching.
102 The point for collecting worm pellets to carry out downstream analysis was defined
103 according to the highest *eud-1* expression point reported in the reference strain PS312
104 (Sun, Rödelsperger and Sommer, 2021). Indeed, differential expression analysis showed
105 that *eud-1* is 1.4x (40% higher) in the Eu parental line, RSA076 (Fig. 4A). Surprisingly,
106 the paralog of *eud-1*, *sul2.2.1*, was 10x higher in the Eu parental line, but note that the
107 expression levels were in general extremely low for this gene. Together, these findings
108 suggest a potential involvement of *eud-1* expression in regulating dimorphism in nature,
109 and in turn a potential polymorphism in the regulatory elements of the switch gene *eud-*
110 *1*.

111 112 **4. Genetic swapping and gene expression analysis indicate additive effects of** 113 **potential forkhead binding motifs in the *eud-1* promoter and the first intron in** 114 **regulating mouth-form response**

115
116 *Cis*-regulatory elements have proven to possess a significant role in evolutionary biology
117 (Wray, 2007; Carroll, Grenier and Weatherbee, 2013). Numerous empirical studies have
118 shown the involvement of *cis*-variations in adaptive divergence, mainly promoter regions
119 and enhancers in close proximity (Gompel *et al.*, 2005; McGregor *et al.*, 2007; Wittkopp
120 and Kalay, 2011). In addition, several reports in the nematode model *C. elegans* have
121 shown the active role of the first intron in regulating gene expression (Fuxman Bass *et*
122 *al.*, 2014). Therefore, we advanced with an attentive analysis on the 5.9 kb region

123 upstream to *eud-1* and the 209 nucleotide-long first intron of *eud-1*. Prior to identifying
124 potential causative lesions in *eud-1* upstream regions and the first intron, we conducted
125 a comparative setup for closely related strains of the two parental lines. We scored the
126 mouth-form ratio of these closely related strains (Fig. 4B), and then used the available
127 sequence data for all scored strains to narrow down variants in the *cis*-regulatory region
128 into 6 potential causative candidates. This includes one variant in the first intron of *eud-1*
129 (Fig. 4C).

130
131 Next, we performed swapping experiments, again using CRISPR/Cas-9 technology.
132 Specifically, we replaced single nucleotides in the Eu parental background RSA076, with
133 the St variants. First, we replaced the intronic variant and created other lesions in the
134 same area. Interestingly, the mouth-form ratio remained highly Eu (*tu1444*, *tu1445*,
135 *tu1446*, *tu1447*) (Fig. 4D; Supplementary table 1). In addition, in a completely new line,
136 we started to accumulate replacement variants in the upstream region of *eud-1*. We
137 started with those variants that are closest to the presumptive transcriptional start site of
138 *eud-1* in the first exon. Interestingly, the first two swapped variants did not produce the St
139 phenotype, 1.14 kb and 1.98 kb upstream to *eud-1* first exon, respectively. In contrast,
140 they all have shown a reduction in mouth-form ratio, specifically different lesions in the
141 second variant, 1.98 kb, showed a significant reduction in the Eu mouth-form ratio (Fig.
142 4D; Supplementary table 1). Notably, this SNP occurs in a previously identified accessible
143 chromatin area by ATAC-seq (Werner, Sieriebriennikov, *et al.*, 2018).

144
145 Notably, the third candidate was not an SNP variant, but rather a deletion of 32
146 nucleotides approximately 3.12 kb upstream of the first exon. Interestingly, these 32
147 nucleotides are repeated twice in the Eu parental line, with only a spacing of 4 nucleotides
148 between the two copies, while only one copy of this element is present in the St parental
149 line (Fig. 4G). A more detailed analysis of this small sequence identified a potential
150 forkhead transcription factor binding element (DBE) (Fig. 4G). The forkhead (FKH)
151 transcription factor family is one of the largest classes of transcription factors (Nakagawa
152 *et al.*, 2013). In metazoans, many studies have shown the involvement of these
153 transcription factors in various vital functions and are often referred to as FOXO (Accili

154 and Arden, 2004). For instance, in the nematode *C. elegans*, *daf-16*, an ortholog to the
155 FOXO family, contains an FKH binding domain and is found to be involved in the
156 insulin/IGF1 signaling pathway and affecting multiple phenotypes, including; longevity,
157 aging and dauer formation (Lin *et al.*, 1997; Fielenbach and Antebi, 2008; Sun, Chen and
158 Wang, 2017). FKH transcription factors can recognize a range of binding elements,
159 however, *in vitro* assays mostly detect a canonical sequence (RYAAAYA), named as FKH
160 primary motif (fkhP) (Nakagawa *et al.*, 2013). In *C. elegans*, this binding motif of *daf-*
161 *16/FOXO* is observed as (GTAAACA) (Sun, Chen and Wang, 2017). Intriguingly, this
162 potential binding motif, (GTAAACA), is also present in the sequence that is duplicated in
163 the Eu parental line RSA076 (Fig. 4G).

164
165 We generated two mutant lines *tu1591* and *tu1621*, where one of the 32 nucleotide
166 repeated sequences are deleted. This led to a significant reduction in the Eu mouth-form
167 ratio in the mutants' population (Fig. 4E; Supplementary table 2). Additionally, we deleted
168 the second copy of the repeated sequence in the *tu1621* background. This generated two
169 mutant lines, *tu1619* and *tu1620*, where the whole 64 nucleotides were deleted. Indeed,
170 these mutants showed even more pronounced Eu reduction phenotypes, i.e., one block
171 deleted on average: *tu1591*= 93.3% Eu, *tu1621*= 81% Eu; while two blocks deleted on
172 average: *tu1619*= 74% Eu, and *tu1620*= 73% Eu. (Fig. 4E; Supplementary table 2).
173 Moreover, when re-inserting one of the 32 blocks in the mutant line *tu1621*, we observed
174 a partial rescue in the resulting line *tu1622*, i.e., mouth-form phenotype on average=
175 92.6% Eu from 81% Eu (Fig. 4E, Supplementary table 2).

176
177 It is important to note that these mutants did not yet reflect the difference in the mouth-
178 form ratio between the parental lines (Fig. 4E; Supplementary table 2). Given the
179 previously mentioned regulatory role of the first intron in many genes in *C. elegans*, we
180 introduced the St nucleotide variant in the first intron into the mutant line *tu1620*. This
181 creates a line that has both potential FKH binding sites deleted, in addition to the first
182 intronic swap as well (lines *tu1625* and *tu1626*). Remarkably, this 'triple' mutant lines
183 showed the St parental phenotype (Fig. 4E, Supplementary table 2). Together, the fine
184 mapping approach by substituting natural variants has identified a cumulative effect of

185 *eud-1* first intron variants and the *eud-1* upstream region controlling mouth-form response
186 in nature.

187

188 Finally, two approaches were taken to strengthen the previous conclusions. First, we
189 explored more the involvement of the first intron in the regulation of mouth-form
190 phenotype. Strikingly, when sequence alignment was performed between the 32-
191 nucleotide block with copy number variation in the *eud-1* promoter and the *eud-1* first
192 intron, a core sequence of 18 bases displayed uniquely high similarity (Fig. 4G).
193 Therefore, we used CRISPR/Cas-9 technology to introduce lesions on this highly similar
194 sequence in the first intron. Indeed, the produced mutants displayed a reduction in mouth-
195 form ratio; however, this reduction seems to be lesion-specific, *tu1631* and *tu1715* (Fig.
196 4E; Supplementary table 2). Thus *eud-1* first intron presumably harbors potential
197 regulatory elements that affect mouth-form phenotype, but a full understanding of the
198 contribution of this region requires more additional experiments. Second, to entirely
199 confirm that the identified *cis*-variations are affecting mouth-form phenotype through *eud*-
200 *1* expression, we performed RT-qPCR on *eud-1* expression in the generated mutants.
201 We normalized our analysis by the expression of the reference gene *Ppa-cdc-42*
202 (Schuster and Sommer, 2012), and measured *eud-1* expression in relation to normalized
203 expression in the Eu parental line RSA076. Indeed, expression analysis of the mutants
204 *tu1625*, *tu1626*, and *tu1715* showed a reduction in *eud-1* expression that is similar to what
205 is detected in the St parental line, RSC011 (Fig. 4F). Together, these findings suggest
206 that *cis*-variations identified in the natural isolates mapping approach act through
207 changing *eud-1* expression, and consequently regulating mouth-form response.

208

209 **5. Comparative analysis of *P. pacificus* wild isolates declare diverged evolutionary** 210 **mechanisms underlying mouth-form response variation across clades**

211

212 Next, we extended our analysis to include representative strains from different *P.*
213 *pacificus* clades. We performed a three-step analysis. First, we scored mouth-form ratios
214 for 30 different *P. pacificus* strains, where 9 strains represented clade B, 6 strains
215 represented clade A, and 14 strains represented the largest *P. pacificus* clade; clade C,

216 and finally, the strain RS5275, which represents an outgroup to the three main clades A,
217 B and C (Fig. 5B). Second, we performed Sanger sequencing on the DNA region
218 containing the previously detected FKH potential binding motifs for all previously
219 mentioned strains. Finally, we used the available whole genome sequencing data to
220 identify the single nucleotide polymorphism within the intronic region for each strain (Fig.
221 5A). In clade B strains, our analysis revealed an association between the number of
222 binding motifs, the type of the intronic polymorphism, and mouth-form ratio (Fig. 5B).
223 Specifically, in the three sister strains RSC011, RSC012 and RSC008 mouth-form ratio
224 was 22.8%, 20%, 12% Eu, respectively (Fig. 5B). In these strains only one 32-nucleotides
225 block was detected, one potential FKH-binding motif, besides a Guanine base (G) on the
226 polymorphic variant of the first intron (Fig. 5A,B). For other strains selected from clade B,
227 the 64-nucleotides block was detected with two potential FKH-binding motifs, besides an
228 Adenine (A) base on the polymorphic variant of the first intron (Fig. 5A,B). In principle,
229 these changes led to a significant increase in the Eu ratio; *e.g.*, four strains displayed on
230 average more than 91% Eu (Fig. 5B). The same pattern was shown in the outgroup strain
231 RS5275 (Fig. 5B). However, the strains RSB0035 and RSC013 did not display an
232 extremely high Eu ratio as the other four strains, mouth-form ratio in these two strains still
233 exhibited a bias towards more Eu; on average 69.2% and 65.6% Eu, respectively (Fig.
234 5B). These results would first argue for the conservation of the machinery controlling
235 mouth-form response within clade B strains, and second, for the involvement of strain-
236 specific tuning modifiers affecting the same response.

237

238 In clade A, the association between the polymorphic intronic region and mouth-form ratio
239 is less perceptible. Nevertheless, a new feature of uniquely possessing three potential
240 FKH-binding motifs could only be detected in some strains of this clade (Fig. 5B). Notably,
241 a change in the phenotype towards preferentially St is noticed when the number of the
242 potential FKH-binding motifs is reduced; *e.g.*, the strain RS5200 where on average
243 mouth-form ratio was 3.6 % Eu, the potential FKH-binding motif only occurs once (Fig.
244 5B). In contrast, when the two potential binding motifs were detected, mouth-form ratio
245 elevates to reach on average between 90.4% to 92.8% Eu in RSA619 and RS5408,
246 respectively (Fig. 5B). This ratio on average was either equal or higher upon the detection

247 of three potential binding motifs; e.g., 88.8%, 99.6%, 100% Eu in RSB071, RS2333, and
248 RSA639, respectively. However, sampling size from this clade might be enlarged in the
249 future, current observations argue for a more pronounced role of the binding motif in clade
250 A strains. In clade C strains, no direct association between the three elements could be
251 detected (Fig. 5B). In all clade C strains used in this analysis, the intronic variation was
252 absent, meaning all strains only contained an Adenine base (A) (Fig. 5B). Furthermore,
253 the number of the binding motifs did not fully reflect the change in the mouth-form bias
254 (Fig. 5B). Together these results suggest a diverged machinery underlying the evolution
255 of mouth-form response between different *P. pacificus* clades.

256

257 **6. FKH-transcription factors knockouts suggest redundant functionality and the** 258 **involvement of multiple factors acting simultaneously in regulating mouth-form** 259 **expression.**

260

261 Next, we performed an amino acid homology test to identify *C. elegans* forkhead-
262 transcription factors orthologous in *P. pacificus*. Our analysis detected 13 different
263 annotated genes with a potential FKH-binding domain in the *P. pacificus* genome (Fig.
264 5C). Furthermore, we used CRISPR/Cas-9 to target the coding sequence for the FKH
265 binding domain, to knockout seven of these 13 genes in the parental Eu background (Fig.
266 5d). We used various criteria to prioritize our selection from the 13 candidates. First, gene
267 location. Given that many mouth-form related genes are localized on the X chromosome
268 (Ragsdale *et al.*, 2013; Kieninger *et al.*, 2016; Sieriebriennikov *et al.*, 2018, 2020), we
269 prioritized our selection for the genes on *P. pacificus* X chromosome; e.g.
270 *fkh2_ppa_stranded_DN24289_c0_g1_i1*. Second, gene expression patterns reported in
271 *C. elegans*. Either if genes were expressed in the pharynx or pharynx-associated
272 neurons, as *eud-1* was reported to be expressed in somatic and pharyngeal neurons of
273 *P. pacificus* (Ragsdale *et al.*, 2013; Sieriebriennikov *et al.*, 2018). For instance, PHA-4
274 orthologs were reported to be required for both early and late *C. elegans* pharynx
275 development (Gaudet and Mango, 2002).

276

277 However, knockouts of some genes resulted in alleles that did not display a mouth-from
278 phenotype; e.g., *daf-16_PPA39986(tu1648)*, *pha-4_PPA14054(tu1707)*, some alleles
279 displayed weak but insignificant reduction in the Eu ratio, e.g. *fkh-*
280 *2_ppa_stranded_DN24289_c0_g1_i1(tu1712)*, *pha-4_PPA39542(tu1709)* (Fig. 5d,
281 Supplementary table 3). Notably, one allele showed the most reduction in the Eu ratio
282 *fkh-9_PPA29963(tu1714)*; on average 84.8% Eu (Fig. 5d, Supplementary table 3). We
283 speculate that the absence or weakness of phenotypes is presumably due to functional
284 redundancy of transcription factors in the regulatory network, and/or the overlap of various
285 regulatory elements over the same multi-gene-locus (Serobyán *et al.*, 2016; Werner,
286 Sieriebriennikov, *et al.*, 2018). Thus, these current findings are yet preliminary and further
287 investigations are necessary for a more conclusive interpretation.

288

289 **7. Discussion and future directions.**

290

291 In this study we could identify *cis*-polymorphic variants underlying mouth-form response
292 differences in natural isolates of *P. pacificus*. Furthermore, we demonstrated a cumulative
293 effect of the upstream intergenic region and first intronic sequence of the switch gene
294 *eud-1*. Moreover, we confirmed that these *cis*-variations act through controlling *eud-1*
295 expression and thus, changing mouth-form ratio in natural populations. Finally, we
296 investigated the involvement of different FKH-transcription factors encoding genes in the
297 regulation of mouth-form expression. Future investigations would aim at four main
298 directions. First, exploring in more detail the role of the additional FKH encoding genes in
299 regulating mouth-form dimorphism. Second, as different lesions in the intronic region
300 generated unequal effects on mouth-form ratio, furthermore analysis of this region will
301 offer additional perspectives on the regulation of the switch gene *eud-1*. Third, across
302 clades comparative analysis revealed potential divergence in the machinery behind
303 mouth-form response evolution. Thus, in principle, further analysis of the expression of
304 *eud-1* in other strains representing different *P. pacificus* clades will provide insight into
305 whether this potential machinery is acting through regulating *eud-1* expression as well.
306 Fourth, however, the triple mutant with 64-nucleotides block deletion besides the intronic
307 swap indeed reflected mouth-form variation in nature, generating a mutant line with only

308 the 32-nucleotides block deleted besides the swap would be more representative for
309 natural lesions. In conclusion, this study provides in depth molecular analysis for the
310 evolution of a dimorphic threshold trait, with a strong support for the involvement of *cis*-
311 regulatory evolutionary mechanisms.

312

313

314 **8. Figures legend**

315

316 **(Figure1) *P. pacificus* as a model to study the molecular evolution of phenotypic**

317 **plasticity. (a)** A simplified scheme of the genetic regulatory network (GRN) underlying

318 mouth-form development in the *P. pacificus* reference strain PS312. The GRN is divided

319 into three developmental modules. First, the perception network; is involved in the

320 sensing of various environmental cues. Second, the switch network integrates the

321 environmental cues and determines one of the alternative morphs. Mutations in switch

322 genes either activate or inhibit the formation of one of the mouth-forms, thus, populations

323 are either 100% Eu or St. Third, the execution network with genes being involved in the

324 formation of the mouth structural components. Genes in yellow boxes are involved in the

325 mouth-form decision but do not fall into any of the three suggested modules. Solid lines

326 indicate an empirically tested relationship between the network's components, either by

327 epistatic tests or expression analyses, whereas dotted lines indicate a suggested

328 relationship with no empirical evidence. Arrows represent the involvement of these genes

329 in forming the same mouth-form, while horizontal lines indicate the involvement in the

330 formation of the opposite mouth-form. **(b)** *P. pacificus* phylogenetic tree representing 323

331 sequenced strains. *P. pacificus* strains were divided into three major clades (A, B, C),

332 with a 1% genomic divergence between clades. Both parental lines used in this study are

333 highlighted: RSC011; the St parental line, and RSA076 the Eu parental line. Adopted from

334 (Rödelsperger *et al.*, 2017).

335

336 **(Figure2) Mapping the causative locus using a RILs & QTL approach (a)** The mouth-

337 form ratio of the two parental lines from clade B. For each parent, 12 biological replicates

338 were scored with 30 animals each; n=12, N=360. **(b)** A summary scheme elucidates the

339 experimental setup implemented to generate recombinant inbred lines from the two
340 parental lines. In the end, all lines were scored for the mouth form phenotype, genomic
341 DNA was isolated, and whole-genome sequencing was performed. All data were used in
342 the downstream QTL analysis (for more details see Materials and Methods). **(c)** Mean
343 phenotypic score of the RILs. Mouth-form phenotypes of 55 different RILs were scored 5
344 times for each line, with 30 animals counted for each replicate. n=5, N=150. **(d)**
345 Quantitative trait loci analysis reveals a significant association of one peak, genomic
346 region, on the left arm of chromosome X with mouth-form dimorphism. While other two
347 narrow peaks are computational artifacts (for more details see supplementary Figure1).

348

349

350 **(Figure3) Knockout mutants of the multi-gene locus (a)** The multi-gene locus
351 structure representing two pairs of paralogous in an inverted tandem arrangement. The
352 two sulfatases encoding genes *eud-1* and *sul2.2.1* in a head-to-head arrangement with
353 the two α -N-acetylglucosaminidase encoding genes *nag-1* and *nag-2*. **(b)** The introduced
354 *nag-2* substitution in the preferentially St parental line RSC011 (*tu1489* and *tu1490*), with
355 other lesions introduced in the same gene (*tu1491*, *tu1492*, *tu1493*). **(c)** Knockout
356 mutants for the both paralogs encoding for sulfatases in the Eu parental line RSA076.
357 (*tu1429*) single mutant of *sul2.2.1*; (*tu1449*) single mutant in the switch gene *eud-1*; In
358 addition, double knockouts for the two sulfatases paralogous, *eud-1* and *sul2.2.1*
359 (*tu1430*, *tu1431*). **(d)** Knockout mutants for the switch gene *eud-1* in the St parental line
360 RSC011 (*tu1262* and *tu1263*). For each mutant line, 3 biological replicates were scored
361 with 50 animals each; n=3, N=150. For statistical analysis *p < 0.05; **p < 0.01, ***p <
362 0.001. And comparisons were made against the corresponding wild-type parent. Only
363 statistically significant comparisons are displayed.

364

365 **(Figure4) Fine mapping of causative cis-variants (a)** Mean expression levels of the
366 four genes in the multi-gene locus as revealed by RNA-seq analysis for the two parental
367 lines RSA076 and RSC011. **(b)** Mouth-form ratio of the selected *P. pacificus* strains that
368 are closely related to the parental lines. For each wild isolate, 5 biological replicates were
369 scored with 30 animals each; n=5, N=150 **(c)** Candidate *cis*-variants shared by the closely

370 related St lines in comparison to the Eu parental line RSA076. **(d)** Mouth-form phenotype
371 of swapping variants in the Eu parental line RSA076. *Eud-1* first intron (*tu1444*, *tu1445*,
372 *tu1446*, *tu1447*) with only *tu1444* displaying the swap, while other mutants contain
373 different lesions in the same region. The 1.14 kb-upstream variant (*tu1460*, *tu1485*,
374 *tu1487*, *tu1488*) with only *tu1485* displaying the swap, while other mutants contain
375 different lesions in the same region. The 1.98 kb-upstream variant (*tu1504*, *tu1505*,
376 *tu1506*, *tu1507*) with only *tu1504* displaying the swap, while other mutants contain
377 different lesions in the same region. For each lesion, 3 biological replicates were scored
378 with 50 animals each; n=3, N=150. **(e)** Mouth-form phenotype for the identified causative
379 variants. The two parental lines RSA076 and RSC011, mutants; *tu1591* and *tu1621*;
380 where the first 32-nucleotides block is deleted, *tu1619* and *tu1620*; where the 64-
381 nucleotides block is deleted, *tu1622* rescue line with introducing one 32-nucleotides block
382 in the *tu1621* background, *tu1625* and *tu1626*; where the 64-nucleotides block is deleted
383 and the intronic swap is introduced, *tu1631* and *tu1714*; where the highly similar region
384 to the 32-nucleotides block in the intronic area is deleted. For each lesion, 6 biological
385 replicates were scored with 50 animals each; n=6, N=300. **(d-e)** For statistical analysis *p
386 < 0.05; **p < 0.01, ***p < 0.001. And comparisons were made against the Eu parental line
387 RSA076. Only statistically significant comparisons are displayed. **(f)** RT-qPCR analysis
388 of *eud-1* expression in the St parental line RSC011, the two lines with the triple mutant
389 *tu1625* and *tu1626*, besides the line *tu1714* where the highly similar region to the 32-
390 nucleotides block in the intronic area is deleted. For each measurement 3 biological
391 reactions were performed with 9 technical replicates. **(g)** Upper panel shows sequence
392 alignment of the 64-nucleotides block region in the Eu parental line RSA076, the St
393 parental line RSC011 and the reference strain PS312. Lower panel shows sequence
394 alignment of the 32-nucleotides block with *eud-1* first intron in the reference strain PS312.
395 In red is the 32-nucleotides block, while in green are bases where we detect nucleotides
396 mismatch.

397

398 **(Figure5) Extending mouth-form analysis to cover other *P. pacificus* clades and to**
399 **identify associated transcription factors (a)** A representation of the identified variants
400 involved in mouth-form response evolution. **(b)** Phylogenetic analysis of *P. pacificus* wild

401 isolates concerning the identified causative variants. Color code represents strains in
402 different clades. Clades B, A, and C are green, yellow, and blue respectively. AOI(area
403 of interest) , where the color code represent the number of potential binding sites; white:
404 one copy of the 32-nucleotide block, grey: two copies of the 32-nucleotide block, black:
405 three copies of the 32-nucleotide block. **(c)** Protein based-tree of the forkhead (fkh)
406 transcription factors in *P. pacificus* **(d)** Mouth-form phenotype of the fkh mutants in the Eu
407 parental line RSA076. For each allele, 5 biological replicates were scored with 50 animals
408 each; n=5, N=250. For statistical analysis *p < 0.05; **p < 0.01, ***p < 0.001. And
409 comparisons were made against the Eu wild-type parent RSA076. Only statistically
410 significant comparisons are displayed.

411

412 **9. Materials and methods**

413

414 **Nematode culture maintenance**

415

416 *P. pacificus* natural isolates were reared on the laboratory *E. coli* strain OP50. Single
417 colony of the OP50 culture was first inoculated into the liquid Lysogeny broth medium
418 (LB) and then incubated at 37°C without shaking. After overnight incubation, 6-cm petri-
419 dishes containing nematode growth medium (NGM) were seeded with 300µl of OP50 and
420 set-off for an incubation night. Nematodes were grown on the seeded NGM plates at
421 20°C. On five days intervals, three nematodes were passed to new OP50 plates to avoid
422 starvation, crowding and their effect on mouth-form.

423

424 **Mouth-form phenotyping**

425

426 Mouth-form was characterized based on the width of the mouth, and the shape of the
427 dorsal tooth as previously described in (Bento, Ogawa and Sommer, 2010). Screening of
428 the population eurystomotaous ratio was performed on a ZEISS SteREO Discovery.V20
429 microscope, PlanApo S 1.5x objective with eyepiece PL 10x/23 Br.foc. At least three
430 replicates were performed for each experiment with a minimum of 150 animals in total.
431 All mouth-form screening was performed at 20°C on 300µl of OP50.

432 **Recombinant inbred lines generation and mouth-form screening**

433

434 To produce recombinant inbred lines, we first set mating plates to conduct crosses
435 between the two parental lines. From the maintenance culture, we isolated 20 J4
436 hermaphrodites of both the preferentially St line RSC011, and the preferentially Eu line
437 RSA076. These 20 animals were isolated into two 100µl OP50 separate plates,
438 representing each wild isolate. Simultaneously, we isolated 40 males from each wild
439 isolate. Then for five constitutive days, we transferred the 20 hermaphrodites on a daily
440 basis; thus, on the 5th day, when no more self-sperms were available to produce self-
441 progeny, we initiated mating plates. Mating plates were initiated in a reciprocal setup,
442 where 5 adult males from RSA076 and 2 hermaphrodites, that do not produce any self-
443 sperms, from RSC011 were added together; and vice versa. For each setup, 8 mating
444 plates were generated, each seeded with 20µl OP50 and incubated at 20°C. After two
445 days, when fertilized eggs were laid, the 5 parents were removed and the plates were
446 kept in the incubator until F1 animals reached the J4 stage.

447

448 From each mating plate of the 16 plates, 10 F1 animals were singled out in a 300µl OP50
449 plate. The 160 animals were isolated in the J4 stage to avoid any possible mating with
450 other F1 males' brothers. After F1 animals had laid eggs, they were lysed to extract DNA.
451 Each worm was placed in an Eppendorf tube with 10µl of single worm lysis buffer (10 mM
452 Tris-HCl at pH 8.3, 50 mM KCl, 2.5 mM MgCl₂, 0.45% NP-40, 0.45% Tween 20, 120
453 µg/ml Proteinase K) then it was placed at -80 for 10min. Afterwards, Eppendorf tubes with
454 worm lysis were incubated at 65°C in the thermocycler machine for 1 hour, followed by
455 15min at 95 °C for the deactivation of the Proteinase K. The produced lysate was used
456 as a template for PCR reaction. We used Qiagen Taq master mix (Cat. No. / ID: 201445)
457 to amplify a genomic sequence on Chr I, where a SNP occurs between the two parental
458 lines RSA076 and RSC011; Guanine (G) in RSA076, while Adenine (A) in RSC011. This
459 amplified region was then sent to Sanger sequencing to confirm heterozygosity in the F1
460 worms; i.e., two peaks in the visualization software, FinchTV, where the SNP occurs.
461 Primers were added from a 10µM stock (**See table below**).

462

Primer name	Primer sequence 5'----->3'	Primer function
MD15650	TCTCGCTTGTGCTATCGGA	Forward PCR primer
MD15652	TGTTGCAGCTGGCTAACTCAC	Reverse PCR primer
MD15653	CGAGTTACCTCCTCA	Sequencing Primer

463

464

465 After heterozygosity was confirmed, one J4 animal from each of 160 lines were
466 transferred to a new NGM-OP50 plate. For at least 12 generations, single worms were
467 transferred from each line. Supposedly at F8, homozygous recombinant inbred lines
468 (RILs) with mosaic genetic background were generated (Broman, 2005). While
469 generating the F12 RILs, we lost 20 lines. Thus, from the 140 remaining RILs, we have
470 randomly chosen 55 lines representing the two parental lines' mouth-form. Mouth-form
471 score was screened for 5 successive generations, from F12 to F16, and 28 lines were
472 selected to represent the highly Eu line RSA076, and 27 lines representing the
473 preferentially St parental line RSC011. These lines were selected according to their
474 consistency in the mouth form ratio between successive generations that in the end will
475 lead to a mean mouth-form value that is covered within one of the parental lines'
476 phenotypes. For instance, in the 27 lines representing the highly St parent, the mouth-
477 form ratio ranged between 5% to 50% Eu. While for the 28 lines representing the highly
478 Eu parent, the mouth-form ratio ranged 73.5% to 100% Eu. Notably, when more strict
479 limits of mouth form were applied by removing lines that showed on average 73.5% to
480 95% Eu, 8 lines from the highly Eu representing side; and lines that range from 37% to
481 50% Eu from the highly St side, 3 lines, the final result did not change.

482

483 **Whole-genome sequencing**

484

485 To prepare the 55 lines for whole genome next generation sequencing, for each line, we
486 used 40 ml 0.9% NaCl solution to wash 5 full grown plates with minimum OP50 residue
487 in 50 ml falcon tubes. Then centrifuged falcon tubes at 1300 rcf for 6 min at 20°C. Another
488 washing step followed by first removing the supernatant then adding 40 ml 0.9% NaCl

489 with 40µl Ampicillin (50µg/ml) and 40µl Chloramphenicol (50µg/ml), and incubated at
490 room temperature while shaking overnight. Next day the worm pellet was obtained
491 through centrifugation as previously mentioned, supernatant was dismissed, and worm
492 pellet was transferred from falcon tubes to 1.5 ml Eppendorf tubes. This was followed by
493 a centrifugation step at 140000 rpm for 1 min at 20 °C, then finally the worm pellet was
494 frozen at -20°C.

495
496 Afterwards, we conducted three freezing/thawing cycles using liquid nitrogen and the
497 thermomixer at 37 °C. Subsequently, DNA was extracted using GeneElute Mammalian
498 Genomic DNA Miniprep Kit (DNA column purification, Sigma G1N70) following
499 manufacturer's protocol but with increasing the the Lysis solution T (B6678) amount from
500 180µl to 200µl, besides increasing the Proteinase K (10 mg/ml) amount from 20µl to 50µl
501 in the digestion step. Next generation DNA sequencing libraries (NGS) were prepared
502 using Nextera DNA Flex Library Prep Kit (illumina). Libraries were prepared following
503 manufacturer's protocol. Libraries were paired-end sequenced using HiSeq 3000
504 machine (Illumina).

505

506 **Identification of the candidate region (QTL mapping) and genomic variants**

507

508 Raw sequence reads were aligned against the *P. pacificus* reference assembly (version
509 El Paco) with the BWA aln and same programs (version 0.7.17-r1188) using default
510 options (Li and Durbin, 2009; Rödelsperger *et al.*, 2017). Informative marker positions
511 between the two parental strains RSC011 and RSA076 were identified using a different
512 variant calling approach (Lenuzzi *et al.*, 2021). The classification of the differential
513 variants into non-coding, nonsynonymous, synonymous substitutions was done as
514 described previously (Rae *et al.*, 2012). Alignments of RILs were genotyped at the
515 informative marker positions using the differential variant calling approach (at least 5X
516 coverage). For markers with at least five instances of each of the parental genotypes,
517 LOD scores were computed as the negative logarithm (base 10) of the P-value, as
518 computed by Fisher's exact test. And a threshold corrected LOD score was set at 6 to
519 signify the association between the genomic region and the phenotype.

520 CRISPR/Cas-9 knockouts and swaps in the multi-gene locus

521
522 First, we used available sequenced genomes for other clad B strains, variants were called
523 against the reference genome of clade B strains RSB0001, to identify candidates in the
524 promoter region of *eud-1*. Genomic Sequence bed files were aligned to the annotated
525 reference genome of RSB001 using the software IGV to identify the candidates.

526 Swapping experiment was conducted using CRISPR/Cas-9 machinery as described in
527 (Witte *et al.*, 2015; Lightfoot *et al.*, 2019). For all swapping experiments a guide RNA
528 complex; which is composed of a 20 bases target specific oligo CRISPR RNA (crRNA)
529 and a universal trans-activating CRISPR RNA (tracrRNA), with a Cas9 protein, and a
530 single strand DNA repair oligo template; were injected in the gonad rachis of a one-day
531 old adult hermaphrodite. The crRNAs were always designed upstream to the protospacer
532 adjacent motifs (PAMs) sequences. Repair templates were designed with 40 bases
533 homology arms to each side of the targeted modified swap base, with a total length of
534 approximately 81 bases. Besides the CRISPR/Cas-9 mix to induce swaps in the genome,
535 *egl-20p::TurboRFP* (PZH009) construct was also injected as a CRISPR/Cas-9 co-
536 injection marker (Han *et al.*, 2020). In general, 40 P0 animals were injected with the
537 CRISPR/Cas-9 mix and the co-injection marker, then singled out in NGM-OP50 plates.
538 After 4-5 days, when F1 animals reached adulthood, we screened for red-fluorescent
539 worms in all 40 plates. Indeed, *egl-20p::TurboRFP* co-injection marker has proven to
540 increase the chance of identifying F1 heterozygous worms up to 77% (Han *et al.*, 2020).
541 Thus, we only singled out F1 animals from the plates we found fluorescent worms in.
542 Afterwards these F1 worms were lysed, and targeted amplicons were amplified, and
543 sanger sequencing was performed; all as previously mentioned at the methodology
544 section. From each heterozygous identified animal, 8 F2 worms were singled out,
545 supposedly 25% of these animals should have a genomic lesion. After F2 animals laid
546 eggs, they were lysed, and targeted amplicons were amplified, and sanger sequencing
547 was performed. To identify the type of the lesion and if the targeted swap was obtained,
548 we used the online pairwise sequence alignment tool EMBOSS Needle with default
549 settings (https://www.ebi.ac.uk/Tools/psa/emboss_needle/).

550

Primer name	Gene/regulatory element	Primer function	Primer sequence 5'--->3'
MD001	<i>eud-1</i> gene	Forward primer	GGTAAACACGCGTAATTGGGAC
MD002	<i>eud-1</i> gene	Reverse primer	GACGGGAAGGCAAATGTG
MD003	<i>eud-1</i> gene	Sequencing primer	ATACAGGTGATCAATGAGAG
MD004	<i>sul2.2.1</i> gene	Forward and sequencing primer	CTGGATTAATCACAACCTTATCCG
MD005	<i>sul2.2.1</i> gene	Reverse primer	TGTTGCGTAACCTGAATTTGC
MD019	<i>nag-2</i> gene	Forward primer	TCGGTGCATCTGGTAAGCT
MD022	<i>nag-2</i> gene	Reverse primer	TGTTATAATCCGACCGAATGC
MD024	<i>nag-2</i> gene	Sequencing primer	CATCTGGTAAGCTTGGTCT
MD007	<i>eud-1</i> intron SNP	Forward primer	CGCTAGTTGGTTCGCTCATA
MD009	<i>eud-1</i> intron SNP	Reverse primer	GTATGATGACGTTGGGATGC
MD013	<i>eud-1</i> intron SNP	Sequencing primer	TAGTTGGTTCGCTCATATC
MD014	<i>eud-1</i> promoter region (1.14kb upstream SNP)	Forward primer	GACACTCTAAACGATGTGGTGC
MD016	<i>eud-1</i> promoter region (1.14kb upstream)	Reverse primer	CCTGCAAGACTGCTAGACTCG
MD015	<i>eud-1</i> promoter region (1.14kb upstream)	Sequencing primer	CCTATATGCACTCGCTTC

MD027	<i>eud-1</i> promoter region (1.98kb upstream SNP)	Forward primer	GGAACCTCACGTAAGGTAAGCTCG
MD029	<i>eud-1</i> promoter region (1.98kb upstream SNP)	Reverse primer	GTCGAAACTTCTAAGAGTCCCG
MD030	<i>eud-1</i> promoter region (1.98kb upstream SNP)	Sequencing primer	CTTCTAAGAGTCCCGTAAG
MD032	<i>eud-1</i> promoter region (3.12kb upstream binding motifs)	Forward primer	GATACAGGCGCTGACGACTG
MD033	<i>eud-1</i> promoter region (3.12kb upstream binding motifs)	Reverse primer	CGCACGGATACACTTCGTCA
MD035	<i>eud-1</i> promoter region (3.12kb upstream binding motifs)	Sequencing primer	TATACTGACTCCAGGCACT
MD044	Highly similar region to the 32-block in <i>eud-1</i> first intron	Forward primer	TCACCAAATATCGTGCCTCTTC
MD042	Highly similar region to the 32-block in <i>eud-1</i> first intron	Reverse primer	AAGGAGCAGAGCTTGAAGAGGA
MD043	Highly similar region to the 32-block in <i>eud-1</i> first intron	Sequencing primer	ATTGACAGTGTCTCTAAGC

551

552

553

554

555 **RNA-seq library preparation**

556

557 The time point of 36hrs after bleaching was reported to show the highest expression of
558 the sulfatase encoding gene *eud-1* in the reference strain PS312 (Sun, Rödelsperger and
559 Sommer, 2021). Thus, we designed our experiments to collect worm pellets 36hrs after
560 bleaching, mostly the worm culture was in the J3 stage with few J4 animals. First, we

561 prepared 6 bleaching plates for each parental strain RSC011 and RSA076. These plates
562 were prepared by picking 20 J4 worms into 10-cm NGM-OP50 plates, for each plate. After
563 6 days, when these plates were full of unhatched eggs, we applied the bleaching protocol
564 as described in (Stiernagle, 2006). Bleached eggs were added to 10, 10-cm NGM-OP50
565 plates, and kept at 20°C for 36hrs. For worm pellet preparation, all NGM plates were
566 spotted with 400µl OP50. After 36hrs the plates were washed with an autoclaved M9
567 buffer, and passed through a 5µm filter to remove bacterial debris. Worm pellet was
568 collected in 1.5ml Eppendorf tubes and centrifuged at maximum speed for 2 min. The
569 supernatant was removed and the worm pellet was flash frozen at liquid nitrogen and kept
570 at -80°C till RNA extraction. For each parental line we prepared two biological replicates.

571

572 RNA extraction was performed using the Direct-zol Zymo RNA miniprep kit (R2050)
573 following the manufacturer's protocol (Quick protocol). Elution step was done in a final
574 volume of 25µl distilled water. RNA quality was checked using Nanodrop, and all samples
575 showed a high purity with an A260/A280 ratio of 1.8 and 2.0. For Library preparation we
576 used Illumina TruSeq RNA Library Prep Kit. We started with a 1ug RNA as an input, and
577 followed the manufacturer's protocol, however we increased time from 7 min to 8 min in
578 the Elute, Prime, Fragment step to obtain larger fragments. And the number of PCR
579 enrichment cycles used was 12 cycles. Samples quantity and quality were checked by
580 Qubit and Bioanalyzer. All samples were diluted to 10nM, then 10ul from each sample
581 were pooled together. The concentration of the pooled library was measured by Qubit
582 and adjusted to 2.5nM before being sequenced in a Hiseq 3000 machine (illumina).

583

584 **Analysis of RNA-seq data**

585

586 Raw RNA-seq reads were aligned against the assembly of the *P. pacificus* strain RSB001
587 (European Nucleotide Archive accession: CAKKKZ010000000) with the tophat2 program
588 (version 2.0.14) using default options (Kim *et al.*, 2013). Evidence-based gene
589 annotations for the RSB001 genome were created by the PPCAC pipeline (version 1)
590 (Rödelsperger, 2021). Specifically, a strain-specific transcriptome assembly
591 (Rödelsperger *et al.*, 2018) and the latest version of the gene annotation for the reference

592 strain PS312 (version: El Paco gene annotation 3) (Athanasouli *et al.*, 2020) were
593 mapped on the RSB001 assembly, and the longest gene model per 100bp window was
594 chosen as the representative gene model. Estimation of expression levels and differential
595 expression analysis was done by the Cufflinks and Cuffdiff programs (version 2.2.1)
596 using default options (Trapnell *et al.*, 2013).

597

598 **RNA extraction and qRT-PCR experiments**

599

600 Worm pellets were obtained and RNA was extracted as previously described in the
601 section (**RNA-seq library preparation**). Time points of collecting worm pellets for RT-
602 qPCR were 36hrs after bleaching as in the section (**RNA-seq library preparation**). We
603 used the iTaq™ Universal SYBR® Green One-Step Kit (#1725150) for measuring the
604 normalized expression of the *eud-1* gene in mutant lines and the St parental line RSC011
605 in relation to its expression in the Eu parental line RSA076. We performed 3 biological
606 replicates and nine technical replicates. We followed the manufacturer's protocol, while
607 using 20 ng RNA input, and a final concentration of primers 0.25uM as reported in
608 (Werner *et al.*, 2017). Measuring gene expression was performed on a Roche LightCycler
609 LC480. And program specifications were as follows: reverse transcription reaction 10 min/
610 50°C; polymerase activation and DNA denaturation 1 min/ 95°C; denaturation 15 sec/
611 95°C; annealing and extension 30 sec/ 60°C; for 45 cycles. Primer sequences used in
612 measuring *eud-1* expression and the reference gene *Ppa-cdc-42* as follows. And relative
613 gene expression was measured by calculating the 2-delta delta Ct.

614

Primer	Sequence 5'----->3'
eud-1_qPCR_F	GGCTGGATTCATCACTGGTCGT
eud-1_qPCR_R	ATTCCCGTTGCGTAACCTCGT
cdc-42_qPCR_F	CTCTCTTATCCACAGACGGAC
cdc-42_qPCR_R	GAAGGGAGTGCGTGAGCAGTG

615

616

617 **Phylogenetic analysis of forkhead genes**

618

619 Homologous proteins encoded by *C. elegans* forkhead genes were identified from
620 BLASTP searches against *C. elegans* on www.wormbase.org and *P. pacificus* on
621 www.pristionchus.org. Protein sequences for the best hits were downloaded after manual
622 inspection of the BLASTP results and a multiple sequence alignment was generated by
623 the MUSCLE program (version 3.8.31) (Edgar, 2004). A maximum likelihood tree was
624 computed with the help of the phangorn R package (version 3.4.4) under the LG
625 substitution model with optimization of topology (optNni=TRUE), base frequencies
626 (optBf=TRUE), proportion of variable sites (optInv=TRUE)(Schliep, 2011).

627

628

629 **Identification of the forkhead coding domain and CRISPR/Cas-9 knockouts of**
630 **potential transcription factors**

631

632 First, we downloaded transcript sequences of the identified genes from
633 www.pristionchus.org. Afterwards we used predicted amino acid sequences from these
634 transcripts to predict exons coding for the forkhead binding domain using
635 www.smart.embl-heidelberg.de. Guide RNA were designed to target exons that were
636 predicted to encode for the forkhead binding domain. Guide RNA were designed and
637 worms were injected as described in the section (**CRISPR/Cas-9 knockouts and swaps**
638 **in the multi-gene locus**). For each produced frameshift mutant line, 5 biological
639 replicates were screened for mouth-form ratio; in total 250 animals. Primers used are as
640 follows:

641

642

Primer name	Gene	Primer function	Primer sequence 5'---->3'
MD045	<i>daf-16_PPA39986</i>	Forward primer	GGTTAATTTATGAGTGGGCCGTTTC

MD049	<i>daf-16_PPA39986</i>	Reverse primer	GGAAATTAATTGAATGAAGTGAATGC C
MD047	<i>daf-16_PPA39986</i>	Sequencing primer	GCGTTCACCTTTGTTATACAC
MD051	<i>fkh-2_ppa_stranded_DN24289_c0_g1_i1</i>	Forward primer	GCCGTATGTGCAAGCTGTC
MD053	<i>fkh-2_ppa_stranded_DN24289_c0_g1_i1</i>	Reverse primer	AAGTGGTTATGCACTGGTTGAGA
MD052	<i>fkh-2_ppa_stranded_DN24289_c0_g1_i1</i>	Sequencing primer	TCTGCTTTCGTTTTGAAAC
MD054	<i>fkh-7_ppa_stranded_DN25328_c0_g1_i2</i>	Forward primer	TTCTGACAAGCATACGGTACTCC
MD056	<i>fkh-7_ppa_stranded_DN25328_c0_g1_i2</i>	Reverse primer	TCGAGTAATCTACGGGCCA
MD055	<i>fkh-7_ppa_stranded_DN25328_c0_g1_i2</i>	Sequencing primer	TTCCTGTGTCAACGTAAGA
MD063	<i>pha-4_PPA14055</i>	Forward primer	TCTCCATTGACTCGACCATCAG
MD064	<i>pha-4_PPA14055</i>	Reverse primer	ATTCCCCAATCCATCAGAGGAGA

MD065	<i>pha-4_PPA14055</i>	Sequencing primer	ATTGACTCGACCATCAGTGT
MD066	<i>pha-4_PPA14054</i>	Forward primer	TATAACCCGACGTCGTATCAGG
MD067	<i>pha-4_PPA14054</i>	Reverse primer	CTTGGAGGAGACCATTTAGCG
MD068	<i>pha-4_PPA14054</i>	Sequencing primer	TATAACCCGACGTCGTATCA
MD069	<i>pha-4_PPA39541</i>	Forward primer	AGACCAATTGACGCCTGTTAT
MD071	<i>pha-4_PPA39541</i>	Reverse primer	TCAACATGACCGTACAGTTCC
MD070	<i>pha-4_PPA39541</i>	Sequencing primer	CAATTGACGCCTGTTATGTG
MD072	<i>fkx-9_PPA29963</i>	Forward primer	CCTGCTGGTGTACTATGGTCGA
MD073	<i>fkx-9_PPA29963</i>	Reverse primer	AGTTGCGACAACAAGAGGCC
MD074	<i>fkx-9_PPA29963</i>	Sequencing primer	ACTATGGTCGATGAGCCAAG

643

644

645 **Statistical analysis**

646

647 Mouth-form ratios of the mutants were statistically tested against mouth-form ratios in the
648 parental lines by using the R package betareg to fit beta regression (Cribari-Neto and
649 Zeileis, 2010) . This was performed as mouth-form ratios in some mutants displayed a 0
650 ratio. Thus, we used this methodology as described in (Smithson and Verkuilen, 2006)
651 .We applied a $(y^*(n-1)+0.5)/n$ transformation, where y is the response variable and n is

652 the sample size. Following we applied ANOVA and Post hoc pairwise comparison by
 653 using the R package car and lsmeans (Fox *et al.*, 2012; Lenth, 2016).

654

655 **Guide RNA and repair templates**

656

657 Following is a table with sequences for all guide RNA and repair templates used in this
 658 chapter.

659

Experiment	Guide RNA seq 5'--->3'	Repair template seq 5'----->3'
<i>eud-1</i> and <i>sul2.2.1</i> knockout	CTTCACGAATGCCTACAGTG	None
<i>nag-2</i> swap	AGAGAATACGAGGGCTTCAT	ATGCCAAATATTTTCGAAATTT CAGAGAATACGAGGGCTTCT TTGGCCACTACTTCATCTGGT GCTTGCTGCAGAACTTTGG
<i>eud-1</i> intron swap	GAGAATGAGGAAGTTGATTA	TGAAGAGGAGTCATCTGGAG AATGAGGAAGTTGATTACGG CAGCCGAGGAAATGGAGAAA ATAAGTCGGGAGGAAAGATT
<i>eud-1</i> promoter region (1.14kb upstream SNP) swap	GCAGACTACGGCTGACAAAT	AGTACGCTGCACAAGTGCGG AAAATGTGCAGACTACGGCTA ACAAATAGGAAACCACATCAG TCTCAGCATCGTAACTACC
<i>eud-1</i> promoter region (1.98kb upstream SNP) swap	TCGGCGAATTGGTAGCAACT	CCAAGTCTTGCTATCCCTCCG GGGTCCGGCAATTGGTAGCA GCTTTGGTTGCGAAAGGTAA GGCTACCCGAGGAAGCATTG
<i>eud-1</i> promoter region (3.12kb upstream binding motifs)	GTTTTTCGATCTCTTGTACA	AAATCTGTGTCACCCCTGCAA ACACATCAGATAATGTGCGTG TTTACAATAGATTAGTTTTTCG ATCTCTTGTACACGGA

Highly similar region to the 32-block in <i>eud-1</i> first intron	TACATGAAAAATTAGACTAT	None
<i>daf-16_PPA39986</i>	TCTCCTTTATCACGGAAATA	None
<i>fkh-2_ppa_stranded_DN24289_c0_g1_i1</i>	CCTCGAACGTACAATGATCC	None
<i>fkh-7_ppa_stranded_DN25328_c0_g1_i2</i>	TCAGAAGAAATGCCGCCACT	None
<i>pha-4_PPA14055</i>	TGATTACGATGGCAATTCAA	None
<i>pha-4_PPA14054</i>	TGATTACGATGGCAATTCAA	None
<i>pha-4_PPA39541</i>	AGCGGTGGCAGAACTCACTT	None
<i>fkh-9_PPA29963</i>	TGCGACCCGACCAGTGGGGC	None

660

661

662

663

664

665

666

667

668

669

670 **10. Supplementary material**

671

672 **(Supplementary Figure 1) Association map for the Chr X, Chr IV and mouth-form**
673 **phenotype as an example of the translocation argument.** The x axis represents the X
674 chromosome coordinates and chromosome IV coordinates. While the y axis represents
675 the designated number of the sequenced RILs. The z axis shows RILs mouth-form
676 phenotype; as 1 means the highly Eu parental phenotype, while 0 means the highly St
677 parental phenotype. Black and white display genomic markers mapped in these
678 coordinates, either similar to the highly Eu parent or the highly St parent. Both Chr X
679 markers and Chr IV markers show the exact same pattern in all RILS, which supports our
680 argument.

681

682 **(Supplementary Table 1) Detailed description of the mutants in *eud-1*, *sul2.2.1*,**
683 **intronic variant, the 1.14kb variant, the 1.98 variant.**

684

685 **(Supplementary Table 2) Detailed description of the mutants in the 3.12kb variant,**
686 **the triple mutant, and the intronic highly similar sequence to the 3.12 block.**

687

688 **(Supplementary Table 3) Detailed description of the mutants in the *fkh* transcription**
689 **factors encoding genes.**

690

691

692

693

694

695

696

697

698

699

700

11. References

1. Accili, D. and Arden, K. C. (2004) "FoxOs at the crossroads of cellular metabolism, differentiation, and transformation," *Cell*, 117(4), pp. 421–426.
2. Athanasouli, M. et al. (2020) "Comparative genomics and community curation further improve gene annotations in the nematode *Pristionchus pacificus*," *BMC genomics*, 21(1), p. 708.
3. Bento, G., Ogawa, A. and Sommer, R. J. (2010) "Co-option of the hormone-signalling module dafachronic acid-DAF-12 in nematode evolution," *Nature*, 466(7305), pp. 494–497.
4. Broman, K. W. (2005) "The genomes of recombinant inbred lines," *Genetics*, 169(2), pp. 1133–1146.
5. Bui, L. T., Ivers, N. A. and Ragsdale, E. J. (2018a) "A sulfotransferase dosage-dependently regulates mouthpart polyphenism in the nematode *Pristionchus pacificus*," *Nature communications*. Nature Publishing Group, 9(1), pp. 1–10.
6. Bui, L. T., Ivers, N. A. and Ragsdale, E. J. (2018b) "Author Correction: A sulfotransferase dosage-dependently regulates mouthpart polyphenism in the nematode *Pristionchus pacificus*," *Nature communications*, 9(1), p. 4835.
7. Carroll, S. B., Grenier, J. K. and Weatherbee, S. D. (2013) *From DNA to Diversity: Molecular Genetics and the Evolution of Animal Design*. John Wiley & Sons.
8. Charlesworth, B. and Charlesworth, D. (2010) "Elements of evolutionary genetics." Roberts and Company. Available at: <https://www.research.ed.ac.uk/en/publications/elements-of-evolutionary-genetics>.
9. Cribari-Neto, F. and Zeileis, A. (2010) "Beta Regression in R," *Journal of statistical software*. Foundation for Open Access Statistics, 034(i02). Available at: <https://EconPapers.repec.org/RePEc:jss:jstsof:v:034:i02> (Accessed: December 18, 2021).
10. Edgar, R. C. (2004) "MUSCLE: multiple sequence alignment with high accuracy and high throughput," *Nucleic acids research*, 32(5), pp. 1792–1797.

11. Fielenbach, N. and Antebi, A. (2008) "C. elegans dauer formation and the molecular basis of plasticity," *Genes & development*, 22(16), pp. 2149–2165.
12. Fox, J. et al. (2012) "Package 'car,'" Vienna: R Foundation for Statistical Computing. [mirrors.uct.ac.za](https://mirrors.uct.ac.za/CRAN/src/contrib/201209/00/car_2.26-1.tar.gz), p. 16.
13. Fuxman Bass, J. I. et al. (2014) "Transcription factor binding to *Caenorhabditis elegans* first introns reveals lack of redundancy with gene promoters," *Nucleic acids research*, 42(1), pp. 153–162.
14. Gaudet, J. and Mango, S. E. (2002) "Regulation of organogenesis by the *Caenorhabditis elegans* FoxA protein PHA-4," *Science*, 295(5556), pp. 821–825.
15. Gompel, N. et al. (2005) "Chance caught on the wing: cis-regulatory evolution and the origin of pigment patterns in *Drosophila*," *Nature*. Nature Publishing Group, 433(7025), pp. 481–487.
16. Han, Z. et al. (2020) "Improving Transgenesis Efficiency and CRISPR-Associated Tools Through Codon Optimization and Native Intron Addition in *Pristionchus Nematodes*," *Genetics*, 216(4), pp. 947–956.
17. Kanzaki, N. et al. (2013) "Two androdioecious and one dioecious new species of *pristionchus* (nematoda: diplogastridae): new reference points for the evolution of reproductive mode," *Journal of nematology*, 45(3), pp. 172–194.
18. Kieninger, M. R. et al. (2016) "The Nuclear Hormone Receptor NHR-40 Acts Downstream of the Sulfatase EUD-1 as Part of a Developmental Plasticity Switch in *Pristionchus*," *Current biology: CB*, 26(16), pp. 2174–2179.
19. Kim, D. et al. (2013) "TopHat2: accurate alignment of transcriptomes in the presence of insertions, deletions and gene fusions," *Genome biology*, 14(4), p. R36.
20. Lenth, R. V. (2016) "Least-Squares Means: The R Package lsmeans," *Journal of statistical software*. Foundation for Open Access Statistics, 069(i01). Available at: <https://EconPapers.repec.org/RePEc:jss:jstsof:v:069:i01> (Accessed: December 18, 2021).

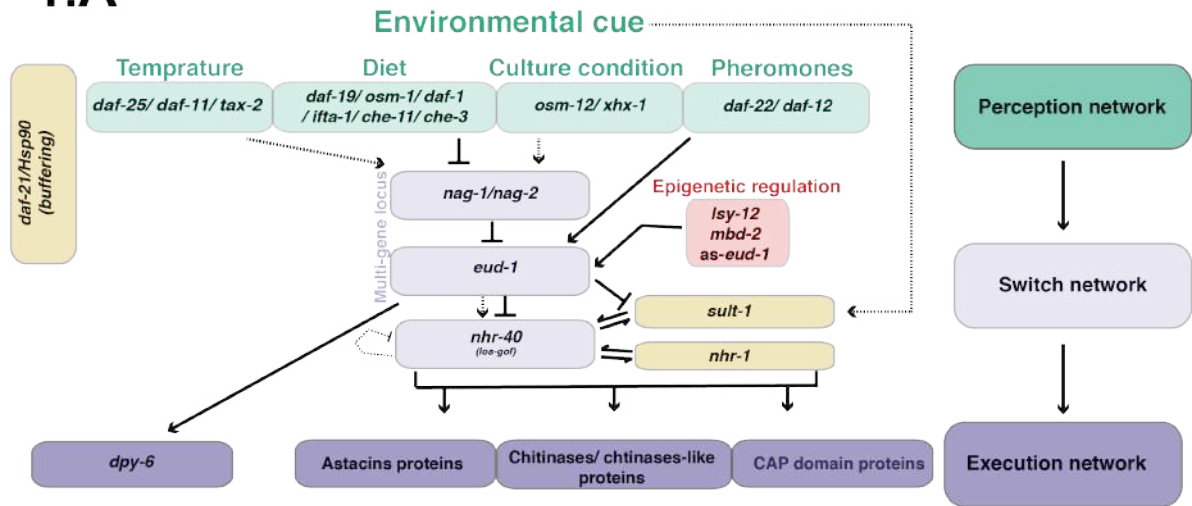
21. Lenuzzi, M. et al. (2021) "Influence of environmental temperature on mouth-form plasticity in *Pristionchus pacificus* acts through daf-11-dependent cGMP signaling," *Journal of experimental zoology. Part B, Molecular and developmental evolution*. John Wiley & Sons, Ltd, n/a(n/a). doi: 10.1002/jez.b.23094.
22. Li, H. and Durbin, R. (2009) "Fast and accurate short read alignment with Burrows–Wheeler transform," *Bioinformatics* . Oxford Academic, 25(14), pp. 1754–1760.
23. Lightfoot, J. W. et al. (2019) "Small peptide-mediated self-recognition prevents cannibalism in predatory nematodes," *Science*, 364(6435), pp. 86–89.
24. Lin, K. et al. (1997) "daf-16: An HNF-3/forkhead family member that can function to double the life-span of *Caenorhabditis elegans*," *Science*, 278(5341), pp. 1319–1322.
25. McGaughran, A. et al. (2016) "Genomic Profiles of Diversification and Genotype–Phenotype Association in Island Nematode Lineages," *Molecular biology and evolution*. Oxford Academic, 33(9), pp. 2257–2272.
26. McGregor, A. P. et al. (2007) "Morphological evolution through multiple cis-regulatory mutations at a single gene," *Nature*. nature.com, 448(7153), pp. 587–590.
27. Moreno, E. et al. (2019) "Cilia drive developmental plasticity and are essential for efficient prey detection in predatory nematodes," *Proceedings. Biological sciences / The Royal Society*, 286(1912), p. 20191089.
28. Nakagawa, S. et al. (2013) "DNA-binding specificity changes in the evolution of forkhead transcription factors," *Proceedings of the National Academy of Sciences of the United States of America*, 110(30), pp. 12349–12354.
29. Namdeo, S. et al. (2018) "Two independent sulfation processes regulate mouth-form plasticity in the nematode *Pristionchus pacificus*," *Development* , 145(13). doi: 10.1242/dev.166272.
30. Rae, R. et al. (2012) "The importance of being regular: *Caenorhabditis elegans* and *Pristionchus pacificus* defecation mutants are hypersusceptible to bacterial pathogens," *International journal for parasitology*, 42(8), pp. 747–753.

31. Ragsdale, E. J. et al. (2013) "A developmental switch coupled to the evolution of plasticity acts through a sulfatase," *Cell*, 155(4), pp. 922–933.
32. Rödelsperger, C. et al. (2017) "Single-Molecule Sequencing Reveals the Chromosome-Scale Genomic Architecture of the Nematode Model Organism *Pristionchus pacificus*," *Cell reports*, 21(3), pp. 834–844.
33. Rödelsperger, C. et al. (2018) "Phylotranscriptomics of *Pristionchus* Nematodes Reveals Parallel Gene Loss in Six Hermaphroditic Lineages," *Current biology: CB*, 28(19), pp. 3123-3127.e5.
34. Rödelsperger, C. (2021) "The community-curated *Pristionchus pacificus* genome facilitates automated gene annotation improvement in related nematodes," *BMC genomics*, 22(1), p. 216.
35. Roff, D. A. (1996) "The Evolution of Threshold Traits in Animals," *The Quarterly review of biology*. University of Chicago Press, 71(1), pp. 3–35.
36. Roff, D. A. (1998) "The maintenance of phenotypic and genetic variation in threshold traits by frequency-dependent selection," *Journal of evolutionary biology*, 11(4), pp. 513–529.
37. Schliep, K. P. (2011) "phangorn: phylogenetic analysis in R," *Bioinformatics*, 27(4), pp. 592–593.
38. Schuster, L. N. and Sommer, R. J. (2012) "Expressional and functional variation of horizontally acquired cellulases in the nematode *Pristionchus pacificus*," *Gene*, 506(2), pp. 274–282.
39. Serobyán, V. et al. (2016) "Chromatin remodelling and antisense-mediated up-regulation of the developmental switch gene *eud-1* control predatory feeding plasticity," *Nature communications*, 7, p. 12337.
40. Sieriebriennikov, B. et al. (2018) "A Developmental Switch Generating Phenotypic Plasticity Is Part of a Conserved Multi-gene Locus," *Cell reports*, 23(10), pp. 2835-2843.e4.

41. Sieriebriennikov, B. et al. (2020) "Conserved nuclear hormone receptors controlling a novel plastic trait target fast-evolving genes expressed in a single cell," *PLoS genetics*, 16(4), p. e1008687.
42. Sieriebriennikov, B. and Sommer, R. J. (2018) "Developmental Plasticity and Robustness of a Nematode Mouth-Form Polyphenism," *Frontiers in genetics*, 9, p. 382.
43. Smithson, M. and Verkuilen, J. (2006) "A better lemon squeezer? Maximum-likelihood regression with beta-distributed dependent variables," *Psychological methods*, 11(1), pp. 54–71.
44. Snell-Rood, E. C. et al. (2018) "Mechanisms of Plastic Rescue in Novel Environments," *Annual Review of Ecology, Evolution, and Systematics*, pp. 331–354. doi: 10.1146/annurev-ecolsys-110617-062622.
45. Stiernagle, T. (2006) Maintenance of *C. elegans*. WormBook.
46. Sun, S. et al. (2021) "The oscillating Mucin-type protein DPY-6 has a conserved role in nematode mouth and cuticle formation," *Genetics*. academic.oup.com. doi: 10.1093/genetics/iyab233.
47. Sun, S., Rödelberger, C. and Sommer, R. J. (2021) "Single worm transcriptomics identifies a developmental core network of oscillating genes with deep conservation across nematodes," *Genome research*, 31(9), pp. 1590–1601.
48. Sun, X., Chen, W.-D. and Wang, Y.-D. (2017) "DAF-16/FOXO Transcription Factor in Aging and Longevity," *Frontiers in pharmacology*, 8, p. 548.
49. Susoy, V. and Sommer, R. J. (2016) "Stochastic and conditional regulation of nematode mouth-form dimorphisms," *Frontiers in Ecology and Evolution*. frontiersin.org. Available at: <https://www.frontiersin.org/articles/10.3389/fevo.2016.00023/full>.
50. Trapnell, C. et al. (2013) "Differential analysis of gene regulation at transcript resolution with RNA-seq," *Nature biotechnology*, 31(1), pp. 46–53.

51. Werner, M. S. et al. (2017) "Environmental influence on *Pristionchus pacificus* mouth form through different culture methods," *Scientific reports*, 7(1), p. 7207.
52. Werner, M. S., Claaßen, M. H., et al. (2018) "Adult Influence on Juvenile Phenotypes by Stage-Specific Pheromone Production," *iScience*, 10, pp. 123–134.
53. Werner, M. S., Sieriebriennikov, B., et al. (2018) "Young genes have distinct gene structure, epigenetic profiles, and transcriptional regulation," *Genome research*, 28(11), pp. 1675–1687. Witte, H. et al. (2015) "Gene inactivation using the CRISPR/Cas9 system in the nematode *Pristionchus pacificus*," *Development genes and evolution. Springer*, 225(1), pp. 55–62.
54. Wittkopp, P. J. and Kalay, G. (2011) "Cis-regulatory elements: molecular mechanisms and evolutionary processes underlying divergence," *Nature reviews. Genetics. nature.com*, 13(1), pp. 59–69.
55. Wray, G. A. (2007) "The evolutionary significance of cis-regulatory mutations," *Nature reviews. Genetics. nature.com*, 8(3), pp. 206–216.

1.A



1.B

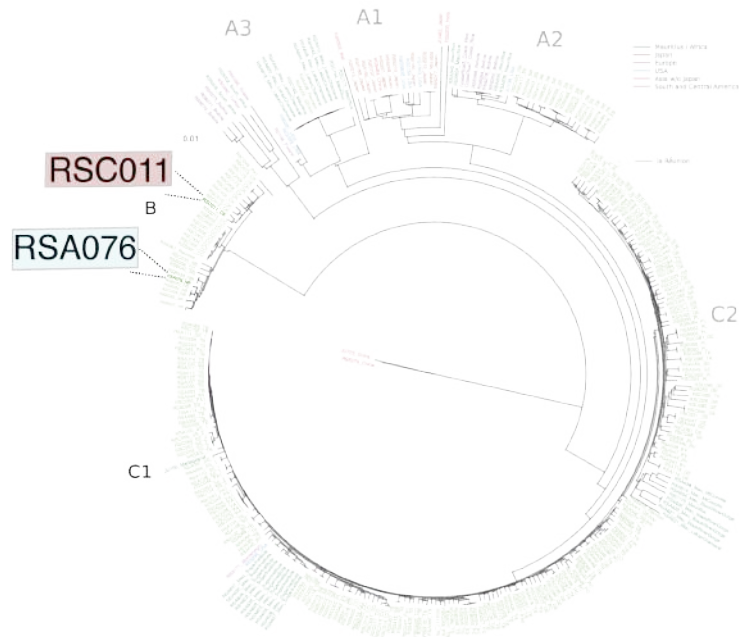
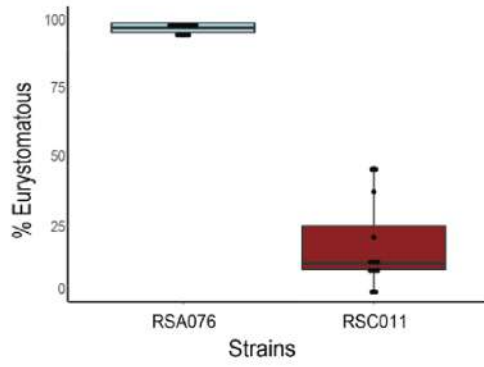
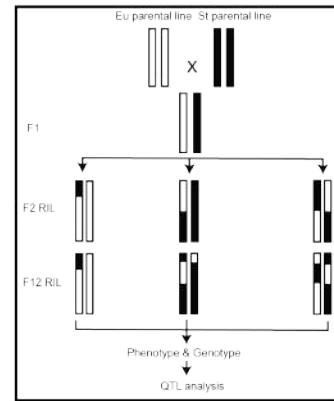


Figure 1

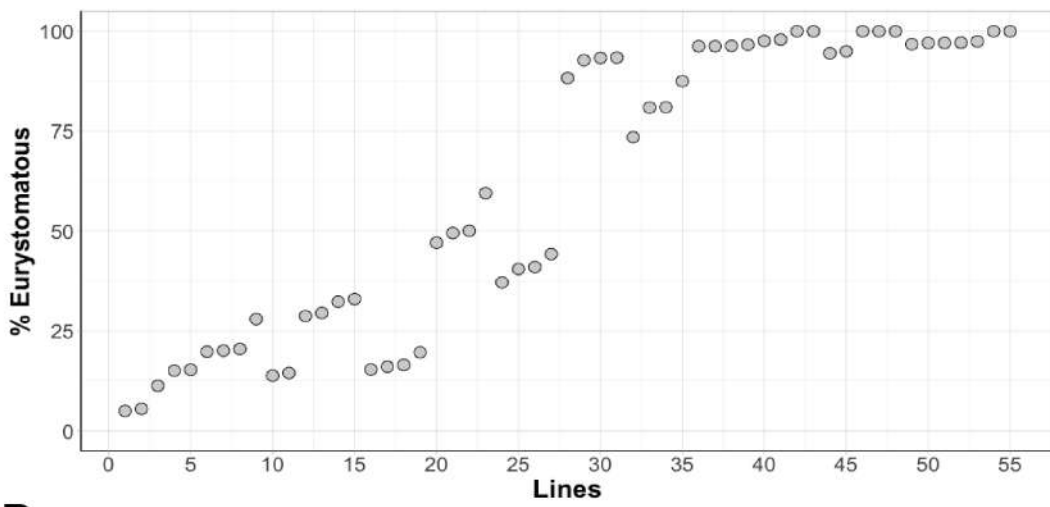
2.A



2.B



2.C



2.D

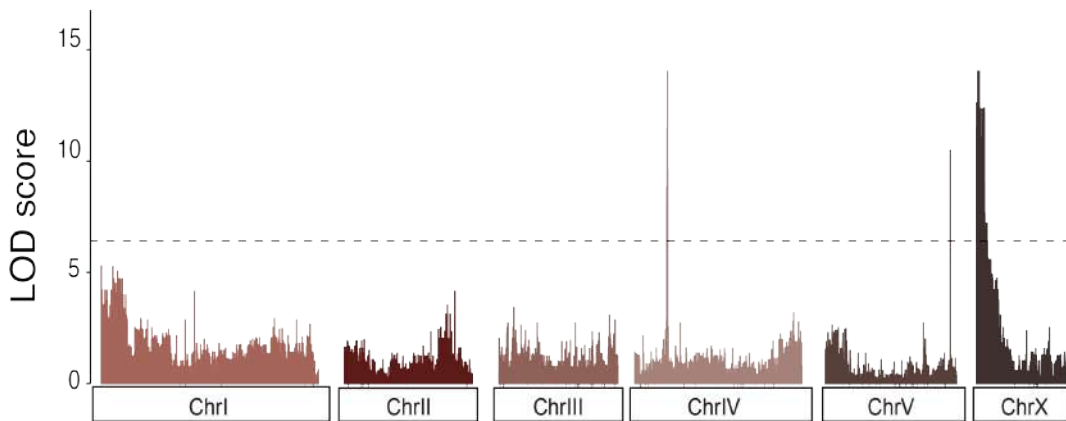
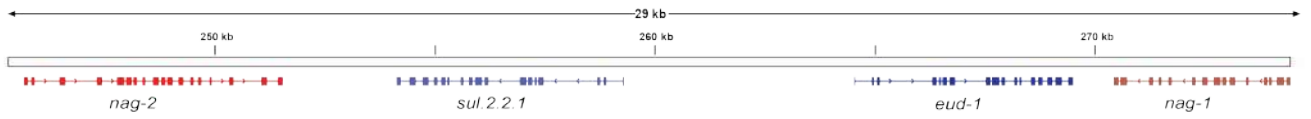
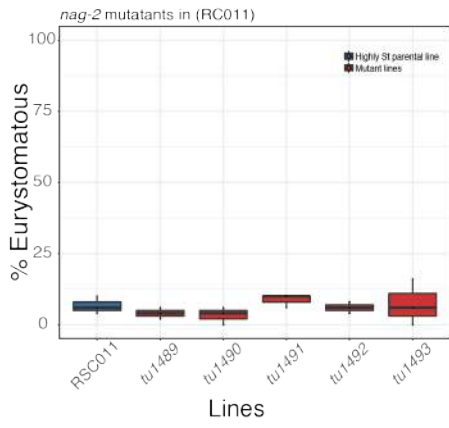


Figure 2

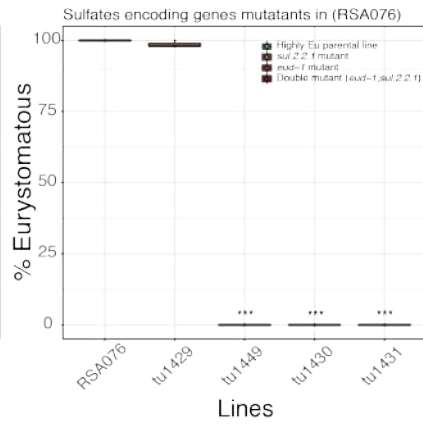
3.A



3.B



3.C



3.D

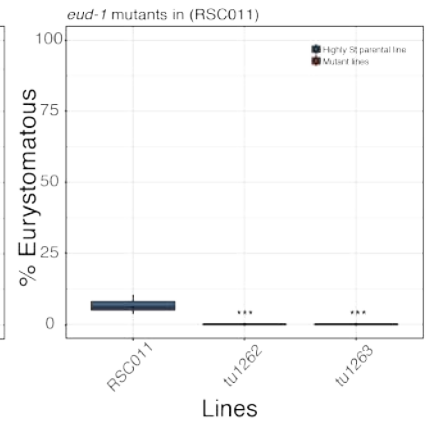


Figure 3

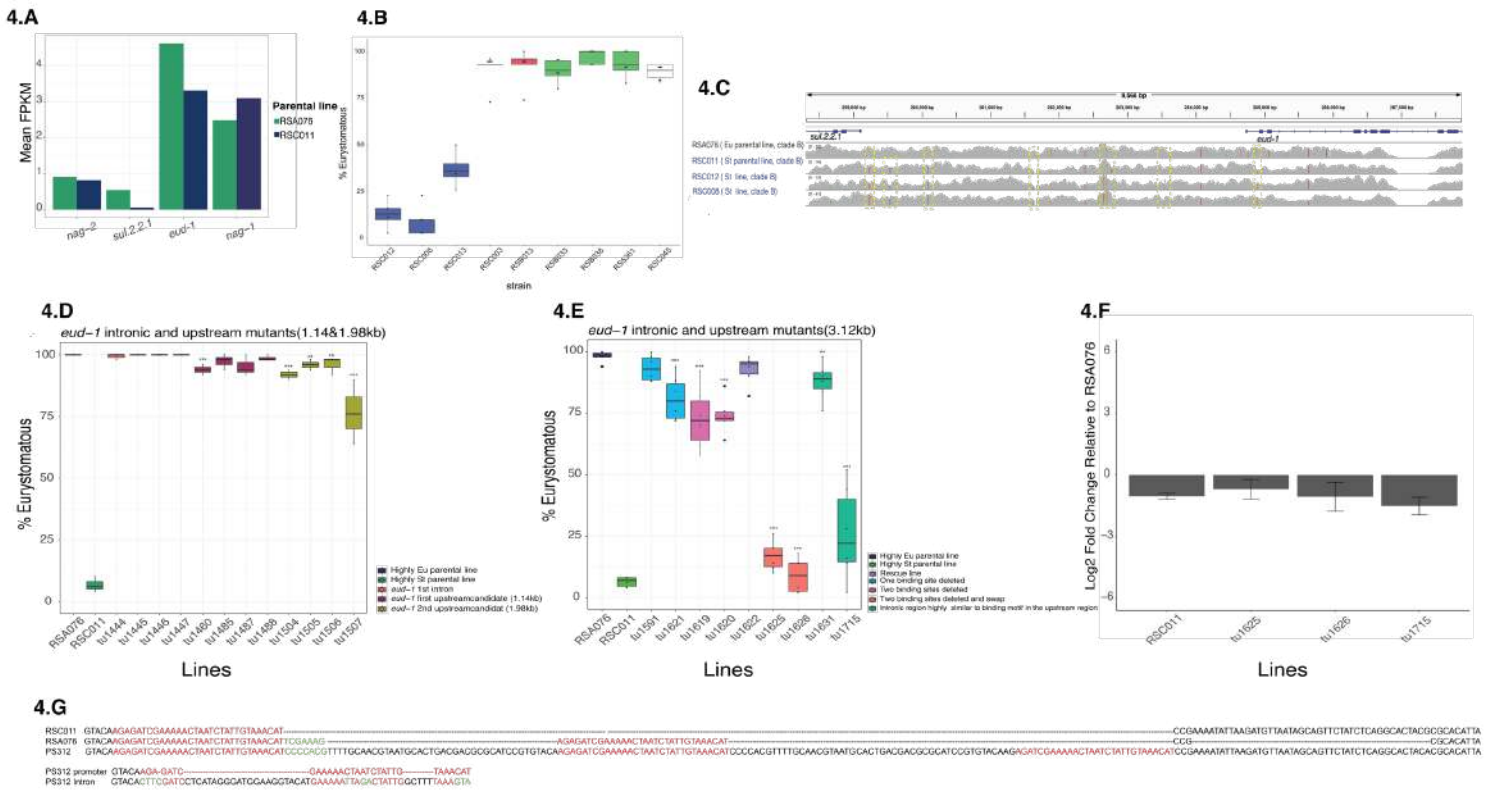
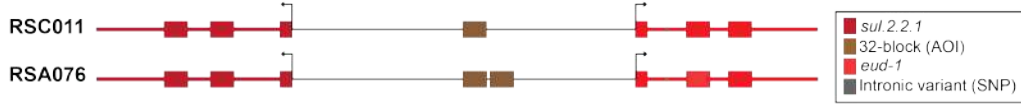
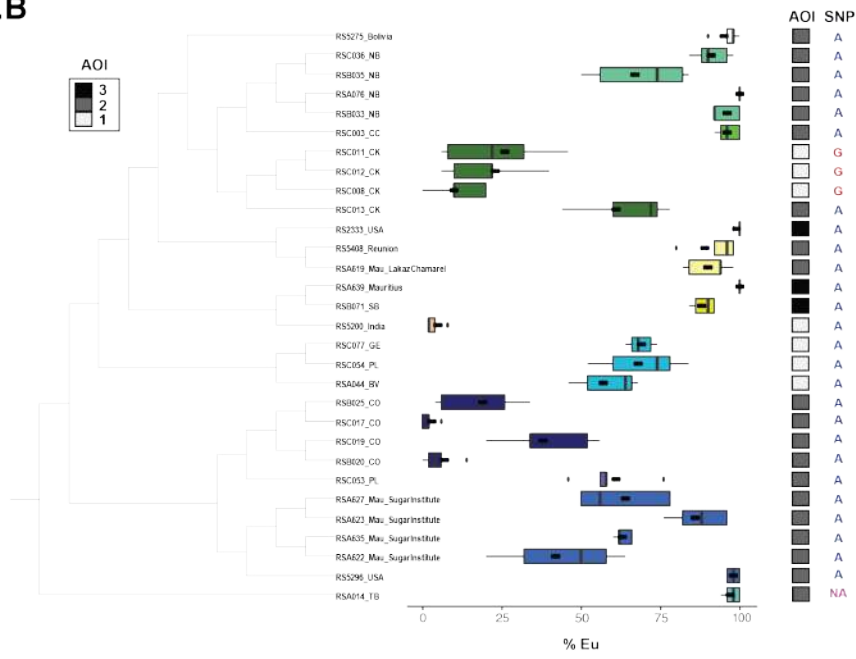


Figure 4

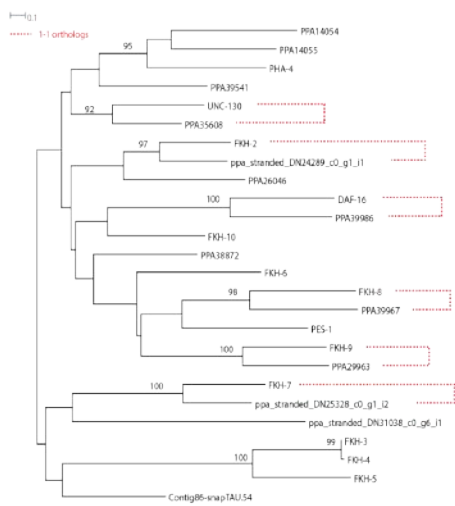
5.A



5.B



5.C



5.D

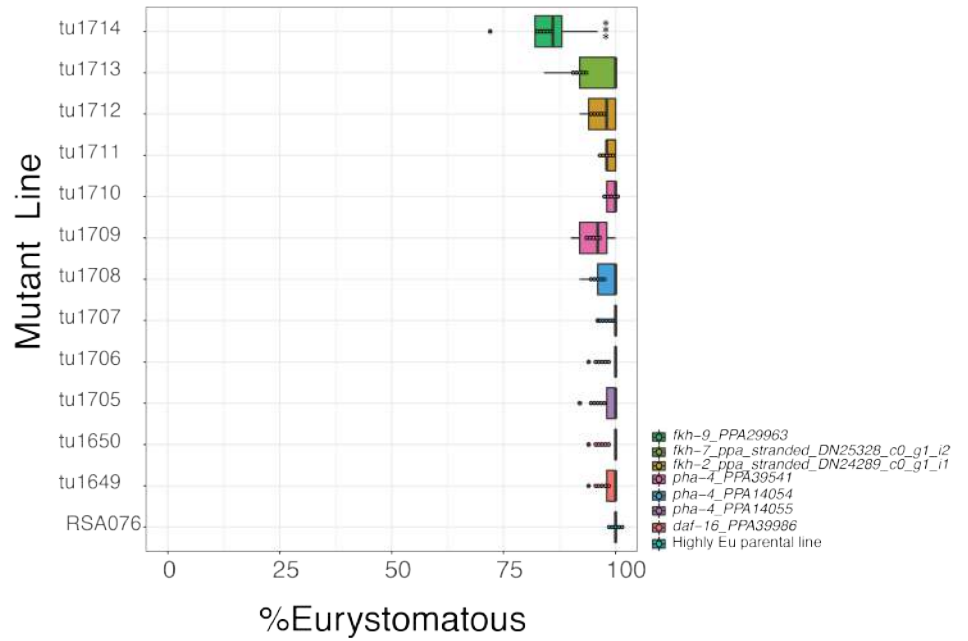
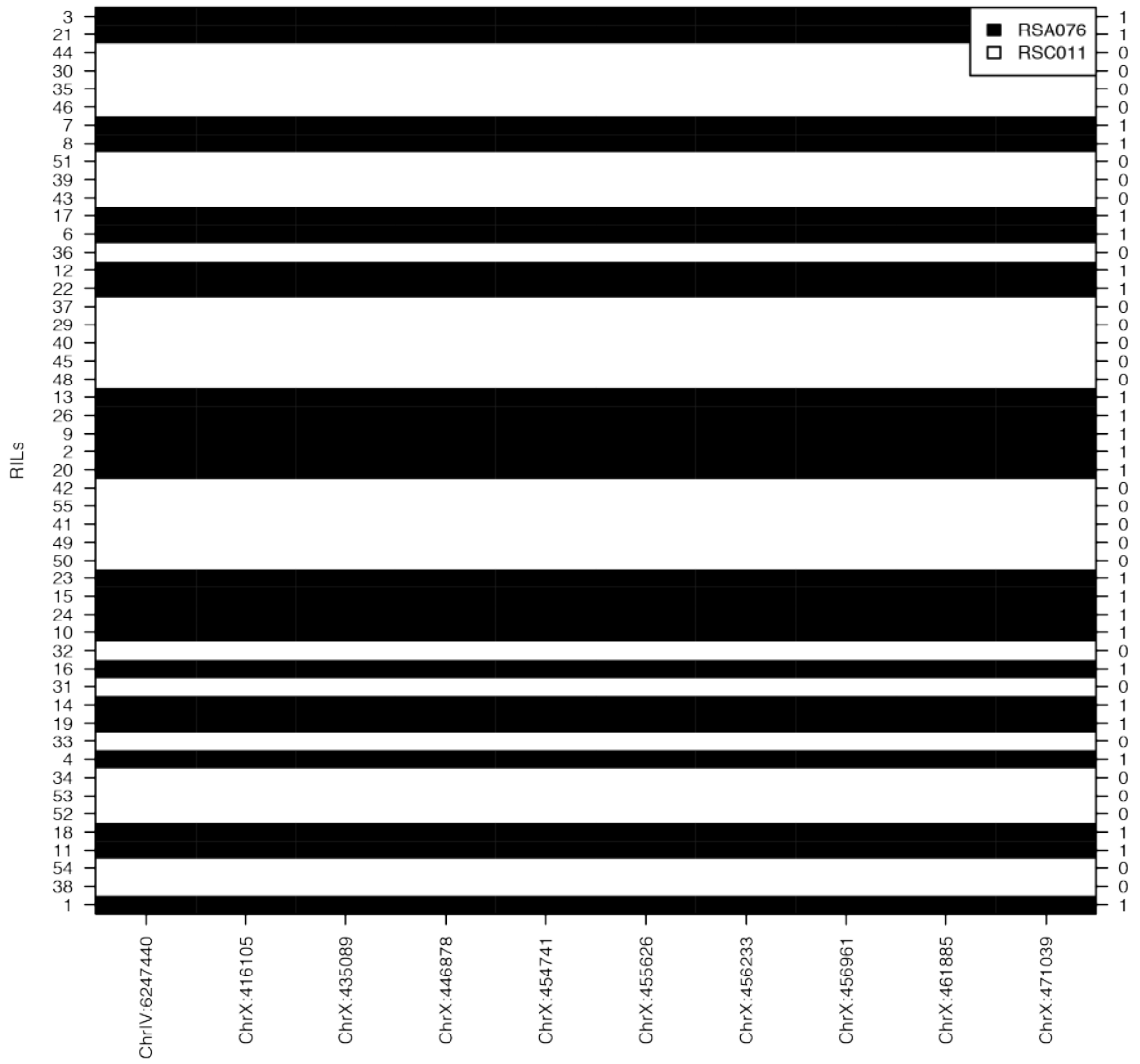


Figure 5



Supplementary Figure 1

Gene/ Regulatory element	Background	Allele	Description/lesion
<i>eud-1</i>	RSC011	<i>tu1262</i>	10bp deletion
<i>eud-1</i>	RSC011	<i>tu1263</i>	24bp insertions + 5 bp deletions = 19 net
<i>eud-1</i>	RSA076	<i>tu1449</i>	7bp deletion + 4bp substitutions
<i>sul.2.2.1</i>	RSA076	<i>tu1429</i>	2bp deletion
double mutant (<i>eud-1; sul.2.2.1</i>)	RSA076	<i>tu1430</i>	<i>eud-1</i> (37bp insertion); <i>sul.2.2.1</i> (5bp deletion)
double mutant (<i>eud-1; sul.2.2.1</i>)	RSA076	<i>tu1431</i>	<i>eud-1</i> (23bp insertion); <i>sul.2.2.1</i> (1bp deletion)
<i>nag-2</i>	RSC011	<i>tu1489</i>	Swap from A to T
<i>nag-2</i>	RSC011	<i>tu1490</i>	Swap from A to T
<i>nag-2</i>	RSC011	<i>tu1491</i>	16bp deletion+ intact targeted SNP (A)
<i>nag-2</i>	RSC011	<i>tu1492</i>	1bp substitution + targeted SNP deleted
<i>nag-2</i>	RSC011	<i>tu1493</i>	9bp deletion including the targeted SNP
<i>eud-1</i> 1st intron	RSA076	<i>tu1444</i>	Swap from A to G
<i>eud-1</i> 1st intron	RSA076	<i>tu1445</i>	1bp deletion + intact targeted SNP (A)
<i>eud-1</i> 1st intron	RSA076	<i>tu1446</i>	2bp deletion + intact targeted SNP (A)
<i>eud-1</i> 1st intron	RSA076	<i>tu1447</i>	4 bp deletion + intact targeted SNP (A)
<i>eud-1</i> first upstream candidate (1.14kb)	RSA076	<i>tu1485</i>	Swap from G to A + 7 bp insertion + 1 substitution
<i>eud-1</i> first upstream candidate (1.14kb)	RSA076	<i>tu1487</i>	8bp deletion including the targeted SNP
<i>eud-1</i> first upstream candidate (1.14kb)	RSA076	<i>tu1488</i>	15bp deletion including the targeted SNP
<i>eud-1</i> first upstream candidate (1.14kb)	RSA076	<i>tu1460</i>	Deletion of the targeted SNP + 2bp substitution
<i>eud-1</i> 2nd upstream candidate (1.98kb)	<i>tu1485</i> (RSA076)	<i>tu1504</i>	Swap from A to G
<i>eud-1</i> 2nd upstream candidate (1.98kb)	<i>tu1485</i> (RSA076)	<i>tu1507</i>	11bp deletion including the targeted SNP
<i>eud-1</i> 2nd upstream candidate (1.98kb)	<i>tu1485</i> (RSA076)	<i>tu1505</i>	3bp deletion including the targeted SNP
<i>eud-1</i> 2nd upstream candidate (1.98kb)	<i>tu1485</i> (RSA076)	<i>tu1506</i>	11bp deletion including the targeted SNP

Supplementary Table 1

Gene/ Regulatory element	Background	Allele	Description/lesion
<i>eud-1</i> 3rd upstream candidate (3.12kb)	<i>tu150</i> (RSA076)	<i>tu1591</i>	One potential Forkhead binding motif deleted (32-block)
<i>eud-1</i> 3rd upstream candidate (3.12kb)	<i>tu150</i> (RSA076)	<i>tu1621</i>	One potential Forkhead binding motif deleted (32-block)
<i>eud-1</i> 3rd upstream candidate (3.12kb)	<i>tu1621</i> (RSA076)	<i>tu1619</i>	Two potential Forkhead binding motif deleted (64-block)
<i>eud-1</i> 3rd upstream candidate (3.12kb)	<i>tu1621</i> (RSA076)	<i>tu1620</i>	Two potential Forkhead binding motif deleted (64-block)
<i>eud-1</i> 3rd upstream candidate (3.12kb)	<i>tu1621</i> (RSA076)	<i>tu1622</i>	Rescue line were the 2nd 32-block is re-inserted
<i>eud-1</i> 3rd upstream candidate (3.12kb) + intronic SNP	<i>tu1620</i> (RSA076)	<i>tu1625</i>	Two potential Forkhead binding motif deleted (64-block) + Swap from A to G
<i>eud-1</i> 3rd upstream candidate (3.12kb) + intronic SNP	<i>tu1620</i> (RSA076)	<i>tu1626</i>	Two potential Forkhead binding motif deleted (64-block) + Swap from A to G
<i>eud-1</i> intronic region highly similar to the 32-block in the upstream region	RSA076	<i>tu1631</i>	6bp deletion
<i>eud-1</i> intronic region highly similar to the 32-block in the upstream region	RSA076	<i>tu1715</i>	4 bases insertion + 1 substitution

Supplementary Table 2

Gene	Background	Allele	Description/lesion
<i>daf-16_PPA39986</i>	RSA076	<i>tu1649</i>	4bp deletion
<i>daf-16_PPA39986</i>	RSA076	<i>tu1650</i>	34 bp insertion + 2bp substitution
<i>fkh2_ppa_stranded_DN24289_c0_g1_i1</i>	RSA076	<i>tu1711</i>	8bp deletion
<i>fkh2_ppa_stranded_DN24289_c0_g1_i1</i>	RSA076	<i>tu1712</i>	2bp insertion
<i>fkh7_ppa_stranded_DN25328_c0_g1_i2</i>	RSA076	<i>tu1713</i>	5bp deletion
<i>Pha-4_PPA14055</i>	RSA076	<i>tu1705</i>	heterozygous animals (homozygous lethal)
<i>Pha-4_PPA14055</i>	RSA076	<i>tu1706</i>	heterozygous animals (homozygous lethal)
<i>Pha-4_PPA14054</i>	RSA076	<i>tu1707</i>	11bp deletion
<i>Pha-4_PPA14054</i>	RSA076	<i>tu1708</i>	10bp deletion
<i>pha-4_PPA39541</i>	RSA076	<i>tu1709</i>	8bp deletion
<i>pha-4_PPA39541</i>	RSA076	<i>tu1710</i>	4bp deletion
<i>fkh-9_PPA29963</i>	RSA076	<i>tu1714</i>	2bp deletion

Supplementary Table 3